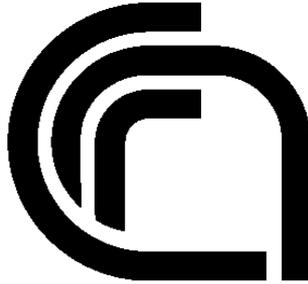# NATIONAL RESEARCH COUNCIL OF ITALY

ADVISORY COMMITTEE
ON TECHNICAL RECOMMENDATIONS FOR CONSTRUCTION

Guide for the assessment of wind actions and effects on structures

CNR-DT 207/2008

ROMA – CNR June 11th, 2010

CNR-DT 207/2008

INDEX

1 GENERAL

1.1 MOTIVATION

The advent of innovative techniques and materials, the development of numerical and experimental methods and the wish to make constructions with striking and stylish formal connotations have given rise to a new generation of increasingly daring and complex structures (low- and high-rise buildings, towers, lighting columns, bridges and footbridges, roofings and shelters, chimneys and tanks, industrial buildings and their structural components, cranes, cables and cable systems, cladding or finishings etc.). These structures are often characterised by exceptional height, length, slenderness, flexibility and lightness, combined with unusual shapes. As such, they are exposed to a wind action that plays a primary role, and whose effects must be assessed in order to ensure the required degree of safety.

These constructions are becoming increasingly common in many countries of the world, including Italy, and they are often built together with more conventional, stiff and bulky structures for which the role of wind loads is far less important, though not negligible. This situation leads to a more and more complex and wider range of structures that requires design principles and rules able of encompassing simple and immediate methods for normal situations, detailed methods for special construction needs and criteria that turn the designer towards advanced numerical, analytical and/or experimental techniques. This occurs especially in those cases involving complex physical phenomena, representing a challenge for the engineer.

Wind Engineering, officially defined as "the rational treatment of interactions between wind in the atmospheric boundary layer and man and his works on the surface of Earth", is a scientific discipline founded in the '60s, that has recorded a tremendous growth over the years. Within its field of activity, it has followed the progress of civil and industrial construction through the development of appropriate solutions to wind-related problems to which man-made structures are prone. Activities in the area of Wind Engineering are coordinated by the *International Association for Wind Engineering* (IAWE) (**www.iawe.org**), a body whose role is recognised worldwide.

Many countries, such as the United States, Japan, Australia, Canada and the United Kingdom, have regularly updated their standards, incorporating into them state-of-the-art tools, adequate with a constantly-developing construction industry. This triggered the attention of the consultancy on wind-related problems. On the other hand, after the release in 1964 of one of the world's first standards on wind actions on structures by the National Research Council, Italy has made no update to a document that, initially ground-breaking, became more and more obsolete and misleading as time passed and knowledge in Wind Engineering grew. This brought to the freezing of technical knowledge and slowed down the growth of those areas of structural engineering related to Wind Engineering.

Given this situation, the implementation of the Eurocodes in the '90s has created conflict in Italy. On the one hand, this introduced principles which were consistent with the state-of-the-art of the time, sometimes indeed advanced; on the other hand, almost without warning, the Italian engineer suddenly found himself face to face with a huge and complex document nearly alien from the regulations applied for years. Having played no part in this process by means of a systematic and progressive development of codes, the Italian engineer has therefore been almost a stranger to it. The release of the new Italian Building Code in 2008, has helped in harmonising Italian and European codes of practice; however, it is not enough to bridge the enormous gap that still exists between two documents of very different complexity and structure. Above all, when dealing with structures that are aerodynamically complex or dynamically susceptible to wind, the engineer is forced to turn to Eurocodes or other documents of similar or greater quality and detail. In addition, in some cases he or she is forced to merge the specifications of several documents.

Acknowledging this situation, the National Research Council has decided it would be expedient, and indeed its official duty, to take an important step on behalf of engineers and the national technical/scientific community by drawing up, with the aid of a Committee open to any form of contribution, Document CNR-DT 207/2008. Such a document meets the general concept of "Guide" in both a "regulatory" and "informative" sense.

From a regulatory point of view, Document CNR-DT 207/2008 is generally consistent with both Italian Building Code (Decreto Ministeriale 14/01/2008) and the Eurocodes as a whole. When it departs from these documents it is to incorporate recent progress recognised worldwide. In addition, it extends to several areas not dealt with by the Italian Building Code and/or by Eurocode 1, acknowledging several aspects of the recent progress in science and in codification that the Eurocode has failed to incorporate in its initial draft (ENV, 1994) and final version (EN 2005). Above all, it brings together in one uniform publication, the set of all those principles and rules the engineers might need when analysing the behaviour of structures and their components under the wind action.

From an informative point of view, in drafting Document CNR-DT 207/2008 an effort has been made to make it not just provide hard-to-understand and difficult-to-apply principles and rules, but also to help the reader to understand and apply its contents. The key to the Document is given in Section 2, summarising the basics of wind actions and effects on structures, and Section 3, explaining design criteria. Examples of application of the Document are given in Section 4, which contains a number of worked examples and Chapter 3, containing equations and diagrams; the former are given for use in automated procedures, whilst the latter allow immediate interpretation of the trends of the relevant parameter and the visual check of the results of the calculations.

Due to their origin and nature, the guide contained in Document CNR-DT 207/2008 is therefore not to be meant as compulsory rules, but rather a tool provided to engineers in sifting through national and international publications, whilst leaving them with the freedom and final responsibility for the choices made.

The National Research Council Advisory Committee on Technical Recommendations for Constructions and the Committee for the drafting of this Document express their appreciation for, and satisfaction with, the Italian technical /scientific community that with great spirit of cooperation has been involved in the preparation of the document and in the public inquiry stage.

This Technical Document was drafted by a Committee comprising:
Prof. Gianni BARTOLI   - University of Florence
Prof. Vittorio GUSELLA   - University of Perugia
Prof. Giuseppe PICCARDO   - University of Genoa
Prof. Pierangelo PISTOLETTI   - Seteco Ingegneria - University of Genoa
Prof. Francesco RICCIARDELLI   - University of Reggio Calabria
Prof. Giovanni SOLARI (*Coordinator*)   - University of Genoa
Ing. Alberto VINTANI   - BCV Progetti - Milan

A preliminary version of the Italian text of the document was approved on January 1, 2008, and presented to a public inquiry, by the "Advisory Committee on Technical Recommendations for Constructions" comprising:

Prof. Franco ANGOTTI   - University of Florence
Prof. Luigi ASCIONE   - University of Salerno
Prof. Alessandro BARATTA   - University of Naples Federico II
Prof. Edoardo COSENZA   - University of Naples Federico II
Prof. Elio GIANGRECO   - University of Naples Federico II

Prof. Ruggiero JAPPELLI   - University of Rome Tor Vergata
Prof. Franco MACERI (*President*)   - University of Rome Tor Vergata
Prof. Federico M. MAZZOLANI   - University of Naples Federico II
Prof. Paolo Emilio PINTO   - University of Rome La Sapienza
Prof. Piero POZZATI   - University of Bologna
Prof. Giovanni SOLARI   - University of Genoa
Prof. Carlo URBANO   - Techical University of Milan
Arch. Roberto VINCI   - National Research Council of Italy
Prof. Paolo   ZANON   - University of Trento

At the end of the public inquiry, the "Advisory Committee on Technical Recommendations for Constructions" approved the final Italian version of the document on February 2, 2009. Meanwhile Professor Elio Giangreco and Professor Piero Pozzati ceased to be members of the Commission.

This updated document has been discussed and approved during the meeting held on June 11, 2010 at the CNR headquarters in Rome by the aforementioned Advisory Committee.

1.2 FIELD OF APPLICATION

Subject to the limitations and requirements specified herein, this Document applies to civil engineering structures of height not exceeding 200 m, industrial structures, including moving and lifting equipment, and bridges with spans not greater than 200 m, and of the types listed in the relevant Sections.

The Document provides wind actions (pressures, forces, moments, etc.) on the whole resisting structure and on its components, including both structural and non-structural parts (Figure 1.1). On the other hand, it generally refers the reader to other technical standards or specialist publications as regards the effects induced by these actions (stresses, displacements, strains, etc.) and the relevant checks (Ultimate Limit States, Serviceability Limit State, Fatigue Limit States, etc.).
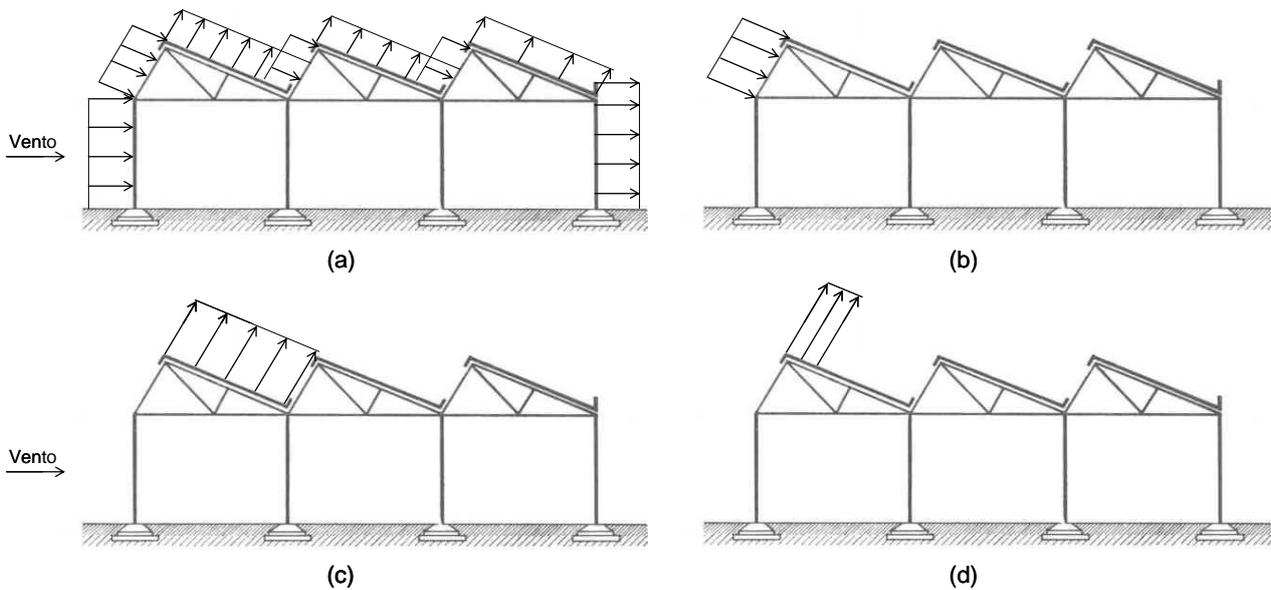
Figure 1.1 - Wind actions: (a) on the whole resisting structure;(b) on an individual structural element; (c) on non-structural roof elements; (d) on roof fasteners.

Furthermore, many parts of the document contain explicit or implicit requirements and criteria associated with the effects of wind actions. This occurs specifically when the effect plays a role in the definition of the action (e.g. in requirements for equivalent static actions, i.e. actions that when applied statically to the structure, or one of its components produce a static effect equal to the maximum corresponding dynamic one) and as part of aeroelastic phenomena in which the wind-structure interaction makes it impossible to separate the action from the effect.

The Document also provides specific guidance on the effects of wind forces and on the relevant checks, should they have any peculiar aspects. Typical examples are the procedure for calculating the number of stress cycles produced by resonant vortex shedding from slender structures or elements with the aim of fatigue checks and the check of serviceability of buildings with respect to floor accelerations.

1.3 ORGANISATION OF THE DOCUMENT AND KEY TO ITS USE

The Document is divided into four Sections.

Section 1 contains general introductory remarks. It places the Document within the framework of the Italian tradition and of the international scenario (1.1), it defines the scope of the Guide (1.2), it illustrates the organisation of the Document and provides a key to its use (1.3), whilst listing the main normative references (1.4) and symbols utilised (1.5).

Section 2 provides basic concepts regarding the actions and effects of wind on structures (2.1-2.8) and provides a summary of essential wind engineering publications (2.9). Experts in the field or persons simply wanting to apply the Instructions directly can skip this Section.

Section 3 contains the body of the Guide. It is divided into two parts: the main body of the text (subsections 3.1 to 3.4) and a set of 15 Annexes (A-Q).

The main body of the text gives explicit criteria for assessing design wind velocity and pressure (3.2); it also explains the general notions of aerodynamic actions (3.3) and dynamic and aeroelastic effects (3.4). Following the approach of the Eurocodes, the Section is arranged in clauses which can be either "principles", identified by the letter "P", or "rules".

The annexes provide guides and criteria that incorporate the current state-of-the-art on how to perform detailed assessments of the characteristics of the oncoming wind (A-F), of the aerodynamic actions (G-H) and of the dynamic and aeroelastic effects (I-P). Annex Q, regarding the use of wind tunnels, is transverse to all topics. The structure chosen for the Document guarantees three main advantages: it simplifies its implementation because only a limited portion of the text has to be used for each application, i.e. the main part and few relevant annexes; this means that, where appropriate, procedures of equal or greater quality and in-depth analysis can be used instead of each particular annex; it helps to extend the validity of the main text and allows limiting maintenance only to those portions requiring it.

Section 4 brings ten worked examples of application of the Guide to ten among the most common structural types. It therefore provides guidance and facilitates the use of the Document, especially for the first-time user.

Figure 1.2 shows the organisation of Sections 2 (Basics) and 3 (Principles and rules).
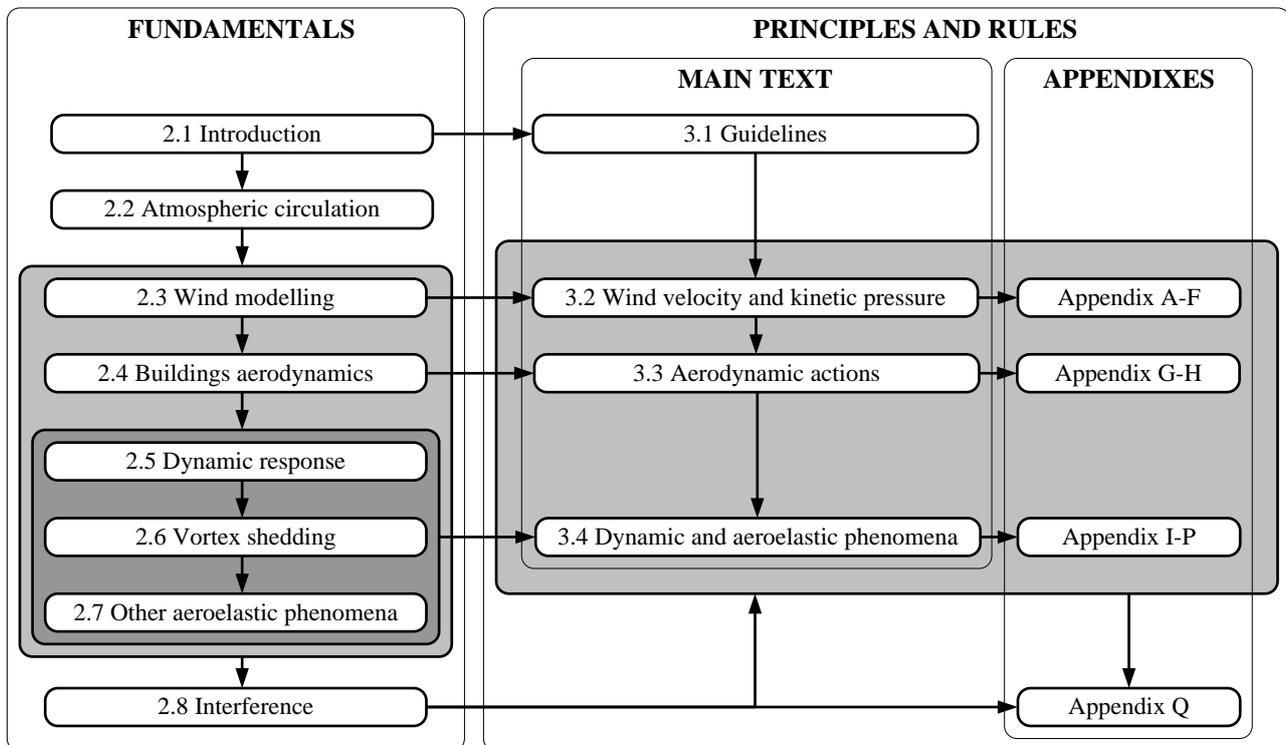
Figure 1.2 – Organisation of Sections 2 and 3.

Whilst the main text (subsections 3.1 to 3.4) applies to all the structures for which an example is given in Section 4, Table 1.I lists the annexes (A through Q) needed in each specific case.

Table 1.I - Application of Annexes to the structures chosen as calculation examples.

Structure	Annex															
	A	B	C	D	E	F	G	H	I	L	M	N	O	P	Q
4.3 Industrial building	#						#	#							
4.4 Residential building	#						#	#		#					
4.5 Multi-storey office block	#						#	#	#	#	#	#			
4.6 Tall building	#						#	#	#	#	#	#			
4.7 Gas tank	#						#		#				#		
4.8 Canopy	#						#	#							
4.9 Reinforced-concrete chimney	#						#		#	#			#		
4.10 Steel chimney	#						#		#	#			#		
4.11 Truss railway bridge	#						#		#	#			#	#	
4.12 Box girder road bridge	#						#		#	#				#	

The overview provided by Table 1.I highlights the different uses of the individual annexes, that can be grouped into four families (Table 1.II):

1. <u>Essential annexes</u>. Annexes A and G are essential in all cases. Annex A (Design return period) provides a guide to the choice of the wind velocity return period according to structural properties and the type of check. Annex G (Overall aerodynamic coefficients) provides the parameters needed to convert wind velocity into aerodynamic actions; only the clause relevant to the type of construction under consideration has to be considered in each case.

2. <u>Specific annexes</u>. Annexes D, H, I, L, M, N, O and P are essential to specific situations only. Annex D (Topographical factor) applies to structures located at the summit of isolated hills, ridges, etc., while Annex H (Detailed and local aerodynamic coefficients) applies to the evaluation of wind actions on individual structural and non-structural members and to the detailed calculation of main structural components. Annex I (Dynamic characteristics of structures) provides preliminary elements to carry out dynamic and aeroelastic assessments. Annex L (Along-wind actions and accelerations) gives the criterion for assessing the along-wind dynamic factor and is far and away the most used of all specific Annexes. Annex M (Cross-wind and torsional actions and accelerations) applies to high-rise, regular-shaped buildings. Annex N (Acceleration and serviceability) is concerned with assessing the serviceability of the top storeys of tall structures. Annex O (Vortex shedding of slender structures) is essential for slender elements and structures. Annex P (Other aeroelastic phenomena) gives essential criteria for structures that are particularly slender, plate-like, flexible, lightweight and lowly damped , and it is aimed at assessing them against aeroelastic instability problems.

3. <u>Informative annexes.</u> Annex Q (Wind tunnel tests) is aimed at guiding those involved in prototype testing.

4. <u>Special purpose annexes.</u> Annexes B (Reference velocity), C (Modelling of wind actions), E (Atmospheric turbulence) and F (Peak wind velocity) have a specialist content, aimed at improving wind knowledge and representation.

Table 1.II – Annex Classification.

Annex	Essential	Specific	Informative	Specialist
A. Design return period	#			
B. Reference velocity				#
C. Wind velocity				#
D. Topographical factor		#		
E. Atmospheric turbulence				#
F. Peak wind velocity				#
G. Overall aerodynamic coefficients	#			
H. Detailed and local aerodynamic coefficients		#		
I. Dynamic characteristics of structures		#		
L. Along-wind actions and accelerations		#		
M. Cross-wind and torsional actions and accelerations		#		
N. Acceleration and serviceability		#		
O. Vortex shedding of slender structures		#		
P. Other aeroelastic phenomena		#		
Q. Wind tunnel tests			#	

1.4   REFERENCES TO OTHER CODES

The Document is consistent with the technical/scientific state-of-the-art in this field (clause 2.9). It also implements the main guide provided by international technical standards and recommendations regarding wind actions and effects on structures.

This clause lists the main codes and standards on wind actions that were considered terms of reference when drafting this Guide. The documents are listed in chronological order of enactment. Documents which now became obsolete are also included. The latest version of the standards and recommendations of other countries and bodies are also specified.

National Research Council Guides

- *Ipotesi di carico sulle costruzioni* (Design loads on structures), CNR-UNI 10012, 1964.
- *Ipotesi di carico sulle costruzioni* (Design loads on structures), CNR-UNI 10012, 1967.
- *Azioni sulle costruzioni* (Actions on structures), CNR Technical Standard 10012/81, 1981.
- *Istruzioni per la valutazione delle azioni sulle costruzioni* (Instructions for assessing actions on structures), CNR 10012/85, 1985.

Italian Standards

- *Ipotesi di carico sulle costruzioni* (Design loads on structures), Ministry of Public Works Circular No. 4773 issued 8th June 1968.
- *Criteri generali per la verifica della sicurezza delle costruzioni e dei carichi e sovraccarichi* (General criteria for the safety check of structures, loads and imposed loads), Ministerial Decree issued 3rd October 1978.
- *Ipotesi relative ai carichi e ai sovraccarichi ed ai criteri generali per la verifica di sicurezza delle costruzioni* (Loads and imposed loads and general criteria for the safety check of structures), Ministry of Public Works Circular No. 18591 dated 9th November 1978.
- *Aggiornamento delle norme tecniche relative ai "Criteri generali per la verifica della sicurezza delle costruzioni e dei carichi e sovraccarichi"* (Revision of technical standards

regarding "General criteria for the safety check of structures, loads and imposed loads"), Ministerial Decree issued 12th February 1982.

- *Ipotesi relative ai carichi e ai sovraccarichi ed ai criteri generali per la verifica di sicurezza delle costruzioni* (Loads and imposed loads and general criteria for the safety check of structures), Ministry of Public Works Circular No. 22631 issued 24th May 1982.

- *Norme tecniche relative ai "Criteri generali per la verifica di sicurezza delle costruzioni e dei carichi e sovraccarichi"* (Technical standards regarding "General criteria for the safety check of structures, loads and imposed loads"), Ministerial Decree issued 16th January 1996.

- *Istruzioni per l'applicazione delle "Norme tecniche relative ai criteri generali per la verifica di sicurezza delle costruzioni e dei carichi e sovraccarichi", di cui al decreto ministeriale 16 gennaio 1996* (Instructions for the implementation of "Technical standards regarding general criteria for the safety check of structures, loads and imposed loads" as per Ministerial Decree issued 16th January 1996), Ministry of Public Works Circular No. 156 General Affairs/ Central Technical Service dated 4th July 1996.

- *Norme tecniche per le costruzioni* (Technical standards for structures), Ministerial Decree issued 23rd September 2005.

- *Norme tecniche per le costruzioni* (Technical standards for structures), Ministerial Decree issued 14th January 2008.

- *Istruzioni per l'applicazione delle "Nuove norme tecniche per le costruzioni", di cui al D.M. 14 gennaio 2008* (Instructions for the implementation of the "Technical standards regarding structures" as per Ministerial Decree issued 14th January 2008), Ministry of Infrastructures and Transportations Circular No. 617 dated 2nd February 2009.

Eurocodes

- Eurocode 1: *Basis of design and actions on structures*. Part 2-4: *Wind actions*, CEN, ENV 1991-2-4, 1994.

- Eurocode 1: *Actions on structures - General actions*. Part 1-4: *Wind actions*, CEN, EN 1991-1-4, 2005.

Other Standards and Recommendations

- *Recommendations for calculating the effects of wind on constructions*, European Convention for Constructional Steelwork, ECCS, N. 52, 1987.
- *Steel stacks*, ASME STS-1-1992, The American Society of Mechanical Engineers, 1992.
- *National Building Code of Canada*, NRC-CNRC, 1995.
- *Loading for buildings*. Part 2: *Code of practice for wind loads*, British Standards Institution, BS 6399, Part 2, 1997.
- *Model code for steel chimneys*, CICIND, 1999.
- *Structural design actions*. Part 2: *Wind actions*, Australian / New Zealand Standard, AS/NZS 1170.2, 2002.
- *Wind actions on structures*, ISO TC 98/SC 3 N254, ISO/CD 4354 (Draft document, 20.4.2005).
- *AIJ Recommendations for loads on buildings*, Architectural Institute of Japan, 2005.
- *Minimum design loads for buildings and other structures*, ASCE/SEI Standard N. 7-05, American Society of Civil Engineers, Structural Engineering Institute, 2005.
- *Wind tunnel studies of buildings and structures*. ASCE manuals and reports on engineering practice No. 67, Isyumov, N. (Ed.), Aerodynamics Committee, American Society of Civil Engineers, 1999.
- *Environmental meteorology. Physical modelling of flow and dispersion processes in the atmospheric boundary layer. Application of wind tunnels*, Verein Deutscher Ingenieure, VDI 3783, 2000.

1.5 Nomenclature

A list follows of the nomenclature used in this Guide (with specific reference to Sections 3 and 4). A definition is given for each symbol along with the physical dimension, either L, T, F or M, identifying, respectively, length, time, force and mass ($M = FT^2/L$).

a_0	reference altitude for the calculation of c_a	L
a_G	factor of galloping instability	---
a_l, $a_{l,0}$	acceleration limit value and its reference value	L/T^2
a_L	normalised limiting amplitude (vortex shedding)	---
a_{pD}, a_{pL}, a_{pM}	peak along-wind, cross-wind and torsional acceleration	L/T^2
a_{pD}^P, a_{pL}^P	peak along-wind and cross-wind acceleration at point P	L/T^2
a_s	altitude above sea level of the construction site	L
A, B, C	coefficients used for orographic location factor	---
b, d, h	reference dimensions for buildings	L
B	quasi-steady response factor	---
c_1, c_2	parameters related to vortex shedding	---
c_a	altitude factor	---
c_d	dynamic factor	---
c_{dD}, c_{dL}, c_{dM}	along-wind, cross-wind and torsional dynamic factors	---
c_D, c_L	aerodynamic drag and lift coefficients	---
c_e	exposure factor	---
c_f	friction coefficient	---
c_{fX}, c_{fY}	force coefficients per unit length in X and Y direction	---
c_{fXo}, c_{fYo}	force coefficients per unit length in X and Y direction for elements of infinite length	---
c_F	force coefficient for canopy calculation	---
c_{FX}, c_{FY}, c_{FZ}	resultant force coefficients in X, Y and Z direction	---
c_{lat}	lateral force coefficient (vortex shedding)	---
$c_L^{'}$	angular derivative of the aerodynamic lift coefficient	---
c_m	mean wind velocity profile coefficient	---
c_{mZ}	moment coefficient (about the Z axis)	---
c_{mZo}	moment coefficient per unit length (about the Z axis) for elements of infinite length	---
$c_{mZ}^{'}$	angular derivative of the aerodynamic moment coefficient	---
c_{MX}, c_{MY}, c_{MZ}	moment coefficients about the X, Y and Z axis	---
c_{pe}, c_{pi}	external and internal pressure coefficients	---
$c_{pe,1}$, $c_{pe,10}$	external pressure coefficients for surfaces of less than or equal to 1 m^2 and greater than or equal to 10 m^2	---
c_{peo}	external pressure coefficient for an infinite cylinder	---
$c_{pe,p}$, $c_{pe,n}$	upwind face and downwind face external pressure coefficients for calculating torsional effects	---
c_{pm}, c_{pb}	parameters for calculating c_{peo}	---
c_{pn}	net pressure coefficient	---
c_r	return factor	---
c_t	topographical factor	---
C_c	non-dimensional parameter for determining the standard deviation of lateral deflection (vortex shedding)	---
C_I	turbulence factor (vortex shedding)	---

C_{jr}	exponential decay coefficient of the turbulent component $j = 1$, 2, 3 in direction $r = x, y, z$	---
C_L, C_M	aerodynamic cross-wind force and torsional moment coefficient for tall buildings	---
$Coh_{11}, Coh_{22}, Coh_{33}$	coherence of longitudinal, lateral and vertical turbulence	---
$C_{TR,i}$	non-dimensional parameter related to the possible occurrence of critical values of the mean wind velocity for long return periods T_R (vortex shedding)	---
d_1, d_2, d_0, D, D_G	bridge deck reference sizes	L
d_x^P, d_y^P	coordinates of point P with respect to the centre of torsion	L
D, L, M	action/effect in along-wind, cross-wind and torsional direction	---
e	geometric parameter for defining the external pressure on buildings	L
E	modulus of elasticity	F/L^2
f_L	equivalent static cross-wind force per unit length	F/L
$f_{L,i}$	equivalent static cross-wind force per unit length for the i-th vibration mode (vortex shedding)	F/L
f_{LM}	ratio of torsional to cross-wind frequency	---
f_X, f_Y	force per unit length in X and Y direction	F/L
F_X, F_Y, F_Z	resultant forces in X, Y and Z direction	F
g	acceleration of gravity	L/T^2
g_{aD}	peak along-wind acceleration factor	---
g_D, g_L, g_M	peak along-wind, cross-wind and torsional factor	---
g_v	peak wind velocity factor	---
G	shear modulus	F/L^2
G_D, G_L, G_M	along-wind, cross-wind and torsional gust factors	---
G_v	wind gust factor	---
h_1, h_2, h_{eff}	reference sizes for chimneys	L
h_p	height of parapet (flat roofs)	L
h_{tot}	total overall height of bridge decks	L
H	height of a topographic feature	L
I_1, I_2, I_3	longitudinal, lateral and vertical turbulence intensities	---
I_f, I_p	bending moment of inertia and polar moment of inertia of mass per unit length	ML
I_i	generalised moment of inertia (bending or polar) of mass for the i-th vibration mode.	$M L^2$
I_M	generalised polar moment of inertia of mass for torsional vibration (first mode)	$M L^2$
I_v	turbulence intensity (longitudinal)	---
J_f, J_p, J_t	bending, polar and torsional moment of inertia	L^4
k	surface roughness	L
k_1, k_2	non-dimensional parameters for determining the resonant response in the cross-wind direction	---
k_a	reference parameter for the calculation of c_a	---
k_r	terrain factor	---
K, K_w	mode shape and effective correlation length factor (vortex shedding)	---
$K_a, K_{a,max}$	aerodynamic damping parameter and its maximum value	---

K_D	factor for determining the standard deviation of along-wind acceleration	---
K_{M1}, K_{M2}	non-dimensional parameters (torsional resonant response)	---
l, L	reference sizes for determining aerodynamic coefficients	L
L_1, L_2, L_3	longitudinal, lateral and vertical turbulence length scales	L
L_d, L_e, L_u	reference lengths of topographic features	L
L_j	correlation length	L
L_v	integral length scale of turbulence (longitudinal)	L
m	mass per unit length	M/L
m_D, m_L	generalised mass (first mode) in along-wind and cross-wind directions	M
$m_{e,i}$	equivalent mass per unit length for the i-th vibration mode	M/L
m_i	generalised mass for the i-th vibration mode	M
m_M	equivalent static torque per unit length	FL/L
M_s	equivalent mass	M
M_X, M_Y, M_Z	moments about the X, Y and Z axis	FL
m_Z	moment per unit length (about the Z axis)	FL/L
n_D, n_L, n_M	frequency of first along-wind, cross-wind and torsional mode	1/T
n_i	frequency of vibration of the i-th mode	1/T
$n_{L,i}$, $n_{M,i}$, $n_{O,i}$	frequency of the i-th cross-wind, torsional and ovalling mode	1/T
n_{LM}	frequency of first cross-wind or torsional mode	1/T
n_s	frequency of vortex shedding	1/T
n_{s1}, n_{s2}	frequency parameters for determining the resonant response in the cross-wind direction	1/T
N, N_i	number of load cycles caused by cross-wind oscillation	---
p_e, p_i, p_n	external, internal and net pressure	F/L^2
P_1, P_2, P_3	non-dimensional parameters for determining the torsional frequency of bridge decks	---
P_v	reduction factor of turbulence intensity	---
q_p	peak velocity pressure	F/L^2
r	radius of curvature	L
r_m	non-dimensional parameter (bridge deck stability)	---
R_b, R_h	parameters for determining the resonant response factor in along-wind direction	---
R_D, R_L, R_M	resonant response factor in along-wind, cross-wind and torsional direction	---
Re	Reynolds number	---
s	orographic location factor	---
S	tension (cables)	F
S_1, S_2, S_3	longitudinal, lateral and vertical turbulence spectra	L^2/T
Sc_i	Scruton number for the i-th vibration mode	---
S_D, S_L	non-dimensional parameters (resonant response in along-wind and cross-wind direction)	---
S_M, S_{M1}, S_{M2}	non-dimensional parameters (torsional resonant response)	---
St	Strouhal number	---
t	thickness of cylindrical shells	L
T	averaging time for the mean wind velocity	T
T_R, $T_{R,0}$, T_0	design, reference and conventional return periods	T
$v_{0,i}$	reference wind velocity for the i-th vibration mode (load cycles caused by vortex shedding)	L/T

v_b, $v_{b,0}$	fundamental basic wind velocity and its value at sea level	L/T
$v_{cr,i}$	critical wind velocity of vortex shedding for i-th mode	L/T
v_D	divergence critical wind velocity	L/T
v_F	flutter critical wind velocity	L/T
$v_{G,i}$	galloping critical wind velocity for the i-th mode	L/T
v_m	mean wind velocity	L/T
v_m^*	reduced mean wind velocity	---
$v_{m,0}$, $v_{m,l}$	mean wind velocity with return period of 1 and 10 times the reference return period	L/T
V_N	nominal design life of the structure	T
$v_{O,i}$	critical wind velocity for ovalling in the i-th mode	L/T
v_p	peak wind velocity	L/T
v_r	design reference wind velocity	L/T
w_f	friction action	F/L^2
W_S, W_T	weight of structural parts and total weight (fundamental frequency of a chimney)	F
x, y, z	coordinates	L
$y_{pL,i}$	peak cross-wind displacement in the i-th vibration mode (vortex shedding)	L
$\bar{z}$, $\bar{z}_e$, $\bar{z}_i$	reference heights for aerodynamic coefficients	L
z_0	roughness length	L
z_e	reference height for calculation of the along-wind response	L
z_g	distance from the ground (calculation of actions on signboards and isolated bodies)	L
$z_{\min}$	minimum height	L
α	inclination (of slopes, parabola axis, wind direction with respect to a reference axis, etc.)	---
α_p, α_m, α_b	angles for calculating the external pressure on structures with circular plan	---
β, γ	coefficients for determining the topographical factor	---
β_1, β_2	parameters for determining the resonant response in the lateral direction	---
β_F	aerodynamic efficiency parameter (bridge decks)	---
β_{M1}, β_{M2}	non-dimensional parameters (torsional resonant response)	---
γ_{LM}	correlation factor between cross-wind and torsional effects	---
ε_0	bandwidth factor (load cycle calculation)	---
ε_I	parameter for determining the fundamental flexural frequency of chimneys	---
ζ	exponent of the first bending mode shape	---
η_h, η_b	parameters for determining the resonant response factor in along-wind direction	---
θ	angle of torsion	---
Θ	wind direction in the horizontal plane	
κ	coefficient for turbulent length scale calculation	---
λ	effective slenderness	---
λ_L, λ_T, λ_V	length, time and velocity scaling factors (wind tunnel tests)	---
λ_p	dimensionless factor for bridge deck configuration	---
μ	non-dimensional parameter (bridge deck stability)	---
υ	kinematic viscosity of air	L^2/T

υ_D	expected up-crossing frequency for the along-wind response	1/T
υ_v	expected up-crossing frequency of turbulence	1/T
ξ, ξ_a, ξ_d, ξ_s	critical damping ratio: total, aerodynamic, due to passive control systems and structural values	---
ξ_D, ξ_L, ξ_M	critical damping ratio for the first along-wind, cross-wind, lateral and torsional vibration mode	---
$\xi_{D,i}, \xi_{L,i}, \xi_{M,i}$	critical damping ratio for the i-th along-wind, cross-wind, and torsional vibration mode	
$\xi_{O,i}$	critical damping ratio for the i-th ovalling mode	---
$\xi_{s,i}$	structural damping ratio for the i-th bending flexural mode	---
ρ	air density	M/L^3
ρ_s	density of material	M/L^3
$\sigma_1, \sigma_2, \sigma_3$	standard deviations of longitudinal, lateral and vertical turbulence	L/T
$\sigma_{aD}, \sigma_{aL}, \sigma_{aM}$	standard deviations of along-wind, cross-wind and torsional acceleration	L/T^2
σ_L	standard deviation of cross-wind deflection (vortex shedding)	L
τ	averaging time for the peak wind velocity	T
φ	density (walls, parapets and trusses) and degree of blockage (canopy roofs)	---
Φ	mean up-wind slope of topography	---
Φ_D, Φ_L, Φ_M	first along-wind, cross-wind and torsional mode shape	---
Φ_i	i-th vibration mode shape	---
$\Phi_{L,i}$	i-th cross-wind vibration mode shape	---
ψ	reduction factor for pressure on buildings	---
ψ_r	reduction factor of force coefficient for sections with rounded edges (elongated slender structures and structural members)	---
ψ_s	sheltering factor	---
ψ_α	correction factor for inclined wind flow (lattice structures)	---
ψ_λ	reduction factor of force coefficient for structural elements with end-effects	---
$\psi_{\lambda\alpha}$	end-effect factor for circular cylinders	---
ω	non-dimensional parameter (cables)	---
Ω	non-dimensional parameter (ovalling)	---
Ω_i	non-dimensional parameter (natural frequencies of cables)	---

2 FUNDAMENTALS

2.1 MOTIVATIONS

The meteorological phenomena that occur in the Earth's atmosphere are caused by solar radiation. Solar radiation gives rise to temperature and pressure fields that are responsible for the displacement of air masses, which are generally classified in accordance with their spatial and temporal scale (section 2.2). The analysis of the actions and effects of wind on constructions is based on the evaluation of wind V at the construction site (section 2.3), wherein the wind is considered as one component of a broader and more complex atmospheric and meteorological system.

Assuming initially that the structure is fixed and not deformable, wind V exerts on the structure, globally and on its components, a system of aerodynamic actions F_s that depend on shape, orientation, and size of the construction (section 2.4).
Assuming also that the structure is subject to deflection due to the action of the wind, but that such deflection is sufficiently small so that the deformed geometry is essentially coincident with respect to its initial configuration, the response R can be established through the classic methods of structural analysis (sections 2.5 and 2.6); the response turns out to be static for stiff and damped structures, and dynamic for flexible and/or low damped structures.

Figure 2.1 shows the flow diagram that transforms wind velocity V into structural response R.
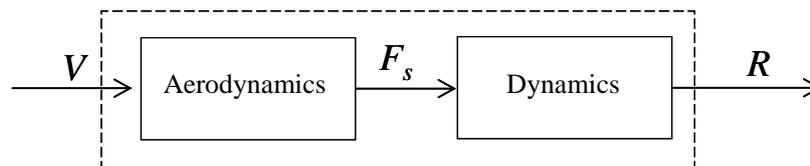
Figure 2.1 – Structural response.

In practice, especially in the case of lightweight, flexible and/or low damped structures having an aerodynamic shape that is susceptible to wind actions, the deflection and the velocity of the structure can be of such a sufficiently large magnitude to give rise to wind-structure interactions phenomena, known as aeroelastic or feedback phenomena (sections 2.6 and 2.7), which modify the oncoming wind V, the aerodynamic actions F_s, and the structural response R. These phenomena are generally schematized by assuming that wind induces global actions $F = F_s + F_a$ on the structure, where F_s are the aerodynamic actions exerted by the wind on the fixed structure and F_a is the aeroelastic or self-excited actions due to the movement of the structure. Figure 2.2 shows the same diagram as Figure 2.1 modified to take the self-excited actions into account.
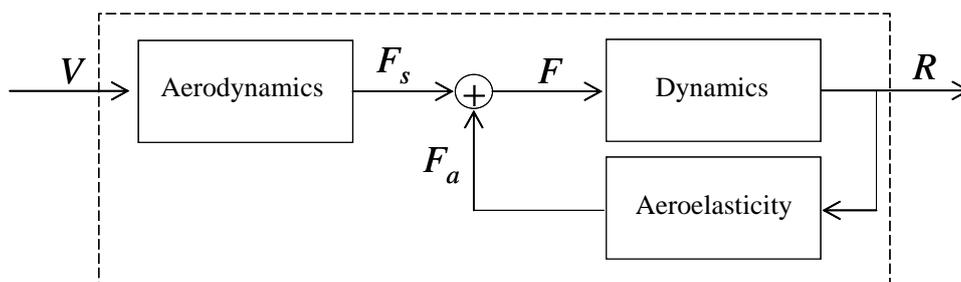
Figure 2.2 – Structural response in presence of aeroelastic phenomena.

Comparison between Figures 2.1 and 2.2 highlights the essential aspects of wind engineering and the basic concepts reported in this Guide. Wind is the cause that produces the response of the construction and of its components. The link between cause and effect depends on aerodynamics, dynamics, and aeroelasticity. Interference between adjacent structures or elements (section 2.8) is of a transverse nature with respect to these sectors. A basic bibliography is given in section 2.9.

2.2   ATMOSPHERIC CIRCULATION

The atmospheric phenomena that occur in the gaseous envelope that surrounds the Earth are caused by solar radiation. Warmed by the Sun, the ground and the atmosphere return the energy they receive and, in turn, emit thermal radiation. The lowest atmospheric layer immediately next to the principal heat source, i.e. land masses, retains higher amounts of heat, giving rise to a vertical profile of the mean temperature value T, shown in Figure 2.3 with the acronym IS for International Standard, which approximately decrease linearly with respect to height z.
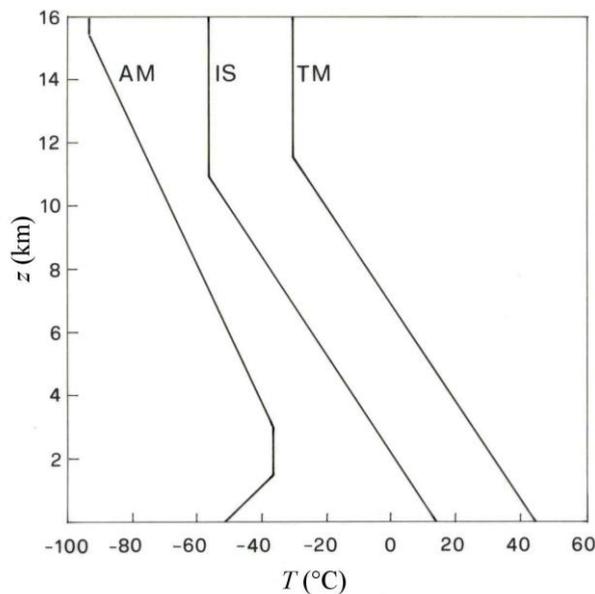
Figure 2.3 – Mean vertical profiles of atmospheric temperature.

The difference between energy received and energy emitted by the earth-atmosphere system varies mainly in accordance with the different angle of the sun rays with respect to the horizon, which results in the highest radiation levels in tropical-equatorial regions and the minimum radiation levels at the poles (Figure 2.3). In the former regions, the average temperature (Tropical Maximum or TM) is greater than the average terrestrial temperature (IS), resulting in the establishment of a low-pressure zone; in the latter case (Arctic Minimum or AM) the temperature is lower than IS, resulting in the creation of a high-pressure zone. If the temperature were unaffected by other factors, air would circulate in each hemisphere in accordance with a single cell running from the pole to the equator (Figure 2.4).
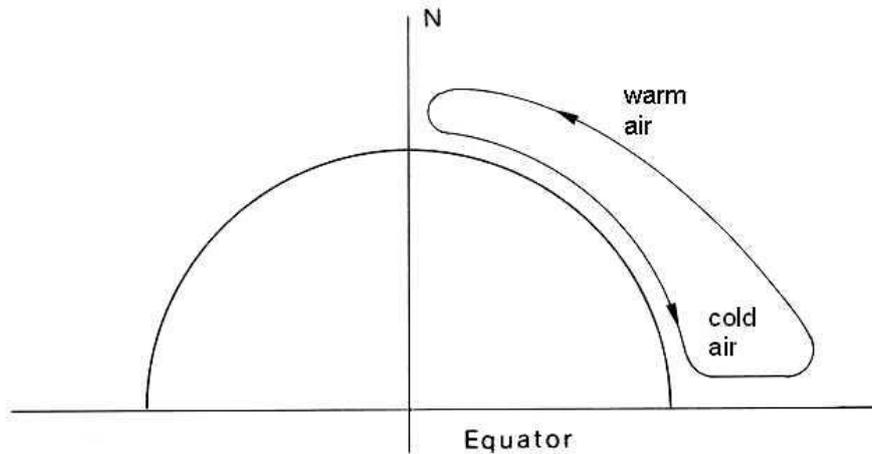
Figure 2.4 – Ideal monocellular circulation.

In practice, the uneven distribution of oceans, continents and clouds, causes the formation of a sub-tropical high-pressure belt and of a sub-polar low-pressure belt. This leads to a tricellular circulation system in each hemisphere (Figure 2.5).
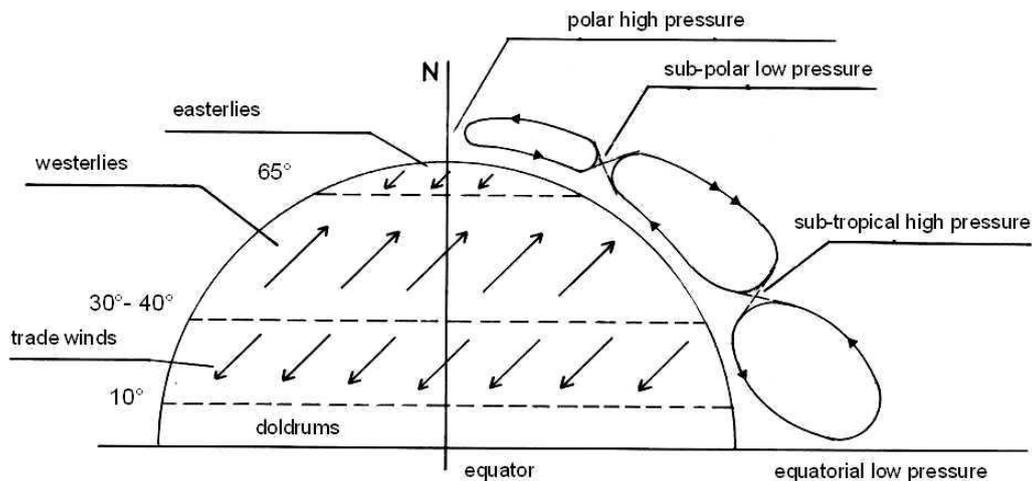
Figure 2.5 – Effective tricellular circulation.

The surface winds of such a tricellular system are called Westerlies, Easterlies or Trade Winds depending on the latitude at which they occur. The set of these winds constitutes the primary circulation and includes winds that develop over monthly or seasonal periods, on areas of planetary scale. These winds are responsible for establishing the Earth's weather patterns. However, they have moderate velocity (normally less than 4-5 m/s) and thus have little influence on structures.

Secondary circulation is defined as the combination of winds that form in low- and high-pressure areas due to local heating or cooling of the lower atmospheric layers (Figure 2.6). These winds develop over periods of between a few days up to one week, on areas sized from several hundred square kilometres up to a thousand square kilometres. These winds include cyclones, anticyclones and monsoons. Unlike the effect of primary circulation, secondary circulation defines local weather patterns.
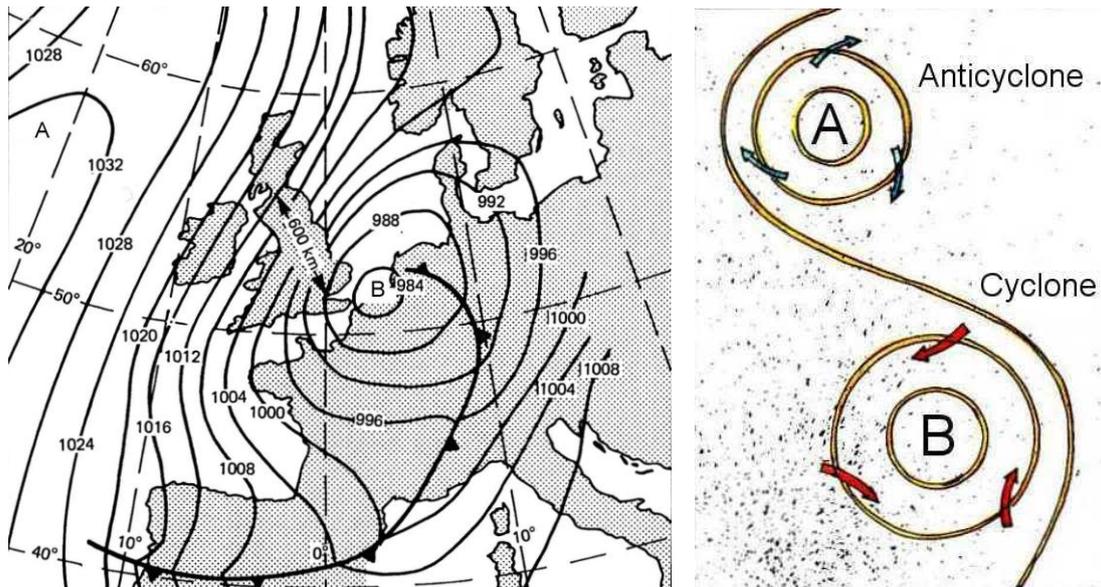
Figure 2.6 - (a) Isobar map; (b) cyclone and anti-cyclone.

.

Cyclones are winds that blow in the direction of concentric isobars, around low-pressure areas (Figure 2.6). The direction of circulation is counter-clockwise in the northern hemisphere and clockwise in the southern hemisphere. Cyclones are divided into extra-tropical and tropical cyclones, depending on the area in which they form.

Extratropical cyclones are formed from the meeting, in the sub-polar belt, of cold polar air carried by the easterlies and hot tropical air carried by the westerlies (Figure 2.5). The meeting of the two air fronts of different temperature can be figuratively construed as a clash between two warring armies. This meeting, in the case in question, will cause a storm.

Tropical cyclones (Figure 2.7) originate in the Doldrums (Figure 2.6), and they draw their power from the latent heat released by condensation of water vapour. With respect to extratropical cyclones, tropical cyclones are normally smaller in size although wind velocities tend to be much higher and their destructive force is far greater. In the US, tropical cyclones are classified as hurricanes when the wind velocity exceeds 120 km/h; the same phenomena in the Far East are called "typhoons", or simply "cyclones" in Australia and in the Indian Ocean.
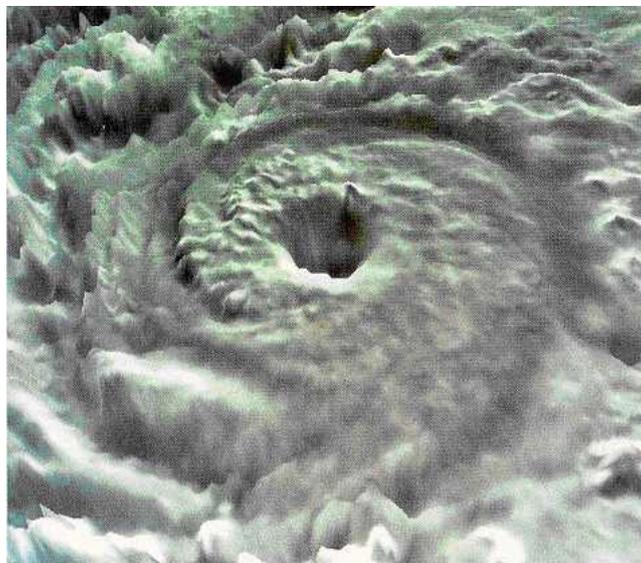
Figure 2.7 – Tropical cyclone.

Anticyclones are winds that blow in the direction of concentric isobars inside high pressure areas (Figure 2.6). The direction of circulation is clockwise in the northern hemisphere and counter-clockwise in the southern hemisphere.

Compared to cyclones, anticyclones are generally larger in size and more passive in nature. They produce relatively calm weather and light winds. Several special considerations must be applied to atmospheric movements of a seasonal nature caused by the temperature difference between oceans and continental land masses. Across Asia and the adjoining Indian Ocean, these movements are of a magnitude and size of sufficient significance to give rise to winds, known as monsoons, which are considered to all effects and purposes as an integral part of the secondary circulation system.

Local winds constitute movements of air masses that arise inside the secondary circulation system without altering the relative properties. These winds cover limited areas of just a few kilometres and tend to be of short duration – usually no more than a couple of hours – although the relative velocity can reach very high values. Local winds are generally divided into two main categories associated, respectively, with specific geographic conditions and special atmospheric conditions.

Winds associated with specific geographic conditions include breezes, the Föhn and the Catabic winds. Breezes occur on a daily basis and are generally of moderate velocity; they manifest themselves in coastal areas, on lake shores, in hill countries or on mountain slopes. The Föhn wind occurs when an air mass climbs over an elevation, thus cooling, and then descends over the opposite side, heating up in a substantially adiabatic manner (Figure 2.8). Catabatic winds, these including the Bora wind, originate when a cold air mass has crossed a mountain chain or plateau and then the ground level drops away to a low lying area with hot stagnant air: at this point the air drops under the effect of gravity and can reach velocities of up to 150-200 km/h.
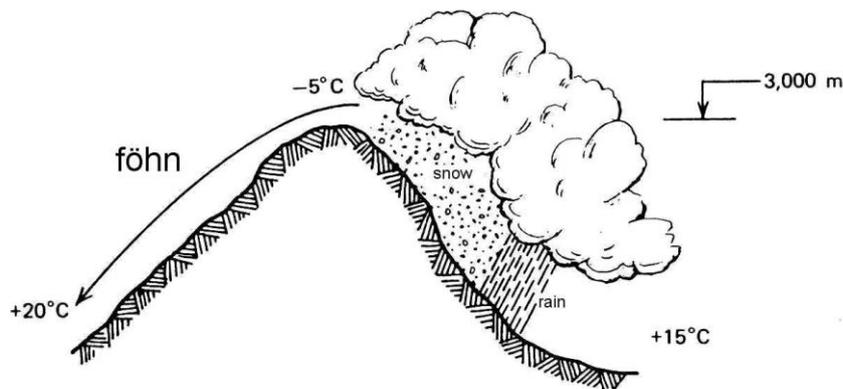
Figure 2.8 -. Föhn wind.

Winds associated with special weather conditions include thunderstorms and tornados. The former group includes frontal winds that occur at the interface between warm and cool air masses which, on meeting, give rise to extratropical cyclones, and convective down currents or downbursts, which create surface gusts in a radial pattern (Figure 2.9) with wind velocities of even up to 100 km/h. The latter, which are called "*trombe d'aria*" (whirlwind) in Italy (Figure 2.10), are the most destructive single natural event; in some parts of the world these can cause wind velocities even greater than 300 km/h, peaking at an estimated value of 700 km/h; it is thus fortunate that the extension of these phenomena is limited, as is the likelihood of their occurrence.
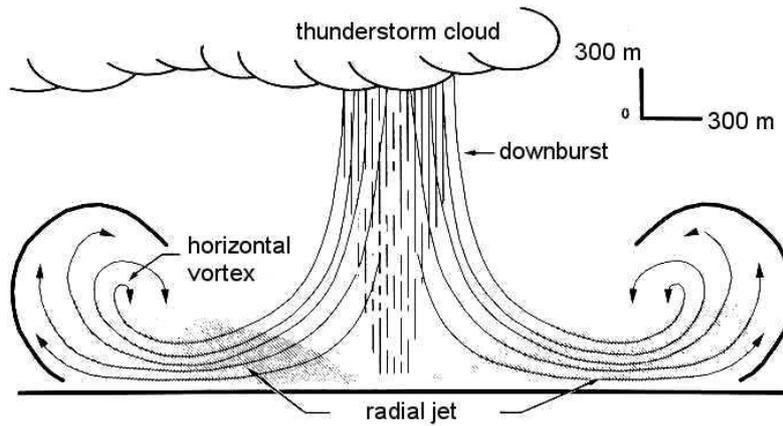
Figure 2.9 – Convective down current or downburst.

Figure 2.10 - Tornado or "tromba d'aria" (whirlwind).

A concise classification of the various wind phenomena described above is given in Table 2.I a.

Table 2.I – Aeolic phenomena: classification.

Primary circulation	Trade winds	
	Westerlies	
	Easterlies	
Secondary circulation	Cyclones	Extra-tropical
		Tropical
	Anti-cyclones	
	Monsoons	
Local winds	Winds associated with specific geographic conditions	Breezes
		Föhn winds
		Catabatic winds (bora, ...)
	Winds associated with specific atmospheric conditions	Frontal winds
		Downbursts
		Tornados or "*tromba d'aria*" (whirlwinds)

In the current state of the art there are no mathematical models capable of encompassing, in a general manner, all the aeolic phenomena mentioned above. In contrast, there exist various different partial models that are capable of representing, with varying degrees of confidence, the single wind types, which are thus presumed to be reciprocally independent. The wind representation adopted in this Guide concerns extratropical cyclones; these are normally the most severe wind events in terms of intensity and likelihood of occurrence, potentially affecting structures in countries with well behaving climate, notably Italy.

2.3   WIND REPRESENTATION

To represent the wind configuration in an extratropical cyclone two atmospheric layers having different properties are considered. The gradient height is defined as the height z_g above which the wind is no longer affected by the ground friction force; this height is between 1000 m and 3000 m depending on the wind velocity and on the roughness length of the terrain, which is expressed by a roughness parameter z_0. The atmosphere between the earth surface and the gradient height is denoted as atmospheric boundary layer. Above the gradient height is free atmosphere.

The wind velocity in free atmosphere is constant, defined as geostrophic, and identified by the symbol V_g. The wind direction is parallel to the isobars and the intensity is the greater the more closely are spaced the isobars. In the atmospheric boundary layer the air flow is affected by the friction force exerted by the terrain, which is opposed to the wind velocity V. Such force is zero at the gradient height and increases descending towards the ground, resulting in lower wind velocities. The resulting tapering velocity profile is overlaid, again due to the effect of friction, by a three-dimensional fluctuation with zero mean, designated atmospheric turbulence (Figure 2.11). Atmospheric turbulence is maximum immediately above the ground, while it tends to zero with increasing height.
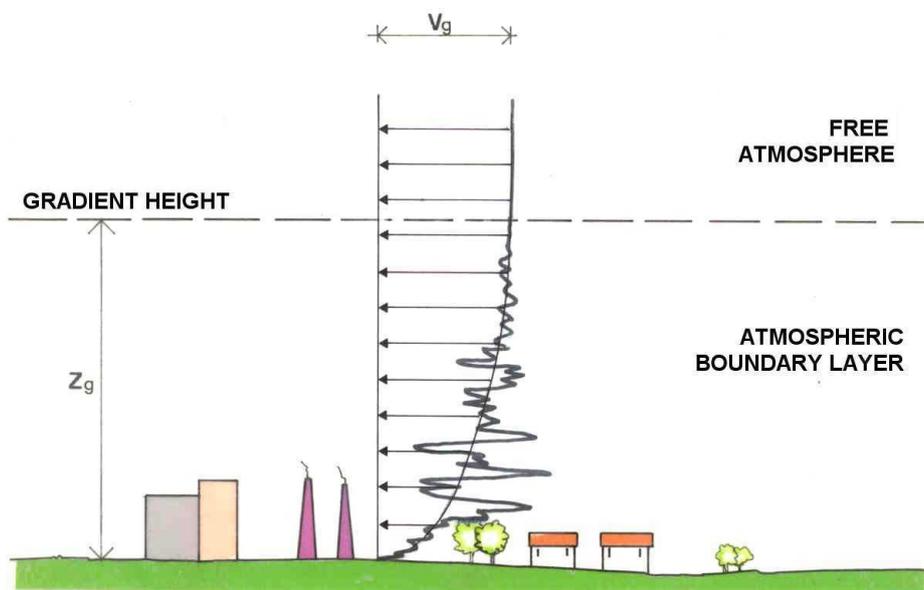
Figure 2.11 – Mean wind velocity and atmospheric turbulence profile.

To define the properties of the wind more precisely two further concepts shall be considered. The first concerns atmospheric equilibrium, while the second concerns the meaning of average velocity and fluctuation.

Let us consider a mass of air in hydrostatic vertical equilibrium under the action of the weight force and the vertical pressure gradient. This column of air is in a stable, unstable or neutral equilibrium

condition, depending on whether the vertical gradient of temperature T is greater, smaller, or equal to the vertical gradient of temperature T_a in adiabatic conditions.

There are two limit situations that can be used to clarify the problem. The first is constituted by the horizontal movement of warm air over cold terrain (Figure 2.12a); this causes a reduction of temperature next to the ground or even the inversion of the temperature gradient, and a tendency towards conditions of stable equilibrium capable of suppressing the turbulence. The second limit situation occurs in the dual condition wherein cold air flows over the warm ground (Figure 2.12b); in this case heating from below results in an increase in the temperature gradient, which makes the atmosphere unstable and increases turbulence.
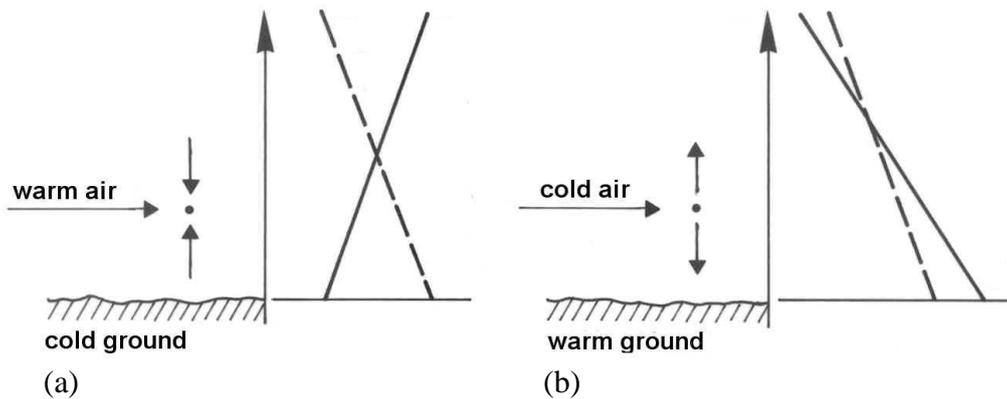
Figure 2.12 – Stable atmosphere (a) and unstable atmosphere (b).

The above situation is modified in relation to the wind velocity. As velocity increases, the friction forces exerted by the ground tend to increase and the turbulent fluctuations become larger and larger. Turbulent fluctuations result in a remixing of the atmosphere that, due to the speed at which it occurs, is of an adiabatic nature. In other words, as the wind velocity increases, the temperature gradient moves towards the adiabatic value and the atmosphere tends towards the neutral condition. When this occurs, wind velocity is independent of temperature.

Wind engineering in general and this Guide in particular are mainly concerned with the effects of high winds. The hypothesis of neutrality is therefore accepted, simplifying the mathematics. This approach, which is generally reliable, may prove inaccurate when applied to vortex shedding response and to aeroelastic phenomena, as both are in general amplified by the absence of turbulence. It can also prove inaccurate for fatigue calculations, as fatigue mainly cumulates due to frequent winds of moderate velocity.

The second key concept concerns the meaning of the mean velocity and of the turbulent fluctuations. When a long time span is taken into consideration and the power spectrum $S_V(n)$ of the wind velocity is evaluated, where n is the frequency (Figure 2.13), it appears that the curve has two separate harmonic contents. The first, which is associated to periods of between approximately one hour and several months, is known as the macro-meteorological peak and it corresponds to the frequency of aeolic events. The second, which is associated with periods of between a few seconds and approximately ten minutes, is called the micro-meteorological peak and it corresponds to turbulent fluctuations. The two peaks are separated by a frequency range that is almost free of harmonic contents, designated as the spectral gap, with periods of between around ten minutes and one hour.
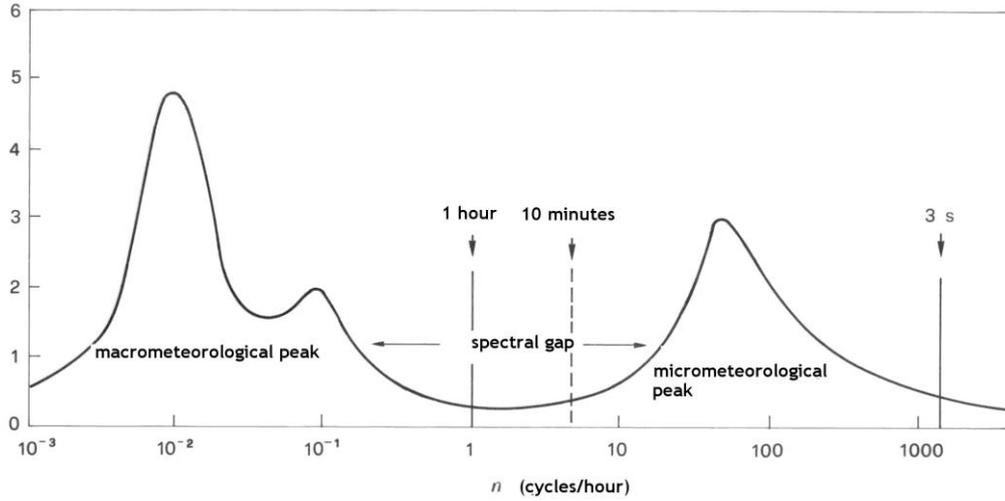
Figure 2.13 – Wind velocity power spectrum.

From this spectral representation derives the possibility of separating the wind velocity (vector) **V** into two contributions. The first contribution describes the mean velocity $\mathbf{V}_m$ over an interval of 10 minutes and it is characterised by long-term variations. The second contribution describes atmospheric turbulence **V'** and it is characterised by high frequency fluctuations. More precisely, in a x, y, z reference system with origin O at the ground, vertical z axis directed upward and x axis parallel to the mean velocity $\mathbf{V}_m$, (Figure 2.14):

$$\mathbf{V}\left(M;t\right) = \mathbf{V}_m\left(z\right) + \mathbf{V}'\left(M;t\right) \tag{2.1}$$

$$\mathbf{V}_m\left(M\right) = \mathbf{i} \cdot v_m\left(z\right) \tag{2.2}$$

$$\mathbf{V}'\left(M;t\right) = \mathbf{i} \cdot v_1'\left(M;t\right) + \mathbf{j} \cdot v_2'\left(M;t\right) + \mathbf{k} \cdot v_3'\left(M;t\right) \tag{2.3}$$

where M is a generic point in space at height z above the ground, t is time, **i**, **j**, **k** are the versors of x, y and z axes; v_m is the mean wind velocity (along x); v_1', v_2', v_3' are the longitudinal (along x), lateral (along y) and vertical (along z) components of turbulence.
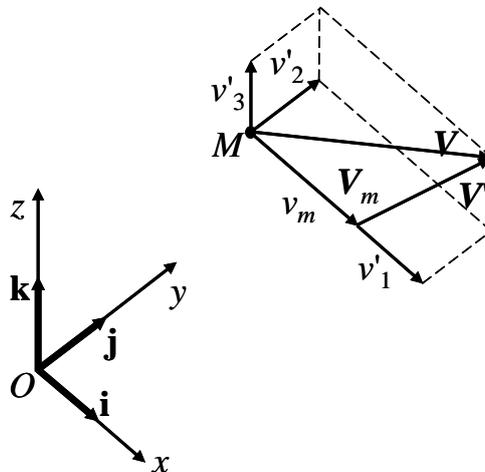
Figure 2.14 – Representation of wind velocity.

Wind engineering usually describes the mean velocity as a random function of time and a deterministic function of space; in contrast, it describes turbulence as a random function of space and time.

Considering the mean velocity as a random function of time, this is defined through a conventional reference value v_r that characterises the windiness of the area and is a function of the probability of exceedence in one year. The chosen reference velocity is the average velocity over a time interval of 10 minutes at a height of 10 m on flat, homogeneous terrain, with roughness length $z_0 = 0.05$ m. The probability of exceedence of this value is assigned by means of a design return period T_R, which is a function of the properties of the structure and the particular limit state under consideration. Values of such parameters are given in this Guide at sections 3.2.1 and 3.2.2, as derived following the procedures of Annexes A and B.

The vertical profile of the mean wind velocity in the site of interest is expressed by means of a deterministic function of the terrain roughness and its local topography.

First of all let us consider the case of flat ground of uniform roughness length. The atmospheric boundary layer is divided into two regions called the inner layer and the outer layer. The inner layer lies between the ground surface and an altitude z_s of approximately 200 m; the average velocity has a logarithmic profile that is a function of the roughness length z_0. In the outer layer, which is located between altitudes z_s and z_g, the mean velocity tends toward the geostrophic velocity V_g following a spiral shaped profile.

Wind engineering practice applies these concepts as follows. If the reference velocity v_r and the relative roughness length are known, from these two values the geostrophic velocity V_g is calculated. It is assumed that this value, regardless of the ground roughness length, remains the same over rather large areas. Starting from V_g it is therefore possible to get down back to the inner layer and evaluate the mean velocity profile associated with the local terrain roughness length (Figure 2.15). This Guide provides the information required to perform such calculations at sections 3.2.3 and 3.2.4. The procedure is valid for heights up to 200 m, in which the wind direction remains constant and the mean velocity profile is of a logarithmic shape.
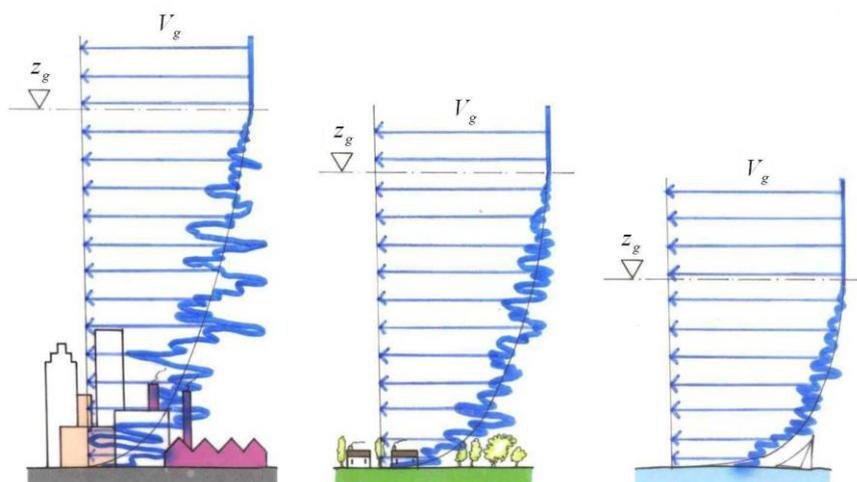
Figure 2.15 – Mean wind velocity profile in sites with different ground roughness.

Real situation is complicated by two factors. First, indefinite areas of uniform roughness do not exist in nature, but rather the ground roughness varies in a complex manner from site to site. Moreover, the territory features topography that is frequently far away from the ideal case of a flat terrain. This Guide addresses the above issues at section 3.2.5 and Annexes C and D.

Coming to velocity fluctuations, wind engineering practice usually describes the three turbulence components v'_1, v'_2, v'_3 as random stationary Gaussian processes (at times ergodic). This Guide provides basic guidance for the modelling of such processes at section 3.2.6 and in Annex E.

The longitudinal component v (parallel to x) of the wind velocity (Eqs. 2.1 to 2.3) is given as:

$$v\left(M;t\right) = v_m\left(z\right) + v'\left(M;t\right) \tag{2.4}$$

where, for the sake of simplicity, $v' = v'_1$. Velocity v is characterised by a Gaussian probability density function $f(v)$. The maximum value v_{max} of v in the time interval $T = 10$ minutes is a random variable whose density function $f(v_{max})$ is usually narrow and sharped.

The wind velocity peak value v_p is defined as the mean value of v_{max} associated with the design return period. This parameter is defined as:

$$v_p\left(z\right) = v_m\left(z\right) + g_v\left(z\right)\cdot\sigma_v\left(z\right) = v_m\left(z\right)\cdot G_v\left(z\right) \tag{2.5}$$

$$G_v\left(z\right) = 1 + g_v\left(z\right)\cdot I_v\left(z\right) \tag{2.6}$$

$$I_v\left(z\right) = \frac{\sigma_v\left(z\right)}{v_m\left(z\right)} \tag{2.7}$$

where I_v is the (longitudinal) turbulence intensity, g_v is the peak factor of v, G_v is the velocity gust factor (Figure 2.16).
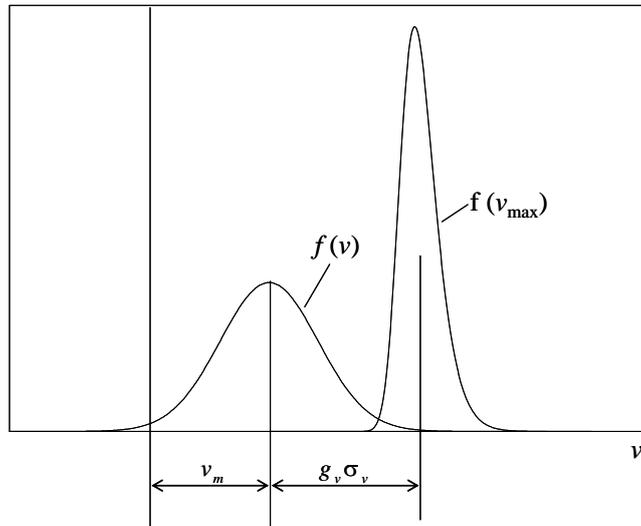
Figure 2.16 – Probability density of wind velocity and its maximum value.

Consequently, as turbulence intensity is usually significantly smaller than 1, the wind peak velocity pressure value can be expressed by the formula:

$$q_p\left(z\right) \cong \frac{1}{2}\rho\cdot v_p^2\left(z\right) \cong \frac{1}{2}\cdot\rho\cdot v_m^2\left(z\right)\cdot\left[1 + 2\cdot g_v\left(z\right)\cdot I_v\left(z\right)\right] \tag{2.8}$$

where ρ is the air density. At section 3.2.of this Guide eq. (2.8) is applied setting $g_v = 3.5$. Annex F explains the role of the approximation involved in eq. (2.6) and the relationship between the wind peak velocity and the peak velocity pressure.

2.4   AERODYNAMICS OF STRUCTURES

Consider a fixed and stiff body immersed in a wind flow. We can identify two associated effects: on the one hand, the body will alter the air flow, changing the local velocity pattern, while on the other hand a pressure P that is different from the static pressure P_0 of the free flow will arise on the surface of the body. The surface of the body is therefore subject to an aerodynamic action associated with the pressure difference $p=P-P_0$. The representation of the physical phenomenon changes depending on whether the body has typically three-dimensional properties (Figure 2.17), or whether it can be associated, at least away from the edges with a two-dimensional regime (Figure 2.18) (in the cross-sectional plane).
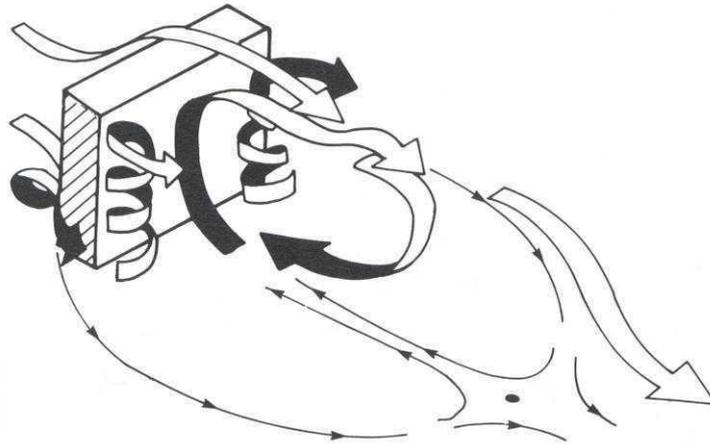
Figure 2.17 – Three-dimensional body in a wind field.
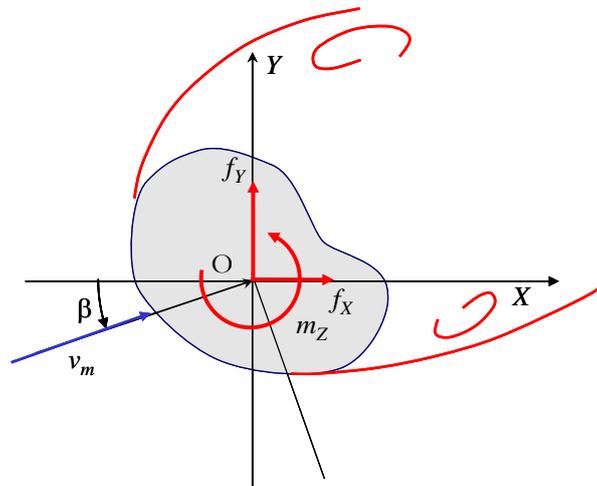
Figure 2.18 – Two-dimensional body in a wind field.

In both cases a laminar or turbulent boundary layer is formed on the surface of the body exposed to the oncoming flow (Figure 2.19), in accordance with the Reynolds number *Re*, defined at section 3.3.7, and with the body surface roughness.

(a) (b)

Figure 2.19 – Laminar (a) and turbulent (b) boundary layer.

When the boundary layer is exposed to a negative pressure gradient along the flow direction, i.e. when the flow tends to accelerate due to Bernoulli's principle, the thickness of the boundary layer tends to diminish and the vorticity that is produced within it is transported towards the surface; in other words, the boundary layer tends to be still further compressed against the surface. The opposite phenomenon occurs when the boundary layer has a positive pressure gradient (adverse pressure gradient); in this case the thickness of the boundary layer increases and the vorticity is transferred from the surface of the body and away from it, giving rise to the phenomenon of boundary layer separation. Downstream the separation point, the flow external to the boundary layer moves away from the surface; it follows that the vorticity is no longer confined to a thin layer adhering to the surface, but it instead occupies a broad area of the flow. This flow area is the turbulent wake and it has a key role in the behaviour of structures exposed to wind.

The occurrence of an adverse pressure gradient has different features depending on whether the surface of the body is rounded or sharp-edged.

For rounded bodies, flow separation depends not only on the body shape but also on the Reynolds number and on the surface roughness. Figure 2.20 shows the classic case of a smooth cylinder of infinite length and circular section, immersed in a smooth wind field (zero turbulence). For $Re < 1$ the boundary layer is laminar and stays attached to the cylinder along the entire perimeter (Figure 2.20a). For $1 < Re < 30$, the laminar boundary layer separates from the cylinder, giving rise to two symmetric stationary laminar vortices (Figure 2.20b). For $30 < Re < 10000$, the boundary layer is still laminar but the vortices, though still laminar, are shed alternatively from the cylinder creating a Von Karman wake, i.e. two streets of vortices (Figure 2.20c) dragged by the mean flow. For $10000 < Re < 200000$ the boundary layer is again laminar, but the vortices are mainly turbulent, with vortex layers hard to identify (Figure 2.20d). For $Re > 200000$ the boundary layer is turbulent and the separation points move downstream, while the wake, which remains turbulent, becomes narrower (Figure 2.20e). An increase in surface roughness brings transition regimes occuring at lower Reynolds numbers.

(a) $Re \sim 1$

(b) $Re \sim 20$

(c) $30 < Re < 10000$

(d) $10000 < Re < 200000$

(e) $Re > 200000$
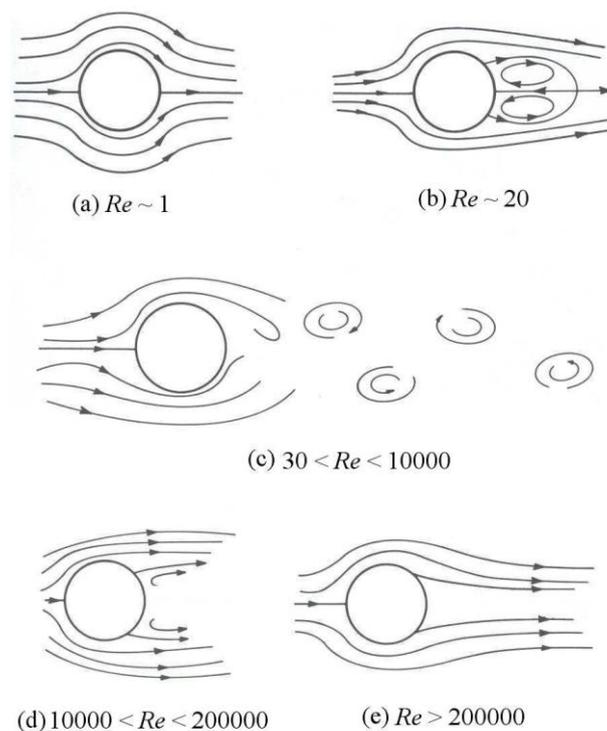
Figure 2.20 – Circular cylinder of infinite length immersed in a wind field.

The flow pattern is dramatically different in the case of sharp-edged bodies. For such bodies separation of the boundary layer occurs because, if the flow were to follow the corner, the velocity of the boundary layer would be very high and the pressure very low. Immediately after the corner the pressure gradient would be of a magnitude such as to be unsustainable without separation. Figure 2.21(a) shows the flow around a square section, in which wake separation occurs at the leading edge. The flow configuration is thus independent of the Reynolds number and of the surface roughness. It should also be noted that elongated shapes may give rise to the formation of separation bubbles after separation from the leading edge (Figure 2.21b); downstream the separation bubble the flow may reattach to the lateral faces of the body, to separate again at the trailing edge.

The broader the turbulent wake, the larger the drag force.
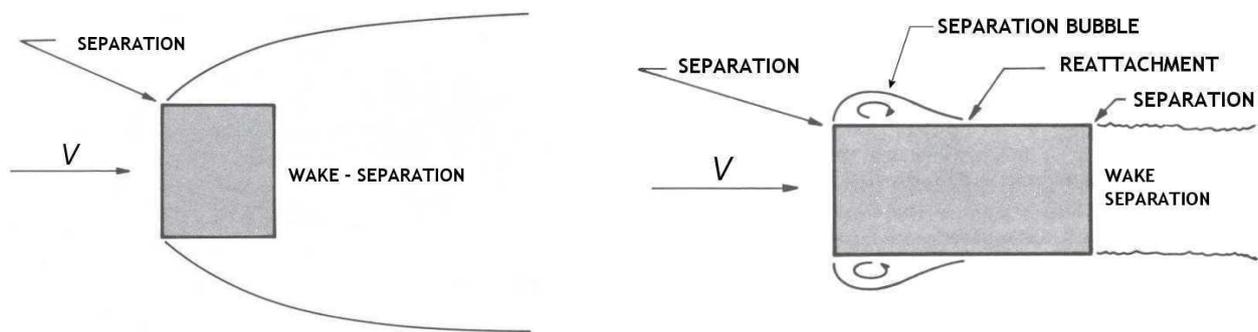
Figure 2.21 – Flow separation from sharp-edged bodies.

As a consequence, the aerodynamic actions on stationary, stiff bodies depend on both the oncoming flow and the turbulent wake. The oncoming flow is characterised by the mean velocity and its fluctuation. The turbulent wake generates actions associated with the so-called signature turbulence. Wind engineering practice usually quantifies these actions through dimensionless parameters termed "aerodynamic coefficients". These include pressure coefficients, net pressure coefficients, force and moment coefficients, coefficients of force and moment per unit length, and friction coefficients.

The following parameter is defined as the pressure coefficient:

$$c_p = \frac{p}{\frac{1}{2} \cdot \rho \cdot V^2} \qquad (2.9)$$

where V is the mean or peak wind velocity hence independent of time, which characterises the free flow. V is evaluated at a conventional reference height.

When $p > 0$ ($P > P_0$), c_p is positive and the point is subjected to inward pressure; this is the case for points of surfaces directly exposed to the oncoming wind and, more generally, of points at which the boundary layer is attached to the body surface. On the othe hand,, when $p < 0$ ($P < P_0$), c_p is negative and the point is subjected to outward pressure or suction; this occurs, e.g., on lateral and downwind surfaces and, more generally, at points were the flow is separated.

Pressure p_e that acts on the outer faces of the body is defined as external; in this case coefficient c_p is designated external pressure coefficient and denoted with symbol c_{pe}.

Pressure p_i that acts on the internal faces of the body is designated internal pressure; in this case coefficient c_p is called the internal pressure coefficient and denoted with symbol c_{pi}. Figure 2.22 shows the typical distribution of the external pressure coefficient of a building.
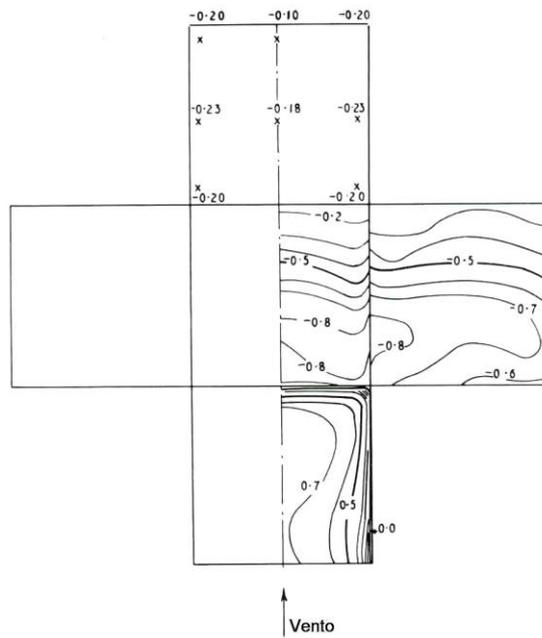
Figure 2.22 – External pressure coefficient of a building.

Net pressure p_n exerted by the wind on a surface is the sum of pressures p_1 and p_2 applied by the wind, respectively, on faces 1 and 2 of the surface. Assuming for p_n the same sign of p_1, $p_n = p_1 - p_2$. The net pressure coefficient is then given as:

$$c_{pn} = \frac{p_n}{\frac{1}{2} \cdot \rho \cdot V^2} = \frac{p_1 - p_2}{\frac{1}{2} \cdot \rho \cdot V^2} \tag{2.10}$$

Pressure coefficients and net pressure coefficients are generally used to represent the distribution of pressure p on the surfaces of large three-dimensional bodies. In the case of compact three-dimensional bodies it is often sufficient to find the three components of resultant force F_X, F_Y and F_Z, and of the resultant moment M_X, M_Y and M_Z, with respect to an X, Y, Z. The following six parameters are defined as force coefficients c_{FX}, c_{FY} and c_{FZ}, and moment coefficients c_{MX}, c_{MY} and c_{MZ}:

$$c_{F\alpha} = \frac{F_\alpha}{\frac{1}{2} \cdot \rho \cdot V^2 \cdot L^2} \; ; \quad c_{M\alpha} = \frac{M_\alpha}{\frac{1}{2} \cdot \rho \cdot V^2 \cdot L^3} \quad (\alpha = X, Y, Z) \tag{2.11}$$

where L is a characteristic length of the compact body.

The formulation is greatly simplified in the case of slender two-dimensional bodies, for which it is often sufficient to find the resultant aerodynamic actions per unit length, referred to the body axis. From Figure 2.18, where the axis of the body coincides with the Z axis, the following three aerodynamic coefficients are defined:

$$c_{fX} = \frac{F_X}{\frac{1}{2} \cdot \rho \cdot V^2 \cdot l} \; ; \quad c_{fY} = \frac{F_Y}{\frac{1}{2} \cdot \rho \cdot V^2 \cdot l} \; ; \quad c_{mZ} = \frac{m_Z}{\frac{1}{2} \cdot \rho \cdot V^2 \cdot l^2} \tag{2.12}$$

where l is a characteristic length of the body cross section. Figure 2.23 shows a sample plot of these aerodynamic coefficients for a bridge deck as a function of the angle of attack β that defines the flow direction.
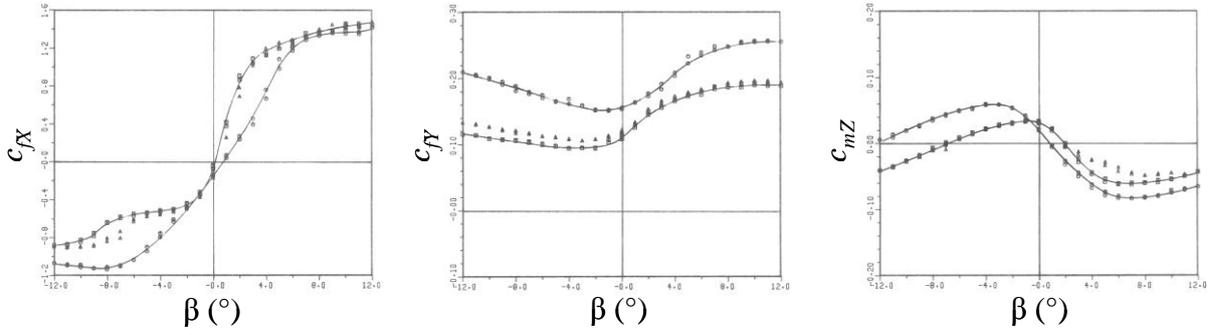
Figure 2.23 – Drag, lift and torque coefficients for a bridge deck.

When axis X coincides with the oncoming wind direction, coefficients c_{fX} and c_{fY} are termed drag and lift coefficient, respectively.

The friction coefficient is defined as:

$$c_f = \frac{w_f}{\frac{1}{2} \cdot \rho \cdot V^2} \tag{2.13}$$

where w_f is the friction action per unit area in the direction of the flow.

The aerodynamic actions can be calculated using eqs. (2.9) through (2.13), once the wind parameters ρ and V, the characteristic body lengths L and l, and the aerodynamic coefficients are known.

In particular, when V is the mean wind velocity ($V = v_m$), eqs. (2.9) through (2.13) provide the mean values of the aerodynamic actions. For example, starting from eq. (2.12), the mean wind force per unit length in the X direction is:

$$f_{Xm} = \frac{1}{2} \cdot \rho \cdot v_m^2 \cdot l \cdot c_{fX} \tag{2.14}$$

Likewise, when V is the peak velocity ($V = v_p$), eqs. (2.9) through (2.13) give the peak values of the aerodynamic actions. For example, using again eq. (2.12), the peak wind force X per unit length in the X direction is:

$$f_{Xp} = \frac{1}{2} \cdot \rho \cdot v_p^2 \cdot l \cdot c_{fX} \tag{2.15}$$

Similar equations are obtained when the remaining eqs. (2.9) through (2.13) are used.

Sections 3.3.1 through 3.3.5 implement eqs. (2.9) through (2.13), to give the peak aerodynamic actions as the product of three parameters: the peak velocity pressure at a given reference height, the appropriate aerodynamic coefficient, and, when applicable, a characteristic length of the body. Annexes G and H contain the global and local aerodynamic coefficients for a broad variety of constructions. Annex Q provides basic information concerning wind tunnels testing.

2.5   DYNAMIC RESPONSE

Let us consider a structure or a structural element that can be modelled, at a first approximation, by the two-dimensional scheme in Figure 2.18. Assuming that the displacements caused by wind are rather small, they can be treated by applying on the body the aerodynamic actions caused by wind assuming that the body is fixed and not deformable (section 2.4). The aerodynamic action per unit length is described by means of an alongwind force F_D (D = drag in the x direction), an across-wind force F_L (L = lift in the y direction) and a torque (M, about axis z) (Figure 2.24). As a result, the structure or structural element experiences a three-dimensional response, with alongwind (D), across-wind (L) and torsional (M) components. The alongwind response and the across-wind response occur, respectively, in the x-z and y-z planes, respectively; torsional rotation occurs about the z axis. For the sake of simplicity, the three response components are dealt with as uncoupled.
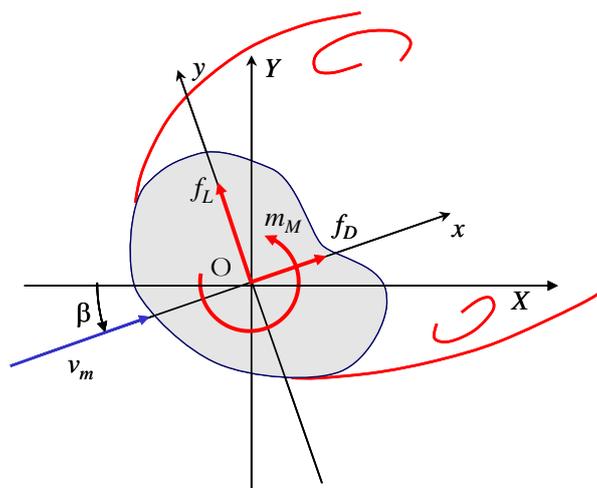
Figure 2.24 – Alongwind, across-wind and torsional response.

For an elastic structure featuring viscous damping, the equation of motion in the alongwind degree of freedom $x(t)$ is:

$$\ddot{x}(t) + 2 \cdot \xi_D \cdot (2\pi \cdot n_D) \cdot \dot{x}(t) + (2\pi \cdot n_D)^2 \cdot x(t) = \frac{1}{m} \cdot f_D(t) \tag{2.16}$$

where m, n_D and ξ_D are the mass, the natural frequency and the damping ratio in the alongwind direction, respectively (Annex I). Like the wind velocity (eq. 2.4), also the aerodynamic action f_D and the dynamic response x are expressed as follows:

$$f_D(t) = f_{Dm} + f_D'(t) \tag{2.17}$$

$$x(t) = x_m + x'(t) \tag{2.18}$$

where f_{Dm} and f_D' are the mean value and the fluctuating component of f_D, respectively, and x_m and x' are the mean value and fluctuating component of x, respectively. The mean value and the fluctuating component of x (eq. 2.18) are respectively due to the mean value and fluctuating component of f_D (eq. 2.17), which are, in turn, associated with the mean value and fluctuating component of v, respectively (eq. 2.4). In particular, (assuming that atmospheric turbulence is small), like velocity, also the aerodynamic action and response can be described as stationary, Gaussian, random processes. Therefore, the peak value of x is given as:

$$x_p = x_m + g_D \cdot \sigma_x = x_m + g_D \cdot \sqrt{\sigma_{Bx}^2 + \sigma_{Rx}^2} = x_m \cdot G_D \tag{2.19}$$

$$G_D = 1 + g_D \cdot \frac{\sigma_x}{x_m} = 1 + 2 \cdot g_D \cdot I_v \cdot \sqrt{B^2 + R_D^2} \tag{2.20}$$

where σ_x and g_D are the standard deviation and the peak factor of x, respectively; σ_{Bx} and σ_{Rx} are the background and resonant parts of the standard deviation of the response, respectively; G_D is the gust factor of the alongwind dynamic response; B and R_D are two coefficients defined as the background response factor and the resonant response factor.

The backgrund response factor B is a coefficient that takes account of the partial correlation of pressures exerted by the wind on the exposed surface of area A. For small values of A, B tends to 1; as A increases, due to the non full correlation of pressure peaks, B tends to zero for A tending to infinite (Figure 2.25a).

The resonant response factor R_D is a coefficient depending on the exposed surface of area A, on the natural frequency n_D and on the damping ratio ξ_D of the structure. Like B, also R_D decreases as A increases due to the non full correlation of pressure peaks. Moreover, for practical values of the natural frequency, this factor is smaller the stiffer is the structure (Figure 2.25b). Finally, R_D decreases as damping increases.

(a)   (b)
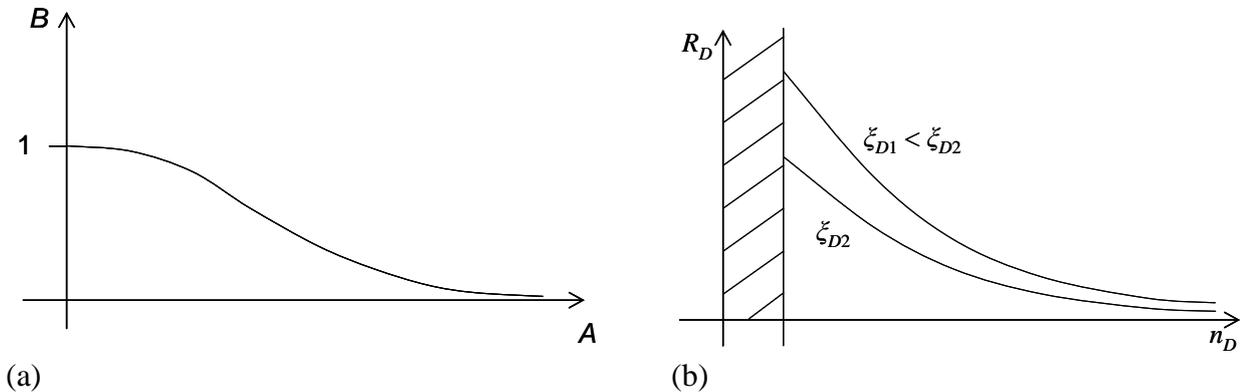
Figure 2.25 – Quasi-static B (a) and resonant R_D (b) response factors.

It can thus be stated that gust factor G_D depends on size, stiffness, and damping of the structure. This factor is large if the structure is small and slender, flexible and/or only moderately damped, and is small if the structure is large, stiff, and highly damped. Table 2.II provides a summary of the values of G_D; in all cases $G_D \geq 1$.

Table 2.II – Alongwind gust factor G_D.

Frequency n_D and damping ξ_D	Exposed surface A		
	pointlike ($B \rightarrow 1$)	medium ($0 < B < 1$)	large ($B \rightarrow 0$)
small ($R_D \square B$)	$G_D = 1 + 2 g_D I_v R_D$	$G_D = 1 + 2 g_D I_v R_D$	-
medium ($R_D > 0$)	$G_D = 1 + 2 g_D I_v \sqrt{1 + R_D^2}$	$G_D = 1 + 2 g_D I_v \sqrt{B^2 + R_D^2}$	$G_D = 1 + 2 g_D I_v R_D$
large ($R_D \rightarrow 0$)	$G_D = 1 + 2 g_D I_v$	$G_D = 1 + 2 g_D I_v B$	1

Observing that the mean dynamic action f_{Dm} gives rise to the mean structural response x_m, the equivalent static load f_{Dse} is defined as an aerodynamic action that, when applied statically to the structure, gives rise to the peak value of response x_p. Due to linearity, the static load is calculated as:

$$f_{Dse} = f_{Dm} \cdot G_D \tag{2.21}$$

where G_D is the gust factor.

As an alternative to eq. (2.21), the equivalent static action can be expressed by the formula:

$$f_{Dse} = f_{Dp} \cdot c_{dD} \tag{2.22}$$

where $f_{Dp} = f_{Dm}(1 + 2 g_v I_v)$ is the peak aerodynamic action and c_{dD} is the dynamic coefficient, given as:

$$c_{dD} = \frac{G_D}{1 + 2 \cdot g_v \cdot I_v} = \frac{1 + 2 \cdot g_D \cdot I_v \cdot \sqrt{B^2 + R_D^2}}{1 + 2 \cdot g_v \cdot I_v} \tag{2.23}$$

Unlike the gust factor G_D, the dynamic coefficient c_{dD} can be greater than, lesser than, or equal to 1. The condition $c_{dD} > 1$ corresponds to $G_D > 1+2g_vI_v$ and leads to equivalent static loads greater than peak aerodynamic actions; this is the case for small, flexible, and low damped structures. The condition $c_{dD} < 1$ corresponds to $G_D < 1+2g_vI_v$ and leads to equivalent static loads smaller than peak aerodynamic actions; this is typical of large, stiff, and highly damped structures. Table 2.III gives a summary of the possible values of c_{dD}, having set $g_D = g_v = 3.5$. This is an average representative value of the alongwind response peak coefficient; $g_v = 3.5$ is the conventional value used in this Guide for the velocity peak coefficient. Figure 2.26 provides a graphic interpretation of the data given in Table 2.III.

Table 2.III - Alongwind dynamic coefficient c_{dD}.

Frequency n_D and damping ξ_D	Exposed surface A		
	pointlike $(B \to 1)$	medium $(0 < B < 1)$	large $(B \to 0)$
small $(R_D \square\ B)$	$c_{dD} = \dfrac{1 + 7 I_v R_D}{1 + 7 I_v}$	$c_{dD} = \dfrac{1 + 7 I_v R_D}{1 + 7 I_v}$	-
medium $(R_D > 0)$	$G_D = 1 + 2 g_D I_v \sqrt{1 + R_D^2}$	$G_D = 1 + 2 g_D I_v \sqrt{B^2 + R_D^2}$	$c_{dD} = \dfrac{1 + 7 I_v R_D}{1 + 7 I_v}$
large $(R_D \to 0)$	$c_{dD} = 1$	$c_{dD} = \dfrac{1 + 7 I_v B}{1 + 7 I_v}$	$c_{dD} = \dfrac{1}{1 + 7 I_v}$
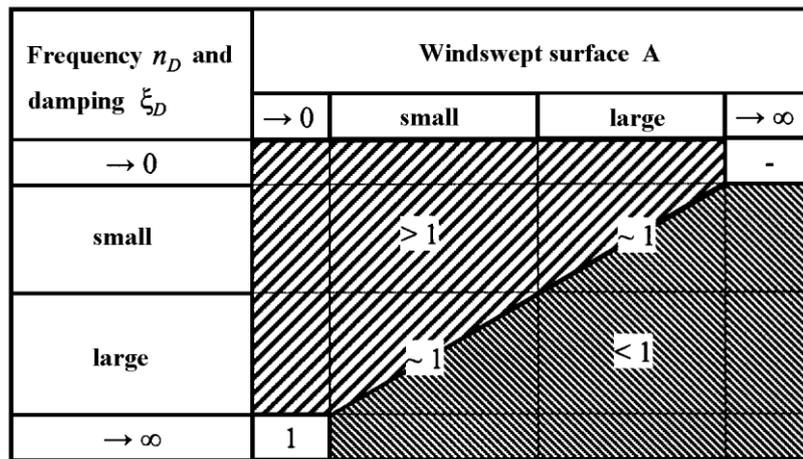
Figure 2.26 – Alongwind dynamic coefficient c_{dD}.

This Guide introduces eq. (2.22) in section 3.4.1, extending it to all wind actions. On the contrary, eq. (2.23) is introduced in Annex L, setting $g_v = 3.5$. In this manner the equivalent static wind force is the product of three parameters characterising the wind at the site (section 3.2), the aerodynamics of the construction (section 3.3) and the structural dynamics (section 3.4): the peak velocity pressure at a reference height (eq. 2.8), the aerodynamic coefficient (eq. 2.9-2.13) and the dynamic coefficient (eq. 2.23).

The distinctive element of this approach is that the alongwind response of the structure is produced by two primary action mechanisms, both of which are associated with the oncoming flow: the mean wind velocity and the alongwind turbulence. The situation is more complex in the case of the across-wind and torsional response, where three additional causes of excitation come into play: lateral turbulence (for high-rise structures), vertical turbulence (for horizontal structures), and, above all, the turbulent wake. There results a set of phenomena, whose evaluation and interpretation is far more complex than that required for the alongwind response. Moreover, it should be noted that, at least for standard structures, the across-wind and torsional response is often less significant than the alongwind response. In general, however, this is not the case for structural types characterised, for example, by significant height (high-rise buildings, towers, stacks, …) or length (bridges, footbridges, elements of large industrial structures, power transmission lines,…); in these cases it often happens that the requirements on the across-wind and torsional responses become more stringent than those on the alongwind response. Annex M of this Guide contains several criteria to evaluate these phenomena in the specific case of high-rise buildings with regular shapes.

The human body does not generally experience major difficulties in supporting significant displacements; it is however extremely sensitive to accelerations, producing reactions that range from perception to intolerability. The assessment of the acceleration induced by the wind on top

floors of high-rise buildings is therefore an essential requirement for serviceability. Together with criteria for evaluating equivalent alongwind, across-wind and torsional static actions, Annexes L and M provide criteria for determining the associated accelerations. Annex N introduces relevant criteria for evaluating the acceptability of the accelerations in relation to the building serviceability.

2.6   VORTEX SHEDDING

The phenomenon of vortex shedding from slender constructions and elements (such as chimneys, lighting poles, elements of lattice structures and power lines) is one of the most specific aspects of wind engineering.

To illustrate this phenomenon, let us consider a slender body, which is therefore essentially two-dimensional in respect to its cross-section, and consider the turbulent wake that forms in the flow separation region (Figure 2.24). The wake is characterised by an alternate shedding of vortices from the structure resulting in an across-wind load, which can be described, at a first approximatio, by means of a sine function:

$$f_{sL}(t) = A_s \cdot \sin(2\pi \cdot n_s \cdot t) \tag{2.24}$$

where A_s is the force amplitude and n_s is the dominant vortex shedding frequency, given by Strouhal law:

$$n_s = \frac{St \cdot v_m}{b} \tag{2.25}$$

where St is a dimensionless parameter, called the Strouhal number, which is primarily a function of the shape of the cross section and of the Reynolds number, v_m is the mean wind velocity, and b is a characteristic length of the cross section.

The most critical conditions occur when the vortex shedding frequency coincides with the frequency of a structural across-wind vibration mode $n_{L,i}$, specifically at the first natural frequency $n_{L,1}$ associated with a vibration mode perpendicular to the wind direction.

The mean wind velocities $v_m = v_{cr,i}$ for which $n_s = n_{L,i}$ are defined as critical and the structure is subjected to a resonant load:

$$v_{cr,i} = \frac{n_{i,L} \cdot b}{St} \tag{2.26}$$

Eq. (2.26) deserves some comments.

The first issue is that the harmonic model of the across-wind force caused by vortex shedding (eq. 2.24) is reasonable only in the case of a smooth flow; on increasing the turbulence, the harmonic content of the force spreads over a broader range of frequencies, indicatively centred on frequency n_s. Therefore, while the alongwind response tends to increase with the level of turbulence, the increase in turbulence mitigates the across-wind response due to vortex shedding.

The second issue concerns the variation of the mean wind velocity with height. Tall structures may have critical values of mean wind velocity which move along the structure as the mean velocity varies (Figure 2.27). This brings the necessity of identifying the position of the critical velocity causing the maximum across-wind response. Practical experience and theory together show that this occurs when the critical velocity occurs at a height where the resonant vibration mode has a maximum. The first vibration mode has, therefore, the maximum excitation when the critical shedding of vortices occurs at the tip of the structure (Figure 2.27a). Vibration in the higher modes, on the other hand, must be analysed for several positions of the critical shedding velocity (Figure 2.27b).
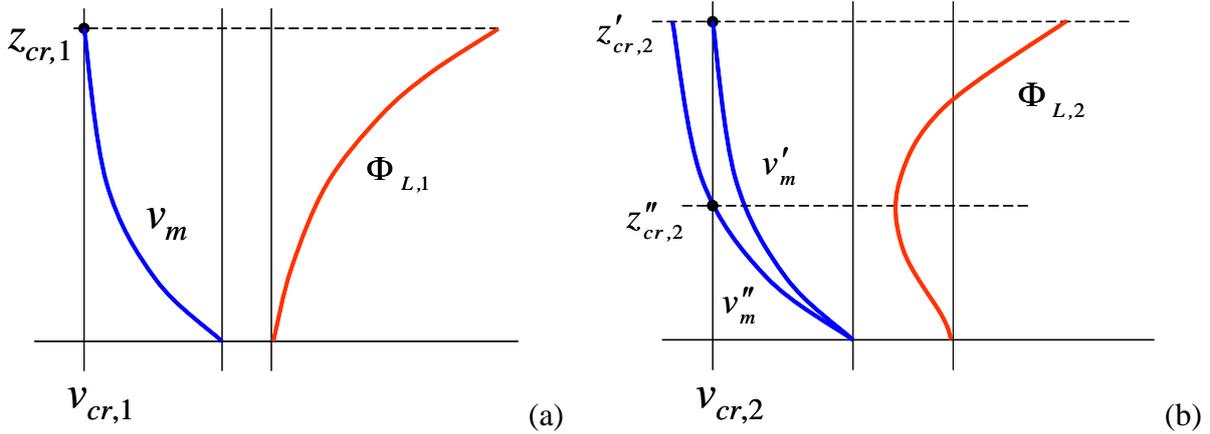
Figure 2.27 – Critical positions at which the resonant shedding of vortices occurs.

The third and main observation is that, in accordance with eq. (2.25), the vortex shedding frequency n_s is a linear function of the mean wind velocity v_m (Figure 2.28a). In practice, this law is violated, starting from wind velocities close to $v_{cr,i}$, within a velocity interval $\Delta v_{cr,i}$ (Figure 2.28b), called lock-in (or synchronization) range, which is broader the smaller the Scruton number:

$$Sc = \frac{4\pi \cdot m \cdot \xi_{L,i}}{\rho \cdot b^2}$$

(2.27)

where m is the mass per unit length of the structure, (which is assumed to be uniform for the sake of simplicity), and $\xi_{L,i}$ is the damping ratio in the i-th across-wind vibration mode.
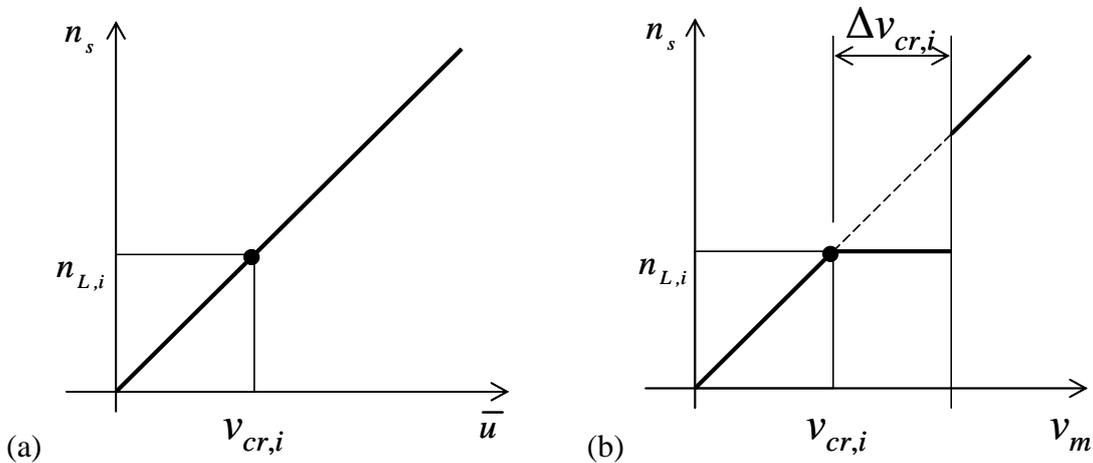
Figure 2.28 – Strouhal law for large (a) and small (b) Scruton numbers.

The above situation has a key physical meaning. When the Scruton number is large (Figure 2.28a), the alternate shedding of vortices causes an across-wind load of the type described above, which in turn gives rise to a resonant vibration; this therefore falls into the category of the typical dynamic structural response phenomena illustrated at section 2.5. In contrast, when the Scruton number is small, the vortex wake produces vibrations of an amplitude such that they themselves trigger the shedding of vortices. Under these circumstances vortex shedding takes place at the vibration frequency, also when the mean wind velocity varies within the range shown in Figure 2.28b, this phenomenon is driven by fluid-structure interaction and as such it falls into the class of problems

addressed at section 2.7. For these reasons, the vibrations caused by vortex shedding may represent a transition between dynamic response and aeroelastic response.

Figure 2.29 may help understanding the different types of behaviour that can occur when the Strouhal law is violated. The figure shows the results of experiments carried out on a model chimney in a wind tunnel. The x and y axes show, respectively, the reduced mean velocity, $v_m / n_{L,1} b$, and the normalised standard deviation of the tip across-wind displacement σ_y / b; the different curves correspond to different values of the Scruton number Sc. When Sc is large, the across-wind response increases only moderately, within a small range around the critical velocity. For lower values of Sc, the across-wind response increases abruptly and the resonance extends to a rather broad range of values of the wind velocity, mainly to the right of the critical value; this means that Strouhal law is violated (Figure 2.28b).
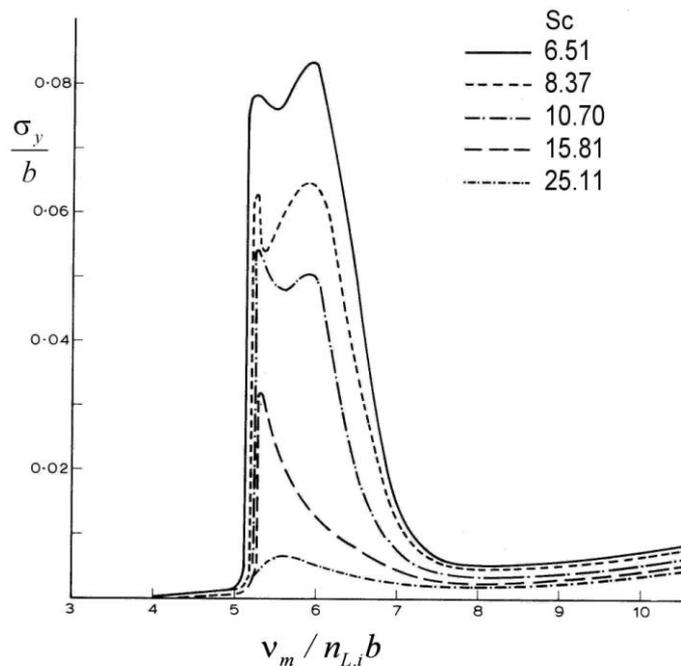
Figure 2.29 – Across-wind response to vortex shedding.

Figure 2.30 presents similar results to those of Figure 2.29, showing the maximum value of normalised standard deviation of the across-wind response at the top of the structure as a function of the Scruton number. Three separate regimes can be identified. For large Sc values vibrations are forced by vortex shedding and they have a random nature (Figure 2.31a). For small Sc values vibrations are self-excited by the structure vibration and they have deterministic characteristics (Figure 2.31b). For intermediate Sc values a transition occurs between the two types of behaviour above and vibrations are of an hybrid nature (Figure 2.31c).
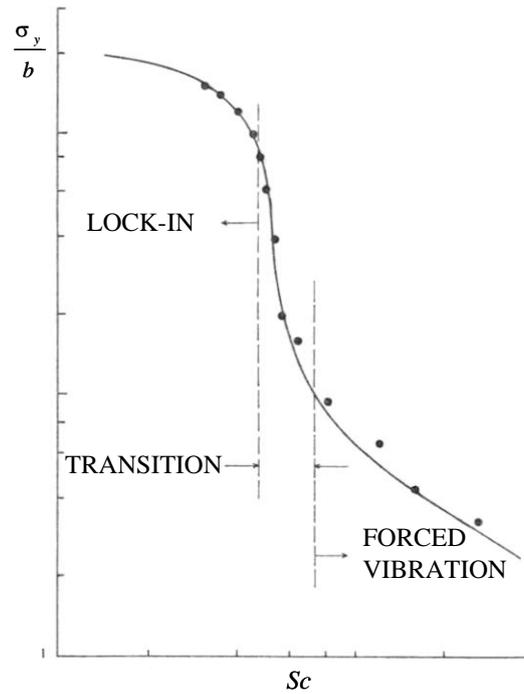
Figure 2.30 – Domains of the across-wind response to vortex shedding.

(a)   (b)   (c)
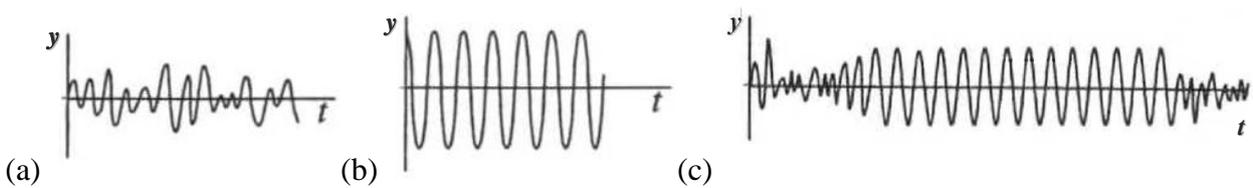
Figure 2.31 – Forced (a), self-excited (b) and transition (c) response regimes.

The transition from forced to aeroelastic response occurs for Scruton numbers indicatively in the order of 5 to 20. In this regime an abrupt increase in the vibration amplitudes takes place, and it is usually a design requirement that the structure should not enter the aeroelastic regime and should instead remain in the field of forced vibrations. It is worth noting the favourable role of turbulence; the increase in turbulence tends to shift the transition towards smaller Scruton numbers, therefore postponing the aeroelastic behaviour.

Given the complexity of the phenomenon, and despite research work that has been carried out over a time span now approaching a century, comprehensive, reliable, and totally agreed formulations able of predicting these phenomena in a quantitatively reasonable manner are still lacking. The two methods that are currently the most commonly used in wind engineering are associated with a number of complementary pros and cons, and they often bring quite different conclusions.

The equation of motion of a linear elastic structure featuring viscous damping, subjected to vortex shedding in resonance with across-wind vibration mode i is:

$$\ddot{y}_i(t) + 2 \cdot \xi_{L,i} \cdot (2\pi \cdot n_{L,i}) \cdot \dot{y}_i(t) + (2\pi \cdot n_{L,i})^2 \cdot y_i(t) = \frac{1}{m} \cdot f_L(t) \tag{2.28}$$

where y_i denotes the deflection associated with across-wind vibration mode i and f_L is the total across-wind load:

$$f_L(t) = f_{sL}(t) + f_{aL}(t) \tag{2.29}$$

f_{sL} being the aerodynamic load exerted by vortex shedding (eq. 2.24) on the stationary structure (therefore not including motion-related forces), and f_{aL} is the aeroelastic force that depends on the structure motion. The latter force can be expressed as:

$$f_{aL}(t) = A_a \cdot K_a \cdot \left[1 - \frac{y_i^2(t)}{y_l^2}\right] \cdot \dot{y}_i(t) \tag{2.30}$$

where the model parameters A_a, K_a, y_l, are calibrated from data available from existing structures, and chosen such to stay on the safe side.

The second method, termed harmonic method, does not consider the explicit presence of an aeroelastic force in eq. (2.29). However, it does take account of the aeroelastic force implicitly by expressing the length of the portion of structure over which vortex shedding is locked as a function of the vibration amplitude. Such length is termed correlation length. Also in this case, the model parameters are calibrated on tests performed on existing structures.

It should be noted that the former method may lead to excessively prudent calculations, while the latter proves to not necessarily be on the safe side. In addition, the harmonic method applies to a broader range of structures than the spectral method. Figure 2.32 shows a qualitative comparison between the typical results of the two methods, highlighting how the largest discrepancies occur within the Scruton number transition range. These concepts are described in detail in Annex O, which also provides operational criteria for the application of both methods.
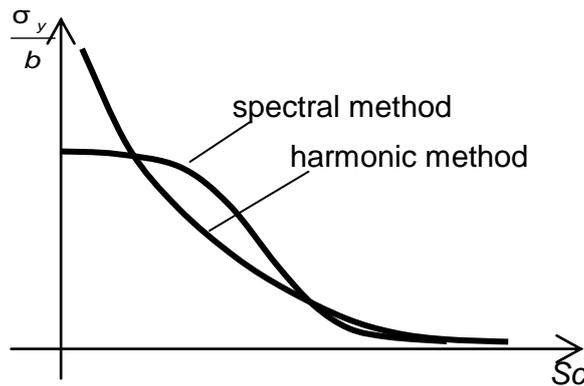
Figure 2.32 – Comparison between typical results of the spectral and harmonic methods.

2.7   OTHER AEROELASTIC PHENOMENA

The term "aeroelastic" describes wind-structure interaction phenomena caused by structural deflections and/or velocities of sufficient magnitude to modify the oncoming flow and aerodynamic actions that the wind would otherwise exert if the body were stationary. Lightweight, flexible and low damped structures are highly susceptible to such phenomena, e.g. masts, chimneys, lighting poles and towers, cable-supported bridges and footbridges, large roofs and cable structures, power transmission lines and individual components of lattice and industrial structures.

Disregarding vibration caused by vortex shedding, already illustrated at section 2.6, and with the aim of illustrating the remaining aeroelastic phenomena in a simple, intuitive, and compact way, let us consider initially a structural system with a single degree of freedom in the direction $\alpha = x$, y or θ, where θ is the torsional rotation about axis z (Figure 2.24). If the structure is linear elastic and viscously damped, the equation of motion is:

$$\ddot{\alpha}(t) + 2 \cdot \xi_\alpha \cdot (2\pi \cdot n_\alpha) \cdot \dot{\alpha}(t) + (2\pi \cdot n_\alpha)^2 \cdot \alpha(t) = \frac{1}{m_\alpha} \cdot f_\alpha(t) \tag{2.31}$$

where m_α, n_α and ξ_α are the mass (or polar mass moment of inertia), the natural frequency, and the damping ratio in direction of movement α; f_α is the global action, given as:

$$f_\alpha(t) = f_{s\alpha}(t) + f_{a\alpha}(t) \tag{2.32}$$

where $f_{s\alpha}$ is the aerodynamic action that the wind would exert if the body were stationary, and $f_{a\alpha}$ is the aeroelastic or self-excited action caused by the body motion; in general, this is a non-linear function of velocity $\dot{\alpha}(t)$ and displacement $\alpha(t)$.

For small values of these parameters, i.e. analysing incipient motion conditions, $f_{a\alpha}$ is given by:

$$f_{a\alpha}(t) = 2 \cdot \beta_\alpha \cdot (2\pi \cdot n_\alpha) \cdot \dot{\alpha}(t) + \gamma_\alpha \cdot (2\pi \cdot n_\alpha)^2 \cdot \alpha(t) \tag{2.33}$$

where β_α and γ_α are coefficients that depend on the structural properties and on the mean wind velocity. Replacing eq. (2.33) into eqs. (2.31) and (2.32), it results:

$$\ddot{\alpha}(t) + 2 \cdot (\xi_\alpha - \beta_\alpha) \cdot (2\pi \cdot n_\alpha) \cdot \dot{\alpha}(t) + (1 - \gamma_\alpha) \cdot (2\pi \cdot n_\alpha)^2 \cdot \alpha(t) = \frac{1}{m_\alpha} \cdot f_{s\alpha}(t) \tag{2.34}$$

from which it appears that the proportionality between $f_{a\alpha}$ and $\dot{\alpha}$ corresponds to a variation of the amount of damping, while the proportionality between $f_{a\alpha}$ and α corresponds to a variation of stiffness, therefore of the natural frequency.

Analysis of eq. (2.34) shows that, if $\beta_\alpha < 0$, the total damping, obtained by summing the structural and aeroelastic components, increases. On the contrary, if $\beta_\alpha > 0$, the total damping reduces and eventually becomes zero for $\beta_\alpha = \xi_\alpha$. This situation gives rise to aeroelastic phenomena of a dynamic nature, called galloping for $\alpha = y$ and torsional flutter for $\alpha = \theta$. The mean wind velocity at which $\beta_\alpha = \xi_\alpha$ is called the critical galloping velocity (for $\alpha = y$) or critical torsional flutter velocity (for $\alpha = \theta$). The probability of occurrence of this velocity must be very low.

In the case in which $\gamma_\alpha < 1$, the total stiffness, obtained by adding the structural part and the aeroelastic part, increases. On the contrary, if $\gamma_\alpha > 1$, the total stiffness reduces and eventually becomes zero for $\gamma_\alpha = 1$. This situation gives rise to an aeroelastic phenomenon of a static nature called divergence. The mean wind velocity at which $\gamma_\alpha = 1$ is called the critical divergence velocity. The probability of occurrence of this velocity must be very low.

When the alongwind, across-wind, and torsional responses are analysed separately it is found that in the alongwind direction $\alpha = x$, $\beta_x \leq 0$ and $\gamma_x \leq 1$. Therefore, neither galloping nor divergence can take place, and aeroelasticity is either ininfluential or it reduces the structural response.

In the across-wind direction $\alpha = y$, usually $\gamma_y \leq 1$, therefore divergence cannot occur. In contrast, β_y can take positive, negative or zero values, the former case leading to galloping. This phenomenon arises mainly with non-circular structural elements, in particular iced cables or cables with water rivulets.

In the torsional direction $\alpha = \theta$, since β_θ can take positive, negative or zero values, and since also γ_θ can be larger, smaller or equal to 1, both galloping and divergence can manifest themselves. Galloping is quite rare, while divergence mainly concerns bridge decks and thin plates.

A form of aeroelastic instability that involves two or more coupled degrees of freedom may be defined as flutter, in the broadest possible meaning of the term. Flutter gives rise to a phenomenon that results in the simultaneous modification of structural damping and stiffness. This is typical of

suspension and cable-stayed bridge decks and wing sections. The properties of flutter are highly complex and call for specialised analysis.

Annex P provides a general description of this topic and, where possible, simple operational analysis criteria.

2.8 INTERFERENCE

The term interference is used to describe those phenomena that modify the aerodynamic actions to which a structure or a structural component would be subject if it were isolated. According to various circumstances, interference may give rise to an increase or a reduction of wind velocity, of aerodynamic actions, of the dynamic response, and of the aeroelastic behaviour.

In relation to the wind velocity, interference occurs primarily when a structure is of a height that is comparable to the surrounding constructions or to the surrounding roughness elements. This situation is associated with specific problems, especially when a low rise structure is located in a wooded area or in a city centre. The surface layer is the portion of the atmosphere in contact with the ground, of thickness $z_s \approx 1,5 z_h$, where z_h is the average height of roughness elements (Figure 2.33). The use of the logarithmic profile for the mean wind velocity is acceptable above this layer. Inside the surface layer the velocity field depends on the orientation and properties of the roughness elements and can therefore be evaluated only by means of experimental tests or numerical simulations. In this regard, this Guide suggests that the wind field can be considered uniform beneath a conventional reference height, termed minimum height, z_{min} (section 3.2.3). This, however, does not take into account the local reductions or increases in velocity around specific distributions of obstacles and specific directions of the oncoming wind.
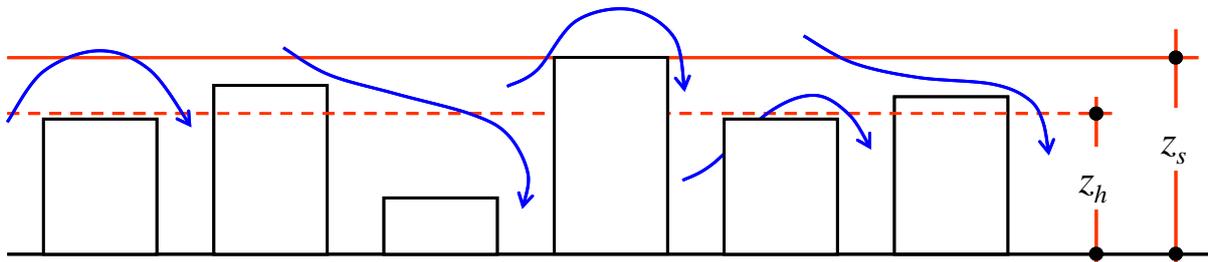
Figure 2.33 – Surface layer.

The phenomenon of aerodynamic interference occurs when two or more fixed and stiff bodies located close together give rise to significant variations of the local flow field and the aerodynamic actions associated with respect to those that would take place on isolated buildings. This phenomenon is of particular importance in the case of buildings of the same shape or type, e.g. tall buildings rising above city skylines, opposing cantilever roof structures on sport arenas, tanks, adjacent cooling towers and bridges, groups of chimneys, closely-spaced parallel power transmission lines, contiguous structural members, and tube bundles. Figure 2.34 shows the case of two adjacent cylinders, highlighting the different flow regimes that occur in accordance with the reciprocal position of the bodies. Each configuration is associated with quite different aerodynamic actions.

(a)   (b)
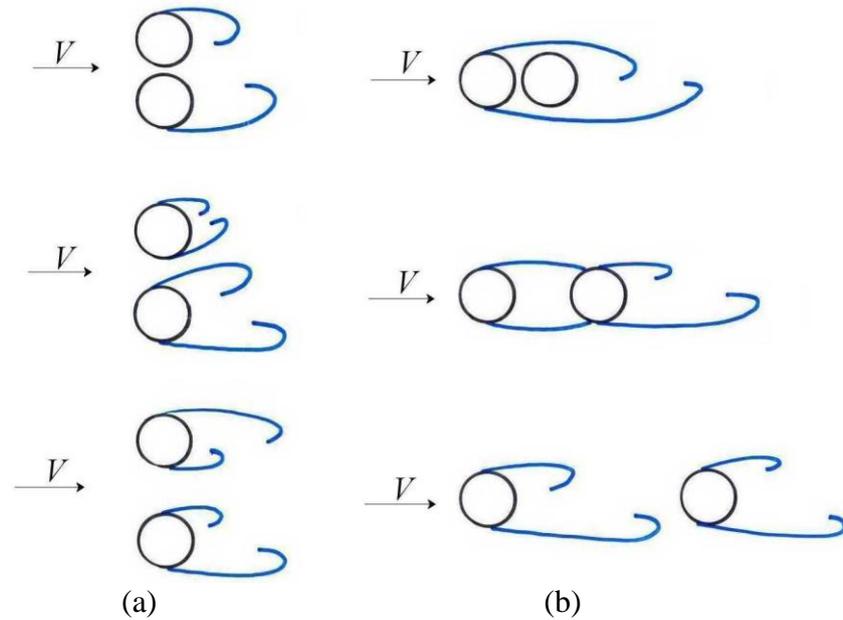
Figure 2.34 – Aerodynamic interference between pairs of cylinders.

Dynamic interference arises as a consequence of aerodynamic interference, when the dynamic response of a structure is modified by the variation of aerodynamic actions to which the structure is subjected due to the presence of an adjacent structure. Among the many phenomena of technical interest, the most well known concerns the case in which a structure or a structural element produces a vortex shedding hitting another structure located downstream (Figure 2.35). If the frequency of vortex shedding from the upstream structure is equal to a natural frequency of the downstream structure, the downstream structure is subject to a resonant action caused by interference. This phenomenon frequently involves pairs of tall buildings emerging above the city skyline, with highly critical consequences in relation to floor accelerations and the relevant serviceability assessments. This phenomenon may occur also following the construction of new bridges adjacent to existing bridges.
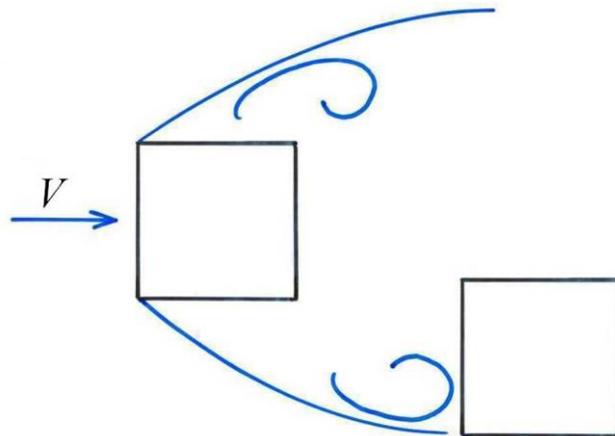
Figure 2.35 – Dynamic interference between adjacent buildings.

Aeroelastic interference is one of the most complex and potentially catastrophic phenomena. It may occur when closely spaced, lightweight, low-damping structures exchange actions, arising from their relative motion through the flow in which they are immersed. This family of actions includes phenomena of lock-in, galloping and flutter, which jointly affect closely spaced structures. In particular, the phenomena of structure-wind-structure interactions occurring in groups of chimneys

(Figure 2.36), closely-spaced slender elements, parallel cables, and adjacent cable-stayed bridge decks, are well known and highly dangerous.

(a) (b) (c)
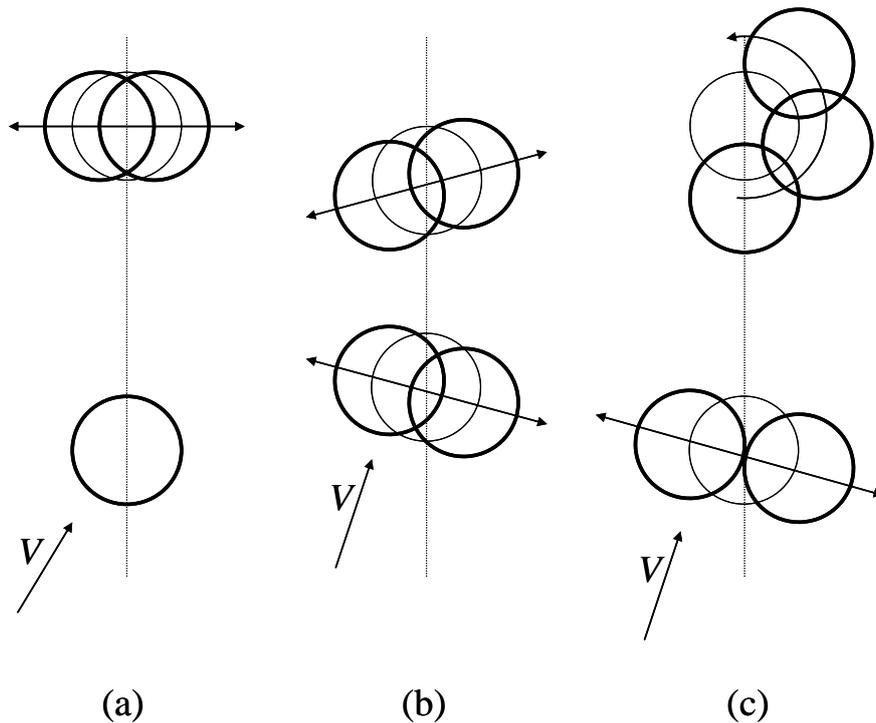
Figure 2.36 – Aeroelastic interference associated with galloping induced by a turbulent wake.

This Guide provides a number of qualitative and at times quantitative examples concerning the phenomena illustrated, and suggest the use of wind tunnel testing and the expert guidance in the most critical cases.

2.9 BIBLIOGRAPHY

This section contains a basic bibliography concerning wind actions and effects on structures. Readers who wish to get a deeper knowledge of the subject can refer to the following books as starting points for a search for information in further literature, specific scientific papers and conference proceedings.

Blevins, R.D. (2001). Flow-induced vibrations. Krieger Publishing Company, Malabar, Florida.

Cook, N.J. (1985). The designer's guide to wind loading of building structures. Part 1: Background, damage survey, wind data and structural classification. Building Research Establishment, Butterworths, U.K.

Cook, N.J. (1990). The designer's guide to wind loading of building structures. Part 2: Static structures. Building Research Establishment, Butterworths, U.K.

Holmes, J.D. (2001). Wind loading of structures. Spon Press, London, U.K.

Simiu, E., Scanlan, R.H. (1996). Wind effects on structures: Fundamentals and applications to design. John Wiley & Sons, New York, N.Y.

Strommen, E. (2006). Theory of bridge aerodynamics. Springer, Berlin, Heidelberg.

More extensive and comprehensive bibliographic references can be found, for example, on the *International Association for Wind Engineering* (IAWE) website at www.iawe.org.

3 PRINCIPLES AND RULES

3.1 GENERAL

(1)P Wind is the movement of air masses characterised by a velocity field that fluctuates randomly in time and space. It exerts aerodynamic actions on whole structures or on individual structural components, due to the oncoming flow and to the turbulent wake generated by the bodies. These actions fluctuate randomly in time and space, and generate dynamic effects. When structures or their components oscillate, they also modify the oncoming flow and the associated aerodynamic actions, resulting in an aeroelastic behaviour, caused by the mutual interaction of wind and structure. Finally, the presence of adjacent structures causes interference phenomena, such as to reduce or increase the actions and effects that the wind would cause on the structure if it were isolated; these phenomena can also affect individual structural components.

(2)P Furthermore, limited to the case of structures and components of regular shape and standard size, having sufficient stiffness and damping to limit dynamic effects and prevent any aeroelastic behaviour and interference effects such as to increase dynamic response, wind effects can be assessed by means of equivalent static actions giving rise to the maximum effects produced by dynamic application of actual actions.

(3)P Assessment of wind actions and effects on structures and their components is performed in the following manner:

(a) based on the characteristics of the construction site, wind design velocity and peak velocity pressure are calculated (clause 3.2);

(b) based on the shape, size and orientation of the structure, the peak aerodynamic actions exerted by the wind on the structure and its components are assessed (clause 3.3);

(c) based on the mechanical properties of the structure and of its components, the following elements are assessed in accordance with the particular situation and when required (clause 3.4):

- equivalent static actions (clause 3.4.1);
- dynamic response to wind actions (clause 3.4.2);
- dynamic and aeroelastic actions and effects caused by vortex shedding from slender structures and components (clause 3.4.3);
- possible occurrence of other aeroelastic phenomena, such as galloping, divergence and flutter, or aeroelastic interference situations (clause 3.4.4).

(4)P The Designer shall ensure the safety and efficiency of the structure and of its components against wind. Consideration should also be given to the problem of building serviceability and to the trust of occupants towards wind-induced accelerations. It is also necessary to ensure the safety of users both inside and outside buildings, e.g. by preventing non-structural elements of building facades and roofs from falling.

(5)P The use of specific analytical, numerical and/or experimental procedures is especially recommended for structures of an unusual shape or type, for tall or long structures, for slender, lightweight, flexible, poorly damped structures, and for structures with large surfaces. It is also recommended for structures of great importance or whose safety is strategic to that of individuals or the community as a whole.

3.2   WIND VELOCITY AND PRESSURE

(1)P   The instantaneous wind velocity fluctuates randomly in time and space. It is the sum of a mean part, varying slowly in time and space, and a zero-mean turbulent component with rapid fluctuations in time and space. Peak velocity pressure is defined as the expected value of the maximum velocity pressure. The design values of the mean wind velocity and of the turbulent fluctuation depend on the geographic location of the construction site, on the altitude above sea level, on the local characteristics of terrain, in particular roughness and topography, on the height above ground, on the annual probability of exceedence or on the return period. The design values of the peak wind velocity pressure depend on the same quantities above and on air density.

(2)P   The following steps are made when assessing the design values of wind velocity and peak velocity pressure:

(a)   based on geographical location and altitude above sea level of the construction site, the fundamental basic wind velocity v_b is calculated (clause 3.2.1);

(b)   based on the design return period T_R, the design reference velocity v_r is calculated (clause 3.2.2);

(c)   based on the local terrain roughness at the construction site, the exposure category is determined (clause 3.2.3);

(d)   based on local topography at the construction site, the topography coefficient c_t is calculated (clause 3.2.4);

(e)   if necessary (for determining aerodynamic actions on bodies with rounded surfaces or for the analysis of dynamic and aeroelastic phenomena), the mean wind velocity v_m is calculated (clause 3.2.5);

(f)   if necessary (for the analysis of dynamic and aeroelastic phenomena), the turbulence intensity I_v and the turbulent length scale L_v are calculated (clause 3.2.6);

(g)   the peak wind velocity pressure q_p is calculated (clause 3.2.7).

3.2.1 Basic reference wind velocity

(1)   The basic reference wind velocity v_b characterises the wind climate of the construction site. It is defined as the 10 minute mean wind velocity at a height of 10 m above flat open country with roughness length $z_0 = 0,05$ m (exposure category II, clause 3.2.3), for a design return period $T_R = 50$ years.

(2)   In the absence of suitable specific statistical analyses (Annex B) that take account of site roughness, terrain topography and wind direction (Annex C), for sites whose altitude is less than 1500 m above sea level, the basic reference wind velocity should be not less than the value given by the equation:

$$v_b = v_{b,0} \cdot c_a \qquad (3.1)$$

where:

$v_{b,0}$ is the value of the basic reference wind velocity at sea level, assigned by Table 3.I according to the construction site characteristics (Figure 3.1);

c_a is the altitude factor provided by the equations:

$$c_a = 1 \qquad \text{for } a_s \leq a_0 \qquad (3.2a)$$

$$c_a = 1 + k_a \cdot \left(\frac{a_s}{a_0} - 1 \right) \qquad \text{for } a_s > a_0 \qquad (3.2b)$$

where:

a_0, k_a are parameters given in Table 3.I according to the construction site characteristics (Figure 3.1);

a_s is the altitude above sea level of the construction site.

Table 3.I – Parameter $v_{b,0}$, a_0 and k_a for Italy.

Area	Zone	$v_{b,0}$ (m/s)	a_0 (m)	k_a
1	Valle d'Aosta, Piemonte, Lombardia, Trentino Alto Adige, Veneto, Friuli Venezia Giulia (except for Trieste Province)	25	1000	0,40
2	Emilia Romagna	25	750	0,45
3	Toscana, Marche, Umbria, Lazio, Abruzzo, Molise, Puglia, Campania, Basilicata, Calabria (except for Reggio Calabria Province)	27	500	0,37
4	Sicilia and Reggio Calabria Province	28	500	0,36
5	Sardegna (area to the east of the line joining Capo Teulada to the island of La Maddalena)	28	750	0,40
6	Sardegna (area to the west of the line joining Capo Teulada to the island of La Maddalena)	28	500	0,36
7	Liguria	28	1000	0,54
8	Trieste Province	30	1500	0,50
9	Islands (except for Sicilia and Sardegna) and open sea	31	500	0,32
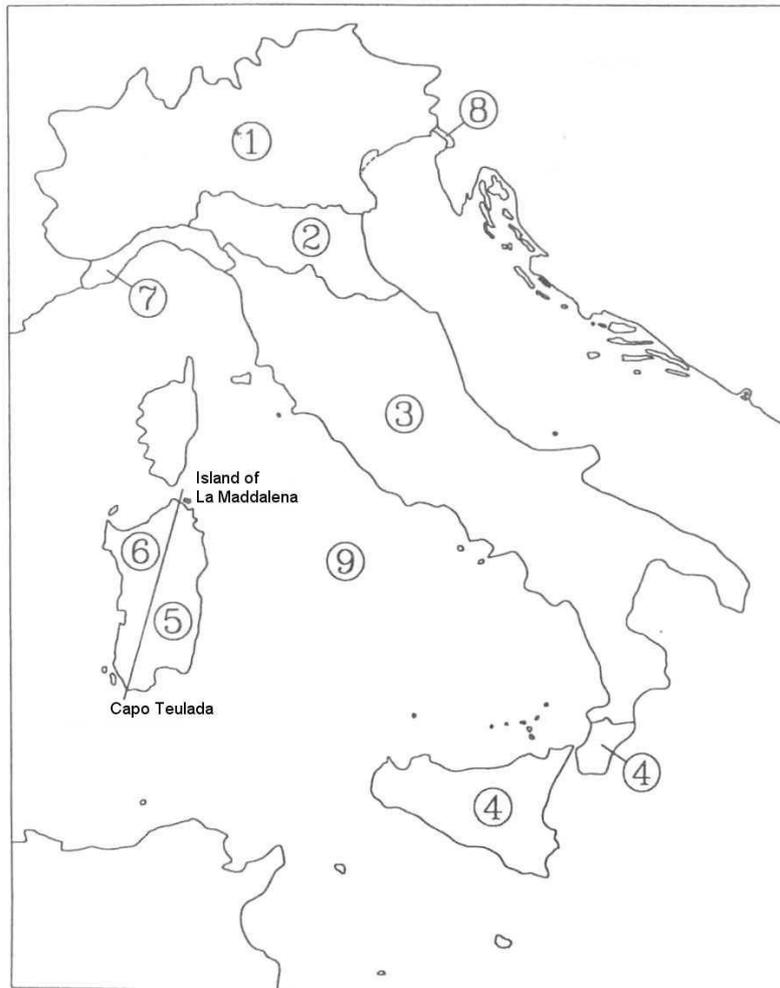
Figure 3.1 – Zones characterised by uniform basic reference wind velocity values.

(3)   For sites whose altitude exceeds 1500 m above sea level, the basic reference wind velocity can be obtained from well documented data or well established statistical analyses (Annex B). This approach is recommended in the proximity of summits and ridges, but the values used should be never less than the one obtained using the procedure above for an altitude of 1500 m.

(4)P   Annex B provides guides for calculating the basic reference wind velocity v_b using well established methods and reliable data.

3.2.2 Design return period and design reference velocity

(1)   The design reference velocity v_r is the maximum value of the 10 minute mean wind velocity at a height of 10 m above flat open terrain with roughness length $z_0 = 0,05$ m (exposure category II, clause 3.2.3), for design return period T_R.

(2)   In the absence of reliable specific statistical analyses (Annex B), this velocity is given by the equation:

$$v_r = v_b \cdot c_r \tag{3.3}$$

where:
v_b is the basic reference wind velocity associated with a return period $T_R = 50$ years (clause 3.2.1);
c_r is the return factor given by the equation (Figure 3.2):

$$c_r = 0,75 \qquad \text{for } T_R = 1 \text{ year} \tag{3.4a}$$

$$c_r = 0,75 + 0,0652 \ln\left(T_R\right) \qquad \text{for } 1 \text{ year} \leq T_R < 5 \text{ years} \tag{3.4b}$$

$$c_r = 0,75 \sqrt{1 - 0,2 \cdot \ln\left[-\ln\left(1 - \frac{1}{T_R}\right)\right]} \qquad \text{for } 5 \text{ years} \leq T_R < 50 \text{ years} \tag{3.4c}$$

$$c_r = 0,65 \left\{1 - 0,138 \cdot \ln\left[-\ln\left(1 - \frac{1}{T_R}\right)\right]\right\} \qquad \text{for } T_R \geq 50 \text{ years} \tag{3.4d}$$

where T_R is the design return period in years.
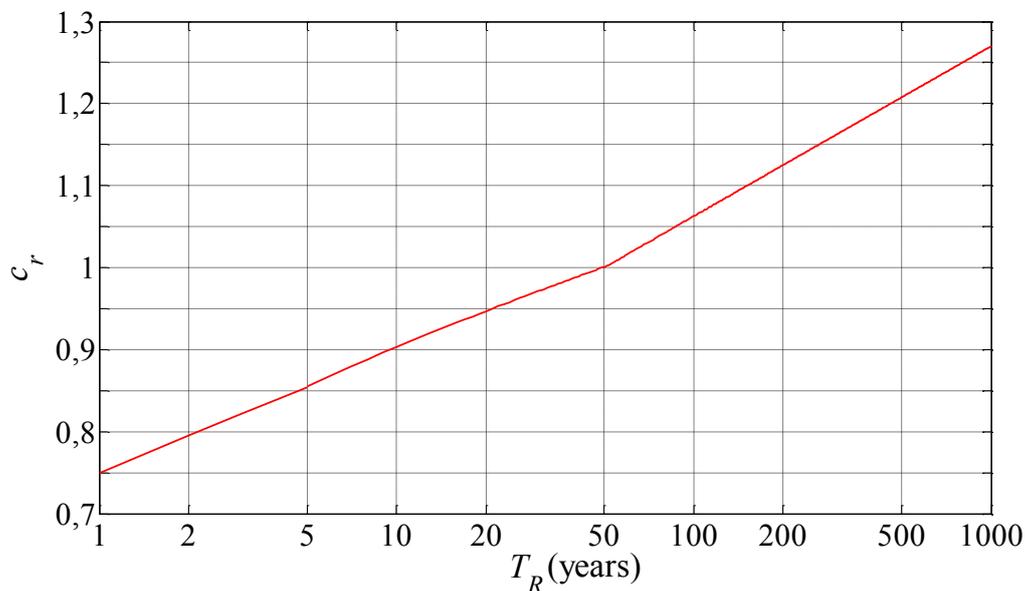
Figure 3.2 – Graph of return factor c_r versus return period T_R.

(3)P   Annex A provides guides for choosing the design return period. Annex B provides guides for calculating the design reference velocity v_R based on well established methods and reliable data.

3.2.3 Exposure category

(1)   In the absence of specific analyses that take account of wind direction and of roughness and topography of the terrain surrounding the construction (Annex C), mean wind velocity, turbulence intensity and peak velocity pressure, defined, respectively, in clauses 3.2.5, 3.2.6 and 3.2.7, depend on three parameters: terrain factor k_r, roughness length z_0 and minimum height z_{min}, given in Table 3.II as a function of the exposure category of the construction site. This is assigned by using the graphs in Figure 3.3, as a function of the site geographical location and of the terrain roughness class specified in Table 3.III.

Table 3.II – Parameter k_r, z_0, and z_{min}

Exposure category	k_r	z_0 (m)	z_{min} (m)
I	0,17	0,01	2
II	0,19	0,05	4
III	0,20	0,10	5
IV	0,22	0,30	8
V	0,23	0,70	12

ZONES 1,2,3,4,5

750 m
500 m
coast
sea
2 km | 10 km | 30 km

A	–	IV	IV	V	V	V
B	–	III	III	IV	IV	IV
C	–	*	III	III	IV	IV
D	I	II	II	II	III	**

* Category II in zone 1,2,3,4
  Category III in zone 5
** Category III in zone 2,3,4,5
  Category IV in zone 1

ZONE 9

coast
sea

A	–	I
B	–	I
C	–	I
D	I	I

ZONE 6

500 m
coast
sea
2 km | 10 km | 30 km

A	–	III	IV	V	V
B	–	II	III	IV	IV
C	–	II	III	III	IV
D	I	I	II	II	III

ZONES 7,8

coast
sea
1.5 km | 0.5 km

A	–	–	IV
B	–	–	IV
C	–	–	III
D	I	II	*

* Category II in zone 6
  Category III in zone 7

Figure 3.3 – Criteria for the assignment of the exposure category for the various zones of Italy.

Table 3.III - Terrain roughness classes.

Roughness class	Description
A	Urban area where at least 15 % of the terrain surface is covered with buildings and their average height exceeds 15 m
B	Urban, suburban, industrial or forest area (not class A)
C	Area with closely-spaced obstacles (such as trees, houses, walls, fences, etc.); areas whose roughness cannot be included in Classes A, B, D.
D	a) Sea and its coastline (no more than 2 km from the shore) b) Lake (with width of at least 1 km) and its shoreline (no more than 1 km from the shore) c) Area with no obstacles or only occasional isolated obstacles (open countryside, airports, farmland, pastures, marshlands or sandy areas, snow- or ice-covered areas, etc.)

(2)   In the absence of more detailed assessments (Annex C), the terrain roughness class can be assigned by applying the following criteria:

(a)   unless otherwise specified, any site belongs to roughness class C;

(b)   it shall be assumed that the site belongs to roughness class D when the structure is built in the areas denoted in Table 3.III by the letters a) or b) or when within a radius of 1 km from the structure there is a sector wide at least 30° in which at least 90% of the terrain is of the type denoted in Table 3.III by the letter c);

(c)   it may be assumed that the site belongs to roughness class A or B, provided that the structure is located in the corresponding area indicated in Table 3.III, within a radius of at least 1 km and never less than 20 times the height of the structure, for all wind direction sectors of at least 30°.

(3)   Where doubts exist regarding the assignment of a roughness class, the most unfavourable class shall be taken (bearing in mind that, generally speaking, wind action is lowest in class A and highest in class D).

3.2.4 Topography coefficient

(1)P   The topography coefficient c_t, generally a function of height above ground z, takes into account the construction site topographic features.

(2)   In most cases, in the absence of more detailed assessments (Annex C), the topography coefficient is set to 1 for both flat areas and undulated, hilly and mountainous areas.

(3)   For construction sites at the top of isolated hills and crests, the topography coefficient c_t should be calculated from reliable and well documented data; Annex D provides some calculation criteria.

(4)   For structures located within valleys where wind funnelling is likely to occur, it is recommended that specific assessments be performed.

3.2.5 Mean velocity

(1)   The mean wind velocity v_m, over a time $T = 10$ minutes, depends on the height above ground z, on local wind climate (clause 3.2.1), on design return period (3.2.2) and on local features of the construction site. Other than in a few special cases, its direction is generally taken to be horizontal.

(2)   In the absence of specific analyses that consider wind direction and effective roughness and topography of the terrain surrounding the construction site (Annex C), for heights above ground not exceeding $z = 200$ m, mean wind velocity is provided by the equation:

$$v_m(z) = v_r \cdot c_m(z) \tag{3.5}$$

where:

v_r is the design reference velocity (clause 3.2.2);

c_m is the mean wind velocity profile coefficient provided by the equation:

$$c_m(z) = k_r \cdot \ln\left(\frac{z_{min}}{z_0}\right) \cdot c_t(z_{min}) \quad \text{for } z \leq z_{min} \tag{3.6a}$$

$$c_m(z) = k_r \cdot \ln\left(\frac{z}{z_0}\right) \cdot c_t(z) \quad \text{for } z > z_{min} \tag{3.6b}$$

where:

k_r, z_0, z_{min} are, respectively, the terrain factor, the roughness length and the minimum height, specified in clause 3.2.3 as a function of the site exposure category;

c_t is the topography coefficient, given in clause 3.2.4 as a function of site topographic features.

Figure 3.4 shows $c_m(z)$ diagrams for various exposure categories where $c_t(z) = 1$.
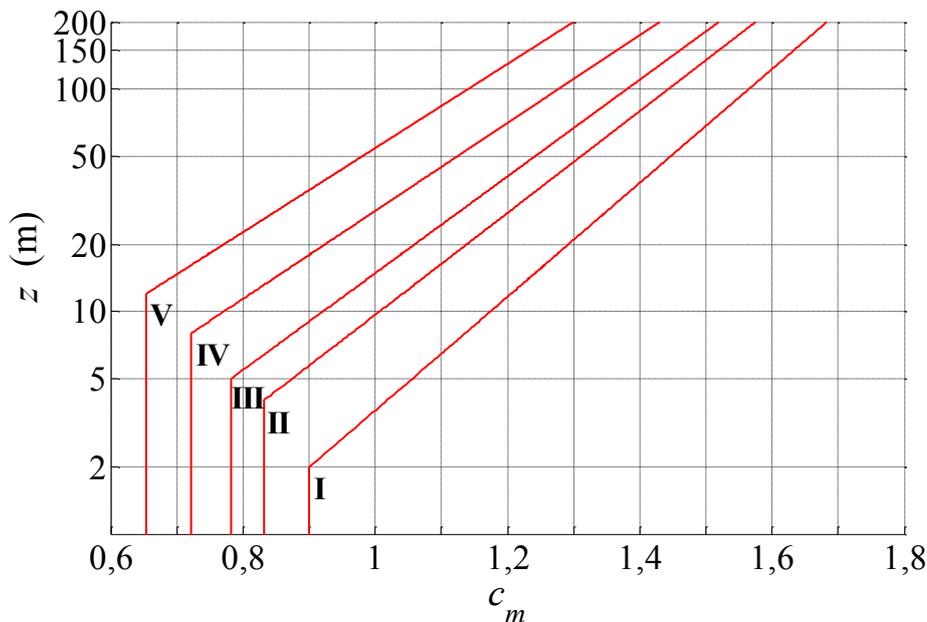
Figure 3.4 – $c_m(z)$ diagrams for various exposure categories where $c_t(z) = 1$.

3.2.6 Atmospheric turbulence

(1)   Atmospheric turbulence is the zero-mean fluctuation of the instantaneous wind velocity (around the mean value v_m). It is mainly characterised by two parameters: the turbulence intensity I_v and the turbulent length scale L_v.

(2)   The turbulence intensity is the standard deviation of the longitudinal turbulent component divided by the mean wind velocity. In the absence of specific analyses that consider wind direction, effective roughness and topography of the terrain surrounding the construction site (Annex C), for heights above ground not exceeding $z = 200$ m, it is provided by the equation:

$$I_v(z) = \frac{1}{\ln\left(\dfrac{z_{min}}{z_0}\right) \cdot c_t(z_{min})} \qquad \text{for } z \le z_{min} \tag{3.7a}$$

$$I_v(z) = \frac{1}{\ln\left(\dfrac{z}{z_0}\right) \cdot c_t(z)} \qquad \text{for } z > z_{min} \tag{3.7b}$$

where:

z_0, z_{min} are, respectively, the roughness length and the minimum height, specified in clause 3.2.3 as a function of the construction site exposure category;

c_t is the topography coefficient, given in clause 3.2.4 as a function of the construction site topographic features.

Figure 3.5 shows $I_v(z)$ diagrams for various exposure categories where $c_t(z) = 1$.
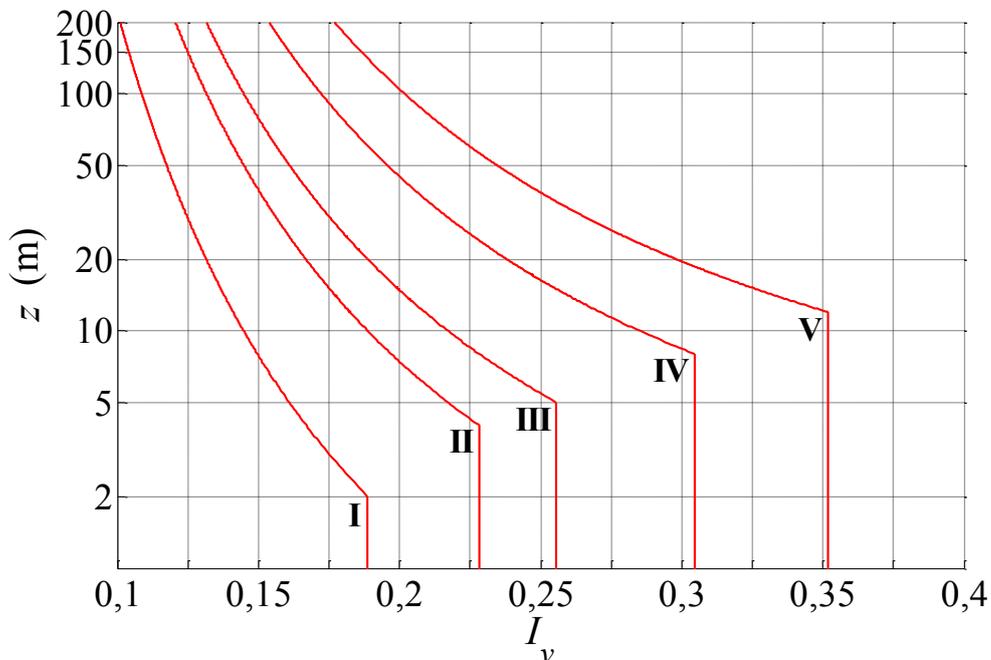
Figure 3.5 – $I_v(z)$ diagrams for various exposure categories where $c_t(z) = 1$.

(3)   The turbulent length scale represents the average size of the eddies forming the atmospheric turbulence. In the absence of specific analyses, it is given by the equations:

$$L_v(z) = \overline{L} \cdot \left(\frac{z_{min}}{\overline{z}} \right)^{\kappa} \qquad \text{for } z \leq z_{min} \tag{3.8a}$$

$$L_v(z) = \overline{L} \cdot \left(\frac{z}{\overline{z}} \right)^{\kappa} \qquad \text{for } z > z_{min} \tag{3.8b}$$

where:

$\overline{z}$ = 200 m is a reference height;

$\overline{L}$ = 300 m is a reference length;

z_{min} is the minimum height, specified in clause 3.2.3 as a function of the exposure category of the construction site;

κ is a coefficient given in Table 3.IV as a function of the exposure category of the construction site (clause 3.2.3).

Table 3.IV – Values of coefficient κ for the various exposure categories.

Site exposure category	κ
I	0,44
II	0,52
III	0,55
IV	0,61
V	0,65

Figure 3.6 shows $L_v(z)$ diagrams for various exposure categories.
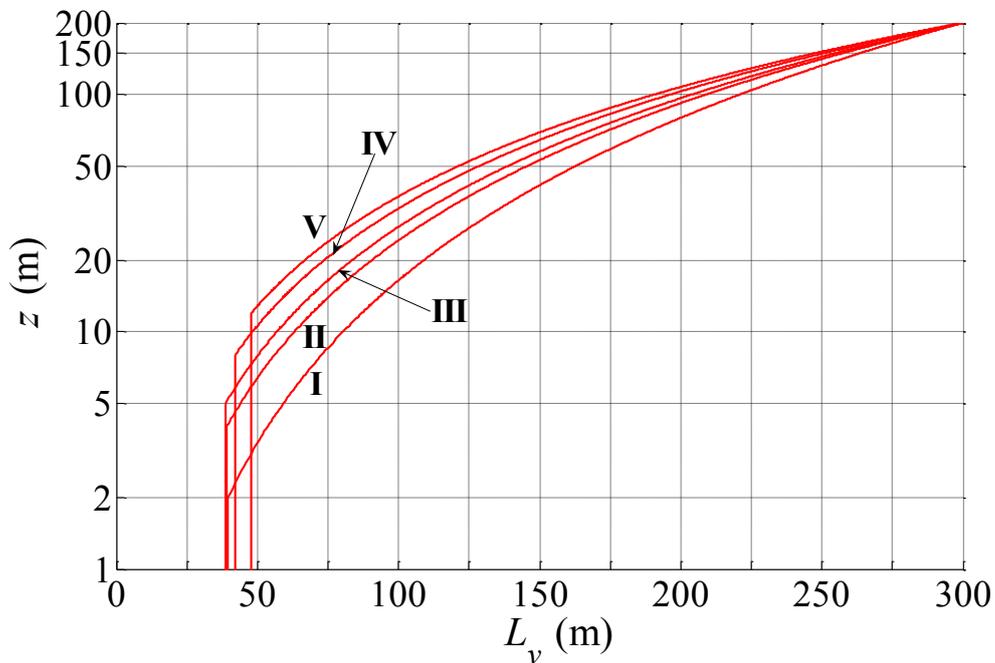
Figure 3.6 – $L_v(z)$ diagrams for various exposure categories.

(4)P   Annex E provides guides on the definition and use of detailed atmospheric turbulence models.

3.2.7 Peak velocity pressure

(1)   The peak wind velocity pressure q_p is the expected value of the maximum wind velocity pressure over a time $T = 10$ minutes. It depends on the height above ground z, on the wind climate (clause 3.2.1), on the design return period (clause 3.2.2), on the local features of the construction site and on air density.

(2)   In the absence of specific analyses that consider wind direction, effective roughness and topography of the terrain surrounding the construction site (Annex C), for heights above ground not exceeding z = 200 m, the peak velocity pressure is given by the equation:

$$q_p(z) = \frac{1}{2} \cdot \rho \cdot v_r^2 \cdot c_e(z) \qquad (3.9)$$

where:

ρ is the mean air density. As a rule, in the absence of more accurate estimates for the specific construction site, $\rho = 1{,}25$ kg/m^3;

v_r is the design reference velocity (clause 3.2.2);

c_e is the exposure factor given by the equation :

$$c_e(z) = k_r^2 \cdot \ln\left(\frac{z_{min}}{z_0}\right) \cdot c_t(z_{min}) \cdot \left[\ln\left(\frac{z_{min}}{z_0}\right) \cdot c_t(z_{min}) + 7\right] \quad \text{for } z \leq z_{min} \qquad (3.10a)$$

$$c_e(z) = k_r^2 \cdot \ln\left(\frac{z}{z_0}\right) \cdot c_t(z) \cdot \left[\ln\left(\frac{z}{z_0}\right) \cdot c_t(z) + 7\right] \quad \text{for } z > z_{min} \qquad (3.10b)$$

where:

k_r, z_0, z_{min} are, respectively, the terrain factor, roughness length and minimum height, specified in clause 3.2.3 as a function of the site exposure category;

c_t is the topography coefficient, given in clause 3.2.4 as a function of site topographic features.

By expressing ρ in kg/m^3 and v_r in m/s, q_p is given in N/m^2.

Figure 3.7 shows $c_e(z)$ diagrams for various exposure categories where $c_t(z) = 1$.
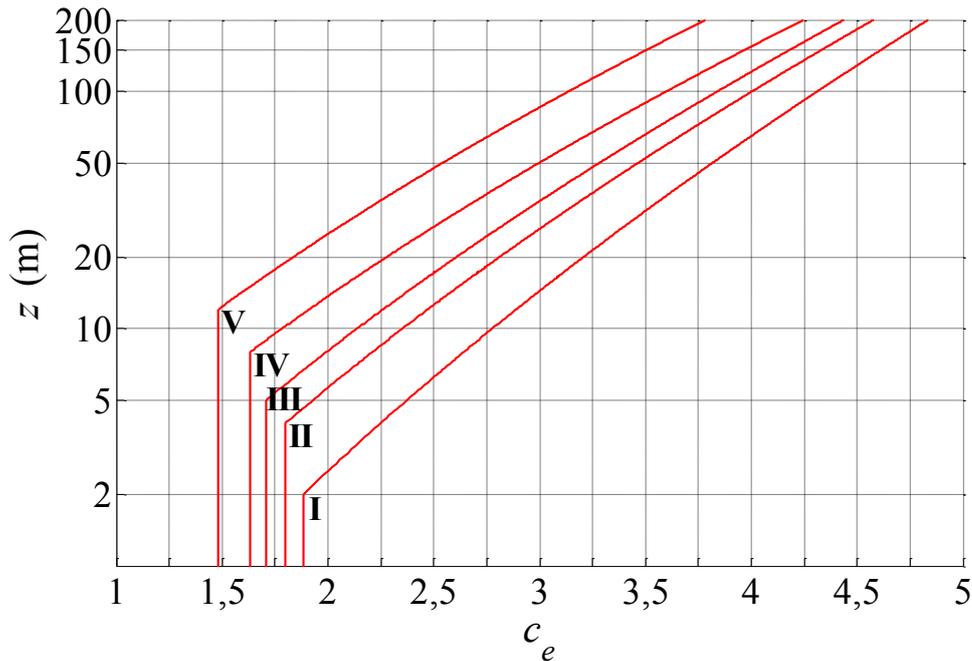
Figure 3.7 – c_e(z) diagrams for various exposure categories where $c_t(z) = 1$.

(3)P   Annex F provides guides for assessing peak wind velocity and explains the relationship that exists between this quantity and peak velocity pressure.

3.3   AERODYNAMIC ACTIONS

(1)P   The wind exerts aerodynamic actions both globally over the whole structure and locally on its components and on non-structural elements. These depend on the shape, size and orientation of the structure and its components with respect to the wind direction. They also depend on wind mean velocity and turbulence. Furthermore, especially in the case of structures and components with rounded surfaces, such actions also depend on the Reynolds number (clause 3.3.7) and surface roughness.

(2)P   As a rule, aerodynamic actions on the entire structure are assessed by assuming the wind directions to be those corresponding to each main axis of the structure considered separately (Figure 3.8). In special cases, like for example square plan towers, the possibility of the wind blowing in the direction of the diagonal also needs to be considered (Figure 3.9). For structures with only one or no axes of symmetry, the wind directions giving rise to the most severe aerodynamic actions and structural effects should be assessed.

(3)P   Local aerodynamic actions on individual structural and non-structural components are assessed by considering from amongst all possible wind directions those which cause the most severe actions. Such actions are often much greater than those applied to individual components in order to assess the global wind action on the structure, particularly near to its edges and corners (Figure 3.10). Under no circumstances should local and overall aerodynamic actions be added together.
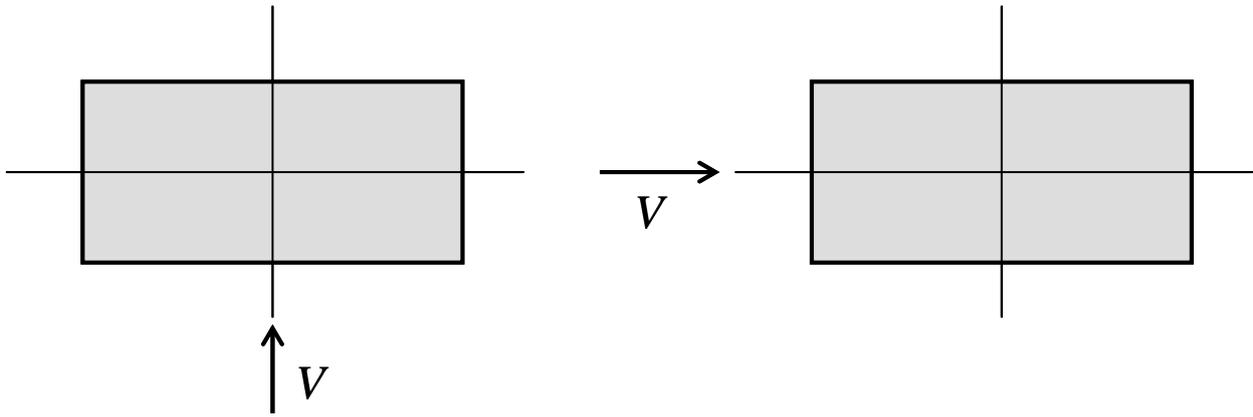
Figure 3.8 – Design wind directions for structures with two axes of symmetry.
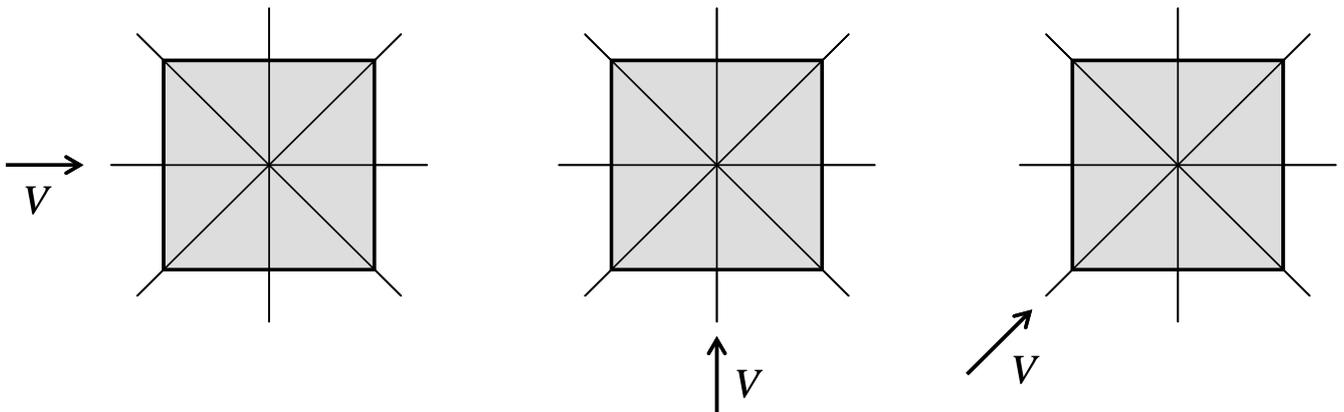
Figure 3.9 – Design wind directions for square plan structures.
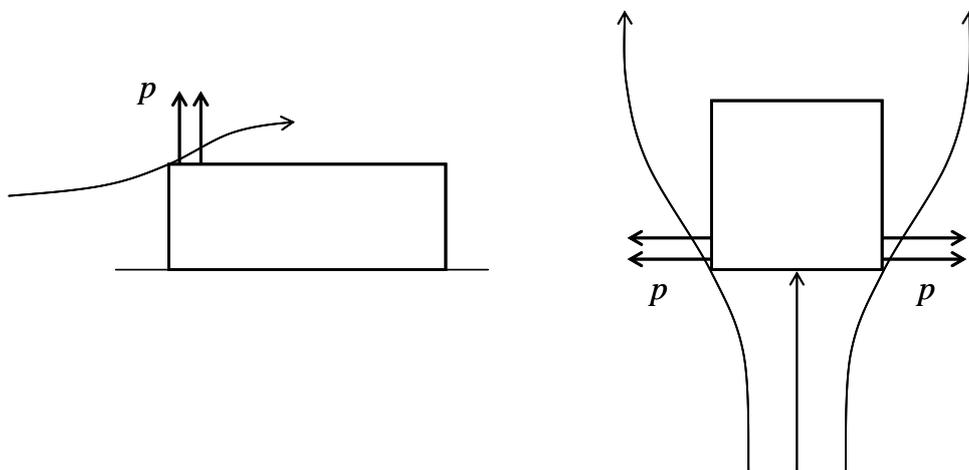
Figure 3.10 – Local wind actions on the structural components.

(4)P   Peak aerodynamic actions on the whole structure or its individual components are defined as the expected values of the maximum 10 minute wind actions, calculated independently of the reduction effects due to partial correlation between maximum local pressure and of the amplification effects associated with structural vibrations (clause 3.4). These are proportional to peak wind velocity pressure q_p (clause 3.2.7) in accordance with specific laws for the following scenarios:

(a)   aerodynamic actions are represented through the wind pressure on each face of the surfaces of a structure or its components (clause 3.3.1), e.g. in the case of buildings and tanks, and generally in the case of structures enclosing an internal volume;

(b)   aerodynamic actions are represented through the net pressure that the wind exerts on the surfaces of the structure and its components; it is the sum of the pressures acting on the opposite faces of the surfaces (clause 3.3.2) and is used, for example, in the case of walls and parapets and generally in the case of structures not enclosing an internal volume;

(c)   aerodynamic actions are represented through the resultant forces and moments that the wind exerts on compact structures or components (clause 3.3.3), e.g. canopies and signboards;

(d)   aerodynamic actions are represented through the forces and moments per unit length that the wind exerts along the axis of slender structures or components (clause 3.3.4), e.g. in the case of chimneys, towers and bridges.

(5)P   It is possible that the same structure can be schematised according to different models, depending on the particular calculations performed. For example, for a chimney, one can fall within case a) when calculating radial actions (Figure 3.11a) and in case d) when calculating overall actions (Figure 3.11b).
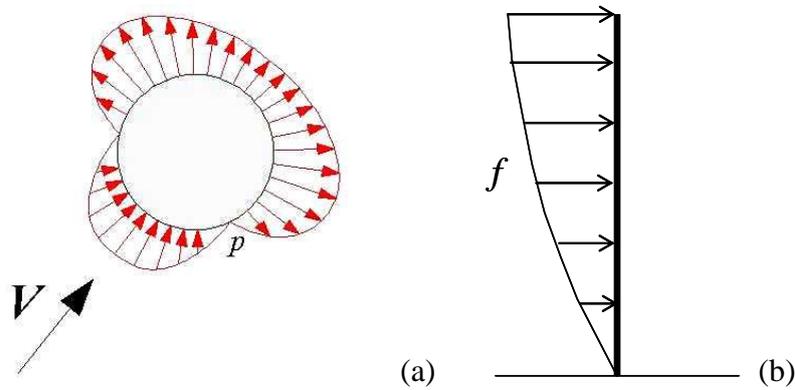
Figure 3.11 – Wind actions on chimneys: (a) local pressure applied radially to the shell; (b) overall forces per unit length applied at the centre line.

(6)P   In the case of structures or components with large surfaces e.g. large industrial buildings and very long walls or parapets, consideration should also be given to the effects of the wind tangential action on the surfaces parallel to the direction of flow (clause 3.3.5).

(7)P   The presence of adjacent structures modifies the oncoming flow and aerodynamic actions that the wind would cause on an isolated structure. Likewise, the presence of adjacent components modifies the oncoming flow and aerodynamic actions that the wind would cause on an isolated component. The actions and effects associated with the interaction between adjacent structures or components causes interference phenomena. Depending on each particular scenario, these can have reducing or increasing effects on the aerodynamic actions on isolated structures or components (clause 3.3.6).

(8)P   For structures with a large or irregular plan, the Designer is responsible for identifying unsymmetrical load scenarios and for taking due account of possible torsional actions (Annex G).

3.3.1 Pressure on each face of a surface

(1)P   The peak aerodynamic actions that the wind exerts on each face of a surface take the form of overpressure and suction p, acting orthogonally on the external and internal faces. By convention, overpressure is considered positive (Figure 3.12a) and suction negative (Figure 3.12b).

(a)   (b)
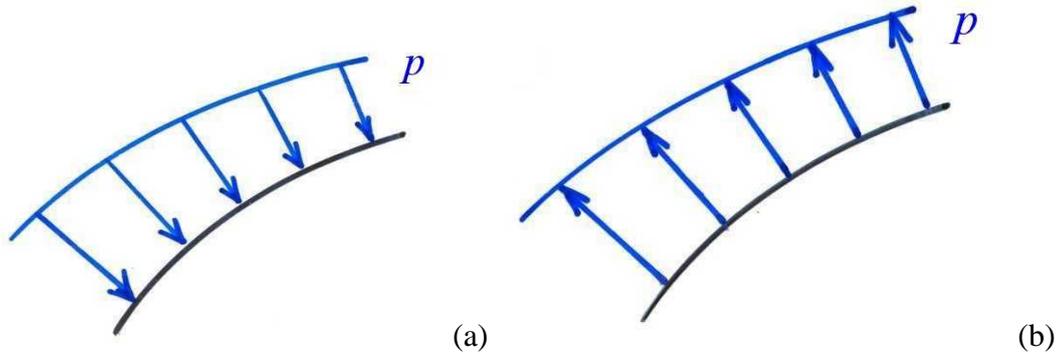
Figure 3.12 – Overpressure (a) and suction (b) on the face of a surface.

(2)   Pressure acting on the external surfaces of a structure is defined external p_e, whilst that acting on the internal surfaces of a structure is defined internal p_i (Figure 3.13). These are given through the expressions:

$$p_e(z) = q_p(\overline{z}_e) \cdot c_{pe} \tag{3.11a}$$

$$p_i(z) = q_p(\overline{z}_i) \cdot c_{pi} \tag{3.11b}$$

where:

q_p is the peak wind velocity pressure (clause 3.2.7);

c_{pe}, c_{pi} are the external and internal pressure coefficients, positive or negative depending on whether corresponding to overpressure (Figure 3.13a) or suction (Figure 3.13b);

$\overline{z}_e, \overline{z}_i$ are the reference heights associated with the definition of c_{pe} and c_{pi}.
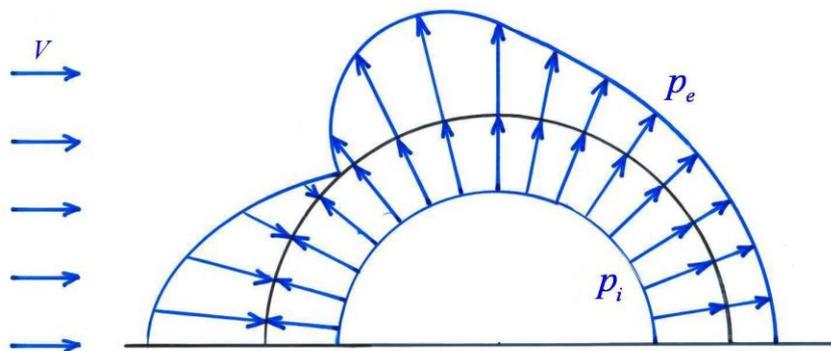
Figure 3.13 – External and internal pressure on the two faces of a surface.

(3)   Wind action on each individual component is determined by considering the worst combination of pressures acting on the two faces of the surface.

(4)P   The external and internal pressure coefficients, c_{pe} and c_{pi}, and the associated reference heights, $\overline{z}_e$ and $\overline{z}_i$, can be obtained from either well documented data or from wind tunnel tests (Annex Q).

(5)P   Annex G contains external and internal pressure coefficients and their corresponding reference heights for regular rectangular-plan buildings and circular-plan structures; these are applicable when assessing overall actions on structures. Annex H contains external pressure coefficients and their corresponding reference heights for irregular buildings; these are applicable when assessing local wind actions on structural and non-structural members, or for the purpose of more accurate global analyses.

3.3.2 Net pressure on a surface

(1)   The peak aerodynamic actions that the wind exerts on the faces of the surfaces of a structure or its components (Figure 3.14a) can be expressed by the net pressure, acting orthogonally on the surfaces (Figure 3.14b). Net pressure is defined as positive or negative according to its direction. It is given by the equation:

$$p_n(z) = q_p(\overline{z}) \cdot c_{pn} \tag{3.12}$$

where:

q_p is the peak wind velocity pressure (clause 3.2.7);

c_{pn} is the net pressure coefficient, positive or negative according to the direction of the resulting pressure acting on the surface;

$\overline{z}$ is the reference height associated with the definition of c_{pn}.
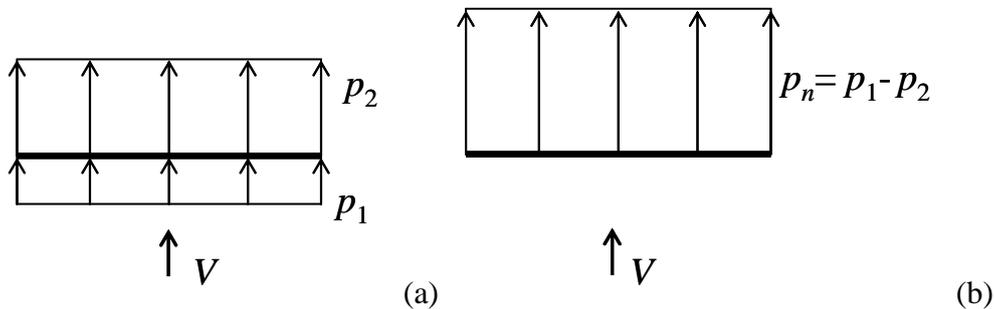
Figure 3.14 – (a) Pressure that the wind exerts on each face of a surface; (b) net pressure on a surface.

(2)P   The net pressure coefficients c_{pn} and the associated reference height $\overline{z}$ can be obtained from either well documented data or from wind tunnel tests (Annex Q).

(3)P   Annex G contains net pressure coefficients and their corresponding reference heights for a variety of structures and components with simple geometry. Annex H contains net pressure coefficients and their corresponding reference heights for canopies with simple geometry.

3.3.3 Global forces and moments

(1)   The peak aerodynamic actions that the wind exerts on compact structures and components can be expressed by a set of three orthogonal forces F_X, F_Y, F_Z and three orthogonal moments M_X, M_Y, M_Z applied at a reference point of the structure or component, in accordance with the scheme illustrated in Figure 3.15. They are given by the expressions:

$$F_X = q_p(\overline{z}) \cdot L^2 \cdot c_{FX} \tag{3.13a}$$

$$F_Y = q_p(\overline{z}) \cdot L^2 \cdot c_{FY} \tag{3.13b}$$

$$F_Z = q_p(\overline{z}) \cdot L^2 \cdot c_{FZ} \tag{3.13c}$$

$$M_X = q_p(\overline{z}) \cdot L^3 \cdot c_{MX} \tag{3.13d}$$

$$M_Y = q_p(\overline{z}) \cdot L^3 \cdot c_{MY} \tag{3.13e}$$

$$M_Z = q_p(\overline{z}) \cdot L^3 \cdot c_{MZ} \tag{3.13f}$$

where:

q_p	is the peak wind velocity pressure (clause 3.2.7);
c_{FX}, c_{FY}, c_{FZ}	are the force coefficients in the three orthogonal directions X, Y, Z;
c_{MX}, c_{MY}, c_{MZ}	are the moment coefficients around the three orthogonal directions X, Y, Z;
$\overline{z}, L$	are the reference height and length associated with the coefficients c_{FX}, c_{FY}, c_{FZ} and c_{MX}, c_{MY}, c_{MZ}.
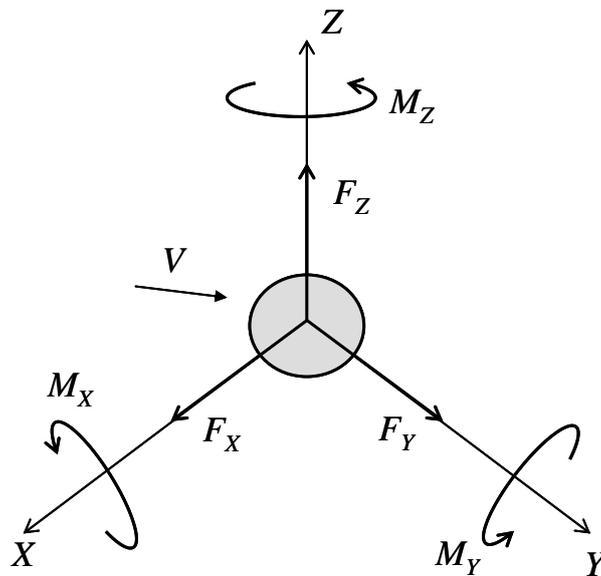
Figure 3.15 – Resulting actions on compact structures and components.

(2)P   The force coefficients c_{FX}, c_{FY}, c_{FZ} and the moment coefficients c_{MX}, c_{MY}, c_{MZ} are defined as positive or negative according to the direction of the force or moment considered in each case.

Their values and respective reference height $\overline{z}$ and length L values can be obtained either from well documented data or from wind tunnel tests (Annex Q).

(3)P   As an alternative to the above method of calculation, the moments (Expressions 3.13d-f) may be represented through the relevant eccentricities of the forces (Expressions 3.13a-c).

(4)P   Annex G contains force and moment coefficients (or equivalent eccentricities) and their corresponding reference height and length values for structures and components with simple geometry.

3.3.4 Forces and moments per unit length

(1)   The peak aerodynamic actions that the wind exerts on slender structures and components can be expressed by a pair of orthogonal forces f_X and f_Y and a torque m_Z per unit length, applied along the reference Z axis of the structure or component in accordance with the scheme illustrated in Figure 3.16. Such forces and moments are conventionally defined as positive or negative according to their direction. They are given by the expressions:

$$f_X(z) = q_p(z) \cdot l \cdot c_{fX} \tag{3.14a}$$

$$f_Y(z) = q_p(z) \cdot l \cdot c_{fY} \tag{3.14b}$$

$$m_Z(z) = q_p(z) \cdot l^2 \cdot c_{mZ} \tag{3.14c}$$

where:
q_p is the peak wind velocity pressure (clause 3.2.7);
z is the height above ground;
c_{fX}, c_{fY}, c_{mZ} are the force coefficients (in accordance with the two orthogonal directions X and Y) and moment coefficient (about the Z axis), conventionally defined as positive or negative according to the direction of the force or moment considered in each case;
l is the reference length associated with the coefficients c_{fX}, c_{fY}, c_{mZ}.
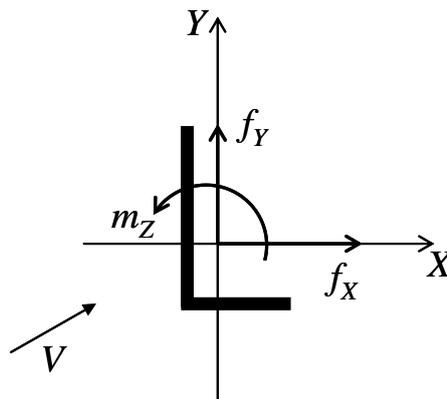
Figure 3.16 – Actions per unit length on slender structures and components.

(2)P   The force and moment coefficients c_{fX}, c_{fY}, c_{mZ} can be obtained either from well documented data or from wind tunnel tests (Annex Q).

(3)P   Annex G contains force and moment coefficients and their corresponding reference lengths for slender structures and components with simple geometry; these apply when the wind blows at right angles to the axis of the structure or component.

(4)P   The assessment of aerodynamic actions on slender structures and components inclined with respect to the the wind direction requires well documented analyses or wind tunnel tests (Annex Q).

3.3.5 Friction action

(1)   The peak friction action per unit area parallel to the wind direction (Figure 17) is given by the equation:

$$w_f(z) = q_p(\overline{z}) \cdot c_f \qquad (3.15)$$

where:

q_p is the peak wind velocity pressure (clause 3.2.7);
c_f is the friction coefficient as a function of surface roughness;
$\overline{z}$ is the reference height associated with the definition of c_f.
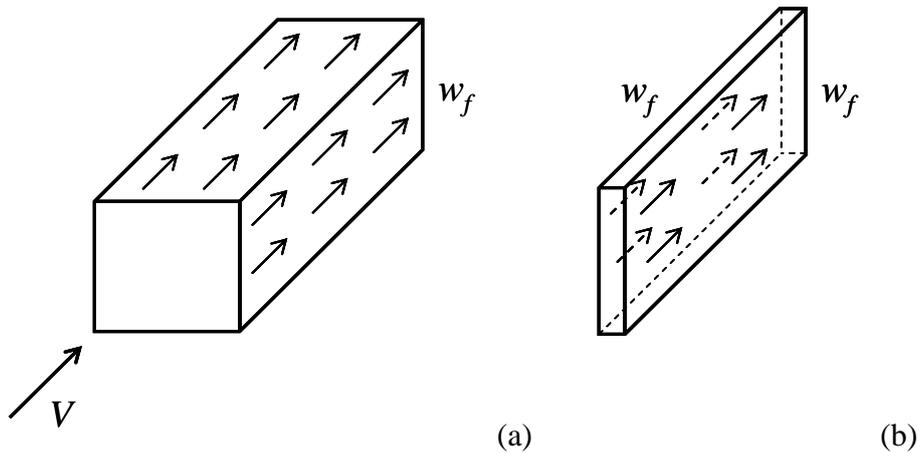
Figure 3.17 – Tangential actions of wind: (a) enclosed structure; (b) individual wall.

(2)P   Friction actions w_f and friction coefficients c_f are conventionally defined as positive if matching the wind direction. They can be obtained either from well documented data or from wind tunnel tests (Annex Q).

(3)P   Annex G contains values of the friction coefficients as a function of the surface roughness, and a criterion for the choice of the reference height.

3.3.6 Interference

(1)P   The term interference is used to describe those phenomena that modify the aerodynamic actions to which an isolated structure or one of its components would be subject if it were isolated. Depending on circumstances, such phenomena may increase or reduce aerodynamic actions.

(2)P   Interference may cause a considerable increase in aerodynamic actions when there are closely-spaced bodies of the same shape or type, e.g. tall buildings emerging from city skylines, tanks, adjacent cooling towers and bridges, grouped chimneys, bundled cables, contiguous structural members, tube bundles. In these cases interference should be considered through well documented data or through assessments based on experimental, numerical or analytical methods.

(3)P   Advantage can be taken of load and response reduction effects arising from interference only if these are accurately assessed. In this case, the Designer is responsible for ensuring that such reduction is not susceptible to changes over the structure nominal life.

3.3.7 Reynolds number

(1)   The Reynolds number Re at height above ground z is given by the equation:

$$Re(z) = \frac{l \cdot v_m(z)}{\upsilon} \tag{3.16}$$

where:
l is a characteristic length of the structure or component considered;
v_m is the mean wind velocity (clause 3.2.5);
υ is the kinematic viscosity of the air. As a rule, in the absence of more accurate estimates of the local site conditions, $\upsilon = 15 \cdot 10^{-6}$ m^2/s.

By expressing l in m and v_m in m/s, Re is a dimensionless quantity.

(2)P   For structures and components with rounded surfaces, Annex G specifies, case by case, the characteristic length l to be used in Equation (3.16).

3.4   DYNAMIC AND AEROELASTIC PHENOMENA

(1)P   The aerodynamic actions defined in clause 3.3 represent the peak values that the wind exerts on the whole structure or on its components.

(2)P   In practice, the lack of full correlation of peak actions gradually reduces overall aerodynamic actions as the size of the loaded surfaces increases. On the other hand, dynamic amplification causes large displacements and stresses when the structure or component is flexible and low damped.

(3)P   Furthermore, turbulent wakes formed downwind from structures and their components, cause mainly across-wind and torsional dynamic actions. These can become particularly severe for tall buildings and slender, lightweight, low damped structures and components subject to alternate vortex shedding in resonance with a vibration mode.

(4)P   In some cases, vibration of highly flexible structures or their components modifies the oncoming flow and aerodynamic actions that the wind would cause it it were fixed. The actions and effects associated with wind-structure interaction give rise to aeroelastic phenomena. Such phenomena, including vortex resonance and the most critical cases of interference, can impair the safety of a structure.

(5)P   Indeed, most structures and their components have sufficiently large stiffness and damping to limit dynamic effects and prevent aeroelastic phenomena. In these cases, wind actions can be represented by equivalent load distributions that when applied statically to the structure or its components produce the maximum displacements and stresses induced by the actual dynamic wind action.

(6)P   Clause 3.4.1 provides guides for assessing equivalent static actions. Clause 3.4.2 deals with the analysis of the dynamic response to wind actions. Clause 3.4.3 describes the dynamic and aeroelastic actions and effects caused by vortex shedding from slender structures and components. Clause 3.4.4 considers other aeroelastic phenomena.

(7)P   Annex I provides assessment criteria for the dynamic parameters of structures.

(8)P   Annex Q provides guides for the analysis of the dynamic behaviour of structures and their components by means of wind tunnel testing.

3.4.1 Equivalent static actions

(1)   Equivalent static actions are defined as those actions that when applied statically to the structure or its components produce displacements and stresses equal to the maximum values induced by the actual dynamic wind action. As a rule, these are given by an equation such as:

$$\text{Equivalent static actions} = \text{Peak aerodynamic actions} \times c_d \qquad (3.17)$$

in which c_d is a non-dimensional parameter called the dynamic factor.

(2)P   For slender, flexible or low damped structures or components, the increase in the dynamic response dominates over the reduction effects due to the partial correlation of peak actions and c_d is generally greater than 1. In this case, the equivalent static actions and/or dynamic factor can be calculated by applying specific well documented theoretical, numerical and/or experimental analyses. In any case, they should also take account of the static and quasi-static part of the response, as well as the contributions associated with all vibration modes likely to cause significant resonance effects.

(3)P   On the other hand, for stiff and/or high damped structures or components, or in the case in which these have large surfaces, the reduction effects due to the partial correlation of peak actions dominates over the increased dynamic response and c_d is generally less than 1. In this case, unless more accurate assessments are carried out, equivalent static actions can be considered equal to peak aerodynamic action, by setting $c_d = 1$ in equation (3.17). Indeed, in these situations, more accurate calculations of the dynamic factor often lead to considerable reductions in design actions.

(4)   In the absence of more accurate, adequately-documented assessments, it is acceptable to take $c_d = 1$ (generally conservative), in the following cases:

- low- to medium-rise civil buildings (less than 40 metres), with regular distribution of stiffness and mass;
- low-rise industrial buildings (less than 20 m) of regular shape, with sufficiently large stiffness (frequency of first vibration mode greater than 1,5 Hz);
- chimneys with circular cross-sections whose height is less than 6 times the diameter and, in any case, less than 50 metres;
- stiff (fundamental frequency of alongwind vibration greater than 2 Hz) and large structures (width of the exposed area exceeding 25 m and height less than 75 m);
- stiff individual structural members and facade support systems (fundamental frequency of alongwind vibration greater than 5 Hz).

(5)P   Annex L contains alongwind equivalent static actions, i.e. parallel to wind direction, for structures and components with specific geometrical and mechanical properties.

(6)P   Annex M contains across-wind and torsional equivalent static actions on rectangular plan buildings. It also provides combination rules for alongwind, across-wind and torsional actions.

3.4.2 Dynamic response analysis

(1)P   Analysis of the dynamic response of structures or their components is an alternative to, or an improvement on the use of equivalent static actions (clause 3.4.1). It can be performed using well documented analytical, numerical and/or experimental methods.

(2)P   Dynamic response analysis can be performed analytically or numerically, based on appropriate models or wind velocity measurements (Annexes C, D, E) that are then transformed either analytically, numerically and/or experimentally into aerodynamic actions. Alternatively, it can be performed analytically or numerically based on appropriate models or measurements of the aerodynamic actions. Dynamic response measurements can also be performed experimentally, in full scale or on a wind tunnel reduced scale model. Use of analytical, numerical and/or experimental procedures requires deep knowledge and experience.

(3)P   Besides alongwind, across-wind and torsional equivalent static actions, Annexes L and M also provide a method for calculating building floor accelerations. Annex N provides guides for using these accelerations for serviceability assessments.

3.4.3 Vortex shedding

(1)P   For slender structures such as chimneys, towers, cables and the chords of lattice structures, account must be taken of the dynamic effects caused by alternate vortex shedding. This produces an almost periodic action perpendicular to the direction of the flow and the axis of the structure or component, whose frequency depends on the mean wind velocity and the section shape and size.

(2)P   When the vortex shedding frequency is close to a natural frequency of vibration, resonance occurs, causing on lightweight and low damped structures or components large amplitude vibrations. Well documented theoretical, numerical and/or experimental analyses must be carried out to ensure safety.

(3)P   Annex O provides guides for the evaluation of actions and effects caused by vortex shedding from slender structures and components. Special attention must be paid to fatigue caused by vortex shedding. Attention must also be paid to interference phenomena associated with adjacent structures or components subject to vortex resonance, especially those of the same shape and size.

(4)P   Where necessary, use is recommended of aerodynamic measures to reduce the regularity of vortex shedding or mechanical devices to mitigate vibrations.

3.4.4 Other aeroelastic phenomena

(1)P   The term "aeroelastic" is used to describe wind-structure interaction phenomena arising when a structure or one of its components has large displacements and/or velocities, such to modify the flow and the aerodynamic actions that the wind would otherwise cause if they were stationary. Lightweight, flexible and low damped structures are prone to such phenomena, e.g. masts, chimneys, lighting columns and towers, cable-supported bridges and footbridges, large roofs and tensile structures, cables and cable structures, individual components of lattice and industrial structures.

(2)P   Generally speaking, the wind action can be represented by superimposing aerodynamic actions (independent of the motion of the structure or its components) and aeroelastic actions (associated with the vibration of the structure or component). These aeroelastic actions depend on the mean wind velocity and modify structural behaviour by modifying its apparent damping and/or stiffness.

(3)P   Leaving aside aeroelastic phenomena due to vortex shedding, dealt with in clause 3.4.3, wind velocities that when reached cause the structure to become unstable are termed "critical". Aeroelastic instabilities associated with a reduction of the total damping (sum of positive structural damping and any negative aerodynamic damping) are termed galloping in the case of across-wind oscillations and torsional flutter in the case of torsional oscillations. The former occurs for non-circular structural members and iced cables or cables with water rivulets, while the latter case is characteristic of suspension and cable-stayed bridge decks. (Torsional) divergence is a static

aeroelastic instability associated with a reduction of the total (torsional) stiffness (sum of positive structural stiffness and any negative aerodynamic stiffness); it is typical of bridge decks and flat plates. Flutter is a dynamic aeroelastic instability associated with a simultaneous modification of the total damping and stiffness; it is typical of suspension and cable-stayed bridge decks and wing sections. The term "aeroelastic interference" describes wind-structure interaction phenomena involving closely spaced bodies; it occurs to grouped chimneys, closely-spaced slender elements, bundled cables, decks of adjacent cable-supported bridges. The above-mentioned phenomena must be studied using well documented experimental, numerical and/or analytical methods.

(4)P   Apart from those associated with vortex shedding (clause 3.4.3), all critical velocities of the structure and its components associated with aeroelastic instability phenomena must be sufficiently larger than the wind design velocity.

(5)P   Annex P provides guides for analysing the main aeroelastic phenomena.

Annex A DESIGN RETURN PERIOD

For well maintained constructions, the nominal lifetime V_N is defined as the time span over which it shall be possible to use the construction for its intended purpose.

Every analysis recommended herein depends on the design reference wind velocity v_r as a function of the design return period T_R in accordance with the criteria given in subclause 3.2.2. The choice of the design return period therefore plays an essential role in assessing wind actions and effects on structures. Such choice depends on the type of analysis performed, on the properties and the nominal lifetime of the construction.

The reference return period is defined as the greater between the conventional return period T_0 given in Table A.I and the nominal lifetime of the construction V_N:

$$T_{R,0} = \max\{T_0, V_N\} \tag{A.1}$$

Table A.I – Conventional return period T_0 .

Properties of the structure	T_0 (years)
Temporary constructionss, structures under construction or being demolished, provided this condition lasts for less than 1 year. For temporary structures, the overall length of all periods in which the structure is reused shall be less than a year	10
Standard constructions	50
Large important constructions	100
Strategic constructions	200

Where not specified herein, or when neither specific standards exist nor, well documented rules apply, it is recommended that the design return period T_R be equal to the reference return period $T_{R,0}$ given by Eq. (A.1), therefore $T_R = T_{R,0}$.

In two specific cases, these Guides recommend the use of design return period T_R values different from the reference return period $T_{R,0}$:

- for building serviceability assessments, Annex N recommends determining peak acceleration for a design return period $T_R = 1$ year;
- for assessing the behaviour of structures and their elements due to vortex shedding and other aeroelastic phenomena, Annexes O and P recommend determining mean wind velocity for a design return period $T_R = 10 T_{R,0}$.

The Consultant and/or the Client are responsible for identifying those situations to which larger design return periods than those specified above should be applied.

Solely in the case of non-structural elements, lower design return periods than those specified above may be implemented, provided such choice does not conflict with other specific regulations, is well justified and specifically declared at the design and/or verification stage, and when failure of the elements would not place structural and/or personal safety at risk.

ANNEX B REFERENCE WIND VELOCITY

The criterion shown in 3.2.1 and 3.2.2 for determining reference wind velocity provides reasonably accurate, often conservative, values, consistent with the level of accuracy usually achieved in standard design analyses. Clause B.1 provides guides on performing a detailed probabilistic analysis. B.2 explains the assumptions and simplifications upon which the simplified method proposed herein is based.

B.1   Detailed method

In principle, accurate calculation of the reference velocity goes through the following three steps:

(a)   acquisition, verification and correction of wind mean speed and direction measurements that characterise the construction site (clause B.1.1);

(b)   transformation of measured data to values consistent with the definition of reference wind velocity (clause B.1.2);

(c)   probabilistic analysis of transformed data.

In all cases, application of the procedure above requires specific knowledge in this field (clause B.1.3).

B.1.1   Acquisition, verification and correction of wind measurements

Reference velocity analysis requires meteorological stations representative of the construction site to be located and acquisition of the respective wind mean speed and direction measurements.

In order for the data measured by a meteorological station to be representative of the construction site, the station should be suitably located, the acquisition period sufficiently long and the collected data uniform and free from errors that could affect the validity of subsequent probabilistic analysis.

The location of a station is suitable provided it is not too far from the construction site (no more than 50-100 km), wind regimes at the station are comparable to those of the construction site (e.g. site and station are not separated by mountain ranges), instruments are correctly installed (e.g. positioned at a height above ground of not less than approx. 10 m and away from bodies that disturb the wind, including those on which the instruments are placed).

The duration of the data acquisition period is commensurate with both the return period at which the reference velocity is to be determined and the probabilistic methods applied for the analysis. In any event, data should be used from stations with long sets of historical records.

Reliable probabilistic analysis requires the use of data that is both uniform (e.g. mean values over the same time interval) and correct (i.e. free from systematic or random errors that could affect the validity of the analysis). When studying extreme winds, verification, correction or deletion of incorrect data regarding the most severe winds is essential. Data smoothing and correction requires the use of reliable and well documented procedures.

B.1.2   Transformation of measured data to reference conditions

The design reference velocity is the maximum 10 minute mean wind velocity at a height of 10 m above flat open country terrain with roughness length $z_0 = 0,05$ m (exposure category II, clause 3.2.3), for design return period T_R. In order to calculate this value it is therefore necessary to transform measured data to values consistent with reference wind conditions.

For this transformation, with mean velocity value measured by the station being known, it is necessary to determine for each wind direction the mean value that would be measured if the anemometer were placed at a height of 10 m above flat open country terrain with roughness length

$z_0 = 0,05$ m. This transformation operation requires the use of wind modelling procedures as described in clause C.1.

B.1.3 Probabilistic analysis of transformed data

Probabilistic analysis of transformed data at each selected meteorological station is aimed at determining the distribution of the maximum annual mean wind velocity, applying well documented procedures, and subsequent derivation of the mean velocity associated with the design return period T_R. Analysis should be performed using databases comprising a number of years at least 1/5 larger than the design return period and in any case longer than 5 years. Analysis based on shorter measurement periods is only possible if well documented statistical methods are applied.

When calculated using data from several weather stations, the reference wind velocity at the construction site may be obtained by applying suitable weight factors (for example related to the distance of the stations from the construction site, to the length of historical records and to the quality of the measurements) to the estimates for each individual station.

It is possible to determine reference velocity as a function of wind direction, applying well documented procedures, provided that the overall risk associated with directional analysis does not exceed the risk arising from a non-directional analysis.

B.2 Simplified method

The reference velocities given in clause 3.2.1 have been obtained by applying the procedure described in clause B.1 to sixtynine meteorological stations uniformly distributed over the Italian country.

The law given in clause 3.2.2 for transforming reference wind velocity (clause 3.2.1) to design reference velocity, has also been based on analyses carried out at numerous national meteorological stations, and it usually results in conservative values.

Annex C   WIND VELOCITY

The criterion utilised herein for determining mean wind velocity (clause 3.2.5), turbulence intensity (3.2.6) and peak velocity pressure (3.2.7) is based on a simplified procedure adopted by international standards, that has been adapted to the Italian orography and wind climate; it provides values consistent with the level of accuracy of standard design analyses. Clause C.1 provides guides on detailed wind models. C.2 explains the assumptions and simplifications upon which the simplified method proposed herein is based.

C.1   Detailed method

The wind characteristics at the construction site may be determined using well documented experimental (clause C.1.1), numerical or analytical (C.1.2) methods.

C.1.1 Experimental assessments

Experimental determination of wind at the construction site can be performed by means of full-scale measurements or wind tunnel testing.

Experimental full-scale measurements require the use of instruments of well documented quality. The acquisition time step should be chosen based on the properties of the data requested. Instruments should be placed in positions that well characterise the oncoming wind, therefore neither disturbed by neighbouring bodies, nor by the instrument supports. The spatial distribution of the instruments has to be related to the geometry and mechanical properties of the construction. Measurements should be carried out over time periods of sufficient length to allow suitable probabilistic interpretations of the data for all wind directions.

Measurements on wind tunnel topographic models (Annex Q) should be carried out at laboratories with a specific know-how. They should be performed by using appropriate geometric and time scales. The geometric scale should be small enough to allow the correct reproduction of an area large enough to properly reproduce the actual wind circulation; at the same time, it should be large enough to allow suitable simulation of the local wind at the site of interest.

C.1.2 Numerical and analytical assessments

Numerical and analytical assessment of the wind at the site of interest depends on three main factors: 1) terrain roughness and topography surrounding the site; 2) thermal conditions of the atmosphere; 3) wind climate of the site.

Roughness modelling requires the building of a model reflecting the roughness length of the terrain surrounding the construction. The accuracy of the model should increase in the proximity of the construction. The taller the construction, the larger the size of the model. The model may be built by utilising visual inspections, photographic records, soil cover data (converted to roughness lengths), cartographic surveys and satellite pictures. Figures C.1-C.5 show descriptions of areas with different roughness lengths z_0 (not necessarily corresponding with each other from a geographical viewpoint), through photographic records (a), satellite pictures (b) and cartographic surveys (c)

(a)

(b)
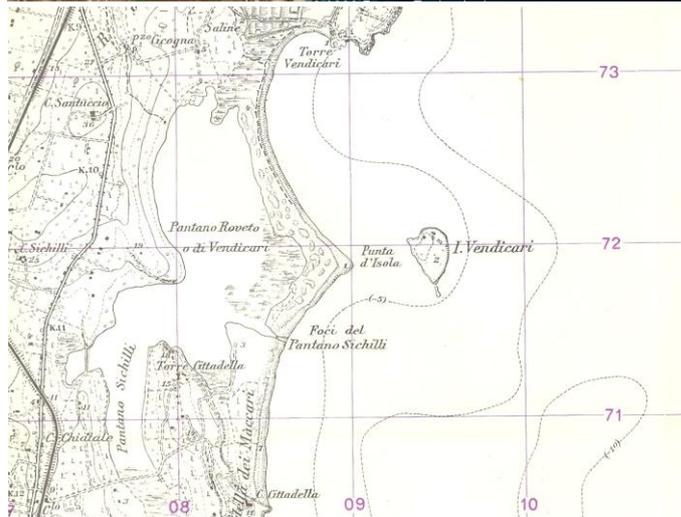
(c)

Figure C.1 – Coastal area ($z_0 \approx 0,01$m).

(a)

(b)

(c)

Figure C.2 – Open country with isolated obstacles ($z_0 \approx 0,05$ m).

(a)

(b)

(c)

Figure C.3 – Countryside with closely-spaced obstacles ($z_0 \approx 0{,}1$ m).

(a)

(b)

(c)
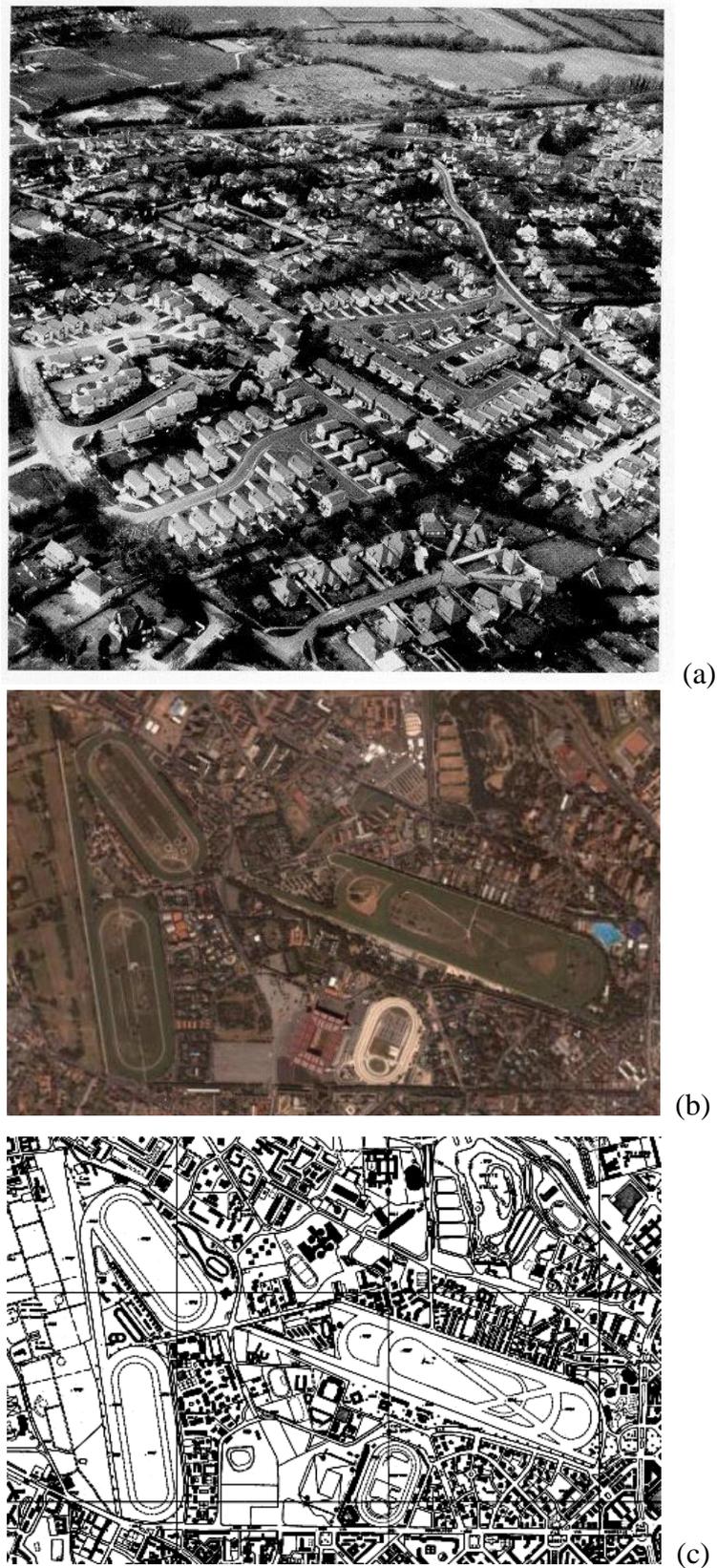
Figure C.4 – Suburban area ($z_0 \approx 0{,}3$ m).

(a)

(b)

(c)
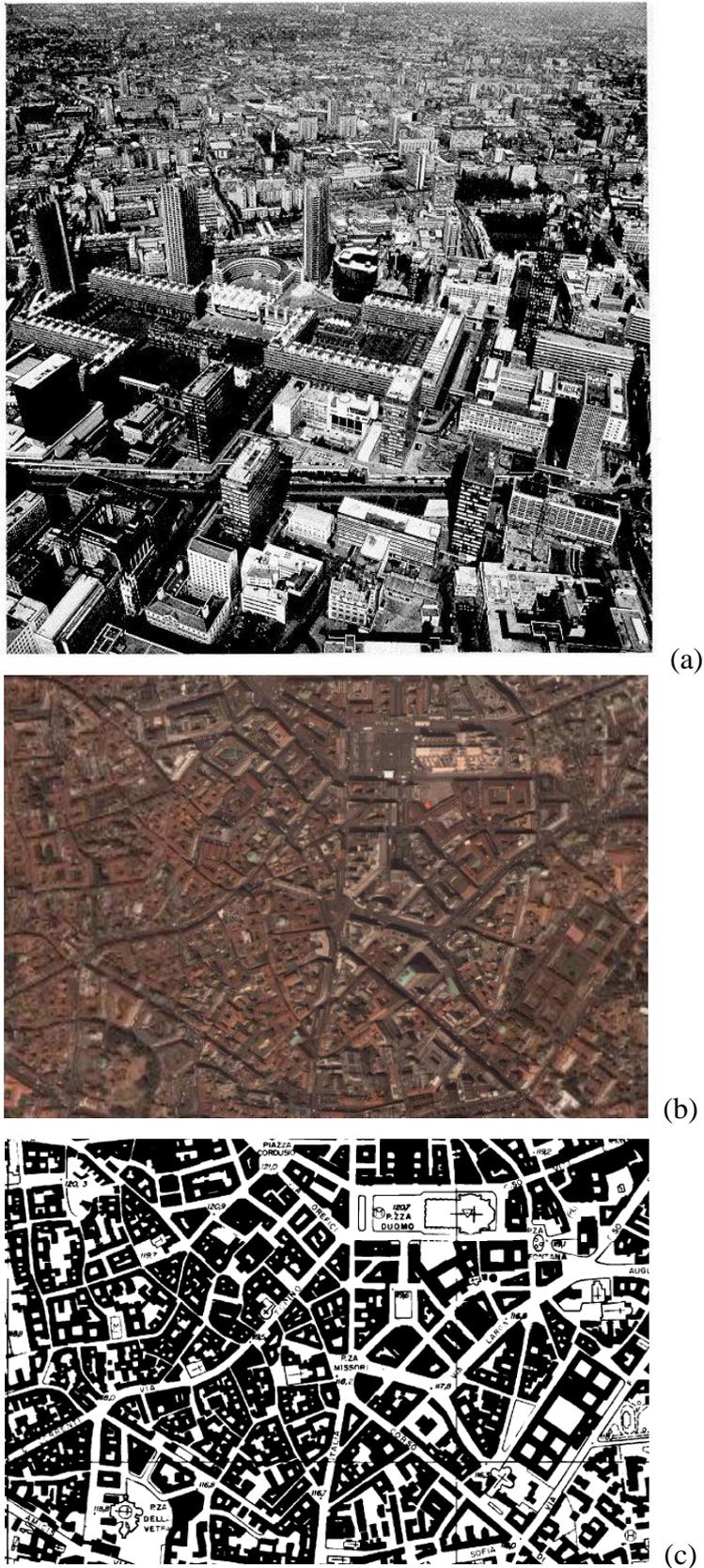
Figure C.5 – Urban area ($z_0 \approx 0{,}7$ m).

Topography modelling requires the building of a model that considers the height of the ground surrounding the construction. The model accuracy should be increased in the proximity of the

construction. The size of the model should be large enough to include the area that influences the local circulation at the site of interest. The model may be built by utilising contour data.

If the area surrounding the construction is flat or only moderately hilly, well documented software or analytical methods may be used that take only terrain roughness into account. In this case, the effects of roughness variations (transitions) for each wind direction must be accounted for.

Should the area surrounding the construction have a complex orograpy, then the determination of the local wind circulation may only be carried out analytically, for each direction of incidence, for two-dimensional, isolated features (hills, ridges, etc.) of simple shape (Annex D). In all other cases it is usually necessary to use well documented softwares that take terrain roughness and topography into account. For areas with moderate slopes it is possible to use codes based on mass conservation equations or linearised Navier-Stokes equations solvers; as a rule, both these approaches only provide the mean wind velocity field. For large terrain slopes the use is recommended of codes based on complete Navier-Stokes equations (CFD codes). In any event, expert advice should be sought when using computational tools.

As regards the atmosphere's thermal conditions, analysis of the wind configuration at the construction site will usually assume a neutral climate, i.e. taking the wind velocity to be independent from the atmosphere's thermal conditions. This assumption is reasonably correct when the mean wind velocity at a height above the ground of 10 m is greater than approx. 10 m/s; this condition is nearly always satisfied for ultimate and serviceability limit state analysis. However, mean wind velocities of less than approx. 10 m/s may assume great importance due to the occurrence of vibrations induced by vortex shedding from slender structures (Annex O); in this case, the creation of low levels of turbulence associated with stable atmospheric regimes may actually cause worse situations than those associated with neutral regimes. Likewise, lower mean wind velocity values can greatly affect structural fatigue characteristics; in this case, the occurrence of stable or unstable atmospheric regimes may actually cause worse situations than those associated with neutral regimes.

Finally, as regards the properties of the weather phenomenon under consideration, it is usually accepted that design wind velocity is established during cyclonic events characteristic of Italian territory: these develop over very wide areas (of around several hundred km) and long periods (at least one or two days). The most popular calculation models are generally based on this assumption. The analysis of wind configuration associated with other weather phenomena, e.g. whirlwinds, thunderstorm winds and downbursts, föhn and bora, requires specific well documented calculations.

C.2 Simplified method

The calculation methods introduced herein for determining mean wind velocity (clause 3.2.5), turbulence intensity (3.2.6) and peak velocity pressure (3.2.7) represents a simplification of the detailed procedure illustrated in clause C.1. This simplification is based on the following assumptions:

- the wind climate which the design wind velocity is associated with is that of extratropical cyclones that develop over very wide areas (of around several hundred km) and long periods (at least one or two days);

- the wind velocity is high, therefore the atmosphere is neutrally stratified and it is independent of temperature;

- the site of interest is flat or includes one isolated topographic feature of simple shape (Annex D). Terrain roughness is uniform in all directions.

Under these circumstances, mean wind velocity (clause 3.2.5), turbulence intensity (3.2.6) and peak velocity pressure (3.2.7) are expressed as a function of the five exposure categories specified in 3.2.3.

The criterion provided in clause 3.2.3 for the choice of the appropriate exposure category is strictly related to the morphology of the Italian territory and specifically considers terrain roughness, geographical area, distance from the coast and altitude above sea level; it also takes the direction of the most severe winds into account.

Annex D   OROGRAPHY COEFFICIENT

This annex applies to isolated topographic features of simple shape.

In the lack of specific detailed assessments, the orography factor c_t, a function of height above ground z, can be calculated using the methods described in clauses D.1- D.3. Clause D.1 shows a detailed calculation method whose parameters are provided through; in clause D.2 analytical expressions are given for these parameters; clause D.3 describes a simplified method, based on the detailed method provided in D.1 and D.2, that usually produces more conservative estimates than the previous ones. Conservatively, all methods proposed assume that the wind direction is perpendicular to the crest of the hill, ridge, cliff or escarpment.

D.1   Detailed method

The orography coefficient for isolated cliffs and escarpments (Figure D.1) and for hills and ridges (Figure D.2) is given by the equations:

$$c_t = 1 \qquad \text{for } \Phi \leq 0,05 \qquad (D.1a)$$

$$c_t = 1 + 2 \cdot s \cdot \Phi \qquad \text{for } 0,05 < \Phi < 0,3 \qquad (D.1b)$$

$$c_t = 1 + 0,6 \cdot s \qquad \text{for } \Phi \geq 0,3 \qquad (D.1c)$$

where:

s is the topographic location factor given by Figure D.1, for cliffs and escarpments, and Figure D.2, for hills and ridges, as a function of the x and z coordinates; alternatively, it is given by the equations provided in clause D.2;

Φ $= H/L_u$, is the mean upwind slope of the relief;

H is the height of the relief;;

L_u is the (horizontal) upwind length of the relief;;

L_e is the effective (horizontal) upwind length of the relief;:

                  $L_e = L_u$ for $\Phi \leq 0,3$;

                  $L_e = H/0,3$ for $\Phi > 0,3$;

L_d is the (horizontal) downwind length of the hill or ridge;

x is the (horizontal) distance of the site from the crest of the relief;;

z is the height above ground.
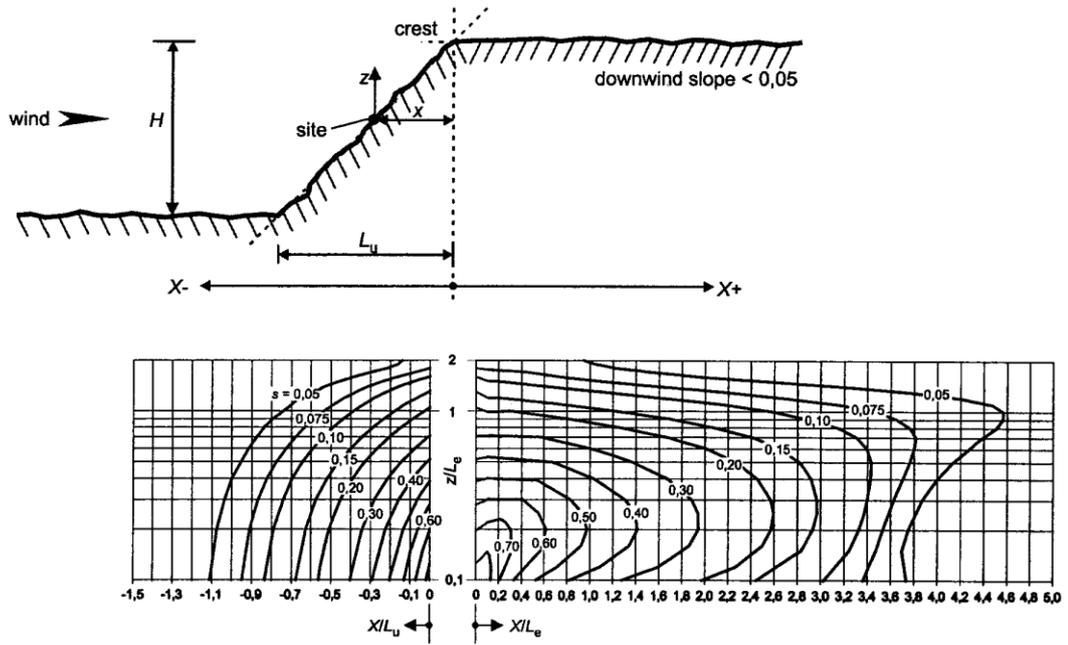
Figure D.1 - Topographic location factor *s* for isolated cliffs and escarpments.
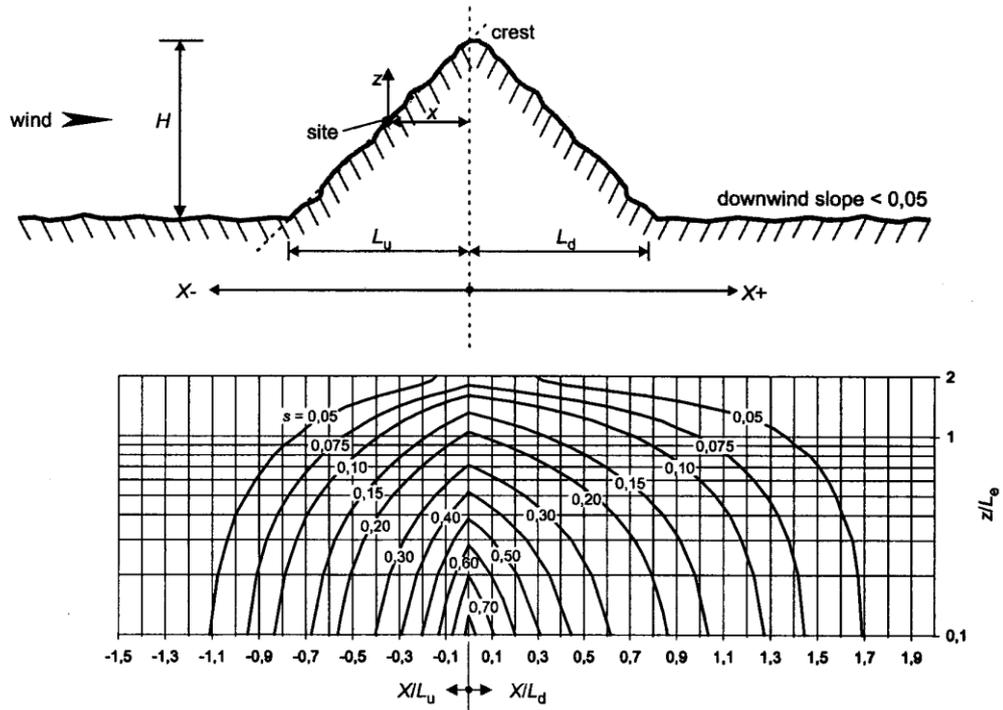
Figure D.2 - Topographic location factor *s* for isolated hills and ridges.

D.2 Topographic location factor equations

As an alternative to the diagrams provided by Figures D.1 and D.2, the topographic location factor s can be calculated by applying the equations set out hereafter. More specifically, clause D.2.1 gives equations for upwind slopes of hills, ridges, cliffs or escarpments.; clauses D.2.2 and D.2.3 give equations for downwind slopes of hills and ridges, respectively. The use of these equations must be restricted to the ranges where they are defined; extrapolation is not possible.

D.2.1 Upwind slope of of hills, ridges, cliffs and escarpments

For $-1,5 \leq x / L_u \leq 0$ and $0 \leq z / L_e \leq 2,0$, the topographic location factor s is given by the equation:

$$s = A \cdot \exp \left(B \cdot \frac{x}{L_u} \right) \tag{D.2}$$

where:

$$A = 0,1552 \cdot \left(\frac{z}{L_e} \right)^4 - 0,8575 \cdot \left(\frac{z}{L_e} \right)^3 - 1,8133 \cdot \left(\frac{z}{L_e} \right)^2 - 1,9115 \cdot \left(\frac{z}{L_e} \right) + 1,0124 \tag{D.3a}$$

$$B = 0,3542 \cdot \left(\frac{z}{L_e} \right)^2 - 1,0577 \cdot \left(\frac{z}{L_e} \right) + 2,6456 \tag{D.3b}$$

For $x / L_u < -1,5$ or $z / L_e > 2$, $s = 0$ has to be assumed.

D.2.2 Downwind slope of cliffs and escarpments

For $0,1 \leq x / L_u \leq 3,5$ and $0,1 \leq z / L_e \leq 2,0$, the topographic location factor s is given by the equation:

$$s = A \cdot \left[\log \left(\frac{x}{L_e} \right) \right]^2 + B \cdot \left[\log \left(\frac{x}{L_e} \right) \right] + C \tag{D.4}$$

where:

$$A = 1,3420 \cdot \left[\log \left(\frac{z}{L_e} \right) \right]^3 - 0,8222 \cdot \left[\log \left(\frac{z}{L_e} \right) \right]^2 + 0,4609 \cdot \log \left(\frac{z}{L_e} \right) - 0,0791 \tag{D.5a}$$

$$B = -1.0196 \cdot \left[\log \left(\frac{z}{L_e} \right) \right]^3 - 0,8910 \cdot \left[\log \left(\frac{z}{L_e} \right) \right]^2 + 0,5343 \cdot \log \left(\frac{z}{L_e} \right) - 0,1156 \tag{D.5b}$$

$$C = 0.8030 \cdot \left[\log \left(\frac{z}{L_e} \right) \right]^3 + 0.4236 \cdot \left[\log \left(\frac{z}{L_e} \right) \right]^2 - 0.5738 \cdot \log \left(\frac{z}{L_e} \right) + 0,1606 \tag{D.5c}$$

For $0 \leq x / L_e \leq 0,1$, the topographic location factor s may be obtained by linear interpolation between the values obtained for $x / L_e = 0$ and $x / L_e = 0,1$.

For $z / L_e < 0,1$, the topographic location factor s takes the value obtained for $z / L_e = 0,1$.

For $x / L_d > 3,5$ or $z / L_e > 2,0$, $s = 0$ has to be assumed.

D.2.3 Downwind slope of hills and ridges

For $0 \leq z / L_d \leq 2,0$ and $0 \leq z / L_e \leq 2,0$, the topographic location factor s is given by the equation:

$$s = A \cdot \exp\left(B \cdot \frac{x}{L_d} \right) \tag{D.6}$$

where:

$$A = 0,1552 \cdot \left(\frac{z}{L_e} \right)^4 - 0,8575 \cdot \left(\frac{z}{L_e} \right)^3 + 1,8133 \cdot \left(\frac{z}{L_e} \right)^2 - 1,9115 \cdot \left(\frac{z}{L_e} \right) + 1,0124 \tag{D.7a}$$

$$B = -0,3056 \cdot \left(\frac{z}{L_e} \right)^2 + 1,0212 \cdot \left(\frac{z}{L_e} \right) - 1,7637 \tag{D.7b}$$

For $x / L_d > 2,0$ or $z / L_e > 2,0$, $s = 0$ has to be assumed.

D.3 Simplified method

For sites on top of isolated cliffs or escarpments (Figure D.1), the orography coefficient is given by the equation:

$$c_t = 1 + \beta \cdot \gamma \cdot \left(1 - 0,1 \cdot \frac{x}{H}\right) \geq 1 \qquad (D.8)$$

For sites on upwind slopes of isolated cliffs or escarpmements, (Figure D.1) and of isolated hills or ridges (Figure D.2), the oroography coefficient is given by the equation:

$$c_t = 1 + \beta \cdot \gamma \cdot \left(1 - \frac{x}{L_u}\right) \geq 1 \qquad (D.9)$$

The parameters used in equations (D.8) and (D.9) have the following meanings:

H is the height of the feature;
L_u is the (horizontal) upwind length of the feature;
β is a coefficient defined as a function of height z above ground (Figure D.3):

$$\beta = 0,5 \qquad \text{for } \frac{z}{H} \leq 0,75 \qquad (D.10a)$$

$$\beta = 0,8 - 0,4 \cdot \frac{z}{H} \qquad \text{for } 0,75 < \frac{z}{H} \leq 2 \qquad (D.10b)$$

$$\beta = 0 \qquad \text{for } \frac{z}{H} > 2 \qquad (D.10c)$$

γ is a coefficient defined as a function of the ratio $\Phi = H/L_u$ (Figure D.3):

$$\gamma = 0 \qquad \text{for } \Phi \leq 0,10 \qquad (D.11a)$$

$$\gamma = 5\left(\Phi - 0,10\right) \qquad \text{for } 0,10 < \Phi \leq 0,30 \qquad (D.11b)$$

$$\gamma = 1 \qquad \text{for } \Phi > 0,30 \qquad (D.11c)$$

x is the (horizontal) distance of the site from the crest of the feature;
z is the height above ground.

Annex E   ATMOSPHERIC TURBULENCE

The instantaneous wind speed fluctuates randomly in time and space, causing dynamic actions and effects on structures. Clauses E.1 and E.2 provide some information regarding the spectral properties of turbulence in neutral atmospheric conditions, respectively, at one and two points in space (Annex C), which apply to heights above the ground not exceeding $z = 200$ m. Clause E.3 provides guides on Monte Carlo turbulence simulation and the use of this technique in time history dynamic analysis of structures (clause 3.4.2).

E.1   Single-point spectral modelling of turbulence

Atmospheric turbulence at a point M is described as a vector whose three components are called, respectively, longitudinal (v_1', horizontal, in the x-direction of the mean wind velocity), lateral (v_2', horizontal, in the y-direction perpendicular to the mean wind velocity) and vertical (v_3', in the vertical z-direction) (Figure E.1). Each turbulent component is usually described by a zero-mean stationary Gaussian random process, given through its power spectrum. As a first approximation, it can be assumed that the three turbulent components are not correlated (in practice, this assumption is not true for the along-wind and the crosswind turbulent component).
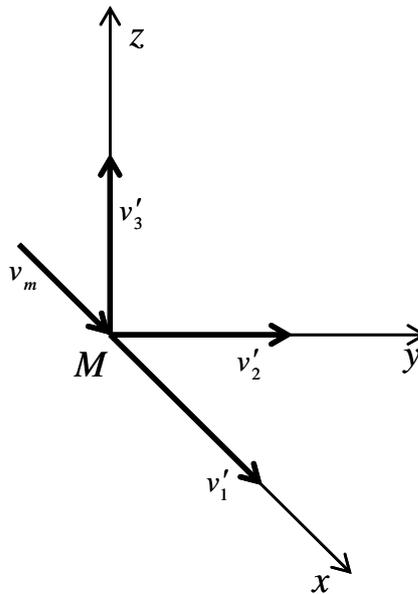
Figure E.1 - Instantaneous wind speed.

In the lack of specific analyses, alongwind, crosswind and vertical turbulence power spectra, S_1, S_2, S_3 (normalised so that the variance is the integral of the power spectrum as frequency n varies from zero to infinity), are given by the equations:

$$\frac{n \cdot S_1(z,n)}{\sigma_1^2(z)} = \frac{n \cdot S_1(z,n)}{I_1^2(z) \cdot v_m^2(z)} = \frac{6,868 \cdot n \cdot L_1(z) / v_m(z)}{\left[1 + 10,302 \cdot n \cdot L_1(z) / v_m(z)\right]^{5/3}} \tag{E.1a}$$

$$\frac{n \cdot S_2(z,n)}{\sigma_2^2(z)} = \frac{n \cdot S_2(z,n)}{I_2^2(z) \cdot v_m^2(z)} = \frac{9,434 \cdot n \cdot L_2(z) / v_m(z)}{\left[1 + 14,151 \cdot n \cdot L_2(z) / v_m(z)\right]^{5/3}} \tag{E.1b}$$

$$\frac{n \cdot S_3(z,n)}{\sigma_3^2(z)} = \frac{n \cdot S_3(z,n)}{I_3^2(z) \cdot v_m^2(z)} = \frac{6,103 \cdot n \cdot L_3(z) / v_m(z)}{1 + 63,181 \cdot \left[n \cdot L_3(z) / v_m(z)\right]^{5/3}} \tag{E.1c}$$

where:

v_m is the mean wind velocity, specified in clause 3.2.5 or calculated by means of specific analyses, e.g. those described in Annex C;

σ_1, σ_2, σ_3 are the standard deviations of longitudinal, lateral and vertical turbulence;

I_1, I_2, I_3 are the longitudinal, lateral and vertical turbulence intensities, defined as the standard deviations of turbulence σ_1, σ_2, σ_3 divided by the mean wind velocity v_m;

L_1, L_2, L_3 are the integral length scales in the direction of the mean wind velocity of the longitudinal, lateral and vertical turbulence

In the lack of specific analyses, the standard deviations of the longitudinal, lateral and vertical turbulent components are given by the equations:

$$\sigma_1(z) = v_r \cdot k_r \tag{E.2a}$$

$$\sigma_2(z) = 0,75 \cdot v_r \cdot k_r \tag{E.2b}$$

$$\sigma_3(z) = 0,50 \cdot v_r \cdot k_r \tag{E.2c}$$

where:

v_r is the design reference velocity (clause 3.2.2);

k_r is the terrain factor (clause 3.2.3).

In accordance with Eq. (E.2), in the lack of specific analyses, the intensities of the longitudinal, lateral and vertical turbulent components are given by the equations:

$$I_1(z) = I_v(z) \tag{E.3a}$$

$$I_2(z) = 0,75 \cdot I_v(z) \tag{E.3b}$$

$$I_3(z) = 0,50 \cdot I_v(z) \tag{E.3c}$$

where I_v is the turbulence intensity specified by clause 3.2.6.

Turbulence integral length scales represent the average gust size in the wind direction for each of the three turbulent components. In the lack of specific analyses, they are given by the equations:

$$L_1(z) = L_v(z) \tag{E.4a}$$

$$L_2(z) = 0.25 \cdot L_v(z) \tag{E.4b}$$

$$L_3(z) = 0.10 \cdot L_v(z) \tag{E.4c}$$

where L_v is the turbulent length scale specified by clause 3.2.6.

Figure E.2 shows longitudinal, lateral and vertical turbulence spectra obtained through Eqs. (E.1) through (E.4). Spectral values are normalised using variance σ_1^2 for the three turbulent components.
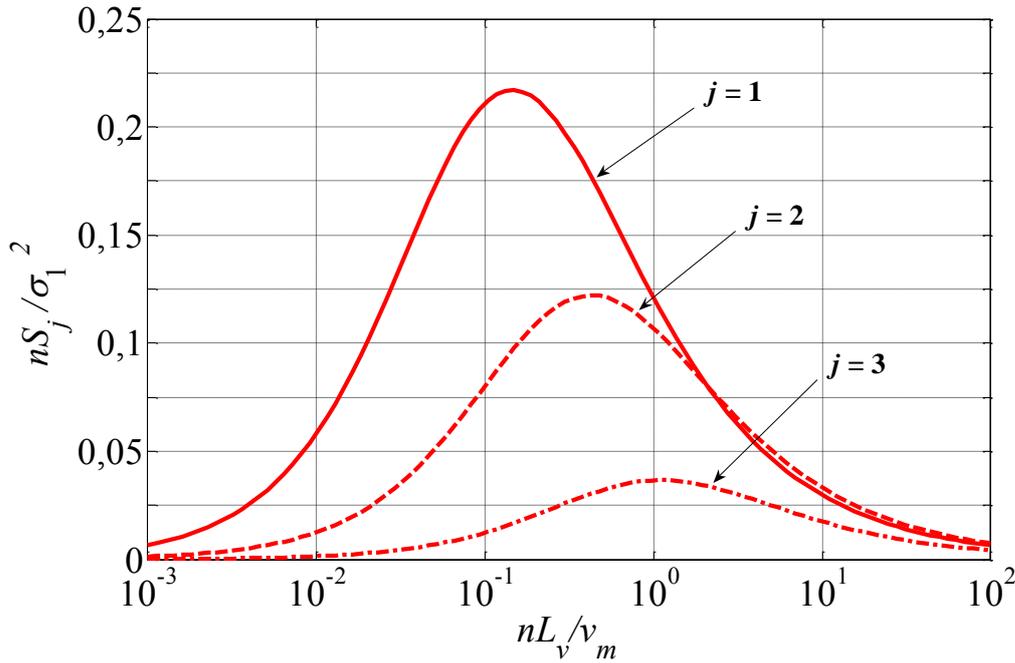
Figure E.2 – Turbulence spectra.

E.2 Two-point spectral modelling of turbulence

Cross-spectral properties of the atmospheric turbulence are usually described through the power spectra of the individual turbulent components (clause E.1) and a coherence function.

In the lack of specific analyses, the coherence functions of longitudinal, lateral and vertical turbulence (defined as the ratio of the cross-power spectrum and the square root of the product of the local power spectra), are given by the equation:

$$Coh_{jj}(M, M', n) = \exp\left\{-\frac{2 \cdot n \cdot \sqrt{C_{jx}^2 \cdot |x - x'|^2 + C_{jy}^2 \cdot |y - y'|^2 + C_{jz}^2 \cdot |z - z'|^2}}{v_m(z) + v_m(z')}\right\} \quad (j = 1, 2, 3) \tag{E.5}$$

where:
M e M' are two points of coordinates (x, y, z) and (x', y', z') (Figure E.3);
C_{jr} are the exponential decay coefficients of the turbulent component $j = 1, 2, 3$ in direction $r = x, y, z$. In the lack of specific analyses, the values given by Table E.I can be used.
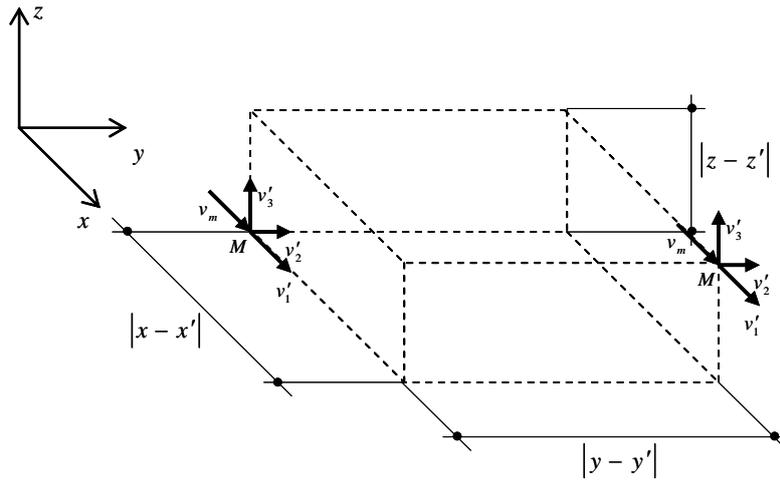
Figure E.3 - Instantaneous wind speed at two points M and M'.

Table E.I – Turbulence exponential decay coefficients.

C_{1x}	C_{1y}	C_{1z}	C_{2x}	C_{2y}	C_{2z}	C_{3x}	C_{3y}	C_{3z}
3	10	10	3	6,5	6,5	0,5	6,5	3

The coherence functions defined by Eq. (E.5) are reasonable approximations for the longitudinal and lateral turbulent components. On the other hand, unlike the results produced by Eq. (E.5), at frequency $n = 0$ the coherence function of the vertical turbulent component usually shows values lower than 1; more accurate assessment of the coherence function of the vertical turbulent component requires specific well documented analytical, numerical and/or experimental methods.

E.3 Monte Carlo turbulence simulation

Computational simulation of wind fields is generally carried out by applying the Monte Carlo method. Various techniques have been developed for representing the wind field as a stationary Gaussian random process. These can be separated into two main classes. The former comprises methods based on spectral representation of the processes; by using such methods, the sample functions as a whole are simulated for all requested time periods; they are normally expressed as the sum of harmonic waves with random phase angle and occasionally with random amplitude. The latter comprises methods based on the construction of recursive models; these simulate sample functions in successive periods with narrow-band-pass filters on white noises – by using, for example, autoregressive (AR) and moving average (MA) methods and a combination of both (ARMA) – or by conditioned simulations of random vectors.

Computational simulation of wind fields requires discretisation of the time and space domains. The use of methods based on spectral representation of processes also requires discretisation of the frequency domain. In this case, by applying an FFT (*Fast Fourier Transform*) algorithm, the two discretisations are not independent, but uniquely linked to the choice of parameters N_t and Δt representing, respectively, the number of time intervals in which the process is simulated and the sampling time; $T_p = N_t \Delta t$ is the duration of the sampled signal. The value $n_c = 1/(2\Delta t)$ is the upper frequency limit of the harmonics reproduced in the simulation (cutoff frequency); $\Delta n = 1/T_p$ is the minimum distance between separate harmonic frequencies. Finite values of the parameters Δt and T_p as necessary in the applications, lead to the respective cancelling out of high- and low-frequency spectral content. Figure E.2 shows how the choice of the most suitable parameters for simulating one turbulence component may be ineffective to simulate another component. Discretisation of the space domain in which the wind field is simulated requires the use of fairly small space steps Δs, in

order to represent in sufficient detail the partial two-point turbulence correlation.

Application of the principles above is the essential requirement for an appropriate representation of turbulence. The generated wind fields are suitable for analysing the static and quasi-static wind actions. When aimed at analysing the dynamic response of structures (clause 3.4.2), simulated wind field should meet additional requirements.

For linear structures, the time step Δt should be small enough not to neglect spectral content capable of exciting vibration modes that significantly contribute to the structure's dynamic response; thus, for example, $1/\Delta t$ should be at least twice the frequency of the largest significant mode. In addition, the signal duration T_p should be much longer than the period of the first vibration mode and it should be increased as damping decreases. Finally, the space step Δs should be sufficiently smaller than the spatial wavelength of modes having a significant effect on the dynamic response.

Wind field simulation for the purpose of analysing the dynamic response of structures with non-linear behaviour requires special care and expert advice.

In any event, the number of wind scenarios simulated should be large enough for accurate statistical treatment.

Annex F   PEAK WIND VELOCITY

Peak wind velocity v_p is the expected maximum wind velocity over a time $T = 10$ minutes, with averaging time τ much less than time T. It depends on the height above ground z, wind climate (clause 3.2.1), design return period (clause 3.2.2) and orography.

In the lack of specific analyses that consider wind direction and effective roughness and orography of the terrain surrounding the site (Annex C), for heights above ground not exceeding $z = 200$ m, peak wind velocity is given by the equation:

$$v_p(z) = v_m(z) \cdot G_v(z) \tag{F.1}$$

where:

v_m is the mean wind velocity (clause 3.2.5);

G_v is the wind velocity gust factor expressed by the equation:

$$G_v(z) = 1 + g_v(z) \cdot I_v(z) \cdot P_v(z) \tag{F.2}$$

where:

g_v is the peak wind velocity factor;

I_v is the turbulence intensity (clause 3.2.6);

P_v is a coefficient taking into account the reduction in turbulence intensity due to the peak velocity averaging time τ.

Coefficients g_v and P_v are given by the equations:

$$g_v(z) = \sqrt{2 \cdot \ln\left[\upsilon_v(z) \cdot T\right]} + \frac{0.5772}{\sqrt{2 \cdot \ln\left[\upsilon_v(z) \cdot T\right]}} \tag{F.3}$$

$$\upsilon_v(z) = 0,032 \frac{v_m(z)}{L_v(z)} \cdot \left[\frac{L_v(z)}{\tau \cdot v_m(z)}\right]^{1,44} \tag{F.4}$$

$$P_v(z) = \frac{1}{1 + 0,56 \cdot \left[\dfrac{\tau \cdot v_m(z)}{L_v(z)}\right]^{0,74}} \tag{F.5}$$

where:

υ_v is the expected turbulence up-crossing rate;

L_v is the turbulent length scale (clause 3.2.6).

In the lack of specific guides, it is recommended to use $\tau = 3$ s. In this case, $G_v = 1,5$ is generally a reasonable approximation of Expression (F.2).

By applying Expressions (F.1) and (F.2), the velocity pressure q_p associated with peak wind velocity v_p is:

$$q_p(z) = \frac{1}{2} \cdot \rho \cdot v_m^2(z) \cdot \left[1 + 2 \cdot g_v(z) \cdot I_v(z) \cdot P_v(z) + g_v^2(z) \cdot I_v^2(z) \cdot P_v^2(z)\right] \tag{F.6}$$

where ρ is the air density.

Eq. (3.9) is derived from Eq. (F.6) by making three assumptions:

1. the third (quadratic) term inside the square brackets is ignored; this assumption is only slightly on the unsafe side since I_v is a small quantity;
2. the conservative value $P_v = 1$ is used;
3. the value $g_v = 3.5$ is used, usually being conservative.

Following these approximations, Eq. (F.6) becomes:

$$q_p(z) = \frac{1}{2} \cdot \rho \cdot v_m^2(z) \cdot \left[1 + 7 \cdot I_v(z) \right] \qquad \text{(F.7)}$$

It can be seen that Eq. (F.7) coincides with Eq. (3.9), and it normally provides a conservative peak wind velocity pressure estimate.

Assumptions 1 and 2 are typical approximations adopted by many standards. On the other hand, assumption 3 has a specific conceptual and practical meaning.

In this Guides, peak wind velocity pressure is transformed firstly into peak aerodynamic actions (clause 3.3) and then into equivalent static actions (clause 3.4) by introducing multiplication factors of, respectively, an aerodynamic and dynamic nature. The expected equivalent static action up-crossing frequency is generally much greater than the expected turbulence up-crossing frequency. Eqs. (F.7) and (3.9) take account of this circumstance, for the assessment of wind actions on structures.

For this reason, Eqs.. (F.7) and (3.9) should not be replaced by Eq. (F.6).

Annex G   GLOBAL AERODYNAMIC COEFFICIENTS

G.1   General

This Annex provides values for the dimensionless coefficients needed to transform wind velocity pressure (clause 3.2) into overall aerodynamic actions on structures (clause 3.3). These coefficients, defined as a whole as global aerodynamic coefficients, include pressure coefficients (used to define external, internal and net pressures), force and moment coefficients (used to define resulting forces and moments per unit length) and friction coefficients (used to define tangential actions). Global aerodynamic coefficients can be used when wind actions can be represented in a simplified form in order to assess the overall actions on large areas of structures or the resultant forces on the major structural components; on the other hand, they should not be used to assess local actions on structural members and cladding for which reference should be made to the values specified in Annex H.

Annex H gives values for the local or detailed aerodynamic coefficients for various structural types; these allow a more realistic representation of the actual pressure field on structural surfaces. They are generally used to assess local aerodynamic actions for use when sizing and verifying individual structural members or cladding and their fixings (façade and roof elements, etc.). Alternatively, for buildings only, they can be used to perform a more detailed assessment of wind action on an entire structure or its individual components.

Pressure coefficients (clause 3.3.1) may be either positive or negative depending on the structure geometry. In particular, external pressure coefficients are positive at all points directly exposed to the oncoming wind; they are negative at all points exposed to separated flow, i.e. on the downwind and lateral surfaces. Positive pressure coefficients commonly range between 0 and 1. Negative pressure coefficients can be greater (in magnitude) and may take values in the range of -3 to 0; even larger negative values (in magnitude) may occur locally over fairly small areas.

Net pressure coefficients (clause 3.3.2) can be positive or negative, depending on geometry of the surface, on wind direction and on orientation of the axis adopted as reference for pressures; when assessing pressure on building surfaces, the net pressure is obtained as the difference between external and internal pressures.

Resulting force and moment coefficients (clause 3.3.3) can be either positive or negative depending on geometry of the structure, on wind direction and on orientation of the axes adopted as reference for forces. When the x axis coincides with the oncoming wind direction, force coefficient c_{FX} is always positive.

Force and moment coefficients per unit length (clause 3.3.4) can be either positive or negative depending on geometry of the structure, on wind direction and on orientation of the axes adopted as reference for forces axes. When the x axis coincides with the oncoming wind direction, force coefficient c_{fX} is always positive.

The friction coefficient is always positive.

The following clauses summarise aerodynamic coefficients for the most common structural types giving, depending on each particular case, pressure coefficients (clauses G.2-G.4), net pressure coefficients (clause G.5), resulting force and moment coefficients (clauses G.6-G.9), coefficients of force and moment per unit length (clauses G.10-G.11) and friction coefficients (clause G.12). More specifically, the following cases are included:

- external pressure coefficients for rectangular-plan buildings (clause G.2);
- external pressure coefficients for circular-plan structures (clause G.3);

- internal pressure coefficients (clause G.4);
- net pressure coefficients for walls and parapets (clause G.5);
- resulting force and moment coefficients for canopies (clause G.6);
- resulting force and moment coefficients for signboards (clause G.7);
- resulting force and moment coefficients for compact bodies (clause G.8);
- resulting force coefficients for plane trusses and lattice structures (clause G.9);
- coefficients of force and moment per unit length for slender structures and elongated components (clause G.10);
- coefficients of force and moment per unit length for bridge decks (clause G.11);
- friction coefficients for plane surfaces (clause G.12).

For structural types and geometries not considered herein, reference should be made to Annex H (irregular buildings only), technical publications or wind tunnel testing (Annex Q).

G.2   Rectangular-plan buildings

G.2.1   General

The wind exerts on the two faces of the surfaces of the building a distribution of external pressure p_e and internal pressure p_i. These pressures are quantified by specifying external c_{pe} and internal c_{pi} pressure coefficients (clause 3.3.1).

External pressure coefficients c_{pe} depend on the shape of the building, on the oncoming wind direction and on the size of the loaded area. In the following, there are reported values that, in the lack of more detailed investigations, can be used to assess overall actions on large areas of buildings with a regular plan and the resultant forces on major structural components. These are derived from the external pressure coefficients $c_{pe,10}$ given in clause H.2 for loaded areas larger than 10 m²; they are different to the latter in that they lead to a simplified and generally conservative definition of the pressure field.

The values given herein refer to wind blowing at right angles to the main faces of a building. In practice, these values represent the most unfavourable ones obtained in a range of wind directions placed ± 45° either side of the relevant orthogonal direction.

Internal pressure coefficients c_{pi} are given in clause G.4.

G.2.2   Side walls

The aerodynamic behaviour of buildings and in particular of their walls mainly depends on the ratio of plan sizes to height. For low-rise buildings a three-dimensional flow is generated. For slender, tall buildings, with the exception of the base and top section, a two-dimensional flow in horizontal planes tends to be generated.

Therefore, as a rule, the pressure coefficients provided herein depend on the h/d ratio, where h is the height of the building and d its along-wind dimension (Figure G.1). These are given in Table G.I and Figure G.2.

For very slender buildings, whose h/d ratio is greater than 5, reference should be made to the provisions of clause G.10 (slender structures and elongated components). In this case, unlike the requirements specified in this clause, wind actions are expressed as forces per unit length.
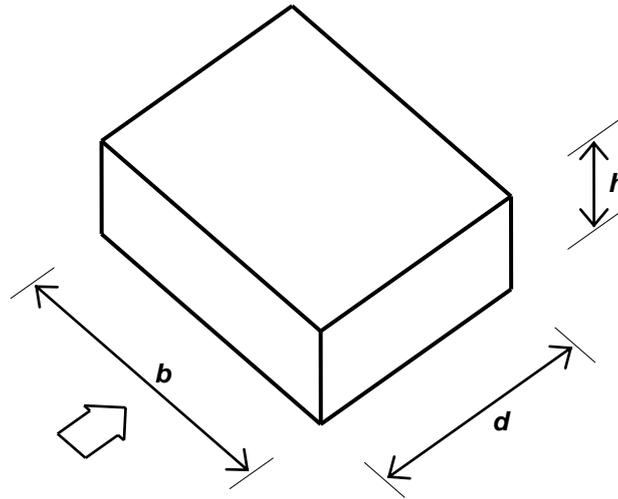
Figure G.1 – Characteristic parameters of rectangular-plan buildings.

Table G.I – Rectangular-plan buildings: c_{pe} for windward, leeward and side faces.

Windward face	Side faces	Leeward face
$h/d \leq 1$: $c_{pe} = 0,7 + 0,1 \cdot h/d$	$h/d \leq 0,5$: $c_{pe} = -0,5 - 0,8 \cdot h/d$	$h/d \leq 1$: $c_{pe} = -0,3 - 0,2 \cdot h/d$
$h/d > 1$: $c_{pe} = 0,8$	$h/d > 0,5$: $c_{pe} = -0,9$	$1 < h/d \leq 5$: $c_{pe} = -0,5 - 0,05 \cdot (h/d\text{-}1)$
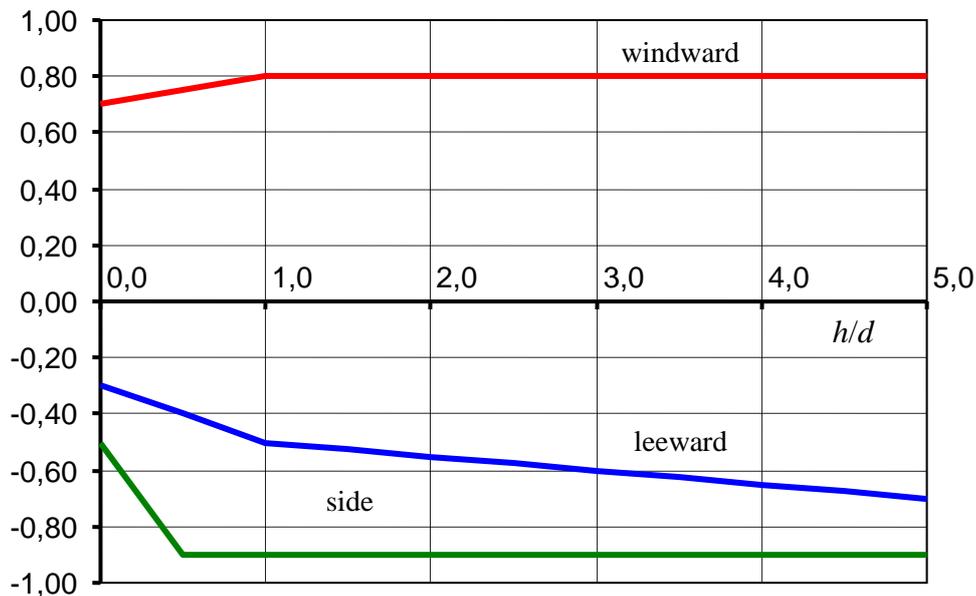
Figure G.2 – Rectangular-plan buildings: c_{pe} for windward, leeward and side faces.

As a rule, besides the aerodynamic actions above, buildings are also subject to torsional actions. These arise not only on buildings with asymmetrical plan, but also on symmetrical and, in particular, rectangular buildings. More specifically, torsional actions can arise when the wind incidence is not parallel to an axis of symmetry or due to the presence of neighboring structures. They also arise when the wind does blow along an axis of symmetry, due to both pressure fluctuations on the side faces and lack of full correlation of the pressure on the windward face. It is recommended to consider such actions especially in the case of elongated plans.

Clauses G.2.2.1 and G.2.2.2 give criteria for assessing the respective reference heights for the windward faces and leeward and side faces of rectangular-plan buildings. Clause G.2.2.3 provides some advice on estimating torsional effects.

G.2.2.1 Reference height for windward face

The flow that is established around buildings is highly complex, especially at the base and top of the windward face. This produces a pressure profile that is generally different to the peak velocity pressure profile of an undisturbed wind (clause 3.3.7). This clause provides a reference height assessment criterion for the windward face, i.e. the height at which peak velocity pressure should be calculated, such as to produce approximate, generally conservative, estimates of the resulting force of such pressure.

For low-rise buildings, i.e. buildings whose height is less than or equal to the plan across-wind size ($h \leq b$), the reference height is constant and equal to the building height ($\bar{z}_e = h$); wind pressure is therefore uniform.

For high-rise buildings, i.e. buildings whose height is between the across-wind plan size and 5 times the in-wind plan size ($b < h \leq 5 \cdot d$), two zones are specified. In the lower part of the building, up to height $z = b$, the reference height is constant and equal to $\bar{z}_e = b$; wind pressure is therefore uniform.

In the top part of the building, for z between b and h, the reference height $\bar{z}_e$ may be selected by applying one of the two following criteria (Figure G.3):

1. The reference height is constant and equal to the top of the building ($\bar{z}_e = h$); wind pressure is therefore uniform between heights $z=b$ and $z=h$. This simplifies the calculation of aerodynamic forces, but the resulting overall force may be largely conservative.

2. The building is divided into sections of arbitrary height, each of which corresponds to a constant reference height equal to the top of the section; if the height of each section coincides with the building interstorey and each individual section is centred on the position of a floor, the reference height may be taken as being equal to the height of the respective floor; in both cases wind pressure is uniform on each section. This makes force calculation more difficult, but the values obtained are more realistic and no greater than those obtained by applying criterion (1).
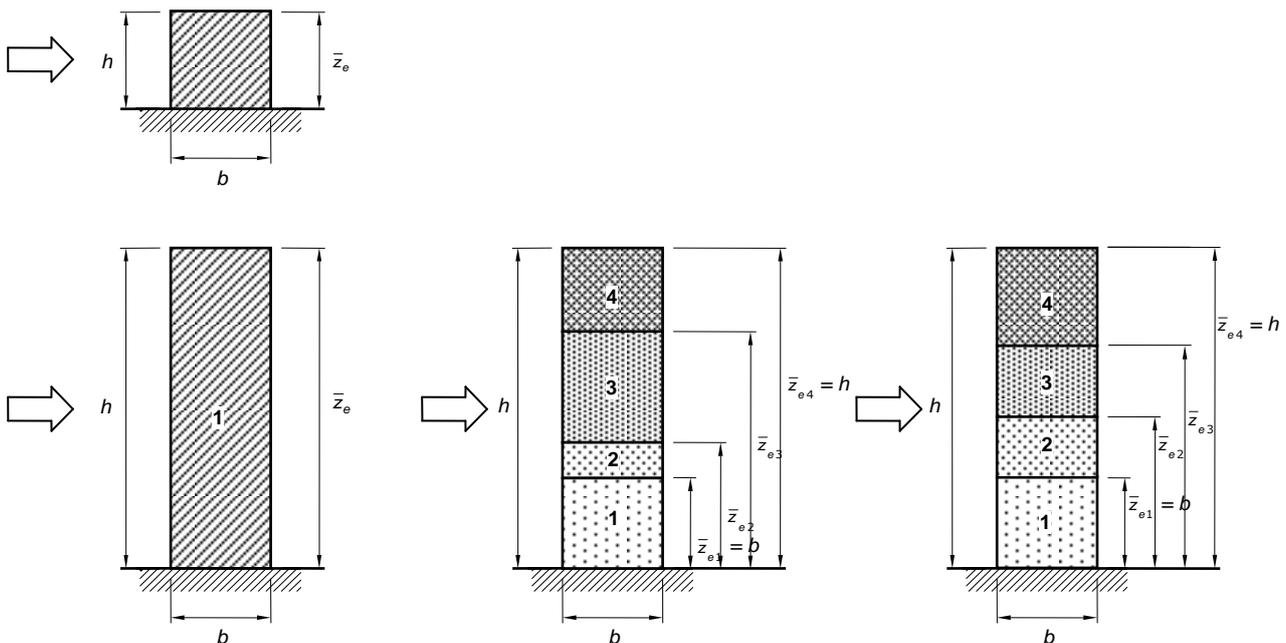
Figure G.3 – Reference heights in low- and high-rise buildings.

G.2.2.2 Reference height for leeward and side faces

Pressure on the leeward and side faces of buildings is associated with the characteristics of separated flow and can, with a good approximation, be considered constant with height. This is taken into account by assuming that the reference height is constant and equal to the height of the top of the building ($\bar{z}_e = h$).

G.2.2.3 Torsional actions

In the case of rectangular-plan buildings, it is possible to account for the presence of torsional actions by modifying the pressure distribution acting on the windward face only.

To this end, in addition to the load case that considers the full pressure distribution on both the windward face (characterised by a pressure coefficient $c_{pe,p}$) and leeward face (characterised by a pressure coefficient $c_{pe,n}$), consideration is also given to the effects induced by an additional load case characterised, on the windward face, by a triangular pressure distribution in plan whose value ranges from $c_{pe,p}$ to zero; on the leeward face, the same uniform pressure distribution as the first load case is applied, characterised by pressure coefficient $c_{pe,n}$ (Figure G.4).
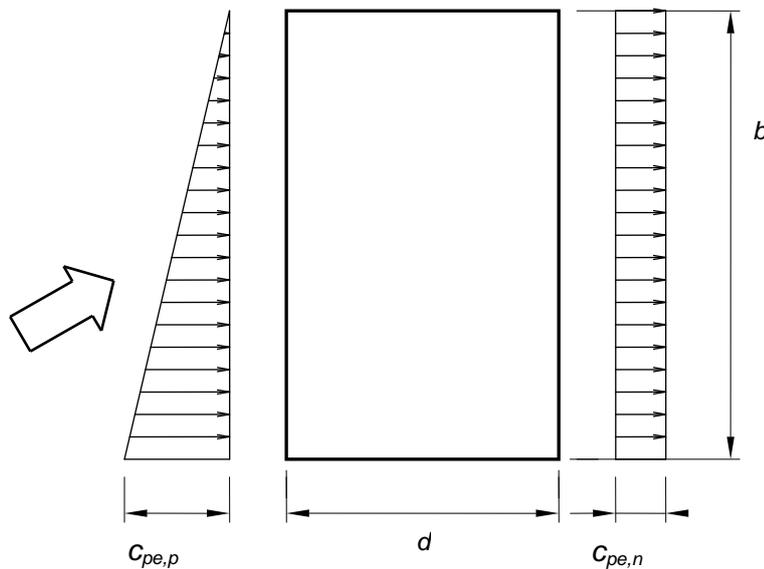
Figure G.4 – Torsional actions on rectangular-plan buildings (plan view).

G.2.3 Roofs

G.2.3.1 Flat roofs

Roofs with a pitch ranging from -5° to +5° are considered as flat.

The reference height $\bar{z}_e$ for flat roofs is equal to the maximum height of the roof itself, including the presence of parapets and other similar elements. Pressure coefficients are given in Table G.II, based on the loaded areas shown in Figure G.5.

Table G.II – Rectangular buildings: c_{pe} for flat roofs.

Upwind strip of depth equal to $b/2$ or h, whichever is smaller:	$c_{pe,A} = -0,80$

Other zones	$c_{pe,B} = \pm 0{,}20$

In the downwind zone, pressure may take both negative and positive values, therefore both cases must be considered.

The presence of parapets whose height exceeds 1/20 of the height of the building (not including the parapet) may lead to reductions in the value of coefficient $c_{pe,A}$, as specified in Annex H.
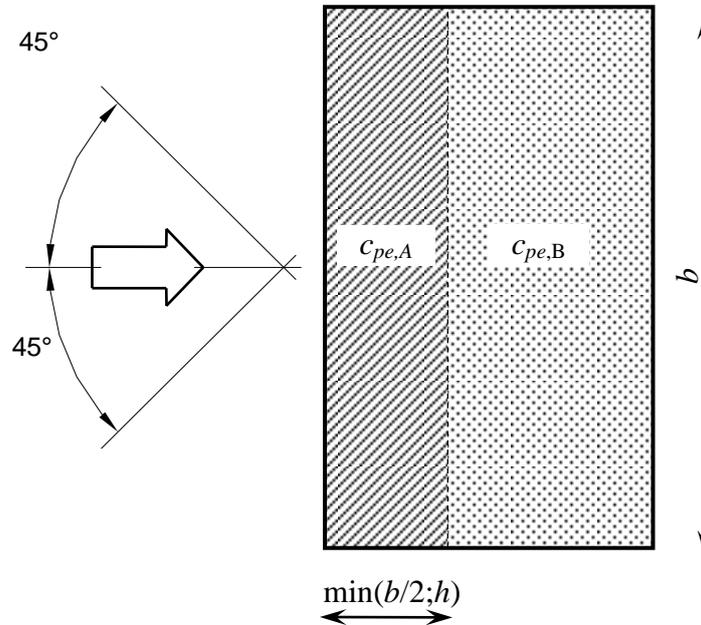
Figure G.5 – Key for flat roofs.

G.2.3.2 Monopitch roofs

The reference height $\bar{z}_e$ for inclined monopitch roofs (Figure G.6) is equal to the maximum height of the roof. For slopes of $-5° \le \alpha \le +5°$, reference has to be made to clause G.2.3.1.

Table G.III and Figure G.7 give pressure coefficients for a wind direction perpendicular to the roof ridge.

For $0° \le \alpha \le 45°$, pressure can easily vary from negative to positive values, therefore pressure coefficients with either signs are provided; as a rule both load cases have to be taken into account, to be sure to consider the worst case scenario.

Table G.IV and Figure G.8 give the pressure coefficients for a wind direction parallel to roof ridge.
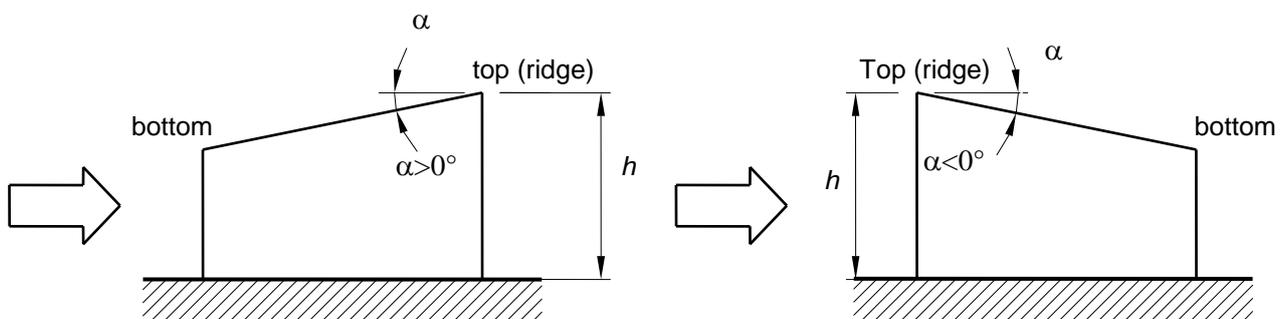
Figure G.6 – Key for monopitch roofs.

Table G.III – Pressure coefficients for monopitch roofs (α in °):

wind perpendicular to the roof ridge.

Negative values		Positive values	
$\alpha \leq -60°$	$c_{pe} = -0,5$		
$-60° \leq \alpha \leq -15°$	$c_{pe} = -0,5 - (\alpha+60)/90$	$0° \leq \alpha \leq 45°$	$c_{pe} = +\alpha/75$
$-15° \leq \alpha \leq 30°$	$c_{pe} = -1,0 + (\alpha+15)/75$	$45° \leq \alpha \leq 75°$	$c_{pe} = +0,6 + (\alpha-45)/150$
$30° \leq \alpha \leq 45°$	$c_{pe} = -0,4 + (\alpha-30)/37,5$		

Figure G.7 – Monopitch roofs: values of coefficient c_{pe}:
wind perpendicular to the roof ridge.

Table G.IV – Pressure coefficients for monopitch roofs (α in °):
wind parallel to the roof ridge.

Upwind zone of depth equal to $b/2$ or h, whichever is smaller	$0° \leq \alpha \leq 15°$	$c_{pe,A} = -0,6 - \alpha/50$
	$15° < \alpha$	$c_{pe,A} = -1,00$
Other zones	$0° \leq \alpha \leq 15°$	$c_{pe,B} = -0,6 - \alpha/30$
	$15° \leq \alpha \leq 45°$	$c_{pe,B} = -0,7 - (\alpha-15)/150$
	$45° \leq \alpha$	$c_{pe,B} = -0,9 + (\alpha-45)/75$
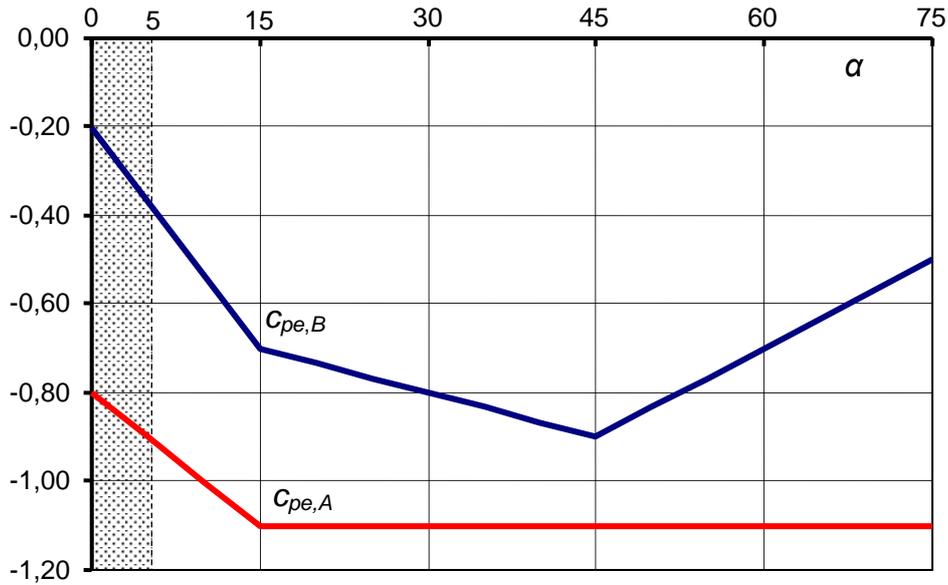
Figure G.8 – Pressure coefficients for monopitch roofs:
wind parallel to the roof ridge.

G.2.3.3   Duopitch roofs

The reference height $\bar{z}_e$ for inclined duopitch roofs (Figure G.9) is equal to the maximum height of the roof. For slopes of $-5°\leq\alpha\leq+5°$, reference has to be made to clause G.2.3.1.

For wind perpendicular to the direction of the roof ridge, pressure coefficients for the upwind area are those given for monopitch roofs (Table G.III, Figure G.7).

For $0°\leq\alpha\leq45°$, pressure can easily vary from negative to positive values, therefore pressure coefficients with either signs are provided; as a rule both load cases have to be taken into account, to be sure to consider the worst case scenario..

For the downwind area refer to the values given in Table G.V and Figure G.10.

Table G.VI and Figure G.11 give pressure coefficients for wind parallel to the roof ridge.
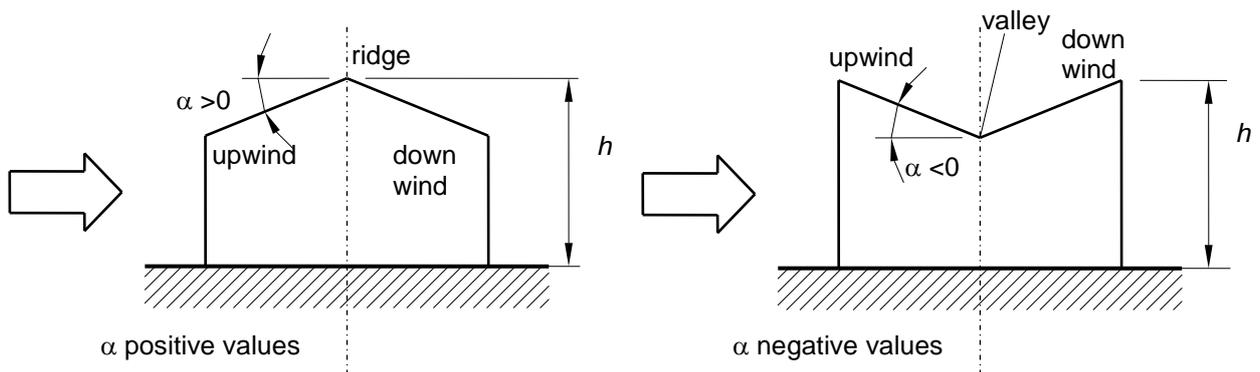
Figure G.9 – Key for duopitch roofs.

Table G.V – Pressure coefficients for duopitch roofs (α in °): downwind area.

$-75° \leq \alpha \leq -15°$	$c_{pe} = -0,85 + (\alpha+60)/180$
$-15° \leq \alpha \leq 15°$	$c_{pe} = -0,6$
$15° \leq \alpha \leq 45°$	$c_{pe} = -0,6 + (\alpha-15)/100$
$45° \leq \alpha$	$c_{pe} = -0,3$
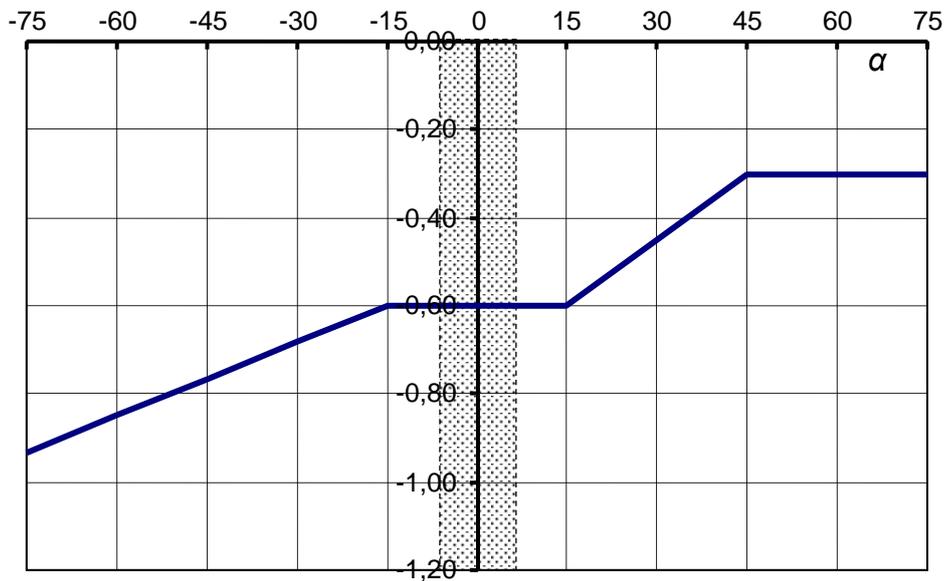
Figure G.10 – Pressure coefficients for duopitch roofs:
downwind area for a wind direction perpendicular to the roof ridge.

Table G.VI – Pressure coefficients for duopitch roofs (α in °):
wind direction parallel to roof ridge.

Upwind area of depth equal to *b*/2 or *h*, whichever is smaller	$\alpha \leq -30°$	$c_{pe,A} = -1,0$
	$-30° \leq \alpha \leq 0°$	$c_{pe,A} = -0,8 + \alpha/150$
	$0° \leq \alpha \leq 30°$	$c_{pe,A} = -0,8 - \alpha/150$
	$30° \leq \alpha$	$c_{pe,A} = -1,0$
Other zones:	$-45° \leq \alpha \leq -30°$	$c_{pe,B} = -0,9$
	$-30° \leq \alpha \leq 10°$	$c_{pe,B} = -0,9 + (\alpha+30)/100$
	$10° \leq \alpha$	$c_{pe,B} = -0,5$
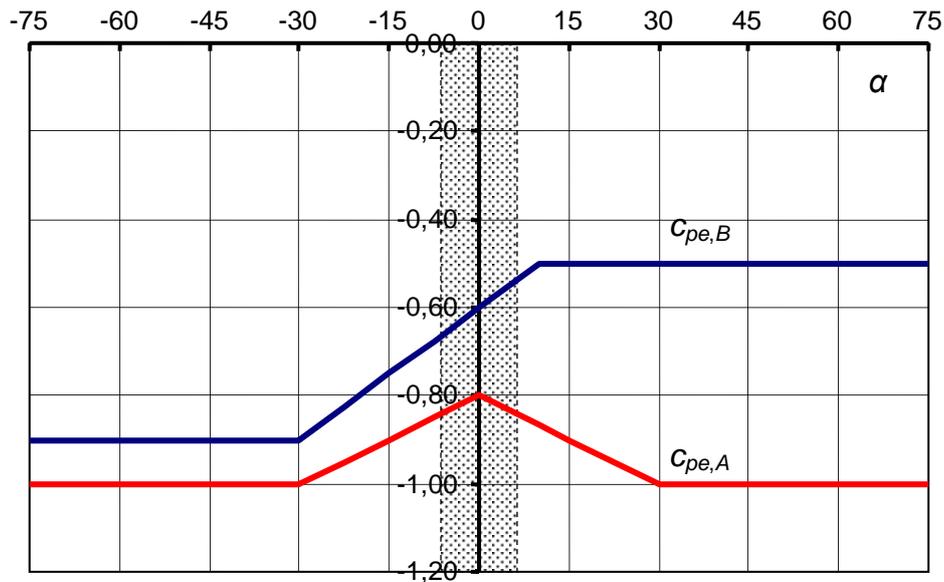
Figure G.11 – Pressure coefficients for duopitch roofs:
wind direction parallel to roof ridge.

G.2.3.4 Hipped roofs

The reference height $\bar{z}_e$ for hipped roofs (Figure G.12) is equal to the maximum height of the roof.

For upwind and downwind areas the same coefficients defined for duopitch roofs (Tables G.III and G.V and Figures G.7 and G.10) shall be used.

For the side faces when the wind direction is parallel to the walls, the pressure coefficients given in Table G.VII and Figure G.13 shall be used.
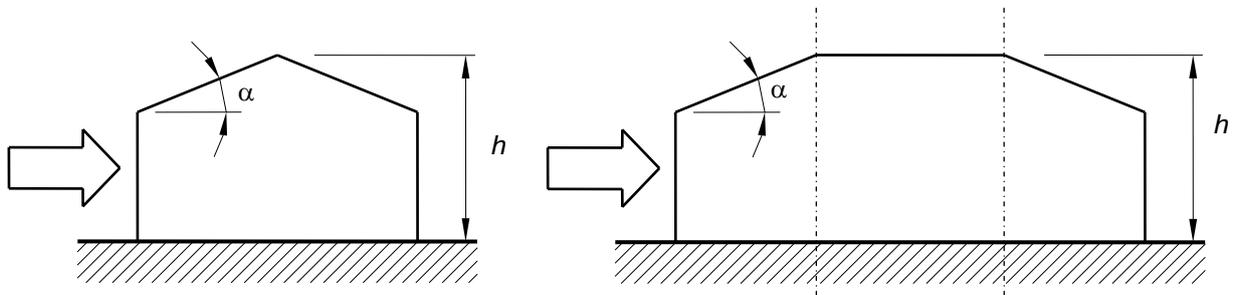
Figure G.12 – Key for hipped roofs.

Table G.VII – Pressure coefficients for hipped roofs (α in °): side faces.

$0° \leq \alpha \leq 30°$	$c_{pe} = -0,6 - \alpha/75$
$30° \leq \alpha \leq 45°$	$c_{pe} = -1,0$
$45° \leq \alpha \leq 60°$	$c_{pe} = -1,0 + (\alpha-45)/37,5$
$60° \leq \alpha$	$c_{pe} = -0,6$
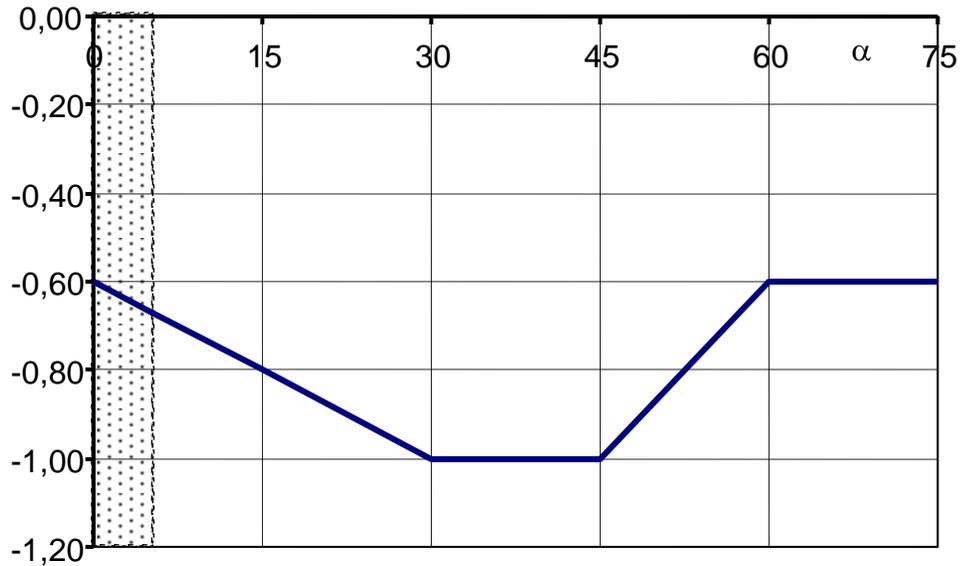
Figure G.13 – Pressure coefficients for hipped roofs: side faces.

G.2.3.5   Multispan roofs

The reference height $\bar{z}_e$ for multipitch roofs, i.e. roofs comprising adjoining groups of mono or duopitch roofs (Figure G.14), is equal to the maximum height *h* of the roof.

As a rule, for multipitch roofs the same pressure coefficients specified for mono or duopitch roofs (clauses G.2.3.2 and G.2.3.3) shall be used.

Only in the case of the wind perpendicular to the direction of the roof ridge , and for the geometries shown in Figure G.14, the above-mentioned pressure coefficients can be multiplied by the reduction factors given in Figure G.14. Specifically:

- for the case shown in Figure G.14a, the pressure coefficients specified in clause G.2.3.2 (monopitch roofs with negative pitch angle) are applied to each span of the roof. These coefficients are multiplied by the reduction factor 0,8 in the second span and by the reduction factor 0,6 in subsequent spans;

- for the case shown in Figure G.14b, the pressure coefficients specified in clause G.2.3.2 (monopitch roofs with positive pitch angle) are applied to each span of the roof. Should such coefficients be positive ($c_{pe} > 0$), in the second and subsequent spans $c_{pe} = $ -0,4 is applied. Should such coefficients be negative ($c_{pe} < 0$), they are multiplied by the reduction factor 0,8 in the second span and by the reduction factor 0,6 in subsequent spans;

- for the case shown in Figure G.14c, the pressure coefficients specified in clause G.2.3.2 (monopitch roofs with positive pitch angle) are applied to the first span of the roof (first upwind slope). In subsequent spans of the roof, the pressure coefficients specified in clause G.2.3.3 (duopitch roofs with negative pitch angle) are applied; these coefficients are multiplied by the reduction factor 0,6 starting from the third span of the roof;

- for the case shown in Figure G.14d, the pressure coefficients specified in clause G.2.3.3 (duopitch roofs with negative pitch angle) are applied to each span of the roof. These coefficients are multiplied by the reduction factor 0,8 in the second span and by the reduction factor 0,6 in subsequent spans.
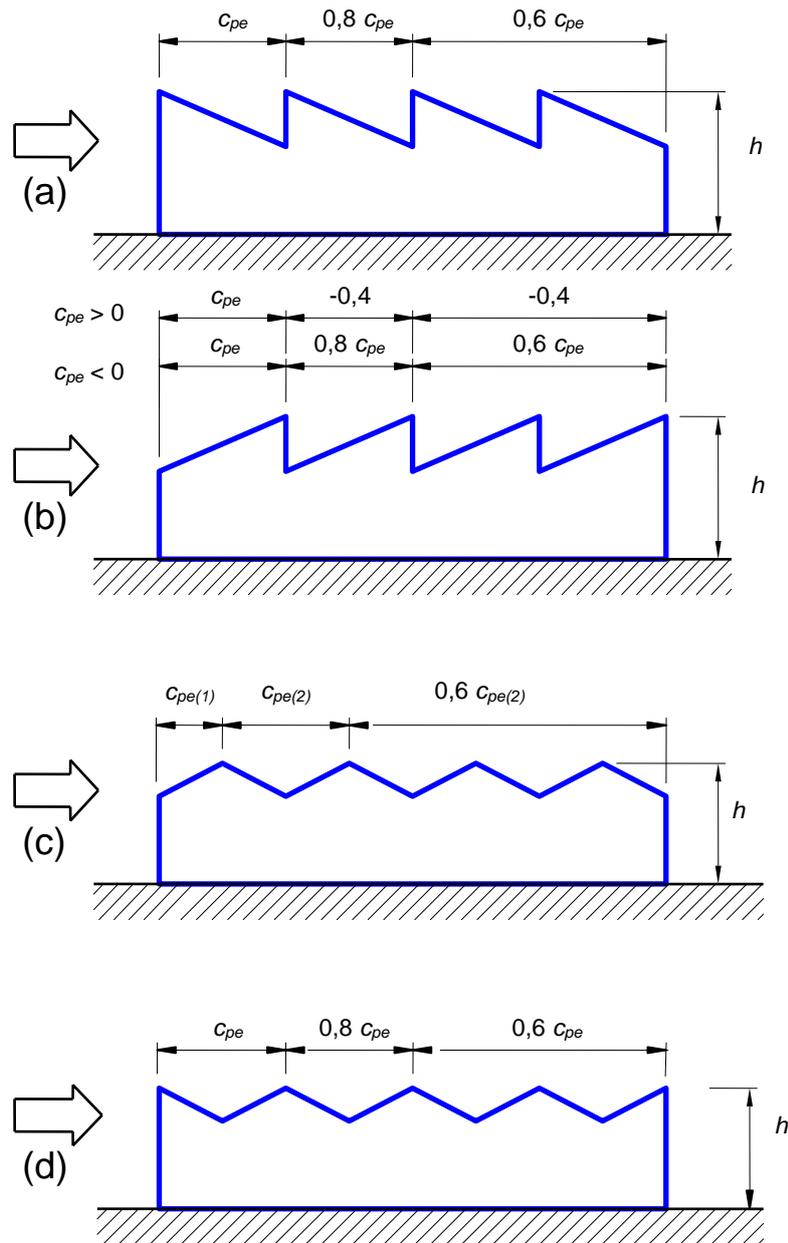
Figure G.14 – Pressure coefficients for multipitch roofs.

G.2.3.6 Vaulted roofs

The reference height for vaulted roofs is $\bar{z}_e = h + f/2$ (Figure G.15).

For a wind direction perpendicular to the roof generatrices, the roof is divided into four zones of equal area:

- in the upwind zone A pressure coefficients $c_{pe,A}$ are adopted;
- in the two intermediate zones B pressure coefficients $c_{pe,B}$ are adopted;
- in the downwind zone C pressure coefficients $c_{pe,C}$ are adopted.

Values for pressure coefficients $c_{pe,A}$, $c_{pe,B}$ and $c_{pe,C}$ are given in Figure G.16 as a function of h/d and f/d ratios (Figure G.15). In particular, for coefficient $c_{pe,A}$:

- when $h/d \geq 0,5$, both values given in the graph shall be used;
- for intermediate values $0 < h/d < 0,5$, linear interpolation of the given values is allowed.

For values of $f/d \leq 0,05$, the pressure coefficients for flat roofs (clause G.2.3.1) shall be used.
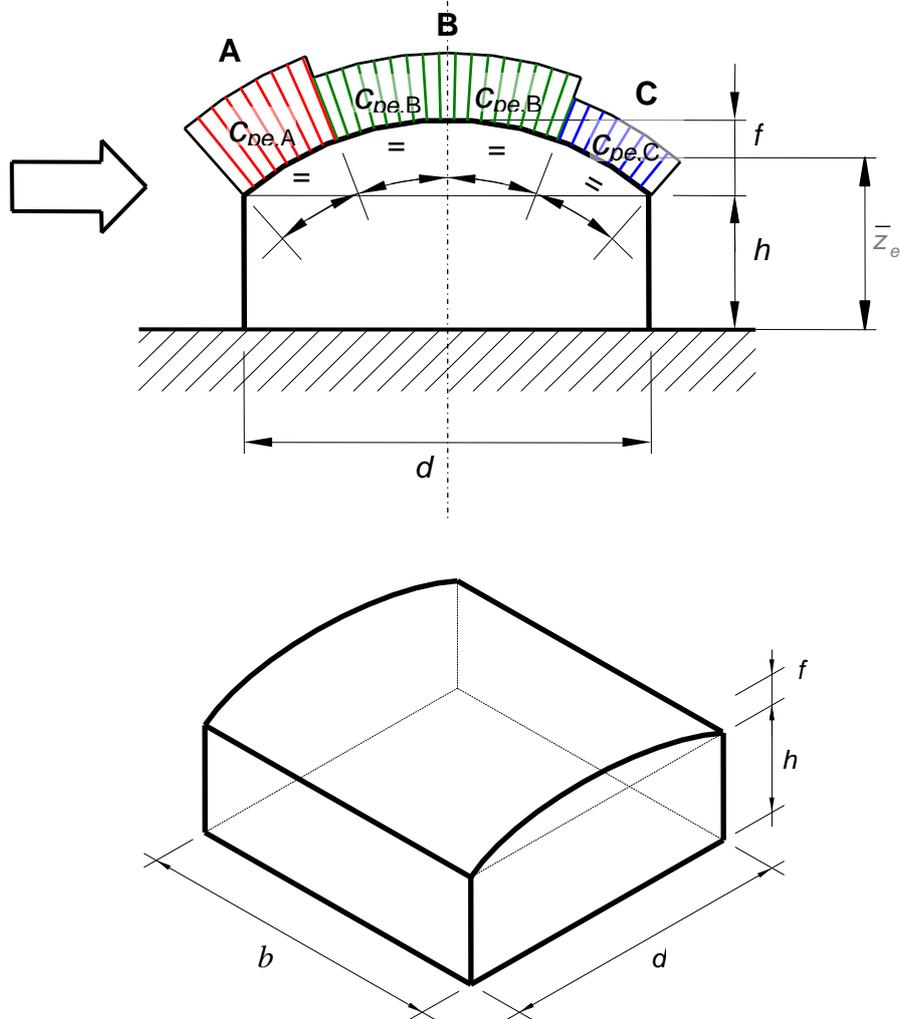
Figure G.15 – Key for vaulted roofs.
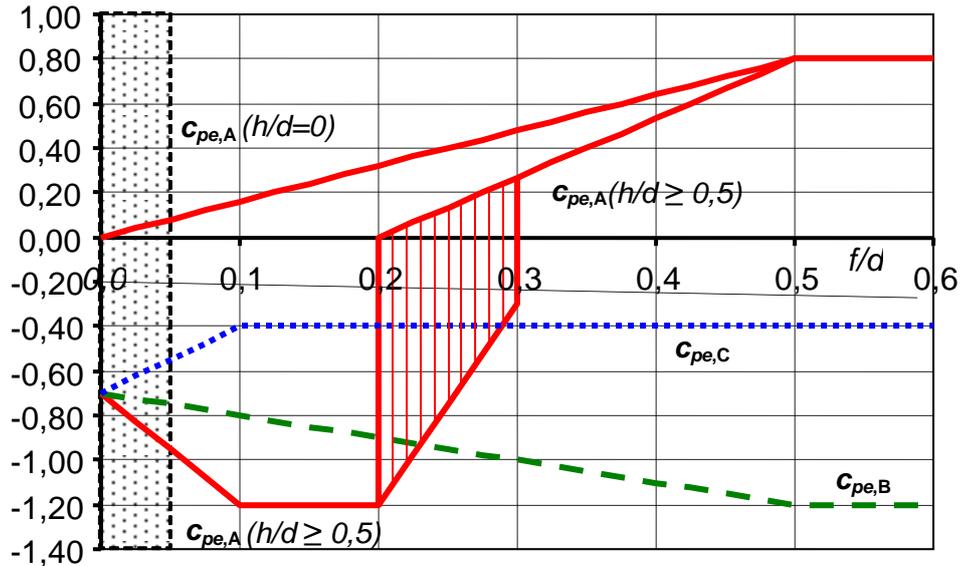
Figure G.16 – Pressure coefficients per vaulted roofs.

For wind parallel to the roof generatrices, as a first approximation, pressure coefficients for flat roofs (clause G.2.3.1) can be used.

G.3   Constructions with circular plan

G.3.1   General

The wind exerts on the two faces of the surfaces of constructions with circular plan a distribution of external pressure p_e and internal pressure p_i. These pressures are quantified by specifying external c_{pe} and internal c_{pi} pressure coefficients (clause 3.3.1). The pressure coefficients specified hereafter refer to external surfaces. Internal pressure coefficients are given in clause G.4.

G.3.2   Vertical surfaces

As in the case of rectangular-plan buildings, the aerodynamic behaviour of constructions with circular plan, in particular their vertical surface, mainly depends on the ratio of plan diameter to height. For low rise constructions, a three-dimensional flow is generated. For slender constructions, with the exception of the base and top portions, a two-dimensional flow in horizontal planes is generated.

Therefore, the pressure coefficients provided herein depend on the h/b ratio, where h is the height of the construction and b its plan diameter. They also depend on the Reynolds number Re and surface roughness k.

For very slender structures, whose h/b ratio is greater than 5, reference should be made to the provisions of clause G.10 (slender structures and elongated structural components). In this case, unlike the requirements specified in this clause, wind actions are expressed as forces per unit length.

G.3.2.1 Reference height

As in the case of constructions with rectangular plan, the flow around circular constructions is highly complex, especially at the base and top. This produces a vertical pressure distribution that is generally different from the peak velocity pressure profile associated with the undisturbed wind (clause 3.3.7). This clause provides a criterion for the assessment of the reference height, such to produce approximated estimates of the resulting force of the pressure, mainly on the safe side.

For low rise buildings, i.e. whose height is less than or equal to the plan diameter ($h \leq b$), the reference height is constant and equal to the height of the construction ($\bar{z}_e = h$); wind pressure is therefore uniform with height.

For tall constructions, i.e. whose height ranges between one and five times the plan diameter ($b < h \leq 5 \cdot b$), two zones are specified. In the lowest part of the construction, up to height $z = b$, the reference height is constant and equal to $\bar{z}_e = b$; wind pressure is therefore uniform with height. In the upper part of the construction, for z of between b and h, the reference height $\bar{z}_e$ may be selected by applying one of the two following criteria (Figure G.3):

1. The reference height is constant and equal to the top of the construction ($\bar{z}_e = h$); wind pressure is therefore uniform between heights $z=b$ and $z=h$. This simplifies the calculation of aerodynamic forces, but the resulting overall force may be largely conservative.
2. The construction is divided into sections of arbitrary height, each of which corresponds to a constant reference height equal to the top of the section. This makes force calculation more articulated, but the values obtained are more realistic and no greater than those obtained by applying criterion (1).

G.3.2.2 Pressure coefficients

The external pressure coefficients c_{pe} are given by the equation:

$$c_{pe} = c_{peo} \psi_{\lambda\alpha} \tag{G.1}$$

where:
c_{peo} is the external pressure coefficient for a circular cylinder of infinite length;
$\psi_{\lambda\alpha}$ is a slenderness factor.

The external pressure coefficient c_{peo} is given by the equation:

$$c_{peo}\left(\alpha_p\right) = 1 - \left(1 - c_{pm}\right) \cdot \sin^2\left(\frac{\pi \cdot \alpha_p}{2 \cdot \alpha_m}\right) \quad \text{for } 0° \leq \alpha_p \leq \alpha_m \tag{G.2a}$$

$$c_{peo}\left(\alpha_p\right) = c_{pb} - \left(c_{pb} - c_{pm}\right) \cdot \cos^2\left(\frac{\pi}{2} \cdot \frac{\alpha_p - \alpha_m}{\alpha_b - \alpha_m}\right) \quad \text{for } \alpha_m \leq \alpha_p \leq \alpha_b \tag{G.2b}$$

$$c_{peo}\left(\alpha_p\right) = c_{pb} \quad \text{for } \alpha_b \leq \alpha_p \leq 180° \tag{G.2c}$$

where α_p is the angle shown in Figure G.17 in degrees (°); the meaning of parameters c_{pm}, c_{pb}, α_m and α_b is illustrated in Figure G.17. Table G.VIII gives some reference values for these parameters, corresponding to different values of the Reynolds numbers Re (clause 3.3.7), calculated by assigning the value of diameter b as the reference length and assuming $k/b \leq 0.5 \cdot 10^{-3}$ (clause G.10.6, Table G.XVII).
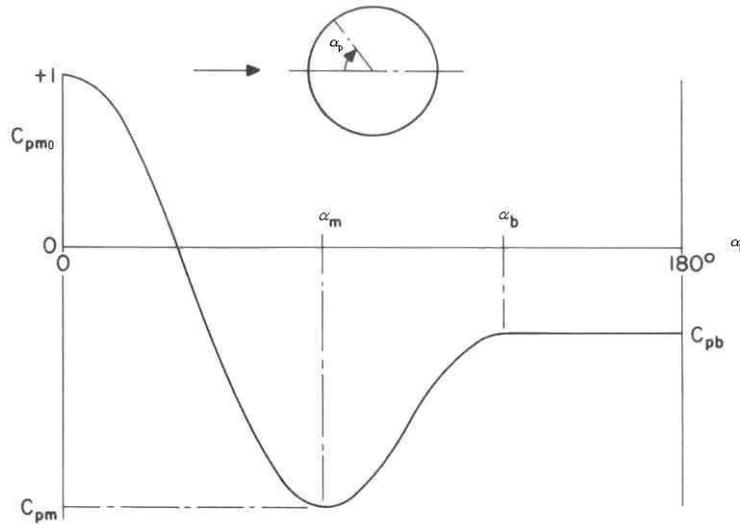
Figure G.17 – External pressure coefficient c_{peo}.

Table G.VIII – Reference values for parameters c_{pm}, c_{pb}, α_m and α_b for $k/b \leq 0.5 \cdot 10^{-3}$.

Re	c_{pm}	c_{pb}	α_m [°]	α_b [°]
$5 \cdot 10^5$	-2,2	-0,4	85	135
$2 \cdot 10^6$	-1,9	-0,7	80	120
10^7	-1,5	-0,8	75	105

Factor $\psi_{\lambda\alpha}$ is given by the equation:

$$\psi_{\lambda\alpha} = 1 \qquad\qquad \text{for} \ \ 0° \leq \alpha_p \leq \alpha_m \qquad \text{(G.3a)}$$

$$\psi_{\lambda\alpha} = \psi_\lambda + \left(1 - \psi_\lambda\right) \cdot \cos\left[\frac{\pi}{2} \cdot \left(\frac{\alpha_p - \alpha_m}{\alpha_b - \alpha_m}\right)\right] \quad \text{for} \ \ \alpha_m \leq \alpha_p \leq \alpha_b \quad \text{(G.3b)}$$

$$\psi_{\lambda\alpha} = \psi_\lambda \qquad\qquad \text{for} \ \ \alpha_b \leq \alpha_p \leq 180° \quad \text{(G.3c)}$$

where α_p is expressed in degrees (°); ψ_λ is a slenderness factor (clause G.10.8). For structures dealt with herein ($h/b \leq 5$), the value $\psi_\lambda = 2/3$ is acceptable.

G.3.3 Roofs

For spherical domes, the reference height is equal to $\bar{z}_e = h + f/2$ (Figure G.18).

A pressure distribution is applied to the roof surface that varies in the wind direction, with values of the pressure coefficient constant along planes perpendicular to the wind (dotted lines in Figure G.18).

Values of the pressure coefficient are given in Figure G.19 and are indicated as $c_{pe,A}$, $c_{pe,B}$ and $c_{pe,C}$; they refer, respectively, to the windward zone A, to the centre of the roof (zone B) and to the downwind zone C. In order to calculate the value of the pressure coefficient along the roof, linear interpolation between the three values indicated can be used.

Intermediate values of h/d with respect to those given in Figure G.19 can be considered by linear interpolation.
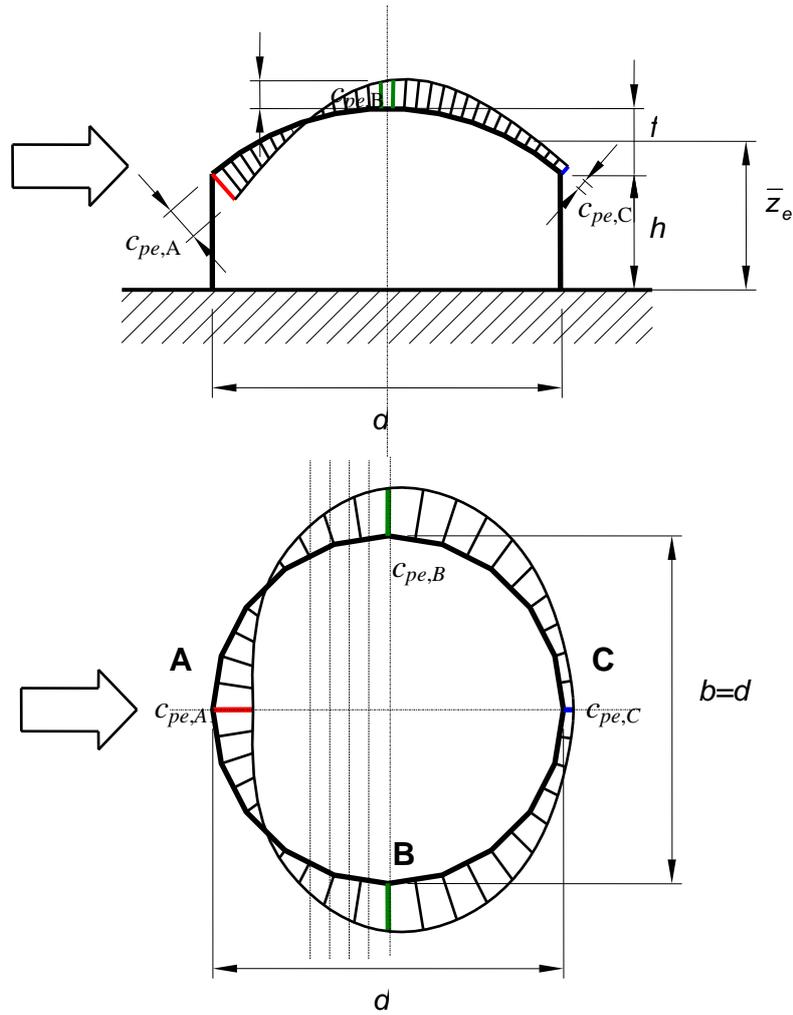
Figure G.18 – Key for spherical domes.
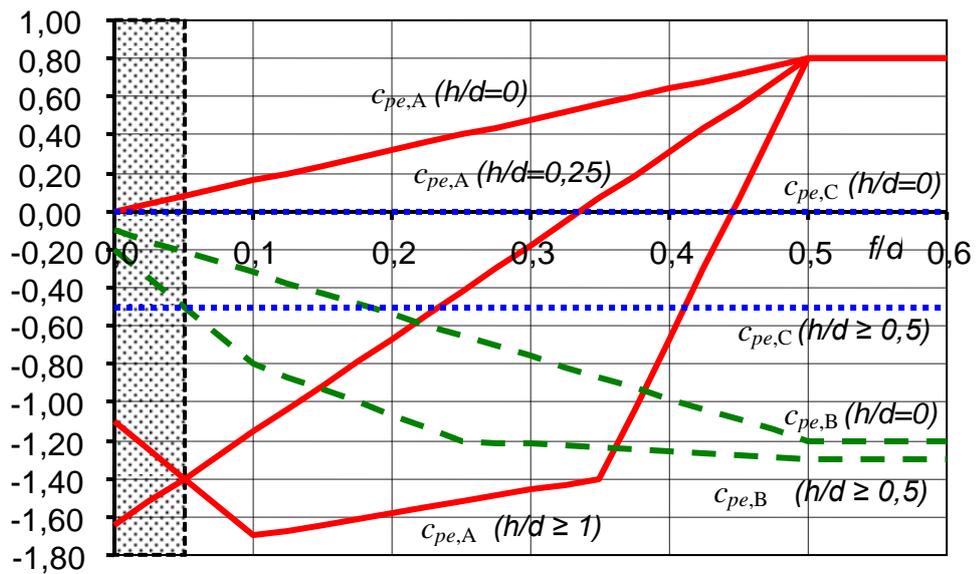
Figure G.19 – Pressure coefficients for spherical domes.

G.4   Internal pressure

The pressure that the wind exerts on the external surfaces of constructions varies from point to point. On the other hand, internal pressure is very uniform, indeed constant on all surfaces of communicating internal volumes. This makes the resulting action from internal pressure distribution vanish. Nevertheless, internal pressure can determine aerodynamic actions that are essential for the design and verification of individual parts and components.

The internal pressure coefficient c_{pi} is used to quantify the internal pressure of a construction. It depends on various factors, above all the size and distribution of the openings in the surfaces of the construction. If the construction has a distributed porosity, this has a filtering effect on external pressure fluctuations, and the internal pressure tends to reach a static equilibrium at a value equal to the area-weighted average external pressure of the openings. On the other hand, if the surfaces have large openings, the internal pressure is influenced by fluctuations of the external pressure at the openings; therefore the internal pressure coefficient takes much higher (absolute) values, and these depend on position and size of the openings.

Internal pressure shall be considered to act simultaneously to external pressure. Design actions on individual parts or components are therefore represented by the worst combination of external and internal pressures.

As a rule, no structure shall be assumed to be fully sealed, therefore a non-zero internal pressure has to be considered. Exeptions are the following two cases, in which the construction can be considered as fully sealed:

- constructions in which the overall area of openings does not exceed 0,0002 ($0,2 \cdot 10^{-3}$) of the overall area of the external surfaces;

- constructions with controlled openings, i.e. openings that are usually kept closed or that can be closed if needed.

In principle, different internal pressure values may be applied in accordance with the particular limit state considered. For example, if large openings are designed to be sealed during high winds, these openings need not be considered when verifying ultimate limit states; on the other hand, the presence of these openings shall be considered under service or accidental conditions. Similar choices shall be carefully assessed and clearly specified at the design or verification stage.

This section provides criteria for the choice of internal pressure coefficient in the four following cases:

- buildings whose total area of openings is more than 30% (clause G.4.1);

- buildings with a dominant surface (clause G.4.2) not belonging to the previous case;

- buildings with uniformly distributed openings (clause G.4.3) not belonging to the two previous cases;

- open silos, chimneys and tanks (clause G.4.4).

In all other cases, use is recommended of assessments based on well documented data or analytical, numerical and/or experimental procedures.

G.4.1 Buildings with more than 30% of openings

When at least two surfaces of the building have more than 30% of their surface represented by openings (Figure G.20a), the rules given in clause G.6 (canopies) shall be used. When the roof has more than 30% of openings (Figure G.20b), the rules given in clause G.5 (walls and parapets) shall be used.
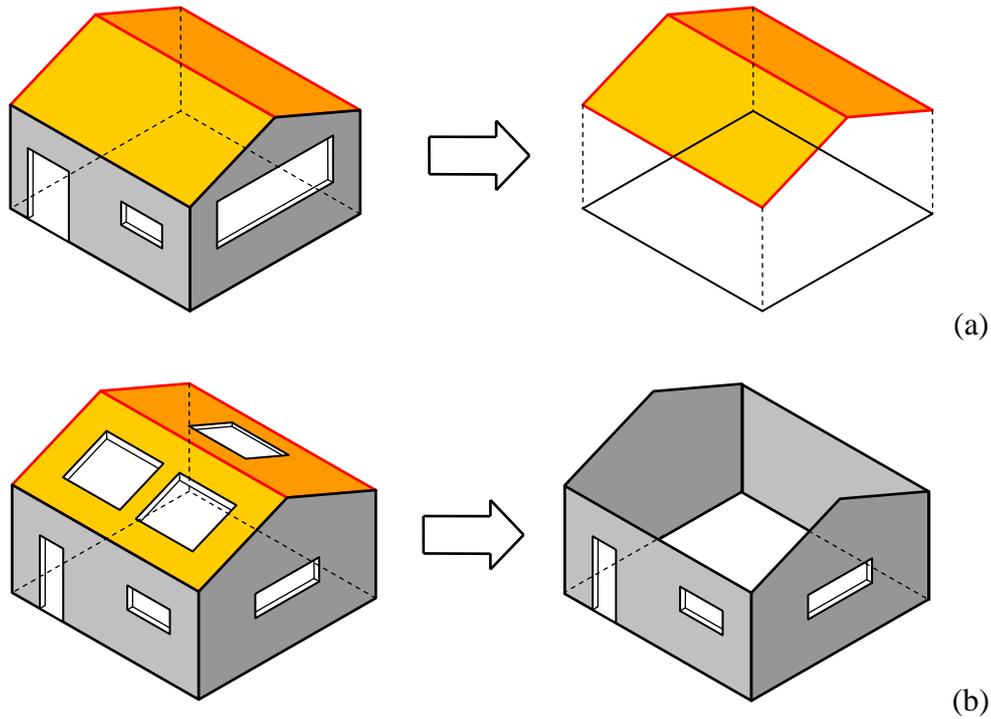
Figure G.20 - Keys for large openings on side walls (a) and the roof (b).

G.4.2 Buildings with a dominant surface

For the purposes of assessing internal pressures, a surface of a building is regarded as dominant (compared to the others) when the area of openings at that surface is at least twice the area of openings in the remaining surfaces.

For buildings not matching one of the cases specified in clause G.4.1 but having a dominant surface, the following rules shall apply.

The total area of openings in a surface is calculated as the sum of the areas of openings (the sum comprising only openings whose area is greater than 1% of the area of the respective surface and greater than 0,2 m^2), increased by the contribution of distributed porosity. The opening area produced by distributed porosity is calculated as the product of the area of the surface and the porosity factor. The porosity factor ranges from 0,0005 (0,5·10^{-3}) to 0,01 (10·10^{-3}), where the smaller value applies to well sealed buildings (good quality windows, ventilation systems) and the larger to buildings with large porosity.

Table G.IX specifies the internal pressure coefficient c_{pi} for buildings with a dominant surface as a function of the corresponding external pressure coefficient c_{pe}.

Table G.IX – Internal pressure coefficients for buildings with a dominant surface.

Area of openings on the dominant surface at least twice the area of openings in the remaining surfaces	$c_{pi} = 0{,}75 \cdot c_{pe}$
Area of openings on the dominant surface at least three times the area of openings in the remaining surfaces	$c_{pi} = 0{,}90 \cdot c_{pe}$

The reference height $\bar{z}_i$ is equal to the reference height $\bar{z}_e$ of the dominant surface.

G.4.3 Buildings with uniformly distributed openings

If the building has a uniformly distributed porosity and therefore does not match anyone of the cases specified in clauses G.4.1 and G.4.2, the internal pressure coefficient is independent of porosity, and is given by the equation:

$$c_{pi} = \frac{A_p^2 \cdot c_{pe,p} + A_n^2 \cdot c_{pe,n}}{A_p^2 + A_n^2} \tag{G.4}$$

where:

A_p is the total area of openings on surfaces with a positive external pressure coefficient;

A_n is the total area of openings on surfaces with a negative external pressure coefficient;

$c_{pe,p}$ is the mean external pressure coefficient for openings subject to positive external pressure;

$c_{pe,n}$ is the mean external pressure coefficient for openings subject to negative external pressure.

The mean external pressure coefficients are given by the following equations:

$$c_{pe,p} = \frac{\displaystyle\sum_{\text{surfaces with } c_{pe}>0} A_{p,j} \cdot c_{pe,p,j}}{\displaystyle\sum_{\text{surfaces with } c_{pe}>0} A_{p,j}} = \frac{\displaystyle\sum_{\text{surfaces with } c_{pe}>0} A_{p,j} \cdot c_{pe,p,j}}{A_p} \tag{G.5a}$$

$$c_{pe,n} = \frac{\displaystyle\sum_{\text{surfaces with } c_{pe}<0} A_{n,j} \cdot c_{pe,n,j}}{\displaystyle\sum_{\text{surfaces with } c_{pe}<0} A_{n,j}} = \frac{\displaystyle\sum_{\text{surfaces with } c_{pe}<0} A_{n,j} \cdot c_{pe,n,j}}{A_n} \tag{G.5b}$$

where:

$A_{p,j}$ is the area of the *j-th* opening with a positive external pressure coefficient;

$A_{n,j}$ is the area of the *j*-th opening with a negative external pressure coefficient;

$c_{pe,p,j}$ is the external pressure coefficient of the *j*-th opening subject to positive external pressure;

$c_{pe,n,j}$ is the external pressure coefficient of the *j*-th opening subject to negative external pressure.

The reference height $\bar{z}_i$ is equal to the height of the building.

When accurate calculations of the internal pressure coefficient are not possible, e.g. because the data needed to apply Eqs. (G.4) and (G.5) is not available, values $c_{pi} = +0,2$ and $c_{pi} = -0,3$ can be used to obtain the worst case scenario for each particular situation.

G.4.4 Open silos, chimneys and tanks

In the case of a distributed leakage, the internal pressure coefficient for open silos and chimneys can be taken as $c_{pi} = -0,60$. The internal pressure coefficient for tanks that are permeable to the wind with small openings can be taken as $c_{pi} = -0,40$.

As an alternative the value $c_{pi} = 0$ shall also be used if it produces the worst load condition.

G.5 Walls and parapets

The wind exerts a net pressure distribution p_n on walls and parapets. This net pressure is quantified through net pressure coefficients c_{pn} (clause 3.3.2). The net pressure coefficients specified hereafter refer to flat walls and parapets.

Net pressure coefficients for flat walls and parapets are greatly influenced by any porosity of the element, i.e. the ratio of the total area of openings to the area of the wall or parapet. This section applies to elements whose porosity does not exceed 20%, i.e. whose density φ is not less than 80%. For elements whose density is less than 80%, reference shall be made to clause G.7 dealing with lattice structures.

Net pressure coefficients are functions of the distance from the edge of the element; this is therefore divided into zones as shown in Figure G.21, where h is the height of the wall or parapet. Net pressure coefficients are also influenced by any return corner (Figure G.22); this has the effect of reducing the magnitude of the negative pressure on the leeward face and, therefore, reducing the net pressure acting on areas close to the edge.
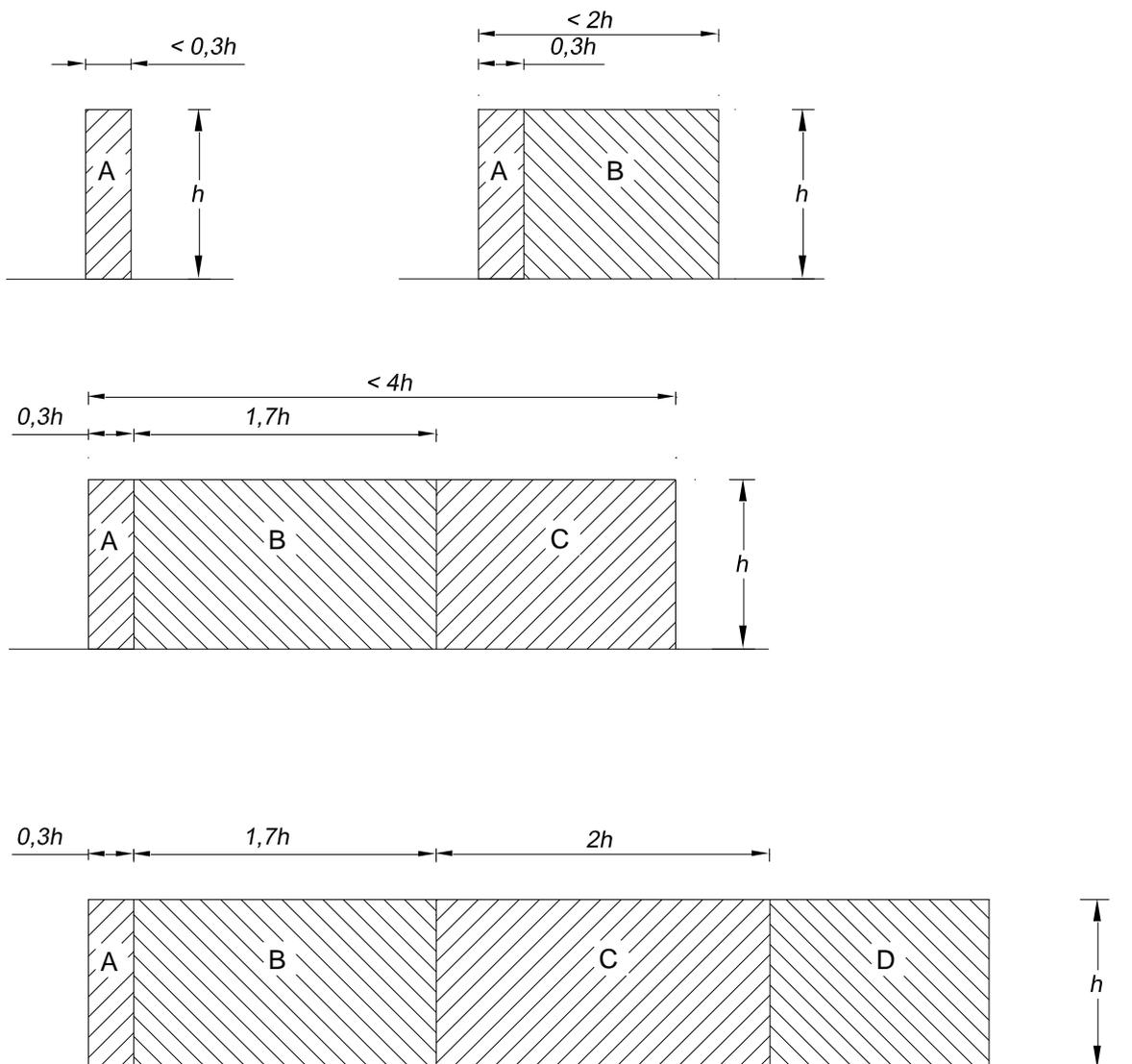
Figure G.21 – Areas of walls and parapets of uniform net pressure.

$$c_{pn} \qquad\qquad c_{pn}$$

Figure G.22 – Walls and parapets without and with return corner.

Table G.X gives net pressure coefficients for each zone of the element, both without and with return corners, for two density φ values of 1 and 0,8; l is the length of the wall or parapet. Intermediate density values can be considered through linear interpolation of net pressure coefficient values.

Table G.X – Net pressure coefficients for walls and parapets.

φ	Return corner	l/h	A	B	C	D
1,0	no	<3	2,3	1,4	1,2	1,2
		5	2,9	1,8	1,4	
		>10	3,4	2,1	1,7	
	yes	all	2,1	1,8	1,4	
0,8	yes/no	all	1,2			

The reference height is $\bar{z}_e = h$.

When the element considered is located downstream another similar element, this may cause a sheltering effect, giving rise to a reduction in net pressure on the downwind element. Such reduction depends on the porosity of the sheltering element and on its distance from the sheltered element. The sheltering effect can be taken into account by multiplying the net pressure coefficients in Table G.X by the reduction factor ψ_s given in Table G.XI and Figure G.23, as a function of the ratio of spacing x between the elements and height h of the sheltered element, and of the density φ of the sheltering element. This reduction can only be applied when the sheltering element is at least as high as the sheltered element and is only applicable in the zones that are more than a distance of h from the edges of the sheltered element (Figure G.24).

Table G.XI – Shelter factor for walls and parapets.

Spacing x/h	φ = 1,0	φ = 0,8
$0 \le x/h \le 5$	$\psi_s = 0,3$	
$5 \le x/h \le 10$	$\psi_s = 0,07 \cdot (x/h) - 0,05$	$\psi_s = 0,03 \cdot (x/h) + 0,15$
$10 \le x/h \le 15$	$\psi_s = 0,04 \cdot (x/h) + 0,25$	$\psi_s = 0,04 \cdot (x/h) + 0,05$
$15 \le x/h \le 20$	$\psi_s = 0,03 \cdot (x/h) + 0,40$	$\psi_s = 0,07 \cdot (x/h) - 0,40$
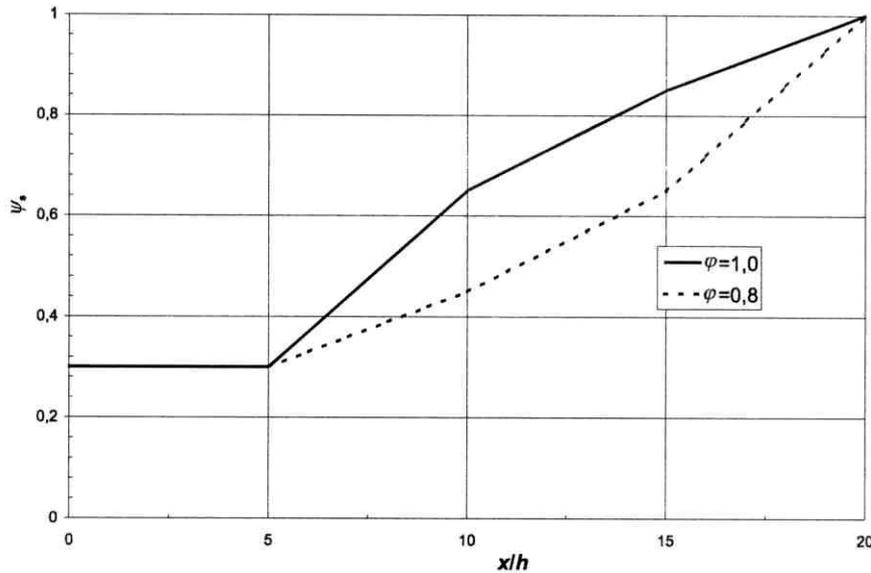
Figure G.23 – Shelter factor ψ_s.
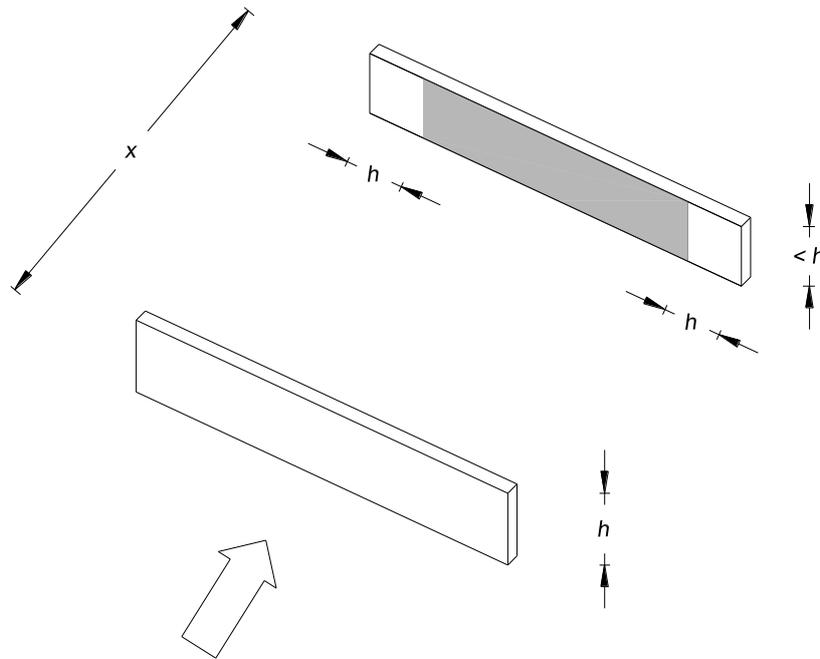
Figure G.24 – Sheltering effect.

G.6 Canopies

This section provides criteria for assessing the overall wind actions on roofs not resting on permanent vertical walls, i.e. whose underlying space is not permanently closed by walls.

Blockage φ is defined as the ratio of the projected area of any obstruction under the canopy and the overall projected area under the canopy (Figure G.25). Two limit cases are identified:

- $\varphi=0$ represents a canopy with no obstructions (empty canopy);
- $\varphi=1$ represents the fully obstructed canopy.

Case $\varphi=1$ is quite different from that specified for buildings, as an obstruction could also be represented by elements that do not enclose space under the canopy.

Downwind of the location of maximum blockage the value $\varphi=0$ shall be used.

The actions that the wind exerts on canopies depend on blockage, as the presence of an obstruction, even on just the downwind side, prevents airflow under the canopy.

Empty canopy, φ=0   *Blocked canopy, φ=1*
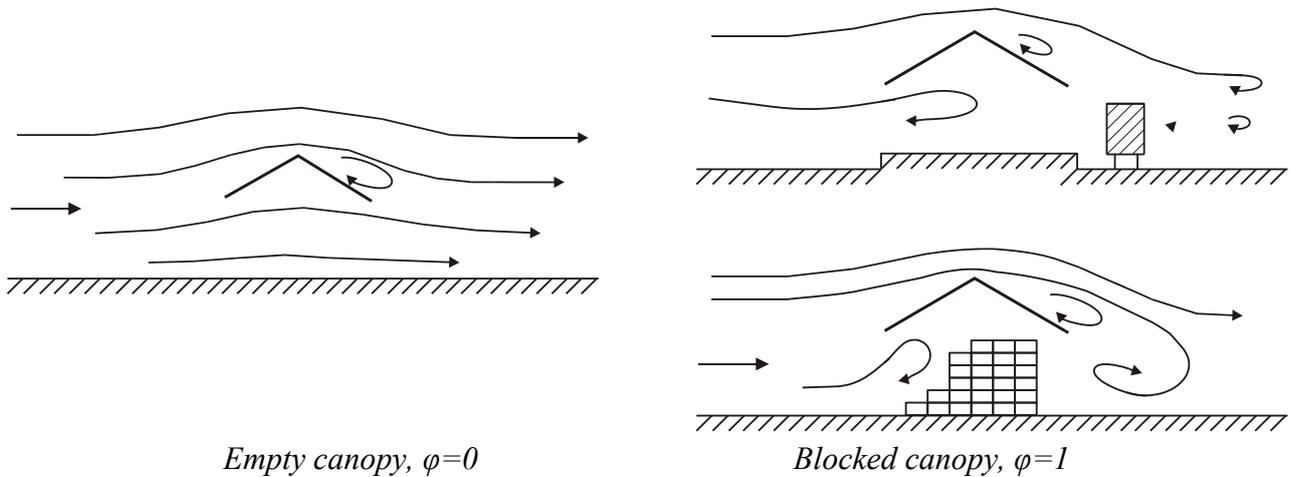
Figure G.25 – Differences in airflow for canopies with φ=0 and φ=1.

This clause describes the wind action on canopies through forces *F* perpendicular to the plane of each canopy slope. These forces are quantified through force coefficients, c_F, and the position of their point of application (clause 3.3.3).

Annex H gives the values of net pressure coefficient that can be used to assess local actions on the elements or sections of single-layer canopies. The calculation of local pressure on the upper and lower sides of double-layer canopies requires specific assessments and, where necessary, wind tunnel testing.

G.6.1 Monopitch canopies

Table G.XII and Figure G.26 give force coefficients for monopitch canopies with wind blowing at right angles to the ridge. Force coefficients are expressed as a function of the degree of blockage φ and pitch angle α of the slope. For intermediate values of φ the force coefficients can be obtained by linear interpolation between the cases φ=0 and φ=1.

The reference height $\bar{z}$ is equal to the maximum height *h* of the canopy. The reference area L^2, i.e. the area on which the resultant force is applied, is equal to the area of the canopy.

Table G.XII – Force coefficients for monopitch canopies (α in °).

Positive values	All values of φ	$c_F = +\,0{,}2 + \alpha/30$
Negative values	φ = 0	$c_F = -\,0{,}5 - 1{,}3 \cdot \alpha/30$
	φ = 1	$c_F = -1{,}4$
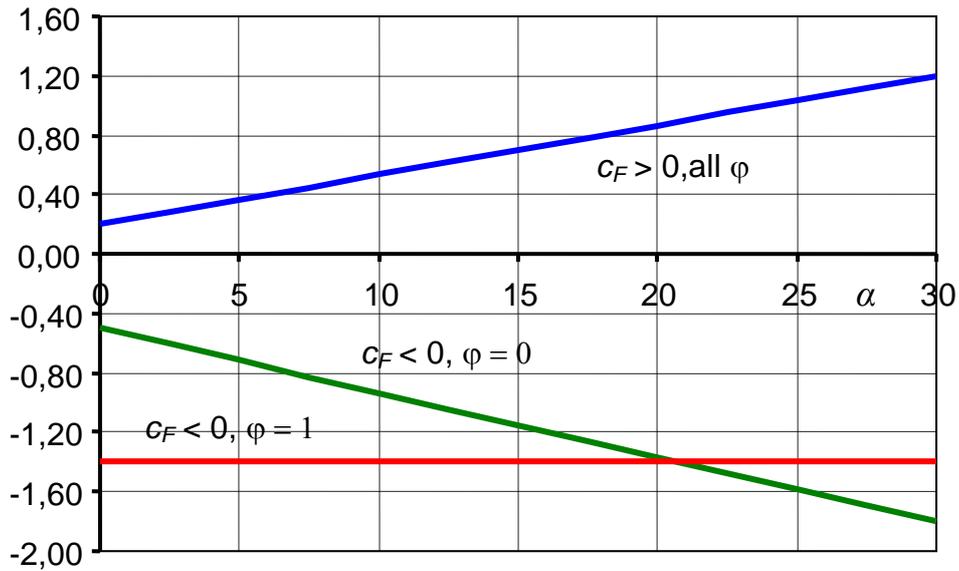
Figure G.26 – Net pressure coefficients for monopitch canopies.

When performing the calculation of the canopy, the worst load cases of the four shown in Figure G.27 has to be considered, where the resultant force $F = q_p(\bar{z}) \cdot L^2 \cdot c_F$ (Eqs 3.13a,b,c) is applied at $d/4$ from the windward edge.
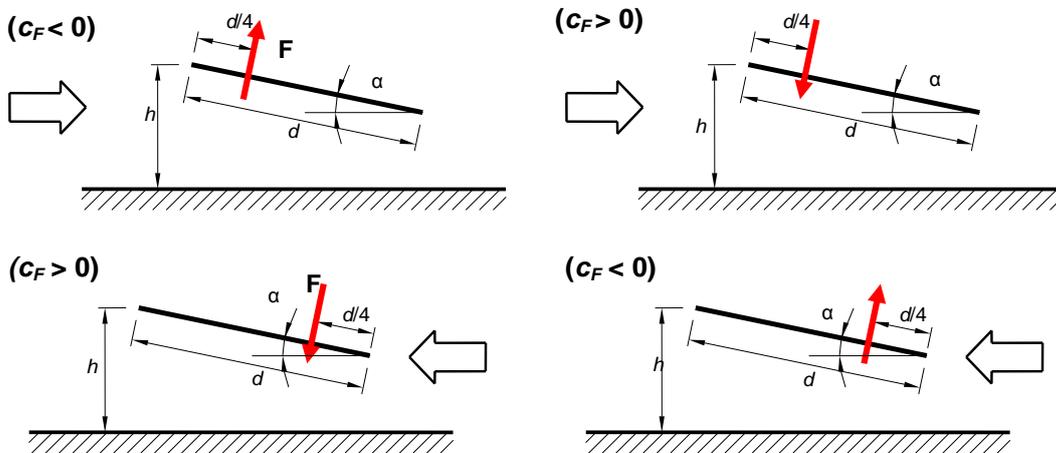
Figure G.27 – Monopitch canopies: location of the resultant force for different wind and force directions.

As a first approximation, monopitch canopies with wind acting parallel to the ridge may be analysed as flat monopitch canopies ($\alpha = 0°$).

G.6.2 Duopitch canopies

Table G.XIII and Figure G.28 give force coefficients for duopitch canopies (of equal pitch) with wind blowing at right angles to the ridge. Force coefficients are expressed as a function of the degree of blockage φ and pitch angle α of the slopes For intermediate values of φ the force coefficients can be obtained by linear interpolation between the cases $\varphi=0$ and $\varphi=1$.

The reference height $\bar{z}$ is equal to the maximum height h of the canopy. The reference area L^2, i.e. the area on which the resultant force is applied, is equal to the area of each canopy slope.

Table G.XIII – Force coefficients for duopitch canopies (α in °).

Positive values	All values of φ	$c_F = +\,0,2 + 0,7 \cdot |\alpha|/30$	
Negative values	$\varphi = 0$	$\alpha \leq 0°$	$c_F = -\,0,5 + 0,1 \cdot \alpha/10$
		$\alpha \geq 0°$	$c_F = -\,0,5 - 0,2 \cdot \alpha/10$
	$\varphi = 1$	all values of α	$c_F = -\,1,4$
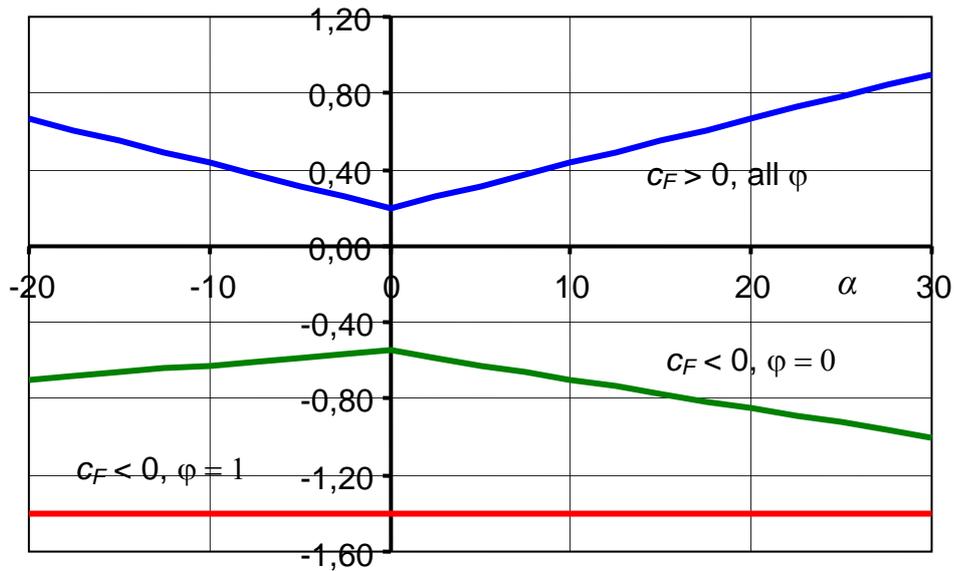
Figure G.28 – Force coefficients for duopitch canopies.
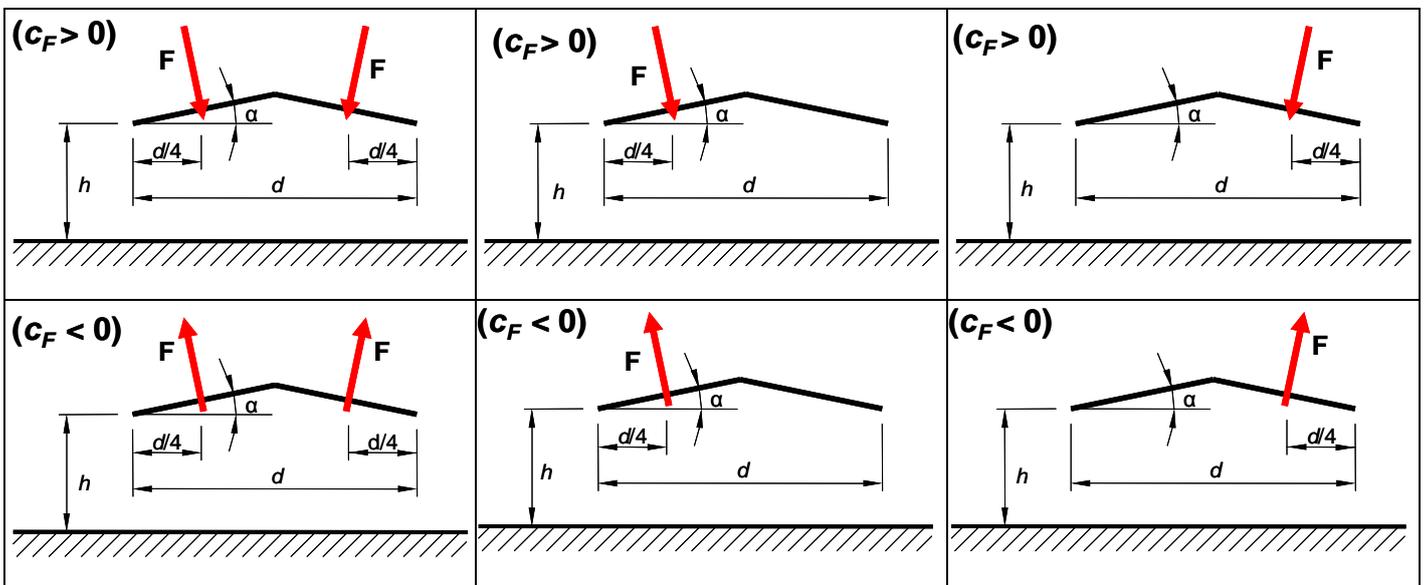
Figure G.29a – Duopitch canopies: location of the resultant force for the different wind and force directions – key for $\alpha > 0°$.
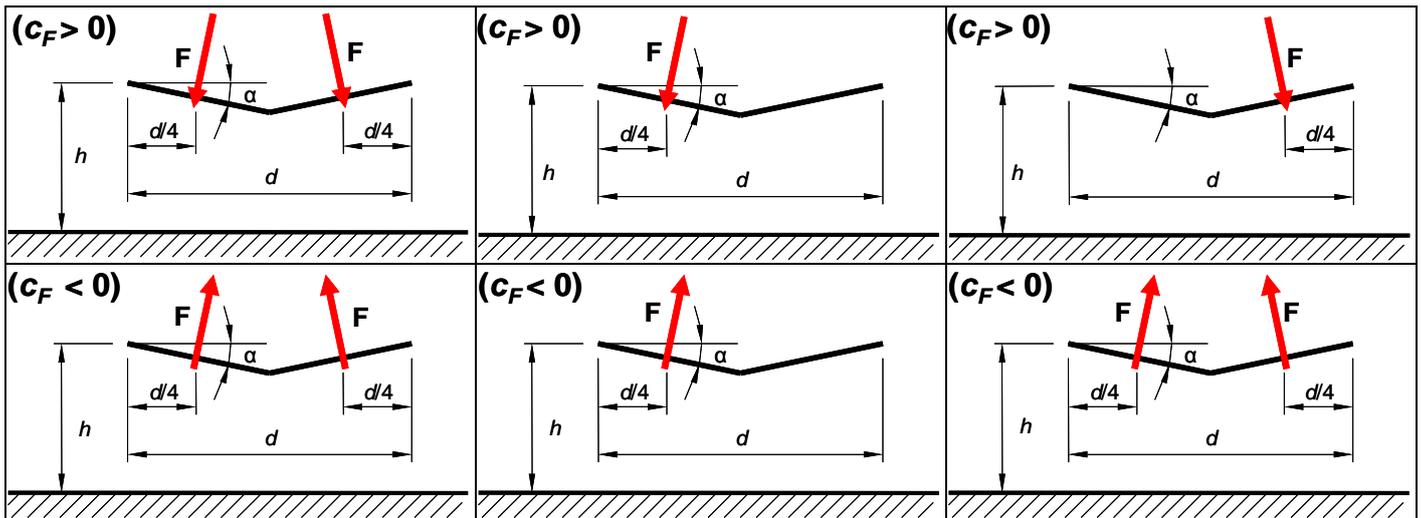
Figure G.29b – Duopitch canopies: location of the resultant force for the different wind and force directions – key for α<0°.

When performing the calculation of the canopy, the worst load cases of those shown in Figure G.29 have to be considered, where the resultant force $F = q_p(\overline{z}) \cdot L^2 \cdot c_F$ (Eqs 3.13a,b,c) is considered to be acting simultaneously on both slopes or on one of them.

As a first approximation, each slope of duopitch canopies with wind acting parallel to the ridge can be analysed as a flat monopitch canopy (α = 0°).

G.6.3 Multibay canopies

As a first approximation, each pair of slopes of canopies made of several pairs of adjoining slopes (of equal pitch) may be analysed as a single duopitch canopy (clause G.6.2).

For wind perpendicular to the direction of the ridges and referring to the geometry of Figure G.30, the force coefficients can be multiplied by the reduction factors given in Table G.XIV, in accordance with the scheme illustrated in Figure G.30.
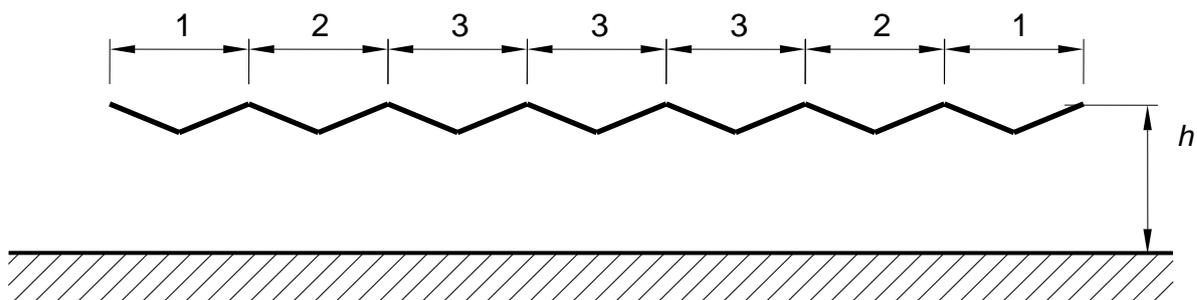
Figure G.30 – Reference scheme for multibay canopies.

Table G.XIV – Force reduction factors for multibay canopies.

Element No.	Location	Reduction factors for all values of φ	
		for $c_F > 0$	for $c_F < 0$
1	End bay	1,0	0,8
2	Second bay	0,9	0,7
3	Third and subsequent bays	0,7	0,7

G.7 Signboards

Signboards are flat elements separated from the ground by a height z_g of at least a quarter of their own height h, $z_g/h \geq 1/4$ (Figure G.31).

This section gives the aerodynamic action through a force F perpendicular to the plane of the element. This force is given through a force coefficient $c_F = 1,8$ and the location of its point of application (clause 3.3.3).

The reference height is equal to $\bar{z} = z_g + 0,5 \cdot h$ (Figure G.31). The reference area L^2, i.e. the area on which the resultant force is applied, is equal to $b \cdot h$, $L^2 = b \cdot h$. The force is to be applied at a height $z = z_g + 0,5 \cdot h$, with a horizontal eccentricity $e = \pm 0,25 \cdot b$.
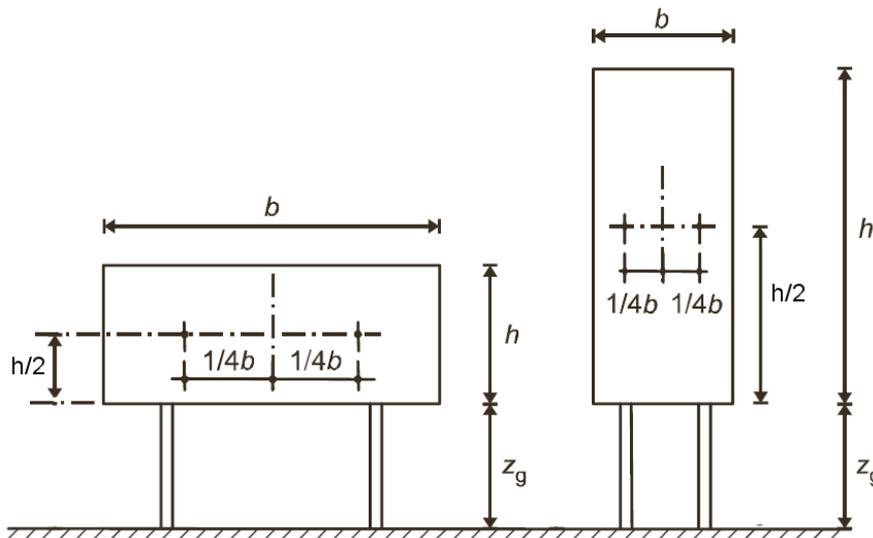
Figure G.31 – Geometry of signboards.

For $z_g/h < 1/4$ there are two possible scenarios. Elements with prevailing horizontal development ($h < b$) can be treated in accordance with clause G.5. Elements with prevailing vertical development ($h > b$) can still be treated as signboards provided the reference height is equal to $\bar{z} = z_g + h$.

G.8 Compact bodies

G.8.1 Spheres

The wind exerts on spherical bodies located not too far from the ground a pair of resultant forces F_X and F_Z acting along the X and Z axes shown in Figure G.32. These forces are given through a pair of force coefficients c_{FX} and c_{FZ} (clause 3.3.3).
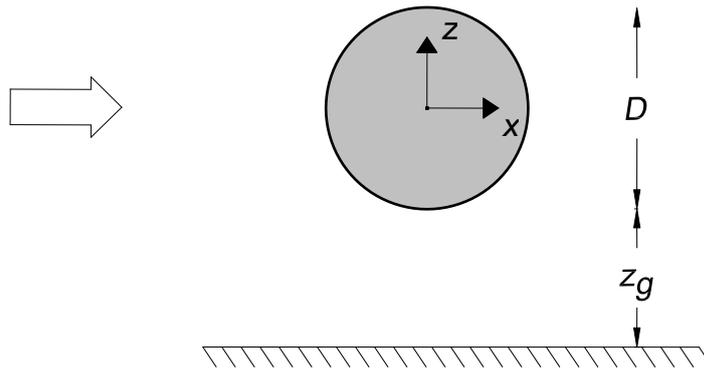
Figure G.32 – Geometry of spheres.

The force coefficient c_{FX} depends on the Reynolds number Re and on the surface roughness k. It is defined by Figure G.33 and by the equation G.6:

$$
\begin{aligned}
c_{FX} &= 0,6 & 10^5 &\leq Re \leq 2,5 \cdot 10^5 \\
c_{FX} &= -1,194 \cdot \log_{10}(Re) + 7,05 & 2,5 \cdot 10^5 &\leq Re \leq 10^7 \\
c_{FX} &\geq 0,2 & k/D &= 10^{-5} \\
c_{FX} &\geq 0,3 & k/D &= 10^{-4} \\
c_{FX} &\geq 0,4 & k/D &= 10^{-3}
\end{aligned}
\tag{G.6}
$$
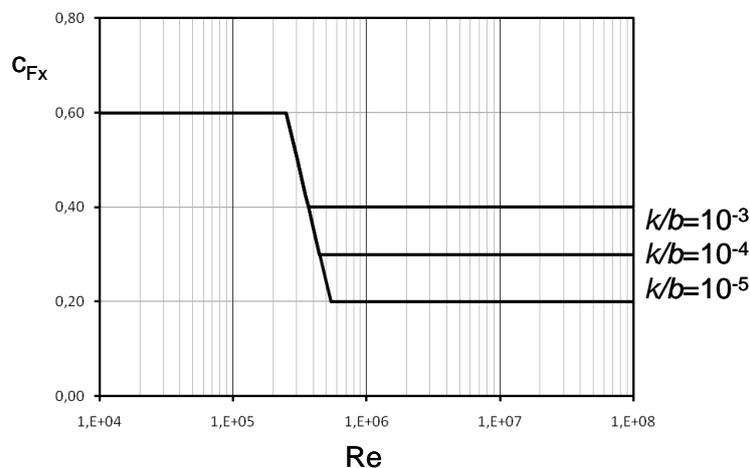
Figure G.33 – Force coefficient c_{FX} for spherical bodies.

The Reynolds number must be calculated in accordance with the equation given in clause 3.3.7 where the reference length is equal to the diameter of the sphere, $l=D$. The reference area L^2, i.e. the area on which the resultant force is applied, is equal to $A = \pi \cdot D^2/4$, $L^2 = A$. The reference height is equal to the height above ground of the centre if the sphere, $\bar{z} = z_g + 0,5 \cdot D$ (Figure G.32).

The values of the force coefficient given by Figure G.33 and Eq. (G.6) are limited to cases where the distance of the centre of the sphere from the horizontal reference surface is more than D. If this is not the case, the values given by Figure G.33 and Eq. (G.6) must be be increased by a factor of 1,6.

The vertical force coefficient c_{FZ} is given by the equation:

$$c_{FZ} = 0 \quad \text{for} \quad z_g \geq \frac{D}{2} \qquad \text{(G.7a)}$$

$$c_{FZ} = 0{,}6 \quad \text{for} \quad z_g < \frac{D}{2} \qquad \text{(G.7b)}$$

In theory, the remaining aerodynamic coefficients should be zero. In practice, even small geometrical imperfections can lead to values of these coefficients other than zero. Therefore, in all cases where such imperfections cannot be excluded, their possible effects must be considered through conservative values of the aerodynamic coefficients.

G.8.2 Parabolic antennas

The wind exerts on parabolic antennas a set of aerodynamic actions defined in clause 3.3.3 using Eq. 3.13. However, when the oncoming wind direction is in the vertical plane of symmetry of the parabola, the aerodynamic action reduces to a force F_X parallel to the axis of the parabola,,a force F_Z perpendicular to the axis of the parabola and in the vertical plane, and a moment in the plane of symmetry, M_Y (Figure G.34). These actions are quantified by a pair of force coefficients, c_{FX} and c_{FZ}, and a moment coefficient, c_{MY}.
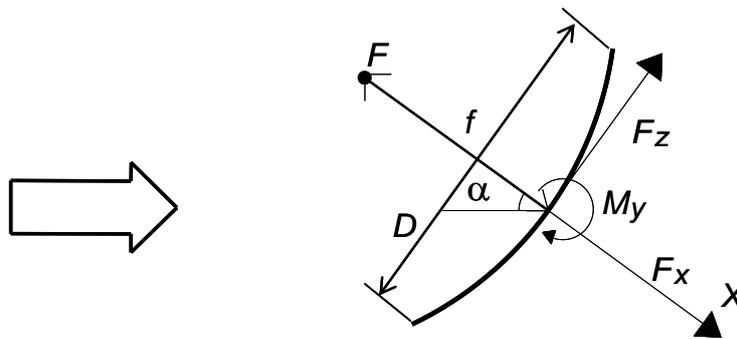
Figure G.34 – Aerodynamic actions on parabolic antennas.

The coefficient c_{FX} depends on the angle α of the parabola axis to the horizontal and on the ratio f/D, where f is the focal length (F is the focal point) and D the diameter of the parabola (Figure G.34). It is defined by Figure G.35 and by the equation G.8:

$$
\begin{aligned}
c_{FX} &= -0{,}0521 \cdot \alpha + 5{,}03 \\
&-0{,}7 \leq c_{FX} \leq 1{,}8 \qquad f/D = 0{,}2 \\
&-1{,}1 \leq c_{FX} \leq 1{,}5 \qquad f/D = 1{,}0
\end{aligned}
\qquad \text{(G.8)}
$$

where α is the angle of inclination in degrees (°).

For ratios f/D ranging from 0,2 to 1,0, linear interpolation of the values given in Figure G.35 is allowed. For values outside the range f/D = 0,2-1,0, the use of values lower than those given in Figure G.35 is not allowed.
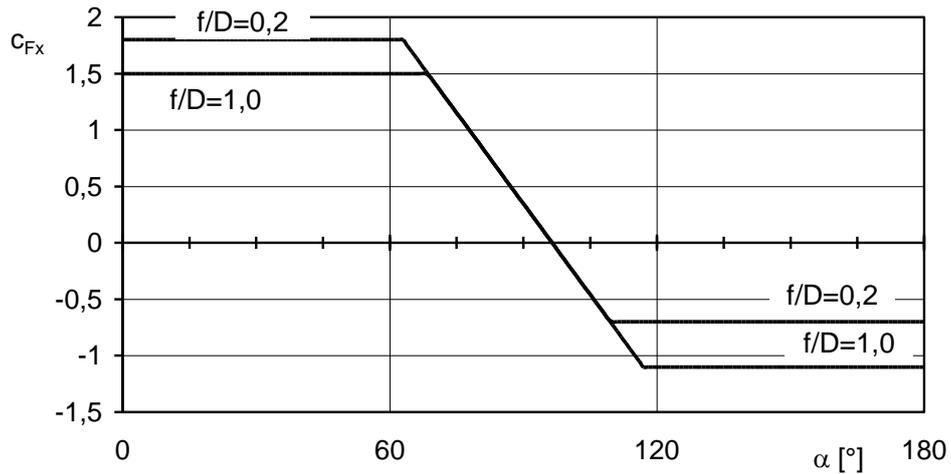
Figure G.35 – Force coefficient c_{FX} for parabolic antennas.

The coefficient c_{FZ} depends on the angle α and on the ratio f/D (Figure G.34). It is defined by Figure G.36 and by the equation G.9:

$$
\begin{aligned}
c_{FZ} &= 0,05 & \alpha &\leq 75° \\
c_{FZ} &= 0,01 \cdot \alpha - 0,7 & 75° &< \alpha \leq 90° \\
c_{FZ} &= 0,0023 \cdot \alpha - 0,0025 & 90° &< \alpha \leq 130° \\
c_{FZ} &= -0,006 \cdot \alpha + 1,08 & 130° &< \alpha \leq 180°
\end{aligned}
\qquad f/D = 0,2
$$

$$
\begin{aligned}
c_{FZ} &= -0,1 & \alpha &\leq 60° \\
c_{FZ} &= 0,005 \cdot \alpha - 0,4 & 60° &< \alpha \leq 80° \\
c_{FZ} &= 0,002 \cdot \alpha - 0,16 & 80° &< \alpha \leq 130° \\
c_{FZ} &= -0,002 \cdot \alpha + 0,36 & 130° &< \alpha \leq 180°
\end{aligned}
\qquad f/D = 1,0
$$

(G.9)

where α is the angle of inclination in degrees (°).
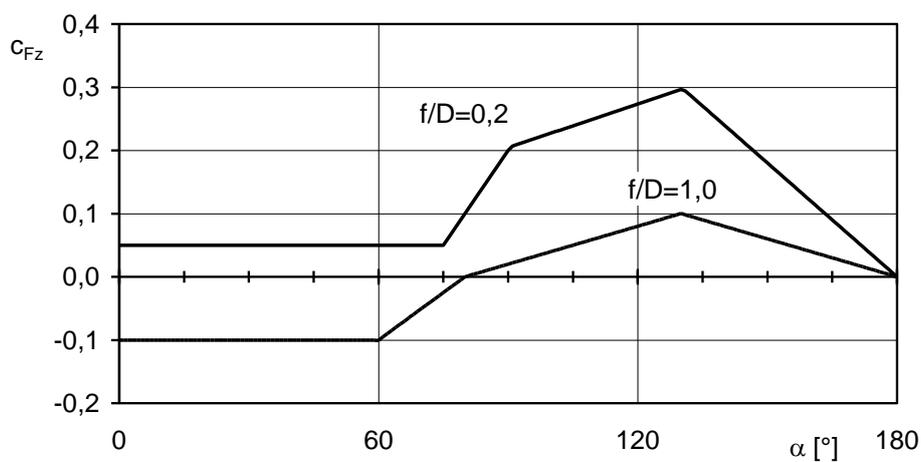
Figure G.36 – Force coefficient c_{FZ} for parabolic antennas.

For ratios f/D ranging from 0,2 to 1,0, linear interpolation of the values given in Figure G.36 is allowed provided they have the same sign, otherwise both values of opposite sign must be

considered. For values outside the range f/D = 0,2-1,0, the use of values lower than those given in Figure G.36 is not allowed.

The moment coefficient c_{MY} is given by the equation:

$$c_{MY} = c_{FZ} \cdot \frac{x_{FZ}}{D}$$

(G.10)

where x_{FZ} is the eccentricity of the transverse force given in Figure G.37.
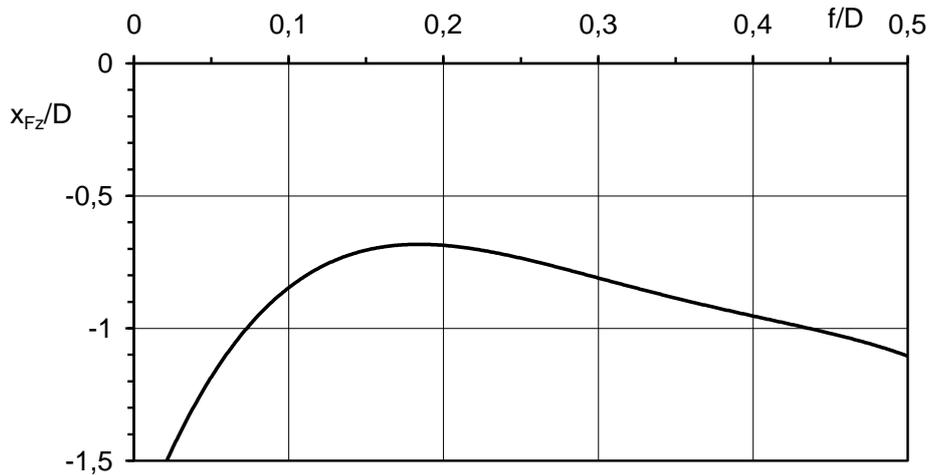
Figure G.37 – Eccentricity of the transverse force F_Z for parabolic antennas.

The reference area L^2, i.e. the area on which the resultant force is applied, is equal to the parabola projected area on a plane perpendicular to its axis, $A = \pi \cdot D^2/4$, $L^2 = A$. The reference height is equal to the height above the ground of the focal point F of the parabola (Figure G.34).

G.9 Lattice structures

G.9.1 General

This section gives aerodynamic coefficient for plane trusses and lattice structures. In both cases, the wind exerts on the structure or structural sections a force F_X applied in direction X that generally coincides with the along-wind direction (clause 3.3.3). This force is quantified by a force coefficient c_{FX} given by the equation:

$$c_{FX} = c_{FXo} \cdot \psi_\lambda$$

(G.11)

where:
c_{FXo} is the force coefficient for structures of infinite length;
ψ_λ is the slenderness factor that takes account of edge effects.

Clause G.9.2 gives force coefficients c_{FXo} for plane trusses. Clause G.9.3 gives force coefficients c_{FXo} for 3-D lattices. Clause G.9.4 gives the slenderness factor. For the aerodynamic coefficients of individual structural members forming the truss, refer to clause G.10.

G.9.2 Plane trusses

The density φ of a plane truss is the ratio between the net projected area A_n (on the plane perpendicular to the wind direction) of the truss elements (members and gusset plates), and the gross projected area A_c. For example, should the wind direction be perpendicular to a rectangular plane truss (Figure G.40), the density φ is given by the equation G.12:

$$\varphi = \frac{A_n}{A_c} = \frac{\sum b_i \cdot \ell_i + \sum A_{gk}}{\ell \cdot d} \tag{G.12}$$

where b_i and ℓ_i are the width and length of the individual member i, A_{gk} is the area of k-th gusset plate and d and ℓ are the width and length of the truss.
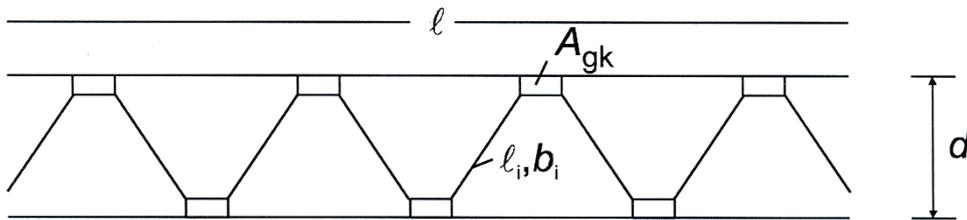
Figure G.38 – Key for rectangular plane trusses.

In the case of flow perpendicular to plane of the truss, the wind exerts on the whole truss, or on a portion of it, a force in direction X perpendicular to the plane of the truss (Eq. G.11). Ignoring edge effects (clause G.9.4), this force is quantified through a force coefficient c_{FXo}, generally a function of the truss density φ, of the shape of structural members and, in the case of rounded sections, of their Reynolds number Re.

The force coefficient c_{FXo} for plane trusses with sharp-edged structural members is given by the equation G.13 (Figure G.39):

$$
\begin{aligned}
c_{FXo} &= -1,778 \cdot \varphi + 2 & 0 \le \varphi \le 0,225 \\
c_{FXo} &= 1,6 & 0,225 \le \varphi \le 0,9 \\
c_{FXo} &= 4 \cdot \varphi - 2 & 0,9 \le \varphi \le 1
\end{aligned}
\tag{G.13}
$$
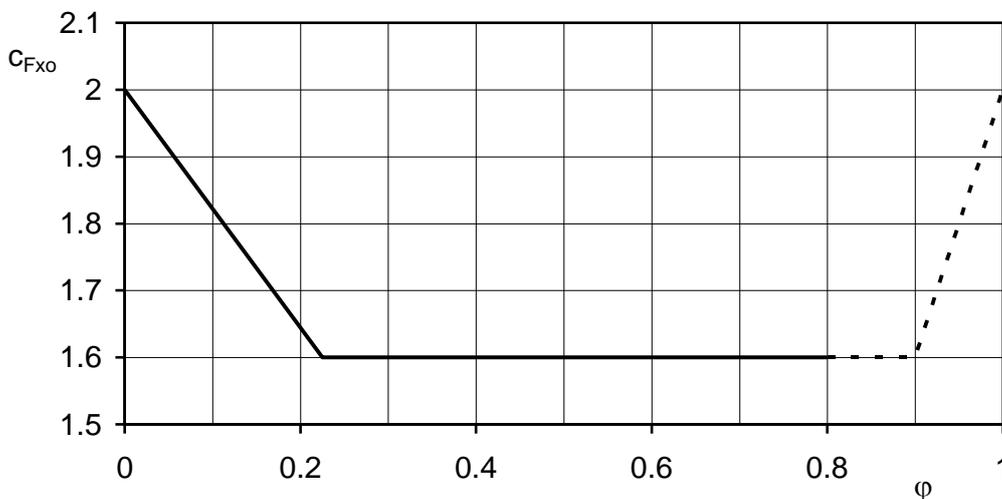
Figure G.39 – Force coefficient c_{FXo} for plane trusses with sharp-edged members.

The force coefficient c_{FXo} for plane trusses with circular structural members and density φ ranging from 0,2 to 0,6 is given by the equation G.14 (Figure 40):

$$
\begin{aligned}
c_{FXo} &= 1,1 & 10^4 \leq Re \leq 2 \cdot 10^5 \\
c_{FXo} &= -1,33 \cdot \log_{10}(Re) + 8,16 & 2 \cdot 10^5 \leq Re \leq 5 \cdot 10^5 \\
c_{FXo} &= 0,2 \cdot \log_{10}(Re) - 0,57 & 5 \cdot 10^5 \leq Re \leq 10^6
\end{aligned}
\tag{G.14}
$$

The reference area L^2, i.e. the area on which the resultant force is applied, is equal to the net area A_n, $L^2 = A_n$. The reference height $\bar{z}$ is equal to the maximum height of the truss, or of its portion, considered in each particular case.
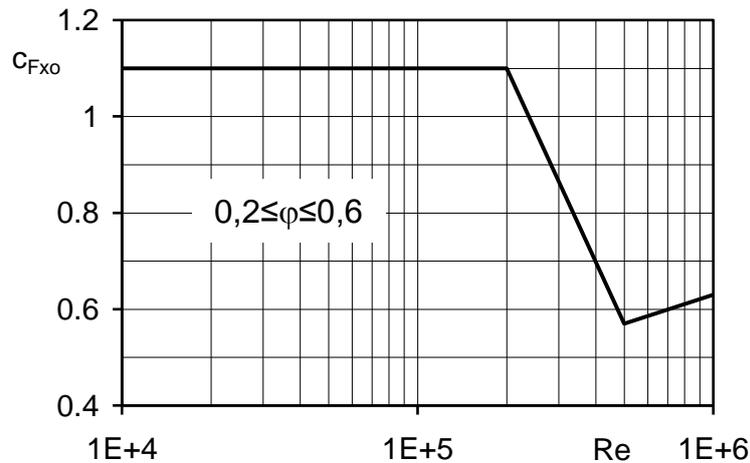
Figure G.40 – Force coefficient c_{FXo} for plane trusses with circular members.

When the flow is not perpendicular to the plane of the truss, the force in the *X* direction (perpendicular to the plane of the truss) is lower than in the case of perpendicular flow (Eq. G.11). This reduction may be taken into account by multiplying the force coefficient c_{FXo}, defined by Eqs. (G.13) and (G.14) and Figures G.39 and G.40, by the factor ψ_α given by the equation G.15 (Figure G.41):

$$
\psi_\alpha = -0,00013 \cdot \alpha^2 + 0,00035 \cdot \alpha + 1
\tag{G.15}
$$

in which α is the angle (°), in the horizontal plane, between the oncoming wind direction and that normal to the plane of the truss.
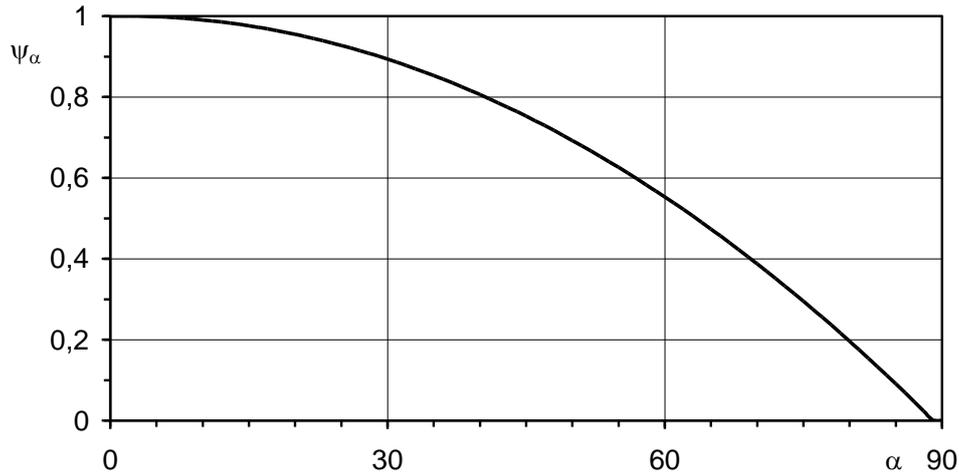
Figure G.41 – Reduction factor for skewed wind.

In the case of several plane trusses parallel to each other and with flow perpendicular to them, the force in X direction (perpendicular to the plane of the trusses) acting on the downstream trusses is lower than that acting on the upstream truss (Eq. G.11). This reduction may be taken into account by multiplying the force coefficient c_{FXo}, defined by Eqs. (G.13) and (G.14) and Figures G.39 and G.40 for the upstream truss, by the sheltering factor ψ_s given by Figure G.42 and the equation G.16:

$$\psi_s = 0,75 - 0,35 \cdot c_{FXo} \qquad\qquad \text{for } x/d \le 3 \qquad\qquad \text{(G.16a)}$$

$$\psi_s = 0,75 - 0,35 \cdot c_{FXo} \quad ; \quad \psi_s > 0,1 \cdot x/d \qquad \text{for } x/d > 3 \qquad\qquad \text{(G.16b)}$$

where:
x is the distance between the downstream and the upstream trusses;
d is the dimension of the truss shown in Figure G.38;
c_{FXo} is the force coefficient of the upstream truss.
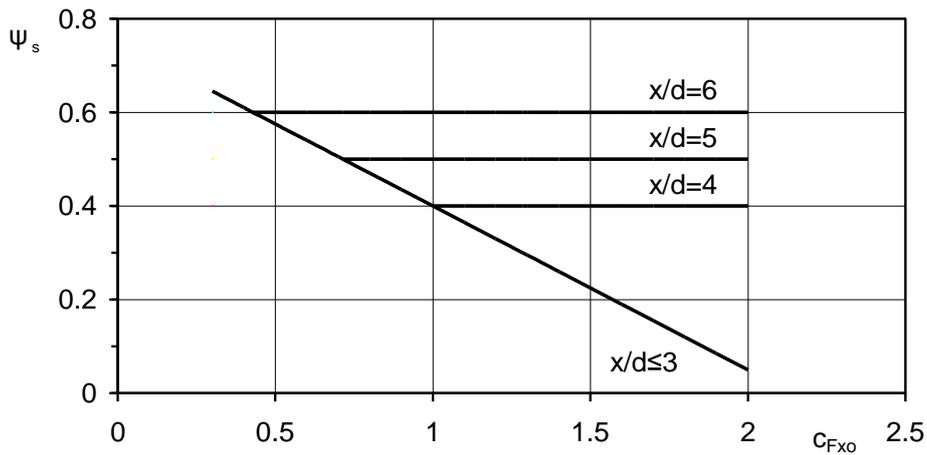
Figure G.42 - Sheltering factor.

Under no circumstances should reduction factors ψ_α and ψ_s be combined. Therefore, in the case of trusses arranged downwind from another truss with flow not perpendicular to their plane, the force coefficient c_{FXo} may be reduced by just one of the two factors ψ_α or ψ_s, whichever is larger.

G.9.3 Lattices

The density φ of all or part of the lattices is calculated by using Eq. (G.12) where the geometrical sizes of elements are those projected on a plane perpendicular to the wind direction (Figure G.43). Elements (members and gusset plates) in the wake of other elements are not included in the calculation.
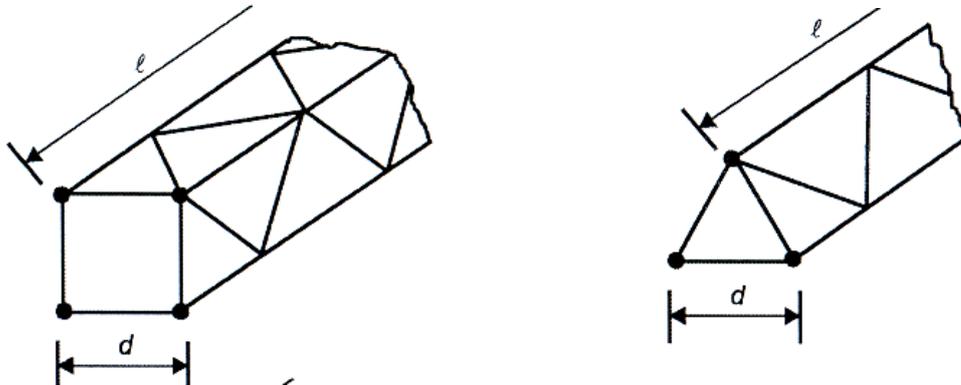
Figure G.43 – Characteristic dimensions of lattice girders.

In the case of lattices with a square or triangular cross section, the wind exerts on all or part of the lattice girder a force in the direction X of the oncoming flow (Eq. G.11). Ignoring edge effects, this force is quantified through a force coefficient c_{FXo}, generally a function of the lattice density φ, of the shape of structural members and, in the case of rounded sections, of their Reynolds number Re.

Figures G.44 and G.45 give typical values of coefficient c_{FXo} for sharp-edged structural members and for circular members, respectively.
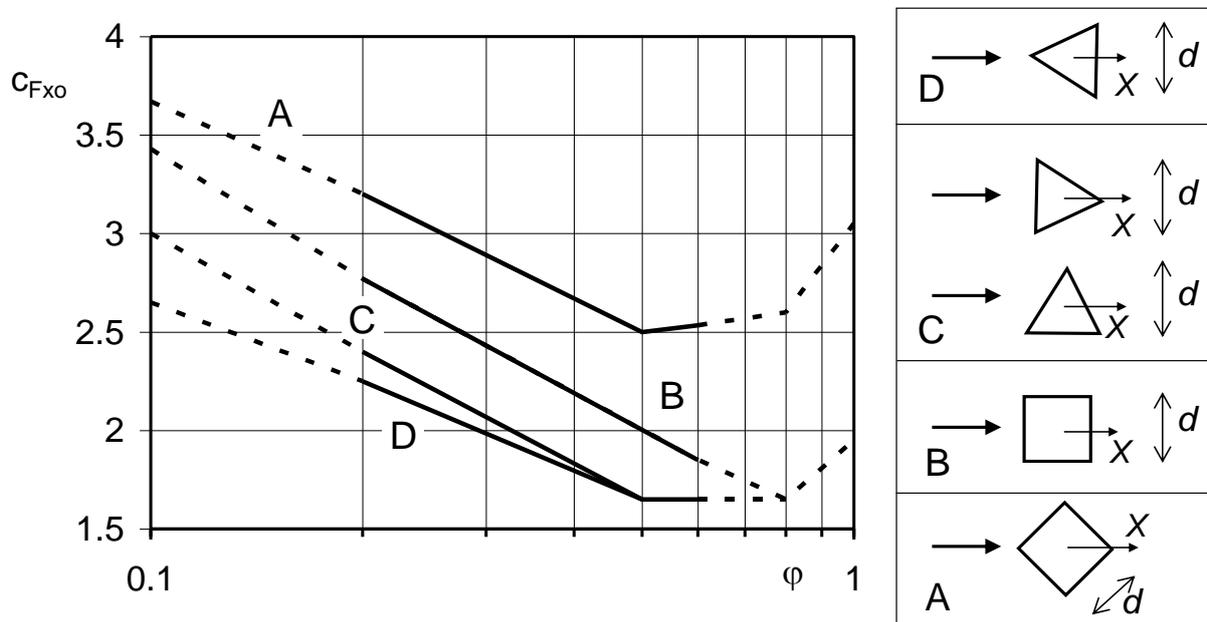
Figure G.44 – Force coefficient c_{FXo} for lattices with sharp-edged members.
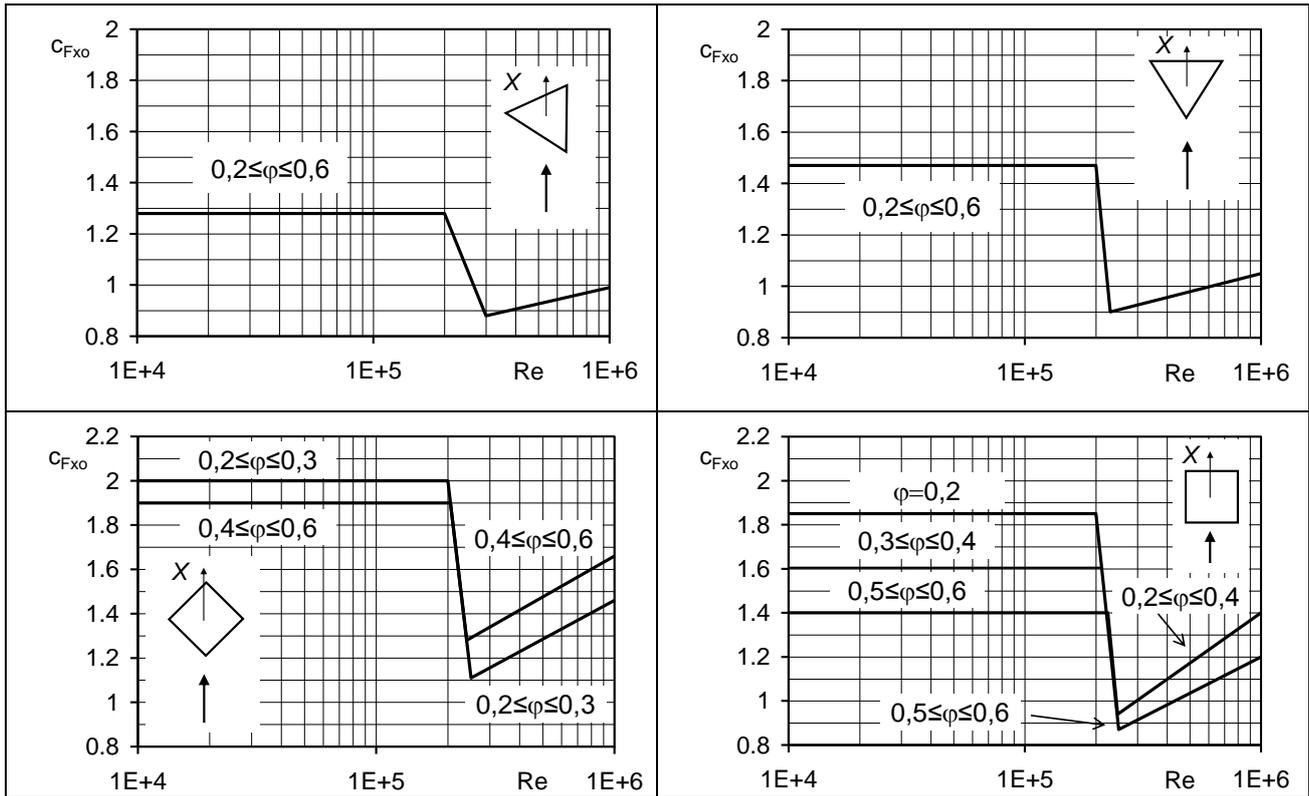
Figure G.45 – Force coefficient c_{FXo} for lattices with circular members.

The reference area L^2, i.e. the area on which the resultant force is applied, is equal to the net area A_n, $L^2 = A_n$. The reference height $\overline{z}$ is equal to the maximum height of the lattice, or of its portion, considered in each particular case.

G.9.4 Slenderness factor

The aerodynamic coefficients given in clauses G.9.2 and G.9.3 apply to trusses and lattices of infinite length. In practice, these structures have finite length and therefore edge reduction effects must be accounted for. Such reduction can be ignored or, otherwise, it can be quantified through the slenderness factor ψ_λ.

The slenderness factor ψ_λ is given by the equation G.17 (Figure G.46):

$$\varphi = 0,1 \quad \begin{cases} \psi_\lambda = 0,005 \cdot \log_{10}(\lambda) + 0,985 & 1 \le \lambda \le 10 \\ \psi_\lambda = 0,01 \cdot \log_{10}(\lambda) + 0,98 & 10 \le \lambda \le 100 \\ \psi_\lambda = 1 & 100 \le \lambda \le 200 \end{cases}$$

$$\varphi = 0,5 \quad \begin{cases} \psi_\lambda = 0,025 \cdot \log_{10}(\lambda) + 0,885 & 1 \le \lambda \le 10 \\ \psi_\lambda = 0,07 \cdot \log_{10}(\lambda) + 0,84 & 10 \le \lambda \le 100 \\ \psi_\lambda = 0,066 \cdot \log_{10}(\lambda) + 0,85 & 100 \le \lambda \le 200 \end{cases} \quad (G.17)$$

$$\varphi = 0,9 \quad \begin{cases} \psi_\lambda = 0,05 \cdot \log_{10}(\lambda) + 0,825 & 1 \le \lambda \le 10 \\ \psi_\lambda = 0,097 \cdot \log_{10}(\lambda) + 0,778 & 10 \le \lambda \le 100 \\ \psi_\lambda = 0,093 \cdot \log_{10}(\lambda) + 0,786 & 100 \le \lambda \le 200 \end{cases}$$

where λ is the dimensionless effective slenderness (Table G.XV).

Regardless of whether the force coefficient c_{FXo} (clauses G.9.2 and G.9.3) has been calculated for all or just a part of the truss or lattice, λ depends on the overall length l of the truss (Figure G.38) or lattice (Figure G.43) and on the ratio l/d, where d is the mean reference dimension of the cross section. For φ values different from those specified in Eq. (G.17) and Figure G.46, ψ_λ can be evaluated by linear interpolation.
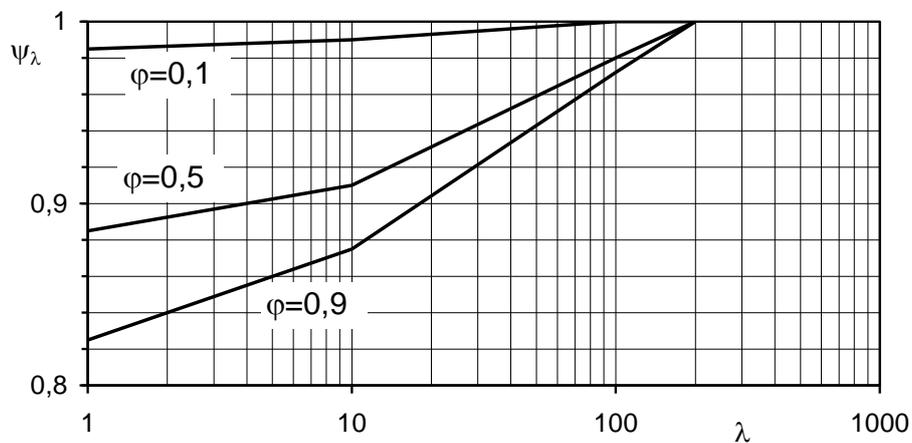
Figure G.46 – Slenderness factor ψ_λ.

Table G.XV – Effective slenderness λ.

$l \le 20$ m	$\lambda = 2 \cdot l / d$
20 m$\le l \le 50$ m	$\lambda = (2,4 - 0,02 \cdot l) \cdot l / d$
50 m $\le l$	$\lambda = 1,4 \cdot l / d$

G.10 Slender structures and elongated structural members

G.10.1 General

This section gives force and moment coefficients to be used in Eqs (3.14) for assessing aerodynamic actions per unit length on slender structures and elongated structural members with polygonal or circular section, and on metallic profiles (clause 3.3.4). These coefficients are defined for isolated structures or structural members. Members forming part of lattices must be calculated both individually, following the provisions of clauses G.10.2-G.10.6, and as part of the lattice structure as a whole, following the provisions of clause G.9. Indeed, clause G.9 considers aerodynamic interference phenomena arising amongst individual elements with consequent deviations of actions from those of an isolated member. Aerodynamic interference may lead to both a reduction or an increase in the overall action; therefore, in cases for which no provision is made herein, it cannot be taken into account other than with the support of reliable experimental data.

Force and moment coefficients per unit length are given by the equations G.18:

$$c_{fX} = c_{fXo} \cdot \psi_{\lambda}$$ (G.18a)

$$c_{fY} = c_{fYo} \cdot \psi_{\lambda}$$ (G.18b)

$$c_{mZ} = c_{mZo} \cdot \psi_{\lambda}$$ (G.18c)

where:

c_{fXo}, c_{fYo}, c_{mZo} are the force and moment coefficients per unit length for structures and components of infinite length, therefore with two-dimensional aerodynamic behaviour in the cross section plane;

ψ_{λ} is the slenderness factor that takes account of edge reduction effects.

Clauses G.10.2-G.10.7 give values of the aerodynamic coefficients c_{fXo}, c_{fYo} and c_{mZo} for the most common geometric shapes, examining case by case the dependence of these parameters on the Reynolds number, surface roughness and wind direction. In particular, clause G.10.2 deals with structures and components with a square cross section and sharp or rounded corners. Clause G.10.3 deals with rectangular structures and components. Clause G.10.4 deals with regular polygonal structures and components. Clause G.10.5 deals with metallic profiles. Clause G.10.6 deals with circular structures and components. Clause G.10.7 deals with cables. Clause G.10.8 gives the slenderness factor.

The reference height of slender structures and elongated members dealt with in clauses G.10.2-G.10.7 is the current height z considered case by case.

G.10.2 Structures and components with a square cross section

In the case of flow perpendicular to a face, the wind exerts on structures and components with a square cross section a force per unit length in the direction of flow X given by Eq. (G.18a). Ignoring edge effects, this force is quantified through a force coefficient c_{fXo}.

For sharp-edged sections, regardless of Reynolds number and surface roughness, the force coefficient is $c_{fXo} = 2,1$.

Although theoretically zero when the wind blows at right angles to one side of the square, the force coefficient transverse to the wind direction, c_{fYo}, and torsional moment coefficient, c_{mZo}, may take values other than zero even in the case of slight deviations of the oncoming wind direction. In order to take account of this situation and any flaws in the geometric configurations, rather than zero, it is recommended that $c_{fYo}= \pm 0,3$ be used.

For sections with rounded corners, aerodynamic parameters depend on the corner radius r, on the Reynolds number and on the surface roughness. Whilst considering just the dependence on the corner radius to be conservative, the coefficient c_{fXo} can be reduced as a function of the ratio r/l of corner radius r and side l of the section, using the multiplication factor ψ_r given by Eq. G.19 (Figure G.47):

$$\psi_r = 1 - 2,5 \cdot \frac{r}{l} \quad ; \quad \psi_r \geq 0,5 \tag{G.19}$$
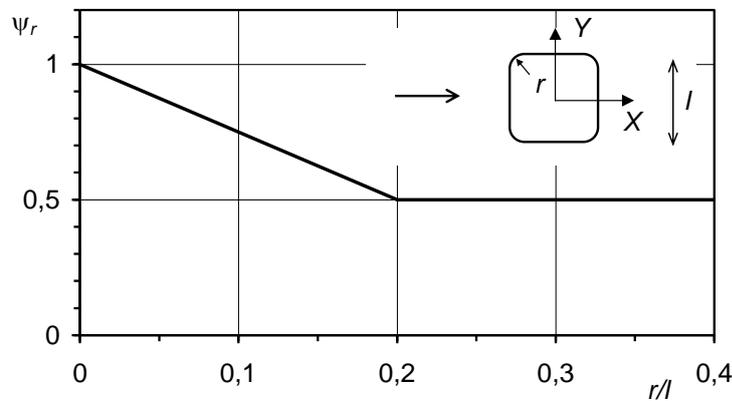
Figure G.47 – Aerodynamic force reduction factor for square sections with rounded corners (wind perpendicular to a face).

In the case of flow along a diagonal, indicating the axes perpendicular to the faces with X and Y, the wind exerts on structures and components with a square cross section a pair of forces per unit length, in directions X and Y, given by Eqs. (G.18a) and (G.18b). Ignoring edge effects, these forces are quantified through a pair of force coefficients c_{fXo} and c_{fYo}.

For sharp-edged sections, regardless of Reynolds number and surface roughness, the force coefficients are $c_{fXo} = c_{fYo} = 1,55$.

For sections with rounded corners, aerodynamic parameters depend on the corner radius r, Reynolds number and surface roughness. Whilst considering just the dependence on the Reynolds number to be conservative, the force coefficients c_{fXo} and c_{fYo} can be reduced as a function of the ratio r/l of corner radius r and side l of the section using the multiplication factor ψ_r given by Eq. G.20 (Figure G.48):

$$\psi_r = 1 - 0,75 \cdot \frac{r}{l} \quad ; \quad \psi_r \geq 0,7 \tag{G.20}$$

In each case the reference dimension l is equal to the side of the section.
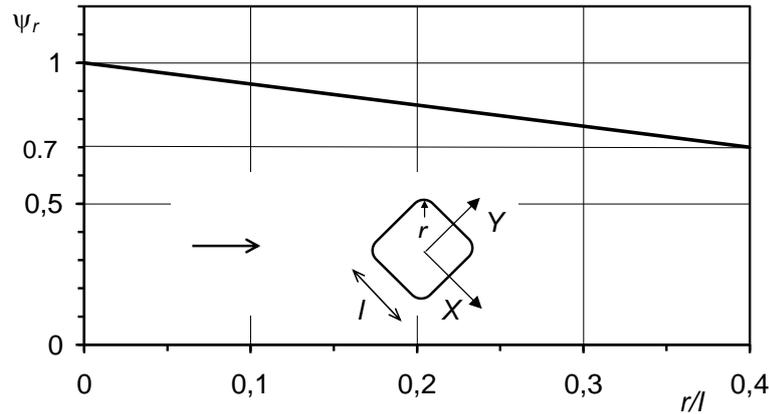
Figure G.48 – Aerodynamic force reduction factor for square sections with rounded corners (diagonal wind direction).

G.10.3 Rectangular structures and components

In the case of flow perpendicular to a face, the wind exerts on rectangular structures and components a force per unit length in the direction of flow X given by Eq.(G.18a). Ignoring edge effects, this force is quantified through a force coefficient c_{fXo}.

For sharp-edged sections, the force coefficient in the wind direction depends on the section aspect ratio d/b (Figure G.49) and to a much lesser extent on the Reynolds number and surface roughness. It is given by the equation G.21 (Figure G.49):

$$c_{fXo} = 2,0 \qquad\qquad 0,1 \le d/b \le 0,2$$

$$c_{fXo} = 0,73 \cdot \log_{10}\left(d/b\right) + 2,51 \qquad 0,2 \le d/b \le 0,7$$

$$c_{fXo} = -1,64 \cdot \log_{10}\left(d/b\right) + 2,15 \qquad 0,7 \le d/b \le 5 \qquad\qquad \text{(G.21)}$$

$$c_{fXo} = -0,33 \cdot \log_{10}\left(d/b\right) + 1,23 \qquad 5 \le d/b \le 10$$

$$c_{fXo} = 0,9 \qquad\qquad 10 \le d/b \le 50$$
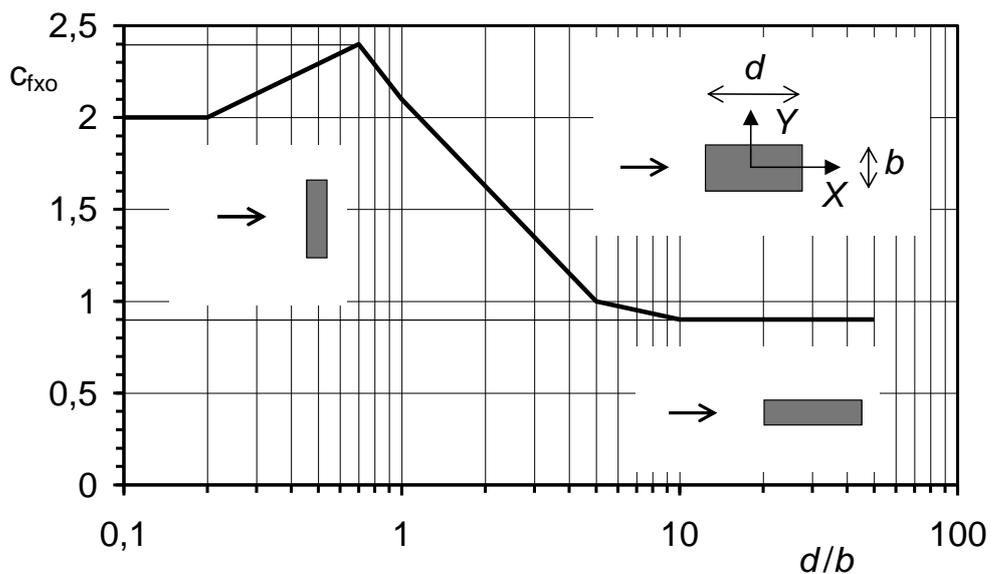
Figure G.49 – Force coefficient c_{fXo} for rectangular sections.

Although theoretically zero when the wind blows at right angles to one side of the rectangle, the transverse force coefficient, c_{fYo}, and torsional moment coefficient, c_{mZo}, may take values other than zero even in the case of slight deviations of the oncoming wind direction. This mainly occurs to plate-like sections in the wind direction. It is recommended that such possibility should be taken into account by using conservative non-zero values for these coefficients.

The reference length for rectangular structures and components is $l=b$ (Figure G.49).

G.10.4 Structures and components with regular polygonal section

In the case of flow perpendicular to a face or along an axis of symmetry, the wind exerts on structures and components with regular polygonal section a force per unit length in the direction of flow X given by Eq. (G.18a). Ignoring edge effects, this force is quantified through a force coefficient c_{fXo}.

For sharp-edged polygonal sections, the flow separation can be dictated by the edges, as in the case of polygons with a small number of faces, or by the flow, as in the case polygons with a large number of faces, whose aerodynamic behaviour approaches that of a circular section. Table G.XVI gives force coefficients c_{fXo} for the most common sections, assuming a smooth surface; these are to be considered the highest values obtained upon varying the angle of the wind direction, except in the case of a triangular section for which two wind directions are considered.

The reference length l is equal to the diameter of circumscribed circle.

Table G.XVI – Force coefficient c_{fXo} for regular polygonal sections.

Section	c_{fXo}
Triangle – upwind vertex	1,5
Triangle – downwind vertex	1,7
Pentagon	1,8
Hexagon	1,6
Octagon	1,4
Decagon	1,3
Dodecagon	1,2

Although theoretically zero when the wind blows along an axis of symmetry of the section, the transverse force coefficient, c_{fYo}, and torsional moment coefficient, c_{mZo}, may take values other than zero even in the case of slight deviations of the oncoming wind direction. This mainly occurs to polygons with a small number of faces. It is recommended that such possibility should be taken into account using conservative non-zero values for these coefficients.

G.10.5 Metallic profiles

The wind exerts on metallic profiles a pair of forces per unit length in directions X and Y in the plane of the cross-section given by Eqs.(G.18a) and (G.18b). Ignoring edge effects, these forces are quantified through a pair of force coefficients c_{fXo} and c_{fYo}.

Figure G.50 gives force coefficients c_{fXo} and c_{fYo} for the most common metallic sections. For some coefficients c_{fYo} a pair of values is given (positive and negative). This is the case of symmetric sections for which, even though theoretically zero, the transverse force coefficient may take non-zero values due to a small deviation of the flow .
The reference length is $l=b$ (Figure G.50).

α [°]	c_{fXo}	c_{fYo}
0	2,0	0
45	1,8	0,1
90	0,1	0

α [°]	c_{fXo}	c_{fYo}
0	2,05	0
45	1,95	0,6
90	$\pm 0,5$	0,9

α [°]	c_{fXo}	c_{fYo}
0	1,6	0
45	1,5	1,5
90	0	1,9

α [°]	c_{fXo}	c_{fYo}
0	2,05	0
45	1,85	0,6
90	0	0,6
135	-1,6	0,4
180	-1,8	0

α [°]	c_{fXo}	c_{fYo}
0	1,8	1,8
45	2,1	1,8
90	-1,9	-1,0
135	-2,0	0,3
180	-1,4	-1,4

α [°]	c_{fXo}	c_{fYo}
0	1,9	0,95
45	1,8	0,8
0	2,0	1,7
135	-1,8	-0,1
180	-2,0	0,1

α [°]	c_{fXo}	c_{fYo}
0	2,0	0
45	1,2	0,0
90	-1,6	2,15
135	-1,1	2,5
180	-1,7	$\pm 2,1$

α [°]	c_{fXo}	c_{fYo}
0	1,75	0,1
45	0,85	0,85
90	-0,1	1,75
135	-0,75	-0,75
180	-1,75	-0,1

α [°]	c_{fXo}	c_{fYo}
0	1,6	0
45	1,5	-0,1
90	-0,95	0,7
135	-0,5	1,05
180	-0,1	-1,5

Figure G.50 – Force coefficients for metallic profiles.

G.10.6 Circular structures and components

The wind exerts on circular structures and components a force per unit length in the direction *X* of flow given by Eq. (G.18a). Ignoring edge effects, this force is quantified through a force coefficient c_{fXo}.

Figure G.51 gives force coefficients c_{fXo} for circular sections as a function of the Reynolds number *Re* and of the ratio *k/b*, where *k* is the surface roughness and *b* the section diameter. Curves A and B shown in Figure G.51 are given by the equations G.22:

$$c_{fXo} = \frac{0,056}{\left(Re/10^6\right)^{1,4}} \leq 1,2 \qquad\qquad (\text{curva A}) \qquad\qquad (G.22a)$$

$$c_{fXo} = 1,255 + \frac{0,197 \cdot \log_{10}\left(10 \cdot k/b\right)}{1 + 0,4 \cdot \log_{10}\left(Re/10^6\right)} \geq 0,4 \quad \left(k/b \geq 10^{-5}\right) \qquad (\text{curva B}) \qquad\qquad (G.22b)$$

The choice between curve A and curve B is made based on the value of the Reynolds number.

The Reynolds number is calculated based on clause 3.3.7, where the reference dimension *l* is the diameter *b*. Table G.XVII gives reference values for the roughness *k* of the most common materials.
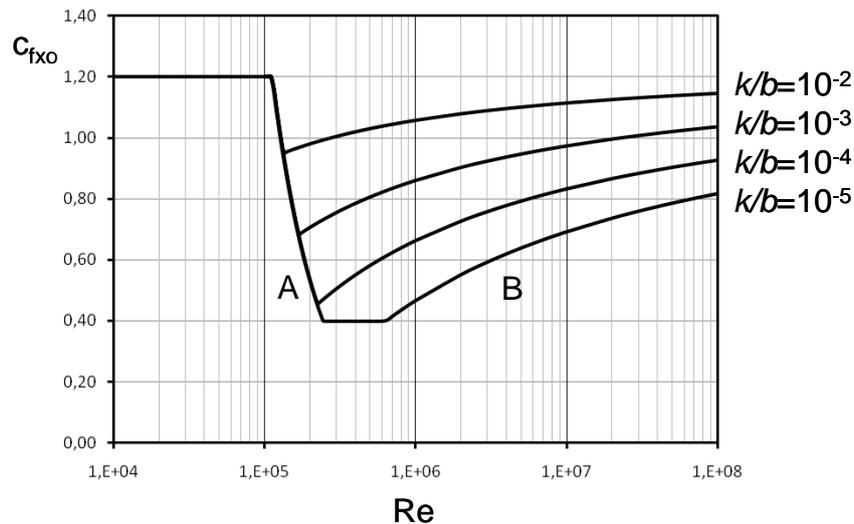
Figure G.51 – Force coefficient c_{fXo} for circular structures and components.

Table G.XVII – Surface roughness k.

Surface area	k [mm]
Glass	0,0015
Polished metal	0,002
Fine paint	0,006
Spray paint	0,02
Bright steel	0,05
Cast iron	
Galvanised steel	0,2
Smooth concrete	
Planed wood	0,5
Rough concrete	1,0
Rough wood	
Rusted surfaces	2,0
Brickwork	3,0

Although theoretically zero, the transverse force coefficient, c_{fYo}, and torsional moment coefficient, c_{mZo}, may take values other than zero due to even very slight imperfections in the shape of a nominally-circular section. They may also be very different from zero, especially in sections of small diameter, due to the formation of ice or water rivulets. It is recommended that such possibilities should be taken into account using conservative non-zero values for these coefficients.

In the case of circular structures with large diameter but moderate wall thickness, it is often necessary to assess the effects produced by radial pressure distribution. To this end, reference should be made to clause G.3 by assigning the values specified in clause G.10.8 to the slenderness factor ψ_λ in Eq. (G.3).

G.10.7 Cables

The wind exerts on cables a force per unit length in the direction of flow X given by Eq. (G.18a). Ignoring edge effects, this force is quantified through a force coefficient c_{fXo}.

As in the case of circular components, the force coefficient of cables depends on the Reynolds number Re and on the surface roughness. In particular, roughness can be expressed by the ratio of the strand diameter d (of the outer layer should not all strands have the same diameter) and the cable external diameter D (Figure G.52). The force coefficient c_{fXo} is given in Table G.XVIII.

The reference length is equal to the external diameter, $l=D$.
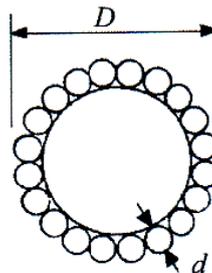
Figure G.52 – Cable geometry.
Table G.XVIII – Force coefficient c_{fXo} for cables.

d/D	$Re < 4 \cdot 10^4$	$Re > 4 \cdot 10^4$
0,07		0,85
0,1	1,2	0,95
0,15		1,05
0,2	1,3	1,11
0,3		1,18

G.10.8 Slenderness factor

The aerodynamic coefficients given in clauses G.10.2-G.10.7 apply to a two-dimensional flow condition, i.e. they can be used for structures or structural members of infinite slenderness. In practice, structures and structural members have finite slenderness which means that edge effects should be taken into account. The finite slenderness of structures and structural members leads to a reduction of the aerodynamic forces that would act on a structure or member of infinite slenderness. Such reduction can generally be ignored or, otherwise, it can be quantified by the slenderness factor ψ_λ.

The slenderness factor ψ_λ is given by the equation G.23 (Figure G.53):

$$\psi_\lambda = 0,6 + 0,1 \cdot \log_{10}(\lambda) \quad \text{for} \quad 1 \leq \lambda \leq 10 \tag{G.23a}$$

$$\psi_\lambda = 0,45 + 0,25 \cdot \log_{10}(\lambda) \quad \text{for} \quad 10 \leq \lambda \leq 100 \tag{G.23b}$$

$$\psi_\lambda = 0,61 + 0,17 \cdot \log_{10}(\lambda) \leq 1 \quad \text{for} \quad 100 \leq \lambda \leq 1000 \tag{G.23c}$$

where λ is the dimensionless effective slenderness (Table G.XV). It depends on the length L of the structure or component, on the ratio L/l, where l is the mean reference dimension of the cross section, on the shape of the cross section and on the flow conditions at the two ends of the structure or component. Two possiblities are considered here: the first is that where the flow is free (in the absence of end constraints) or only slightly obstructed (e.g. in the case of ordinary unconstrained nodes of trusses) at at least one end; the second includes situations in which flow is essentially blocked at both ends (e.g. in the case of members supported by large plates or walls).
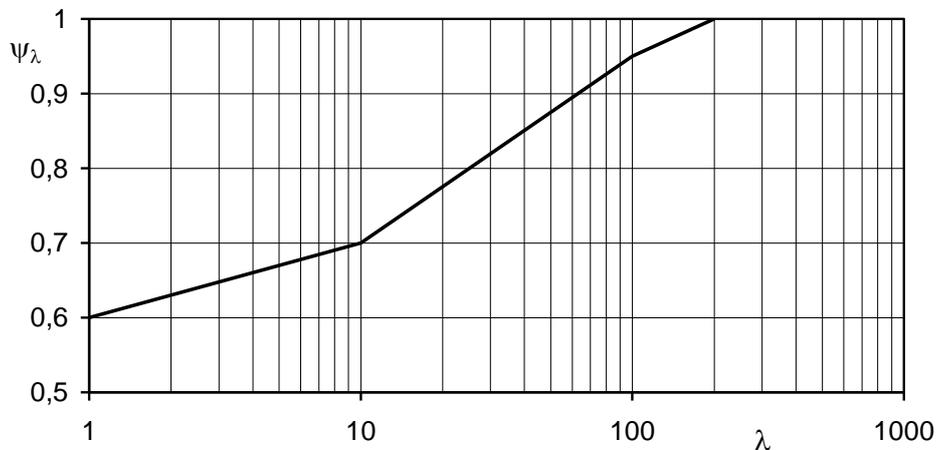
Figure G.53 – Slenderness factor ψ_λ.

Table G.XIX – Effective slenderness λ.

Length L (m)	Free flow at least one end		Flow blocked at both ends
	Sharp-edged section	Circular section	
$L \leq 20$ m	$\lambda = 2 \cdot L / l$	$\lambda = L / l$	$\lambda = L / l \geq 70$
20 m$\leq L \leq 50$ m	$\lambda = \left(2,4 - 0,02 \cdot L \right) \cdot L / l$	$\lambda = \left(1,2 - 0,01 \cdot L \right) \cdot L / l$	$\lambda = \left(1,2 - 0,01 \cdot L \right) \cdot L / l$ $\lambda \geq 70$
50 m $\leq L$	$\lambda = 1,4 \cdot L / l$	$\lambda = 0,7 \cdot L / l$	$\lambda = 0,7 \cdot L / l \geq 70$

G.11 Bridge decks

The wind flow around a bridge deck and the associated pressure distribution are very complex phenomena, highly dependent on the shape of the deck and of non structural components (e.g. wind- and noise-screens, barriers and Jersey barriers), the presence and spacing of any adjacent deck and the presence and distribution of crossing vehicles or trains. Technical and scientific publications on this subject still lack experimental data and calculation criteria that can be applied generally and with reasonable accuracy at the design and/or verification stage.

In the lack of more specific and detailed analyses and assessments, the criteria provided herein should therefore be taken as a simple preliminary, generally conservative, guide; under no circumstances should they be considered mandatory provisions. They apply to bridge decks with uniform cross sections, and of the types specified in Figure G.54 only for single or multiple span bridges of length not exceeding 200 m.

This section does not cover other bridge types such as arch bridges, suspension and cable-stayed bridges, covered or moving bridges, bridges with significantly curved decks and bridges with several adjacent decks not comparable to the simple scheme illustrated in clause G.11.2. All these structural types require specific assessments.
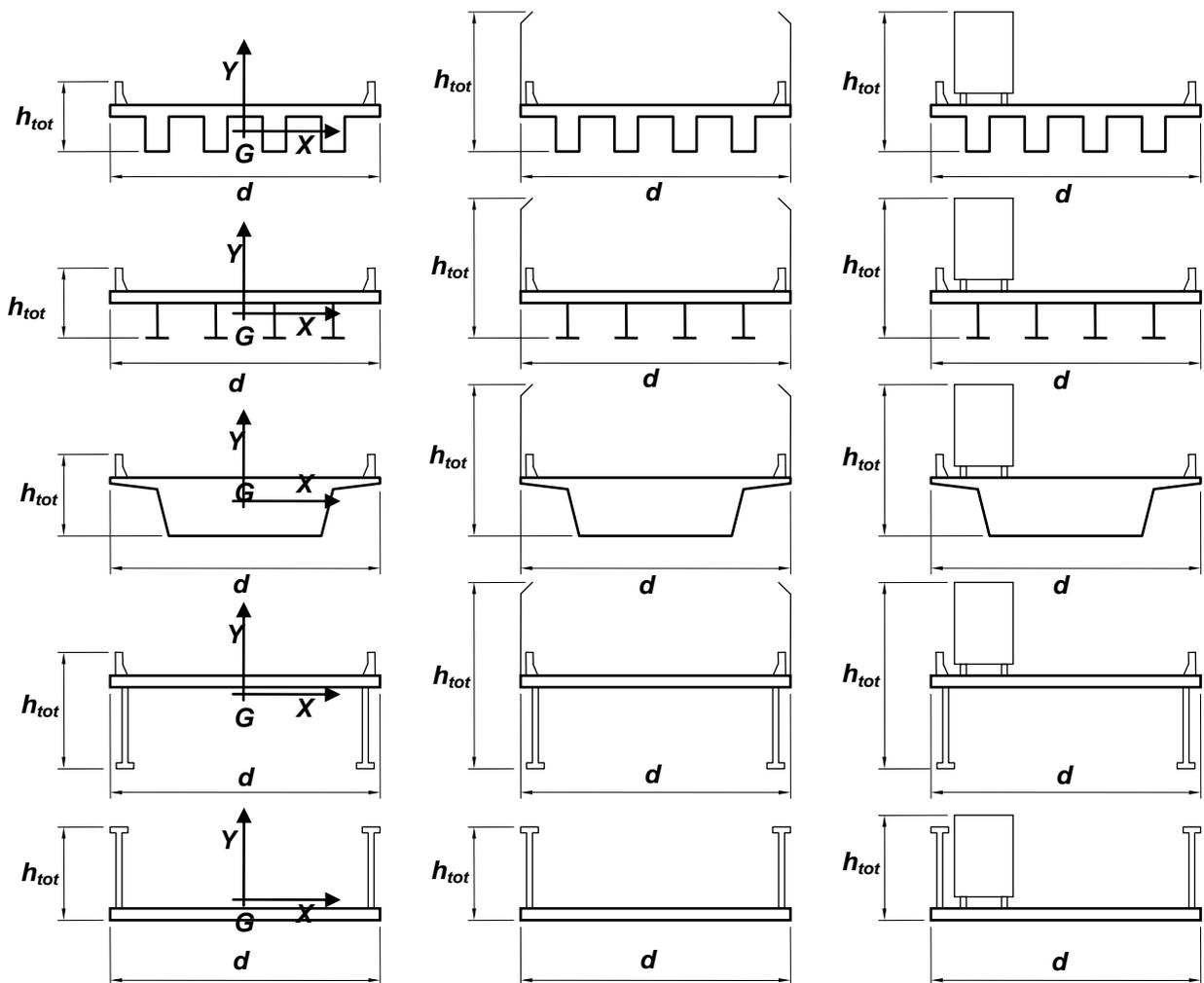
Figure G.54 – Types of bridge decks covered in this section: the last two cases refer to both plate and truss girders.

In the case of road bridges, it is assumed that the height of vehicles is 3 m along the entire bridge span.

In the case of railway bridges, it is assumed that the height of trains is 4 m along the entire bridge span.

When the wind action occurs simultaneously to road or railway loads, it should be reduced using combination factors that take into account the probability of design wind and traffic loads occurring simultaneously.

Clause G.11.1 deals with the case of an isolated deck. Clause G.11.2 examines the case of a pair of adjacent decks of similar shape.

G.11.1 Isolated deck

Assuming that the wind acts horizontally and perpendicular to the deck axis, it exerts a set of aerodynamic actions per unit length equal to an along-wind force f_X, an across-wind (vertical) force f_Y, and a torque m_Z (Figure G.54, Eq. (3.14), clause 3.3.4). These actions are quantified through a pair of force coefficients, c_{fX} and c_{fY}, and a moment coefficient, c_{mZ}.

In the lack of more accurate assessments, force and moment coefficients per unit length are given by the equations G.24:

$$c_{fX} = \begin{cases} \dfrac{1,85}{d/h_{tot}} - 0,10 & 2 \leq d/h_{tot} \leq 5 \\[4mm] \dfrac{1,35}{d/h_{tot}} & d/h_{tot} > 5 \end{cases} \tag{G.24a}$$

$$c_{fY} = \begin{cases} \pm\left(0,7 + 0,1\dfrac{d}{h_{tot}}\right) & 0 \leq d/h_{tot} \leq 5 \\[4mm] \mp 1,2 & d/h_{tot} > 5 \end{cases} \tag{G.24b}$$

$$c_{mZ} = \pm 0,2 \tag{G.24c}$$

where:
d is the deck width (Figure G.54);
h_{tot} is the overall deck height (possibly including vehicles) (Figure G.54).

Eq. (G.24a) and Figure G.55 apply for values $d/h_{tot} \geq 2$; for values $d/h_{tot} < 2$, reference can be made to the coefficients of force per unit length for rectangular slender structures and elongated members (clause G.10.3).

The aerodynamic actions f_X, f_Y and m_Z are simultaneous and shall be combined in a way such to produce the most severe effects.

If wind loads are combined with traffic loads, the height h_{tot} shall include the height of vehicles or trains. If wind loads are not combined with traffic loads, the height h_{tot} shall include the height of barriers.

The reference length l is equal to the deck width d (Figure G.54).

The reference height $\bar{z}$ is equal to the distance from the lowest ground level to the centre of the bridge deck structure increased by $h_{tot}/2$.
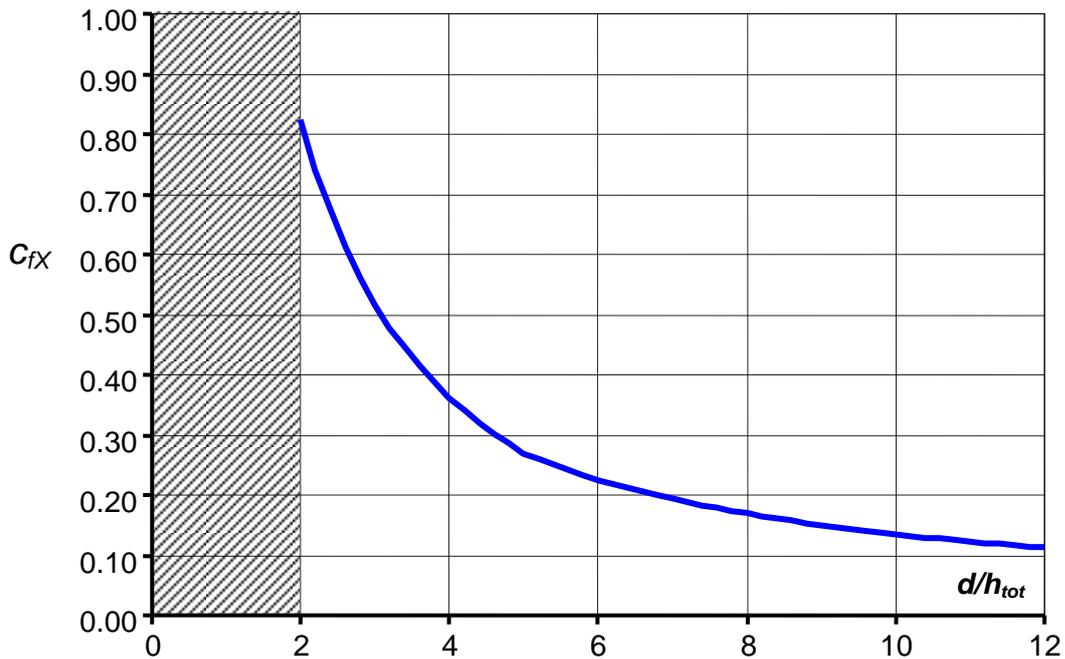
Figure G.55 – Values of coefficient c_{fX}.

G.11.2 Adjacent decks

In the case of adjacent decks (Figure G.56), considerable interference effects occur. In the case in which the two decks are similar to each other, in the lack of more detailed analyses, the provisions specified hereafter can be applied for preliminary calculations.
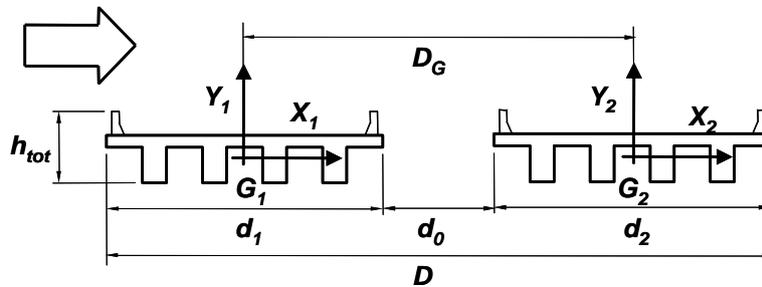
Figure G.56 – Reference dimensions for adjacent decks.

When assessing wind actions on decks, the following three cases should be considered:

a) If the gap between the decks meets the requirement (Figure G.56):

$$\frac{d_0}{\max\{d_1, d_2\}} \geq \frac{1}{4} \tag{G.25}$$

the wind actions on each deck are those that would act on the deck if it were isolated (clause G.11.1).

b) If the gap between the decks does not meet the requirement of Eq. (G.25) and the two decks are structurally independent (ignoring any connections at piers and/or abutments), the wind actions on each deck are assessed by using the following procedure:

1. wind actions on each deck are calculated as if the decks were isolated (clause G.11.1); these actions are designated by f_{X1}, f_{Y1} and m_{Z1};

2. wind actions are calculated as if the two separate decks were one single deck of overall width D (clause G.11.1); these actions are designated by f_{X2}, f_{Y2} and m_{Z2};

3. wind actions on each deck are given by the equations:

$$f_X = max \begin{cases} f_{X1} \\ 0,75 \cdot f_{X2} \end{cases}$$

(G.26a)

$$f_Y = \pm max \begin{cases} \left| f_{Y1} \right| \\ 0,5 \cdot \left| f_{Y2} \right| + \dfrac{\left| m_{Z2} \right| - \left| m_{Z1} \right|}{D_G} \end{cases}$$

(G.26b)

$$m_Z = m_{Z1}$$

(G.26c)

where D_G is the centre-to-centre distance between the two decks (Figure G.56).

c) If the gap between the decks does not meet the requirement of Eq. (G.25) and the two decks are structurally connected (either continuously or at a number of sections), the along-wind force f_X is equal to either the force calculated as if the two decks were one single deck of overall width D (Figure G.56) or the force calculated for the upstream deck as if it were isolated, whichever is greater; the across-wind force f_Y and the torque m_Z are calculated as if the two decks were one single deck of overall width D (clause G.11.1).

In order to calculate the overall actions transferred by the two decks to common supporting structures (e.g. piers or abutments common to both decks), the following procedure can be used. For cases a) and c) above, the actions exerted from the decks to common supporting structures are the resultant of wind actions on the adjacent decks. In case b) these actions are calculated by applying the criterion specified under case c) above.

G.12 Friction coefficients

The friction coefficients c_f for use in Eq. (3.15) (clause 3.3.5) are given in Table G.XX.

Table G.XX – Friction coefficients.

Surface	c_f
Steel, smooth concrete	0,01
Rough concrete, tarred surfaces	0,02
Corrugated surfaces	0,04

For the surfaces of flat elements having no flow separation (e.g. signboards and canopies), the reference area coincides with the surface area (Figure G.56). In the case of surfaces of elements subject to flow separation (e.g. roofs and side walls of buildings), the reference area is limited to that portion of the surface subjected to an attached flow; more specifically, it is assumed that area A_r subjected to friction is on the leeward side of the building and has an in-wind length equal to the smallest value of 2*b* or 4*h* (Figure G.57).

The reference height for the friction force is equal to the highest point above ground of the surface, $\bar{z} = h$ (Figure G.57).
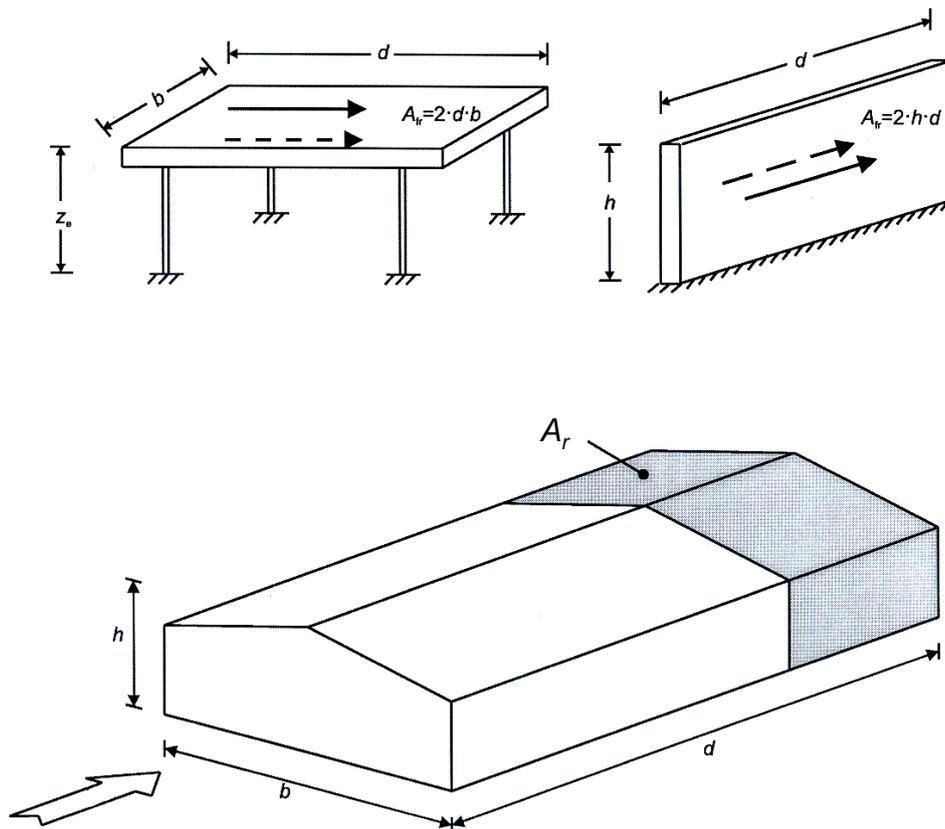
Figure G.57 – Reference area for calculating friction forces.

Annex H   DETAILED AND LOCAL AERODYNAMIC COEFFICIENTS

H.1   Introduction

This Annex provides values for the dimensionless coefficients needed to transform wind velocity pressure (clause 3.2) into local and/or detailed aerodynamic actions on buildings (both regular and irregular in shape) and canopies.

These values can be used to quantify local pressure on small structural and non-structural components of limited surface area, e.g. for assessing wind actions on individual members, cladding or their fixings.

Furthermore, only for buildings, they can be used as an alternative to the values given in Annex G when, using the equations given in clause 3.3, the pressure field has to be described in major detail; in particular, the values given in Annex G are obtained from those specified in Annex H with the aim of providing a simplified and generally conservative definition of the force or pressure field.

The values given hereinafter refer to nominal oncoming wind directions Θ perpendicular to the main faces of the structure. these directions are denoted on each occasion by $\Theta = 0°$, $\Theta = 90°$ and $\Theta = 270°$. In practice, these represent the most unfavourable values obtained in a range of wind direction $\Delta\Theta = \pm45°$ either side of the relevant orthogonal direction.

The following sections provide aerodynamic coefficients for:

- buildings with rectangular plan and uniform height (clause H.2);
- buildings with a non-rectangular plan or non-uniform height (clause H.3);
- canopies with rectangular plan (clause H.4).

For the internal pressure coefficients, reference should be made to Annex G.4. For structural types and geometries not considered herein, reference should be made to technical publications and/or to wind tunnel testing (Annex Q).

H.2   Buildings with rectangular plan and uniform height

H.2.1   General

This section gives external pressure coefficients for the walls and roof of buildings with rectangular plan and uniform height.

In addition to the shape of the building and to the oncoming wind direction, external pressure coefficients depend on the size of the loaded area. The following sections give pressure coefficients for loaded areas of 1 m^2 and 10 m^2; the corresponding values are given as $c_{pe,1}$ and $c_{pe,10}$. External pressure coefficients for different reference areas may be calculated by using the equations given in Table H.I.

Table H.I – Pressure coefficients as a function of the size of the loaded area A.

Area	External pressure coefficient
$A \leq 1\ \mathrm{m}^2$	$c_{pe} = c_{pe,1}$
$1\ \mathrm{m}^2 < A < 10\ \mathrm{m}^2$	$c_{pe} = c_{pe,1} - (c_{pe,1} - c_{pe,10}) \cdot \log_{10}(A)$
$A \geq 10\ \mathrm{m}^2$	$c_{pe} = c_{pe,10}$

Values of $c_{pe,1}$ are generally used when calculating aerodynamic actions on small elements and fixings (cladding elements, roofing elements, etc.). Values of $c_{pe,10}$ (denoted in Annex G as c_{pe}) are

used in all cases in which a less detailed representation of the pressure field on the structure is possible, e.g. when assessing overall actions on large areas of buildings or the resultant wind forces on major structural components.

For protruding eaves the following criterion is applied (Figure H.1):

- the pressure coefficient on the lower face of the eave is equal to the pressure coefficient on the vertical wall below the eave;

- the pressure coefficient on the upper face of the eave is equal to the pressure coefficient on the neighbouring area of the roof.
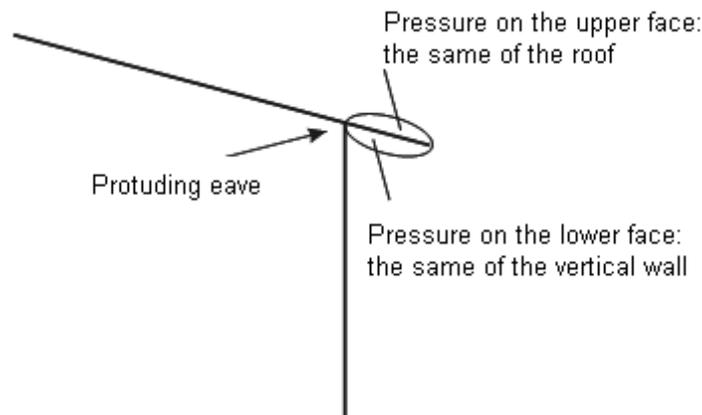
Figure H.1 – Pressure on protruding parts roof eaves.

H.2.2. Walls

The side walls of buildings with rectangular plan (Figure H.2) are divided in zones of uniform pressure coefficient as shown in Figures H.3 and H.4. External pressure coefficients for each zone are given in Table H.II as a function of h/d, where h is the height of the building and d is its along-wind plan size. For intermediate values of h/d, linear interpolation may be used.

For very slender buildings, whose h/d ratio is greater than 5, reference should be made to the provisions of clause G.10 (slender structures and elongated structural components). In this case, unlike the requirements specified in this clause, wind actions are expressed as forces per unit length.

The value of geometric parameter e shown in Figure H.4 is equal either to b or $2 \cdot h$, whichever is smaller

$$e = \min \begin{cases} b \\ 2 \cdot h \end{cases} \tag{H.1}$$

where b is the building across-wind size (Figure H.2).

The reference height $\bar{z}_e$ shall be calculated following clauses G.2.2.1 and G.2.2.2.

Where overall forces on the building are calculated as the sum of the forces acting on the windward and leeward faces, the effect of the lack of full correlation between the two actions can be taken into account by reducing the values of both pressure coefficients using a multiplication factor ψ of:

$$\psi = \begin{cases} 0,85 & \text{for} \quad h/d \leq 1 \\ 0,0375 \cdot h/d + 0,8125 & \text{for} \quad 1 < h/d \leq 5 \end{cases} \tag{H.2}$$

Torsional actions arising when the wind does not blow along an axis of symmetry, due to pressure fluctuations on the side faces or due to the partial correlation of pressures on the windward face, can be taken into account by applying the criterion specified in clause G.2.2.3.
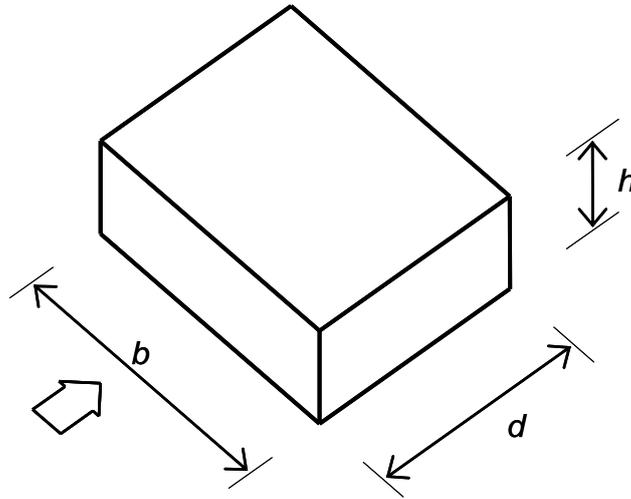
Figure H.2 – Sizes of buildings with rectangular plan.
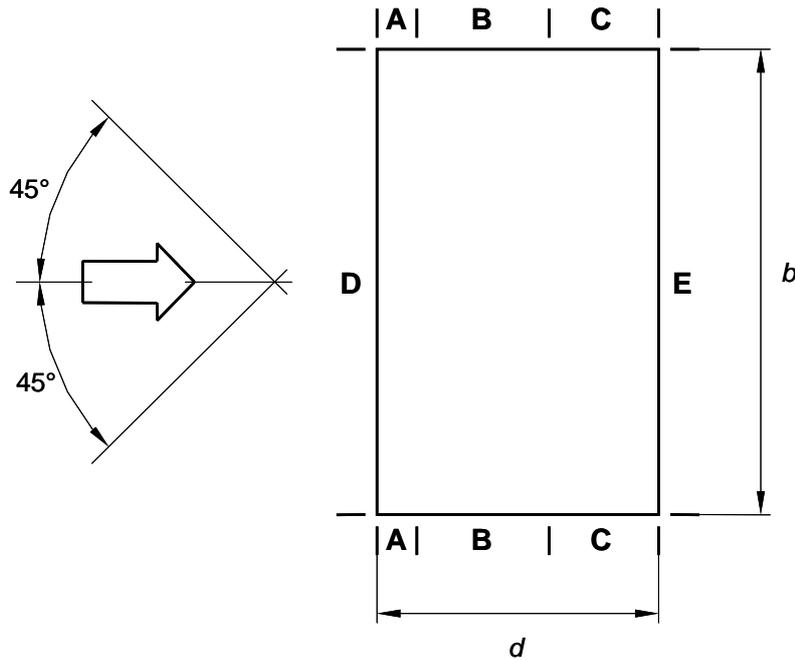
Figure H.3 – Walls of buildings with rectangular plan: areas of uniform pressure coefficient (plan view).
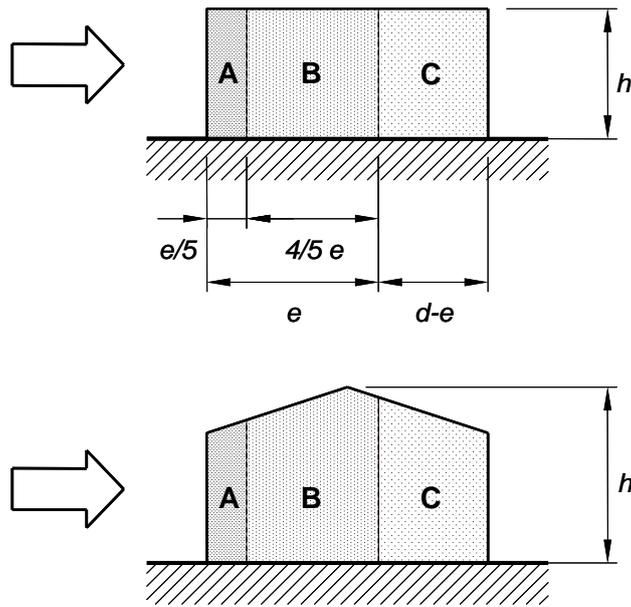
Figure H.4 – Walls of buildings with rectangular plan: areas of uniform pressure coefficient (elevation).

Table H.II – Pressure coefficients for the vertical walls of buildings with rectangular plan.

Zone	A		B		C		D		E	
h/d	$c_{pe,10}$	$c_{pe,1}$	$c_{pe,10}$	$c_{pe,1}$	$c_{pe,10}$	$c_{pe,1}$	$c_{pe,10}$	$c_{pe,1}$	$c_{pe,10}$	$c_{pe,1}$
5	−1,2	−1,4	−0,8	−1,1	−0,5		+0.8	+1,0	−0,7	
1	−1,2	−1,4	−0,8	−1,1	−0,5		+0,8	+1,0	−0,5	
≤ 0,25	−1,2	−1,4	−0,8	−1,1	−0,5		+0,7	+1,0	−0,3	

H.2.3 Roofs

H.2.3.1 Flat roofs

Roofs with a pitch ranging from −5° to +5° are considered flat.

The roof is divided in areas of uniform pressure coefficent as shown in Figures H.5 and H.6. The external pressure coefficients for each zone are given in Table H.III.

The value of geometric parameter e shown in Figure H.5 is equal either to b or $2 \cdot h$, whichever is smaller:

$$e = \min \begin{cases} b \\ 2 \cdot h \end{cases} \tag{H.3}$$

The reference height $\bar{z}_e$ for flat roofs (Figure H.6) is equal to the maximum height h of the roof above the ground. For roofs with parapets, the reference height is equal to $\bar{z}_e = h + h_p$, where h_p is the height of the parapets; wind action on the parapet shall be calculated following the provisions of clause G.5.
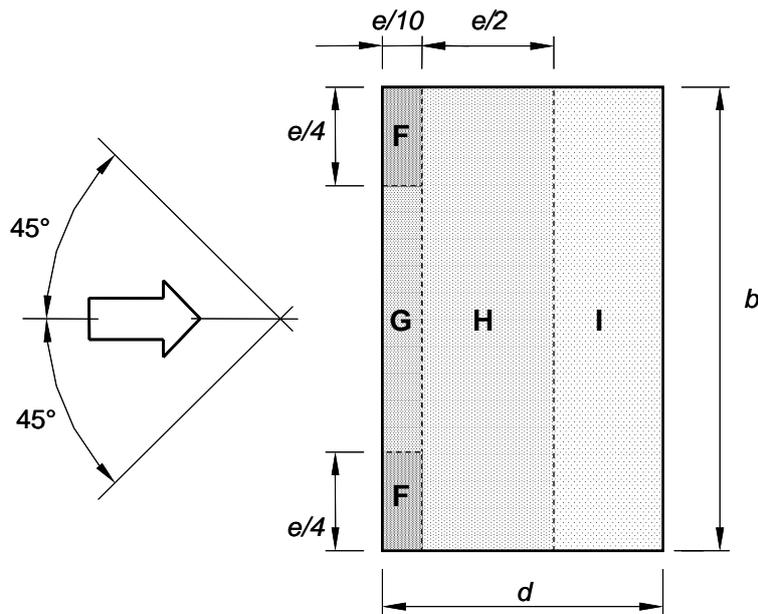
Figure H.5 – Flat roofs of buildings with rectangular plan: areas of uniform pressure coefficient.
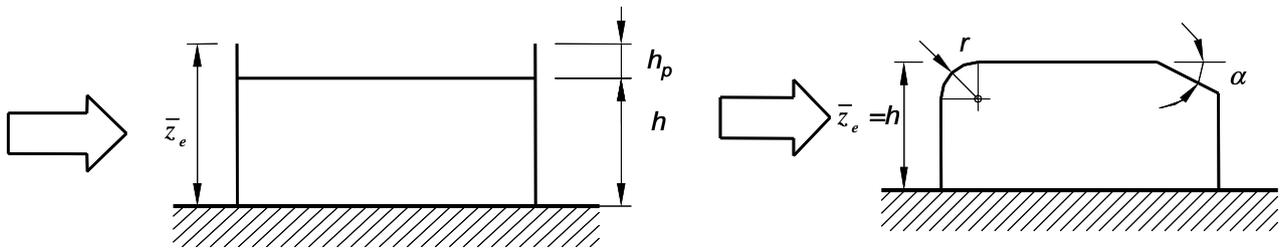
Figure H.6 – Reference height for flat roofs with parapets or curved or mansard eaves.

Table H.III – Pressure coefficients for flat roofs.

		Zone							
		F		G		H		I	
		$c_{pe,10}$	$c_{pe,1}$	$c_{pe,10}$	$c_{pe,1}$	$c_{pe,10}$	$c_{pe,1}$	$c_{pe,10}$	$c_{pe,1}$
Sharp edges		−1,8	−2,5	−1,2	−2,0	−0,7	−1,2	±0,2	
With parapets	$h_p/h = 0,025$	−1,6	−2,2	−1,1	−1,8	−0,7	−1,2	± 0.2	
	$h_p/h = 0,05$	−1,4	−2,0	−0,9	−1,6	−0,7	−1,2		
	$h_p/h = 0,10$	−1,2	−1,8	−0,8	−1,4	−0,7	−1,2		
Curved eaves	$r/h = 0,05$	−1,0	−1,5	−1,2	−1,8	−0,4		±0,2	
	$r/h = 0,10$	−0,7	−1,2	−0,8	−1,4	−0,3			
	$r/h = 0,20$	−0,5	−0,8	−0,5	−0,8	−0,3			
Mansard eaves	$\alpha = 30°$	−1,0	−1,5	−1,0	−1,5	−0,3		±0,2	
	$\alpha = 45°$	−1,2	−1,8	−1,3	−1,9	−0,4			
	$\alpha = 60°$	−1,3	−1,9	−1,3	−1,9	−0,5			

In zone I, both cases of positive and negative pressure coefficient shall be considered.

For roofs with parapets, linear interpolation can be used for intermediate values of h_p/h.

For roofs with curved eaves, linear interpolation can be used for intermediate values of r/h, where r is the radius of curvature; furthermore, along the curved portion of the eave, linear interpolation can be used between values on the vertical wall and on the roof.

For roofs with mansard eaves, linear interpolation can be used for intermediate values of angle α; For $\alpha > 60°$ linear interpolation between the values for $\alpha = 60°$ and the values for flat roofs featuring sharp eaves can be used. Along the mansard eave, the pressure coefficients values given in clause H.2.3.3 shall apply (duopitch roofs, values for $\Theta = 0°$) for the two zones F and G in accordance with the pitch angle α of the mansard eave.

H.2.3.2 Monopitch roofs

Monopitch roofs (Figure H.7) are divided in areas of uniform pressure coeffect as shown in Figure H.8. The external pressure coefficients for each zone are given in Tables H.IVa and H.IVb.

The value of geometric parameter e shown in Figure H.8 is equal either to b or $2 \cdot h$, whichever is smaller:

$$e = \min \begin{cases} b \\ 2 \cdot h \end{cases} \tag{H.4}$$

The reference height for inclined monopitch roofs (Figure H.7) is equal to the maximum height of the roof above the ground $\overline{z}_e = h$.

For slopes of $-5° \leq \alpha \leq +5°$, reference shall be made to clause H.2.3.1.

For $5° \leq \alpha \leq 45°$, pressure can fluctuate from negative to positive values, therefore pressure coefficients with both signs are provided; the value bringing to the largest effect for the structure or element shall be considered in each case.

Figure H.7 – Key for monopitch roofs.

Figure H.8 – Monopitch roofs of buildings with rectangular plan: areas of uniform pressure coefficient.

Table H.IVa – Pressure coefficients for monopitch roofs ($\Theta = 0°$ and $\Theta = 180°$).

α	Wind direction $\Theta = 0°$						Wind direction $\Theta = 180°$					
	F		G		H		F		G		H	
	$c_{pe,10}$	$c_{pe,1}$	$c_{pe,10}$	$c_{pe,1}$	$c_{pe,10}$	$c_{pe,1}$	$c_{pe,10}$	$c_{pe,1}$	$c_{pe,10}$	$c_{pe,1}$	$c_{pe,10}$	$c_{pe,1}$
5°	−1,7	−2,5	−1,2	−2,0	−0,6	−1,2	−2,3	−2,5	−1,3	−2,0	−0,8	−1,2
	0		0		0							
15°	−0,9	−2,0	−0,8	−1,5	−0,3		−2,5	−2,8	−1,3	−2,0	−0,9	−1,2
	+0,2		+0,2		+ 0,2							
30°	−0,5	−1,5	−0,5	−1,5	−0,2		−1,1	−2,3	−0,8	−1,5	−0,8	
	+0,7		+0,7		+0,4							
45°	0		0		0		−0,6	−1,3	−0,5		−0,7	
	+0,7		+0,7		+0,6							
60°	+0,7		+0,7		+0,7		−0,5	−1,0	−0,5		−0,5	
75°	+0,8		+0,8		+0,8		−0,5	−1,0	−0,5		−0,5	

Table H.IVb – Pressure coefficients for monopitch roofs ($\Theta = 90°$).

α	Wind direction $\Theta = 90°$									
	F_a		F_b		G		H		I	
	$c_{pe,10}$	$c_{pe,1}$	$c_{pe,10}$	$c_{pe,1}$	$c_{pe,10}$	$c_{pe,1}$	$c_{pe,10}$	$c_{pe,1}$	$c_{pe,10}$	$c_{pe,1}$
5°	−2,1	−2,6	−2,1	−2,4	−1,8	−2,0	−0,6	−1,2	−0,5	
15°	−2,4	−2,9	−1,6	−2,4	−1,9	−2,5	−0,8	−1,2	−0,7	−1,2
30°	−2,1	−2,9	−1,3	−2,0	−1,5	−2,0	−1,0	−1,3	−0,8	−1,2
45°	−1,5	−2,4	−1,3	−2,0	−1,4	−2,0	−1,0	−1,3	−0,9	−1,2
60°	−1,2	−2,0	−1,2	−2,0	−1,2	−2,0	−1,0	−1,3	−0,7	−1,2
75°	−1,2	−2,0	−1,2	−2,0	−1,2	−2,0	−1,0	−1,3	−0,5	

For intermediate values of pitch angle α, pressure coefficients can be obtained by linear interpolation between values of the same sign.

H.2.3.3 Duopitch roofs

Duopitch roofs (Figure H.9) are divided in areas of uniform pressure coefficent as shown in Figures H.10a and H.10b. The external pressure coefficients for each zone are given in Tables H.Va and H.Vb.

The value of geometric parameter e shown in Figure H.9 is equal either to b or $2 \cdot h$, whichever is smaller:

$$e = \min \begin{cases} b \\ 2 \cdot h \end{cases} \qquad (H.5)$$

The reference height for inclined duopitch roofs (Figure H.9) is equal to the maximum height of the roof above the ground, $\overline{z}_e = h$.

For slopes of $-5° \leq \alpha \leq +5°$ reference shall be made to clause H.2.3.1.

In the zone $5° \leq \alpha \leq 45°$, pressure can fluctuate from negative to positive values, therefore pressure coefficients with both signs are provided; ; the value bringing to the largest effect for the structure or element shall be considered in each case.

Figure H.9 – Key for duopitch roofs.

Figure H.10a – Duopitch roofs of buildings with rectangular plan: areas of uniform pressure coefficient for wind direction perpendicular to the ridge.

Table H.Va – Pressure coefficients for duopitch roofs:
wind direction perpendicular to the ridge.

α	Wind direction $\Theta = 0°$									
	F		G		H		I		J	
	$c_{pe,10}$	$c_{pe,1}$	$c_{pe,10}$	$c_{pe,1}$	$c_{pe,10}$	$c_{pe,1}$	$c_{pe,10}$	$c_{pe,1}$	$c_{pe,10}$	$c_{pe,1}$
−45°	−0,6		−0,6		−0,8		−0,7		−1,0	−1,5
−30°	−1,1	−2,0	−0,8	−1,5	−0,8		−0,6		−0,8	−1,4
−15°	−2,5	−2,8	−1,3	−2,0	−0,9	−1,2	−0,5		−0,7	−1,2
−5°	−2,3	−2,5	−1,2	−2,0	−0,8	−1,2	−0,6 / +0,2		−0,6 / +0,2	
5°	−1,7 / 0	−2,5	−1,2 / 0	−2,0	−0,6 / 0	−1,2	−0,6		−0,6 / +0,2	
15°	−0,9 / +0,2	−2,0	−0,8 / +0,2	−1,5	−0,3 / +0,2		−0,4 / 0		−1,0 / 0	−1,5
30°	−0,5 / +0,7	−1,5	−0,5 / +0,7	−1,5	−0,2 / +0,4		−0,4 / 0		−0,5 / 0	
45°	0 / +0,7		0 / +0,7		0 / +0,6		−0,2 / 0		−0,3 / 0	
60°	+0,7		+0,7		+0,7		−0,2		−0,3	
75°	+0,8		+0,8		+0,8		−0,2		−0,3	
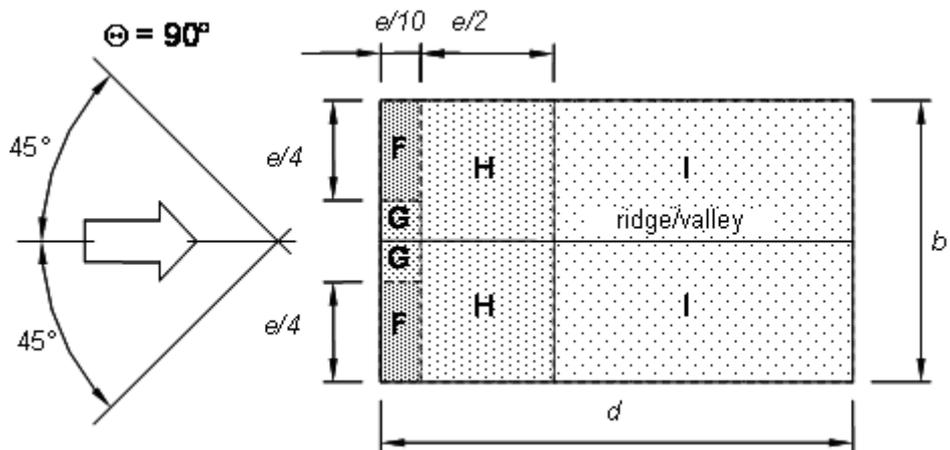
Figure H.10b – Duopitch roofs of buildings with rectangular plan: areas of uniform pressure coefficient for wind direction parallel to the ridge.

Table H.Vb – Pressure coefficients for duopitch roofs:
wind direction parallel to the ridge

α	Wind direction Θ = 90°							
	F		G		H		I	
	$c_{pe,10}$	$c_{pe,1}$	$c_{pe,10}$	$c_{pe,1}$	$c_{pe,10}$	$c_{pe,1}$	$c_{pe,10}$	$c_{pe,1}$
−45°	−1,4	−2,0	−1,2	−2,0	−1,0	−1,3	−0,9	−1,2
−30°	−1,5	−2,1	−1,2	−2,0	−1,0	−1,3	−0,9	−1,2
−15°	−1,9	−2,5	−1,2	−2,0	−0,8	−1,2	−0,8	−1,2
−5°	−1,8	−2,5	−1,2	−2,0	−0,7	−1,2	−0,6	−1,2
5°	−1,6	−2,2	−1,3	−2,0	−0,7	−1,2	−0,6	
15°	−1,3	−2,0	−1,3	−2,0	−0,6	−1,2	−0,5	
30°	−1,1	−1,5	−1,4	−2,0	−0,8	−1,2	−0,5	
45°	−1,1	−1,5	−1,4	−2,0	−0,9	−1,2	−0,5	
60°	−1,1	−1,5	−1,2	−2,0	−0,8	−1,0	−0,5	
75°	−1,1	−1,5	−1,2	−2,0	−0,8	−1,0	−0,5	

For a wind direction Θ = 0°, when 5° ≤ α ≤ 45° two values are given for the pressure coefficient. The largest values for the areas F, G and H are combined with the largest values for the areas I and J, the smallest with the smallest; positive and negative pressure coefficient shall not be combined for the same face.

For a wind direction Θ = 0° and for intermediate values of pitch angle α, pressure coefficients can be obtained by linear interpolation between values of the same sign.

H.2.3.4 Hipped roofs

Hipped roofs are divided in areas of uniform pressure coefficent as shown in Figure H.11 and H.12. The external pressure coefficients for each zone are given in Table H.VI.

The value of geometric parameter e shown in Figures H.11 and H.12 is equal either to b or $2 \cdot h$, whichever is smaller:

$$e = \min \begin{cases} b \\ 2 \cdot h \end{cases} \tag{H.6}$$

The reference height for hipped roofs (Figures H.11 and H.12) is equal to the maximum height of the roof above the ground $\overline{z}_e = h$.

For slopes of −5° ≤ α ≤ +5°, reference shall be made to clause H.2.3.1.

In the zone 5° ≤ α ≤ 45°, pressure can fluctuate from negative to positive values, therefore pressure coefficients with both signs are provided; the value bringing to the largest effect for the structure or element shall be considered in each case.
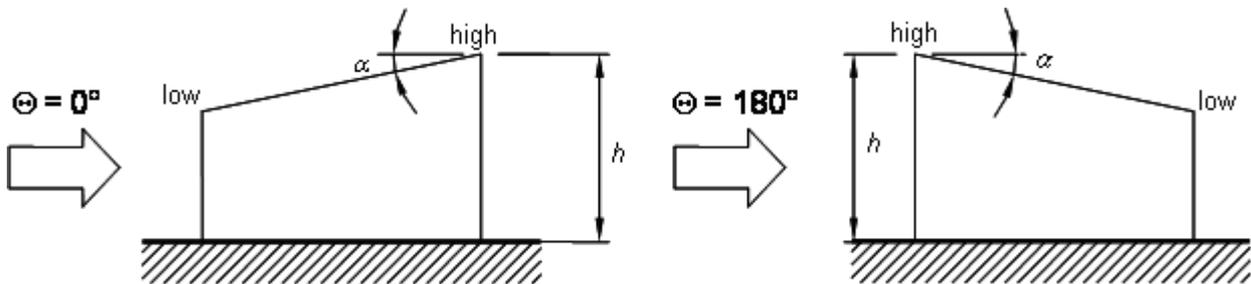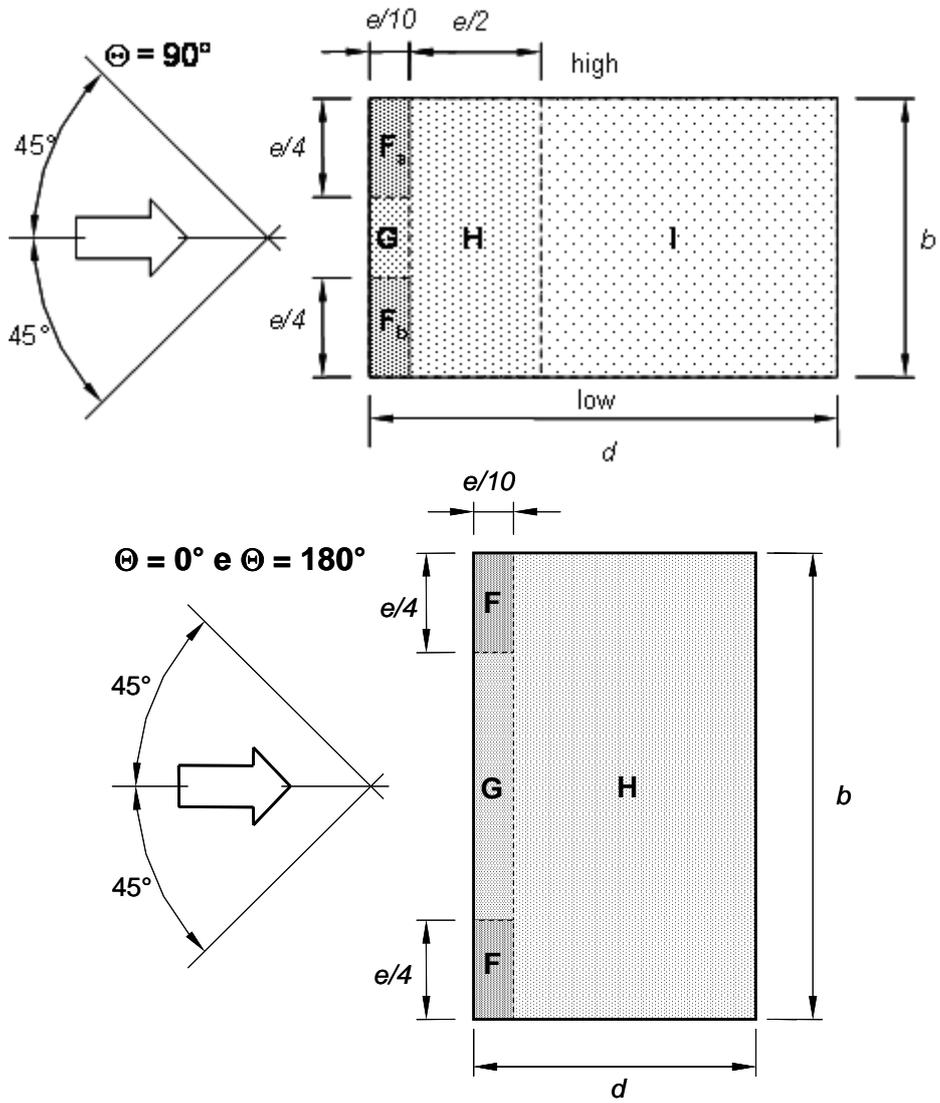
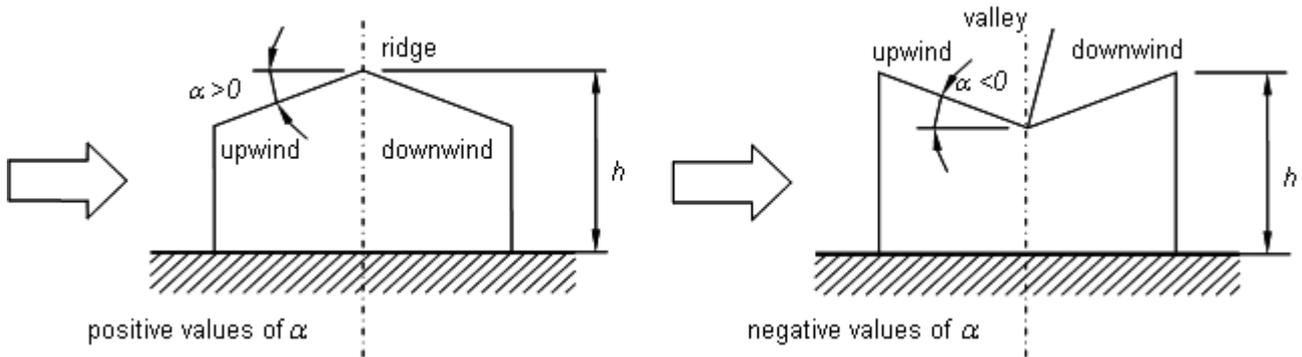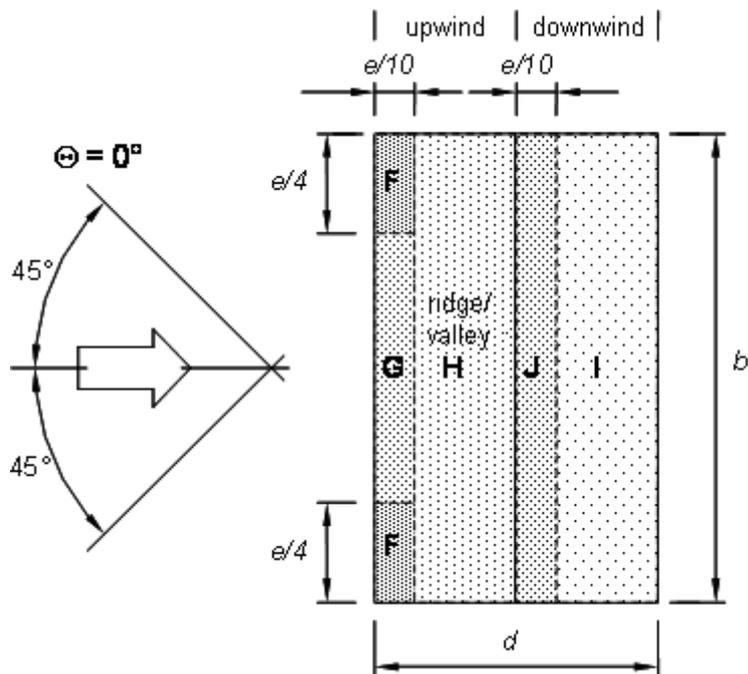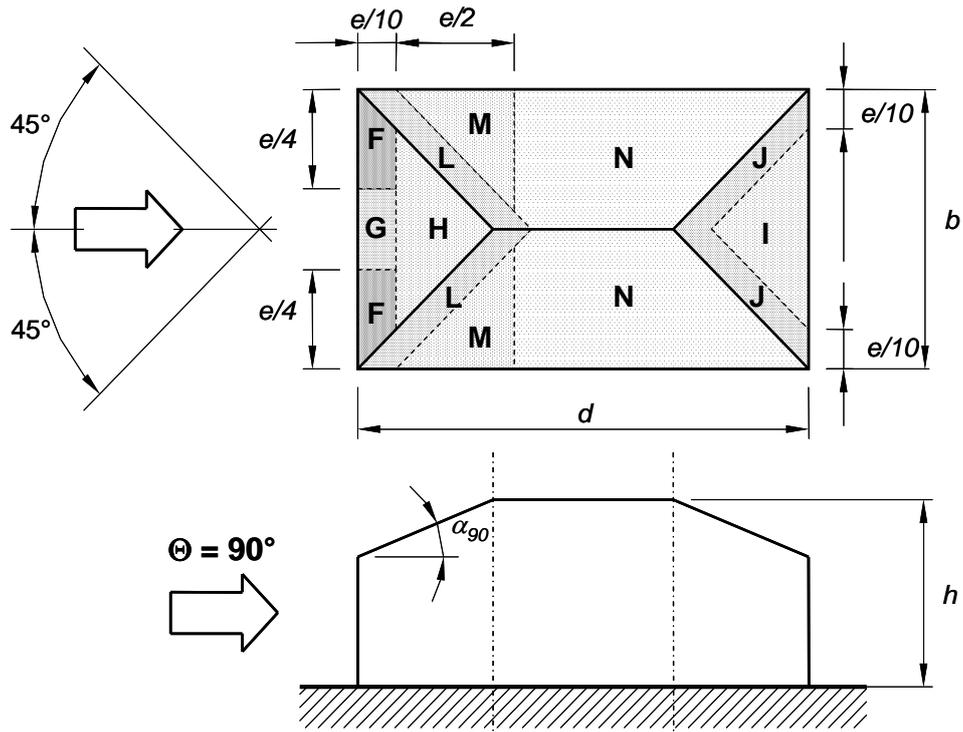**Figure H.11.** – Hipped roofs of buildings with rectangular plan: areas of uniform pressure coefficient ($\Theta = 90°$).
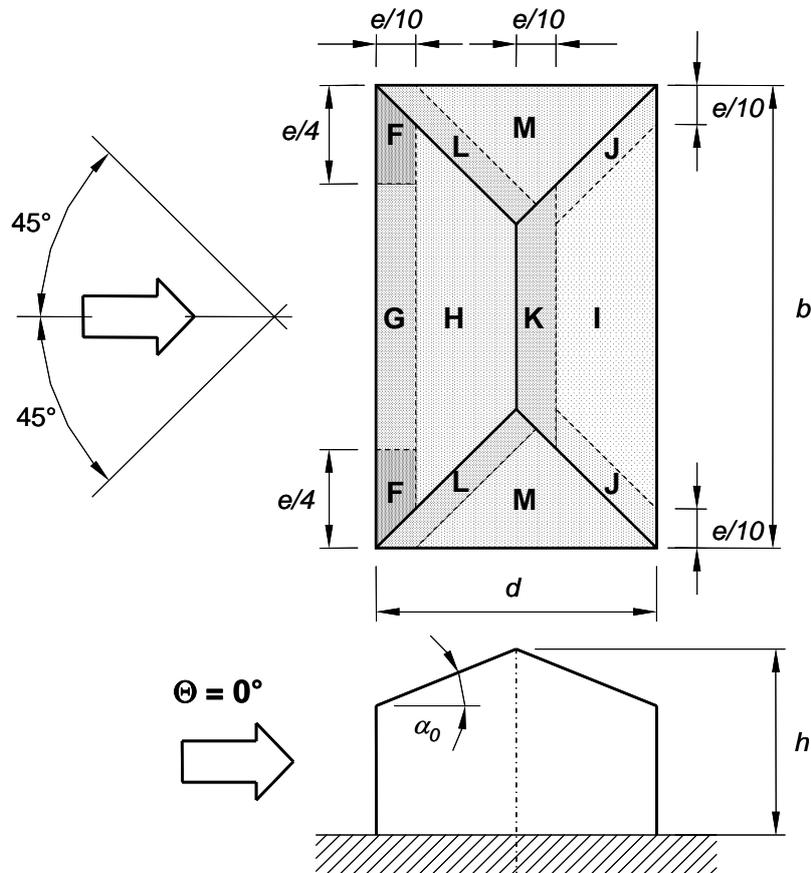
Figure H.12. – Hipped roofs of buildings with rectangular plan: areas of uniform pressure coefficient ($\Theta = 0°$).

Table H.VI – Pressure coefficients for hipped roofs.

α_0 for $\Theta=0°$, α_{90} for $\Theta=90°$	Wind direction $\Theta = 0°$ and $\Theta = 90°$																	
	F		G		H		I		J		K		L		M		N	
	$c_{pe,10}$	$c_{pe,1}$	$c_{pe,10}$	$c_{pe,1}$	$c_{pe,10}$	$c_{pe,1}$	$c_{pe,10}$	$c_{pe,1}$	$c_{pe,10}$	$c_{pe,1}$	$c_{pe,10}$	$c_{pe,1}$	$c_{pe,10}$	$c_{pe,1}$	$c_{pe,10}$	$c_{pe,1}$	$c_{pe,10}$	$c_{pe,1}$
+ 5°	-1,7	-2,5	-1,2	-2,0	-0,6	-1,2	-0,3		-0,6		-0,6		-1,2	-2,0	-0,6	-1,2	-0,4	
	0		0		0													
+ 15°	-0,9	-2,0	-0,8	-1,5	-0,3		-0,5		-1,0	-1,5	-1,2	-2,0	-1,4	-2,0	-0,6	-1,2	-0,3	
	+0,2		+0,2		+0,2													
+ 30°	-0,5	-1,5	-0,5	-1,5	-0,2		-0,4		-0,7	-1,2	-0,5		-1,4	-2,0	-0,8	-1,2	-0,2	
	+0,5		+0,7		+0,4													
+ 45°	0		0		0		-0,3		-0,6		-0,3		-1,3	-2,0	-0,8	-1,2	-0,2	
	+0,7		+0,7		+0,6													
+ 60°	+0,7		+0,7		+0,7		-0,3		-0,6		-0,3		-1,2	-2,0	-0,4		-0,2	
+ 75°	+0,8		+0,8		+0,8		-0,3		-0,6		-0,3		-1,2	-2,0	-0,4		-0,2	

For a wind direction $\Theta = 0°$ and pitch angles $5° \leq \alpha \leq 45°$ two values are given for the pressure coefficient. Two cases should be considered: one with all positive pressure coefficient and one with all negative values; positive and negative pressure coefficient shall not be combined.

For intermediate values of pitch angle α pressure coefficients can be obtained by linear interpolation between values of the same sign.

The pressure coefficients shall be chosen based on the pitch angle of the windward face of the building.

H.3 Buildings with a non-rectangular plan or non-uniform height

The distribution of external pressure on buildings depends significantly on their geometry. Therefore, for buildings other than those with a rectangular plan and uniform height (clauses G.2 and H.2), attention must be paid in selecting external pressure coefficients.

For buildings with a complex plan geometry, as for those with non uniform height, pressure coefficients cannot be quantified in a simple manner; in these cases, their assessment may require wind tunnel testing.

This clause deals with two particular types of irregular building. Clause H.3.1 refers to buildings of uniform height but with a ground plan which is a combination of rectangular elements. Clause H.3.2 refers to buildings having a rectangular plan but made of elements of different height (clause H.3.2.1) or recessed bodies (clause H.3.2.2). For these cases knowledge of the flow pattern and available experimental data allow to infer general criteria for selecting pressure coefficients from the values given in clauses H.2.2 (walls of buildings with a rectangular ground plan and regular elevation) and H.2.3.1 (flat roofs).

In general, re-entrant corners and recessed bays can create local flow modifications giving rise to areas where pressure is very different from that which would occur in the absence of such features.

With reference to the building shown in Figure H.2, the geometric parameter e is introduced, equal either to b or $2 \cdot h$, whichever is smaller:

$$e = \min \begin{cases} b \\ 2 \cdot h \end{cases} \qquad \text{(H.7)}$$

Re-entrant corners and recessed bays less than $e/20$ can generally be ignored in the assessment of the pressure distribution around the building.

On the other hand, for re-entrant corners and recessed bays greater than $e/20$, and in the absence of more accurate data, reference can be made to the criteria given in the following clauses.

H.3.1 Buildings with non-rectangular plan

For buildings that can be included in one of the cases shown in Figure H.13, pressure coefficients for the vertical walls can be assessed by adopting the criteria given below.

If the plan of the building comprises a body with a rectangular plan (generally of larger dimensions) from which other bodies with a rectangular plan protrude (generally of smaller dimensions as in cases a, b and c in Figure H.13), the following rules apply. From the windward corner of the building from which the flow separates, 45° angle lines are drawn with respect to the direction of the oncoming flow. The surfaces inside the sector identified by these lines can be broken down into two zones: the first, indicated as X, belong to body A (with parameters b_A and d_A) from which the lines were plotted; the second, indicated as Y, belong to the rest of the building (body B, with geometric parameters b_B and d_B).

In the X zones, the pressure coefficient is the same as it would be in the absence of body B.

In the Y zones, both the following situations are considered:
1) the pressure coefficient is the same as that in X zones of body A (and therefore generally negative);
2) the pressure coefficient is the same as that which would act on body B in the absence of body A (therefore generally positive).

In all other areas of body B, pressure coefficients are the same as they would be in the absence of body A.

The pressure coefficients on all the leeward faces of body B (downwind with respect to body A) are equal to the pressure coefficient on the leeward face of a rectangular building of across-wind dimensions equal to those of body B.

If the ground plan of the building has recessed bays (as in case d in Figure H.13), geometric parameter e, is equal either to b_2 or $2 \cdot h$, whichever is smaller:

$$e = \min \begin{cases} b_2 \\ 2 \cdot h \end{cases} \qquad \text{(H.8)}$$

If the recess sizes (b_1 and d_1) do not exceed the value of $e/10$:
- on the faces of the recess bay (indicated as X), the pressure coefficient is equal to that of the adjacent portion of the roof;
- on the other faces of the building, the pressure coefficient is the same as it would be in the absence of the recess.

If the sizes of the recess are more than $e/10$, reference should be made to specific data or wind tunnel tests.
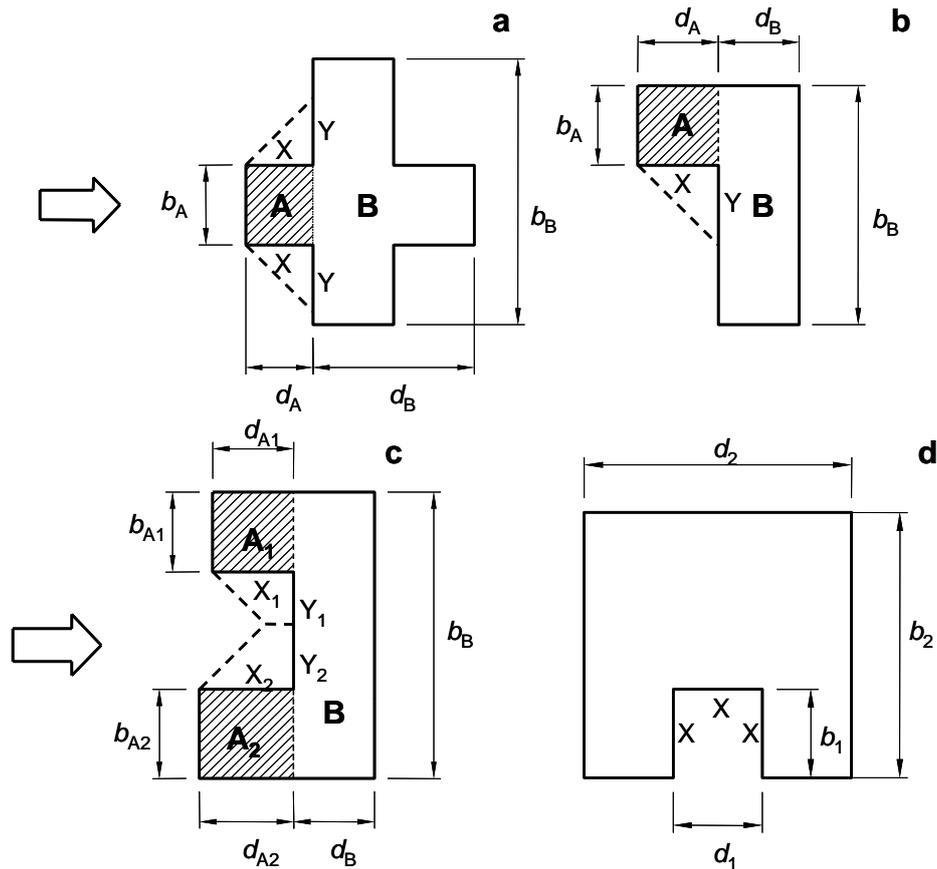
Figure H.13 - Reference diagrams for buildings with an irregular plan.

H.3.2 Buildings of non-uniform height

H.3.2.1 Buildings with irregular or inset faces

The criteria set down below apply to buildings with a rectangular plan, having flush walls with corner cut-outs in elevation, as in the cases shown in Figures H.14 and H.15.

If the lower portion of the building is located downwind (cut-out downwind), the lateral faces of the building are divided into zones of uniform pressure coefficient (Figure H.14) in accordance with geometric parameter *e* given as:

$$e = \min \begin{cases} b \\ 2 \cdot h \end{cases} \tag{H.9}$$

where *b* is the building width (across-wind dimension) and *h* is the maximum height.

The pressure coefficients on the upwind face of the taller portion are the same as they would be in the absence of the lower portion. The pressure coefficients on the downwind faces of the taller body and the lower body must be calculated with reference to the maximum height *h* and to the longitudinal dimension *d* of the building, following heading H.2.
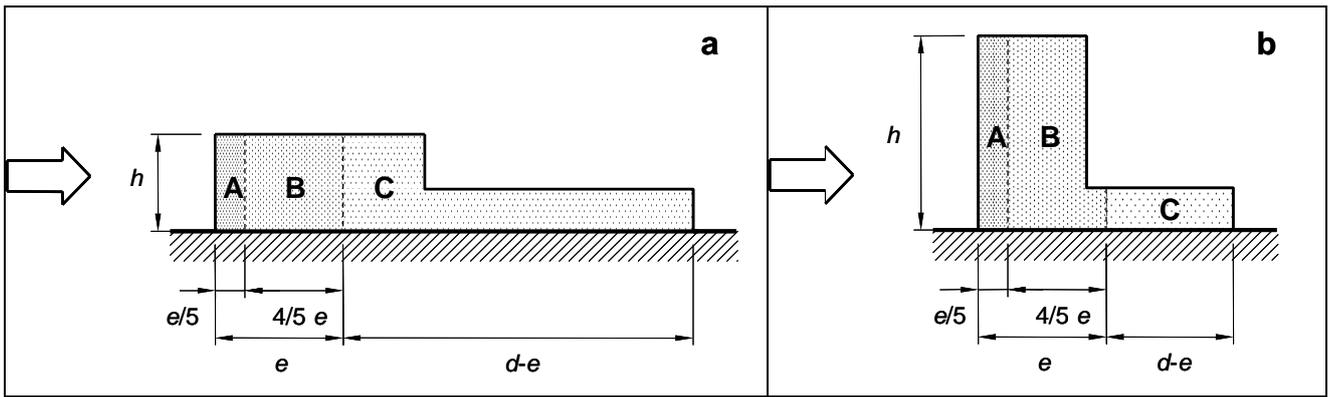
Figure H.14 - Buildings with a rectangular plan and portions of different heights (cut-out downwind)).

If the lower portion of the building is located upwind (cut-out upwind), the lateral faces of the building are divided into zones of uniform pressure coefficient (Figure H.15) in accordance with geometric parameters e_1 and e_2 given as:

$$e_1 = \min \begin{cases} b_1 \\ 2 \cdot h_1 \end{cases} \quad ; \quad e_2 = \min \begin{cases} b_2 \\ 2 \cdot h_2 \end{cases} \tag{H.10}$$

where b_1 and b_2 are respectively the width exposed to the wind of the upper and lower portions of the building. The reference heights for each of the two zones are the heights h_1 and h_2 of each portion of the building.

The pressure on the upwind face of the lower portion of the building is calculated as if the taller portion were not present. The pressure on the upwind and downwind faces of the taller portion body is calculated as if the lower body were not present.
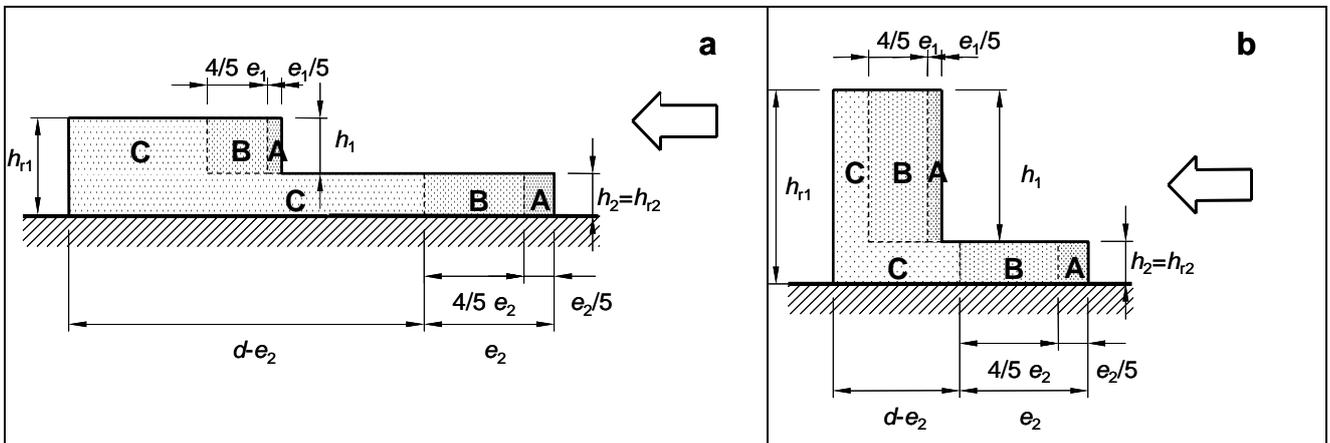
Figure H.15 - Buildings with a rectangular plan and portions of different heights (cut-out upwind).

H.3.2.2 Buildings with inset storeys

For buildings with inset storeys with respect to the storeys below, as in the cases shown in Figure H.16, use can be made of the following criteria, in which geometric parameters e_1 and e_2 are defined as:

$$e_1 = \min \begin{cases} b_1 \\ 2 \cdot h_1 \end{cases} \qquad ; \qquad e_2 = \min \begin{cases} b_2 \\ 2 \cdot h_2 \end{cases} \qquad \text{(H.11)}$$

For edge of face inset from edge of lower storey, provided that the upwind edge of the wall is inset a distance of at least $0{,}2 \cdot e_1$ (Figure H.16a), the pressure distribution on that portion of the building are the same as a rectangular building of uniform height (heading H.2) with base located at the level of the roof of the lower portion of the building. The reference height is the total height of the building.

Where the upwind edge of lower storey is flush, or inset, a distance less than $0{,}2 \cdot e_1$ (Figure H.16a), or is aligned along the upwind face (Figure H.16b), the same division into uniform zones is used as for the previous point, although in this case inserting a zone, indicated by E in Figure H.16b, in which a pressure coefficient $c_{pe} = -2{,}0$ is used; this zone extends from the roof level of the underlying body for a height equivalent to $e_2/3$.
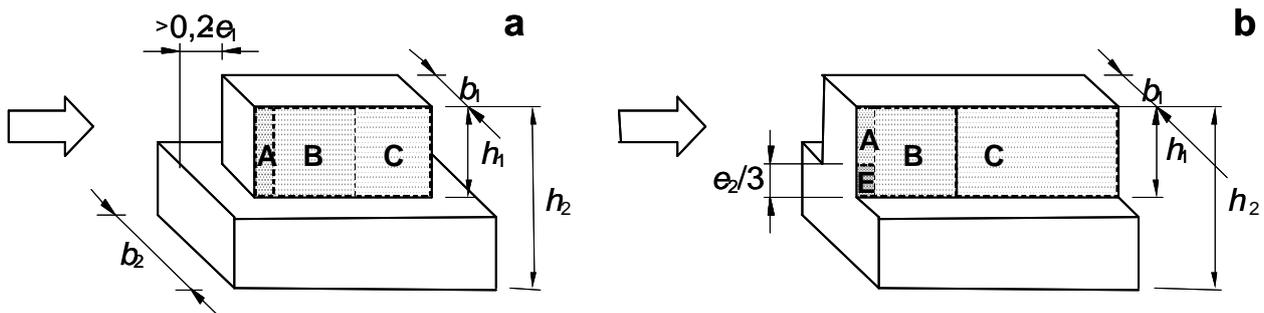
Figure H.16 – Division into zones of uniform pressure coefficient of the lateral walls of buildings with edge of face inset or flush with edge of lower storey.

The pressure coefficients on the roof of the lower portion of the building are the same as they would be in the absence of the inset storeys, except for an area of width $e_1/2$, indicated by the broken line in Figure H.17, around the perimeter of the inset storeys. In this area, the pressure coefficients are the same as those acting on the adjacent vertical walls of the upper storeys.
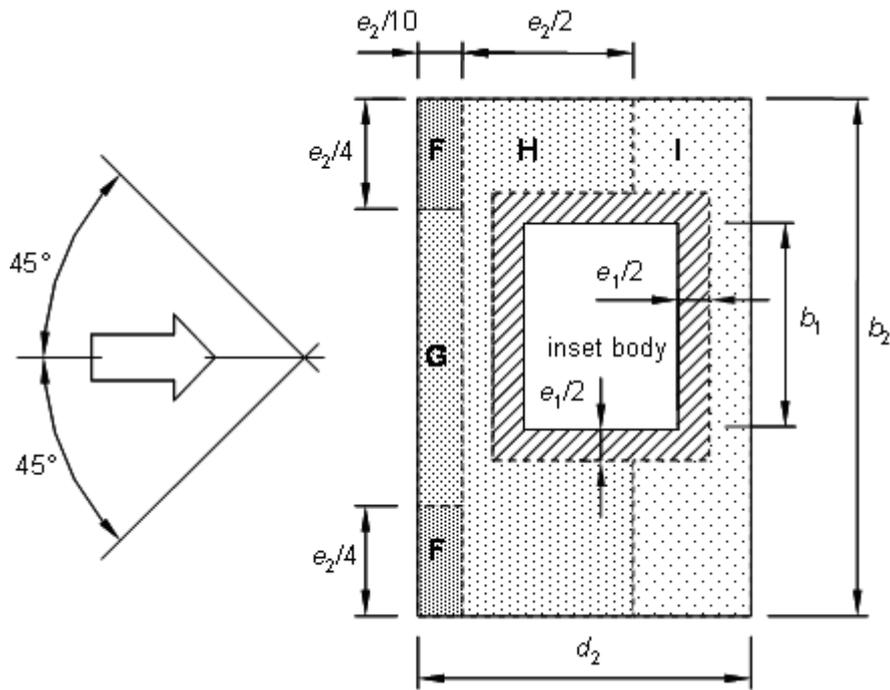
Figure H.17 – Pressure distribution on the roof of a building having inset storeys (plan view).

H.4 Canopies

This heading gives net pressure coefficients to be used to assess local actions on elements or portions of canopies composed of a single layer roof. Evaluation of local pressures on the upper and lower face of canopies with a double roof layer requires specific assessments and, if necessary, wind tunnel tests.

Net pressure coefficients c_{pn} given below are functions of the blockage arising from the presence of constructions or obstacles underneath the canopy; the blockage φ is the ratio between the obstructed area underneath the canopy and the total area underneath the canopy, as shown in heading G.6.

Positive net pressure coefficients are associated with downward pressures, negative net pressure coefficients with upward pressures.

In no case should net pressure coefficients be used to assess the global action exerted by wind on the canopy.

H.4.1 Monopitch canopies

Local net pressure coefficients on monopitch canopies are given in Table H.VII, for the areas of uniform pressure shown in Figure H.18.

Table H.VII gives the values of net pressure coefficients as a function of the blockage ratio φ and of the slope α of the canopy (Figure H.19). Linear interpolation is allowed for intermediate values of α; for intermediate values of φ, linear interpolation is allowed between the values φ=0 and φ=1.

The reference height is equal to the maximum height of the canopy above the ground, $\bar{z} = h$ (Figure H.19).

Figure H.18 –Monopitch canopies: areas of uniform pressure coefficients.

Table H.VII – Net pressure coefficients for monopitch canopies.

α	Blockage φ	Net pressure coefficient c_{pn}		
		A	B	C
0°	Maximum, all values of φ	+0,5	+1,8	+1,1
	Minimum, φ = 0	−0,6	−1,3	−1,4
	Minimum, φ = 1	−1,5	−1,8	−2,2
5°	Maximum, all values of φ	+0,8	+2,1	+1,3
	Minimum, φ = 0	−1,1	−1,7	−1,8
	Minimum, φ = 1	−1,6	−2,2	−2,5
10°	Maximum, all values of φ	+1,2	+2,4	+1,6
	Minimum, φ = 0	−1,5	−2,0	−2,1
	Minimum, φ = 1	−2,1	−2,6	−2,7
15°	Maximum, all values of φ	+1,4	+2,7	+1,8
	Minimum, φ = 0	−1,8	−2,4	−2,5
	Minimum, φ = 1	−1,6	−2,9	−3,0
20°	Maximum, all values of φ	+1,7	+2,9	+2,1
	Minimum, φ = 0	−2,2	−2,8	−2,9
	Minimum, φ = 1	−1,6	−2,9	−3,0
25°	Maximum, all values of φ	+2,0	+3,1	+2,3
	Minimum, φ = 0	−2,6	−3,2	−3,2
	Minimum, φ = 1	−1,5	−2,5	−2,8
30°	Maximum, all values of φ	+2,2	+3,2	+2,4
	Minimum, φ = 0	−3,0	−3,8	−3,6
	Minimum, φ = 1	−1,5	−2,2	−2,7
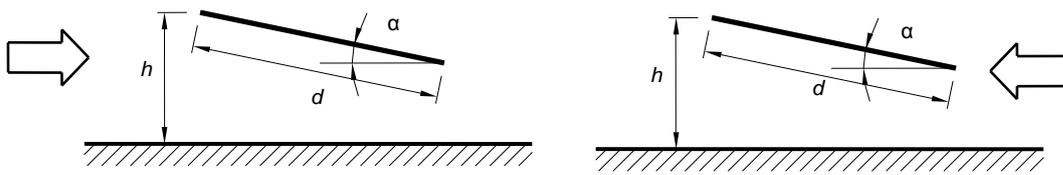
Figure H.19 – Key for monopitch canopies.

H.4.2 Duopitch canopies

Local net pressure coefficients on duopitch canopies are given in Tables H.VIIIa and H.VIIIb, for the areas uf uniform pressure shown in Figure H.20.

Tables H.VIIIa and H.VIIIb give the values of net pressure coefficients as a function of the blockage ratio φ and of the slope α of the canopy (Figure H.21). Linear interpolation is allowed for intermediate values of α; for intermediate values of φ, linear interpolation is allowed between the values $\varphi=0$ and $\varphi=1$.

The reference height is equal to the maximum height of the canopy above the ground, $\overline{z} = h$ (Figure H.19).
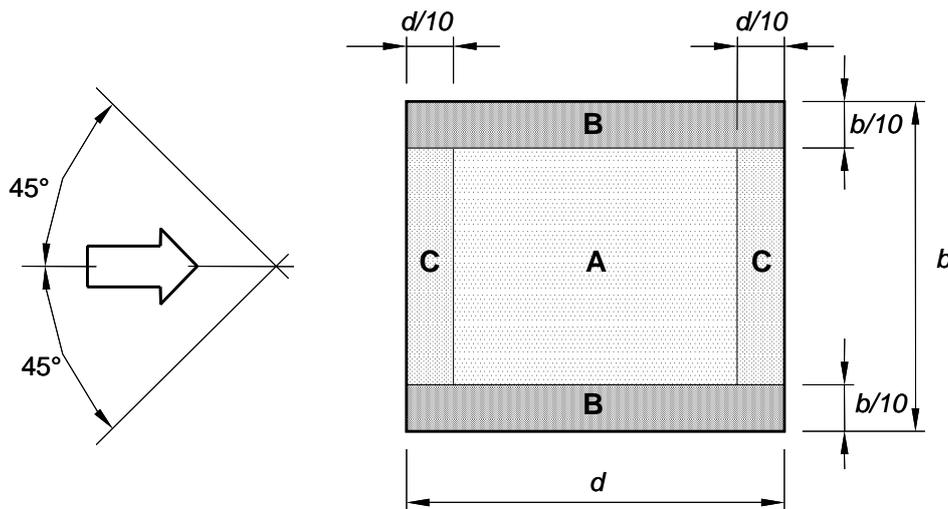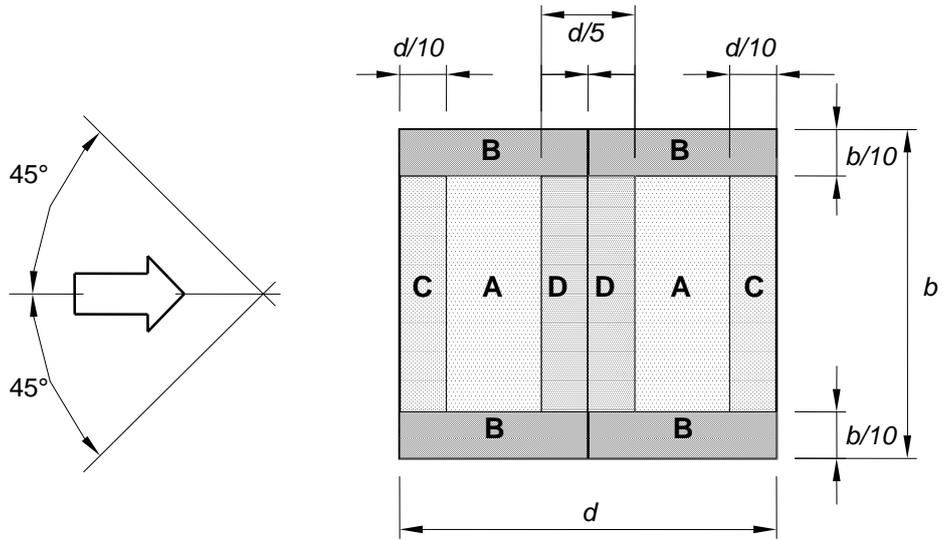
Figure H.20 –Duopitch canopies areas of uniform pressure coefficients.
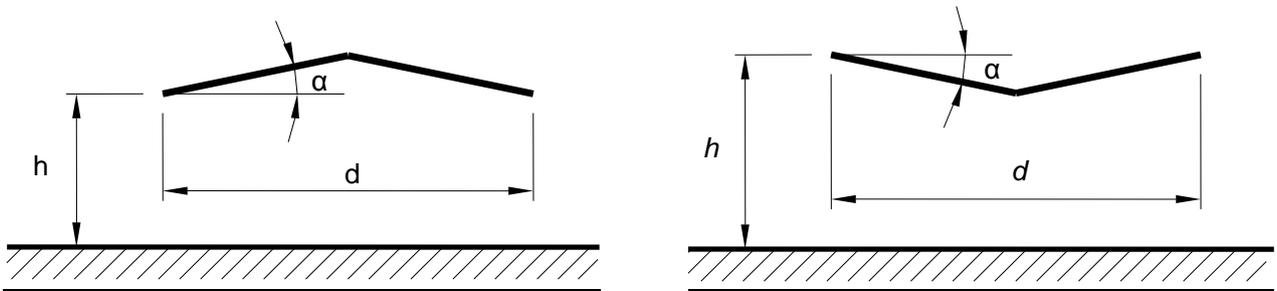
Figure H.21 – Key for duopitch canopies.

Table H.VIIIa - Net pressure coefficients for duopitch canopies: values for $\alpha > 0°$.

α	Blockage φ	Net pressure coefficient c_{pn}			
		A	B	C	D
5°	Maximum, all values of φ	+0,6	+1,8	+1,3	+0,4
	Minimum, φ = 0	−0,6	−1,4	−1,4	−1,1
	Minimum, φ = 1	−1,3	−2,0	−1,8	−1,5
10°	Maximum, all values of φ	+0,7	+1,8	+1,4	+0,4
	Minimum, φ = 0	−0,7	−1,5	−1,4	−1,4
	Minimum, φ = 1	−1,3	−2,0	−1,8	−1,8
15°	Maximum, all values of φ	+0,9	+1,9	+1,4	+0,4
	Minimum, φ = 0	−0,9	−1,7	−1,4	−1,8
	Minimum, φ = 1	−1,3	−2,2	−1,6	−2,1
20°	Maximum, all values of φ	+1,1	+1,9	+1,5	+0,4
	Minimum, φ = 0	−1,2	−1,8	−1,4	−2,0
	Minimum, φ = 1	−1,4	−2,2	−1,6	−2,1
25°	Maximum, all values of φ	+1,2	+1,9	+1,6	+0,5
	Minimum, φ = 0	−1,4	−1,9	−1,4	−2,0
	Minimum, φ = 1	−1,4	−2,0	−1,5	−2,0
30°	Maximum, all values of φ	+1,3	+1,9	+1,6	+0,7
	Minimum, φ = 0	−1,4	−1,9	−1,4	−2,0
	Minimum, φ = 1	−1,4	−1,8	−1,4	−2,0

Table H.VIIIb – Net pressure coefficients for duopitch canopies: values for $\alpha < 0°$.

α	Blockage φ	Net pressure coefficient c_{pn}			
		A	B	C	D
−20°	Maximum, all values of φ	+0,8	+1,6	+0,6	+1,7
	Minimum, φ = 0	−0,9	−1,3	−1,6	−0,6
	Minimum, φ = 1	−1,5	−2,4	−2,4	−0,6
−15°	Maximum, all values of φ	+0,6	+1,5	+0,7	+1,4
	Minimum, φ = 0	−0,8	−1,3	−1,6	−0,6
	Minimum, φ = 1	−1,6	−2,7	−2,6	−0,6
−10°	Maximum, all values of φ	+0,6	+1,4	+0,8	+1,1
	Minimum, φ = 0	−0,8	−1,3	−1,5	−0,6
	Minimum, φ = 1	−1,6	−2,7	−2,6	−0,6
−5°	Maximum, all values of φ	+0,5	+1,5	+0,8	+0,8
	Minimum, φ = 0	−0,7	−1,3	−1,6	−0,6
	Minimum, φ = 1	−1,5	−2,4	−2,4	−0,6

H.4.3 Multibay canopies

As a first approximation, the net pressure coefficients on each bay of multibay canopies (all with the same pitch angle) can be considered the same as those of an isolated duopitch canopy (heading H.4.2).

Only in the case of wind perpendicular to the direction of the ridges, and only for the geometries shown in Figure G.30, the net pressure coefficients defined in heading H.4.2 can be multiplied by the reduction factors given in Table G.XIV, in accordance with the diagram in Figure G.30.

Annex I   DYNAMIC PROPERTIES OF STRUCTURES

I.1   Introduction

This Annex applies to structures featuring a linear elastic behaviour and classic vibration modes. The dynamic properties of the structure are therefore:

- the natural frequencies,
- the mode shapes,
- the generalised and equivalent masses,
- the generalised moments of inertia,
- the critical damping ratios.

The following headings provide estimates of these parameters and specify their applicability.

I.2   Natural frequencies

I.2.1   Natural frequencies for cantilevered structures with mass concentrated at the free end

An approximate equation for the first natural frequency of a mass supported by a cantilever of uniform mass and stiffness (Figure I.1) is given by Eq. I.1 :

$$n_1 = \frac{1}{2\pi} \cdot \sqrt{\frac{3 \cdot E \cdot J_f}{M_s \cdot h^3}} \tag{I.1}$$

where:
h is the height of the structure;
E is the modulus of elasticity of the material;
J_f is the moment of inertia of the cross-section of the cantilever;
M_s is the equivalent mass, approximately equal to $M_s = M + m \cdot h / 2$, where M is the concentrated mass and m is the mass per unit length of the cantilever.

When the structural sizes are expressed in m, the modulus of elasticity in N/m^2 and the mass in kg, then in Eq. (I.1) the frequency n_1 is in Hz.
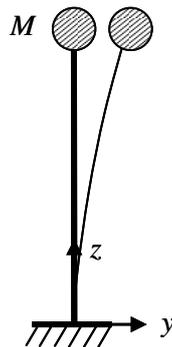
Figure I.1 – Vibration of a cantilever of uniform cross-section
with mass concentrated at the free end.

I.2.2 Bending natural frequencies for slender structures

The *i*-th bending natural frequency of a slender structure (beam-like structure) of uniform cross section is given by Eq. I.2:

$$n_i = \frac{\lambda_i^2}{2\pi \cdot l^2} \cdot \sqrt{\frac{E \cdot J_f}{m}}$$

(I.2)

where:

l   is the length of the structure;
E   is the modulus of elasticity of the material;
J_f is the moment of inertia of the cross-section of the structure;
m   is the mass per unit length;
λ_i is a coefficient depending on boundary conditions (Table I.I).

Table I.I. λ_i coefficients.

Boundary condition	λ_1	λ_2	λ_3	λ_4	λ_i $(i>4)$
Hinge-hinge	π	2π	3π	4π	$i\pi$
Fixed-fixed	4,730	7,853	10,996	14,137	$(2i+1)\pi/2$
Fixed-hinge	3,927	7,069	10,210	13,352	$(4i+1)\pi/4$
Fixed-free	1,875	4,694	7,855	10,996	$(2i-1)\pi/2$

When the structural sizes are expressed in m, the modulus of elasticity in N/m^2 and the mass in kg, then in Eq. (I.2) the frequency n_i is in Hz.

I.2.3 Torsional natural frequencies for slender structures

The *i*-th torsional natural frequency of a slender structure (beam-like structure) of uniform cross section is given by Eq. I.3:

$$n_{M,i} = \frac{\lambda_{M,i}}{2\pi \cdot l} \sqrt{\frac{G \cdot J_t}{I_p}}$$

(I.3)

where:

G   is the shear modulus of the material;
J_t is the torsional moment of inertia of the cross-section of the structure; for circular cross-sections, this is equal to the polar moment of inertia J_p; in general $J_t < J_p$;
I_p is the polar mass moment of inertia per unit length about the torsion axis; this can be calculated as $I_p = I_p' + m \cdot d^2$, were I_p' is the polar mass moment of inertia per unit length about the centre of mass, *m* is the mass per unit length and *d* is the distance of the centre of mass to the centre of torsion;
l   is the length of the structure;
$\lambda_{M,i}$ is a coefficient that depends on boundary conditions; in particular, for cantilever structures, $\lambda_{M,i} = (2 \cdot i - 1) \cdot (\pi / 2)$.

When the structural sizes are expressed in m, the shear modulus in N/m^2 and the polar mass moment of inertia per unit length in kg·m^2/m, then in Eq. (I.3) the frequency $n_{M,i}$ is in Hz.

I.2.4 Natural frequencies for multi-storey buildings

This heading applies only to buildings having uncoupled sway and torsional modes. As an example, this is the case of buildings having two planes of symmetry.

The first sway natural frequency n_1 decreases with increasing height h of the building and can be approximated as:

$$n_1 = \frac{1}{0,015 \cdot h} \div \frac{1}{0,018 \cdot h} \quad \text{for RC or composite steel/RC buildings} \tag{I.4}$$

$$n_1 = \frac{1}{0,020 \cdot h} \div \frac{1}{0,024 \cdot h} \quad \text{for steel buildings} \tag{I.5}$$

where h is in m and n_1 is in Hz.

The former estimates (larger frequency values) apply to small amplitude of oscillations and are thus appropriate for abitability assessments (Annex N); the latter estimates (smaller frequency values) apply to large amplitudes of oscillation and are therefore appropriate for ultimate limit states, to be in any case carried out in the elastic range.

Only for steel buildings, the frequencies of higher modes can be assumed proportional to the first natural frequency, by applying the equations I.6:

$$n_2 = 3,05 \cdot n_1, \quad n_3 = 5,46 \cdot n_1, \quad n_4 = 7,69 \cdot n_1 \tag{I.6}$$

The frequency of the first torsional mode for reinforced concrete, composite and steel buildings may be estimated by Eq. I.7:

$$n_M = 1,35 \cdot n_1 \tag{I.7}$$

Equations I.4 through I.7 interpolate an extensive collection of full-scale experimental measurements in existing buildings. Dynamic numerical analyses (e.g. FEM analyses) must be carried out properly accounting for the contribution of non-structural elements.

I.2.5 Fundamental bending frequency for chimneys

The fundamental bending frequency of chimneys can be calculated by using Eq. I.8:

$$n_1 = \frac{\varepsilon_1 \cdot b}{h_{\text{eff}}^2} \cdot \sqrt{\frac{W_S}{W_T}} \tag{I.8}$$

with:

$$h_{\text{eff}} = h_1 + \frac{h_2}{3} \tag{I.9}$$

where:
b is the top diameter of the chimney;
h_{eff} is the effective height of the chimney (see Figure I.2);
W_S is the weight of structural parts only, i.e. those also contributing to the stiffness of the chimney;
W_T is the total weight of the chimney, calculated by adding to W_S the weight of all non structural parts;

ε_1 = 1000 m/s, for steel chimneys;

      = 700 m/s, for concrete and masonry chimneys.

When structural sizes are in m, frequency n_1 is obtained in Hz.
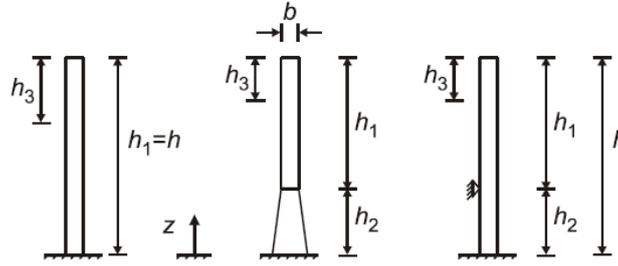
Figure I.2 - Geometric parameters for chimneys ($h_3=h_1/3$).

I.2.6 Ovalling frequency for cylindrical shells

The fundamental ovalling frequency for an unstiffened cylindrical shell is given by Eq. I.10:

$$n_{O,1} = 0,49 \cdot \frac{t}{b^2} \cdot \sqrt{\frac{E}{\rho_s}}$$

(I.10)

where:

t is the shell thickness;

b is the shell diameter;

E is the modulus of elasticity of the material;

ρ_s is the density of the material of the structure.

When structural sizes are in m, the modulus of elasticity in N/m^2 and the density in kg/m^3, frequency $n_{O,1}$ is obtained in Hz.

For steel shells (assuming $E = 0,21 \cdot 10^{12}$ N/m^2, $\rho_s = 7.850$ kg/m^3), Equation (I.10) becomes:

$$n_{O,1} = 2534 \cdot \frac{t}{b^2}$$

(I.11)

where, expressing t and b in m, frequency $n_{O,1}$ is obtained in Hz.

I.2.7 Fundamental bending frequency for bridge girders

The fundamental vertical bending frequency for bridge girders having sufficient torsional stiffness (e.g. box girders), even if with non-uniform cross-section, can be approximated by Eq. I.12:

$$n_1 = \frac{\lambda_p^2}{2\pi \cdot L^2} \cdot \sqrt{\frac{E \cdot J_f}{m}}$$

(I.12)

where:

L is length of the main span;

E is the modulus of elasticity of the material;

J_f is the moment of inertia of the cross-section (evaluated at midspan for variable sections);

m is the mass per unit length of the total cross-section of the bridge deck at midspan (including dead and live loads);

λ_p is a dimensionless configuration factor, depending on support condition. The following cases can be considered:

(a) for single span bridges:
$\lambda_p = \pi$ for simply supported girders;
$\lambda_p = 3,927$ for girders clamped at one end and supported at the other end;
$\lambda_p = 4,730$ for girders clamped at both ends;

(b) for two-span bridges, λ_p is obtained from Figure I.3, where $L \geq L_1$;

(c) for three-span bridges, λ_p is obtained from Figure I.3, where L_1 is the length of the longer side span and $L \geq L_1 \geq L_2$. This value applies also to bridges with a cantilevered or suspended main span. If $L_1 \geq L$, the factor λ_p may be obtained by considering only two spans, neglecting the shortest side span and considering the largest side span as the main span of an equivalent two-span bridge;

(d) for symmetrical four-span continuous girders (i.e. bridges symmetrical about the central support), factor λ_p can be obtained from the curves for two-span bridges, considering each half of the bridge as an equivalent two-span bridge;

(e) for non symmetrical four-span continuous girders and continuous girders with more than four spans, factor λ_p can be obtained from Figure I.3 using the curve appropriate to three-span bridges, taking as main span the largest internal span.
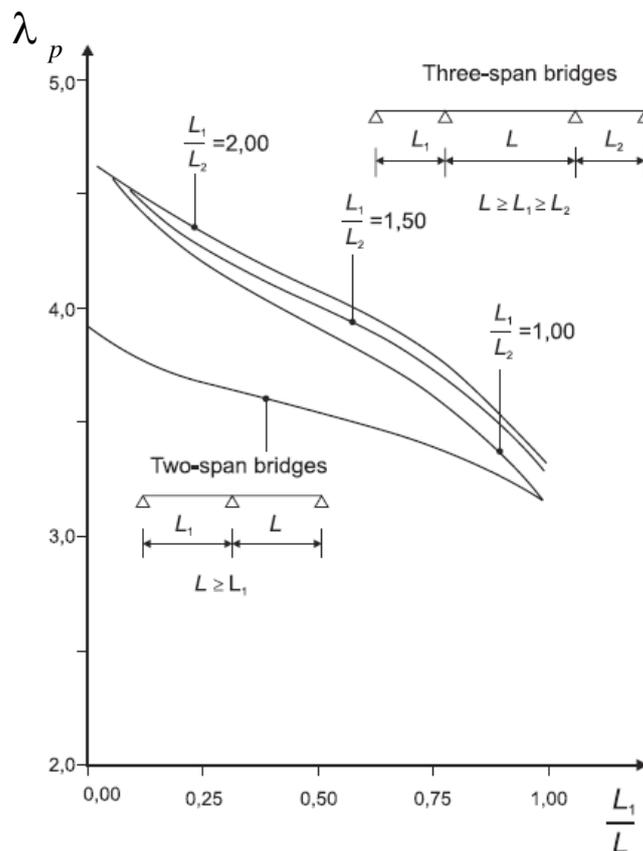
Figure I.3 - Dimensionless configuration factor λ_p.

If the value of $\sqrt{E \cdot J_f / m}$ at the girder supports is less than 0.8 times or exceeds twice the value at midspan, Equation (I.12) becomes inaccurate, and should not be used.

If structural dimensions are in m, the modulus of elasticity in N/m^2 and the mass per unit length in kg/m, the frequency n_1 is obtained in Hz.

The equations given in this heading are applicable only to cases in which the girder rests on stiff shoulders or piers. For bridge girders resting on flexible piers it is essential to use models that take jointly into account the deck and the piers.

I.2.8   Fundamental torsional frequency for bridge girders

The fundamental torsional frequency for bridge box girders can be approximated by Eq. I.13:

$$n_{M,1} = n_1 \cdot \sqrt{P_1 \cdot (P_2 + P_3)} \tag{I.13}$$

in which:

$$P_1 = \frac{m \cdot b^2}{I_f}, \quad P_2 = \frac{\sum_j r_j^2 \cdot I_{fj}}{b^2 \cdot I_f}, \quad P_3 = \frac{L^2 \cdot \sum_j J_{fj}}{2 \cdot \lambda_p \cdot b^2 \cdot I_f \cdot (1+\nu)} \tag{I.14}$$

where:
n_1 is the fundamental bending frequency;
b is the total width of the bridge;
m is the total mass per unit length of the bridge at midspan (including dead and live loads) in kg/m;
λ_p is the dimensionless configuration factor of heading I.2.7;
ν is the Poisson ratio of the girder material;
j is an index identifying the box girder;
r_j is the offset of the j-th box centre-line with respect to the bridge centre-line;
I_{fj} is the mass moment of inertia per unit length of the j-th box girder at midspan, including the effective width of deck;
I_f is the girder mass moment of inertia per unit length, given by Eq. I.15:

$$I_f = \frac{m_d \cdot b^2}{12} + \sum_j \left(I_{fj} + m_j \cdot r_j^2 \right) \tag{I.15}$$

where:
m_d is the mass per unit length of the girder at midspan;
I_{fj} is the mass moment of inertia of box j at midspan;
m_j is the mass per unit length of box j at midspan with an associated portion of deck;
J_{tj} is the torsional moment of inertia of box j at midspan, given by Eq. I.16:

$$J_{tj} = \frac{4 \cdot A_j^2}{\oint \frac{ds}{t}} \tag{I.16}$$

where A_j is the area enclosed by the j-th box at midspan; in the integral the chord thickness t is that of the midspan section.

Equation (I.13) may loose accuracy if applied to multi-box bridges having a span-to-width ratio of more than 6.

The dimensions of the parameters involved must be uniform so that the coefficients P_1, P_2, P_3 are dimensionless.

I.2.9 Oscillation frequencies for taut cables

This heading refers to cables subjected to a dead load and whose suspension points are at the same height (Figure I.4). In addition the condition expressed by Eq. I.17 must apply:

$$\frac{d}{L} \leq \frac{1}{8}$$

(I.17)

where:
d is the cable sag;
L is the distance between the ends of the cable.
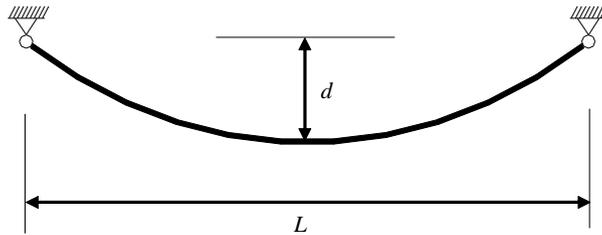
Figure I.4 – Cable with sag d.

The cable can have in-plane and out-of-plane oscillations. The natural frequency in the i-th out-of-plane mode is given by Eq. I.18:

$$n_i = \frac{i}{2 \cdot L} \cdot \sqrt{\frac{S}{m}}$$

(I.18)

where:
S is the cable tension;
m is the cable mass per unit length;
L is the distance between the ends of the cable.

When the cable tension is in N, the cable length in metres and the cable mass in kg/m, the frequency n_i is obtained in Hz.

In-plane oscillations can be further divided into anti-symmetric modes and symmetric modes. Anti-symmetric modes are characterised by vertical and longitudinal displacement components of the cable sections, which are respectively anti-symmetric and symmetric with respect to the cable midspan section. For these modes, the length of the cable does not vary, therefore no increase in tension is associated with them.

The natural frequency of the i-th anti-symmetric in-plane mode is given by Eq. I.19:

$$n_i = \frac{i}{L} \cdot \sqrt{\frac{S}{m}}$$

(I.19)

Symmetric modes are characterised by vertical and longitudinal displacement components, which are symmetric and anti-symmetric in respect to the centre point of the cable, respectively. When vibrating in a symmetric mode the cable is subject to a time-varying tension regime. Assuming this as constant along the cable, the natural frequency of the i-th symmetric mode is given by Eq. I.20:

$$n_i = \frac{\Omega_i}{2 \cdot L} \cdot \sqrt{\frac{S}{m}} \qquad (I.20)$$

Ω_i being a dimensionless coefficient given by Table I.II, depending on parameter ω^2:

$$\omega^2 = \frac{(m \cdot g)^2 \cdot L^3 \cdot E \cdot A}{S^3 \cdot L_e} \qquad (I.21)$$

where:

$$L_e \cong L \cdot \left(1 + 8\left(d/L\right)^2\right) \qquad (I.22)$$

where:
E is the modulus of elasticity of the cable;
A is the cable cross section;
g is the gravity acceleration.

For intermediate values of ω^2 linear interpolation is allowed.

Table I.II – Non-dimensional coefficient Ω_i as a function of ω^2.

ω^2	Ω_1	Ω_2	Ω_3	Ω_4	Ω_5	Ω_6	Ω_7	Ω_8
∞	2,86	4,92	6,94	8,95	10,96	12,97	14,97	16,98
$256\,\pi^2$	2,86	4,91	6,93	8,93	10,93	12,91	14,81	16,00
$196\,\pi^2$	2,85	4,91	6,92	8,92	10,91	12,81	14,00	15,15
$144\,\pi^2$	2,85	4,90	6,91	8,90	10,81	12,00	13,15	15,05
$100\,\pi^2$	2,85	4,89	6,89	8,80	10,00	11,15	13,04	15,02
$64\,\pi^2$	2,84	4,87	6,79	8,00	9,14	11,04	13,02	15,01
$36\,\pi^2$	2,82	4,78	6,00	7,14	9,04	11,02	13,01	15,01
$16\,\pi^2$	2,74	4,00	5,12	7,03	9,01	11,01	13,00	15,00
100	2,60	3,48	5,05	7,01	9,01	-	-	-
80	2,48	3,31	5,04	7,01	9,01	-	-	-
60	2,29	3,18	5,03	7,01	-	-	-	-
$4\,\pi^2$	2,00	3,09	5,02	7,01	-	-	-	-
20	1,61	3,04	5,01	7,00	-	-	-	-
10	1,35	3,02	5,00	-	-	-	-	-
8	1,28	3,01	-	-	-	-	-	-
6	1,22	-	-	-	-	-	-	-
4	1,15	-	-	-	-	-	-	-
2	1,08	-	-	-	-	-	-	-
1	1,04	-	-	-	-	-	-	-
0	1,00	3,00	5,00	7,00	9,00	11,00	13,00	15,00

I.3 Mode shapes

I.3.1 Fundamental mode shape of cantilevered structures

The fundamental mode shape $\Phi_1(z)$ of free-standing vertical structures, e.g. buildings, towers and chimneys, can be approximated by Eq. I.23 (Figure I.5):

$$\Phi_1(z) = \left(\frac{z}{h}\right)^{\zeta} \tag{I.23}$$

where:

z is the vertical coordinate;

h is the total height of the structure;

ζ is a parameter that defines the shape of the mode. The following values are proposed:

     ζ=0,6   for slender framed structures without shear walls;

     ζ=1,0   for framed buildings with central core or wind-bracing;

     ζ=1,5   for slender buildings with cantilever behaviour and buildings with RC core;

     ζ=2,0   for towers and chimneys;

     ζ=2,5   for steel lattice towers.

In the lack of more accurate estimates, the first torsional mode shape $\Phi_1(z)$ for buildings can also be approximated by Equation (I.23), with ζ=1,0.
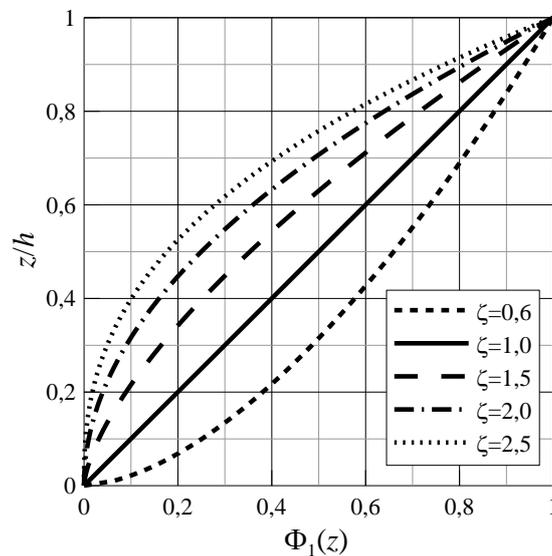
Figure I.5 – First lateral mode shape for buildings, towers and chimneys.

I.3.2   First bending mode shape of single-span beams

The first bending mode *s*hape $\Phi_1(s)$ of single-span beams is given in Table I.III for different support conditions.

Table I.III – First bending mode shape for single-span beams.

Support condition	Mode shape	$\Phi_1(s)$
		$\sin\left(\pi \cdot \dfrac{s}{\ell}\right)$
		$\dfrac{1}{2}\cdot\left[1-\cos\left(2\pi\cdot\dfrac{s}{\ell}\right)\right]$
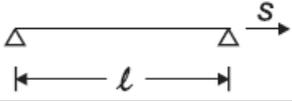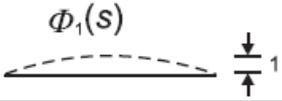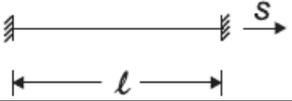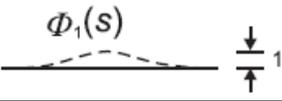
I.3.3 Second mode shape of cantilevered structures

The second mode shape $\Phi_2(z)$ of cantilevered structures, e.g. towers and chimneys, can be approximated by Eq. I.24 (Figure I.6):

$$\Phi_2(z) = -5.5\cdot\left(\frac{z}{h}\right)^2 + 8\cdot\left(\frac{z}{h}\right)^3 - 1.5\cdot\left(\frac{z}{h}\right)^4 \tag{I.24}$$

where:
z is the vertical coordinate;
h is the total height of the structure.

Equation (I.24) derives from data gathered from a large number of existing metal chimneys with a fundamental oscillation mode characterised by Equation (I.23), with ζ in the range of 1.6 to 2.2. The shape described by Equation (I.24) has maximum displacement at the tip of the structure (Figure I.6).
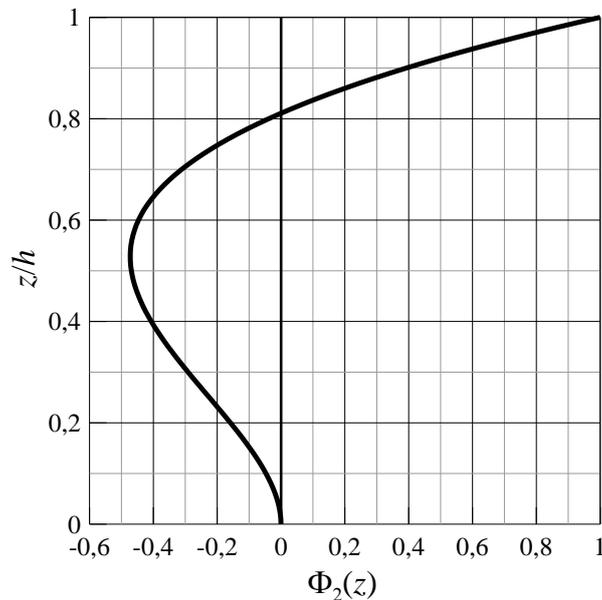
Figure I.6 – Second mode shape of towers and chimneys.

I.4   Generalised mass and equivalent mass

The generalised mass of the structure, m_i, in the i-th vibration mode $\Phi_i(s)$, is given by Eq. I.25:

$$m_i = \int_0^\ell m(s) \cdot \Phi_i^2(s)\, \mathrm{d}s \qquad (\text{I.25})$$

where:

$m(s)$ is the structural mass per unit length, as a rule a function of the s coordinate

ℓ is the height of the structure (or the length of the structural element).

The equivalent mass per unit length, $m_{e,i}$, in the i-th vibration mode $\Phi_i(s)$, is given by Eq. I.26:

$$m_{e,i} = \frac{m_i}{\int_0^\ell \Phi_i^2(s) \cdot \mathrm{d}s} \qquad (\text{I.26})$$

For cantilevered structures with non-constant mass per unit length, the value of the equivalent mass in the fundamental mode, $m_{e,1}$, can be approximated by the mean value of $m(s)$ over one third of the structure length towards the free end (h_3 in Figure I.2 for vertical structures).

For structures supported at both ends and having variable mass per unit length, the value of the equivalent mass in the first mode, $m_{e,1}$, can be approximated from the mean value of $m(s)$ over one third of the structure length centred at the section of maximum modal displacement.

I.5   Generalised mass moment of inertia

The generalised mass moment of inertia (flexural or polar) I_i, in the i-th mode $\Phi_i(s)$ is given by Eq. I.27:

$$I_i = \int_0^\ell I(s) \cdot \Phi_i^2(s) \cdot \mathrm{d}s \qquad (\text{I.27})$$

where:

$I(s)$ is the mass moment of inertia (flexural or polar) of the structure per unit length, as a rule a function of coordinate s;

ℓ is the height of the structure (or length of the structural element).

I.6   Damping ratio

The damping ratio ξ in the fundamental mode is given by Eq. I.28:

$$\xi = \xi_s + \xi_a + \xi_d \qquad (\text{I.28})$$

where:

ξ_s is the structural damping ratio;

ξ_a is the aerodynamic damping ratio;

ξ_d is the damping ratio associated with the presence of damping devices.

Headings I.6.1-I.6.4 provide approximate values of the structural damping ratio ξ_s, for a variety of structural types of interest in wind engineering. Heading I.6.5 provides some guidance on the

calculation of the aerodynamic damping ratio. The additional damping ratio associated with the presence of damping devices must be calculated through specific theoretical, numerical and/or experimental analyses.

Headings I.6.1-I.6.4 provide the value of the structural damping ratio for the fundamental mode or for the first few modes. In the lack of more accurate estimates for the higher modes, an initial approximation can be made by considering a structural damping ratio equal to that of the highest mode considered. This simplified criterion cannot be applied to the evaluation of the aerodynamic damping and of the damping associated with damping devices.

I.6.1 Structural damping ratio for multi-storey buildings

For small oscillations, the structural damping ratio $\xi_{s,1}$, in the first flexural mode of buildings can be approximately taken as linearly increasing with the fundamental frequency n_1. Moreover, experimental results have shown that the damping ratio tends to increase with the amplitude of the oscillations. With the goal of considering values on the safe side, valid also for verifications at serviceability and abitability limit states (where the role of the amplitude of oscillations on damping is not significant), the values reported in Eqs. I.29 and I.30 can be taken:

$$\xi_{s,1} = \frac{1}{100} \cdot \frac{68}{h} \geq 0,01 \qquad \text{for reinforced concrete buildings, } h \geq 30 \text{ m} \tag{I.29}$$

$$\xi_{s,1} = \frac{1}{100} \cdot \frac{56}{h} \geq 0,008 \qquad \text{for steel buildings, } h \geq 30 \text{ m} \tag{I.30}$$

The values given by Equations (I.29) and (I.30) include also the effects of soil-structure interaction.

For buildings of height h less than 30 m, the values calculated through Equations (I.29) and (I.30) for h=30 m shall be taken. Larger values can be taken for ultimate limit state assessments (always to be carried out in the elastic range), based on the results of specific analyses.

For the higher modes of high-rise buildings, damping can be significantly larger than that in the fundamental mode; the damping ratio in the higher modes can be approximated by Eqs. I.31 and I.32:

$$\xi_{s,i} = 1,4 \cdot \xi_{s,i-1} \quad (i = 2,3) \quad \text{for reinforced concrete buildings, } h \geq 50 \text{ m} \tag{I.31}$$

$$\xi_{s,i} = 1,3 \cdot \xi_{s,i-1} \quad (i = 2,3) \quad \text{for steel buildings, } h \geq 50 \text{ m} \tag{I.32}$$

Equations (I.31) and (I.32) do not correspond to proportional damping, which is a typical assumption in structural analyses.

The damping ratio in torsional modes is very much dependent on the fundamental lateral frequency n_1; in the lack of more detailed data, on the safe side, it can be taken as equal to the damping ratio relative to the fundamental mode, by using Equations (I.29) and (I.30).

I.6.2 Structural damping ratio for chimneys

Table I.IV provides approximate, generally conservative, values of the damping ratio ξ_s in the first mode of reinforced concrete and steel chimneys.

Table I.IV – Structural damping ratios for chimneys.

Structural type		ξ_s
Reinforced concrete chimneys and towers		0.005
Unlined welded steel stacks without external thermal insulation		0.002
Unlined welded steel stacks with external thermal insulation		0.003
Steel stacks with one liner with external thermal insulation (*)	$h/b < 18$	0.003
	$20 \leq h/b < 24$	0.006
	$h/b > 26$	0.,002
Steel stacks with two or more liners with external thermal insulation (*)	$h/b < 18$	0.003
	$20 \leq h/b < 24$	0.006
	$h/b > 26$	0.004
Steel stacks with internal brick liner		0.011
Steel stacks with internal gunite		0.005
Unlined coupled stacks		0.002
Unlined guyed steel stacks		0.006

(*) *For intermediate values of the h/b ratio, linear interpolation is allowed*

In the lack of more accurate data, and as a first approximation, the values given in Table I.IV can also be used for ovalling modes.

I.6.3 Structural damping ratio for bridges

Table I.V gives approximate, generally conservative, values of the damping ratio ξ_s in the first bending mode of bridge girders made of different structural materials.

For timber, glass and plastic bridges, the values given in Table I.V are indicative; the actual values may be substantially different.

Table I.V – Structural damping ratio values for bridge decks.

Structural type		ξ_s
Steel bridges (welded)		0.003
Steel bridges (high strength bolts)		0.005
Steel bridges (standard bolts)		0.008
Composite bridges		0.006
Concrete bridges	Prestressed or uncracked	0.006
	Cracked	0.016
Timber bridges		0.009
Aluminium alloy bridges		0.003
Bridges in glass or fibre-reinforced plastic		0.006

I.6.4 Structural damping ratio for cables

The damping ratio for cables is generally very small and difficult to assess. Table I.VI gives conservative values, to be taken as a first approximation. These values apply to all oscillation modes.

Table I.VI – Structural damping ratio for cables.

Structural type	ξ_s
parallel cables	0.001
spiral cables	0.003

I.6.5 Aerodynamic damping ratio

For slender structures (where the length is much greater than cross-sectional dimensions), the aerodynamic damping ratio ξ_a in the first along-wind vibration mode is given by Eq. I.33:

$$\xi_a = \frac{c_{fX} \cdot \rho \cdot b \cdot v_m \left(z_e \right)}{4 \cdot \pi \cdot n_1 \cdot m_{e,1}} \tag{I.33}$$

where:
c_{fX} is the along-wind force coefficient (Annex G);
ρ is the air density; the recommended value is 1,25 kg/m³;
b is the width of the structure (size perpendicular to the direction of the oncoming wind);
v_m is the mean wind velocity (heading 3.2.5) calculated at the equivalent height z_e defined in heading L.1 (Figure L.2);
n_1 is the oscillation frequency;
$m_{e,1}$ is the equivalent mass per unit length in the first along-wind mode, Equation (I.26).

Equation (I.33) can also be used for buildings; in this case, $c_{fX} = (c_{pe,p} - c_{pe,n})$, where $c_{pe,p}$ and $c_{pe,n}$ are pressure coefficients on the upwind and downwind faces respectively (Annex G).

In no case Equation (I.33) should be generalised to the assessment of aerodynamic damping for lateral and torsional vibrations (Annexes M and O). In these cases assessment of aerodynamic damping requires specialist advice and/or experimental assessments.

Annex L   ALONG-WIND EQUIVALENT STATIC ACTIONS AND ALONG-WIND ACCELERATIONS

L.1   General principles

Along-wind equivalent static actions, according to Equation (3.17), can be expressed in the form given by Eq. L.1:

$$\text{Along-wind equivalent static actions} = \text{Peak along-wind aerodynamic actions} \times c_{dD} \qquad \text{(L.1)}$$

where by "peak along-wind aerodynamic actions" it is meant the pressure acting on the external faces of the building ($p_e(z)$, heading 3.3.1), the net pressure on a surface ($p_n(z)$, heading 3.3.2), the resulting along-wind force on constructions and compact elements (heading 3.3.3), the along-wind force per unit length on constructions and slender elements (heading 3.3.4). The along-wind dynamic factor c_{dD} is a dimensionless parameter that modifies peak aerodynamic actions, to account for the partial correlation of wind action and for the amplification of the resonant load. In general, $c_{dD} > 1$ for small, slender, flexible and/or low damped structures and elements; $c_{dD} < 1$ for stiff and/or high damped structures and elements with large exposed surfaces.

The along-wind dynamic factor c_{dD} does not apply to all the peak actions above, but only to components in the along-wind direction (Figure L.1); moreover, it is not applicable to internal pressure and shear actions.
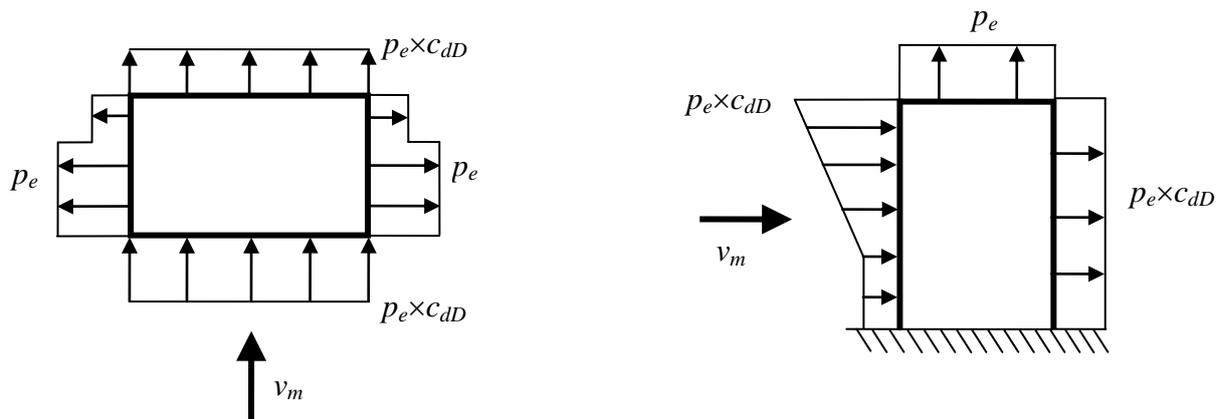
Figure L.1 – Examples of use of the along-wind dynamic factor
(note that this is not applied to the lateral walls and to the roof).

In the lack of more accurate estimates, this Annex provides two different calculation methods for the along-wind dynamic factor c_{dD}.

The first method (heading L.2) concerns a detailed calculation procedure that can be used for the structural types indicated in Figure L.2; it is valid only if the along-wind response is mostly associated with one vibration mode with constant sign (no nodes in the mode shape, Figure L.3); this usually occurs for the fundamental mode, checking that higher modes have no influence on the response (the second along-wind natural frequency shall be at least twice the fundamental frequency).

Vertical structures   Horizontal structures   Point-like structures

$z_e=0.6\,h \geq z_{min}$ $z_e=h_1+h/2 \geq z_{min}$ $z_e=h_1+h/2 \geq z_{min}$
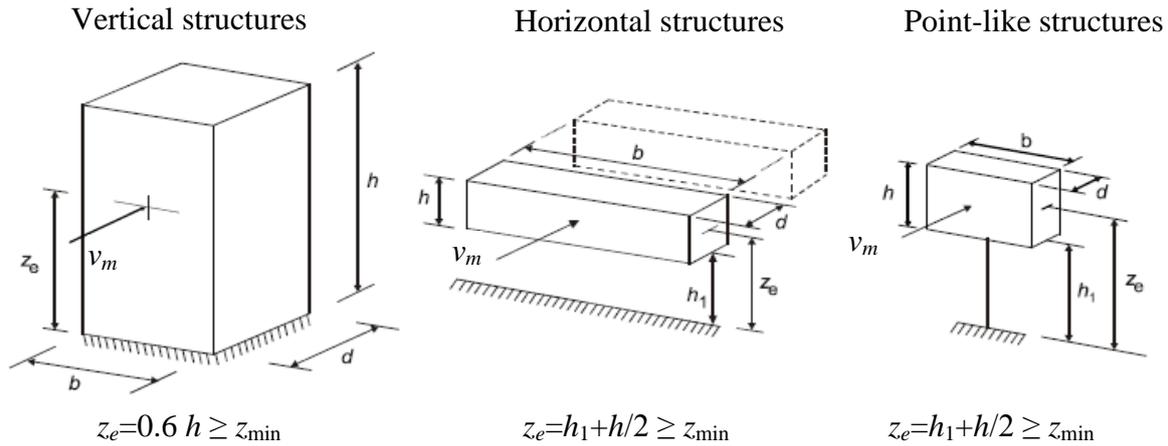
Figure L.2 – Structural types subject to the detailed calculation procedure.
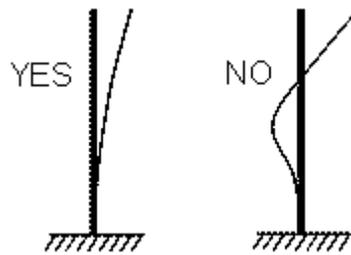
Figure L.3 – Vibration modes to which the detailed procedure can be or cannot be applied (buildings and point-like structures).

The second method (heading L.3) is a simplified, conservative calculation procedure, valid only for rectangular plan buildings with regular distribution of stiffness and mass.

For buildings and other vertical structures to which the detailed procedure can be applied, heading L.4 provides a method for calculating wind-induced acceleration at each storey level, to be used in abitability assessments (Annex N).

For all structural types not considered above, reliable analytical, numerical and/or experimental methods should be used.

L.2 Detailed method

The along-wind dynamic factor c_{dD} is given by Eqs. L.2 and L.3

$$c_{dD} = \frac{G_D}{1 + 7 \cdot I_v(z_e)} \tag{L.2}$$

$$G_D = 1 + 2 \cdot g_D \cdot I_v(z_e) \cdot \sqrt{B^2 + R_D^2} \tag{L.3}$$

where:
G_D is the along-wind gust factor;
z_e is the reference height (Figure L.2);
$I_v(z_e)$ is the turbulence intensity (heading 3.2.6) calculated at height $z = z_e$;
g_D is the along-wind peak factor, defined as the ratio between the maximum value of the fluctuating part of the response and its standard deviation;
B is the background factor, taking into account the partial correlation of the pressure acting on the structure;

R_D is the resonant response factor, taking into account the resonant response of the first vibration mode.

The background factor B is given by Eq. L.4 (Figure L.4):

$$B^2 = \frac{1}{1 + 0,9 \cdot \left(\dfrac{b + h}{L_v(z_e)} \right)^{0,63}}$$

(L.4)

where:
b is the width of the structure (across-wind) (Figure L.2);
h is the height of the structure (Figure L.2);
z_e is the reference height (Figure L.2);
$I_v(z_e)$ is the turbulence length scale (heading 3.2.6), calculated at height z = z_e.

B is in general less than 1, therefore B=1 is a conservative estimate (full pressure correlation).
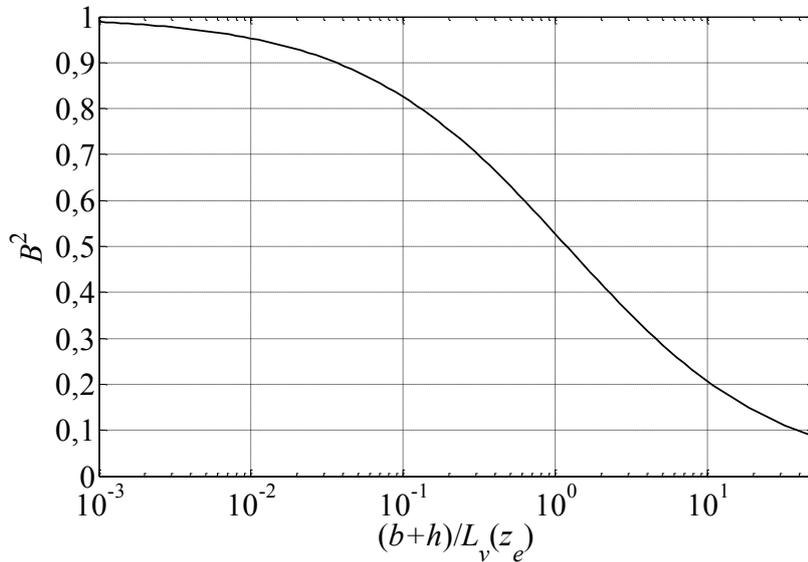
Figure L.4 - Square of background factor B.

The resonant response factor R_D is given by Eqs. L.5-L.9:

$$R_D^2 = \frac{\pi}{4 \cdot \xi_D} S_D \cdot R_h \cdot R_b$$

(L.5)

$$S_D = \frac{6,868 \cdot n_D \cdot L_v(z_e) / v_m(z_e)}{\left[1 + 10,302 \cdot n_D \cdot L_v(z_e) / v_m(z_e) \right]^{5/3}}$$

(L.6)

$$R_h = \begin{cases} 0 & \text{for} \quad \eta_h = 0 \\ \dfrac{1}{\eta_h} - \dfrac{1}{2 \cdot \eta_h^2}(1 - e^{-2 \cdot \eta_h}) & \text{for} \quad \eta_h > 0 \end{cases} \qquad (L.7)$$

$$R_b = \begin{cases} 0 & \text{per} \quad \eta_b = 0 \\ \dfrac{1}{\eta_b} - \dfrac{1}{2 \cdot \eta_b^2}(1 - e^{-2 \cdot \eta_b}) & \text{per} \quad \eta_b > 0 \end{cases} \qquad (L.8)$$

$$\eta_h = 4 \cdot \frac{n_D \cdot h}{v_m(z_e)}, \qquad \eta_b = 4 \cdot \frac{n_D \cdot b}{v_m(z_e)} \qquad (L.9)$$

where:

ξ_D is the damping ratio in the first along-wind vibration mode (Annex I);

n_D is the fundamental along-wind frequency(Annex I);

$v_m(z_e)$ is the mean wind velocity (clause 3.2.5), calculated at height $z=z_e$;

$L_v(z_e)$ is the turbulence length scale (clause 3.2.6), calculated at height $z=z_e$;

S_D is a dimensionless parameter, given in Figure L.5, accounting for the spectral content of longitudinal turbulence (Equation E.1a);

R_h and R_b are two dimensionless parameters, given in Figure L.6, accounting for the partial coherence (i.e. lack of correlation) of the longitudinal turbulence (Equation E.5).
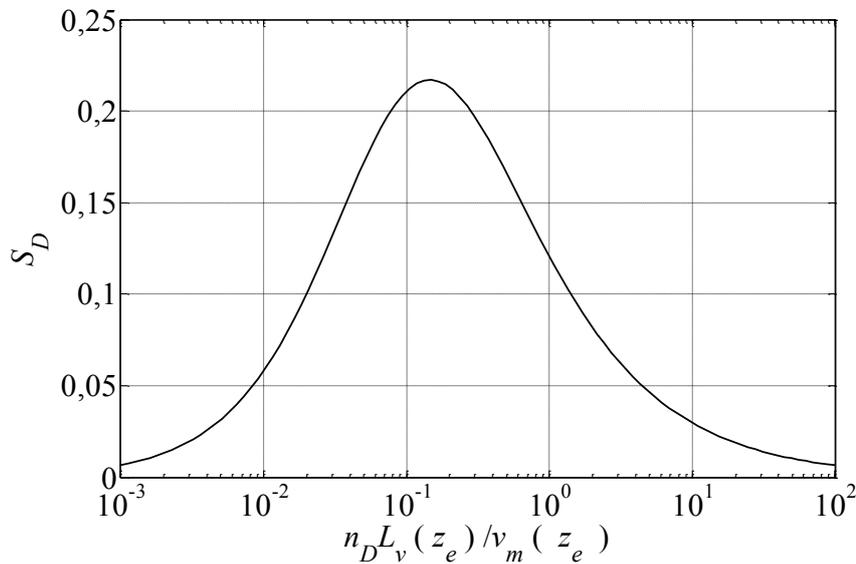
Figure L.5 - Graph of S_D.
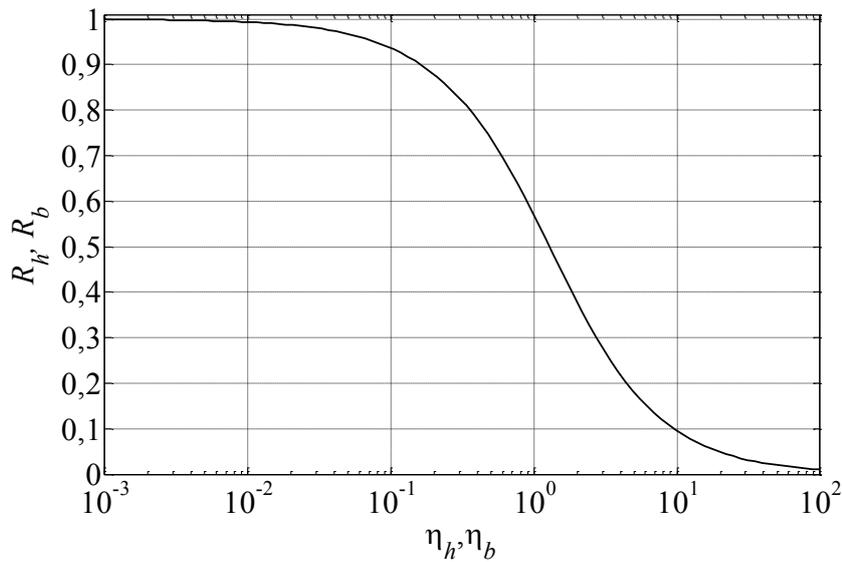
Figure L.6 - Graph of R_h and R_b.

The peak factor in the along-wind direction is given by Eqs. L.10 and L.11 (Figure L.7):

$$g_D = \sqrt{2 \cdot \ln(\upsilon_D \cdot T)} + \frac{0,5772}{\sqrt{2 \cdot \ln(\upsilon_D \cdot T)}} \geq 3 \qquad (L.10)$$

$$\upsilon_D = n_D \cdot \sqrt{\frac{R_D^2}{B^2 + R_D^2}} \geq 0,08 \text{ Hz} \qquad (L.11)$$

where:
υ_D is the expected frequency of the along-wind response;
T is the mean wind velocity averaging time, T=600 s.
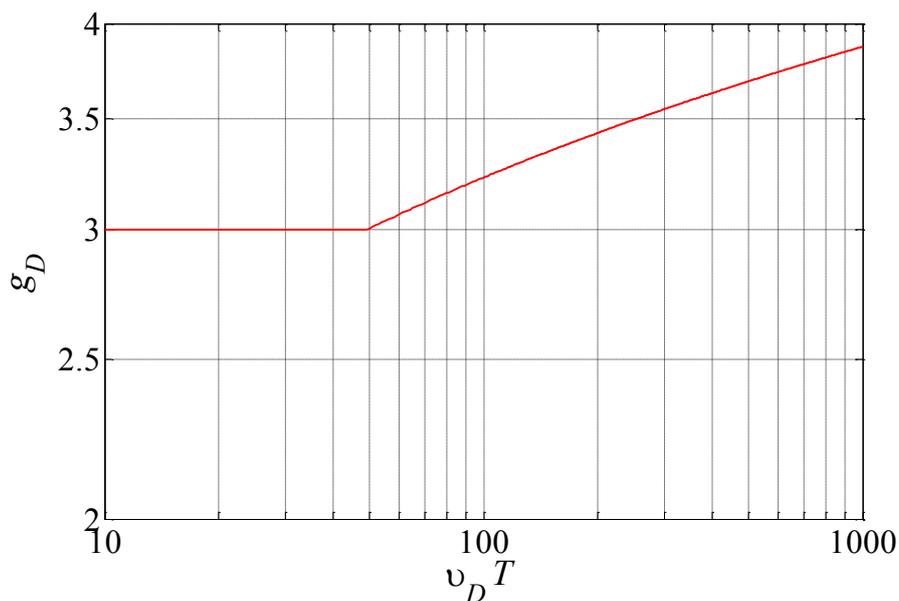
Figure L.7 – Along-wind peak factor g_D.

In Table L.I the calculation procedure for the along-wind dynamic factor is shown.

Table L.I - Calculation procedure for the along-wind dynamic factor.

Step	Operation
1	Choice of the reference structural model (Figure L.2)
2	Evaluation of the geometric parameters b, h, z_e (Figure L.2)
3	Evaluation of the mean wind velocity $v_m(z_e)$ (Heading 3.2.5)
4	Evaluation of the turbulence intensity $I_v(z_e)$ (Heading 3.2.6)
5	Evaluation of the turbulence length scale $L_v(z_e)$ (Heading 3.2.6)
6	Evaluation of dynamic parameters n_D and ξ_D (Annex I)
7	Evaluation of the background factor B (Equation L.4, Figure L.4)
8	Evaluation of the parameter S_D (Equation L.6, Figure L.5)
9	Evaluation of parameters η_h and η_b (Equation L.9)
10	Evaluation of parameters R_h (Equation L.7) and R_b (Equation L.8) (Figure L.6)
11	Evaluation of the resonant response factor R_D (Equation L.5)
12	Evaluation of the expected frequency υ_D (Equation L.11)
13	Evaluation of the peak factor g_D (Equation L.10)
14	Evaluation of the gust factor G_D (Equation L.3)
15	Evaluation of the dynamic factor c_{dD} (Equation L.2)

L.3 Simplified procedure for buildings

Starting from the detailed procedure reported in heading L.2, a conservative value of the along-wind dynamic factor can be derived, which applies to rectangular plan buildings with regular distribution of stiffness and mass, even in the case in which the exact dynamic characteristics of the structure are not known. The figures reported in this heading were obtained by using the detailed procedure, as an envelope for all possible situations associated with different values of the base reference wind velocity and of the roughness length (assuming a unit value for the topography coefficient). The values of the vibration frequencies are calculated through Equations (I.4) and (I.5) on the safe side; the values of the damping ratios are taken from Equations (I.29) and (I.30). Figure L.8 applies to multi-storey steel buildings. Figure L.9 applies to multi-storey reinforced concrete or composite buildings.
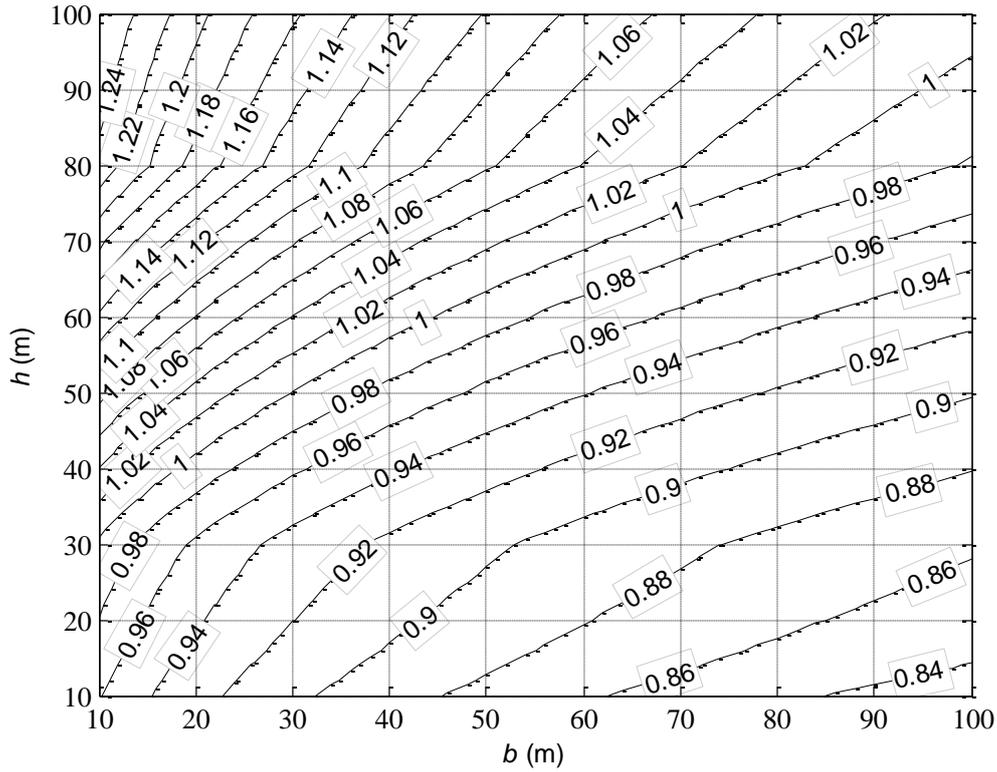
Figure L.8 – Along-wind dynamic factor c_{dD} for rectangular plan steel buildings.
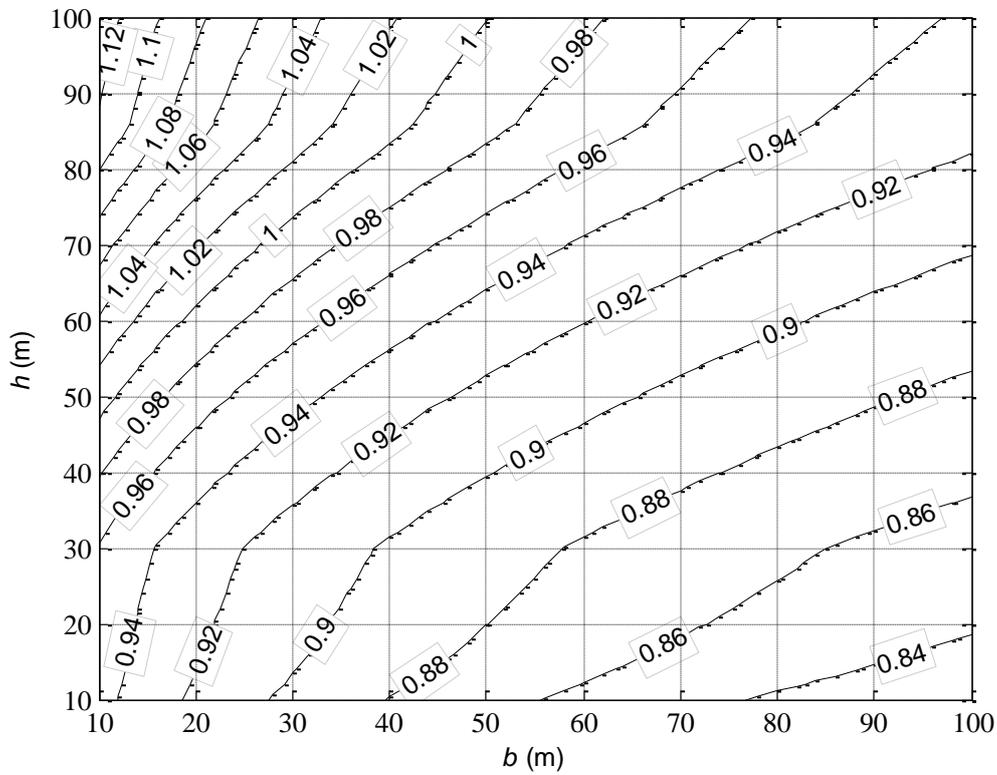
Figure L.9 – Along-wind dynamic factor c_{dD} for rectangular plan RC or composite buildings.

L.4 Acceleration of vertical structures

The application of equivalent static actions to the structure allows assessment of the maximum along-wind deflection and of the associated stresses. In any case, especially for high-rise building, and more in general for vertical constructions designed to accommodate people, it may also be important to determine the wind-induced accelerations, for abitability assessments (Annex N).

The peak value of the along-wind acceleration at height z is given by Eq. L.12:

$$a_{pD}(z) = g_{aD} \cdot \sigma_{aD}(z) \tag{L.12}$$

where:
g_{aD} is the acceleration peak factor:

$$g_{aD} = \sqrt{2 \cdot \ln(n_D \cdot T)} + \frac{0,5772}{\sqrt{2 \cdot \ln(n_D \cdot T)}} \geq 3 \tag{L.13}$$

σ_{aD} is the standard deviation of the along-wind acceleration at height z:

$$\sigma_{aD}(z) = \frac{\rho \cdot v_m^2(z_e) \cdot b \cdot h}{m_D} \cdot c_{fD} \cdot I_v(z_e) \cdot R_D \cdot K_D \cdot \Phi_D(z) \tag{L.14}$$

where:
n_D is the fundamental along-wind frequency (Annex I);
T is the mean wind velocity averaging time interval, T=600 s;
ρ is the air density, ρ=1.25 kg/m^3 (heading 3.2.7);
$v_m(z_e)$ is the mean wind velocity (clause 3.2.5), evaluated for $z = z_e$, for a design return period T_R suitable for abitability assessment (Annex N);
b is the width of the structure (Figure L.2);
h is the height of the structure (Figure L.2);
m_D is the generalised mass in the first along-wind mode (Annex I);
c_{fD} is the coefficient of along-wind force per unit length (Annex G); for buildings, $c_{fD} = (c_{pe,p} - c_{pe,n})$, where $c_{pe,p}$ and $c_{pe,n}$ are respectively the pressure coefficients of the windward and leeward face (Annex G);
$I_v(z_e)$ is the turbulence intensity (clause 3.2.6), evaluated at height $z = z_e$;
R_D is the resonant response factor, the square of which is given by Equation L.5 for a design return period T_R suitable for abitability assessment (Annex N);
$\Phi_D(z)$ is the first along-wind mode shape (Annex I);
K_D is a dimensionless coefficient defined by Eq. L.15:

$$K_D = \frac{\int_0^h v_m(z) \cdot \Phi_D(z) \cdot \mathrm{d}z}{h \cdot v_m(z_e)} \tag{L.15}$$

Only when the fundamental mode shape can be written as $\Phi_D(z)=(z/h)^\zeta$ (Annex I), and the topography coefficient is $c_t = 1$ (heading 3.2.4), Eq. L.15 can be approximated by Eq. L.16 (Figure L.10):

$$K_D = \frac{(\zeta+1)\left[\ln\left(\dfrac{z_e}{z_0}\right)+0,5\right]-1}{(\zeta+1)^2\ln\left(\dfrac{z_e}{z_0}\right)}$$

(L.16)

where z_0 is the roughness length of the site, defined at heading (3.2.4).
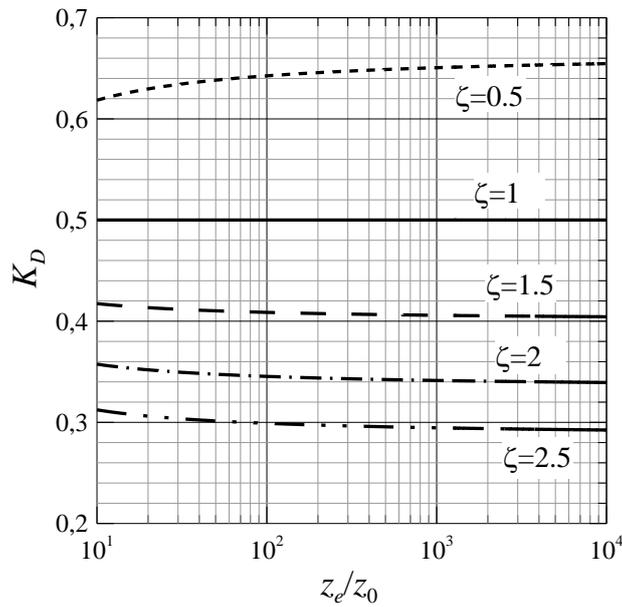
Figure L.10 – Dimensionless coefficient K_D.

Annex M   ACROSS-WIND AND TORSIONAL EQUIVALENT STATIC ACTIONS AND ACCELERATIONS

M.1   General Principles

In general, wind exerts along-wind, across-wind and torsional actions on buildings. Across-wind (*L*, *lift*) and torsional (*M*, *moment*) actions become more important the higher, more slender and flexible the building, mainly because of the wake induced by vortex shedding.

This Annex contains procedures applicable to rectangular plan buildings (Figure M.1). The effects of across-wind and torsional actions shall be assessed if:

$$\frac{h}{\sqrt{b \cdot d}} \geq 3 \tag{M.1}$$

where:
b   is the width of the building (across-wind size);
d   is the depth of the building (along-wind size);
h   is the height of the building.
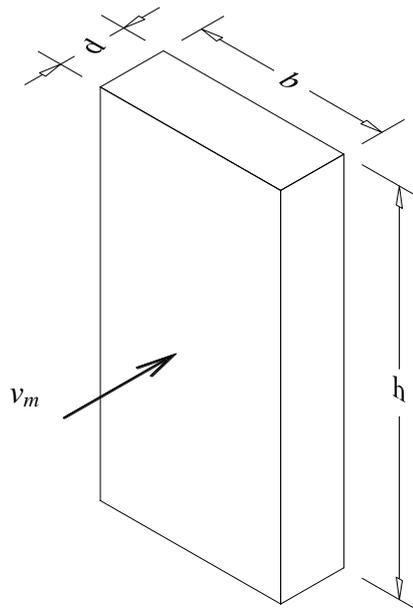
Figure M.1 – Key for rectangular plan buildings.

The procedures given below to calculate equivalent static actions and across-wind and torsional accelerations are applicable when:

(a)   the wind direction is orthogonal to a face of the building (this is usually the most unfavourable load case);

(b)   the building has a uniform vertical mass distribution;

(c)   the building sizes meet the requirements given by Eqs. M.2 to M.4:

$$\frac{h}{\sqrt{b \cdot d}} \leq 6 \tag{M.2}$$

$$0,2 \leq \frac{d}{b} \leq 5 \qquad (\text{M.3})$$

$$\frac{v_m(h)}{n_{LM} \cdot \sqrt{b \cdot d}} \leq 10 \qquad (\text{M.4})$$

where:

$v_m(h)$ is the mean wind velocity (clause 3.2.5), evaluated at the tip of the building, $z=h$;

n_{LM} is the first across-wind or the first torsional frequency, depending on the analysis to carry out. Estimates of the flexural or torsional vibration frequencies are given in Annex I.

When b and d are in m, v_m in m/s and n_{LM} in Hz, the first member of Equation M.4 is dimensionless.

For buildings meeting the requirements of Equations M.2 to M.4, headings M.2 and M.3 contain two detailed calculation procedures to assess the equivalent static across-wind forces and torsional moments, respectively. Heading M.4 contains a simplified conservative procedure to assess static equivalent across-wind forces and torsional moments on square plan buildings. Heading M.5 contains a procedure for the evaluation of across-wind and torsional accelerations for use in abitability assessments of buildings (Annex N). Heading M.6 contains the criteria for combining along-wind, across-wind and torsional actions and their associated effects.

For buildings not meeting the requirements of Equations M.2 to M.4, aeroelastic phenomena may arise. In these cases, use should be made of reliable experimental, numerical and/or theoretical methods.

M.2   Detailed procedure for across-wind actions

Across-wind vibrations are caused by the lateral turbulence and by the turbulent wake. This heading contains a procedure for estimating the static forces equivalent to the actions generated by wind in the across-wind direction.

The equivalent across-wind static force per unit length is given by Eq. M.5:

$$f_L(z) = 3 \cdot q_p(h) \cdot C_L \cdot b \cdot \left(\frac{z}{h}\right) \cdot c_{dL} \qquad (\text{M.5})$$

where:

$q_p(h)$ is the peak velocity pressure (heading 3.2.7), evaluated at height $z=h$;

C_L is the aerodynamic force coefficient (associated with the fluctuating overturning moment, Figure M.1), given by Eq. M.6:

$$C_L = 0,0082 \cdot \left(\frac{d}{b}\right)^3 - 0,071 \cdot \left(\frac{d}{b}\right)^2 + 0,22 \cdot \frac{d}{b} \qquad (\text{M.6})$$

c_{dL} is the across-wind dynamic factor, given by Eqs. M.7 and M.8:

$$c_{dL} = \frac{G_L}{1 + 7 \cdot I_v(h)}$$ (M.7)

$$G_L = g_L \cdot \sqrt{1 + R_L^2}$$ (M.8)

where:
G_L is the across-wind gust factor;
g_L is the across-wind peak factor;
R_L is the across-wind resonant response factor;
$I_v(h)$ is the turbulence intensity (clause 3.2.6) at height $z=h$.
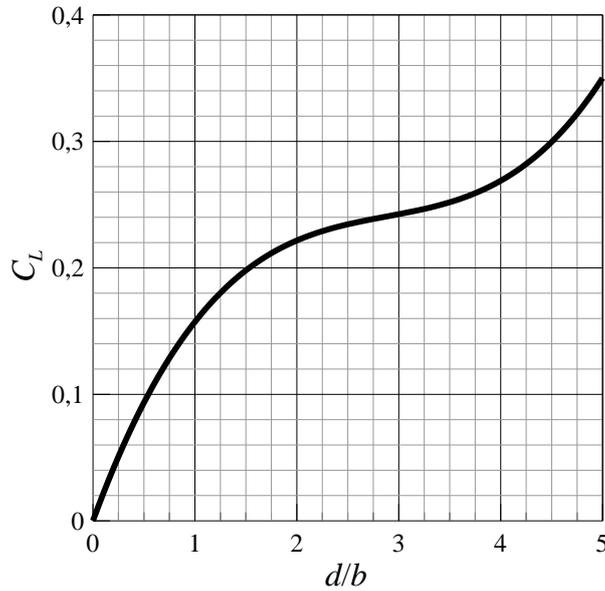
Figure M.2 – Aerodynamic force coefficient C_L.

The resonant response factor in the across-wind direction is given by Eqs. M.9 to M.14:

$$R_L^2 = \frac{\pi \cdot S_L}{4 \cdot \xi_L}$$ (M.9)

$$S_L = \sum_{j=1}^{m} \frac{4 k_j \cdot (1 + 0,6 \cdot \beta_j) \cdot \beta_j}{\pi} \frac{\left(\frac{n_L}{n_{sj}} \right)^2}{\left[1 - \left(\frac{n_L}{n_{sj}} \right)^2 \right]^2 + 4 \cdot \beta_j^2 \cdot \left(\frac{n_L}{n_{sj}} \right)^2}$$ (M.10)

$$m = \begin{cases} 1 & d/b < 3 \\ 2 & d/b \geq 3 \end{cases}$$ (M.11)

$$k_1 = 0,85, \quad k_2 = 0,02$$ (M.12)

$$\beta_1 = \frac{\left(\dfrac{d}{b}\right)^4 + 2,3 \cdot \left(\dfrac{d}{b}\right)^2}{\left[2,4 \cdot \left(\dfrac{d}{b}\right)^4 - 9,2 \cdot \left(\dfrac{d}{b}\right)^3 + 18 \cdot \left(\dfrac{d}{b}\right)^2 + 9,5 \cdot \left(\dfrac{d}{b}\right) - 0,15\right]} + \frac{0,12}{\left(\dfrac{d}{b}\right)}, \quad \beta_2 = 0,28 \cdot \left(\dfrac{d}{b}\right)^{-0,34} \qquad \text{(M.13)}$$

$$n_{s1} = \frac{0,12}{\left\{1 + 0,38 \cdot \left(\dfrac{d}{b}\right)^2\right\}^{0,89}} \frac{v_m(h)}{b}, \quad n_{s2} = \frac{0,56}{\left(\dfrac{d}{b}\right)^{0,85}} \frac{v_m(h)}{b} \qquad \text{(M.14)}$$

where:

ξ_L is the damping ratio in the first across-wind mode (Annex I);

n_L is the first across-wind frequency (Annex I);

$v_m(h)$ is the mean wind velocity (Clause 3.2.5), evaluated at height $z=h$;

β_1, β_2 are dimensionless coefficients given in Figure M.3;

n_{s1}, n_{s2} are parameters given, in a dimensionless form, in Figure M.4.
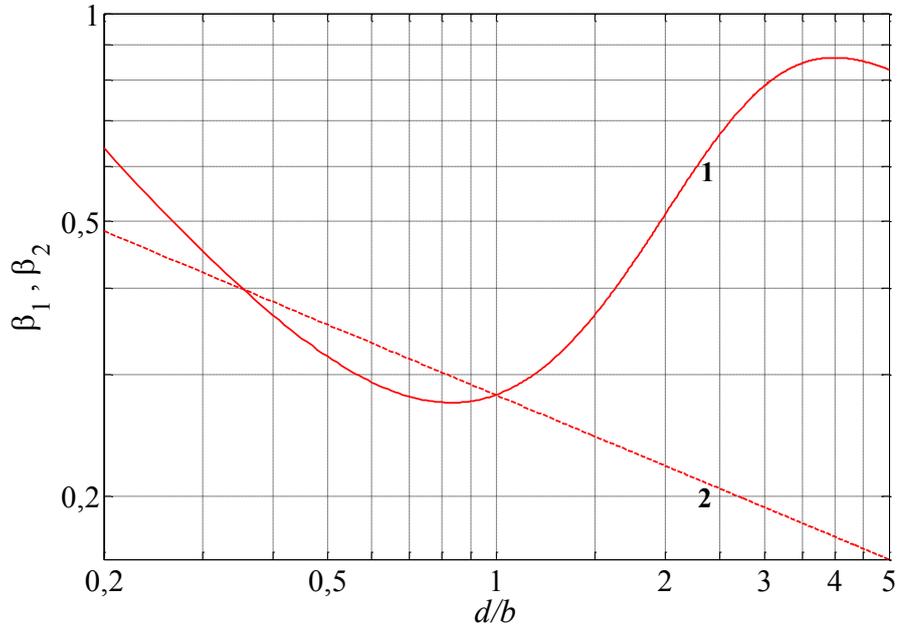
Figure M.3 - Graphs of β_1 and β_2.
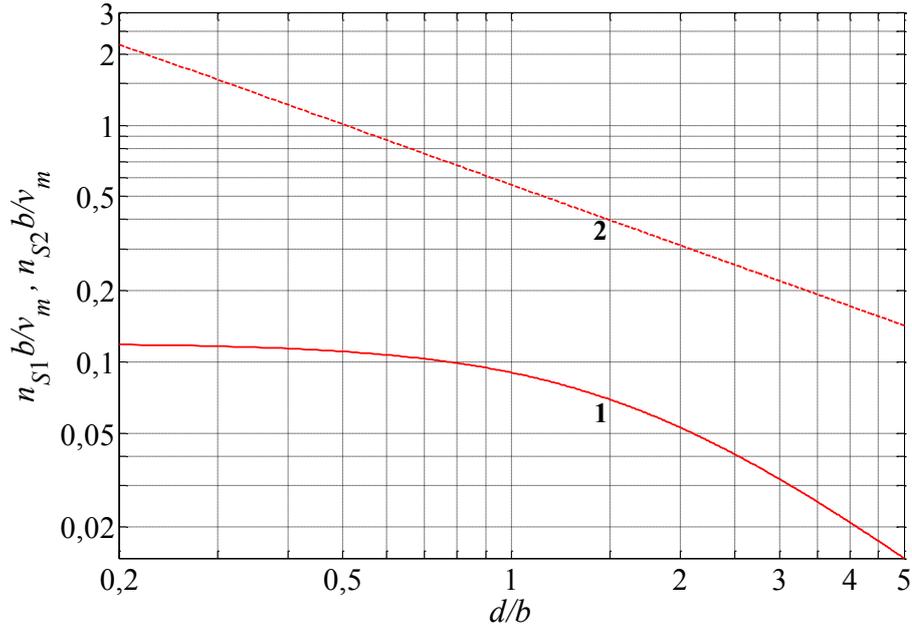
Figure M.4 - Graphs of $n_{s1}b/v_m(h)$ and $n_{s2}b/v_m(h)$.

The across-wind peak factor is given by Eq. M.15:

$$g_L = \sqrt{2 \cdot \ln\left(n_L \cdot T\right)} + \frac{0,5772}{\sqrt{2 \cdot \ln\left(n_L \cdot T\right)}} \geq 3 \qquad (M.15)$$

where:
n_L is the fundamental across-wind frequency (Annex I);
T is the mean wind velocity averaging time interval, T=600 s;

In Table M.I the calculation procedure of the across-wind dynamic factor is shown.

Table M.I - Across-wind dynamic factor calculation procedure.

Step	Operation
1	Evaluation of geometric parameters b, d, h (Figure M.1)
2	Evaluation of the mean wind velocity $v_m(h)$ (Heading 3.2.5)
3	Evaluation of the turbulence intensity $I_v(h)$ (Heading 3.2.6)
4	Evaluation of dynamic parameters n_L and ξ_L (Annex I)
5	Evaluation of parameter m (Equation M.11)
6	Evaluation of parameters k_1 and k_2 (if m=2) (Equation M.12)
7	Evaluation of parameters β_1 and β_2 (if m=2) (Equation M.13, Figure M.3)
8	Evaluation of parameter n_{s1} and n_{s2} (if m=2) (Equation M.14, Figure M.4)
9	Evaluation of parameter S_L (Equation M.10)
10	Evaluation of resonant response factor R_L (Equation M.9)
11	Evaluation of peak factor g_L (Equation M.15)
12	Evaluation of gust factor G_L (Equation M.8)
13	Evaluation of dynamic coefficient c_{dL} (Equation M.7)

M.3 Detailed procedure for torsional actions

Torsional vibrations are caused by the wind turbulence and by the vortex wake. This heading provides a procedure for estimating the static torque equivalent to the actions generated by wind through torsional vibrations.

The equivalent static torque per unit length is given by Eq. M.16:

$$m_M(z) = 1,8 \cdot q_p(h) \cdot C_M \cdot b^2 \cdot \left(\frac{z}{h}\right) \cdot c_{dM} \tag{M.16}$$

where:

$q_p(h)$ is the peak velocity pressure (heading 3.2.7), evaluated at height $z=h$;

C_M is the aerodynamic moment coefficient (associated with the fluctuating base torque, Figure M.5), given by Eq. M.17:

$$C_M = \left[0,0066 + 0,015 \cdot \left(\frac{d}{b}\right)^2\right]^{0,78} \tag{M.17}$$

c_{dM} is the torsional dynamic factor given by Eqs. M.18 and M.19:

$$c_{dM} = \frac{G_M}{1 + 7 \cdot I_v(h)} \tag{M.18}$$

$$G_M = g_M \cdot \sqrt{1 + R_M^2} \tag{M.19}$$

where:

G_M is the torsional gust factor;

g_M is the torsional peak factor;

R_M is the torsional resonant response factor;

$I_v(h)$ is the turbulence intensity (Heading 3.2.6) at the tip of the building.
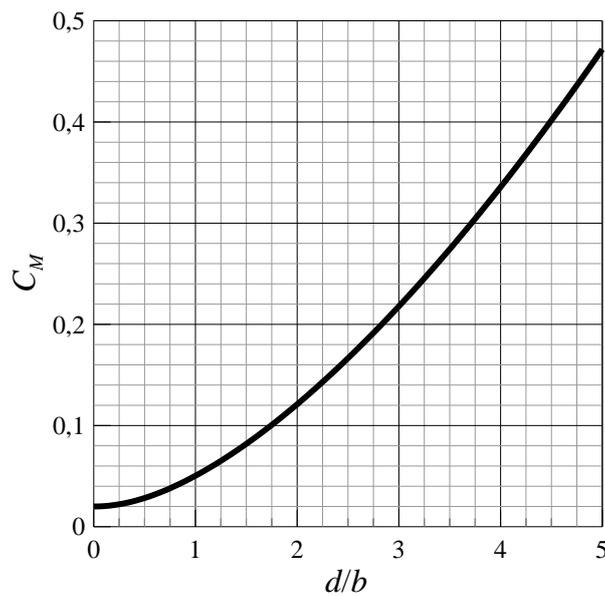
Figure M.5 – Aerodynamic moment coefficient C_M.

The torsional resonant response factor is given by Eqs. M.20 to M.25:

$$R_M^2 = \frac{\pi \cdot S_M}{4 \cdot \xi_M} \tag{M.20}$$

$$S_M = \begin{cases} S_{M1} \cdot \left(\dfrac{v_m^*}{4,5} \right)^{2 \cdot \beta_{M1}} & \text{per } v_m^* \le 4,5 \\[4mm] S_{M1} \cdot \exp \left\{ 3,5 \cdot \ln \left(\dfrac{S_{M2}}{S_{M1}} \right) \cdot \ln \left(\dfrac{v_m^*}{4,5} \right) \right\} & \text{per } 4,5 < v_m^* < 6 \\[4mm] S_{M2} \cdot \left(\dfrac{v_m^*}{6} \right)^{2 \cdot \beta_{M2}} & \text{per } 6 \le v_m^* \le 10 \end{cases} \tag{M.21}$$

$$v_m^* = \frac{v_m(h)}{n_M \cdot \sqrt{b \cdot d}} \tag{M.22}$$

$$S_{M1} = \frac{0,14 \cdot K_{M1}^2 \cdot d \cdot \left(b^2 + d^2 \right)^2}{\pi \cdot \ell^2 \cdot b^3} \cdot (4,5)^{2 \cdot \beta_{M1}} \;, \quad S_{M2} = \frac{0,14 \cdot K_{M2}^2 \cdot d \cdot \left(b^2 + d^2 \right)^2}{\pi \cdot \ell^2 \cdot b^3} \cdot (6)^{2 \cdot \beta_{M2}} \tag{M.23}$$

$$\beta_{M1} = \frac{(d/b) + 3,6}{(d/b)^2 - 5,1 \cdot (d/b) + 9,1} + \frac{0,14}{(d/b)} + 0,14, \quad \beta_{M2} = \frac{0,044 \cdot (d/b)^2 - 0,0064}{(d/b)^4 - 0,26 \cdot (d/b)^2 + 0,1} + 0,2 \tag{M.24}$$

$$K_{M1} = \frac{-1,1 \cdot (d/b) + 0,97}{(d/b)^2 + 0,85 \cdot (d/b) + 3,3} + 0,17, \quad K_{M2} = \frac{0,077 \cdot (d/b) - 0,16}{(d/b)^2 - 0,96 \cdot (d/b) + 0,42} + \frac{0,35}{(d/b)} + 0,095 \tag{M.25}$$

where:

ξ_M is the damping ratio in the first torsional mode (Annex I);

n_L is the first torsional frequency (Annex I);

ℓ is the larger of sizes d and b;

$v_m(h)$ is the mean wind velocity (heading 3.2.5), evaluated at height $z=h$;

v_m^* is the reduced mean velocity, evaluated at height $z=h$;

β_{M1}, β_{M2} are dimensionless coefficients given in Figure M.6;

K_{M1}, K_{M2} are dimensionless coefficients given in Figure M.7.
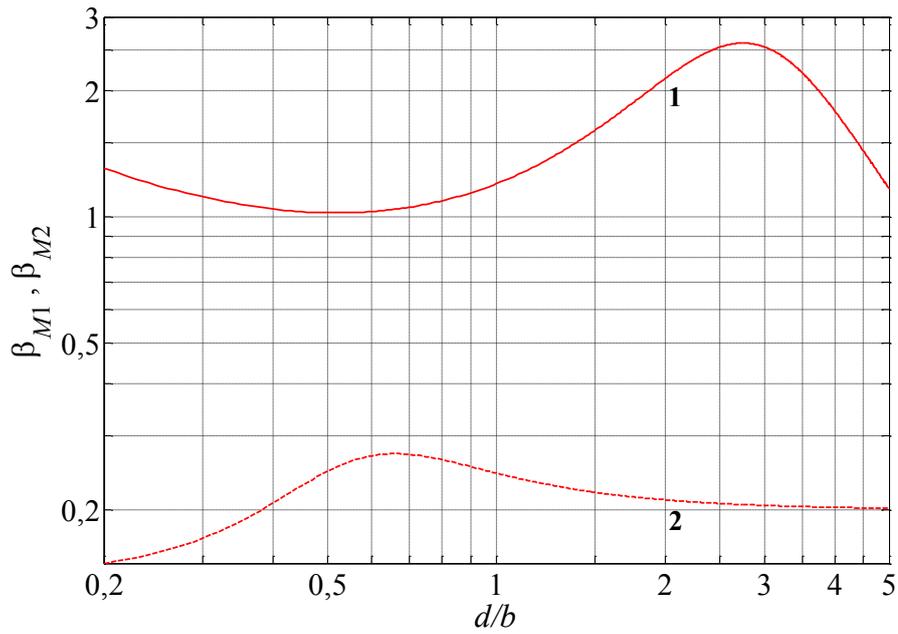
Figure M.6 - Dimensionless coefficients β_{M1} and β_{M2}.
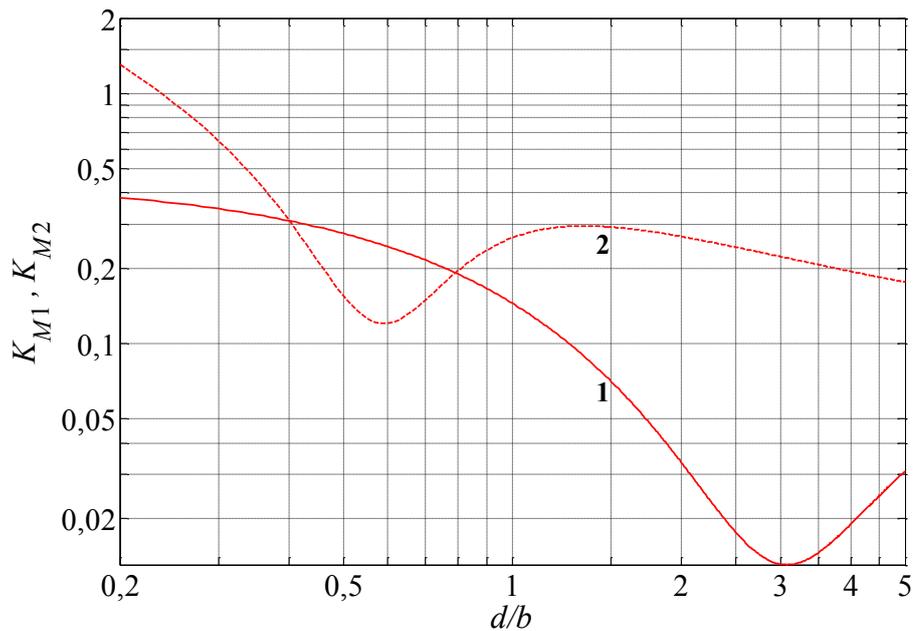
Figure M.7 – Dimensionless coefficients K_{M1} and K_{M2}.

The torsional peak factor is given by Eq. M.26:

$$g_M = \sqrt{2 \cdot \ln\left(n_M \cdot T\right)} + \frac{0,5772}{\sqrt{2 \cdot \ln\left(n_M \cdot T\right)}} \geq 3 \tag{M.26}$$

where:
n_L is the first torsional frequency (Annex I);
T is the mean wind velocity averaging time interval, $T=600$ s;

In Table M.II the calculation procedure of the torsional dynamic factor is shown.

Table M.II - Dynamic torsional coefficient calculation procedure.

Step	Operation
1	Evaluation of geometric parameters b, d, h, (Figure M.1) and $\ell = \max(b,d)$
2	Evaluation of the mean wind velocity $v_m(h)$ (Heading 3.2.5)
3	Evaluation of turbulence intensity $I_v(h)$ (Heading 3.2.6)
4	Evaluation of dynamic parameters n_M and ξ_M (Annex I)
5	Evaluation of parameter v_M^* (Equation M.22)
6	Evaluation of parameters β_{M1} (if $v_M^* \leq 6$) and β_{M2} (if $v_M^* \geq 4.5$) (Equation M.24, Figure M.6)
7	Evaluation of parameters K_{M1} (if $v_M^* \leq 6$) and K_{M2} (if $v_M^* \geq 4.5$) (Equation M.25, Figure M.7)
8	Evaluation of parameters S_{M1} (if $v_M^* \leq 6$) and S_{M2} (if $v_M^* \geq 4.5$) (Equation M.23)
9	Evaluation of parameter S_M (Equation M.21)
10	Evaluation of the resonant response factor R_M (Equation M.20)
11	Evaluation of peak factor g_M (Equation M.26)
12	Evaluation of gust factor G_M (Equation M.19)
13	Evaluation of dynamic coefficient c_{dM} (Equation M.18)

M.4   Simplified procedure for across-wind and torsional actions

Starting from the detailed procedure of heading M.2 and M.3, conservative values of the across-wind and torsional dynamic factors can be derived for square plan buildings with regular distribution of stiffness and mass, even in the case in which the exact dynamic characteristics of the structure are not known. The figures reported in this heading were obtained using the detailed procedure, as an envelope for all possible situations associated with different values of the base reference wind velocity and of the roughness length (assuming a unit value for the topography coefficient). The values of the vibration frequencies are calculated through Equations I.4 and I.5 for across-wind frequencies, and through Equation I.7 for torsional frequencies; the values of the damping ratios are taken from Equations I.29 and I.30 for both across-wind and torsional vibrations. The value of the across-wind and torsional dynamic factors given in the following graphs apply to buildings satisfying Equations M.1, M.2 and M.4, therefore buildings with a square plan and $h \leq 6b$.

Figure M.8 and Figure M.9 show the across-wind dynamic factor for multi-storey steel buildings and for multi-storey reinforced concrete or composite buildings, respectively. The shaded areas in these figures indicate situations in which it is not strictly necessary to assess the effects of across-wind actions, as $h < 3b$ (Equation M.1).

Figure M.10 and Figure M.11 show the torsional dynamic factor for steel multi-storey buildings and for multi-storey reinforced concrete or composite buildings, respectively. The shaded areas in these figures indicate situations in which it is not strictly necessary to assess the effects of torsional actions, as $h < 3b$ (Equation M.1).
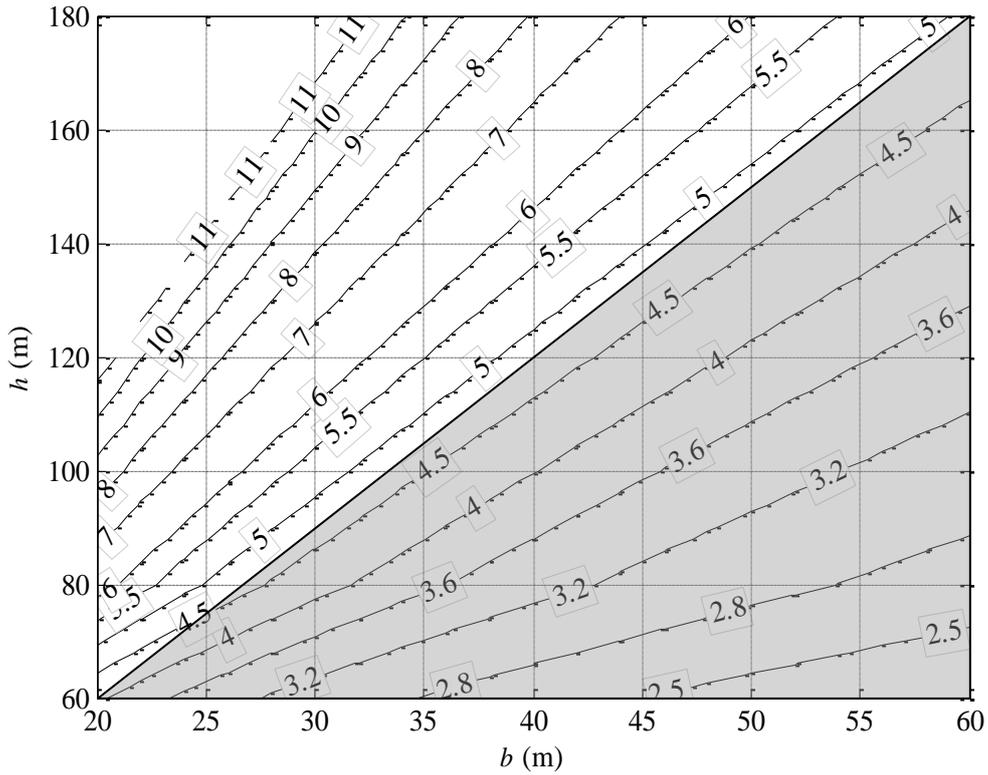
Figure M.8 – Values for the across-wind dynamic coefficient c_{dL} for square plan steel buildings.
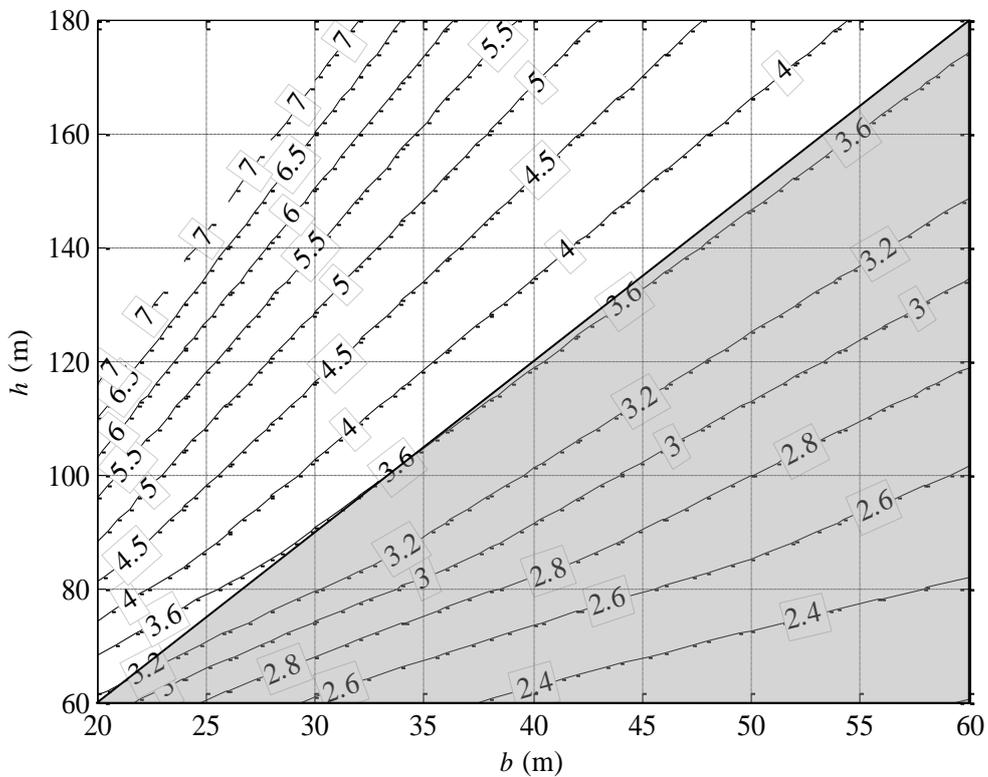
Figure M.9 – Values for the across-wind dynamic coefficient c_{dL} for square plan reinforced concrete or composite buildings.
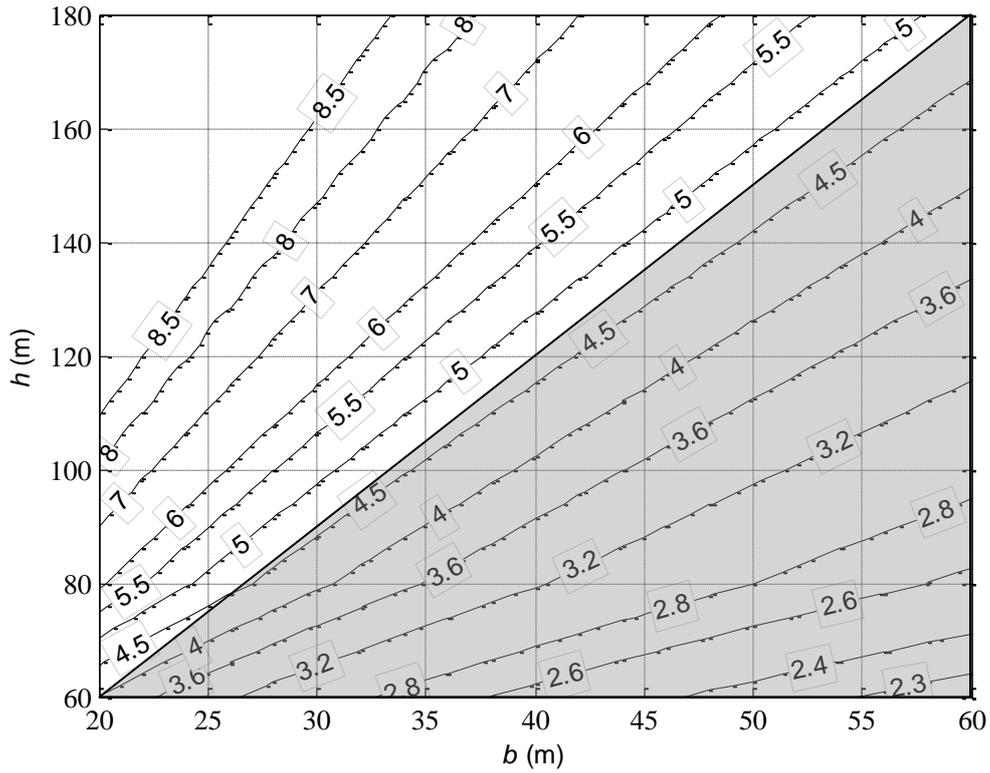
Figure M.10 – Values for the torsional dynamic coefficient c_{dM} for square plan steel buildings.
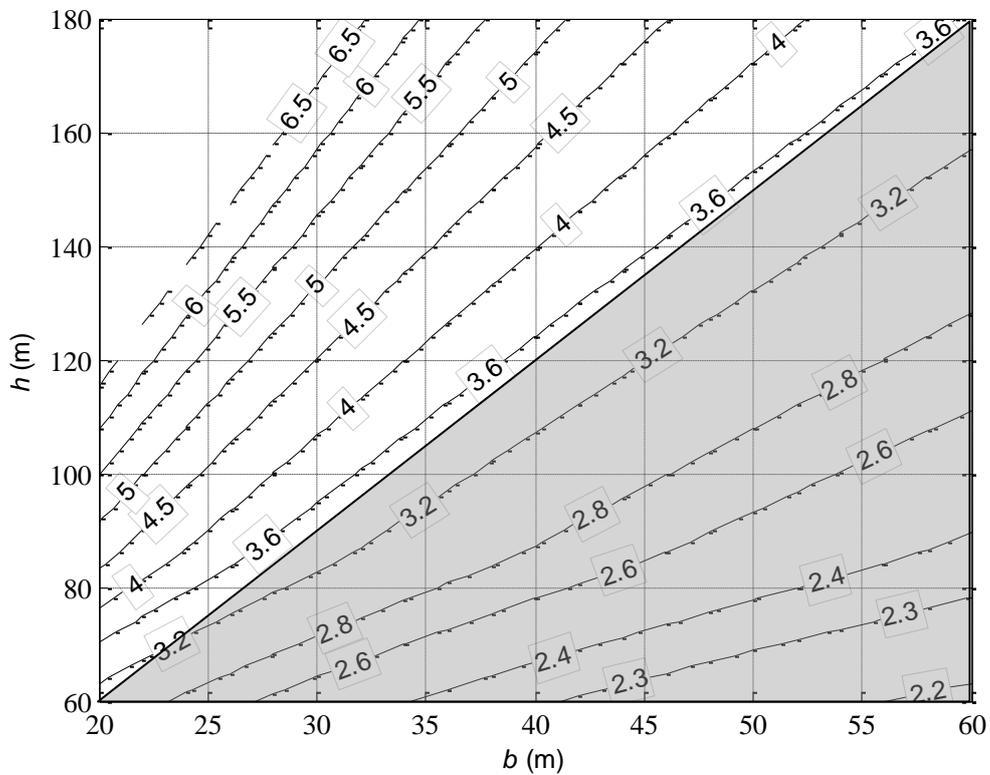
Figure M.11 – Values for the torsional dynamic coefficient c_{dM} for square plan reinforced concrete or composite buildings.

M.5 Across-wind and torsional accelerations

The peak value of the across-wind acceleration at height z of the building is given by Eq. M.27:

$$a_{pL}(z) = g_L \cdot \sigma_{aL}(z) \qquad (M.27)$$

where:
g_L is the across-wind peak factor, Equation (M.15);
σ_{aL} is the standard deviation of the across-wind acceleration at height z:

$$\sigma_{aL}(z) = \frac{0,5 \cdot \rho \cdot v_m^2(h) \cdot b \cdot h}{m_L} C_L \cdot R_L \cdot \Phi_L(h) \cdot \Phi_L(z) \qquad (M.28)$$

where:
ρ is the air density, $\rho = 1{,}25$ kg/m^3 (heading 3.2.7);
$v_m(h)$ is the mean wind velocity (heading 3.2.5), evaluated at $z=h$, for a design return period T_R suitable for abitability assessment (Annex N);
b is the width of the building (Figure M.1);
h is the height of the building (Figure M.1);
m_L is the generalised mass of the building in the first across-wind mode (Annex I);
C_L is the aerodynamic force coefficient, Equation (M.6);
R_D is the across-wind resonant response factor, the square of which is given by Equation M.9 for a design return period T_R suitable for abitability assessment (Annex N);
$\Phi_L(z)$ is the first across-wind mode shape (Annex I).

The peak value of the torsional acceleration at height z of the building is given by Eq. M.29:

$$a_{pM}(z) = g_M \cdot \sigma_{aM}(z) \qquad (M.29)$$

where:
g_M is the torsional peak factor, Equation (M.22);
σ_{aM} is the standard deviation of the across-wind acceleration at height z:

$$\sigma_{aM}(z) = \frac{0,3 \cdot \rho \cdot v_m^2(h) \cdot b^2 \cdot h}{I_M} C_M \cdot R_M \cdot \Phi_M(h) \cdot \Phi_M(z) \qquad (M.30)$$

where:
ρ is the air density, $\rho = 1{,}25$ kg/m^3 (heading 3.2.7);
$v_m(h)$ is the mean wind velocity (heading 2.5.5), evaluated at $z=h$, for a design return period T_R suitable for abitability assessment (Annex N);
b is the width of the building (Figure M.1);
h is the height of the building (Figure M.1);
I_M is the generalised polar mass moment of inertia of the building in the first torsional mode (Annex I);
C_M is the torsional moment aerodynamic coefficient, Equation M.17;
R_M is the torsional resonant response factor, the square of which is given by Equation M.9 for a design return period T_R suitable for abitability assessment (Annex N);
$\Phi_L(z)$ is the first torsional mode shape (Annex I).

M.6 Combination of actions and effects

Across-wind and torsional actions have to be combined with each other and with along-wind actions (Annex L). Similarly, the associated effects have to be combined (displacements, rotations, stress resultants, accelerations, …).

It is recommended to apply the three combination rules given in Table M.III.

Table M.III - Combination rules for actions and effects.

Combination	Along-wind action/effect	Across-wind action/effect	Torsional action/effect
1	D	$0.4 \cdot L$	$0.4 \cdot M$
2	$D \cdot \left(0,4 + \dfrac{0,6}{G_D} \right)$	L	$\gamma_{LM} \cdot M$
3	$D \cdot \left(0,4 + \dfrac{0,6}{G_D} \right)$	$\gamma_{LM} \cdot L$	M

The symbols in Table M.III have the following meanings:

D, L, M indicate, depending on circumstances, respectively an along-wind, across-wind or torsional action, or its effect (displacement, rotation, stress, acceleration, …);

G_D is the along-wind gust factor (heading L.3);

γ_{LM} is the dimensionless combination coefficient of across-wind and torsional actions and effects, given in Table M.IV.

Table M.IV - Combination coefficients of L and M.

d/b	$n_1 \cdot b / v_m(h)$	γ_{LM}		
		$f_{LM} = 1,0$	$f_{LM} = 1,1$	$f_{LM} \geq 1,4$
≤ 0.5	$\leq 0,1$	0,95	0,61	0,55
	0,2	0,55	0,67	0,61
	0,3	0,55	0,73	0,67
	0,6	0,79	0,79	0,79
	≥ 1	0,84	0,84	0,84
1	$\leq 0,1$	0,84	0,55	0,55
	0,2	0,61	0,55	0,55
	0,3	0,55	0,55	0,55
	0,6	0,67	0,67	0,67
	≥ 1	0,73	0,73	0,73
≥ 2	$\leq 0,05$	0,79	0,55	0,55
	$\geq 0,1$	0,55	0,55	0,55

The symbols in Table M.IV have the following meanings:

n_1 is the lowest frequency between n_L and n_M;

f_{LM} is the ratio between the across-wind and torsional frequencies:

$$f_{LM} = \begin{cases} n_L / n_M & \text{per} \quad n_L \geq n_M \\ \\ n_M / n_L & \text{per} \quad n_L < n_M \end{cases} \tag{M.31}$$

Linear interpolation can be used for intermediate values between those given in Table M.IV.

Annex N   ACCELERATION AND ABITABILITY

Constructions occupied by people, especially buildings, must ensure comfort of occupants. The human body generally does not experience difficulties in tolerating significant displacements and velocities; it is, on the other hand, very sensitive to accelerations, giving rise to a series of reactions ranging from perception to discomfort and, in some cases, intolerability. These reactions depend on the frequency with which oscillation occurs plus various other factors, mainly physiological and psychological, associated with the characteristics of individuals. It is the task of the designer to ensure comfort of the occupants or users by limiting physiologically disturbing conditions to exceptional and rare situations.

Therefore, it is recommended to evaluate, by applying well estabilished analytical, numerical and/or experimental methods, the peak values of along-wind a_{pD}, across-wind a_{pL} and torsional a_{pM} acceleration at the centre of twist of the top storey of the building, associated with the mean wind velocity having a return period $T_R = 1$ year (heading 3.2.2). Annexes L and M provide several calculation criteria to this goal, which can be applied to constructions characterised by simple geometric and mechanical properties.

Heading N.1 provides estimates of the acceleration perception thresholds. Heading N.2 suggests possible choices for acceleration limit values, to be used in serviceability assessments. Heading N.3 provides guidance for the evaluation of the acceleration at points other than the centre of twist of the building.

N.1   Acceleration perception thresholds

Figure N.1 gives the peak acceleration perception threshold a_p as a function of the vibration frequency n_0. In particular:

$n_0 = n_D$ for along-wind acceleration a_{pD} ;

$n_0 = n_L$ for across-wind acceleration a_{pL} ;

n_D, n_L first along-wind and across-wind frequencies, respectively.

The curves identified in Figure N.1 by H-10, H-30, H-50, H-70 and H-90 correspond to the 10%, 30%, 50%, 70% and 90% fractiles of the perceived peak acceleration.
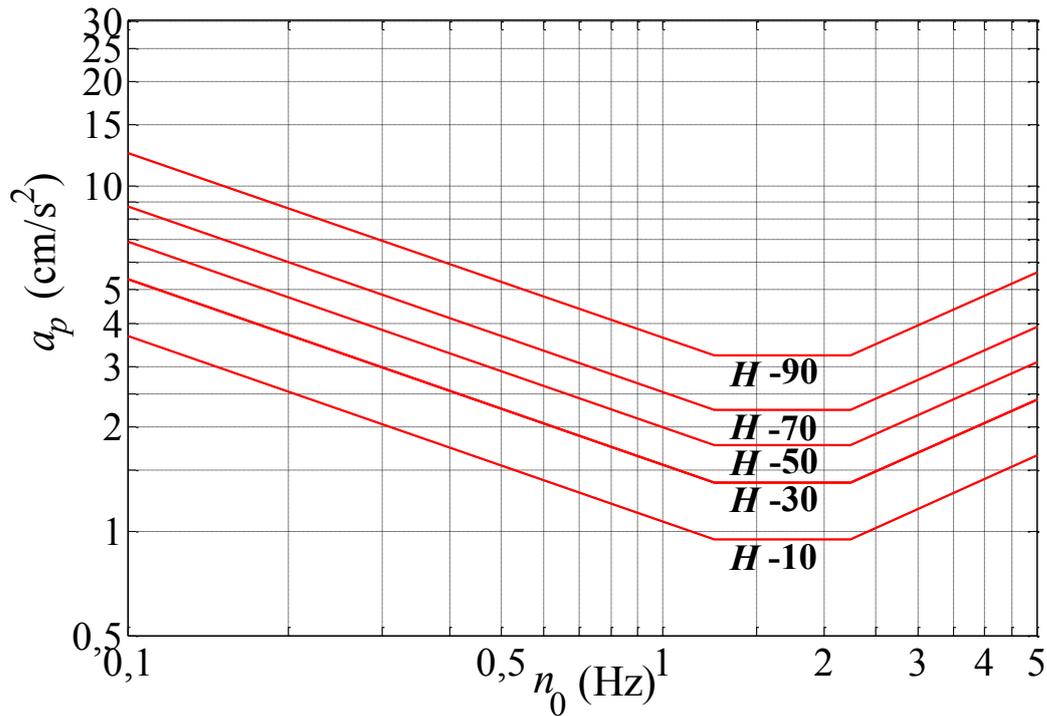
Figure N.1. Peak acceleration perception thresholds.

N.2 Acceleration limit values

To ensure serviceability of a building, each peak value of along-wind and across-wind acceleration at the centre of twist, a_{pD} and a_{pL}, should not exceed the threshold value given by Eq. N.1 and Figure N.2:

$$a_l = \begin{cases} \dfrac{a_0}{n_0^{0,56}} & \text{for } n_0 < 1\,\text{Hz} \\[2mm] a_0 & \text{for } 1\,\text{Hz} \leq n_0 \leq 2\,\text{Hz} \\[2mm] 0,5 \cdot a_0 \cdot n_0 & \text{for } n_0 \geq 2\,\text{Hz} \end{cases} \tag{N.1}$$

where:
a_0 is the reference limit value of acceleration:
      $a_0 = 6\,\text{cm/s}^2$ for office buildings (curve (a) in Figure N.2);
      $a_0 = 4\,\text{cm/s}^2$ for apartment buildings (curve (b) in Figure N.2);
n_0 is the dominant frequency defined at heading N.1 and expressed in Hz.
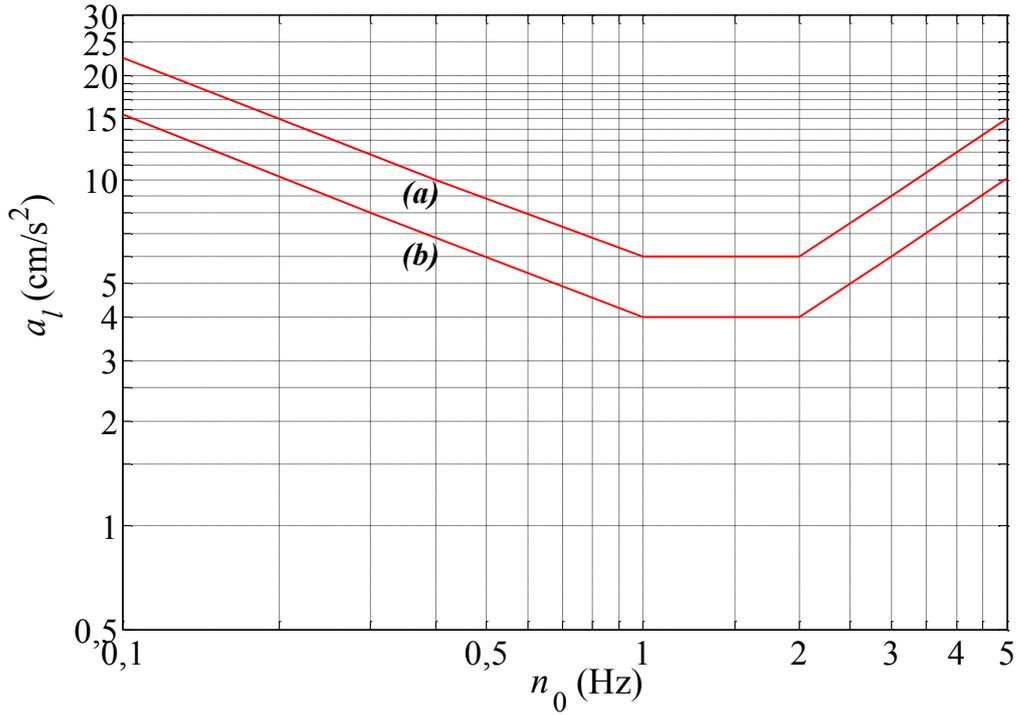
Figure N.2 - Peak acceleration thresholds for $T_R = 1$ year.

N.3 Acceleration at points other than the centre of twist

At points other than the centre of twist, especially in the proximity of corners, the peak values of along-wind and across-wind acceleration are increased due to the effect of torsional acceleration.

At a point P of the building, the peak values of along-wind and across-wind acceleration are given by Eq. N.2:

$$a_{pD}^{P} = a_{pD} + \left| d_{x}^{P} \right| a_{pM} \tag{N.2a}$$

$$a_{pL}^{P} = a_{pL} + \left| d_{y}^{P} \right| a_{pM} \tag{N.2b}$$

where:

a_{pD}, a_{pL}, a_{pM} are the peak values of the along-wind, across-wind and torsional accelerations at the centre of twist, combined through the rules given in heading M.6;

d_{x}^{P}, d_{y}^{P} are the coordinates of point P in respect to the centre of twist (Figure N.3).

Except for special cases, where it is advisable to adopt particular prudence as regards local peak acceleration, for example at the corners of the top storeys of buildings having unusual functions, it is not necessary to perform any verification of the type suggested in heading N.2 as regards the values given by Equation N.2.
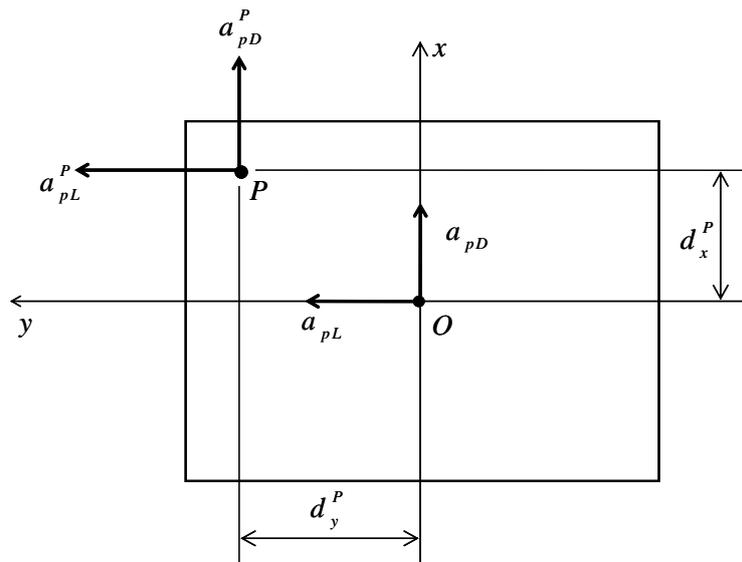
Figure N.3 - Wind-induced floor acceleration.

Annex O   VORTEX SHEDDING FROM SLENDER STRUCTURES

O.1   General

An elongated body immersed in a flow produces, in general, a wake formed by vortex streets (von Karman wake) with alternating shedding (Figure O.1) at a frequency n_s given by the Strouhal law:

$$n_s = \frac{St \cdot v_m}{b}$$ (O.1)

where:
St is a dimensionless parameter, known as the Strouhal number (heading O.2), that essentially depends on the sectional shape of the body;
v_m is the mean wind velocity (heading 3.2.5);
b is the reference dimension (width) of the cross-section (heading O.2).

Alternating vortex shedding generates instantaneous fluctuating pressures on the surface of the body, the integration of which gives forces and moments. These actions can be large, especially for slender structures and structural elements. Even though strictly three-dimensional in nature, vortex shedding can be simplified into a bi-dimensional phenomenon in the plane of the section (Figure O.2). The main action on the body is an across-wind force, L, with a dominant frequency equal to the shedding frequency n_s. An along-wind action, D, also exists, generally of a lesser magnitude, having a dominant frequency $2 \cdot n_s$, together with a torsional action, M, having a dominant frequency equal to about n_s. The following heading considers only the across-wind fluctuating force, perpendicular to the mean direction of flow and to the axis of the structure or element considered.
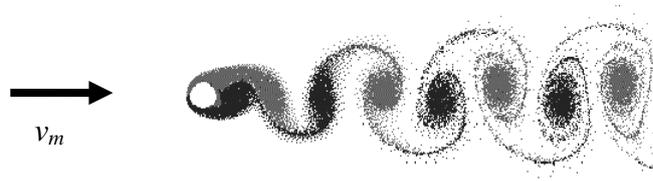
Figure O.1 – Von Kármán wake for a circular cross-section.
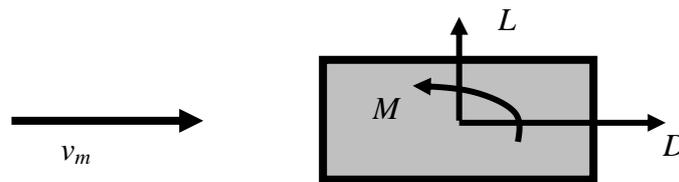
Figure O.2 – Overall fluctuating sectional forces.

If the structure or structural element has an across-wind natural frequency $n_{L,i}$, close to the shedding frequency n_s, the across-wind force L becomes resonant with the vibration. The critical velocity of vortex shedding in the i-th across-wind mode is defined as the mean wind velocity that gives rise to the resonance condition $n_s = n_{L,i}$. Using Equation (O.1), this value is given by Eq. O.2:

$$v_{cr,i} = \frac{n_{L,i} \cdot b}{St}$$ (O.2)

As the mean wind velocity varies with height (heading 3.2.5), vertical structures have critical values for mean wind velocity at different positions along their axes. For a conservative estimate of the critical condition, critical wind velocity shall be considered at the positions of maximum modal displacement. For example, for vertical cantilevered structures and elements (Annex I.3.1), excitation of the first mode is maximum when vortex shedding is resonant at the tip (Figure O.3a); excitation of the second mode may be maximum when vortex shedding is resonant at the tip (Figure O.3b) or at the position of maximum displacement in the second mode (Figure O.3c). Likewise, for supported or fixed structures and structural elements (Annex I.3.2), excitation of the first mode is maximum when vortex shedding is resonant at midspan.
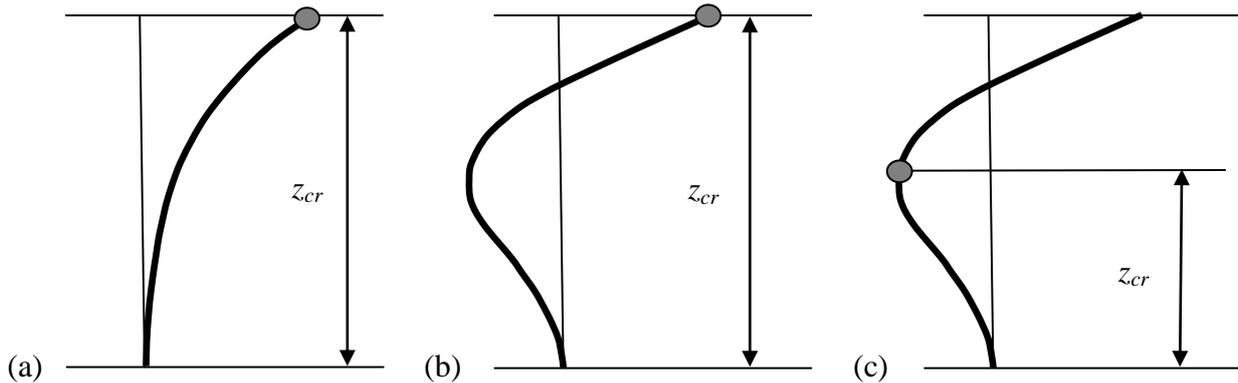
Figure O.3 – Worst-case position of critical vortex shedding for different mode shapes.

The effects of vortex shedding should be assessed for all critical velocities satisfying the condition reported in Eq. O.3:

$$v_{cr,i} < v_{m,l} \tag{O.3}$$

where:

$v_{cr,i}$ is the critical velocity of vortex shedding for the mode i, in the most unfavourable position, Equation O.2;

$v_{m,l}$ is the mean wind velocity (heading 3.2.5) evaluated at the height where critical velocity occurs, for a return period T_R equal to 10 times the reference return period $T_{R0.0}$ (Annex A), $T_R = 10 \cdot T_{R0.0}$.

When vortex shedding is resonant with a lightweight and/or low damped structure, therefore characterised by a low Scruton number (heading O.3), the resonance may turn into self-excitation of fluid-structure interaction type, causing synchronisation (or lock-in). In these cases, vortex shedding no longer excites the structure but rather the structure triggers vortex shedding, giving rise to significant oscillation amplitudes of around 5-10% of the reference size b. The Scruton number is therefore a very important technical parameter, since small values of this quantity are indicative of possible damage phenomena (even up to collapse) in chimneys, towers, elements of lattice structures, off-shore pipelines, heat exchangers and bridge decks, especially those of cable-supported bridges.

This Annex is organised as follows. Heading O.2 gives the values of the Strouhal number for a variety of cross-sections of technical interest. In heading O.3 the Scruton number is defined and discussed. Heading O.4 defines the equivalent across-wind static load and introduces two methods for calculating the peak deflection value induced by vortex shedding, the spectral (heading O.5) and the harmonic method (heading O.6), respectively. Vortex shedding for grouped cylindrical structures or structural elements is discussed in heading O.7. Heading O.8 provides a method for

estimating the number of load cycles induced by vortex shedding, with the aim of fatigue analyses. Heading O.9 briefly discusses response mitigation techniques. Heading O.10 analyses the ovalling phenomenon of shell structures.

O.2 Strouhal number

The Strouhal number St is a dimensionless parameter; it is a function of the aerodynamic behaviour of the structure or structural element. In general, the Strouhal number depends on the shape of the section, on the characteristics of turbulence, on the Reynolds number Re (heading 3.3.7), calculated for critical velocity $v_{cr,i}$, Equation O.2, and on the roughness length k of the surface (heading G.10.6, Table G.XVII). For sharp-edged structures and structural elements, the Strouhal number can be considered as a function of the shape of the section and, to a lesser extent, of the characteristics of turbulence. In Table O.I, together with Figures O.4 (for circular cross-sections) and O.5 (for rectangular cross-sections), reference values St for the most common cross-sections are given.

The value St=0.22 given in Table O.I and Figure O.4 for circular cross-sections with Re>1.6·10⁶, applies to structures or structural elements having mean roughness length, $k/b \cong 0.1 \cdot 10^{-3}$; this value may increase (up to 0.25) or decrease (down to 0.20) for structures or structural elements having lower or higher roughness lengths, respectively.

For circular cylinders, it is acceptable to set $St = 0.2$, regardless of the Reynolds number and of the roughness length of the surface. More accurate assessments can be achieved by applying the following procedure:

1)   set $St = 0.2$ and assess critical velocity $v_{cr,i}$, Equation O.2;

2)   use critical velocity $v_{cr,i}$ to assess the Reynolds number Re (heading 3.3.7);

3)   evaluate St using the Equation given in Table O.I or Figure O.4;

4)   if necessary, iterate the procedure until convergence is achieved.

Table O.I – Strouhal numbers.

Section	St		
	$10^5 \leq Re \leq 4\cdot10^5$ $4\cdot10^5 \leq Re \leq 10^6$ $10^6 \leq Re \leq 1,6\cdot10^6$ $Re > 1,6\cdot10^6$		0,19 $-0,7674+0,1709\cdot\log_{10}(Re)$ $1,3752-0,1862\cdot\log_{10}(Re)$ 0,22 (Figure O.4)
	$0<d/b<1$ $1\leq d/b<2$ $2\leq d/b<3$ $3\leq d/b\leq3,5$ $3,5<d/b<5$ $5\leq d/b<10$ $d/b\geq10$		0,12 $0,18-0,06\cdot d/b$ 0,06 $-0,48+0,18\cdot d/b$ $0,2433-0,02667\cdot d/b$ $0,13-0,004\cdot d/b$ 0,09 (Figure O.5)
	$d/b=1$ $d/b=1,5$ $d/b=2$		0,11 0,10 0,14
	$d/b=1$ $d/b=2$		0,13 0,08
	$d/b=1$ $d/b=2$		0,16 0,12
	$d/b=1,3$ $d/b=2$		0,11 0,07
	d/b=0,5-1 (IPE, HE)		0,14
	equal sides ($d=b$), any α		0,14
NOTE: Linear interpolation of the values given are allowed, but not extrapolation			
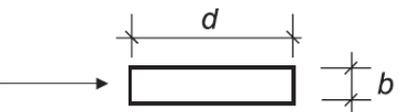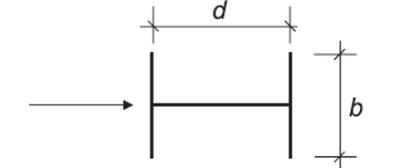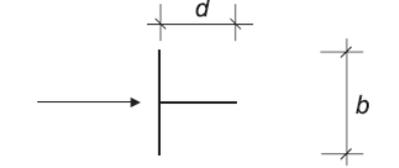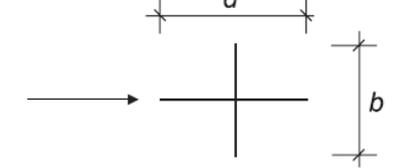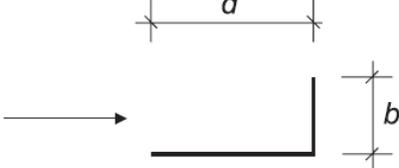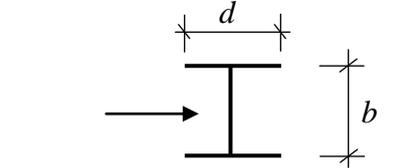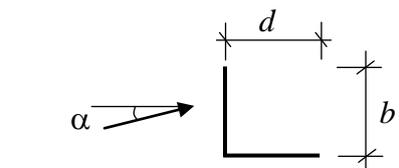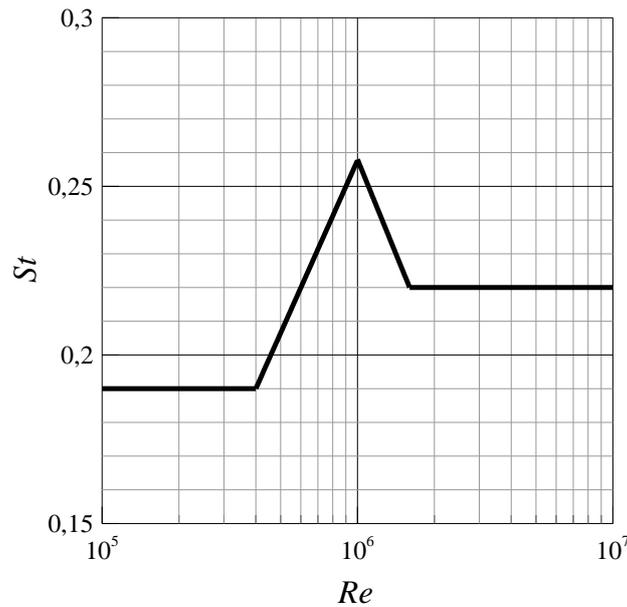
Figure O.4 – Strouhal number for circular cylinders.
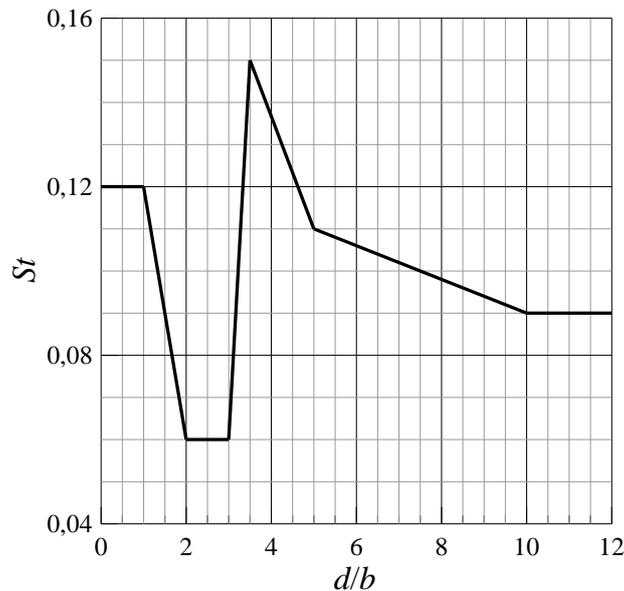
Figure O.5 – Strouhal number for rectangular cross-sections.

O.3   Scruton number

The Scruton number *Sc* is a dimensionless parameter that depends on the equivalent mass, on the damping ratio and on the reference size (width) of the section where critical vortex shedding occurs. As these parameters depend on the vibration mode with which critical shedding is associated, *Sc* in turn depends on the vibration mode *i*. It is indicated by Sc_i and given by Eq. O.4:

$$Sc_i = \frac{4\pi \cdot m_{e,i} \cdot \xi_i}{\rho \cdot b^2}$$
(O.4)

where:

$m_{e,i}$ is the equivalent mass per unit length in the *i*-th across-wind vibration mode (Annex I.4);

ξ_i is the critical structural damping ratio in the *i*-th mode (excluding aerodynamic damping) (Annex I.6);

ρ is the air density; the recommended value is 1,25 kg/m^3 (heading 3.2.7);

b   is the reference size (width) of the cross-section at the position of critical vortex shedding.

In resonance conditions, the smaller the Scruton number (and therefore the lighter and/or low damped the structure) the greater the response. In particular, the following cases can be identified:

- if the Scruton number is higher than 30, the probability of lock-in is quite low and the vortex shedding is not the critical load case; it is nevertheless advisable to perform the checks;

- if the Scruton number is between 5 and 30, the vortex shedding phenomenon is very sensitive to different parameters, first of all turbulence intensity. High values of turbulence intensity reduce the risk of strong vibrations; small values of turbulence intensity, usually associated with small values of critical velocities, may amplify the critical vortex shedding phenomenon. In any case, specific analyses must be performed to ensure that the vibrations do not induce large stresses in the structure and that fatigue limits are not exceeded (heading O.8);

- if the Scruton number is less than 5, vibrations induced by vortex shedding may be very large and dangerous; it is thus advisable to address the problem with the utmost attention and prudence, or seek specialist advice.

O.4   Equivalent static load

The effect of across-wind vibrations induced by resonant vortex shedding in the *i*-th mode can be calculated through application of an equivalent static force per unit length, perpendicular to the mean wind direction and to the axis of the structure or structural element. This is given by Eq. O.5:

$$F_{L,i}(s) = m(s) \cdot (2\pi \cdot n_{L,i})^2 \cdot \Phi_{L,i}(s) \cdot y_{pL,i} \cdot C_{TR,i} \tag{O.5}$$

where:

s   is a coordinate along the structure axis;

$m(s)$ is the mass per unit length of the structure;

$n_{L,i}$ is the *i*-th across-wind natural frequency of the structure;

$\Phi_{L,i}(s)$ is the *i*-th across-wind structural mode shape, normalized such as to be 1 at the position $\bar{s}$ of maximum displacement, $\Phi_{L,i}(\bar{s})=1$;

$y_{pL,i}$ is the peak deflection of the structure, evaluated at $\bar{s}$ (headings O.4.1, O.5 and O.6);

$C_{TR,i}$ is a dimensionless parameter associated with the critical values of the mean wind velocity for long return periods T_R (heading O.4.2).

Expressing the mass in kg/m, the frequency in Hz and the peak deflection value in m, the force $f_{L,i}$ is obtained in N/m (being the mode shape of the structure dimensionless).

O.4.1 Peak deflection

Technical-scientific literature reports a number of procedures for calculating the peak deflection caused by vortex shedding. Most of these have complementary advantages and disadvantages; none may claim to be fully shared and recognised. The spectral method and the harmonic method are among the best-known and most applied.

The spectral method, described at heading O.5, is calibrated on experimental data from tests on cantilevered structures (for example, chimneys, towers and masts), with regular variation of the section properties along the axis, and oscillating in the first vibration mode. In this case, in which application of this method is recommended, it generally gives conservative, and sometime very conservative values.

The harmonic method, described at heading O.6, is calibrated on experimental data from a broader class of structures, oscillating in any vibration mode. On average, it gives an accurate estimate of the structural response; however it may lead to underestimate the effects of vortex shedding. For this reason, it is advisable to limit its use to the cases in which the spectral method cannot be applied. In other situations, application of this method is suggested together with the spectral method to estimate, for example, the uncertainties associated with the two procedures.

When analysis of the response to critical vortex shedding is performed by applying the spectral method and/or the harmonic method, the most conservative result shall be taken.

O.4.2 Reductive coefficient for high return periods

Coefficient $C_{TR,i}$ is a dimensionless parameter introduced for two purposes: to consider critical phenomena at mean wind velocities with a return period larger than the design return period used for standard safety assessments (Annex A); to reduce the calculated response for high values of the mean wind velocity, for which the flow tends to become significantly turbulent and therefore to attenuate vortex shedding. As a first approximation, the coefficient $C_{TR,i}$ can be calculated by using Eq. O.6 (Figure O.6):

$$
\begin{aligned}
C_{TR,i} &= 1 \quad \text{per} \quad v_{cr,i} \leq v_{m,0} \\
C_{TR,i} &= \frac{v_{m,l} - v_{cr,i}}{v_{m,l} - v_{m,0}} \quad \text{per} \quad v_{m,0} \leq v_{cr,i} \leq v_{m,l} \\
C_{TR,i} &= 0 \quad \text{per} \quad v_{m,l} \leq v_{cr,i}
\end{aligned}
\tag{O.6}
$$

where:

$v_{cr,i}$ is the critical vortex shedding mean wind velocity, for mode i, in the most unfavourable position, Equation (O.2);

$v_{m,0}$ is the mean wind velocity (heading 3.2.5), evaluated at the height at which the critical velocity occurs, in correspondence with the design return period T_R equal to the reference return period $T_{R0.0}$ (Annex A), $T_R = T_{R0.0}$.

$v_{m,l}$ is the mean wind velocity (heading 3.2.5), evaluated at the height where the critical velocity occurs, for a design return period T_R equal to 10 times the reference return period $T_{R0.0}$ (Annex A), $T_R = 10 \cdot T_{R0.0}$.
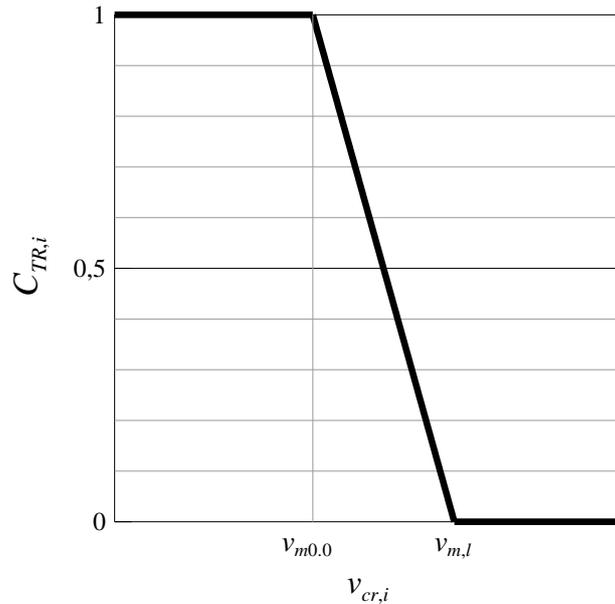
Figure O.6 – Values of coefficient $C_{TR,i}$.

O.5 Spectral method

The spectral method can be applied to cantilevered structures (for example chimneys, towers and masts) with regular variation of the section properties along the axis, only when the first vibration mode is taken into account. The peak deflection value $y_{pL,1}$ induced by critical vortex shedding in the first across-wind vibration mode is given by Eq. O.7:

$$y_{pL,1} = g_L \cdot \sigma_L \tag{O.7}$$

where:
g_L is the peak deflection factor (heading O.5.1);
σ_L is the standard deviation of the deflection (heading O.5.2).

O.5.1 Peak deflection factor

The peak deflection factor g_L is given by Eq. O.8 and Figure O.7:

$$g_L = \sqrt{2} \cdot \left\{ 1 + \left[\arctan\left(0,7 \cdot \left(\frac{Sc_1}{4\pi \cdot K_a} \right)^{2,5} \right) \right]^{1,4} \right\} \tag{O.8}$$

where:
Sc_1 is the Scruton number in the first across-wind vibration mode, Equation O.4;
K_a is the dimensionless aerodynamic damping parameter, given by Eq. O.9 :

$$K_a = K_{a,\max} \cdot C_I \tag{O.9}$$

where:
$K_{a,max}$ is the maximum value of the aerodynamic damping parameter, that is the value of K_a corresponding to the absence of atmospheric turbulence;
C_I is the turbulence factor, less than or equal to 1, associated with critical vortex shedding in the first mode.

Parameter $K_{a,max}$ depends on the shape of the section and possibly on the Reynolds number. It is given in Table O.II and by Figure O.8 (for circular cross-sections).

Table O.II – Value of the aerodynamic damping parameter $K_{a,max}$.

Circular cross-section	$K_{a,max}=1,5$ for $Re \leq 10^5$
	$K_{a,max}=5,075-0,715 \cdot \log_{10}(Re)$ for $10^5 < Re < 5 \cdot 10^5$
	$K_{a,max}=1$ for $Re \geq 5 \cdot 10^5$
	(Figure O.8)
Square cross-section	$K_{a,max}=6$

The turbulence factor C_I takes into account the fact that, for moderate values of critical velocity $v_{cr,1}$, atmospheric turbulence can be very low; for large critical velocities, turbulence is also large and mitigates the vortex shedding phenomenon. In the absence of more accurate assessments, the turbulence factor C_I can be approximated by using Eq. O.10 and Figure O.9:

$$C_I = 1 \qquad\qquad \text{for } v_{cr,i} \leq 5 \text{ m/s}$$
$$C_I = 1.3 - 0.06 \cdot v_{cr,i} \qquad\qquad \text{for } 5 < v_{cr,i} < 10 \text{ m/s} \qquad\qquad (O.10)$$
$$C_I = 0.7 \qquad\qquad \text{for } v_{cr,i} > 10 \text{ m/s}$$

where $v_{cr,1}$ is the critical velocity of vortex shedding, Equation O.2, for the first across-wind vibration mode.
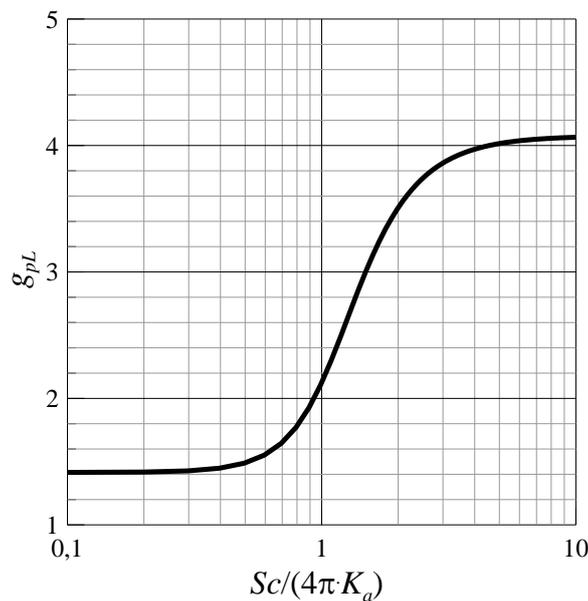
Figure O.7 – Peak factor g_L.
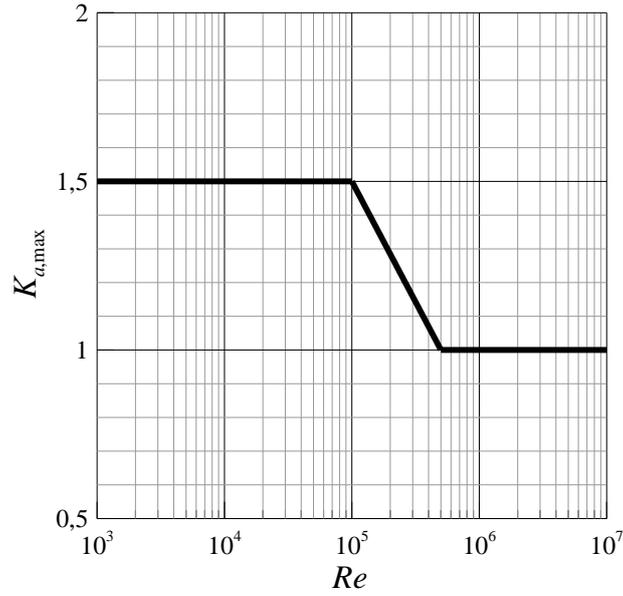
Figure O.8 – Value of the aerodynamic damping parameter $K_{a,max}$ for circular cylinders.
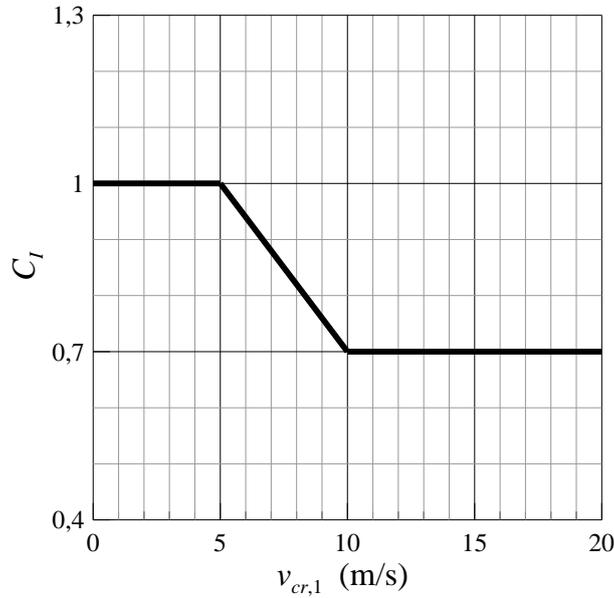
Figure O.9 – Turbulence factor C_I.

O.5.2 Standard deviation of the deflection

The normalised standard deviation of the deflection is given by Eq. O.11:

$$\frac{\sigma_L}{b} = \sqrt{c_1 + \sqrt{c_1^2 + c_2}} \tag{O.11}$$

where c_1 and c_2 are the dimensionless coefficients given by Eqs. O.12 and O.13:

$$c_1 = \frac{a_L^2}{2} \cdot \left(1 - \frac{Sc_1}{4\pi \cdot K_a}\right) \tag{O.12}$$

$$c_2 = \frac{a_L^2}{K_a} \cdot \frac{\rho \cdot b^3}{m_{ie} h} \cdot \frac{C_c^2}{St^4} \tag{O.13}$$

where:

b is the reference size (width) of the cross-section, at the section where the critical vortex shedding occurs;

a_L is the normalized (dimensionless) limiting amplitude, i.e. the maximum deflection divided by the corresponding reference size (width), for Sc going to zero; it is suggested to take $a_L=0.4$;

Sc_1 is the Scruton number for the first across-wind mode, Equation O.4;

K_a is the aerodynamic damping parameter, Equation O.9;

ρ is the air density; the recommended value is 1.25 kg/m^3 (heading.3.2.7);

$m_{e,i}$ is the equivalent mass per unit length in the first across-wind mode (Annex I.4);

St is the Strouhal number (heading O.2);

h is the height of the structure;

C_c is a dimensionless parameter, function of the shape of the cross-section and possibly of the Reynolds number. It is given in Table O.III and by Figure O.10 (for circular cross-sections).

Table O.III – Parameter C_c.

Circular cross-section	$C_c=0.02$ for $Re \leq 10^5$
	$C_c=0{,}07-001 \cdot \log_{10}(Re)$ for $10^5 < Re < 10^6$
	$C_c=0{,}01$ for $Re \geq 10^6$
	(Figure O.10)
Square cross-section	$C_c=0.04$
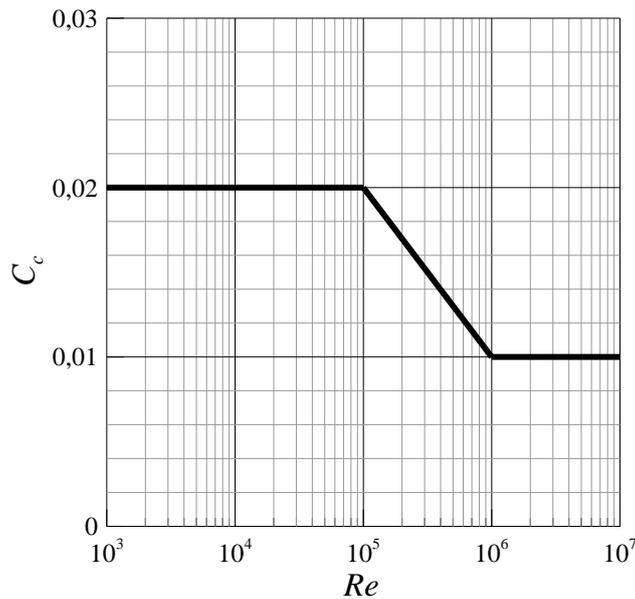
Figure O.10 – Parameter C_c.

O.6 Harmonic method

When applying the harmonic method, the peak deflection $y_{pL,i}$ induced by critical vortex shedding in the i-th across-wind vibration mode is given by Eq. O.14:

$$\frac{y_{pL,i}}{b} = \frac{1}{St^2} \cdot \frac{1}{Sc_i} \cdot K \cdot K_w \cdot c_{lat} \tag{O.14}$$

where:

b is the reference size (width) of the cross-section where the critical vortex shedding occurs;

St is the Strouhal number (heading O.2);

Sc_i is the Scruton number for the across-wind vibration mode *i*, Equation O.4;

K is the mode shape factor (heading O.6.1);

K_w is the effective correlation length factor, a function of the correlation length L_j associated with the portion of the structure where critical vortex shedding occurs (heading O.6.1);

c_{lat} is the lateral force coefficient (heading O.6.2).

As the correlation length of the forces induced by resonant vortex shedding increases, on increasing the vibration amplitude, the across-wind response depends on the parameter K_w, a function of the correlation length L_j, which in turn depends on the peak deflection value $y_{pL,i}$. The solution of Equation O.14 shall therefore be sought through iterations, following this procedure:

1) set $y_{pL,i}/b \leq 0,1$, thereby assuming $L_j/b = 6$ (heading O.6.1); then apply the Equation O.14 to obtain a second estimate of $y_{pL,i}$;

2) if $y_{pL,i}/b \leq 0,1$, convergence is already achieved and the procedure is complete;

3) otherwise, calculate L_j/b for the vibration amplitude $y_{pL,i}$ obtained in the previous step (heading O.6.1) and iterate the solution in Equation O.14 until convergence is achieved.

In general, for structures or structural elements that are moderately sensitive to vortex shedding, $y_{pL,i}/b < 0.1$. Consequently, the procedure described above stops at step 2), without any need for iteration. If this does not occur, attention must be paid to the situation dealt with.

O.6.1 Mode shape factors and effective correlation length

Consider a structure or structural element of length *l*, and divide this length into *m* segments of length l_j, whose sum on *j* from 1 to *m* is equal to *l* (Figure O.11); every segment of length l_j is delimited by a pair of points corresponding to nodes, i.e. points where mode shape $\Phi_{L,i}$ vanishes, or by the ends (either constraints or free). The points of the axis of a structure or structural elements where mode shape $\Phi_{L,i}$ takes absolute or relative maximum values are defined as antinodes (Figure O.11). The number of antinodes coincides with the number *m* of adjacent segments where the structure or the structural element is divided.

The effective correlation length L_j is defined as a portion of a generic segment l_j ($j = 1, ...m$), $L_j \leq l_j$, where vortex shedding occurs, uniformly and regularly, with the frequency $n_{L,i}$ associated with the mode shape $\Phi_{L,i}$ (Figure O.11). The correlation length L_j depends on the amplitude of vibrations, $y_{pL,i}$ (Table O.IV and Figure O.12). On the safe side, it is assumed that the effective correlation length is located in the most unfavourable position, i.e. close to an antinode. The number $n \leq m$ is defined as the number of segments *j* where resonant vortex shedding can take place simultaneously. In this case, one considers, for safety purposes, that the action caused by critical vortex shedding is applied simultaneously at *n* lengths of correlation L_j ($j = 1, ...n$).

The mode shape factor K is a dimensionless parameter, function of the mode shape $\Phi_{L,i}$ considered. The effective correlation length factor K_w is a dimensionless parameter, function of the mode shape $\Phi_{L,i}$ considered and of the correlation lengths L_j ($j = 1, ...n$). These factors are given in Eqs. O.15 and O.16:

$$K = \frac{\sum_{j=1}^{m} \int_{\ell_j} \left| \Phi_{L,i}(s) \right| \cdot \mathrm{d}s}{4\pi \cdot \sum_{j=1}^{m} \int_{\ell_j} \Phi_{L,i}^2(s) \cdot \mathrm{d}s} \tag{O.15}$$

$$K_w = \frac{\sum_{j=1}^{n} \int_{L_j} \left| \Phi_{L,i}(s) \right| \cdot \mathrm{d}s}{\sum_{j=1}^{m} \int_{\ell_j} \left| \Phi_{L,i}(s) \right| \cdot \mathrm{d}s} \leq 0,6 \tag{O.16}$$

where:

s is a coordinate along the structure axis;

$\Phi_{L,i}$ is the i-th across-wind mode shape;

m is the number of segments in which the structure or structural element is divided (Figure O.11);

ℓ_j is the length of the j-th segment (Figure O.11);

n is the number of segments where critical vortex shedding can simultaneously take place (Figure O.11).

L_j is the correlation length (Figures O.11 and O.12, Table O.IV).

Note that the integral at the numerator of Equation O.16 is performed on the portion of length L_j of segment j. All other integrals in Equations O.15 and O.16 are performed on the entire length of the segment l_j; their sum on j from 1 to m therefore gives an integral along the entire length of the structure or structural element.

Table O.V gives the mode shape factors K and the effective correlation length K_w for a number of simple structures, associated with the first across-wind mode.
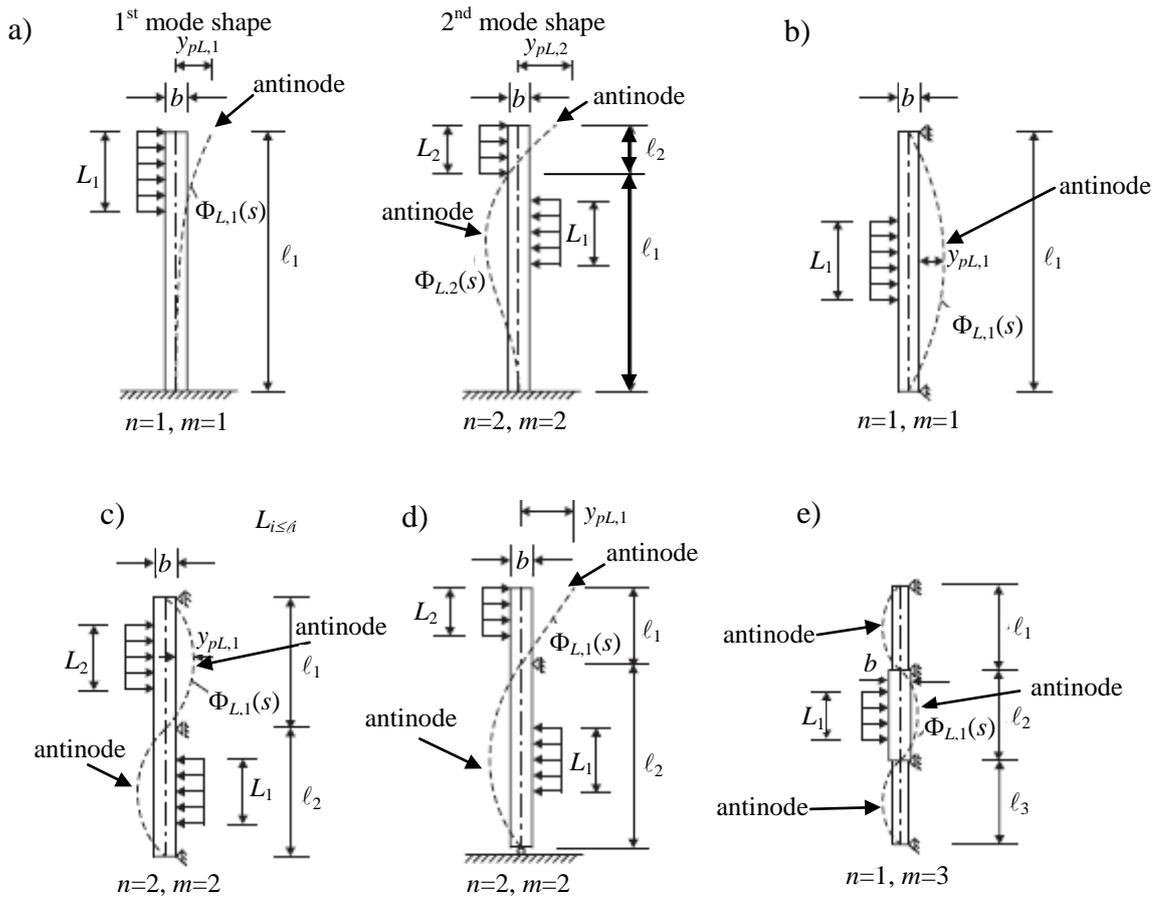
Figure O.11 − Examples of division of the structure or structural element into segments and positioning of the antinodes and correlation lengths.

Table O.IV − Correlation length L_j.

$y_{pL,i}/b$	L_j/b
<0,1	6
0,1-0,6	$4,8+12 \cdot y_{pL,i}/b$
>0,6	12
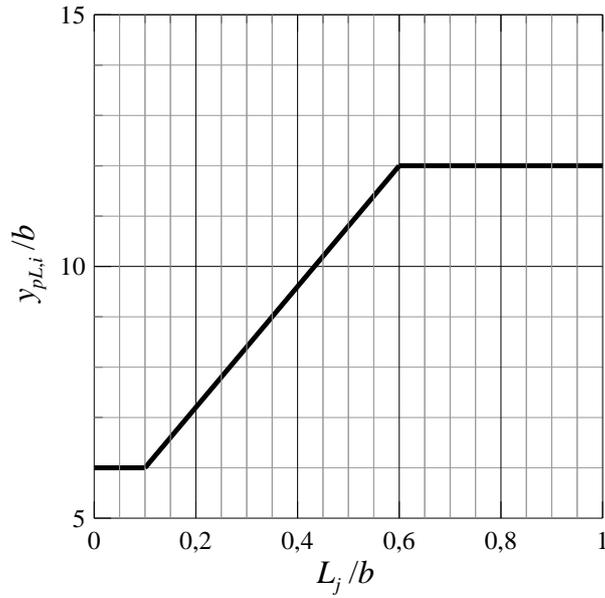
Figure O.12 – Correlation length L_j.

Table O.V – Mode shape factors K and effective correlation length factor K_w for several simple structures.

Structure	Mode shape $\Phi_{L,i}(s)$	K_w	K
	Heading I.3.1 with $\zeta=2$ $n=1$, $m=1$	$3 \cdot \dfrac{L_j/b}{\lambda}\left[1 - \dfrac{L_j/b}{\lambda} + \dfrac{1}{3}\cdot\left(\dfrac{L_j/b}{\lambda}\right)^2\right] \le 0,6$	0.13
	Heading I.3.2 $n=1$, $m=1$	$\cos\left[\dfrac{\pi}{2}\cdot\left(1 - \dfrac{L_j/b}{\lambda}\right)\right] \le 0,6$	0.10
	Heading I.3.2 $n=1$, $m=1$	$\dfrac{L_j/b}{\lambda} + \dfrac{1}{\pi}\cdot\sin\left[\pi\cdot\left(1 - \dfrac{L_j/b}{\lambda}\right)\right] \le 0,6$	0.11
Note: Parameters n and m are defined in Equations O.15 and O.16, $\lambda=\ell/b$			

O.6.2 Lateral force coefficient

The lateral force coefficient c_{lat} is a dimensionless parameter, a function of the shape of the cross-section and possibly of the Reynolds number (heading 3.3.7), calculated for the i-th critical velocity $v_{cr,i}$, Equation O.2, in the cross-section where critical vortex shedding occurs. This parameter is given by Table O.VI and Figure O.13 (for circular cross-sections).

Table O.VI – Values of the lateral force coefficient c_{lat} for several cross-sections.

Section	c_{lat}	
	$10^4 \leq Re \leq 3 \cdot 10^5$	0.7
	$3 \cdot 10^5 < Re < 5 \cdot 10^5$	$13{,}0454 - 2{,}254 \cdot \log_{10}(Re)$
	$5 \cdot 10^5 \leq Re \leq 5 \cdot 10^6$	0.2
	$5 \cdot 10^6 < Re < 10^7$	$-2{,}0241 + 0{,}332 \cdot \log_{10}(Re)$
	$Re \geq 10^7$	0,3
		(Figure O.13)
	1.1 $(0{,}5 \leq d/b \leq 10)$	
	$d/b=1$	0,8
	$d/b=1{,}5$	1,2
	$d/b=2$	0,3
	$d/b=1$	1,6
	$d/b=2$	2,3
	$d/b=1$	1,4
	$d/b=2$	1,1
	$d/b=1{,}3$	0,8
	$d/b=2$	1,0
NOTE: Linear interpolation of the values given are allowed, but not extrapolation.		
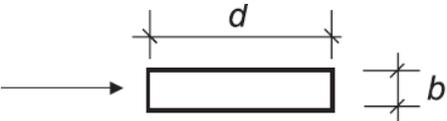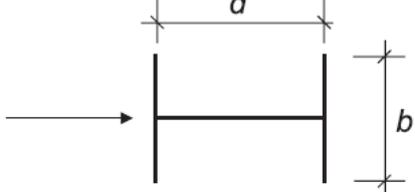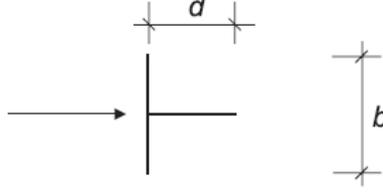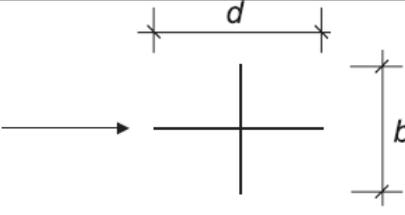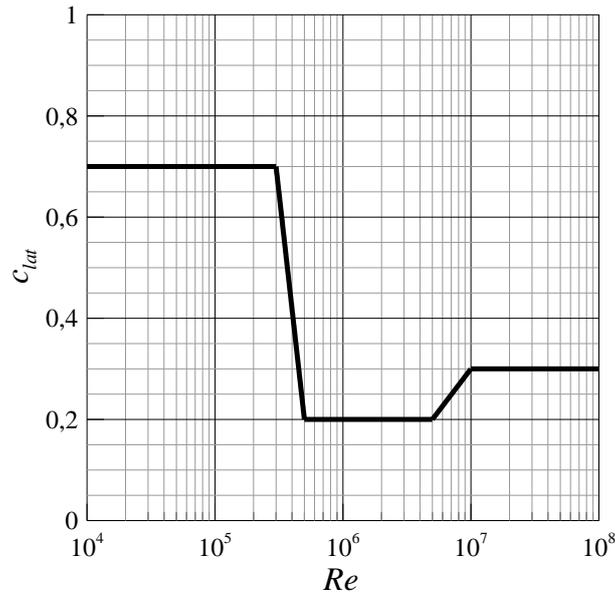
Figure O.13 - Values of the lateral force coefficient c_{lat} for circular cross-sections.

O.7   Circular cylinders in a tandem or grouped

Circular cylinders in tandem or grouped (Figure O.14), with or without structural connections, may give rise to interference phenomena associated with vortex shedding and the corresponding wakes. Especially if the cylinders are closely spaced, vortex shedding may give rise to significantly different actions and effects in respect to those occuring on an isolated cylinder, Equation O.5. These cases must be analysed with due attention.
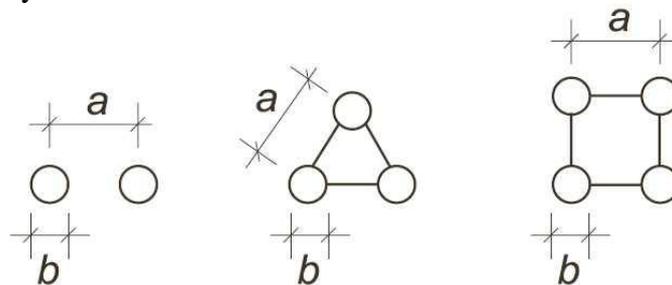
Figure O.14 – Examples of vertical cylinders in tandem (not structurally connected) or grouped (structurally coupled).

For non structurally connected cylinders, in the lack of more accurate information:

- if the distance a between the centres is more than 10 times the largest diameter b, the wake interference phenomenon between the cylinders can be disregarded;

- if the distance a between the centres of the cylinders is between 3 and 10 times the largest diameter b, it is recommended to increase the across-wind action evaluated for the isolated cylinder, Equation O.5, by a factor equal to:

    1,6   when the distance a is between 3 and 4 times the diameter b;

    [2-a/(10·b)]   when the distance a is between 4 and 10 times the diameter b;

- if the distance a between the centres of the cylinders is less than 3 times the largest diameter b, it is recommended to evaluate the response using well documented experimental methods (for example, wind tunnel tests) or seek specialist advice.

For cylinders structurally connected, limited to the case of two cylinders with a distance a between the centres of between 1 and 3 times the largest diameter b, it is recommended to apply the across-wind action evaluated for the single cylinder, Equation O.5, multiplied by a factor of 1.5. For all

other cases, in particular if the distance between the centres is more than 3 times the maximum diameter, it is recommended to evaluate wind-induced actions using well documented experimental methods (for example, wind tunnel tests) or seek specialist advice.

O.8   Number of load cycles

Resonant vortex shedding can generate large structural oscillations even at moderate and then frequent critical velocities. Therefore it may lead to fatigue damage to metal structures, the occurrence and consequences of which must be accurately assessed. The number of load cycles N caused by oscillations induced by resonant vortex shedding is the sum of load cycles N_i, caused by resonant vortex shedding on each across-wind vibration mode i. In the lack of a more accurate approach, these values can be estimated by using Eqs. O.17 and O.18:

$$N = \sum_i N_i \geq 10^4 \tag{O.17}$$

$$N_i = 2 \cdot V_N \cdot n_{L,i} \cdot \varepsilon_0 \cdot \left(\frac{v_{cr,i}}{v_{0,i}}\right)^2 \cdot \exp\left[-\left(\frac{v_{cr,i}}{v_{0,i}}\right)^2\right] \tag{O.18}$$

where:
V_N is the nominal lifetime of the structure or structural element (Annex A);
$n_{L,i}$ is the i-th across-wind natural frequency;
ε_0 is the bandwidth factor, which may be taken equal to 0.3;
$v_{cr,i}$ is the i-th critical velocity of vortex shedding, Equation O.2;
$v_{0,i}$ is a reference value of the wind velocity, indicatively equal to 0.2 times the mean wind velocity (heading 3.2.5) with a design return period T_R=50 years, calculated in the cross-section where the i-th critical vortex shedding phenomenon occurs.

Expressing V_N in s (equal to the nominal life expressed in years, multiplied by $32 \cdot 10^6$) and $n_{L,i}$ in Hz, N_i and N turn out to be dimensionless parameters.

O.9   Techniques for mitigating the effects of vortex shedding

Large across-wind vibrations caused by vortex shedding can be mitigated through the use of passive control systems and even by active or hybrid control systems. It is recommended that structures with poor accessibility (for example, chimneys) be designed such to minimise maintenance.

Passive systems for the control of vortex shedding response can be divided into:

- aerodynamic stabilizers (for example, helical vanes, Figure O.15, or shrouds, Figure O.16) designed to contrast regular vortex shedding. Their effectiveness is only demonstrated for Scruton number values higher than 10; in no case can these solutions be used to mitigate the effects of wake interference caused by neighbouring structures or structural elements. These devices generally increase along-wind loads;

- Tuned Mass Dampers (TMD, Figure O.17) and Tuned Liquid Dampers (TLD) designed to increase the damping ratio and therefore to significantly reduce all types of vibration, including vibration arising from interference phenomena as well as vibration in the along-wind direction. These devices are particularly effective in reducing self-excited vibrations.

For the use of active and/or hybrid control systems it is recommended that specialist advice be sought.

0.10*b* − 0.12*b*

h

b
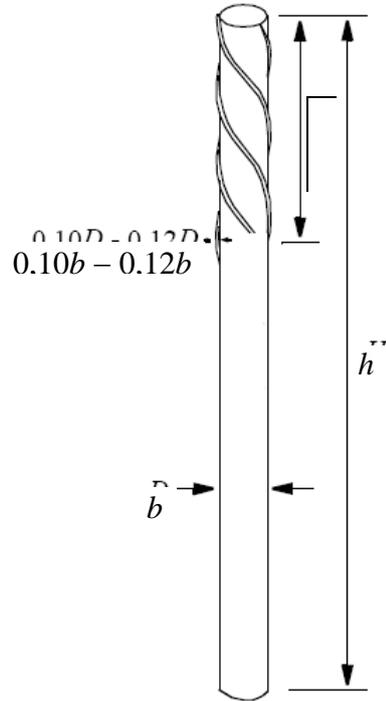
Figure O.15 – Aerodynamic stabilizer: helical vanes.

Porous cladding

Toggle-bolt cladding

0,087*b*

Square apertures
having a side of about
0,07*b*,

Porosity (open area
ratio) equal to 40%

0,12*b*

0,14*b*
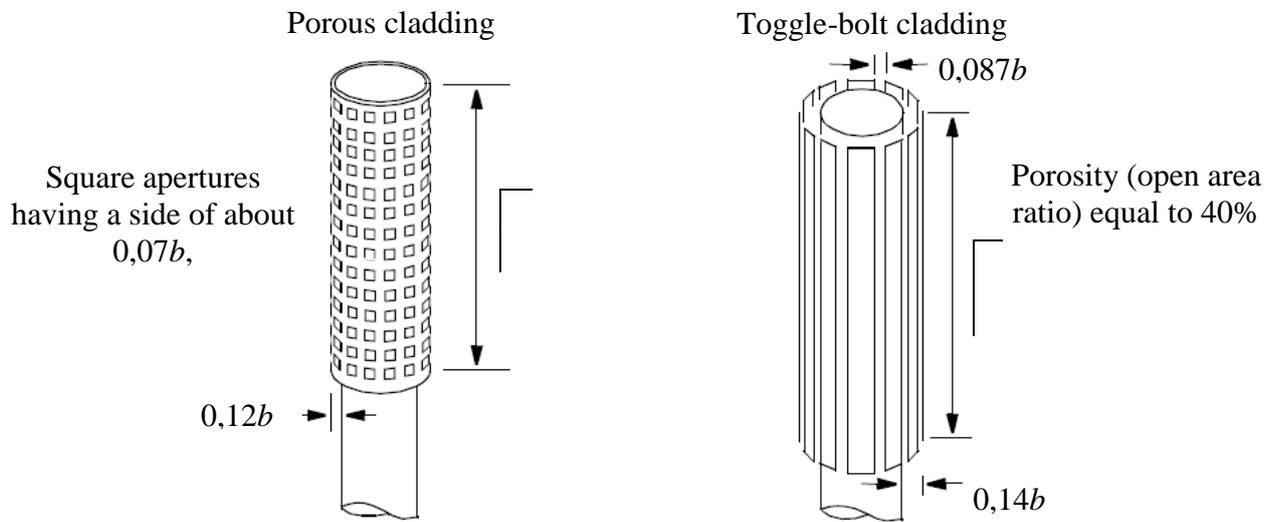
Figure O.16 – Aerodynamic stabilizer: shrouds.
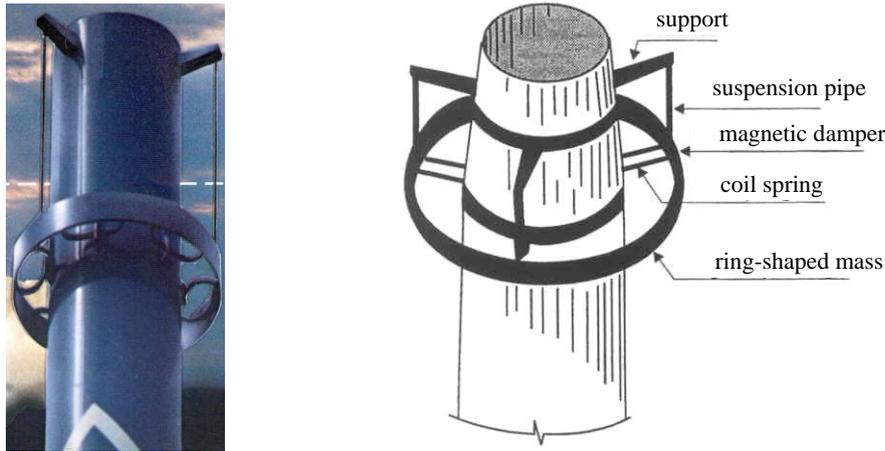
Figure O.17 – Tuned Mass Damper (TMD).

O.10 Ovalling

Circular cylindrical shells (e.g. chimneys, tanks and metal silos) can be subject to ovalling phenomena of static or dynamic nature.

The static ovalling phenomenon is an effect of the pressure distribution on the surface of cylindrical shells with a circular cross-section; it can be assessed by applying the criteria given in headings G.3.2, G.10.6 and G.10.8.

The dynamic ovalling phenomenon, which is the subject of this heading, generally occurs in the first ovalling modes, i.e. the first modes associated with displacements in the cross-section plane in a radial direction (Figure O.18), often coupled with flexural vibration modes with respect to the axis of the cylinder. It can give rise to vibrations that may cause the collapse of the structure through local or global instability, or because of fatigue. This phenomenon occurs at ovalling frequencies that are multiples of the vortex shedding frequency (Equation O.1). From a conceptual point of view, as for the vortex shedding phenomenon, the ovalling phenomenon is located in an intermediate position between a classic dynamic excitation, arising from actions caused by vortex shedding, and a form of aeroelastic instability, associated with the occurrence of fluid-structure interaction due to the shell vibration (Annex P).
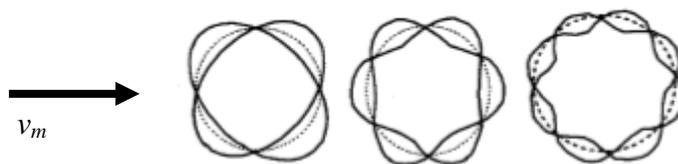
Figure O.18 – Ovalling modes (cross-section of the circular shell).

Critical ovalling velocities are defined as the mean wind velocities that give rise to the dynamic ovalling phenomenon. Technical-scientific literature reports a number of methods for calculating critical ovalling velocities. Most of these have complementary advantages and disadvantages; none may claim to be fully shared and recognised. There follow two alternative assessment criteria. Due to the uncertainties still affecting this phenomenon, these criteria shall be considered as indicative. It is suggested that the most conservative, between the results obtained through the application of the two criteria, has to be considered.

Applying the first criterion, the critical velocity for the *i*-th ovalling mode is given by Eq. O.19:

$$v_{O,i} = \frac{n_{O,i} \cdot b}{\Omega \cdot St} \tag{O.19}$$

where:

$n_{O,i}$ is the i-th ovalling frequency (Annex I);

b is the cylinder diameter;

St is the Strouhal number (heading O.2);

Ω is a dimensionless parameter that, depending on the phenomenon occurring, may be equal to $\Omega = 1, 2, 3, 4$.

The ovalling phenomenon usually occurs for $\Omega = 2$; in less common cases, it may occur for $\Omega = 1, 3$ and 4.

Applying the second criterion, arising from the results of wind tunnel tests on slender cylinders, the i-th ovalling critical velocity is given by Eq. O.20:

$$v_{O,i} = n_{O,i} \cdot b \left(25,66 \cdot \frac{\rho_s}{\rho} \cdot \frac{t}{b} \cdot \xi_{O,i} + 0,3 \right) \tag{O.20}$$

where:

ρ_s is the density of the material of the shell;

ρ is the air density; the recommended value is 1,25 kg/m^3 (heading.3.2.7);

t is the thickness of the shell;

$\xi_{O,i}$ is the critical structural damping ratio in the i-th ovalling mode (not including aerodynamic damping) (Annex I.6).

To avoid ovalling phenomena, or at least to make them extremely unlikely, the condition given by Eq. O.21 should be met:

$$v_{O,i} > v_{m,l} \tag{O.21}$$

where:

$v_{m,l,}$ is the mean wind velocity (heading 3.2.5), evaluated at the top of the cylinder h, for a design return period T_R equal to 10 times the reference return period $T_{R0.0}$ (Annex A), $T_R = 10 \cdot T_{R0.0}$.

Increasing the stiffness of the shell (and thereby increasing the frequencies $n_{O,i}$) reduces the risk of ovalling. A possible solution to the problem of ovalling is therefore the use of stiffening rings, whose size and distance shall be chosen based on the diameter of the cylinder.

Annex P.   OTHER AEROELASTIC PHENOMENA

P.1   General

Aeroelastic phenomena are phenomena of fluid-structure interaction that occur when deflections and/or velocities of a structure or structural element are such as to heavily modify the wind flow and the pressure field. Lightweight, very flexible and low damped structures are therefore prone to these phenomena.

Aeroelastic phenomena may be described through the use of aeroelastic (or self-excited) actions, generally non-linear, that depend on deflections and on velocities of the structure, as well as on the mean wind velocity and on the aerodynamic parameters. In the hypothesis of small deflections, aeroelastic actions can be linearized, giving rise to terms that are directly proportional to the deflections and the velocities of the structure.

The dependence on the structural motion (deflection and velocity) means that linearized aeroelastic actions can be described through parameters that modify the mechanical properties of the structure, in particular damping, when the self-excited action is proportional to velocity, and stiffness when the self-excited action is proportional to deflection.

As the mean wind velocity increases, the above phenomena are such as to reduce and possibly cancel the total stiffness and/or the damping of the structure, generating critical conditions of incipient instability (aeroelastic instability).

The values of mean wind velocity at which instability arises are defined as critical and depend on the geometric and mechanical characteristics of the structure. It is the Designer's duty to ensure that all critical velocities of the construction are considerably higher than the design wind velocity. In particular, as instability phenomena may give rise to collapse, it is important to ensure that the probability of critical velocities is extremely small.

Aeroelastic instabilities can be classified in three main categories, on the basis of their physics:

- galloping: is an aeroelastic phenomenon characterised by the vanishing of damping. Galloping is a dynamic instability that affects slender, lightweight structures and structural elements with low structural damping, having non-circular cross-sections that, in given conditions, may manifest large amplitude across-wind oscillations. This phenomenon may arise, even at low velocities, for all cables whose cross-section can be modified by icing, and for the inclined cables of cable-stayed bridges where the cross-section can be modified by the presence of a water rivulet. It can also manifest itself, at high critical velocities, in high-rise and slender structures, isolated structural elements and lighting poles;

- torsional divergence: is an aeroelastic phenomenon characterised by the vanishing of torsional stiffness. Torsional divergence is a static instability affecting flexible, flat structures oriented in the direction of the oncoming flow. To divergence are prone flexible plate-like structures, such as signboards, shelters, canopies and cable-supported bridge decks;

- flutter: is an aeroelastic phenomenon associated with the modification of both the stiffness and the damping of the structure. Flutter is a dynamic instability, generally in two coupled degrees of freedom of heaving and pitching (classic flutter). In particular cases, flutter can manifest in one single degree of freedom (stall flutter). Stall flutter has been observed in a large variety of plate-like structures such as canopies, road signs and cable-supported bridge decks, especially for torsional vibration modes. Classic flutter is very hazardous for suspension and cable-stayed bridges where the coupling can occur between a heaving and a pitching degree of freedom. In general, classic flutter occurs for modes having closely spaced frequencies and similar mode shapes, with the same number (and approximately the same location) of nodes.

Note that lock-in caused by vortex shedding (Annex O) is a phenomenon of an aeroelastic nature (i.e. caused by flow-structure interaction) with very different characteristics compared to those of the other aeroelastic phenomena described above (galloping, torsional divergence, flutter). It arises at discrete values of the mean wind velocity and the structure may be designed and/or verified to withstand the actions associated with it. Vice versa, the phenomena discussed in this Annex lead to situations of instability (static or dynamic), starting from a critical velocity, that the structure must not reach.

P.2   Galloping

Galloping is an aeroelastic instability phenomenon that can arise in slender structures and structural elements with a non-circular cross-section (for example rectangular, L-shaped, I-shaped, U-shaped, T-shaped). Ice or a water rivulet on a circular section can cause instability of an otherwise stable cross-section (for example, cables). The former case is a classic galloping phenomenon; the latter, which proves very hazardous for the inclined cables of cable-stayed bridges, and which is still not entirely clarified, is a form of instability similar to galloping. Aeroelastic instabilities similar to galloping can also appear on yawed elements with circular cross-sections.

Heading P.2.1 defines the galloping condition. Heading P.2.2 provides a criterion for the evaluation of the critical velocity. Heading P.2.3 defines verification criteria. Headings P.2.4 and P.2.5 deal with the galloping of coupled cylinders.

P.2.1   Galloping condition

The galloping phenomenon is caused by aerodynamic actions orthogonal to the direction of the mean wind velocity, acting on the cross-section of the structure or the structural element.

Considering a generic fixed cross-section (Figure P.1a) in a bi-dimensional flow regime and assuming that the mean value of drag force D and lift force L (associated with the mean wind velocity v_m), acting with generic angle of attack α are known. Forces D and L are proportional to the drag, $c_D(\alpha)$, and lift, $c_L(\alpha)$, coefficients, which in turn depend on the shape of the body and on the angle of attack of the flow α (Figure P.1b). Drag c_D and lift c_L coefficients coincide with the coefficients of force per unit length c_{fX} and c_{fY} (heading 3.3.4), respectively, when axis X in the section plane coincides with the direction of the oncoming wind.

When the cross-section is free to move, the apparent angle of attack becomes a function of the velocity of the across-wind motion; this gives rise to an equivalent aerodynamic damping, that combines with structural damping. The galloping phenomenon occurs when the total damping vanishes. The across-wind galloping condition is given by Eq. P.1 and Figure P.1c:

$$\left[c_L' + c_D \right] \le 0 \tag{P.1}$$

where:
c_L' is the angular derivative of the lift coefficient c_L, evaluated for a fixed value of the angle of attack α;
c_D is the drag coefficient c_D, evaluated for the same value of the angle of attack α.
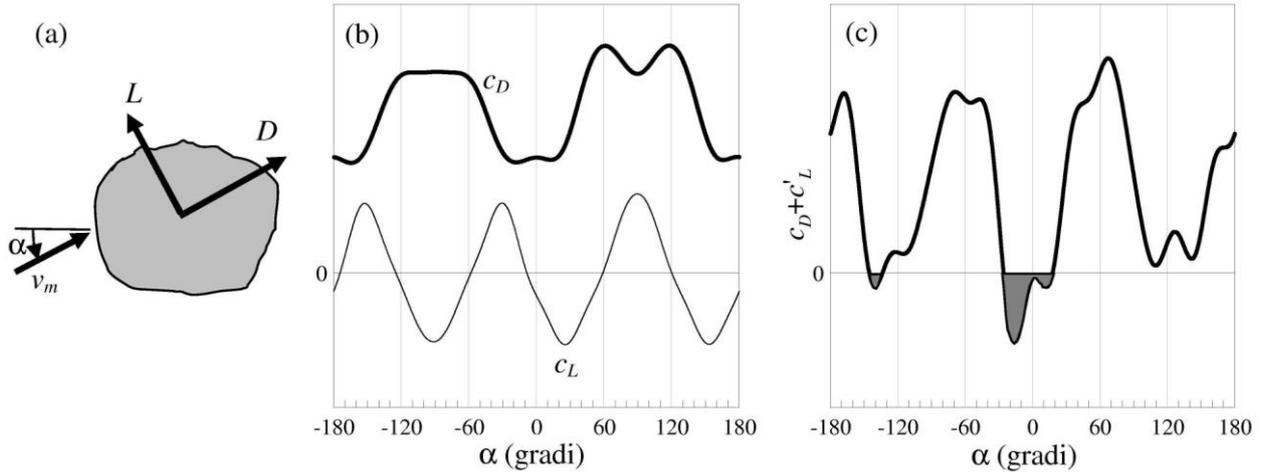
Figure P.1 – Galloping: (a) forces on a fixed cross-section; (b) drag c_D and lift c_L coefficients evaluated on the fixed cross-section;
(c) galloping condition, Equation P.1.

Equation P.1 is known as the Den Hartog criterion, and it represents a necessary condition for the galloping phenomenon to occur. The shaded areas in Figure P.1c highlight the values of the angle of attack α for which Equation P.1 is fulfilled, so the cross-section in question may be subject to galloping instability.

Since the drag coefficient c_D is always positive, regardless of the shape of the cross-section and of the wind direction, a structure or structural element is prone to across-wind galloping only if the angular derivative of the lift coefficient c_L is negative and has a modulus larger than the drag coefficient c_D. In particular, isolated circular elements (e.g. cables) cannot be prone to galloping because of their polar-symmetry. On the other hand, when the cross-section of the cable is ice-coated or carries a water rivulet, galloping similar dynamic instability phenomena can arise.

P.2.2 Critical galloping velocity

Assuming that the X axis in the section plane coincides with the wind direction, acting in general along a main axis of the cross-section of the structure, heading 3.3, in the direction of which the response is more readily described, and that the oncoming flow is perpendicular to Z axis of the structure. It is also assumed that the natural frequencies of the structure are well spaced (absence of internal resonance conditions) so to allow describing the vibrations of the structure by means of a single across-wind bending mode.

Galloping instability occurs when the total damping in the i-th mode vanishes (critical galloping condition). This situation occurs when the mean wind velocity v_m is equal to the critical galloping velocity $v_{G,I}$, given by Eq. P.2:

$$v_{G,i} = \frac{8\pi \cdot m_{e,i} \cdot n_{L,i} \cdot \xi_{L,i}}{\rho \cdot b \cdot a_G} = \frac{2 \cdot n_{L,i} \cdot b \cdot Sc_i}{a_G} \tag{P.2}$$

where:
$m_{e,i}$ is the equivalent mass per unit length in the i-th across-wind mode (Annex I.4);
$n_{L,i}$ is the natural frequency in the i-th across-wind mode(Annex I.2);
$\xi_{L,i}$ is the critical structural damping ratio in the i-th across-wind mode (not including aerodynamic damping) (Annex I.6);
ρ is the air density; the recommended value is 1.25 kg/m^3 (heading 3.2.7);

b is the reference width of the cross-section, corresponding to the galloping instability factor (Table P.I), evaluated at the location of maximum modal displacement;

Sc_i is the Scruton number for the *i*-th across-wind vibration mode, Equation O.4;

a_G is the galloping instability factor; this parameter is equal to the sum (with sign changed) of the angular derivative of the lift coefficient c_L and of the drag coefficient c_D, evaluated for an angle of attack α=0 with respect to axis *X*:

$$a_G = -\left[c_L' + c_D \right]_{\alpha=0} = -\left[c_{fY}' + c_{fX} \right] \qquad (P.3)$$

In the lack of more accurate assessments, Table P.I gives values of a_G for the most common structural shapes. For structural shapes not shown in the Table, taking $a_G = 10$ should give a conservative estimate.

Note the essential role of the Scruton number in describing the sensitivity of structures and structural elements to aeroelastic phenomena: in the case of galloping, structures with a low Scruton number are subjected to low critical velocities and are therefore more sensitive to this type of instability; in the case of vortex shedding, the Scruton number does not influence the critical shedding velocity, Equation (O.2), but governs the amplitude of oscillation at lock-in (oscillation amplitudes increase significantly for small values of the Scruton number).

Table P.I - Galloping instability factor a_G.

Section	a_G		Section	a_G	
ice / iced cables / ice	1,0			1,0	
				4,0	
linear interpolation	$d/b=2$	2,0		$d/b=2$	0,7
	$d/b=1,5$	1,7		$d/b=2,7$	5,0
	$d/b=1$	1,2		$d/b=5$	7,0
linear interpolation	$d/b=2/3$	1,0		$d/b=3$	7,5
	$d/b=1/2$	0,7		$d/b=3/4$	3,2
	$d/b=1/3$	0,4		$d/b=2$	1,0
N.B.: Linear interpolation is allowed (but not extrapolation) of a_G as a function of d/b					
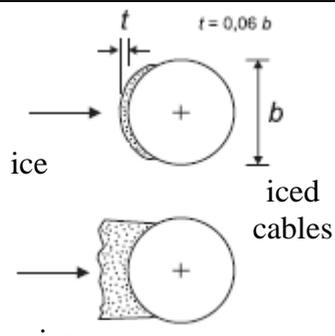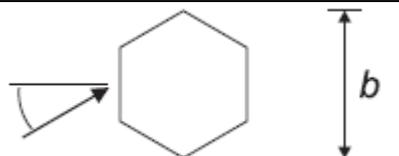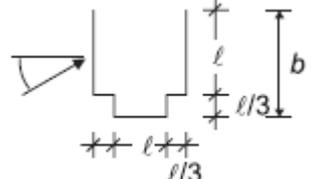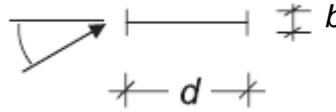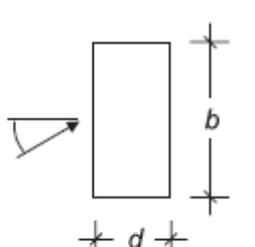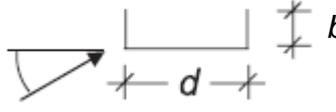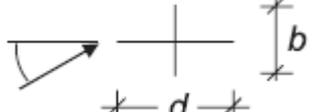
P.2.3 Verification criteria

In order to avoid galloping instability, or make it quite unlikely, the condition given by Eq. P.4 should be met:

$$v_{G,i} > v_{m,l} \qquad \text{(P.4)}$$

where:

$v_{G,i}$ is the critical galloping velocity in the i-th across-wind vibration mode, Equation P.2;

$v_{m,l}$ is the mean wind velocity (heading 3.2.5), evaluated at the height of the section of maximum modal displacement, for a return period T_R equal to 10 times the reference return period $T_{R0.0}$ (Annex A), $T_R = 10 \cdot T_{R0.0}$.

In general, the lowest critical velocity corresponds to the first across-wind vibration mode. Hence the most stringent condition, Equation P.4, corresponds to the critical velocity $v_{G,1}$.

If the critical velocity of vortex shedding $v_{cr,i}$, Equation O.2, is close to the critical velocity of galloping $v_{G,i}$ (for the same across-wind vibration mode), e.g. condition reported in Eq. P.5 is met

$$0,7 < \frac{v_{G,i}}{v_{cr,i}} < 1,5 \qquad\qquad (P.5)$$

an interaction between the two aeroelastic phenomena may occur. In this case, well documented experimental studies are required, and specialist advice shall be sought.

P.2.4   Galloping of coupled circular cylinders

Coupled or grouped circular cylinders may be subject to classic galloping phenomena. The critical galloping velocity can be assessed with Equation P.2, where the galloping instability factor a_G and the reference size (width) b are specified by Table P.II. The verification criterion is the same as that given in heading P.2.3.

Table P.II - Galloping instability factor for coupled cylinders.

Number of coupled cylinders	a_G	
	$a/b \leq 1,5$	$a/b \geq 2,5$
i=2	1,5	3,0
i=3	6,0	3,0
i=4	1,0	2,0
N.B.: Linear interpolation is allowed (but not extrapolation) of a_G as a function of a/b		
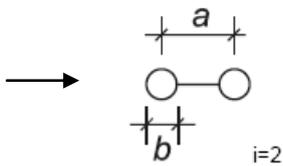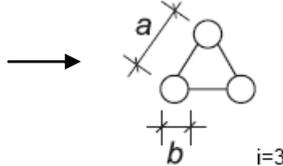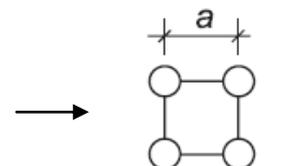
P.2.5   Interference galloping for non-coupled circular cylinders

Circular cylinders in a row, though not structurally connected, can give rise to an instability phenomenon known as wake galloping. Wake galloping is a quite dangerous phenomenon and can be avoided by connecting the cylinders in order to create one of the configurations discussed in heading P.2.4.

Otherwise, if the angle of attack is close to the critical direction $\alpha \cong 10°$, and if $a/b<3$ (Figure P.2), then the critical velocity causing wake galloping instability, v_{IG}, is given by Eq. P.6:

$$v_{IG} = 3,5 \cdot n_{L,1} \cdot \sqrt{a \cdot b \cdot \frac{Sc_1}{a_G}}$$

(P.6)

where:

$n_{L,1}$ is the first across-wind natural frequency (Annex I.2);

Sc_1 is the Scruton number in the first across-wind vibration mode, Equation O.4;

a is the centre-to-centre distance of the cylinders (Figure P.2);

b is the diameter of the cylinders (Figure P.2);

a_G is the galloping instability factor caused by interference; in the lack of more accurate assessments, this parameter can be taken as equal to 3.
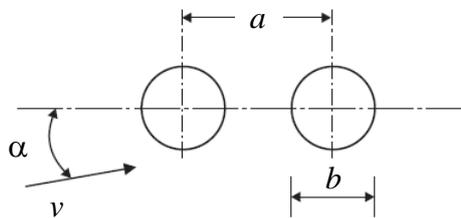
Figure P.2 – Geometric parameters in wake galloping.

The assessment criterion is the same as that given in heading P.2.3.

P.3   Torsional divergence

Torsional divergence is an aeroelastic instability of structures with a streamwise elongated section (e.g. signboards and cable-suported bridge decks)

Heading P.3.1 defines the condition of torsional divergence. Heading P.3.2 contains an evaluation criterion for the divergence critical velocity. Heading P.3.3 defines verification criteria.

P.3.1   Condition for torsional divergence

Torsional divergence is associated with the action of aerodynamic torque on the cross-section of the structure or structural element.

Consider a fixed plate-like cross-section (Figure P.3a) in a bi-dimensional flow regime, and assume that the mean value of the aerodynamic torque M (per unit length), associated with a mean wind velocity v_m acting at an angle α, is known. Aerodynamic torque M is a function of the aerodynamic moment coefficient, $c_{mZ}(\alpha)$, which in turn depends on the section shape and on the angle of attack α (Figure P.3b).

When the cross-section is free to rotate around the structure axis Z, and under the assumption of small rotations, the aerodynamic torque is proportional to the angle of twist θ (with the same direction of the angle of attack α); there arises an equivalent aerodynamic stiffness that combines with the structural stiffness. The phenomenon of torsional divergence occurs when the total stiffness vanishes. A necessary condition of possible instability is then given by Eq. P.7 and Figure P.3c:

$$c'_{mZ} \leq 0$$

(P.7)

where:

c'_{mZ} is the angular derivative of the moment coefficient c_{mZ}, evaluated at the angle of attack α.
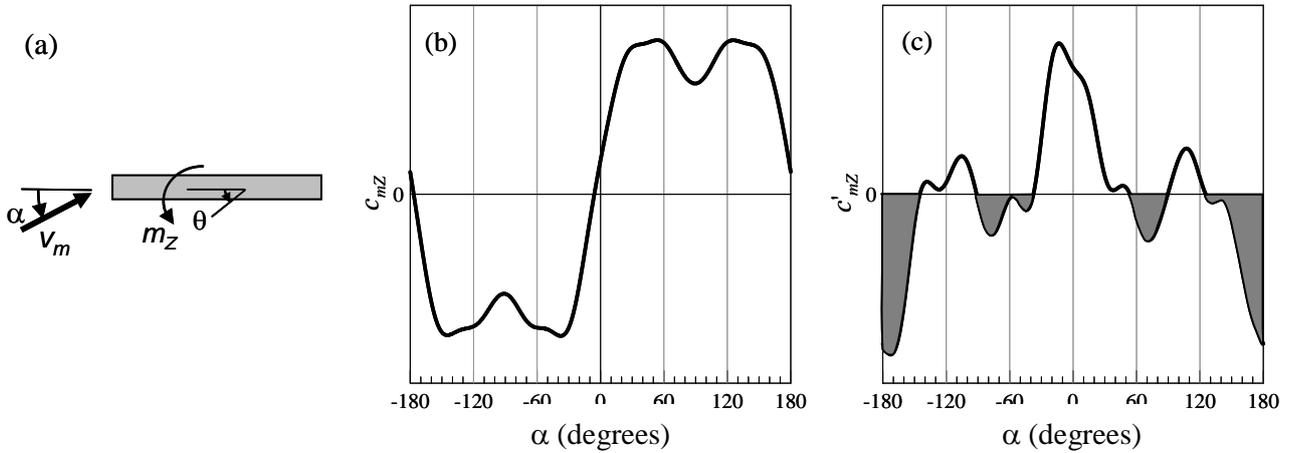
Figure P.3 – Torsional divergence: (a) torque on a fixed section; (b) aerodynamic moment coefficient c_{mZ}, evaluated on the fixed section; (c) condition of torsional divergence, Equation (P.7).

The shaded areas in Figure P.3c show the values of the angle of attack α for which the condition of Equation P.7 is met, therefore giving rise to possible torsional divergence instability.

P.3.2 Critical velocity of torsional divergence

Torsional divergence occurs when the total stiffness vanishes (critical torsional divergence condition). This situation occurs when the mean wind velocity v_m is equal to the critical torsional divergence velocity v_D given by Eq. P.8:

$$v_D = \sqrt{-\frac{2 \cdot G \cdot J_t}{\rho \cdot d^2 \cdot c'_{mZ}}}$$ (P.8)

where:

G is the shear modulus of the material;

J_t is the torsional moment of inertia of the cross-section (heading I.2.3);

ρ is the air density; the recommended value is 1,25 kg/m^3 (heading.3.2.7);

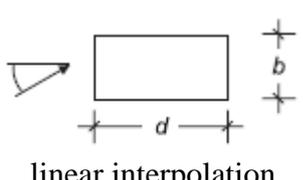d is the chord of the structure (size parallel to the wind direction);

c'_{mZ} is the angular derivative of the aerodynamic moment coefficient c_{mZ} (associated with the reference length $l = d$), evaluated for the angle of attack α.

Expressing the torsional stiffness in N·m^2, the air density in kg/m^3 and the chord in m, the critical velocity v_D is expressed in m/s.

For a rectangular section having sides b and d, at $\alpha = 0$ (Figure P.4) and in the lack of more accurate assessments, c'_{mZ} is given by Eq. P.9 and Figure P.5:

$$c'_{mZ} = 6,3\left(\frac{b}{d}\right)^2 + 0,38\left(\frac{b}{d}\right) - 1,6$$ (P.9)
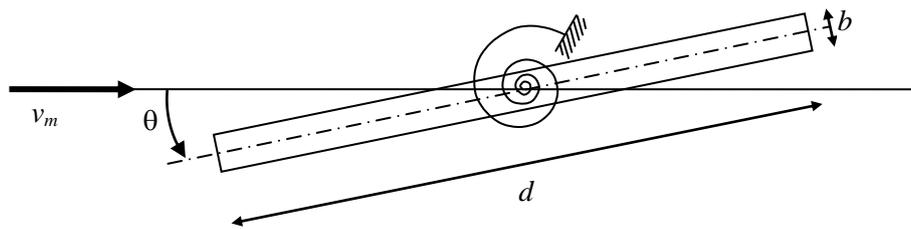
Figure P.4 – Rectangular section subject to torsional divergence.
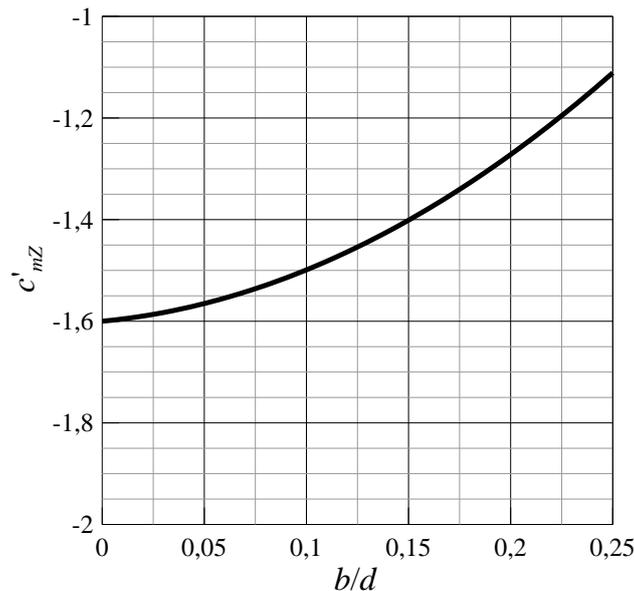
Figure P.5 – Angular derivative of the aerodynamic moment coefficient for a rectangular section.

P.3.3 Verification criterion

To avoid torsional divergence, or make it quite unlikely, the condition given by Eq. P.10 should be met:

$$v_D > 1,2 \cdot v_{m,l} \tag{P.10}$$

where:

v_D is the critical torsional divergence velocity, Equation P.8;

$v_{m,l}$ is the mean wind velocity (heading 3.2.5), evaluated at the mean height of the structure or structural element, for a return period T_R equal to 10 times the reference return period $T_{R0.0}$ (Annex A), $T_R = 10 \cdot T_{R0.0}$.

P.4 Flutter

Flutter is an aeroelastic instability that can arise for particular combinations of sectional geometries and dynamic characteristics of the structure or structural element. With reference to bridge decks, this phenomenon is generally limited to very flexible structures with large spans, such as suspension or cable-stayed bridges.

Headings P.4.1 and P.4.2 give some general criteria to evaluate the susceptibility of bridge decks to torsional flutter (stall flutter) and to coupled flutter (classical flutter), only for the most common

deck geometries and in the absence of vehicles. Heading P.4.3 discusses the general principles concerning verification criteria for flutter.

P.4.1 Sensitivity to stall flutter

For bridge decks with a span of no more than 200 m, stall flutter is unlikely to occur if condition given by Eq. P.11 is met:

$$\frac{1,2 \cdot v_{m,l}}{d \cdot n_{M,1}} \leq 3 \tag{P.11}$$

where:

$v_{m,l}$ is the mean wind velocity (heading 3.2.5), evaluated at the mean height of the deck, for a return period T_R equal to 10 times the reference return period $T_{R,0}$ (Annex A), $T_R = 10 \cdot T_{R,0}$.

d is the size of the deck in the wind direction;

$n_{M,1}$ is the first torsional frequency of the bridge deck.

P.4.2 Sensitivity to coupled flutter

For bridge decks with a span of no more than 200 m, heaving-pitching coupled flutter in the first modes is unlikely to occur if the conditions given by Eqs. P.12 to P.14 are simultaneously met:

$$\frac{n_{M,1}}{n_{L,1}} \geq 1,5 \tag{P.12}$$

$$\frac{1,2 \cdot v_{m,l}}{d \cdot n_{L,1}} \leq 20 \tag{P.13}$$

$$\frac{1,2 \cdot v_{m,l}}{d \cdot n_{M,1}} \leq 2,5 \cdot \beta_F \cdot \sqrt{\left[1 - \left(\frac{n_{L,1}}{n_{M,1}}\right)^2\right] \cdot r_m \cdot \mu} \tag{P.14}$$

in which:

$$r_m = \sqrt{\frac{I}{m \cdot d^2}}, \quad \mu = \frac{2 \cdot m}{\rho \cdot d^2} \tag{P.15}$$

where:

$n_{M,1}$ is the first torsional (pitching) frequency of the deck;

$n_{L,1}$ is the first vertical bending (heaving) frequency of the deck;

$v_{m,l}$ is the mean wind velocity (heading 3.2.5), evaluated at the mean height of the deck, for a return period T_R equal to 10 times the reference return period $T_{R,0}$ (Annex A), $T_R = 10 \; T_{R,0}$;

d is the size of the deck in the wind direction;

I is the deck mass moment of inertia per unit length;

m is the deck mass per unit length;

p is the air density; the recommended value is 1,25 kg/m^3 (heading.3.2.7);

β_F is an aerodynamic efficiency parameter. This parameter is given by Figure P.6 for common decks as a function of the ratio h/d, where h is the height of the deck, including permanent furniture (barriers, guard-rails, Jersey barriers, etc.).
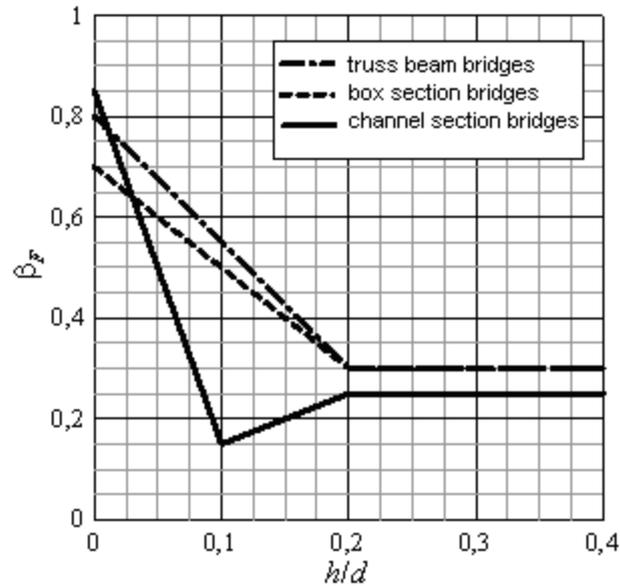
Figure P.6 – Value of aerodynamic efficiency parameter β$_F$.

P.4.3 Verification criterion

When it is not possible to exclude flutter by applying the criteria given in headings P.4.1 and P.4.2, accurate analyses must be carried out based on wind tunnel tests, and specialist advice must be sought. In any case, it is always good practice to ensure that the critical flutter velocity v_F, i.e. the mean wind velocity causing instability, meets the condition given by Eq. P.16:

$$v_F > 1,2 \cdot v_{m,l} \tag{P.16}$$

where:
v_F is the critical velocity of flutter, evaluated through well documented experimental and numerical methods;
$v_{m,l}$ is the mean wind velocity (heading 3.2.5), evaluated at the mean height of the deck, for a return period T_R equal to 10 times the reference return period $T_{R,0}$ (Annex A), $T_R = 10 \cdot T_{R0.0}$.

Annex Q   WIND TUNNEL TESTS

Q.1   Introduction

Calculation of wind action on structures and of the associated structural response cannot be performed without experimental data measured in the wind tunnel. For the most common cases, such data are available in the literature and summarised in this Guide, ready for use in the design. In less common cases, or for large and/or complex structures, it is recommended that design analyses and/or verifications be based on well documented data or on specific experimental tests performed in accordance with the criteria described below. In addition, wind tunnel tests are a useful tool for checking the results of calculations and for optimising aerodynamic and structural performances, often leading to an economic advantage and/or an increase in safety margins.

Wind tunnel testing is based on the reduced-scale reproduction of the physical phenomena that occur in actual cases. Scale reduction must not only concern geometry but all the physical aspects found in the interaction process between wind and structures. Therefore, in wind tunnel modelling, the engineer must appropriately scale all physical dimensions involved in the phenomena under investigation; in this context scaling is performed with different rules depending on individual cases. It should be noted that scaling must be applied to both structural parameters and also wind flow properties. To this end, scales of the different physical entities involved in the problem under investigation should be defined as the ratio between the value that a given quantity takes in the wind tunnel and its corresponding full–scale value.

In view of their interdisciplinary and highly specialised nature, the design, execution and interpretation of wind tunnel tests must be carried out by specialists or specialist laboratories. This Annex aims at providing the Designer with basic elements needed to understand the method of execution of the most common wind tunnel tests and to interface with the specialist in charge of the testing procedure. The Annex also contains some of the minimum conditions that the designer must request for the execution of the wind tunnel experiment. More details about experimental techniques may be found in the technical literature.

Q.2   Wind tunnels and flow characteristics in the tunnel

In order to correctly measure the actions of wind on constructions, and/or the associated structural response, the wind tunnel must reproduce the features of the wind flow in the atmospheric boundary layer. In particular, for vertical structures, the mean velocity and turbulence intensity profiles must be reproduced. Moreover, the turbulence characteristics for all structures must be reproduced in terms of frequency content and length scales. The tunnels capable of best meeting these requisites are defined as Boundary Layer Wind Tunnels (BLWT) and are generally used for testing in Civil and Environmental engineering. Only in cases (to be verified) where the vertical distribution of wind flow characteristics is not relevant, is it possible to use standard (non-boundary layer) tunnels, such as those for mechanical or aeronautical applications. In any case, the flow features reproduced in the tunnel shall be constant along the test chamber. Figure Q.1 gives a photograph of the test chamber in a boundary layer wind tunnel.
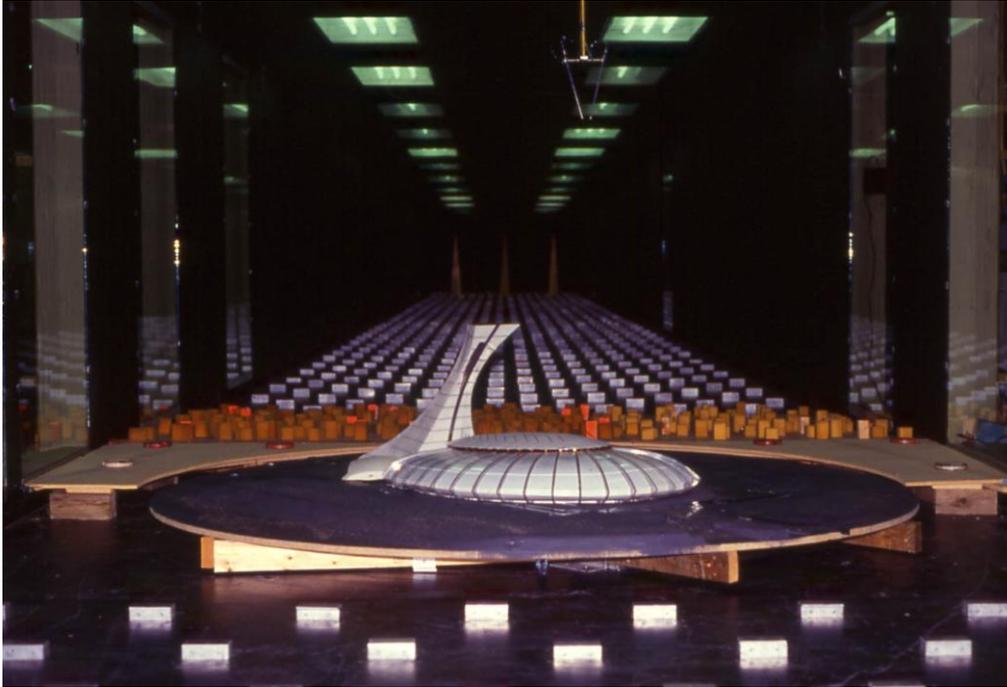
Figure Q.1 – Test chamber in a boundary layer wind tunnel.

For an appropriate reproduction of physical phenomena, the flow parameters in the tunnel must represent, after scaling, those of the actual flow. This means that the following rules must be observed:

1. dimensionless parameters (for example, Reynolds number, Strouhal number, turbulence intensity, etc.) in the tunnel must have the same value as at full-scale;

2. to parameters having the same physical dimensions, the same scale must be applied; this means, for example, that parameters having length dimensions (geometric dimensions of the model, turbulence length scale, depth of the atmospheric boundary layer, etc.) must all be scaled by the same magnitude, indicated as the length scale, λ_L, which is the ratio between the lengths used during tests and the corresponding full–scale values;

3. scales of different physical dimensions must meet the dimensional equations; this means that, for example, the velocity scale, λ_V (ratio between the mean flow velocity during the test and at full-scale), must be equal to the length scale, λ_L, divided by the time scale, λ_T (defined by the ratio between the duration of wind tunnel tests and equivalent full-scale durations).

In general, it is not possible to satisfy all the above requisites simultaneously; it is therefore standard practice to use a distorted modelling to fulfill only some of the scaling constraints. The selection of which scaling constraints can be violated in each situation is extremely complex and largely determines the quality of the results of the experiment. Experimentalists must therefore justify the choices made. In particular, it must be ensured that:

1. for vertical structures, the mean velocity and turbulence intensity profiles shall reproduce full-scale conditions up to a height equal to at least 1,5 times the maximum height of the structure;

2. for all structures, the longitudinal turbulence length scale in the tunnel must be as close as possible to the full-scale one, reduced through the geometric scale of the structural model.

For an accurate reproduction of the aerodynamic behaviour of constructions, the value of the Reynolds number in the tunnel should coincide with the full-scale value. This requisite is frequently not satisfied, leading to negligible errors for sharp-edged geometries with however significant errors for rounded geometries, in which case attention must be paid in the design of tests and in the interpretation of results. It must also be guaranteed that the experimentalist has considered the problem adequately. One of the possible techniques for reducing the error associated with a lower value of the Reynolds number in the wind tunnel is to increase the roughness of the surfaces of the model with respect to the actual value. The result obtained is associated with the roughness given to surfaces and may lead to an apparent value of the Reynolds number 3 or 4 times higher than the effective value in the tunnel.

The confining effect the tunnel has on the flow (blockage) leads to a variation in the magnitude of pressure acting on the surfaces of the models, which must be taken into account when defining the length scale. In particular, the projection of the volume occupied by the model on the cross-section plane of the tunnel (blockage ratio) must not exceed 5% of the area of the cross-section itself. For slightly higher values of the blockage ratio, in any case less than 10%, measurements are affected by small errors and can still be considered as acceptable, provided they are suitably corrected. For blockage ratios exceeding 10%, measurements must be considered to be potentially unreliable.

In addition, the static pressure must be kept constant along the entire tunnel. Variations of static pressure arising from blockage by the model and the formation of a shear layer along the floor, ceiling and lateral walls can be compensated if the tunnel is equipped with mobile lateral walls or ceiling. These features make it possible to create a variable cross-section along the tunnel and such variability can be adjusted to obtain an uniform static pressure along the tunnel .

Q.3   Modelling of wind fields over complex orographies

If the construction is located in an area characterised by complex orography, it may be unreliable, for the purposes of analytical calculation or for the wind tunnel testing, to consider the features of an atmospheric boundary layer developed over a flat surface. This is because the actual local flow may depart significantly from that over a flat surface. For a better understanding of the wind field characteristics at the site of interest, the effects of orography on local flow can be measured in the wind tunnel using topographic models. These models, which are usually made with length scales of between 1:5000 and 1:1000, reproduce the area surrounding the construction and are designed to measure the mean and fluctuating characteristics of the flow at the site of the construction.

The incoming flow must correspond to the flow that would develop at the site in the absence of orography.

Measurements must be carried out by means of anemometers with a high sampling frequency and at a sufficient number of points to reconstruct the mean fluctuating features of the flow. Measurement points should preferably be arranged along vertical or horizontal lines, depending on geometry of the construction. The sampling frequency must be at least twice the largest frequency characterising the aerodynamic loading process. The duration of the test must be between 600 s and 3600 s at full-scale, then reduced through the time scale $\lambda_T = \lambda_L/\lambda_V$.

The tests should be carried out for different oncoming wind directions, generally with angle steps between 10° and 45°.

As an alternative to anemometric measurements, it is possible to use either flow visualisation techniques, which provide only qualitative results, or Particle Image Velocimetry (PIV) techniques, which allow measurement of wind velocity fields in a given plane.

When the aim of the flow characterisation test is the analysis of a structure in complex orography, tests at a larger scale are then performed on the structural model, in which the local flow conditions found in the topographic test are reproduced.

Figure Q.2 shows a wind field modelling test over complex orography.

Figure Q.2 – Wind field modelling test over complex orography.

Q.4   Pressure measurements

The distribution of the pressure induced by wind on the surface of a building can be measured in the tunnel by means of a high sampling frequency pressure acquisition system. The acquisition system comprises a number of pressure taps located on the surface under investigation, each connected through tubing to a pressure scanner. This converts the pressure signal into an electrical analogue signal that is sent to an analogue-digital converter and then stored on mass memory media. Figure Q.3 shows a pressure model with tubing.

The accuracy of data measured depends on the characteristics of the entire measurement chain; however tubing plays a decisive role. An inadequately designed tubing can introduce a significant error in the pressure measurements. To ensure acceptable accuracy of measurements, tubing must be able to transmit, without distortion, pressure fluctuations up to the largest frequency of interest.

The geometric scale of the model (length scale) depends on the sizes of the structure, or the portion of the structure considered, as well as on the sizes of the wind tunnel. For buildings, the geometric scale is usually between 1:400 and 1:50, where the first value applies to tall buildings and the second value to low-rise buildings. The duration of each test must be such to allow adequate statistical processing of the measured data. Except for those cases in which it is possible to exploit symmetries in the structure, the measurements must be performed for all possible oncoming wind directions, with angle steps between 10° and 30°.

Figure Q.3 – Pressure model with tubing.

The models used are usually stiff, so the pressure measured does not take account of the fluid-structure interaction. Possible deformability of the model may give rise to errors in the measured pressure.

The measured pressure is used to obtain the pressure coefficients given by Eq. Q.1:

$$c_p(t) = \frac{P(t) - P_0}{\frac{1}{2}\rho V^2} \qquad (Q.1)$$

where t is time, P the measured pressure, P_0 the reference static pressure and $1/2\rho V^2$ the reference velocity pressure, where ρ the air density and V is the reference wind velocity. Equation Q.1 can be used to obtain the power spectra of the pressure coefficient and the required statistics. Usually, the mean value, the standard deviation and the minimum and maximum values are calculated. More rarely, skewness and curtosis have to be calculated. The minimum and maximum values depend on the time interval in which they are measured, and are usually given as functions of the probability of exceedance.

For example, in order to define wind loads on a surface, reference is often made to the mean value of the pressure coefficient. If, on the other hand, a local load must be defined (load on a portion of the surface), reference is generally made to the maximum or minimum peak value of the pressure coefficient.

The sampling frequency must be at least twice the largest frequency characterising the aerodynamic loading process of the structure. The duration of the test must be between 600 s and 3600 s at full-scale, then reduced through the time scale $\lambda_T = \lambda_L/\lambda_V$.

When calculating the total force acting on a structure, or on a portion of it, the number of pressure taps used in the tests, their positioning and the choice of tributary areas for each tap play a decisive role. The number of pressure taps to be used depends on structural geometry and ranges from a minimum of several dozen to many hundreds. The experimentalist shall identify the minimum number of pressure taps to be used to achieve an adequate description of the pressure field acting on the surfaces of the construction. The distribution of the pressure taps is usually not uniform but taps tend to be more concentrated in areas where there is a higher spatial variation of pressures, i.e. in

the vicinity of sharp edges. When the measurements are aimed at evaluating the dynamic response of the structure, the distribution of pressure taps must be consistent with the mode shape of the structure most excited by the wind.

Pressure transducers can also be used to characterise pressures inside buildings. Their features depend on the number, size and position of the openings of the building (porosity ratio), as well as the possible deformability of the walls and of the roof. Characterisation of the mean pressure inside a building can be performed in the wind tunnel in a sufficiently accurate manner provided the porosity ratio of the building is adequately reproduced. Reproduction of internal pressure dynamics is more complex and must be analysed through analytical and/or numerical models. For characterisation of the pressure inside a building, a lower number of pressure taps will be sufficient than used for characterisation of external pressure. This is because the internal pressure has a more uniform spatial distribution.

Figure Q.4 shows a pressure test.

Figure Q.4 – Pressure test.

Q.5   Force measurements

At the final design stage, the overall forces and the resulting stresses acting on given cross-sections of the main elements of a structure must be known These can be calculated by integrating the pressure measured using the procedure indicated at heading Q.4.

Alternatively, for buildings and other vertical structures, it is possible to use high frequency balance tests. If the structure has linear first along-wind or across-wind mode, then the measured base bending moments are representative of the generalised forces associated with these modes. The wind tunnel test therefore consists in the measurement of the time histories of base bending moments and possibly of base shear forces on a rigid model, and on the deduction from these of the generalised force spectra in the first two bending modes. On the other hand, if the mode shapes depart from being linear, correction factors must be applied, accounting for the effective mode shape. These factors are the result of subsequent analysis and cannot be defined in a general way. Similar considerations can be applied to a generalised force in the first torsional mode, although the non-coincidence of torsional mode with uniform rotation requests the application of correction

factors. In any case attention must be paid to all those cases wherein the structure has coupled modes. Figure Q.5 shows a building model on a base balance.
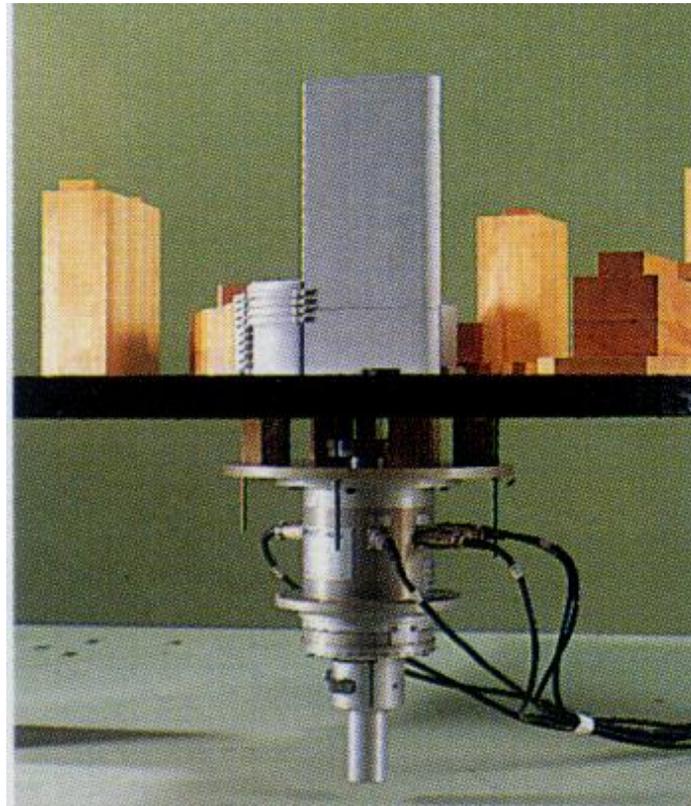
Figure Q.5. – Building model on a base balance.

The models used to measure aerodynamic forces must be stiff and have a small mass. These models are mounted on a balance capable of measuring force components at the base of the building. The geometric scale (length scale) is usually between 1:400 and 1:100. The sampling frequency must be at least twice the largest frequency characterising the aerodynamic loading process of the structure. The duration of the test must be between 600 s and 3600 s at full-scale, then reduced through the time scale $\lambda_T = \lambda_L/\lambda_V$.

Except for cases in which symmetries in the structure can be exploited, measurements must be performed for all possible oncoming wind directions, at angle steps between 10° and 30°.

Force measurements are also made in the case of bridge decks and in general for all elongated structures characterised by a two-dimensional aerodynamic behaviour in their cross-sections. For these structures, the coefficients of force and moment per unit length must be known, defined by Eq. Q.2:

$$c_{fX}(t) = \frac{f_X(t)}{\frac{1}{2}\rho V^2 l} \qquad (Q.2a)$$

$$c_{fY}(t) = \frac{f_Y(t)}{\frac{1}{2}\rho V^2 l} \qquad (Q.2b)$$

$$c_{mZ}(t) = \frac{m_Z(t)}{\frac{1}{2}\rho V^2 l^2}$$

(Q.2c)

where f_X, f_Y and m_Z are the along-wind and across-wind forces and torque per unit length; l is a reference dimension (width).

The tests are performed on a sectional model of the structure. The model must be rigid and of low mass; it is mounted on a pair of balances capable of measuring the three components of the load associated with the forces f_X, f_Y and m_Z. The geometric scale (length scale) depends on the geometric sizes of the structure or structural element, and on the width of the tunnel test section. In any case, the length of the model should be no less than 2.5 times its width. The sampling frequency must be at least twice the largest frequency characterising the aerodynamic loading process of the structure. The full-scale duration of the test should be between 600 s and 3600 s, then reduced through the time scale $\lambda_T = \lambda_L/\lambda_V$.

Tests on sectional models of bridge decks and elongated elements do not require the reproduction in the wind tunnel of the profiles of the mean velocity and turbulence intensity; therefore they can be performed also in non-boundary layer wind tunnels. In any case, it shall be ensured that turbulence characteristics be appropriately scaled, i.e. that integral length scales of turbulence in the tunnel are as close as possible to the full-scale values, in accordance with the length scale of the model. In addition to tests in a turbulent regime, it is also appropriate, in some cases, to repeat the tests in smooth flow conditions. Even though this may represent an unrealistic condition, it helps to point out aeroelastic phenomena, which are enhanced by the absence of turbulence, providing the designer with useful information concerning the ultimate behaviour of the structure.

Tests on bridge decks are usually performed not only by positioning the deck horizontally but also at different angles of attack (that is, turning the model around its axis), so to analyse the effect of a small variation of the wind incidence (possible because of local orography) and to calculate the angular derivative of the aerodynamic coeffcieints. The range of angle of attack considered is usually ±8° or ±12°, with steps of 1° around the zero, and possibly larger steps afterwards.

Except for the cases in which it is possible to exploit the symmetry properties of the cross-section, tests on elongated elements are usually performed for all possible wind directions in steps between 1° and 15°. Lower values are generally used when the angular derivatives of aerodynamic factors must be calculated, especially in cases in which instability phenomena can occur such as galloping, divergence and flutter (Annex P). Larger values apply to elements that are relatively insensitive to the variation in oncoming flow direction.

It is essential to ensure that the coupling between the balance and the model does not give rise to dynamic amplifications of the actions measured. Should this be the case, and should it be impossible to eliminate the phenomenon, suitable procedures must be applied to the results to remove resonant components.

Figure Q.6 shows a test on a bridge deck sectional model.

Figure Q.6 – Test on a bridge deck sectional model.

Q.6 Measurement of the structural response

As an alternative to the measurement of actions (headings Q.4 and Q.5) used for the analytical and/or numeric calculation of the structural response, the static and dynamic response of the structure can be directly measured in the wind tunnel.

In addition, since in some cases the deformability of the structure causes aeroelastic interaction, whenever response is calculated analytically and/or numerically the interaction must be taken into account in the mathematical models used. Direct measurement of the structural response in the wind tunnel automatically takes aeroelastic interaction into account.

To this purpose, deformable or aeroelastic models are used reproducing the scaled dynamic properties of the actual structure, i.e. the frequencies and modes of vibration, as well as structural damping. The aeroelastic models and testing procedures may be very different from case to case, depending on the structure and on the parameters to be measured. The measured parameters can be either actions or response parameters. If the structural response is measured, the tests must be conducted at different wind velocities so as to analyse possible changes in the response with varying velocities.

For tests on an aeroelastic model, attention must be paid not only to scaling of lengths and velocities but also to scaling of masses (representing inertia forces) and stiffnesses (representing elastic forces). It is also essential to accurately reproduce the damping ratios of the modes effectively excited by wind, making especially sure that in the wind tunnel these parameters are no higher than the real values. In most cases, it is not possible to obtain correct scaling of all the physical parameters so it is necessary to use a distorted model, i.e. a model that does not comply with all the scaling rules. The choice of parameters that will be subject to distortion depends on the type of test and is decisive for the quality of the results.

Acquisition of the structural response is usually performed by means of accelerometers or displacement transducers. The former must be lightweight and connected to the acquisition system so as not to affect the dynamics of the model. The latter are usually based on laser technology so they are located outside the model and are not in contact with it. The sampling frequency must be at least twice the largest structural frequency it is intended to reproduce.

There follows a short list of the main types of model and tests currently in use.

Aeroelastic replicas. They are models with internal elasticity, so as to reproduce the geometry and the dynamic properties of the entire structure or part of it. They are used for high-rise buildings, medium- and long-span bridges, towers, chimneys, and large-span roofs. The model must be able to reproduce all vibration modes that significantly contribute to the structural response. Figure Q.7 shows an aeroelastic bridge replica set up for testing.

Figure Q.7 – Test on an aeroelastic replica model of a suspension bridge.

Sectional models. These are models with external elasticity, representing a portion of an elongated structure. The sectional model is rigid, while flexibility and energy dissipation are concentrated in the model supports. Because of the stiffness of the model, the maximum number of degrees of freedom that can be taken into account is equal to six, even if in the majority of cases only two or three modes are effectively considered. They are especially used for medium- to long-span bridges, but also for buildings, towers and chimneys. Figure Q.8 shows the picture of an aeroelastic test on a sectional model of a bridge deck.

Pivot models. These are models of buildings with external elasticity. A rigid model of the building (often the same used for base balance tests) is fitted with a pivot at the base; the pivot reproduces the flexibility and dissipation of the structure. The system obtained has one or two degrees of freedom, and simulates the dynamic behaviour of a building in which the first along-wind and across-wind modes are both linear with height. If these modes depart from being linear, it is necessary to apply correction factors that take the effective mode shape into account. Figure Q.9 shows a test on a pivot model of a building.
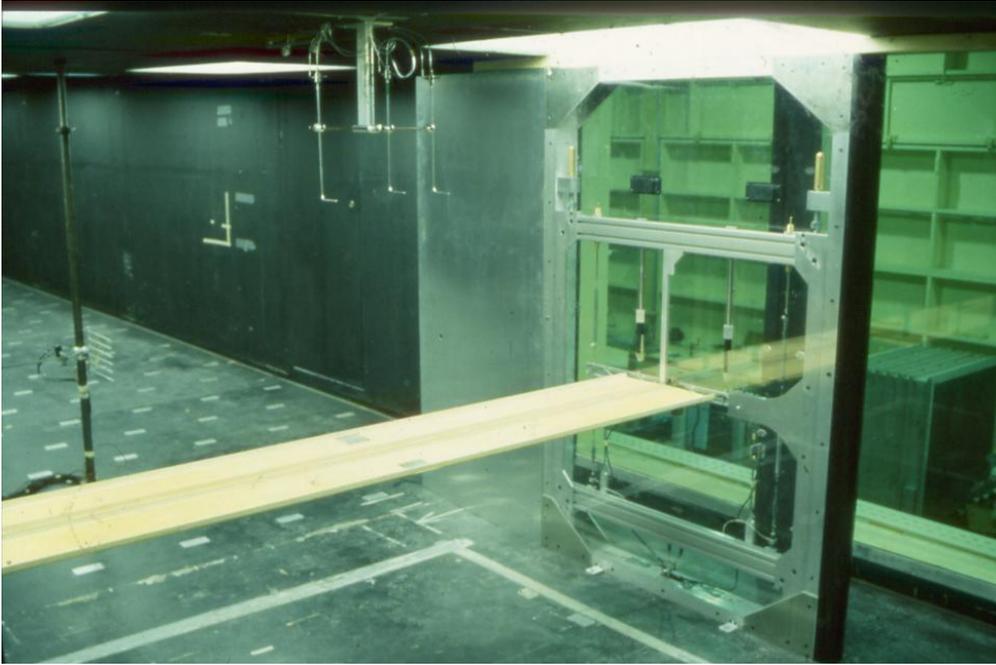
Figure Q.8 – Bridge deck sectional model test.

Figure Q.9 –Building pivot model test.

Taut-strip models. Taut-strip models are used to represent long-span bridge decks and are based on the reproduction of the bending and torsional stiffness of the deck-cable system through the stiffness deriving from taut cables in the model. Figure Q.10 shows a bridge deck taut-strip model test.

Figure Q.10 – Suspension bridge taut-strip model test.

When designing tests on an aeroelastic model, the experimentalist must reproduce the dynamic features (shape, mass, frequency, damping) of the modes that make a significant contribution to the structural response. These properties are those measured in still air and must be set up before the test. In the presence of wind, the dynamic properties of the model vary as a result of the aeroelastic interaction that occurs.

If the action associated with vortex shedding is significant, attention must also be paid to reproducing in the wind tunnel the value of Scruton number (heading O.3) of the actual structure.

The geometric scale (length scale) usually depends on the sizes of the tunnel and of the structure or structural element.

Q.7   Using wind tunnel measurement data

When aerodynamic coefficients, aerodynamic forces or the structural response based on wind tunnel measurements are used for design calculations, these values must be well documented.

In particular, the following must be clearly documented:

*   the type of test performed (in terms of wind tunnel characteristics, model scaling, blockage ratio);

*   the flow characteristics (in terms of mean velocity profiles, longitudinal turbulence intensity and longitudinal turbulence integral length scale);

*   data acquisition modes (sampling frequencies and durations);

*   the scale factors used and the analyses performed on the raw data for calculating the aerodynamic coefficients and the design forces, or for calculating the structural response.

4 EXAMPLES

4.1 INTRODUCTION

To illustrate the use of the CNR-DT 207/2008 Guide, this section provides a number of worked examples concerning some of the most common structural types.

To simplify the analyses, all the structures are assumed to be of standard types, with a nominal lifetime $V_N = 50$ years. Thus, when applying Annex A the reference return period is equal to $T_{R0} = 50$ years.

This section is organised as follows. Clause 4.2 defines the wind velocity and the wind pressure, common to all of the examined structures. Each subsequent clause considers a different structure, in particular:

- 4.3   - Industrial building;
- 4.4   - Apartment building;
- 4.5   - Multi-storey office building;
- 4.6   - Tall building;
- 4.7   - Gasholder;
- 4.8   - Canopy roof;
- 4.9   - Reinforced concrete chimney;
- 4.10   - Metal chimney;
- 4.11   - Truss girder railway bridge;
- 4.12   - Box girder road bridge.

For each example, reference is made to the clauses and Annexes used for the calculations.

The examples do not cover every type of situation. The aim is to highlight the most typical aspects of the calculations performed in a variety of situations, in order to cover a sufficiently broad set of cases.

4.2 WIND VELOCITY AND VELOCITY PRESSURE

The following clauses 4.2.X correspond, respectively, to clauses 3.2.X (X = 1.2,...7). As mentioned in clause 3.2, the use of clauses 3.2.5 and 4.2.5 is limited to cases of rounded surfaces, for which it is necessary to determine the Reynolds number for the evaluation of the aerodynamic coefficients, or to cases in which it is necessary to analyse dynamic and/or aeroelastic phenomena. The use of clauses 3.2.6 and 4.2.6 is limited to the sole case in which it is necessary to analyse dynamic and/or aeroelastic phenomena.

4.2.1 Basic reference wind velocity

The constructions are all located in central Italy at sea level. Applying the rules given in clause 3.2.1, this corresponds to Zone 3 (Figure 3.1).
In the lack of more specific data that take into account site roughness, terrain topography and wind direction, the basic reference wind velocity v_b is given by equation (3.1), where the basic reference wind velocity at sea level is $v_{b,0} = 27$ m/s (Table 3.I), and the altitude coefficient is $c_a = 1$ (Equation 3.2, Table 3.I, with $k_a = 0.37$, $a_s = 0$ m, $a_0 = 500$ m). Thus, $v_b = v_{b,0} = 27$ m/s.

4.2.2 Design return period and reference wind velocity

With reference to Annex A, the design return period T_R is generally assumed as equal to the value of the reference return period $T_{R,0}$, and thus $T_R = T_{R,0} = 50$ years.

In the lack of more specific data, the rules given in clause 3.2.2 express the design reference wind velocity v_r by Equation (3.3), where $v_b = 27$ m/s and the return coefficient is $c_r = 1$ (Equation 3.4, Figure 3.2). Thus, $v_r = v_b = 27$ m/s.

Analysis concerning the abitability of buildings requires that the mean wind velocity be determined for a design return period $T_R = 1$ year. In this case, in the lack of more accurate assessments, $c_r = 0.75$ (Equation 3.4). Thus, $v_r = 0,75 \cdot v_b = 20.25$ m/s.

Analysis concerning vortex shedding and other aeroelastic phenomena requires that the mean wind velocity be determined for a design return period $T_R = 10 \cdot T_{R,0} = 500$ years. In this case, again in the lack of more accurate assessments, $c_r = 1,207$ (Equation 3.4, Figure 3.2). Thus, $v_r = 1,207 \cdot v_b = 32.59$ m/s.

4.2.3 Exposure category

Applying the criterion given at point (2) of clause 3.2.3, it is assumed that, in the lack of more detailed assessments, the structures are located in roughness class C (Table 3.III). It is also assumed that they are located 20 km from the coast. Thus, by using Figure 3.3, the structures are located in the exposure category III. Consequently, applying Table 3.II, the terrain factor is $k_r = 0,20$, the roughness length is $z_0 = 0,10$ m and the minimum height is $z_{\min} = 5$ m.

4.2.4 Topography coefficient

Applying the rules given at point (2) of clause 3.2.4, it is assumed that the structures are located in a flat zone. Therefore, in the lack of more detailed assessments, the topography coefficient is $c_t = 1$.

4.2.5 Mean velocity

Applying the rules given at clause 3.2.5, in the lack of specific analyses that take into account wind direction and the effective local surrounding roughness and topography, the vertical profile of the mean wind velocity v_m, with $T_R = 50$ years, is given by Equation (3.5), where $v_r = 27$ m/s and c_m is the mean wind profile coefficient given by Equation (3.6) and by Figure 3.4. It takes the following form:

$$c_m(z) = 0,782 \qquad \text{for } z \leq 5 \text{ m}$$

$$c_m(z) = 0,20 \cdot \ln\left(\frac{z}{0,10}\right) \qquad \text{for } z > 5 \text{ m}$$

where z is the height above the ground in m. Thus:

$$v_m(z) = 21,125 \qquad \text{for } z \leq 5 \text{ m}$$

$$v_m(z) = 5,4 \cdot \ln\left(\frac{z}{0,10}\right) \qquad \text{for } z > 5 \text{ m}$$

where z is expressed in m and v_m in m/s.

The mean wind velocity profile associated with the design return periods $T_R = 1$ year and $T_R = 500$ years can be determined by multiplying this profile, respectively, by the factors $c_r = 0,75$ and $c_r = 1,207$.

Figures 4.2.1 and 4.2.2 show the graphs of $c_m(z)$ and $v_m(z)$.
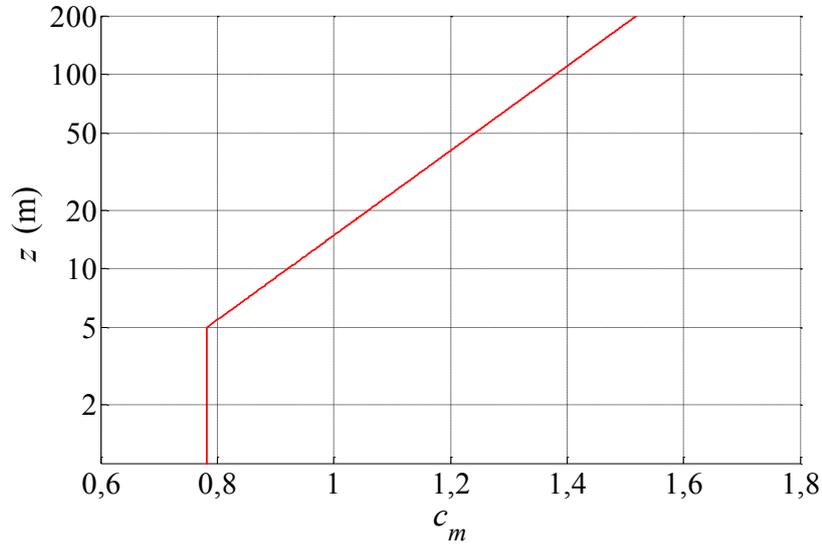
Figure 4.2.1 – Graph of $c_m(z)$.
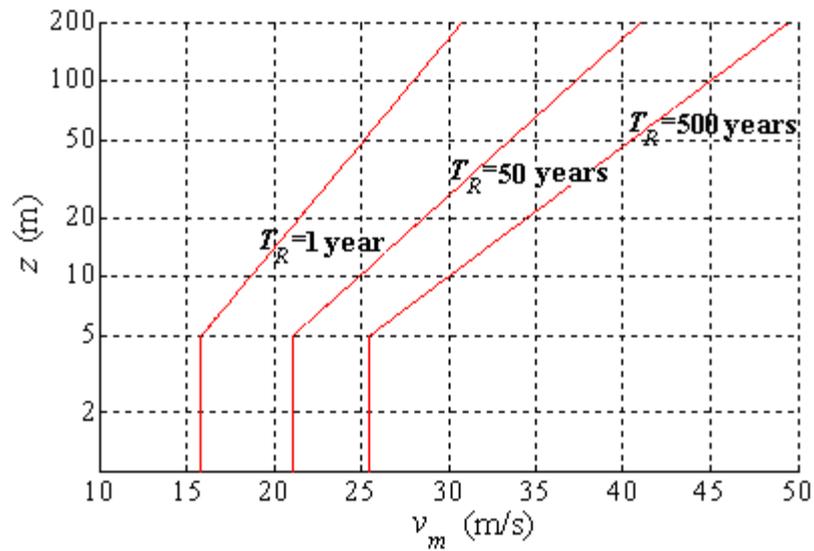
Figure 4.2.2 - Graph of mean velocity $v_m(z)$.

4.2.6 Atmospheric turbulence

Applying the rules given by clause 3.2.6, in the lack of specific analyses that take into account the wind direction and the effective local surrounding roughness and topography, the turbulence intensity I_v is given by Equation (3.7) and by Figure 3.5. It takes the following form:

$$I_v(z) = 0,256 \qquad \text{for } z \le 5 \text{ m}$$

$$I_v(z) = \frac{1}{\ln\left(\dfrac{z}{0,10}\right)} \qquad \text{for } z > 5 \text{ m}$$

where z is the height above the ground in m. Figure 4.2.3 shows the graph of $I_v(z)$.
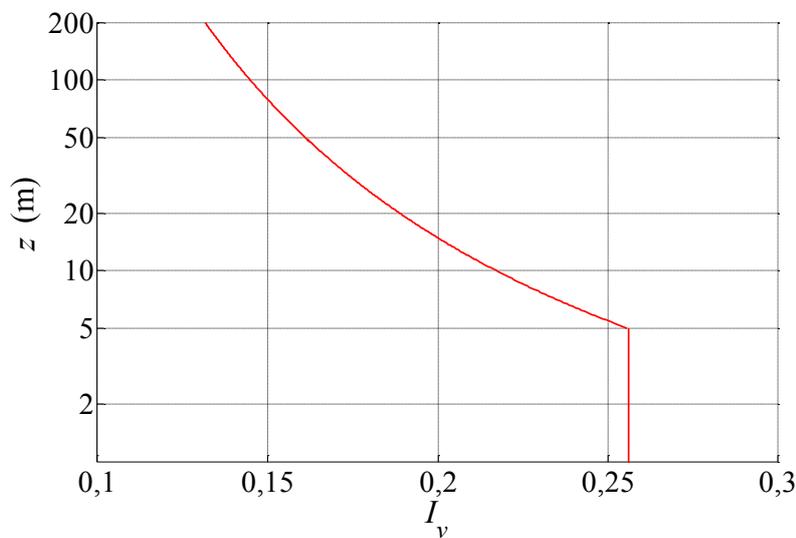
Figure 4.2.3 - Graph of turbulence intensity $I_v(z)$.

In the lack of specific analyses, the turbulence length scale L_v is given by Equation (3.8) and by Figure 3.6. It takes the following form:

$$L_v(z) = 39,44 \qquad \text{for } z \le 5 \text{ m}$$

$$L_v(z) = 300 \cdot \left(\frac{z}{200}\right)^{0,55} \qquad \text{for } z > 5 \text{ m}$$

where L_v and z are expressed in m. Figure 4.2.4 shows the graph of $L_v(z)$.
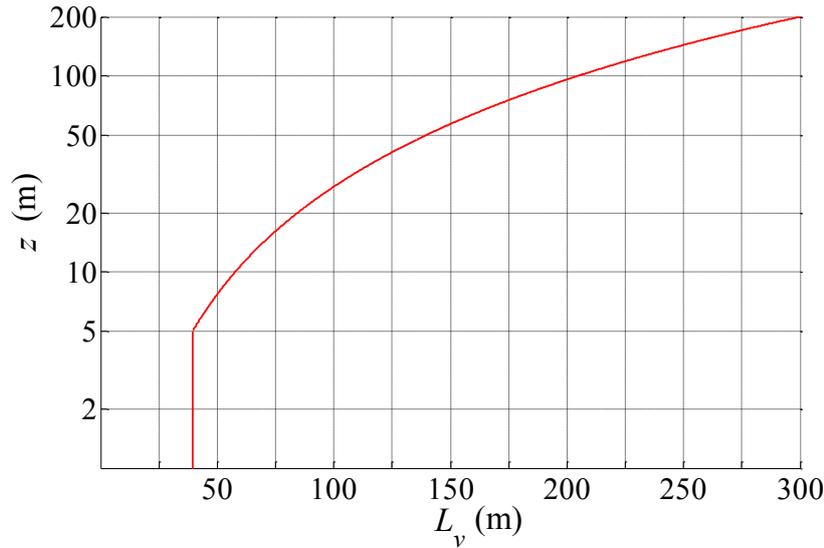
Figure 4.2.4 - Graph of the integral scale of turbulence $L_v(z)$.

4.2.7 Peak velocity pressure

Applying the rules given in clause 3.2.7, in the lack of specific analyses that take into account the wind direction and the effective local surrounding roughness and topography, the peak wind velocity pressure q_p, with $T_R = 50$ years, is given by Equation (3.9), where $\rho = 1.25$ kg/m³, $v_r = 27$ m/s, c_e is the exposure coefficient given by Equation (3.10) and by Figure 3.7. It takes the following form:

$$c_e(z) = 1,708 \qquad\qquad\qquad \text{for } z \leq 5 \text{ m}$$

$$c_e(z) = 0,04 \cdot \ln\left(\frac{z}{0,1}\right) \cdot \left[\ln\left(\frac{z}{0,1}\right) + 7\right] \qquad \text{for } z > 5 \text{ m}$$

where z is expressed in m. Thus:

$$q_p(z) = 778,21 \qquad\qquad\qquad \text{for } z \leq 5 \text{ m}$$

$$q_p(z) = 18,22 \cdot \ln\left(\frac{z}{0,1}\right) \cdot \left[\ln\left(\frac{z}{0,1}\right) + 7\right] \qquad \text{for } z > 5 \text{ m}$$

where z is expressed in m and q_p is expressed in N/m².

The peak velocity pressure profile, associated with the design return periods $T_R = 1$ year and $T_R = 500$ years, can be determined by multiplying this profile, respectively, by the factors $c_r^2 = 0,75^2 = 0,562$ and $c_r^2 = 1,207^2 = 1,457$.

Figures 4.2.5 and 4.2.6 show the graphs of $c_e(z)$ and $q_p(z)$.
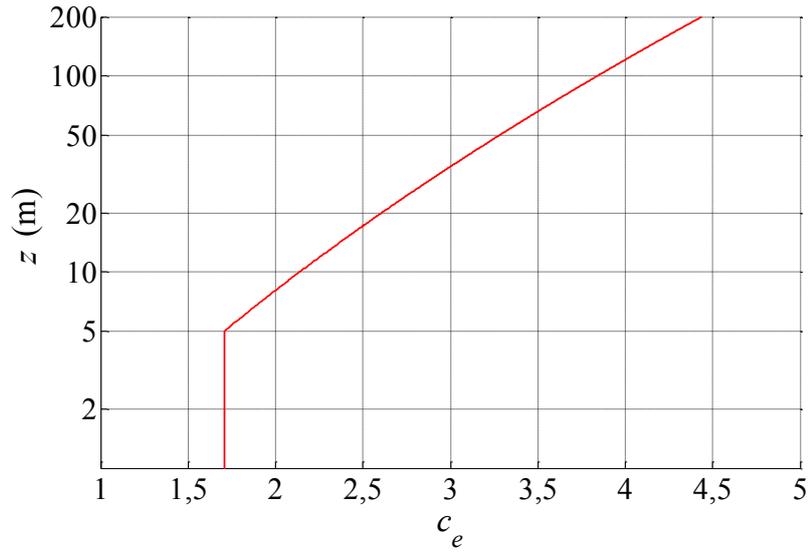
Figure 4.2.5 - Graph of the exposure coefficient $c_e(z)$.
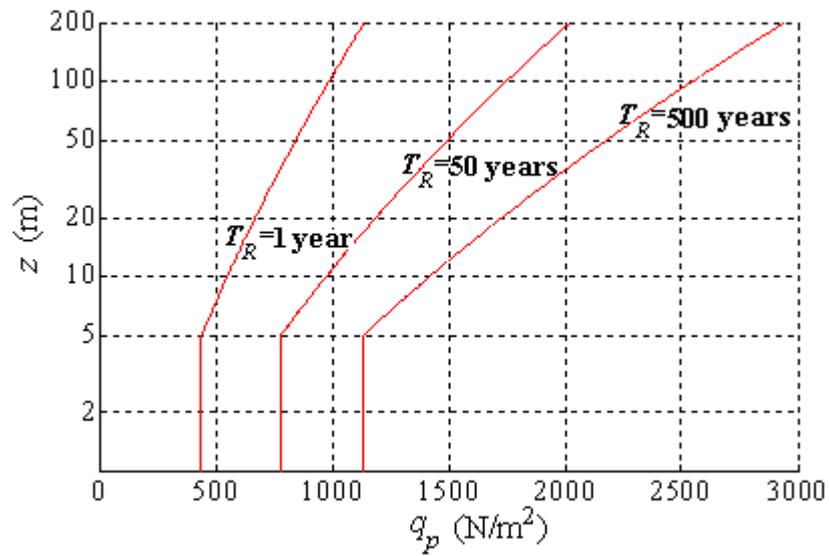
Figure 4.2.6 - Graph of the peak velocity pressure $q_p(z)$.

4.3   INDUSTRIAL BUILDING

The structure examined in this clause is an industrial building used as a warehouse for finished products, described in the technical publication *"Particolari costruttivi di strutture in acciaio"* (Detailing of Steel Structures), published by CISIA - *Centro Italiano Sviluppo Impieghi Acciaio* (Italian Centre for the Development of Steel Applications) - Milan (Figures 4.3.1 and 4.3.2).

The building has a rectangular plan of 54 × 91 m. The roof is duopitch with a 4° slope. The ridge line is in a central position, parallel to the long side of the building, at a height of 13,54 m. The height of the lateral eaves, parallel to the long side of the building, is 11,66 m.

The structural scheme consists of a fixed three-bays portal frame, with truss beams and columns made of I proiles. Longitudinal stability is provided by roof bracing at the top chord of the trusses, by intermediate bracing at the bottom chord, and by bracing between the intermediate columns. The roof joists consist of continuous steel sections.

The roof decking is composed by galvanised, corrugated roofing sheets, with overlying rigid insulation panels in rock wool, and waterproofing with reinforced bituminous felt and gravel ballast. Solid brick masonry walls are placed over a steel framework, with puttyless metal window fittings.

Analysis was based on clauses 3.1-3.4 and Annexes G, H.

Peak aerodynamic actions were determined by means of clause 3.3. More precisely, by using the rules given in clause 3.3.1, the external and internal pressure is given by Equation (3.11), where q_p is the peak velocity pressure, c_{pe} and c_{pi} are the external and internal pressure coefficients, and $\overline{z}_e$ e $\overline{z}_i$ are the associated reference heights. Aerodynamic coefficients were determined by applying Annex G, as regards the overall actions on the structure; Annex H, on the other hand, was used for determining local external actions on the structural and non-structural elements.

The dynamic wind actions were determined by means of clause 3.4. More precisely, by using the rules given in clause 3.4.1, the equivalent static actions are expressed by Equation (3.17), where c_d is the dynamic coefficient.

All the analyses reported below concern the case where wind is at right angles to the long side of the building; calculations need to be repeated for wind at right angles to the short side.

Clause 4.3.1 gives the calculation of the overall external pressure on the structure. Clause 4.3.2 gives the calculation of the local external pressure on the building elements. Clause 4.3.3 gives the calculation of internal pressure. In clause 4.3.4 the net total and local pressure is calculated. Clause 4.3.5 gives the calculation of the dynamic factor and the equivalent static actions.
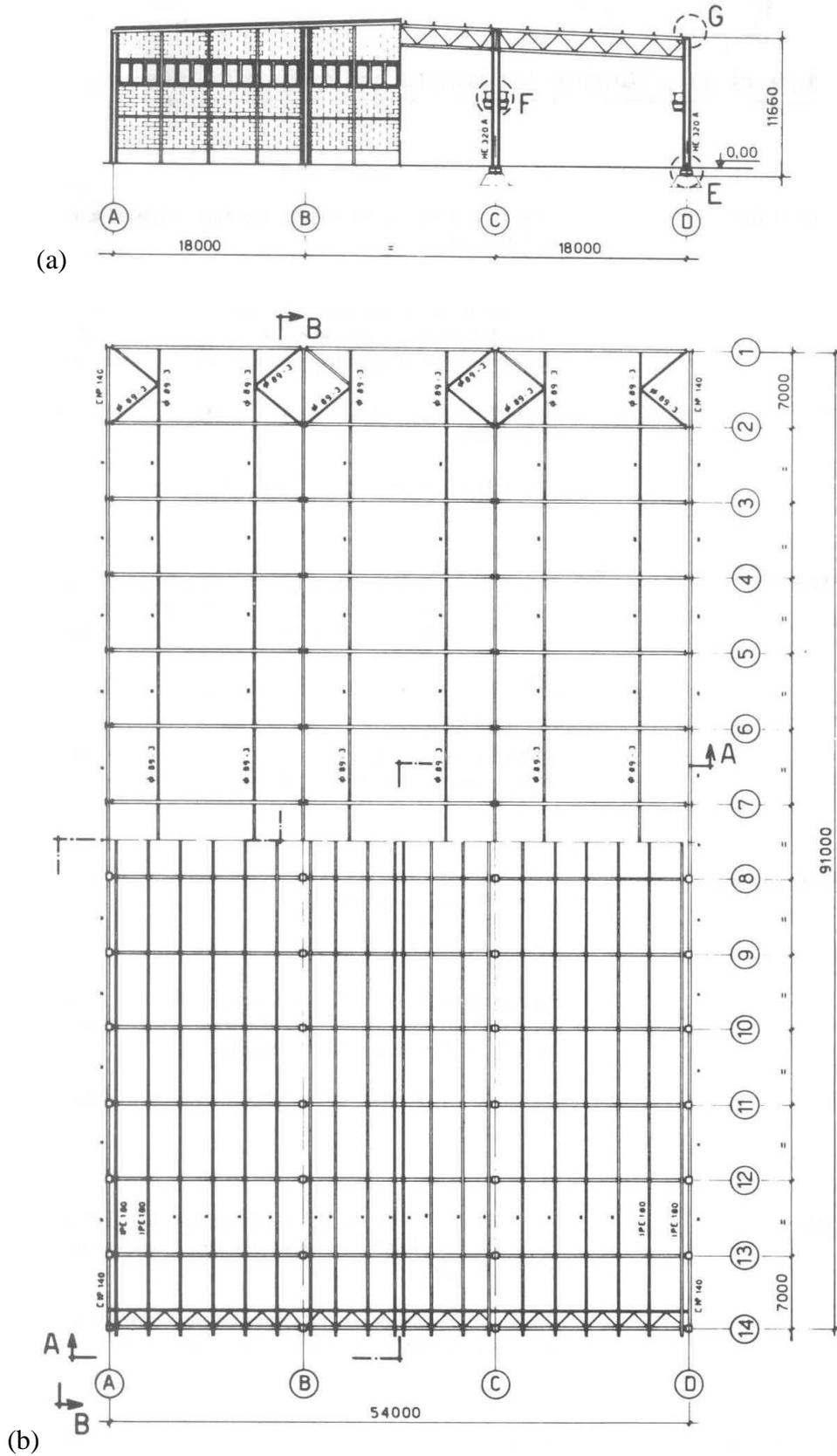
Figure 4.3.1 - Industrial building: (a) view (left) and section A-A (right); (b) roof framing at the level of the top chord (below) and roof bracing at the level of the bottom chord (above).

(a)

(b)
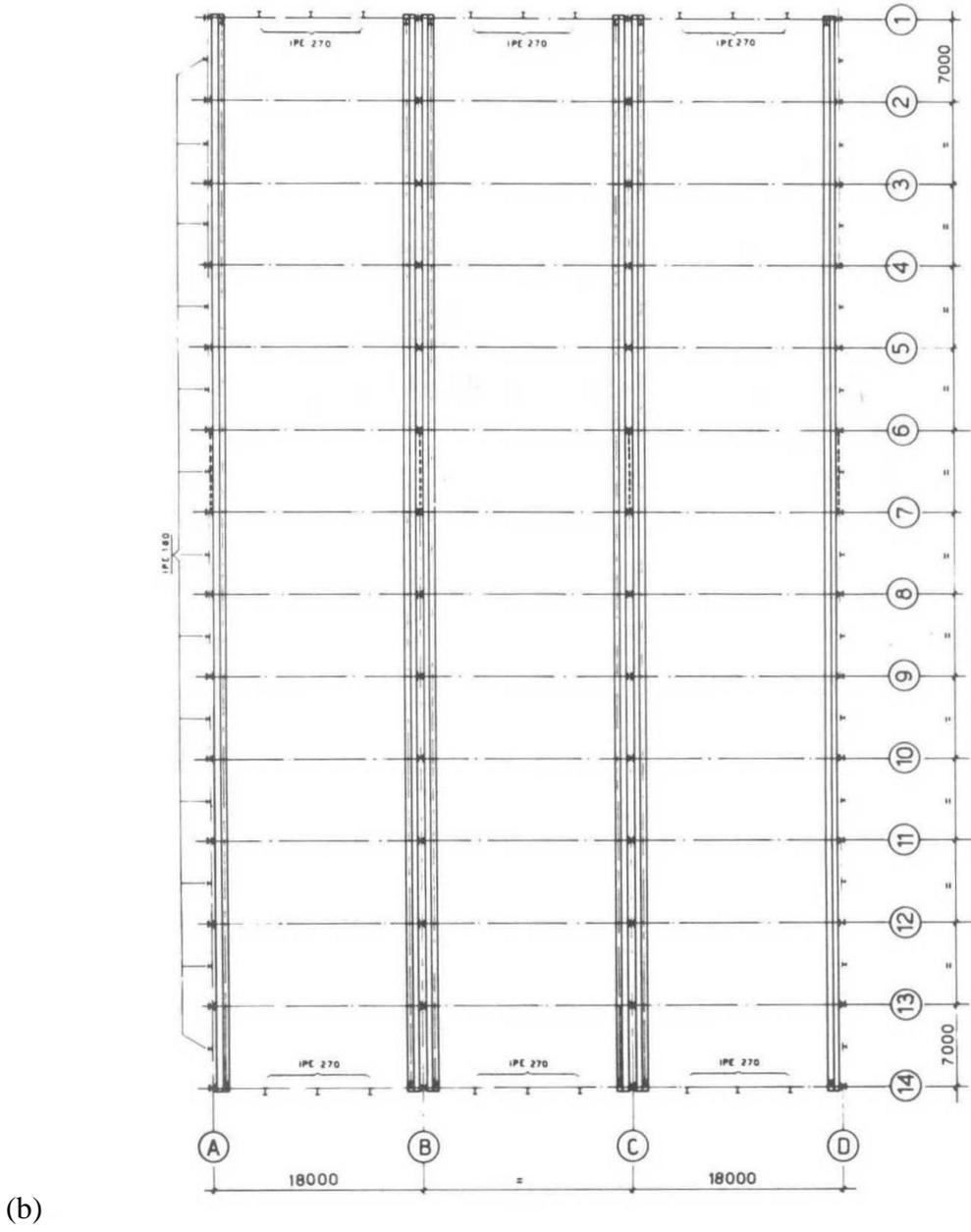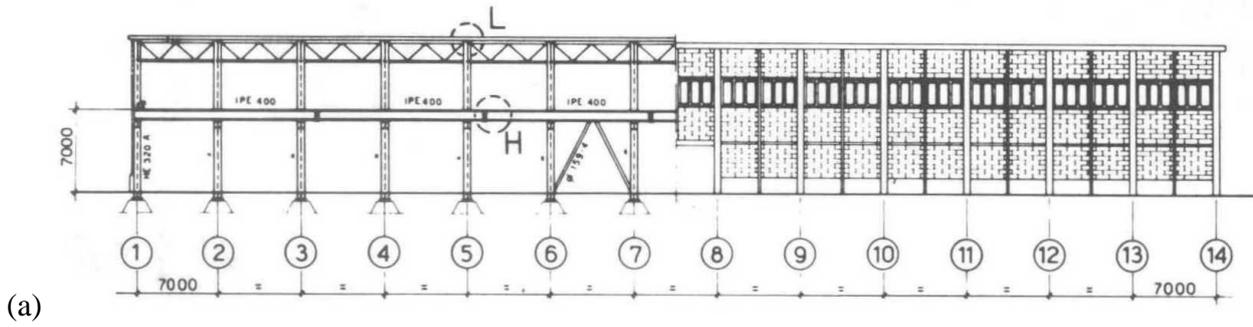
Figure 4.3.2 - Industrial building: (a) section (left) and elevation (right); (b) plan of the columns and sliding planes.

4.3.1 Overall external pressure on the structure

The external pressure on the lateral walls is calculated by applying the rules given in clause G.2.2. With reference to Figure G.1, $b = 91$ m, $d = 54$ m, $h = 13,54$ m; therefore, $h/d = 0,251$. Thus, Table G.I provides the external pressure coefficients given in the second column of Table 4.3.I.

Applying the criterion illustrated in clause G.2.2.1, the reference height for pressure on the upwind face is $\overline{z}_e = h = 13,54$ m. Similarly, applying the criterion illustrated in clause G.2.2.2, the reference height for pressure on the downwind and lateral faces is $\overline{z}_e = h = 13,54$ m. Thus, $q_p(\overline{z}_e) = 1,065$ N/m^2 for all lateral walls. Applying Equation (3.11a), the external pressure on the walls takes the values given in the third column of Table 4.3.I.

Table 4.3.I - External pressure coefficients and external pressure on the walls.

Face	c_{pe}	p_e (N/m^2)
Upwind	+0,7	+745
Lateral	-0,7	-745
Downwind	-0,3	-320

As the roof slope is 4°, it is treated as flat. By applying the criteria illustrated in clause G.2.3.1, the roof is subdivided into the two zones shown in Figure 4.3.3; the obtained external pressure coefficients are given in the second column of Table 4.3.II. Moreover, the reference height for the external pressure on the roof is $\overline{z}_e = h = 13,54$ m. Thus, at all points of the roof, $q_p(\overline{z}_e) = 1,065$ N/m^2. Applying Equation (3.11a), the external pressure on the roof takes the values given in the third column of Table 4.3.II.

Figure 4.3.3 - Zones of the roof with uniform external pressure.

Table 4.3.II - External pressure coefficients and external pressure on the roof.

Zone	c_{pe}	p_e (N/m^2)
A	-0,80	-852
B	±0,20	±213

4.3.2 Local external pressure on the building elements

The external pressure on the lateral wall elements is calculated by means of the rules given in clause H.2.2. With reference to Figure H.2, $b = 91$ m, $d = 54$ m, $h = 13,54$ m; therefore, $h/d = 0,251$, $\bar{z}_e = h = 13,54$ m, $e = 27,08$ m (Equation H.1). Thus, at all points of the lateral walls, $q_p(\bar{z}_e) = 1.065$ N/m². It follows that, by using the criterion indicated in Figures H.3 and H.4, the walls are divided into the zones illustrated in Figure 4.3.4; by means of Table H.II, the corresponding external pressure coefficients for each of these zones are given in the second and fourth columns of Table 4.3.III. Lastly, by applying Equation (3.11a), the external pressure on the walls takes the values given in the third and fifth columns of Table 4.3.III. The pressure coefficients $c_{pe,10}$ and the pressure $p_{e,10}$ refer to elements having an area $A \geq 10$ m²; the pressure coefficients $c_{pe,1}$ and the pressure $p_{e,1}$ refer to elements having an area $A \leq 1$ m²; for elements having an area between 1 and 10 m², the criterion indicated in Table H.I is adopted.
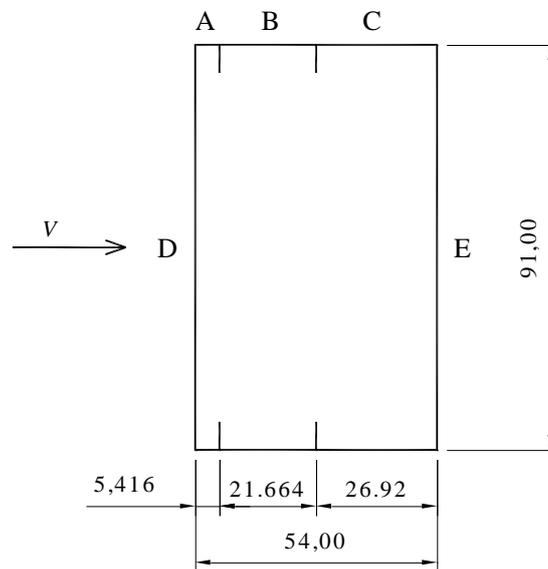
Figure 4.3.4 - Zones of the wall with uniform external pressure (plan view).

Table 4.3.III - External pressure coefficients and external pressure on the walls.

Zone	$c_{pe0.10}$	$p_{e,10}$ (N/m²)	$c_{pe,1}$	$p_{e,1}$ (N/m²)
A	-1,2	-1.278	-1.4	-1.491
B	-0,8	-852	-1,1	-1.171
C	-0,5	-532	-0,5	-532
D	+0,7	+745	+1.0	+1.065
E	-0,3	-319	-0,3	-319

Once again, as the roof slope is 4°, it is treated as flat. The external pressure on the roof elements is therefore assessed by means of the rules given in clause H.2.3.1. Also in this case, $b = 91$ m, $d = 54$ m, $h = 13,54$ m; therefore, $h/d = 0,251$, $\bar{z}_e = h = 13,54$ m, $e = 27,08$ m (Equation H.3), $q_p(\bar{z}_e) = 1.065$ N/m². It is also assumed that the roof has sharp edges . It follows that, by using the criterion reported in Figure H.5, the roof is divided into the zones illustrated in Figure 4.3.5; by means of Table H.III, the corresponding external pressure coefficients for each of these zones are given in the second and fourth columns of Table 4.3.IV. Lastly, by applying the Equation (3.11a), the external pressure on the roof takes the values given in the third and fifth columns of Table 4.3.IV.
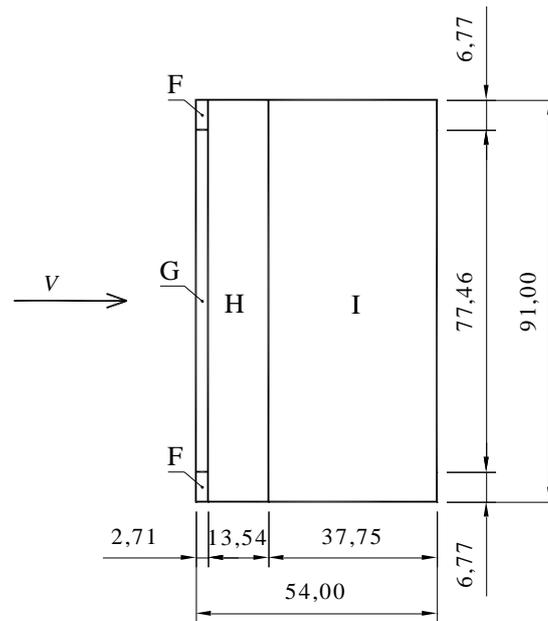
Figure 4.3.5 – Zones of the roof with uniform external pressure.

Table 4.3.IV - External pressure coefficients and external pressure on the roof.

Zone	$c_{pe0.10}$	$p_{e,10}$ (N/m^2)	$c_{pe,1}$	$p_{e,1}$ (N/m^2)
F	-1,8	-1.917	-2,5	-2.662
G	-1,2	-1.278	-2,0	-2.130
H	-0,7	-745	-1,2	-1.278
I	±0,2	±213	±0,2	±213

4.3.3 Internal pressure

The internal pressure in the building depends on the distribution and the size of the openings. It has been estimated, by applying the criteria given in clause G.4, for two different scenarios.

In the first scenario, the distribution and size of the openings are not known but it can be assumed that: a) the openings on each face do not exceed 30% of the surface of the face (clause G.4.1); b) the building does not have dominant surfaces (clause G.4.2). In this case, by applying the criterion provided in clause G.4.3, $c_{pi} = +0,2$ or $c_{pi} = -0,3$. Therefore, as $\overline{z_i} = h = 13,54$ m and $q_p(\overline{z_i}) = 1.065$ N/m^2, there are two internal load cases: $p_i = +213$ N/m^2 and $p_i = -319$ N/m^2.

In the second scenario, it is excluded that the openings on each face exceed 30% of the surface of the face (clause G.4.1); it is assumed, however, that the building has a dominant surface (clause G.4.2). In particular, it is assumed that the area of the openings on the dominant face is between 2 and 3 times the area of the openings in the other faces. If the dominant surface coincides with the upwind face, $c_{pi} = 0,75 \cdot c_{pe} = 0,75 \cdot (+0.7) = 0,525$; if the dominant surface coincides with the downwind face, $c_{pi} = 0,75 \cdot c_{pe} = 0,75 \cdot (-0.3) = -0,225$. Therefore, since $\overline{z_i} = h = 13,54$ m, and $q_p(\overline{z_i}) = 1.065$ N/m^2, there are two internal load cases: $p_i = +559$ N/m^2 and $p_i = -240$ N/m^2. The first value corresponds to the case in which the dominant surface is located upwind; the second value corresponds to the case in which the dominant wall is located downwind.

4.3.4 Net total and local pressure

Internal pressure must be combined with the external pressure in accordance with the outline in Figure 3.13. Thus, considering for example the first condition of internal pressure for the second scenario (p_i = +559 N/m^2), the net wind actions on the roof and its elements (clause 3.3.2) are summarised, respectively, in Tables 4.3.V and 4.3.VI; the values are positive when the net pressure is directed downwards.

Table 4.3.V - Net total pressure on the roof.

Zone	p_n (N/m^2)
1	-1.411
2	-772/-346

Table 4.3.VI - Net local pressure on the roof elements

Zone	$p_{n0.10}$ (N/m^2)	$p_{n,1}$ (N/m^2)
F	-2.476	-3.221
G	-1.837	-2.689
H	-1.304	-1.837
I	-772/-346	-772/-346

4.3.5 Dynamic factor and equivalent static actions

As the height of the structure is less than 20 m and assuming that the frequency of the first vibration mode is greater than 1.5 Hz, in the lack of more accurate assessments, clause 3.4.1 allows the dynamic factor to be given the value c_d = 1. Thus, according to Equation (3.17), the equivalent static actions coincide with the peak aerodynamic actions.

4.4 APARTMENT BUILDING

The structure examined in this clause is a 7-storey apartment building, described in the technical publication "*Particolari construttivi in acciaio*" (Detailing of Steel Structures), published by CISIA - *Centro Italiano Sviluppo Impieghi Acciaio* (Italian Centre for the Development of Steel Applications) - Milan (Figures 4.4.1 and 4.4.2).

The building has a rectangular plan of 48×11 m. The flat roof is located at a height of 26,4 m.

The structural scheme consists of two symmetrical reinforced concrete cores and a steel structure with pinned columns and simply supported beams. The reinforced concrete cores contain the stairwells and lifts, and carry all horizontal actions. The steel columns are made with square box profile, with holes for the bolted connections to the beams. The main beams have an I-shaped cross-section (I profile, according to European Standards). The floors are hollow tiles and reinforced concrete ones.

(a)

(b)
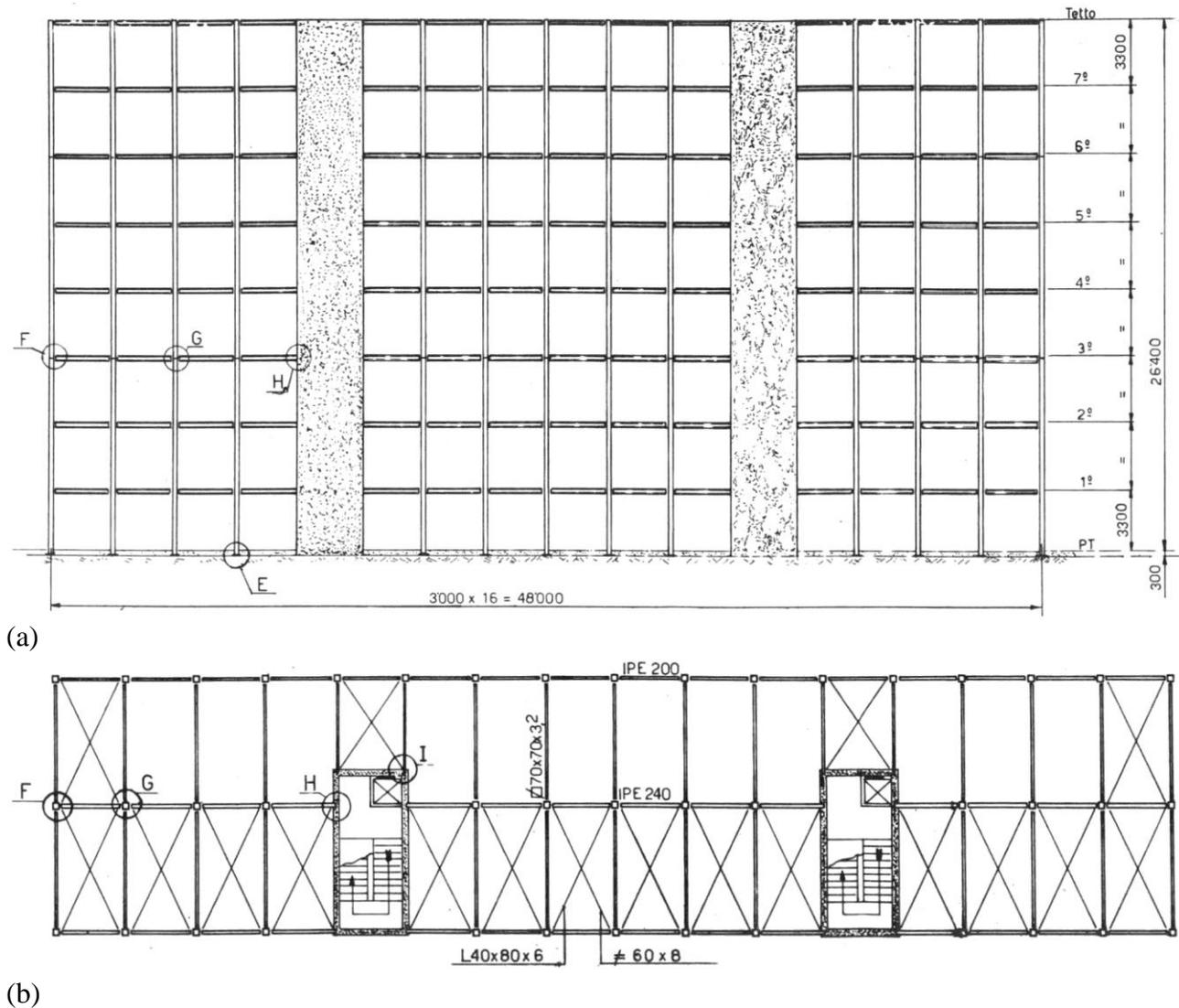
Figure 4.4.1 - Apartment building: (a) longitudinal section; (b) plan.
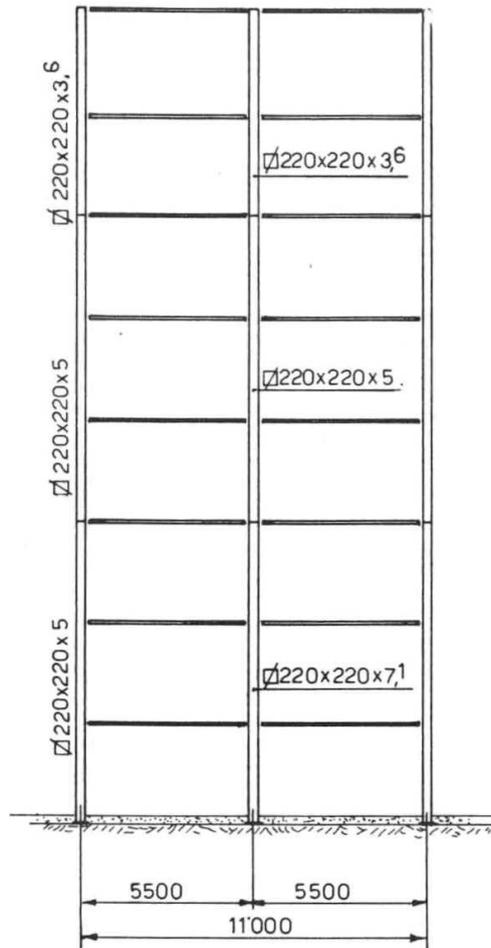
Figure 4.4.2 - Apartment building: transverse section.

The analyses are based on clauses 3.1-3.4 and Annexes G, L.

Peak aerodynamic actions are calculated by means of clause 3.3. More precisely, using the rules given in clause 3.3.1, the external pressure is given by the Equation (3.11a), where q_p is the peak velocity pressure, c_{pe} is the external pressure coefficient, $\overline{z}_e$ is the reference height. The aerodynamic coefficients for the overall wind actions are calculated by means of Annex G.

The dynamic wind actions are calculated by means of clause 3.4. More precisely, by using the rules given in clause 3.4.1, the equivalent static actions are expressed by the Equation (3.17), where c_d is the dynamic factor, assessed by means of the same clause 3.4.1, that is by applying the criteria given in Annex L.

All of the analyses given below concern the case in which the wind is at right angles to the long side of the building; calculations need to be repeated for wind at right angles to the short sides.

Clause 4.4.1 gives the calculation of the peak external aerodynamic actions on the structure. Clause 4.4.2 gives the calculation of the dynamic factor and the equivalent static actions.

4.4.1 Peak aerodynamic actions

The external pressure on the lateral walls is calculated by applying the rules given in clause G.2.2. With reference to Figure G.1, $b = 48$ m, $d = 11$ m, $h = 26{,}4$ m; therefore, $h/d = 2.4$. Thus, Table G.I provides the external pressure coefficients given in the second column of Table 4.3.I.

By applying the criteria illustrated in clauses G.2.2.1 and G.2.2.2, the reference height for the pressure on all faces of the building is $\overline{z}_e = h = 26{,}4$ m. Thus, $q_p(\overline{z}_e) = 1.277$ N/m^2. Applying Equation (3.11a), the external pressure on the walls takes the values given in the third column of Table 4.4.I.

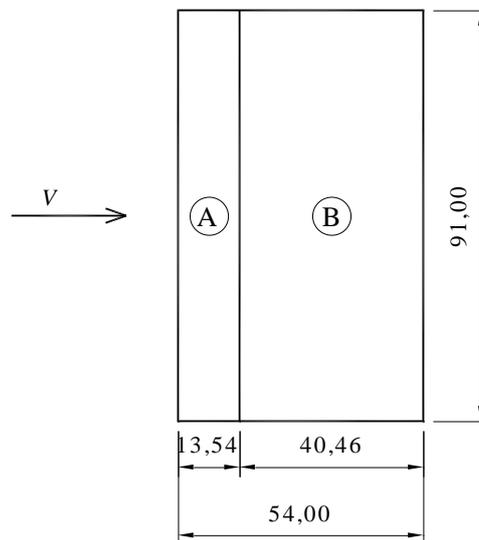**Table 4.3.I** - External pressure coefficients and external pressure on the walls.

Face	c_{pe}	p_e (N/m^2)
Upwind	+0,8	+1.022
Lateral	-0,9	-1.149
Downwind	-0,57	-728

In the case of apartment buildings, the presence of ceilings and partition walls divides the internal volume into a number of smaller volumes. In this situation, the role of internal pressure is normally negligible, and in the lack of more specific assessments, it can be ignored.

4.4.2 Dynamic factor and equivalent static actions

The structure has a regular distribution of stiffness and mass, and a limited height (less than 40 m). Thus, clause 3.4.1 allows the dynamic factor be given the value $c_d = 1$. It follows that, according to Equation (3.17), the equivalent static actions coincide with the peak aerodynamic actions.

In any case, assuming $c_d = 1$ is not mandatory but for sure conservative. Applying Annex L, and in particular the simplified method illustrated in clause L.3, Figure L.8 for metal box-shaped structures with a rectangular plan, gives $c_d = c_{dD} = 0{,}9$. Observing that this coefficient is only applied to actions in the along-wind direction (Figure L.1), the equivalent static actions are expressed by the pressures indicated in Table 4.4.II.

Table 4.4.II - External pressure on the walls.

Face	p_e (N/m^2)	$p_e \times c_{dD}$ (N/m^2)
Upwind	+1.022	+920
Lateral	-1.149	-1.149
Downwind	-728	-655

Also the assumption $c_d = c_{dD} = 0{,}9$ is not mandatory but for sure conservative. Values for this parameter and the equivalent static actions may be further reduced by applying the detailed method illustrated in clause L.2. In the case of the building under consideration, this does not seem to be necessary.

4.5 MULTI-STOREY OFFICE BUILDING

The structure examined in this clause is a 20-storey office building, described in the technical publication "*Particolari costruttivi di strutture in acciaio*" (Detailing of Steel Structures), published by CISIA - *Centro Italiano Sviluppo Impieghi Acciaio* (Italian Centre for the Development of Steel Applications) - Milan (Figures 4.5.1 and 4.5.2).

The building has a square plan, 21,6 m per side. The flat roof is located at a height of 67,44 m. There is a 1 m high parapet around its perimeter.

The structural scheme consists of a central reinforced concrete core and a steel structure with pinned columns and simply supported beams. The reinforced concrete core contains the stairwell and lifts, and it carries all horizontal actions. All connections in the steel structure are bolted and built on site. The floors are hollow tile and reinforced concrete ones.

The analyses are based on the Annexes G, H, I, L, M and N.
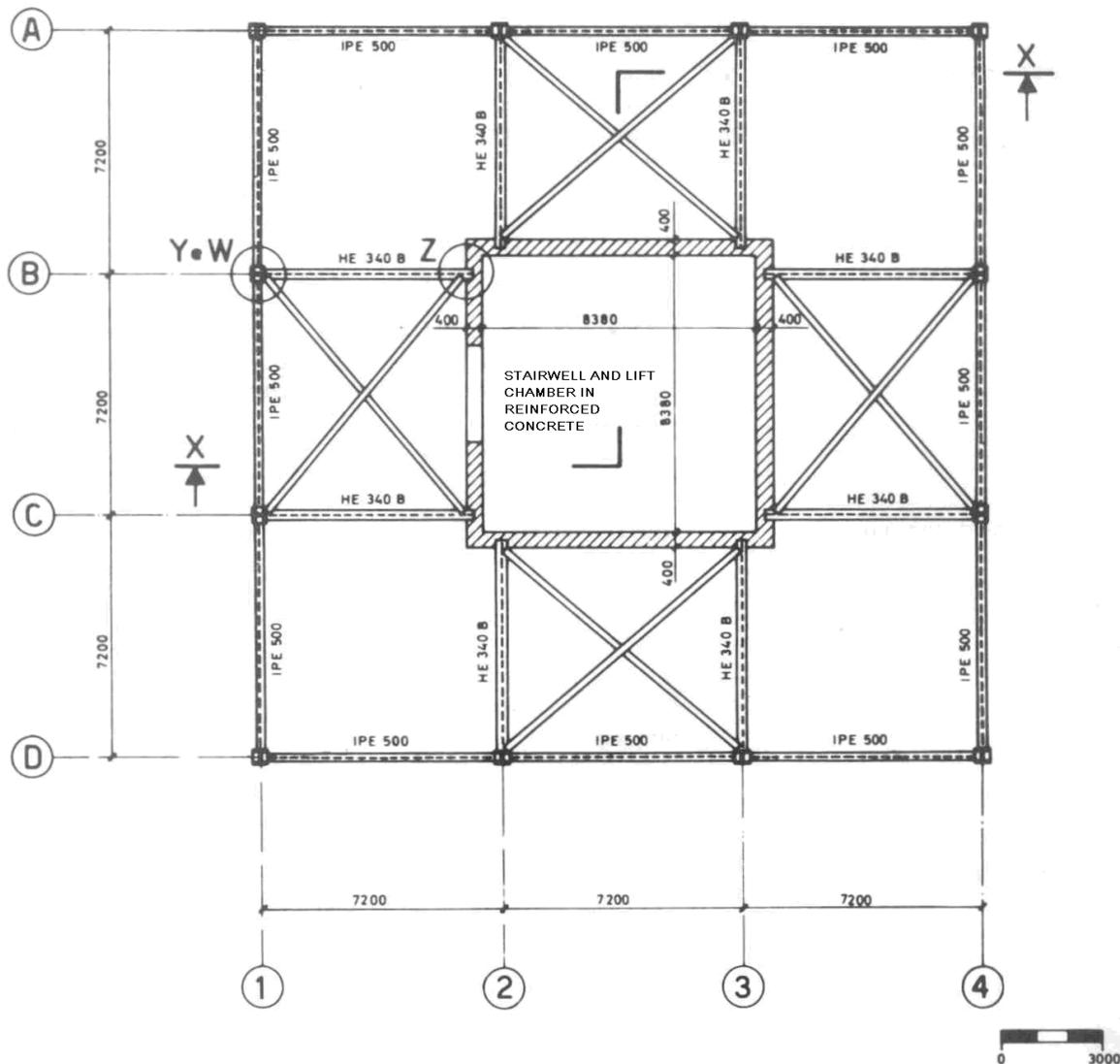
Figure 4.5.1 - Ground plan.
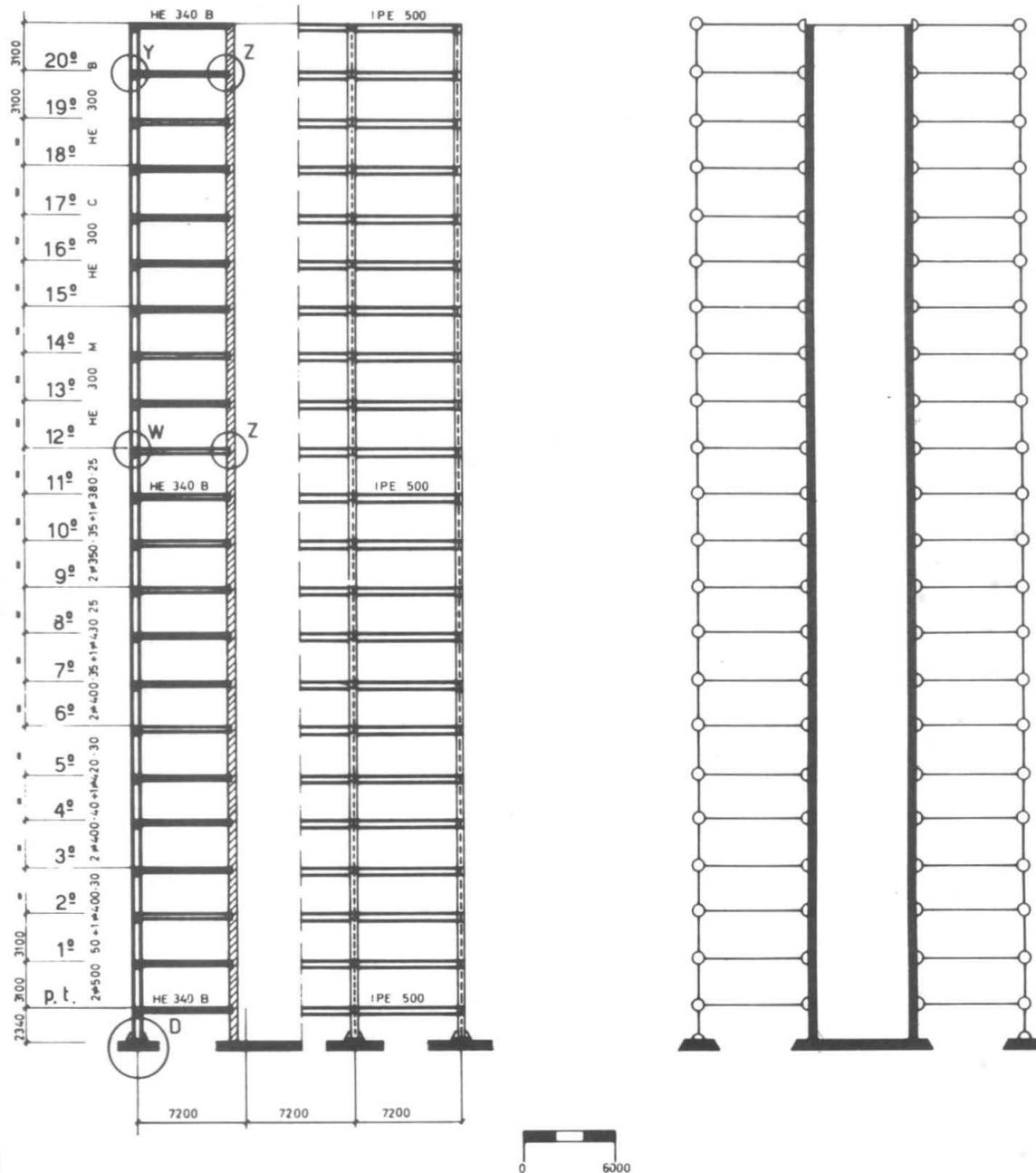
Figure 4.5.2 - (a) Section X-X; (b) Structural scheme.

Starting from the calculations made in clause 4.2, the analysis proceeds in two stages.

In the first stage, the peak aerodynamic actions on the stiff structure (clause 3.3) are calculated. More precisely, by applying the rules given in clause 3.3.1, the wind pressure on the external surfaces of the building are given by the Equation (3.11a), where q_p is the peak velocity pressure, c_{pe} is the external pressure coefficient and $\overline{z}_e$ is the reference height. In the lack of specific and well documented data, or of wind tunnel results, these quantities are calculated by applying Annex G as regards overall external pressure on the structure and Annex H as regards the external pressure on the elements. All analyses given below refer to the case in which the wind acts perpendicularly on one face of the building. Due to the symmetry properties of the building plan, they also apply for a perpendicular wind direction.

The second stage initially estimates the dynamic parameters of the structure (Annex I). Subsequently, the dynamic effects of wind on the flexible structure (clause 3.4) are analysed. In particular, not only the along-wind response (Annex L) is analysed, but also the across-wind and torsional response (Annex M). In any case, the equivalent static actions are calculated, to be used in Ultimate Limit State (ULS) and Serviceability Limit State (SLS) verifications, as well as the accelerations of the top storey of the building, to be used for the SLS check (Annex N). The actions and the effects caused by the various components of the actions are combined by applying the criteria given in Annex M.

Clause 4.5.1 gives the calculation of the overall external pressure on the structure. Clause 4.5.2 gives the calculation of the local external pressure on the elements. Clause 4.5.3 gives an estimate of the dynamic parameters of the building. In clauses 4.5.4, 4.5.5 and 4.5.6 the along-wind, across-wind and torsional equivalent static actions and accelerations are calculated. Clause 4.5.7 determines the combination rules of along-wind, across-wind and torsional actions and effects. Clause 4.5.8 illustrates abitability verification of the building.

4.5.1 Overall external pressure on the structure

The external pressure on the lateral walls is calculated by applying the rules given in clause G.2.2. With reference to Figure G.1, $b = d = 21,6$ m, $h = 67,44$ m; therefore, $h/d = 3.122$. Thus, Table G.I provides the external pressure coefficients given in Table 4.5.I.

Table 4.5.I - External pressure coefficients on the walls.

Face	c_{pe}
Upwind	+0,800
Downwind	-0,606

By applying the criterion illustrated in clause G.2.2.1, the reference height for pressure on the upwind face is $\bar{z}_e = b = 21,6$ m for all points at height $z \leq b$; thus, in this zone, $q_p(\bar{z}_e) = q'_p(\bar{z}_e) = 1.212$ N/m². Where $z > b$, the upwind face of the building is divided into sections of height Δ equal to the inter-storey height; the reference height $\bar{z}_e$ of each section is equal to the height of the storey above ground.

The reference height for pressure on the downwind face is $\bar{z}_e = h = 67,44$ m. Thus, $q_p(\bar{z}_e) = q''_p(\bar{z}_e) = 1.604$ N/m².

The resulting storey force (peak aerodynamic action) is therefore given as:

$$F_D = \left(0,8 \cdot q'_p - 0,606 \cdot q''_p\right) b \Delta$$

Table 4.5.II gives the height above the ground of each storey, the inter-storey height, the peak velocity pressure referred to the upwind and downwind faces and the resulting storey force.

Table 4.5.II - Calculation of storey forces.

Storey	z_e (m)	Δ (m)	q_p' (N/m^2)	q_p'' (N/m^2)	F_D (kN)
ground level	2,34	2,72	1.212	1.604	114
1	5,44	3,10	1.212	1.604	130
2	8,54	3,10	1.212	1.604	130
3	11,64	3,10	1.212	1.604	130
4	14,74	3,10	1.212	1.604	130
5	17,84	3,10	1.212	1.604	130
6	20,94	3,10	1.212	1.604	130
7	24,04	3,10	1.247	1.604	132
8	27,14	3,10	1.287	1.604	134
9	30,24	3,10	1.323	1.604	136
10	33,34	3,10	1.356	1.604	138
11	36,44	3,10	1.386	1.604	139
12	39,54	3,10	1.414	1.604	141
13	42,64	3,10	1.440	1.604	142
14	45,74	3,10	1.462	1.604	144
15	48,84	3,10	1.488	1.604	145
16	51,94	3,10	1.510	1.604	146
17	55,04	3,10	1.530	1.604	147
18	58,14	3,10	1.550	1.604	148
19	61,24	3,10	1.569	1.604	149
20	64,34	3,10	1.587	1.604	150
roof	67,44	2,55	1.604	1.604	124

4.5.2 Local external pressure on the elements

The external pressure on the elements of the lateral walls is calculated by means of the rules given in clause H.2.2. With reference to Figure H.2, $b = d = 21,6$ m, $h = 67,44$ m; then, $h/d = 3,122$, $e = 21,6$ m (Equation H.1). It follows that, by using the criterion shown in Figures H.3 and H.4, the walls are divided into the zones reported in Figure 4.5.3; by means of Table H.II, the corresponding external pressure coefficients for each of these zones are given in Table 4.3.III.
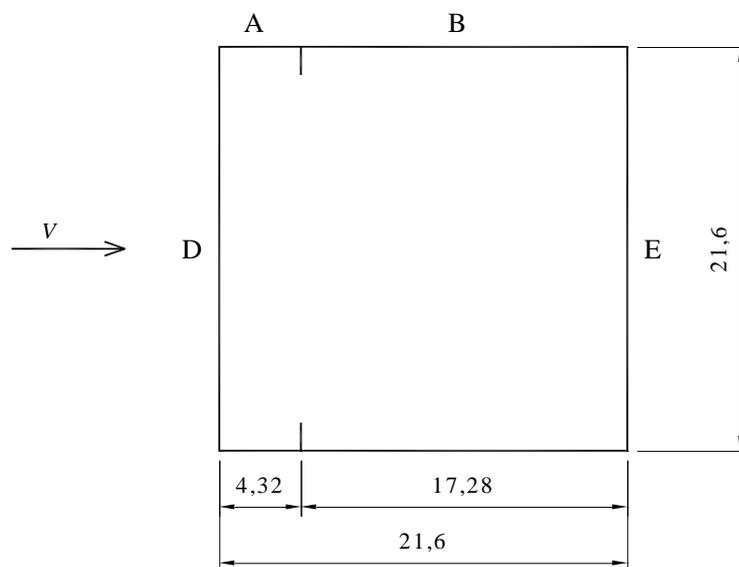
Figure 4.5.3 - Zones of the walls with uniform external pressure.

Table 4.5.III - External pressure coefficients on the walls.

Zone	$c_{pe0.10}$	$c_{pe,1}$
A	-1,2	-1,4
B	-0,8	-1,1
D	+0,8	+1,0
E	-0,606	-0,606

The reference height for pressure on the windward and leeward faces is the same as that calculated in Clause 4.5.1. The reference height for pressure on the lateral faces is $\overline{z}_e = h = 67,44$ m.

The values of local pressure in zone D (upwind face) are therefore the product of the peak velocity pressure in Table 4.5.II and the pressure coefficients in Table 4.5.III (for zone D). They are summarised in Table 4.5.IV. In the other four zones, the peak velocity pressure is constant, $q_p(h) = 1.604$ N/m^2, and local pressure takes the values given in Table 4.5.V.

Table 4.5.IV - Local pressure on the upwind face.

Storey	z_e (m)	Δ (m)	q'_p (N/m^2)	$p_{e,10}$ (N/m^2)	$p_{e,1}$ (N/m^2)
ground level	2,34	2,72	1.212	970	1.212
1	5,44	3,10	1.212	970	1.212
2	8,54	3,10	1.212	970	1.212
3	11,64	3,10	1.212	970	1.212
4	14,74	3,10	1.212	970	1.212
5	17,84	3,10	1.212	970	1.212
6	20,94	3,10	1.212	970	1.212
7	24,04	3,10	1.247	997	1.247
8	27,14	3,10	1.287	1.029	1.287
9	30,24	3,10	1.323	1.058	1.323
10	33,34	3,10	1.356	1.085	1.356
11	36,44	3,10	1.386	1.109	1.386
12	39,54	3,10	1.414	1.131	1.414
13	42,64	3,10	1.440	1.152	1.440
14	45,74	3,10	1.462	1.172	1.462
15	48,84	3,10	1.488	1.190	1.488
16	51,94	3,10	1.510	1.208	1.510
17	55,04	3,10	1.530	1.224	1.530
18	58,14	3,10	1.550	1.240	1.550
19	61,24	3,10	1.569	1.255	1.569
20	64,34	3,10	1.587	1.269	1.587
roof	67,44	2,55	1.604	1.283	1.604

Table 4.5.V - Local pressure on the walls.

Zone	$p_{e,10}$ (N/m^2)	$p_{e,1}$ (N/m^2)
A	-1.925	-2.246
B	-1.283	-1.764
D	see Table 5.IV	
E	-972	-972

The pressure coefficients $c_{pe,10}$ and the pressure $p_{e,10}$ refer to elements having an area $A \geq 10$ m^2; the pressure coefficients $c_{pe,1}$ and the pressure $p_{e,1}$ refer to elements having an area $A \leq 1$ m^2; for elements having an area between 1 and 10 m^2, the criterion indicated in Table H.I is adopted.

As the roof is flat, the external pressure on its elements is determined through the rules given in clause H.2.3.1. Also in this case, $b = d = 21,6$ m, $h = 67,44$ m; therefore, $h/d = 3.122$, and $e = 21,6$ m (Equation H.3). In any case, the roof has a parapet $h_p = 1$ m high; thus $h_p/h = 0,015$, $\overline{z}_e = h + h_p = 68,44$ m, $q_p(\overline{z}_e) = 1.609$ N/m^2. It follows that, by using the criterion shown in Figure H.5, the roof is divided into the zones reported in Figure 4.5.4; by means of Table H.III, the corresponding external pressure coefficients for each of these zones are given in the second and fourth columns of Table 4.5.VI. Lastly, according to Equation (3.11a), the external pressure on the roof takes the values given in the third and fifth columns of Table 4.5.IV
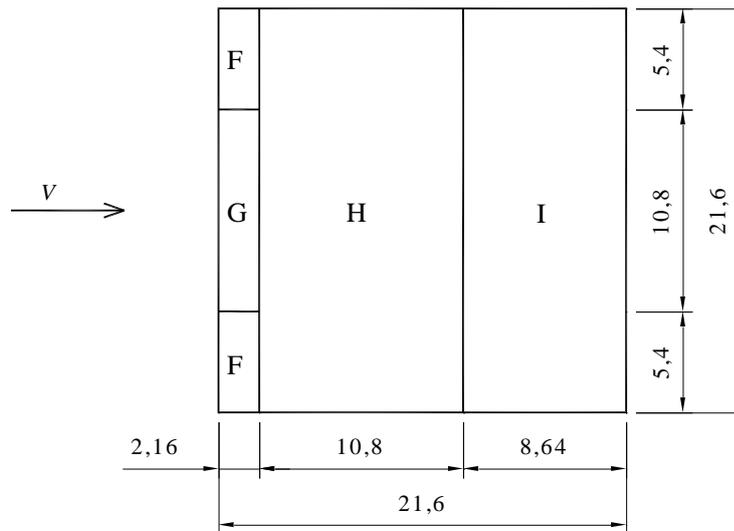
Figure 4.5.4 - Zones of the roof with uniform external pressure.

Table 4.5.IV - External pressure coefficients and external pressure on the roof.

Zone	$c_{pe,10}$	$p_{e,10}$ (N/m^2)	$c_{pe,1}$	$p_{e,1}$ (N/m^2)
F	-1,6	-2.574	-2,2	-3.540
G	-1,1	-1.770	-1,8	-2.896
H	-0,7	-1.126	-1,2	-1.931
I	±0,2	-322	±0,2	-322

4.5.3 Dynamic parameters

In the preliminary design stage, the dynamic parameters of the building are estimated by means of the criteria given in Annex I.

By applying the Equation (I.3), the first longitudinal and lateral frequencies are taken as equal to n_1 = 0.9 Hz for both ULS and SLS checks. The second longitudinal and lateral frequencies are n_2 = 3,05·n_1 = 2,75 Hz (Equation I.6). The first torsional frequency is n_M = 1,35·n_1 = 1,2 Hz (Equation I.7).

By applying the criterion of clause I.3.1, Equation (I.23), the first longitudinal and lateral mode shapes are:

$$\Phi_1(z) = \left(\frac{z}{h}\right)^{\zeta}$$

where ζ = 1. The same mode shape also is applied, as a first approximation, to the first torsional mode.

It is assumed that the building has an average mass density of (distributed in the total volume) ρ_m = 250 kg/m^3. Therefore, the mass of the building per unit height is:

$$m = \rho_m \cdot b \cdot d = 117 \cdot 10^3 \text{ kg/m}$$

Consequently, the generalised mass for the first longitudinal and lateral modes is (Equation I.25):

$$m_1 = \frac{mh}{2\zeta + 1} = 2,62 \cdot 10^6 \text{ kg}$$

The polar mass moment of inertia per unit height is:

$$I = \frac{1}{12} \cdot m \cdot \left(b^2 + d^2 \right) = 9,07 \cdot 10^6 \text{ kg·m}$$

Consequently, the generalised polar mass moment of inertia in the first torsional mode is (Equation I.27):

$$I_1 = \frac{I \cdot h}{2 \cdot \zeta + 1} = 204 \cdot 10^6 \text{ kg·m}^2$$

Lastly, the critical damping ratio is calculated by applying the rules given in clause I.6. In accordance with Equation (I.28), it is given by the sum of three contributions.

Applying Equation (I.29), the structural damping ratio for the first longitudinal and lateral modes is $\xi_{s1} = 0,01$. In accordance with the rules given in clause I.6.1, it is also assumed that the structural damping ratio for the first torsional mode is $\xi_{s1} = 0,01$.

Aerodynamic damping (clause I.6.5) is ignored, leading to a conservative result.

It is lastly assumed that there are no damping devices in the building. Therefore, the overall damping ratio coincides with the structural damping ratio.

4.5.4 Along-wind equivalent static action and acceleration

The dynamic actions and effects in the along-wind direction are assessed by means of the rules given in clause 3.4.

In accordance with Equation (3.17), the equivalent static actions are expressed as the product of the peak pressure determined according to Clause 4.5.1 and the dynamic factor c_d. In this case $c_d = c_{dD}$, since c_{dD} is the along-wind dynamic coefficient. In the lack of more accurate assessments, it is determined by applying the criteria illustrated in Annex L. Since the possibility of using $c_{dD} = 1$ (clause L.1) does not apply, this indicates the application of two different methods, defined, respectively, as the detailed method and the simplified method (used only for buildings).

By applying the detailed method (clause L.2), the dynamic factor c_{dD} is given by the Equation L.2. It is determined by applying the procedure indicated in Table L.I. The building corresponds to the worst case in Figure L.2. Table 4.5.VII summarises the steps towards the calculation of c_{dD}.

Table 4.5.VII - Calculation of the alongwind dynamic factor.

Equation	Parameter
Figure L.2	$h = 67{,}44$ m
	$b = 21{,}60$ m
	$z_e = 40{,}464$ m
(3.5)	$v_m(z_e) = 32{,}417$ m/s
(3.7)	$I_v(z_e) = 0{,}167$
(3.8)	$L_v(z_e) = 123{,}613$ m
(I.4)	$n_D = 0{,}9$ Hz
(I.28)	$\xi_D = 0{,}01$
(L.4)	$B^2 = 0{,}577$
(L.6)	$S_D = 0{,}059$
(L.9)	$\eta_h = 7{,}490$
(L.9)	$\eta_b = 2{,}399$
(L.7)	$R_h = 0{,}125$
(L.8)	$R_b = 0{,}331$
(L.5)	$R_D^2 = 0{,}191$
(L.11)	$\upsilon_D = 0{,}449$ Hz
(L.10)	$g_D = 3{,}518$
(L.3)	$G_D = 2{,}028$
(L.2)	$c_{dD} = 0{,}935$

Note that the simplified method (clause L.3) leads to the estimate $c_{dD} = 1{,}01$ (Figure L.4). This is larger than the value given by the detailed method (Table 4.5.VII).

The determination of along-wind acceleration, for the purpose of the abitability verification, is performed by applying the criterion given in clause L.4. This uses quantities whose value has apparently already been determined when calculating the dynamic factor. In reality, many of these are different for two reasons: 1) the frequency of the first vibration mode can be assumed higher that the one used to assess the dynamic factor (this option is not applied to this case); 2) the mean wind velocity shall be calculated for a design return period $T_R = 1$ year; thus, the values of the mean velocity and the velocity pressure for $T_R = 50$ years shall be scaled, respectively, by the factors 0,75 and $0{,}75^2 = 0{,}562$ (Clauses 4.2.2, 4.2.5 and 4.2.7).

Table 4.5.VIII summarises the steps towards the calculation of the peak acceleration value a_{pD} (Equation L.12), at the height $z_c = 64{,}34$ m of the building top storey.

Table 4.5.VIII - Calculation of the peak alongwind acceleration.

Equation	Parameter
Figure L.2	$h = 67,44$ m
	$b = 21,60$ m
	$d = 21,6$ m
	$z_e = 40,464$ m
(3.5)	$v_m(z_e) = 24,312$ m/s
(3.7)	$I_v(z_e) = 0,167$
(3.8)	$L_v(z_e) = 123,613$ m
(I.4)	$n_D = 0,9$ Hz
(I.25)	$m_D = 2,62 \cdot 10^6$ kg
(I.28)	$\xi_D = 0,01$
(L.6)	$S_D = 0,049$
(L.9)	$\eta_h = 9,986$
(L.9)	$\eta_b = 3,198$
(L.7)	$R_h = 0,095$
(L.8)	$R_b = 0,264$
(L.5)	$R_D^2 = 0,097$
(L.5)	$R_D = 0,312$
-	$c_{fD} = 1,606$
(L.16)	$K_D = 0,5$
(I.23)	$\Phi_D(z_c) = 0,954$
(L.14)	$\sigma_{aD} = 0,0143$ m/s^2
(L.13)	$g_{aD} = 3,710$
(L.12)	$a_{pD} = 0,053$ m/s^2

4.5.5 Across-wind equivalent static action and acceleration

The dynamic actions and effects in the across-wind direction are determined by applying the criteria given in Annex M, provided the building meets the requirements of Equations (M.1)-(M.4). As in Annex L, Annex M introduces two methods defined, respectively, as the detailed method and the simplified method (only for square plan buildings).

By applying the detailed method (clause M.2), the equivalent static across-wind force per unit height f_L is given by the Equation (M.5) where $q_p(h) = 1.604$ N/m^2 (Equation 2.8), $C_L = 0,157$ (Equation M.6), c_{dL} is the dynamic factor given by the Equation (M.7). It is determined by applying the procedure shown in Table M.I. Table 4.5.IX summarises the steps towards the calculation of c_{dL}.

Table 4.5.IX – Calculation of the across-wind dynamic coefficient.

Equation	Parameter
Figure M.1	$h = 67,44$ m
	$b = 21,60$ m
	$d = 21,6$ m
(3.5)	$v_m(h) = 35,175$ m/s
(3.7)	$I_v(h) = 0,154$
(I.4)	$n_L = 0,9$ Hz
(I.28)	$\xi_L = 0,01$
(M.11)	$m = 1$
(M.12)	$k_1 = 0,85$
(M.13)	$\beta_1 = 0,281$
(M.14)	$n_{s1} = 0,147$
(M.10)	$S_L = 0,010$
(M.9)	$R_L^2 = 0,775$
(M.15)	$g_L = 3,710$
(M.8)	$G_L = 4,942$
(M.7)	$c_{dL} = 2,378$

Thus, the equivalent static force per unit height is linear with respect to the height, and its maximum value at the top of the building is $f_L(h) = 38,3$ kN/m.

Note that the simplified method (clause M.4) leads to the estimate $c_{dL} \cong 4$ (Figure M.8). This value is clearly conservative but, unlike the case of the longitudinal (along-wind) dynamic coefficient, it turns out to be much greater than the value given by the detailed method (Table 4.5.IX).

The determination of the across-wind acceleration, for purposes of the abitability verification, is performed by applying the criterion given in clause M.5. This uses quantities whose value has apparently already been determined when calculating the dynamic factor. In reality, many of these are different for two reasons: 1) the frequency of the first vibration mode can be assumed greater that the one used to assess the dynamic factor (this option is not applied in this case); 2) the mean wind velocity shall be calculated for a design return period $T_R = 1$ year; thus, the values of the mean velocity and the velocity pressure for $T_R = 50$ years shall be scaled, respectively, by the factors 0,75 and $0,75^2 = 0,562$ (Clauses 4.2.2, 4.2.5 and 4.2.7).

Table 4.5.X summarises the steps towards the calculation of the peak acceleration a_{pL} (Equation M.27), at height $z_c = 64,34$ m of the building top storey.

Table 4.5.X - Calculation of the peak across-wind acceleration.

Equation	Parameter
Figure M.1	$h = 67,44$ m
	$b = 21,60$ m
	$d = 21,6$ m
(2.5)	$v_m(h) = 26,381$ m/s
(2.7)	$I_v(h) = 0,154$
(I.4)	$n_L = 0,9$ Hz
(I.25)	$m_L = 2,62 \cdot 10^6$ kg
(I.28)	$\xi_L = 0,010$
(M.11)	$m = 1$
(M.12)	$k_1 = 0,85$
(M.13)	$\beta_1 = 0,281$
(M.14)	$n_{s1} = 0,110$
(M.10)	$S_L = 0,005$
(M.9)	$R_L^2 = 0,427$
(M.9)	$R_L = 0,654$
(3.9)	$q_p(h) = 1604$ N/m^2
(M.6)	$C_L = 0,157$
(I.23)	$\Phi_L(h) = 1$
(I.23)	$\Phi_L(z_c) = 0,954$
(M.28)	$\sigma_{aL} = 0,0239$ m/s^2
(M.15)	$g_L = 3,710$
(M.27)	$a_{pL} = 0,088$ m/s^2

4.5.6 Torsional equivalent static action and acceleration

The torsional dynamic actions and effects are calculated by applying the criteria given in Annex M, provided that the building meets the requirements of Equations (M.1)-(M.4). As in Annex L, Annex M introduces two methods defined, respectively, as the detailed method and the simplified method (only for square plan buildings).

By applying the detailed method (clause M.3), the equivalent static torque per unit height m_M is given by the Equation (M.16) where $q_p(h) = 1.604$ N/m^2 (Equation 3.9), $C_M = 0.050$ (Equation M.17), c_{dM} is the dynamic factor given by the Equation (M.18). It is calculated by applying the method shown in Table M.II. Table 4.5.XI summarises the steps towards the calculation of c_{dM}.

Table 4.5.XI - Calculation of the torsional dynamic coefficient.

Equation	Parameter
Figure M.1	$h = 67,44$ m
	$b = 21,60$ m
	$d = 21,6$ m
(3.5)	$v_m(h) = 35,175$ m/s
(3.7)	$I_v(h) = 0,154$
(I.7)	$n_M = 1,2$ Hz
(I.28)	$\xi_M = 0,01$
-	$l = 21,60$ m
(M.22)	$v_m^* = 1,357$
(M.24)	$\beta_{M1} = 1,200$
(M.24)	$\beta_{M2} = 0,716$
(M.25)	$K_{M1} = 0,145$
(M.25)	$K_{M2} = 0,265$
(M.23)	$S_{M1} = 0,138$
(M.23)	$S_{M2} = 0,162$
(M.21)	$S_M = 0,008$
(M.20)	$R_M^2 = 0,610$
(M.26)	$g_M = 3,787$
(M.19)	$G_M = 4,805$
(M.18)	$c_{dM} = 2,312$

Thus, the equivalent static torque per unit height is linear with height and its maximum value at the top of the building is $m_M(h) = 156$ kN·m/m

Note that the simplified method (clause M.4) leads to the estimate $c_{dM} \cong 4$ (Figure M.10). This value is clearly conservative, but, as for the across-wind dynamic coefficient, it is much greater than the value given by the detailed method (Table 4.5.XI).

Aimed at the abitability verification, torsional acceleration is calculated by applying the criterion given in clause M.5. This uses quantities whose value has apparently already been determined when calculating the dynamic factor. In reality, many of these are different for two reasons: 1) the frequency of the first vibration mode can be assumed greater than the one used to assess the dynamic factor (this option is not applied to this case); 2) the mean wind velocity shall be calculated for a design return period $T_R = 1$ year; therefore, the values of the mean velocity and the velocity pressure for $T_R = 50$ years shall be scaled, respectively, by the factors 0,75 and $0,75^2 = 0,562$ (Clauses 4.2.2, 4.2.5 and 4.2.7).

Table 4.5.XII summarises the steps towards the calculation of the peak acceleration value a_{pM} (Equation M.29), at height $z_c = 64,34$ m of the building top storey.

Table 4.5.XII - Calculation of the peak torsional acceleration.

Equation	Parameter
Figure M.1	$h = 67,44$ m
	$b = 21,60$ m
	$d = 21,6$ m
(3.5)	$v_m(h) = 26,381$ m/s
(3.7)	$I_v(h) = 0,154$
(I.7)	$n_M = 1,2$ Hz
(I.27)	$I_M = 204 \cdot 10^6$ kg m^2
(I.28)	$\xi_M = 0,01$
-	$l = 21,60$ m
(M.22)	$v_m^* = 1,018$
(M.24)	$\beta_{M1} = 1,200$
(M.24)	$\beta_{M2} = 0,716$
(M.25)	$K_{M1} = 0,145$
(M.25)	$K_{M2} = 0,265$
(M.23)	$S_{M1} = 0,138$
(M.23)	$S_{M2} = 0,162$
(M.21)	$S_M = 0,004$
(M.20)	$R_M^2 = 0,306$
(M.20)	$R_M = 0,553$
(3.9)	$q_p(h) = 1604$ N/m^2
(M.18)	$C_M = 0,050$
(I.23)	$\Phi_M(h) = 1$
(I.23)	$\Phi_M(z_c) = 0,954$
(M.30)	$\sigma_{aM} = 0,0107$ rad/s^2
(M.26)	$g_M = 3,787$
(M.29)	$a_{pM} = 0,0040$ rad/s^2

Calculation of torsional acceleration is required only if the serviceability of the building has to be estimated at a location other than the centre of torsion. Otherwise, this quantity is an indicator to be considered qualitatively.

4.5.7 Combination of actions and effects

To perform strength and deformability checks, appropriate rules shall be applied for the combination of actions and effects associated with along-wind (*D*), across-wind (*L*) and torsional (*M*) responses. These rules are based on the criterion introduced in clause M.6. On the basis of this criterion $n_1 = \min(n_L, n_M) = 0,9$ Hz, $f_{LM} = 1,35$ (Equation M.31), $n_1 b / v_m(h) = 0,553$, $d / b = 1$. Therefore, by using Table M.IV, $\gamma_{LM} = 0,65$. Bearing in mind that $G_D = 2,028$ (Table 4.5.VII), Table M.III gives the combination rules in Table 4.5.XIII.

Table 4.5.XIII - Action and effect combination rules for safety checks.

Combination	D	L	M
1	D	0,4L	0,4M
2	0,7D	L	0,65M
3	0,7D	0,65L	M

The application of the combination rules of Table 4.5.XIII to base shear, bending moment and torque (Figure 4.5.5) gives the results summarised in Table 4.5.XIV.
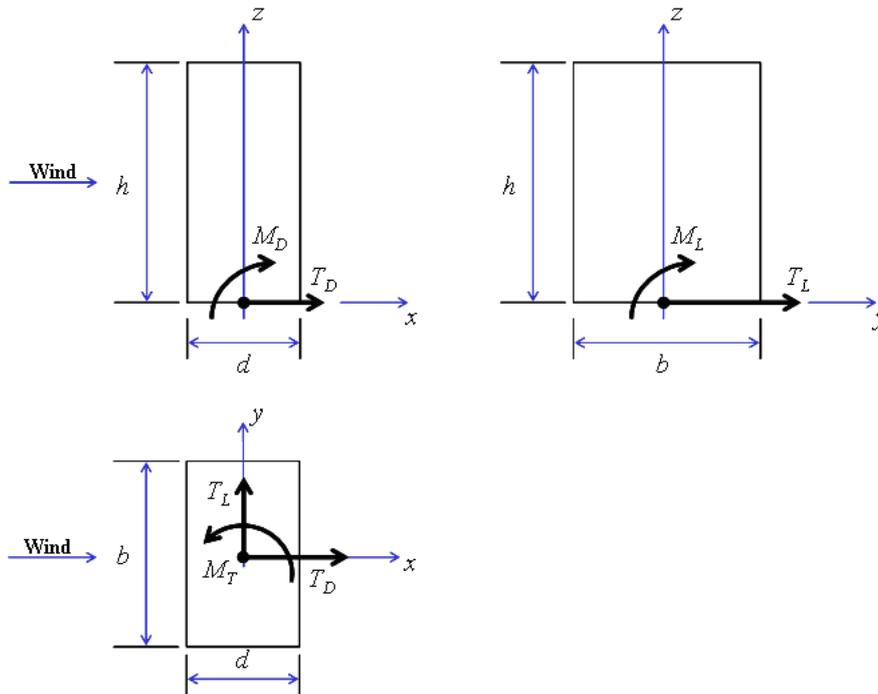
Figure 4.5.5 - Reactions at the base of the building.

Table 4.5.XIV - Combination rules for base reactions.

Combination	F_D (kN)	F_L (kN)	M_D (kN·m)	M_L (kN·m)	M_T (kN·m)
1	2.813	525	100.854	23.600	2.114
2	1.969	1.313	70.598	59.000	3.435
3	1.969	853	70.598	38.350	5.285

Note that, for the purposes of strength and deformability checks, the along-wind wind actions prevail over across-wind actions. This situation is characteristic of low- to medium-rise buildings.

4.5.8 Abitability verification

The abitability verification is performed by applying the criteria indicated in Annex N. Note that this Annex provides purely indicative suggestions that should be interpreted for the situations as they arise.

Clause N.2 suggests making sure that each of the peak values for along-wind and across-wind acceleration in the centre of rotation (torsion), a_{pD} and a_{pL}, do not exceed the limit value given by the Equation (N.1) and in Figure N.2.

In this particular case, at the top storey, $a_{pD} = 0,053$ m/s^2 (Table 4.5.VIII) and $a_{pL} = 0,088$ m/s^2 (Table 4.5.X). The dominant frequency of oscillation is $n_0 = n_D = n_L = 0,9$ Hz.

Note that, unlike the actions and the internal forces (clause 4.5.7), across-wind acceleration prevails over alongwind acceleration. This situation is typical of low- to medium-rise buildings, provided that they are sufficiently slender.

Figure 4.5.6 compares the maximum values of the accelerations given above with the limit indicated by the Equation (N.1) and in Figure N.2. For an office building the reference limit is given by curve (a).
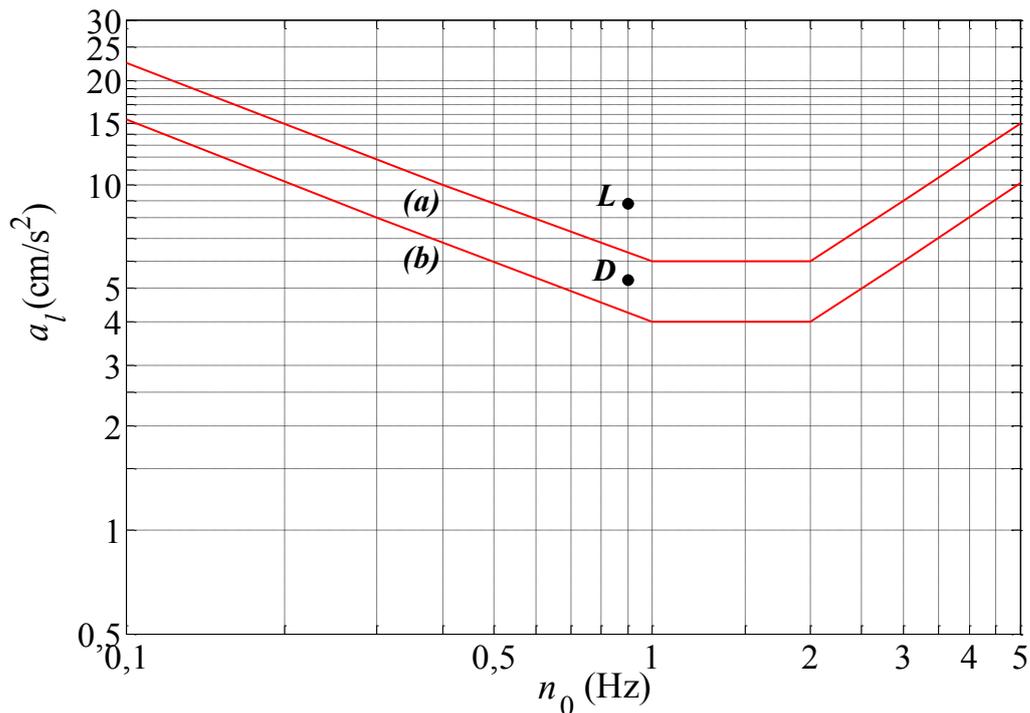
Figure 4.5.6 - Abitability verification of the building top storey.

Note that peak along-wind acceleration is less than the recommended limit; the peak across-wind acceleration, on the other hand, is moderately greater than the limit. It is suggested that the analysis be repeated using more accurate assessments of the natural frequencies, of the mode shapes and of the damping ratios than those given in Annex I.

4.6 TALL BUILDING

The structure examined in this clause is an ideal tall building identified in the literature with the code name C.A.A.R.C. (Commonwealth Aeronautic Advisory Research Council). Over the years, it has been the subject of numerous comparative analytical, numerical and experimental studies conducted by various specialist laboratories all over the world. It is still today used in various standards and projects intended to harmonise international standards for wind action as a term for comparison and illustration of the methods used.

The building is a prism (Figure 4.6.1) with sides $b = 46$ m, $d = 30$ m, $h = 183$ m.
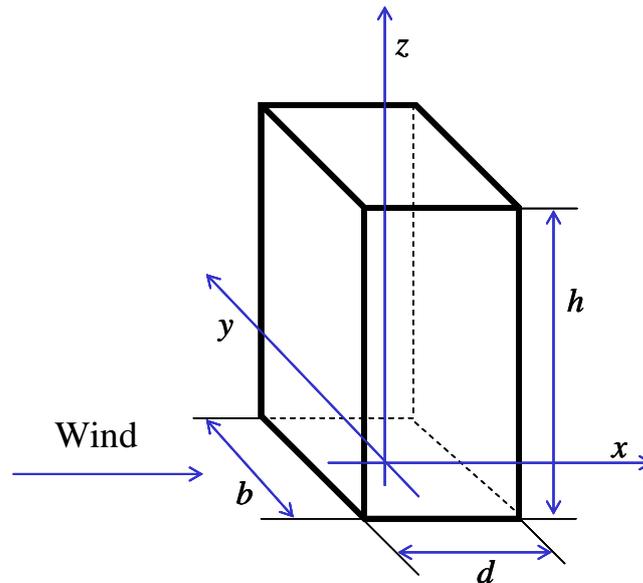
Figure 4.6.1 - C.A.A.R.C. Building

It is assumed that the structure consists of a pair of reinforced concrete cores and a steel pinned column system. It is also assumed that the building has an average mass density (distributed in the total volume) $\rho_m = 200$ kg/m^3.

Aiming to preliminary design calculations only, the analysis concerns tip accelerations. The calculations are made by applying Annexes G, I, L, M and N.

Starting from the calculations made in clause 4.2, the analysis proceeds in two stages.

In the first stage, the peak aerodynamic actions (clause 3.3) are determined. More precisely, by applying the rules given in clause 3.3.1, the overall pressure on the external surfaces of the building is given by Equation (3.11a), where q_p is the peak velocity pressure, c_{pe} is the external pressure coefficient, $\bar{z}_e$ is the reference height. These quantities are determined by applying Annex G. Analysis was performed by considering, separately, the oncoming wind perpendicular to the long side (A) and to the short side (B) of the building, respectively.

The second stage initially estimates the dynamic parameters of the structure (Annex I). Subsequently, the dynamic wind effects (clause 3.4) in along-wind (Annex L), across-wind and torsional (Annex M) directions are evaluated, focusing attention on the building tip acceleration (Annex N).

Clause 4.6.1 gives the calculation of overall external pressure on the structure. Clause 4.6.2 gives an estimate of the dynamic parameters of the building. Clause 4.6.3 gives the calculation of the alongwind gust factor. In clauses 4.6.4, 4.6.5 and 4.6.6 the along-wind, across-wind and torsional accelerations are assessed. Clause 4.6.7 illustrates the abitability verification of the building. Clause 4.6.8 analyses a possible vibration mitigation strategy.

4.6.1 Overall external pressure on the structure

The external pressure on the lateral walls is calculated by applying the rules given in clause G.2.2.

With reference to Figure G.1, considering the case where the wind is perpendicular to the long side (A), b = 46 m, d = 30 m, h = 183 m; therefore, h/d = 6.1. Thus, Table G.I provides the external pressure coefficients given in Table 4.5.I.

Table 4.6.I - External pressure coefficients on the walls (case A).

Face	c_{pe}
Upwind	+0,8
Downwind	-0,7

By applying the criterion illustrated in clause G.2.2.1, the reference height for pressure on the upwind face is $\overline{z}_e = b$ = 46 m for all points at height $z \leq b$, where $q_p(\overline{z}_e)$ = 1.467 N/m^2. Where $z > b$, the peak velocity pressure varies in accordance with the law given in clause 4.2.7; it reaches the maximum value at the building tip, $q_p(h)$ = 1.986 N/m^2. The reference height for pressure on the downwind face is $\overline{z}_e = h$ = 67,44 m. Thus, $q_p(\overline{z}_e) = q_p(h)$ = 1.986 N/m^2.

Similarly, considering the case where the wind is perpendicular to the short side (B), b = 30 m, d = 46 m, h = 183 m; therefore, h/d = 3,98. Thus, Table G.I provides the external pressure coefficients given in Table 4.6.II.

Table 4.6.II - External pressure coefficients on walls (Example B).

Face	c_{pe}
Upwind	+0,800
Downwind	-0,649

By applying the criterion illustrated in clause G.2.2.1, the reference height for pressure on the upwind face is $\overline{z}_e = b$ = 30 m. for all points at height $z \leq b$, where $q_p(\overline{z}_e)$ = 1.320 N/m^2. Where $z > b$, the peak velocity pressure varies in accordance with the law given in clause 4.2.7; it reaches the maximum value at the building tip, $q_p(h)$ = 1.986 N/m^2. The reference height for pressure on the downwind face is $\overline{z}_e = h$ = 67,44 m. Thus, $q_p(\overline{z}_e) = q_p(h)$ = 1.986 N/m^2.

4.6.2 Dynamic parameters

In the preliminary design stage, the dynamic parameters of the building are estimated by means of the criteria given in Annex I.

By applying the Equation (I.4), the first lateral frequency is $n_1 = 0,25$ Hz for both the main orthogonal directions of vibration. The second lateral frequency is $n_2 = 3,05 \cdot n_1 = 4,12$ Hz (Equation I.6). The first torsional frequency is $n_M = 1,35 n_1 = 0,34$ Hz (Equation I.7).

By applying the criterion indicated in clause I.3.1, Equation (I.23), the first lateral mode shape is:

$$\Phi_1(z) = \left(\frac{z}{h} \right)^{\zeta}$$

where $\zeta = 1$. The same mode shape can be applied, as a first approximation, to the first torsional vibration mode.

Assuming that the building has an average mass density (distributed in the total volume) $\rho_m = 200$ kg/m^3, the mass of the building per unit height is:

$$m = \rho_m \cdot b \cdot d = 276 \cdot 10^3 \text{ kg/m}$$

Consequently, the generalised mass in the first lateral mode is (Equation I.25):

$$m_1 = \frac{m \cdot h}{2 \cdot \zeta + 1} = 16,8 \cdot 10^6 \text{ kg}$$

The polar mass moment of inertia per unit height is:

$$I = \frac{1}{12} \cdot m \cdot \left(b^2 + d^2 \right) = 69,4 \cdot 10^6 \text{ kg·m}$$

Consequently, the generalised polar mass moment of inertia for the first torsional mode is (Equation I.18):

$$I_1 = \frac{I \cdot h}{2 \cdot \zeta + 1} = 4,23 \cdot 10^9 \text{ kg·m}^2$$

Lastly, the damping ratio is determined by applying the rules given in clause I.6. In accordance with Equation (I.28), it is given by the sum of three contributions.

By applying Equation (I.29), the structural damping ratio for the first lateral mode is $\xi_{s1} = 0,008$. In accordance with the rules given in clause I.6.1, it is also assumed that the structural damping ratio for the first torsional mode is $\xi_{s1} = 0.008$.

Aerodynamic damping (clause I.6.5) is ignored, leading to a conservative result.

Lastly, it is initially assumed that there are no damping devices in the building. Thus, the total damping ratio coincides with the structural damping ratio.

4.6.3 Longitudinal gust factor

While the objective of analysis is to estimate structural acceleration, the definition of combination rules for effects (clause M.6) requires preliminary calculation of the gust factor G_D in the along-wind direction.

The analysis is performed by applying the criterion given in clause L.2 to the two cases identified by (A) and (B) (clause 4.6.1). Table 4.6.III summarises the steps towards the calculation of the gust factor G_D (Equation L.3) and, though not necessary for the objectives of this Annex, the dynamic factor c_{dD} (Equation L.2).

Table 4.6.III - Calculation of the along-wind dynamic coefficient.

Equation	Parameter (case A)	Parameter (case B)
Figure L.2	$h = 183$ m	$h = 183$ m
	$b = 46$ m	$b = 30$ m
	$z_e = 109,8$ m	$z_e = 109,8$ m
(3.5)	$v_m(z_e) = 37,807$ m/s	$v_m(z_e) = 37,807$ m/s
(3.7)	$I_v(z_e) = 0,143$	$I_v(z_e) = 0,143$
(3.8)	$L_v(z_e) = 215,089$ m	$L_v(z_e) = 215,089$ m
(I.4)	$n_D = 0,25$ Hz	$n_D = 0,25$ Hz
(I.28)	$\xi_D = 0,008$	$\xi_D = 0,008$
(L.4)	$B^2 = 0,516$	$B^2 = 0,528$
(L.6)	$S_D = 0,100$	$S_D = 0,100$
(L.9)	$\eta_h = 4,840$	$\eta_h = 4,840$
(L.9)	$\eta_b = 1,217$	$\eta_b = 0,794$
(L.7)	$R_h = 0,185$	$R_h = 0,185$
(L.8)	$R_b = 0,514$	$R_b = 0,629$
(L.5)	$R_D^2 = 0,932$	$R_D^2 = 1,140$
(L.11)	$\upsilon_D = 0,201$ Hz	$\upsilon_D = 0,207$ Hz
(L.10)	$g_D = 3,282$	$g_D = 3,291$
(L.3)	$G_D = 2,128$	$G_D = 2,214$
(L.2)	$c_{dD} = 1,063$	$c_{dD} = 1,106$

4.6.4 Longitudinal acceleration

Along-wind acceleration is calculated by applying the criterion given in clause L.4. Table 4.5.IV summarises the steps towards the calculation of the peak acceleration value a_{pD} (Equation L.12) at height $z_c = h$ of the building tip.

Table 4.6.IV - Calculation of the peak along-wind acceleration.

Equation	Parameter (case A)	Parameter (case B)
Figure L.2	$h = 183$ m	$h = 183$ m
	$b = 46$ m	$b = 30$ m
	$d = 30$ m	$d = 46$ m
	$z_e = 109,8$ m	$z_e = 109,80$ m
(3.5)	$v_m(z_e) = 28,355$ m/s	$v_m(z_e) = 28,355$ m/s
(3.7)	$I_v(z_e) = 0,143$	$I_v(z_e) = 0,143$
(3.8)	$L_v(z_e) = 215,089$ m	$L_v(z_e) = 215,089$ m
(I.4)	$n_D = 0,25$ Hz	$n_D = 0,25$ Hz
(I.25)	$m_D = 16,8 \cdot 10^6$ kg	$m_D = 16,8 \cdot 10^6$ kg
(I.28)	$\xi_D = 0,008$	$\xi_D = 0,008$
(L.6)	$S_D = 0,085$	$S_D = 0,085$
(L.9)	$\eta_h = 6,454$	$\eta_h = 6,454$
(L.9)	$\eta_b = 1,622$	$\eta_b = 1,058$
(L.7)	$R_h = 0,143$	$R_h = 0,143$
(L.8)	$R_b = 0,434$	$R_b = 0,552$
(L.5)	$R_D^2 = 0,515$	$R_D^2 = 0,655$
(L.5)	$R_D = 0,718$	$R_D = 0,810$
-	$c_{fD} = 1,5$	$c_{fD} = 1,449$
(L.16)	$K_D = 0,5$	$K_D = 0,5$
(I.23)	$\Phi_D(z_c) = 1$	$\Phi_D(z_c) = 1$
(L.14)	$\sigma_{aD} = 0,0386$ m/s^2	$\sigma_{aD} = 0,0275$ m/s^2
(L.13)	$g_{aD} = 3,348$	$g_{aD} = 3,348$
(L.12)	$a_{pD} = 0,129$ m/s^2	$a_{pD} = 0,092$ m/s^2

4.6.5 Across-wind acceleration

Across-wind acceleration is calculated by applying the criterion given in clause M.5, provided that the building meets the requirements of Equations (M.1)-(M.4). Table 4.6.V summarises the steps towards the calculation of the peak acceleration value a_{pL} (Equation M.27) at height $z_c = h$ of the building tip.

Table 4.6.V - Calculation of peak across-wind acceleration.

Equation	Parameter (case A)	Parameter (case B)
Figure M.1	$h = 183$ m	$h = 183$ m
	$b = 46$ m	$b = 30$ m
	$d = 30$ m	$d = 46$ m
(2.5)	$v_m(h) = 30{,}424$ m/s	$v_m(h) = 30{,}424$ m/s
(2.7)	$I_v(h) = 0{,}133$	$I_v(h) = 0{,}133$
(I.4)	$n_L = 0{,}25$ Hz	$n_L = 0{,}25$ Hz
(I.25)	$m_L = 16{,}8 \cdot 10^6$ kg	$m_L = 16{,}8 \cdot 10^6$ kg
(I.28)	$\xi_L = 0{,}008$	$\xi_L = 0{,}008$
(M.11)	$m = 1$	$m = 1$
(M.12)	$k_1 = 0{,}85$	$k_1 = 0{,}85$
(M.13)	$\beta_1 = 0{,}284$	$\beta_1 = 0{,}375$
(M.14)	$n_{s1} = 0{,}069$	$n_{s1} = 0{,}069$
(M.10)	$S_L = 0{,}032$	$S_L = 0{,}042$
(M.9)	$R_L^2 = 3{,}111$	$R_L^2 = 4{,}143$
(M.9)	$R_L = 1{,}764$	$R_L = 2{,}035$
(3.9)	$q_p(h) = 1986$ N/m^2	$q_p(h) = 1986$ N/m^2
(M.6)	$C_L = 0{,}116$	$C_L = 0{,}2$
(I.23)	$\Phi_L(h) = \Phi_L(z_c) = 1$	$\Phi_L(h) = \Phi_L(z_c) = 1$
(M.28)	$\sigma_{aL} = 0{,}059$ m/s^2	$\sigma_{aL} = 0{,}077$ m/s^2
(M.15)	$g_L = 3{,}348$	$g_L = 3{,}348$
(M.27)	$a_{pL} = 0{,}197$ m/s^2	$a_{pL} = 0{,}257$ m/s^2

4.6.6 Torsional acceleration

Torsional acceleration is calculated by applying the criterion given in clause M.5, provided that the building meets the requirements of Equations (M.1)-(M.4). Table 4.6.VI summarises the steps towards the calculation of the peak acceleration value a_{pM} (Equation M.29) at height $z_c = h$ of the building tip.

Table 4.6.VI - Calculation of peak torsional acceleration.

Equation	Parameter (case A)	Parameter (case B)
Figure M.1	$h = 183$ m	$h = 183$ m
	$b = 46$ m	$b = 30$ m
	$d = 30$ m	$d = 46$ m
(3.5)	$v_m(h) = 30,424$ m/s	$v_m(h) = 30,424$ m/s
(3.7)	$I_v(h) = 0,133$	$I_v(h) = 0,133$
(I.7)	$n_M = 0,34$ Hz	$n_M = 0,34$ Hz
(I.27)	$I_M = 4,23 \cdot 10^9$ kg·m^2	$I_M = 4,23 \cdot 10^9$ kg·m^2
(I.28)	$\xi_M = 0,008$	$\xi_M = 0,008$
-	$l = 46$ m	$l = 46$ m
(M.22)	$v_m^* = 2,409$	$v_m^* = 2,409$
(M.24)	$\beta_{M1} = 1,041$	$\beta_{M1} = 1,645$
(M.24)	$\beta_{M2} = 1,261$	$\beta_{M2} = 0,405$
(M.25)	$K_{M1} = 0,229$	$K_{M1} = 0,067$
(M.25)	$K_{M2} = 0,131$	$K_{M2} = 0,291$
(M.23)	$S_{M1} = 0,071$	$S_{M1} = 0,206$
(M.23)	$S_{M2} = 0,093$	$S_{M2} = 0,118$
(M.21)	$S_M = 0,019$	$S_M = 0,026$
(M.20)	$R_M^2 = 1,895$	$R_M^2 = 2,590$
(M.20)	$R_M = 1,376$	$R_M = 1,609$
(3.9)	$q_p(h) = 1986$ N/m^2	$q_p(h) = 1986$ N/m^2
(M.18)	$C_M = 0.034$	$C_M = 0.084$
(I.23)	$\Phi_M(h) = \Phi_M(z_c) = 1$	$\Phi_M(h) = \Phi_M(z_c) = 1$
(M.30)	$\sigma_{aM} = 0,0148$ rad/s^2	$\sigma_{aM} = 0,0183$ rad/s^2
(M.26)	$g_M = 3,438$	$g_M = 3,438$
(M.29)	$a_{pM} = 0,0051$ rad/s^2	$a_{pM} = 0,0063$ rad/s^2

The calculation of torsional acceleration is required only if the serviceability of the building has to be estimated at locations far from the centre of torsion. Otherwise, this value is an indicator to be considered qualitatively.

4.6.7 Abitability verification

The serviceability check is performed by applying the criteria indicated in Annex N. It gives indicative suggestions that should be interpreted for the situations that arise from time to time. This is especially valid in this case, where preliminary serviceability check is performed to estimate the expected performances of the building.

Clause N.2 suggests making sure that each of the peak values for along-wind and across-wind acceleration in the centre of rotation (torsion), a_{pD} and a_{pL}, do not exceed the limit value given by Equation (N.1) and Figure N.2.

Table 4.6.VII summarises the peak acceleration values at the building tip, estimated by using clauses 4.6.4 (Table 4.6.IV) and 4.6.5 (Table 4.6.V). In any case, the dominant frequency of oscillation is $n_0 = n_D = n_L = 0,25$ Hz.

Table 4.6.VII – Peak values of along-wind and across-wind acceleration at the building tip.

Case (A)	Case (B)
$a_{pD} = 0{,}129$ m/s^2	$a_{pD} = 0{,}092$ m/s^2
$a_{pL} = 0{,}197$ m/s^2	$a_{pL} = 0{,}257$ m/s^2

Note that across-wind acceleration always significantly prevails over along-wind acceleration because of the considerable height of the building.

Figure 4.5.6 compares the maximum values of the accelerations given in Table 4.6.VII with the limit indicated by the Equation (N.1) and in Figure N.2. Since the intended use of the building top floors was not defined, reference should be made to curve (a) for office use and to curve (b) for residential use.
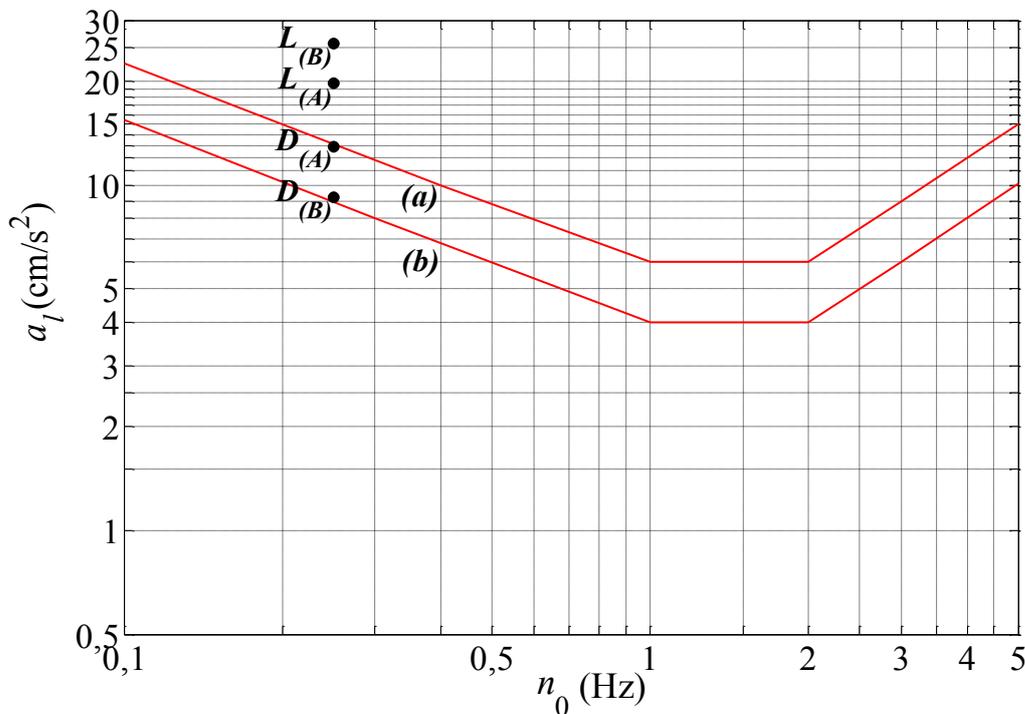
Figure 4.6.2 – Abitability verification of the top storey of the building.

Peak along-wind acceleration is less than the recommended limits if the top storeys are used as offices. Peak across-wind acceleration, on the other hand, is much larger than the recommended limit, especially in case (B) where the wind is perpendicular to the short side of the building. In this case, even repeating the analyses using more accurate assessments of the natural frequencies, of the mode shapes and and of the damping ratios than those given in Annex I, might not be sufficient to obtain accelerations within adequate limits.

4.6.8 Mitigation of vibrations

To mitigate the building accelerations without modifying its main structure, it is possible to add a *Tuned Mass Damper* (TMD) at the top of the building. It is reasonable to assume that proper design of this device can increase the equivalent overall damping ratio of the building at least to $\xi_D = \xi_L = 0,03$.

Table 4.6.VIII summarises the peak tip accelerations, for the building with TMD, still for an oscillation frequency $n_0 = n_D = n_L = 0,25$ Hz.

Table 4.6.VIII – Peak values of along-wind and across-wind tip acceleration of the building with TMD.

Case (A)	Case (B)
$a_{pD} = 0,067$ m/s^2	$a_{pD} = 0,047$ m/s^2
$a_{pL} = 0,109$ m/s^2	$a_{pL} = 0,133$ m/s^2

Note that across-wind acceleration always and significantly prevails over along-wind acceleration. In any case, the peak accelerations are heavily reduced.

Figure 4.6.3 compares the maximum values of the accelerations given in Table 4.6.VIII with the limit indicated by the Equation (N.1) and in Figure N.2.
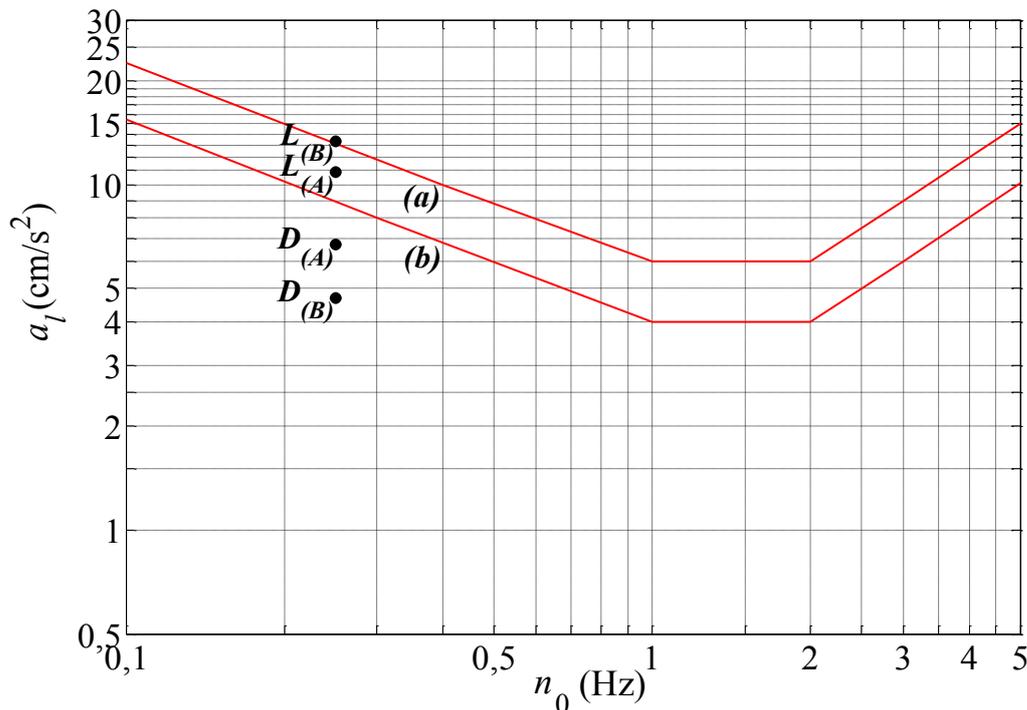
Figure 4.6.3 - Serviceability check of the building top storey..

The addition of a TMD system capable of increasing the damping ratio to 3% is sufficient to ensure that serviceability check is satisfied for office use. It is reasonable to assume that an increase in TMD efficiency can also ensure that the top storeys may be used as apartments.

4.7 GASHOLDER

The structure examined in this clause is a 50,000 m³ dry gasholder (Figure 4.7.1).
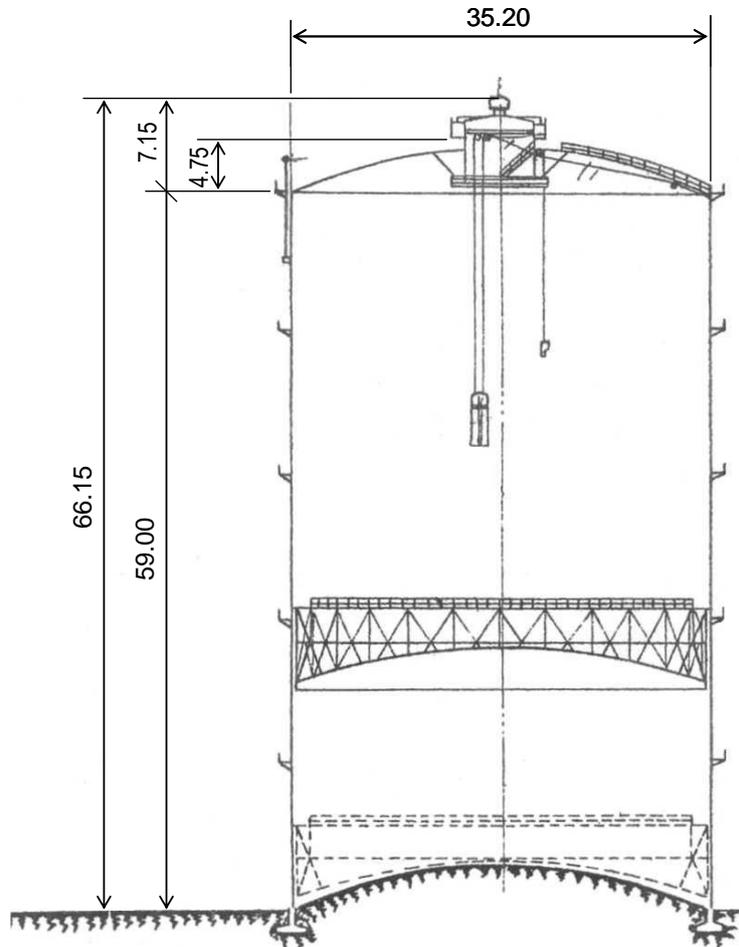
Figure 4.7.1 - 50,000 m³ gasholder.

The gasholder has a diameter of 35,20 m; the height of the shell is 59 m; the maximum height of the dome is 63,75 m; the overall height at the top of the summit fairing is 66,15 m. It is in carbon steel assembled with riveted joints. The resisting structure consists of 22 HEA140 columns (I-shaped cross-section according to European Standards) , riveted to the shell by means of one of the flanges and secured to the foundation with tie-bolts. The columns are connected at approximately 12 m on centre to 5 circumferential stiffeners that form the inspection gangways; 7 secondary stiffeners made from 110 mm [-shaped cross-section profiles are located between two adjacent gangways. Containment is ensured by 5 mm thick calendared sheet steel riveted to the frame members. The sheet steel also acts as shear bracing for the main structure. The upper order of sheet steel has rectangular openings, used for ventilation of the gasholder above the internal piston.

The roof is made from a lattice of radial and circumferential beams in [-shaped cross-section profiles, 140 mm in height, and 3 mm thick sheet steel. At the top of the roof there is a fairing with lateral windows for ventilation and lighting of the internal volume.

The piston is in metalwork. The structural scheme of the shell is similar to that used for the roof; the circumference of the piston is stiffened by a truss beam that supports the guide and seal devices.

Analysis was performed by applying Annexes G, I and O.

Peak aerodynamic actions are calculated by means of clause 3.3. More precisely, by using the rules given in clause 3.3.1, the wind pressure on the external and internal faces of the surfaces of the structure is given by the Equation (3.11), where q_p is the peak velocity pressure, c_{pe} and c_{pi} are external and internal pressure coefficients, and $\overline{z}_e$ and $\overline{z}_i$ are the associated reference heights. The aerodynamic coefficients are determined by applying Annex G.

The dynamic wind actions are calculated by means of clause 3.4. More precisely, by using the rules given in clause 3.4.1, the equivalent static actions are expressed by the Equation (3.17), where c_d is the dynamic factor. The dynamic parameters of the structure are calculated by means of finite element models and the criteria given in Annex I. The possibility of dynamic phenomena caused by vortex shedding and ovalling are also studied with reference to Annex O.

Clause 4.7.1 gives the analysis of the external pressure on the shell. Clause 4.7.2 gives the calculation of external pressure on the dome. Clause 4.7.3 gives the calculation of internal pressure. Clause 4.7.4 estimates the dynamic parameters of the structure. Clause 4.7.5 gives the calculation of the dynamic factor and the equivalent static actions. In clauses 4.7.6 and 4.7.7, respectively, the dynamic phenomena associated with vortex shedding and ovalling of the shell are analysed.

4.7.1 External pressure on the shell

In the following, $h = 59$ m has been assumed as the height of the shell and $b = 35{,}2$ m as its diameter. By applying the criterion illustrated in clause G.3.2.1, the reference height for external pressure on the shell is $\overline{z}_e = b = 35{,}2$ m for all points at height $z \le b$, where $q_p(\overline{z}_e) = q_p(b) =$ 1.374 N/m^2. For $z > b$, the reference height is the current height, therefore $\overline{z}_e = z$; in particular, when $z = h$, $q_p(\overline{z}_e) = q_p(h) = 1.555$ N/m^2.

The external pressure on the shell is calculated by applying the rules given in clause G.3.2.2. With reference to Equation G.1, the external pressure coefficient c_{pe} is given by the product of the external pressure coefficient c_{peo}, with reference to a circular cylinder of an infinite length, and a coefficient $\psi_{\lambda\alpha}$ that takes into account the finite length of the cylinder.

The coefficient c_{peo} depends on Reynolds number Re and on surface roughness of the cylinder k. By applying the rules provided in clause 3.3.7, the Reynolds number Re is given by Equation (3.16), where $b = 35{,}2$ m; the mean wind velocity is calculated, for simplicity, at height $z = h$, therefore $v_m(h) = 34{,}45$ m/s; $\upsilon = 15 \cdot 10^{-6}$ m^2/s. Thus, $Re = 80{,}8 \cdot 10^6$. Considering the presence of the vertical ribs along the shell, it is assumed that $k = 0.16$ m; thus $k/b = 4{,}55 \cdot 10^{-3}$. Lastly, in the lack of more detailed data and more accurate assessments, the parameters given in Table G.VIII are applied for $Re = 10^7$ and $k/b = 0{,}5 \cdot 10^{-3}$: $c_{pm} = -1.5$, $c_{pb} = -0.8$, $\alpha_m = 75°$, $\alpha_b = 105°$. The external pressure coefficient c_{peo} thus is (Equation G.2):

$$c_{peo}(\alpha_p) = 1 - 2{,}5 \cdot \sin^2\left(\frac{\pi \cdot \alpha_p}{150}\right) \qquad \text{for } 0 \le \alpha_p \le 75°$$

$$c_{peo}(\alpha_p) = -0{,}8 - 0{,}7 \cdot \cos^2\left(\frac{\pi}{2} \cdot \frac{\alpha_p - 75}{30}\right) \qquad \text{for } 75° \le \alpha_p \le 105°$$

$$c_{peo}(\alpha_p) = -0{,}8 \qquad \text{for } 105° \le \alpha_p \le 180°$$

where α_p is expressed in degrees (°).

By applying the Equation (G.3) with $\psi_\lambda = 2/3$, the coefficient $\psi_{\lambda\alpha}$ is:

$$\psi_{\lambda\alpha} = 1 \qquad\qquad\qquad\text{for} \quad 0° \leq \alpha_p \leq 75°$$

$$\psi_{\lambda\alpha} = \frac{2}{3} + \frac{1}{3} \cdot \cos\left[\frac{\pi}{2} \cdot \left(\frac{\alpha_p - 75}{30}\right)\right] \qquad\qquad \text{for} \quad 75° \leq \alpha_p \leq 105°$$

$$\psi_{\lambda\alpha} = \frac{2}{3} \qquad\qquad\qquad\text{for} \quad 105° \leq \alpha_p \leq 180°$$

where α_p is expressed in degrees (°).

Figure 4.7.2 shows the graphs of c_{peo}, $\psi_{\lambda\alpha}$ and c_{pe} as functions of the angle α_p.
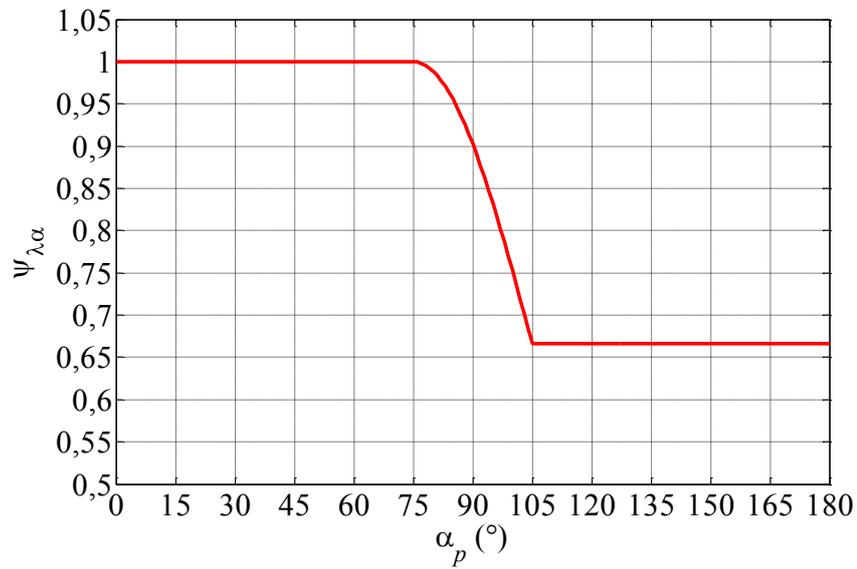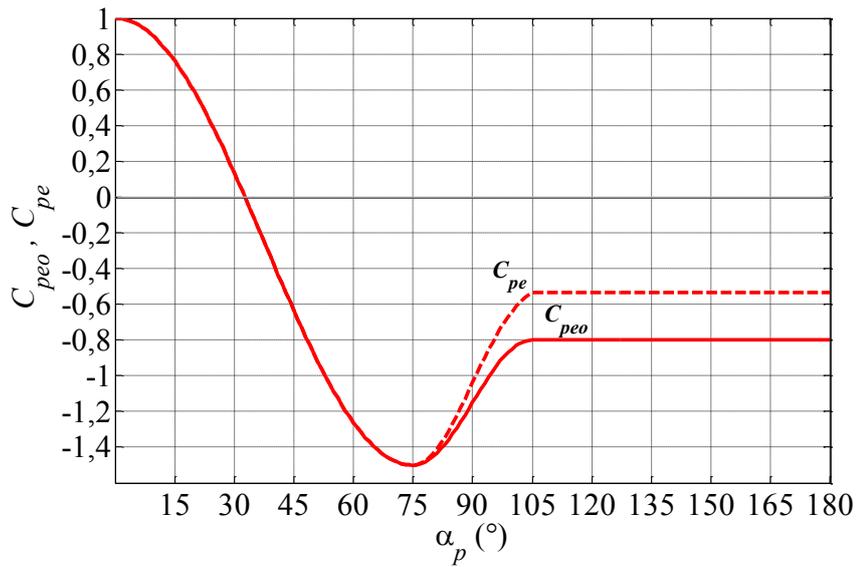
Figure 4.7.2 - Graphs of: (a) c_{peo} and c_{pe}; (b) $\psi_{\lambda\alpha}$;.

4.7.2 External pressure on the dome

Assuming $f = 4.75$ m as the height of the dome in respect to the top of the shell, and by using the criterion illustrated in clause G.3.3, the reference height for the external pressure on the dome is $\overline{z}_e = h + f/2 = 61{,}375$ m (Figure G.18); therefore, $q_p(\overline{z}_e) = 1.570$ N/m^2.

The external pressure coefficients on the dome are calculated by means of the criterion illustrated in Figures G.18 and G.19, having set $h/d = 59/35{,}2 = 1.68$ and $f/d = 4{,}75/35{,}2 = 0{,}135$. Table 4.7.I gives the values of the pressure coefficients and the pressure in the three reference positions indicated, in Figure G.18, with codes A, B and C.

Table 4.7.I - External pressure coefficients and external pressure.

Position	c_{pe}	p_e (N/m^2)
A	-1,65	-2.590
B	-0,9	-1.413
C	-0,5	-785

4.7.3 Internal pressure

Internal pressure is calculated by applying the criterion given in clause G.4.4.

Given the presence of openings at the top of the shell and in the fairing, the reference height of internal pressure is assumed $\overline{z}_e = h + f = 63{,}75$ m; therefore, $q_p(\overline{z}_e) = 1.583$ N/m^2.

The internal pressure coefficient assumes the values $c_{pi} = -0.4$ and $c_{pi} = 0$, for the worst load case. Consequently, $p_i = -633$ N/m^2 and $p_i = 0$.

4.7.4 Dynamic parameters

The dynamic parameters of the gasholder were calculated by means of finite element modelling and by applying the criteria given in Annex I.

Figure 4.7.3 gives a finite element model that ignores, for simplicity, the presence of the internal piston. As a first approximation, this is equivalent to suppose that the piston is located at the base.

Figure 4.7.4 illustrates the first mode shapes of the structure. Given the double symmetry, the mode shapes are presented in pairs. The first 2 modes, with frequency $n_1 = n_2 = 4.70$ Hz, represent an overall crosswind bending (Figure 4.7.4a). Modes 3 and 4 ($n_3 = n_4 = 5{,}28$ Hz, Figure 4.7.4b), 5 and 6 ($n_5 = n_6 = 6{,}29$ Hz, Figure 4.7.4c) and 7 and 8 ($n_7 = n_8 = 6{,}70$ Hz, Figure 4.7.4d) represent ovalling modes with deformation at 3, 4 and 2 lobes, respectively.

In the lack of more accurate data, the structural damping ratio is set equal to the minimum value of those provided for metal chimneys (clause I.6.2), therefore $\xi_s = 0{,}002$. This value is applied to all vibration modes.

(a)   (b)
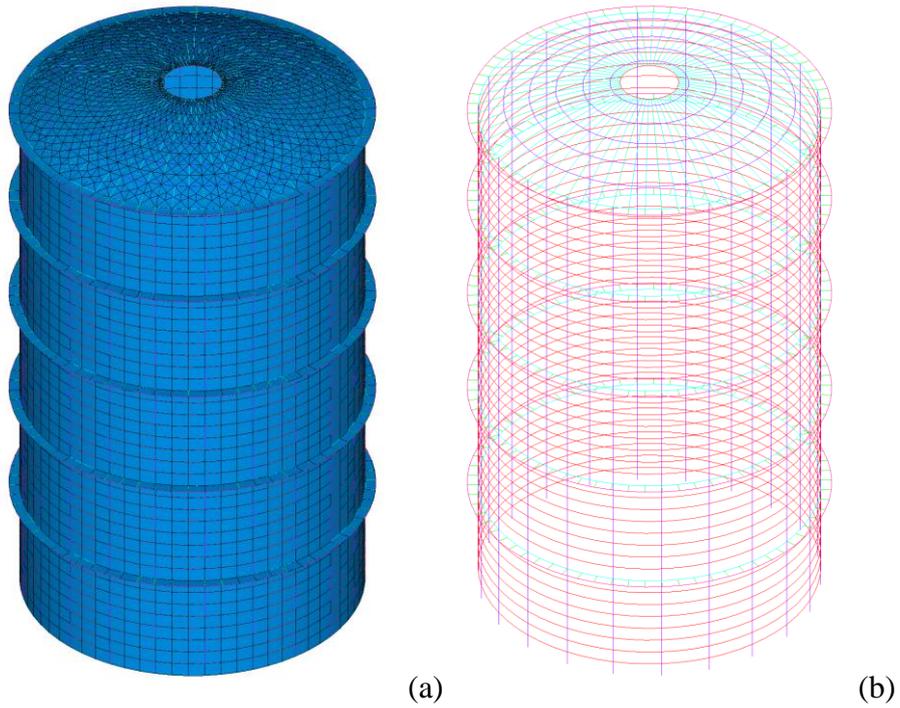
Figure 4.7.3 - Finite element model: shell (a) and beam (b) elements.

(a)   (b)
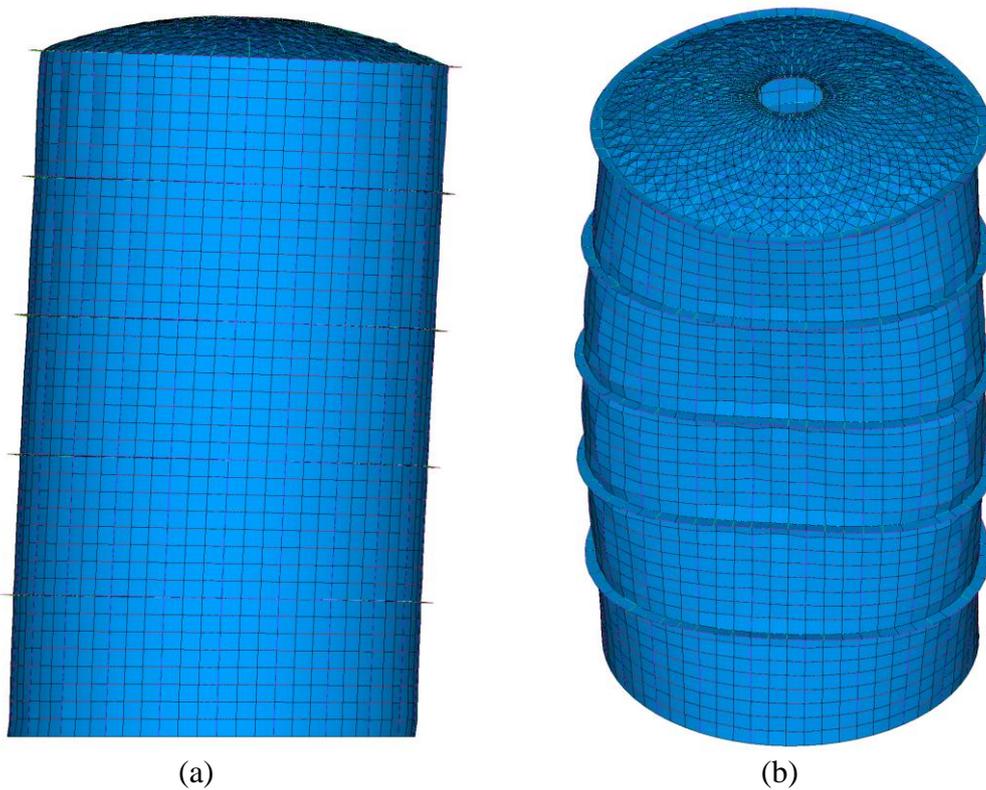
Figure 4.7.4 - Mode shapes 1 and 2 ($n_1 = n_2 = 4{,}70$ Hz) (a);
mode shapes 3 and 4 ($n_3 = n_4 = 5{,}28$ Hz) (b).
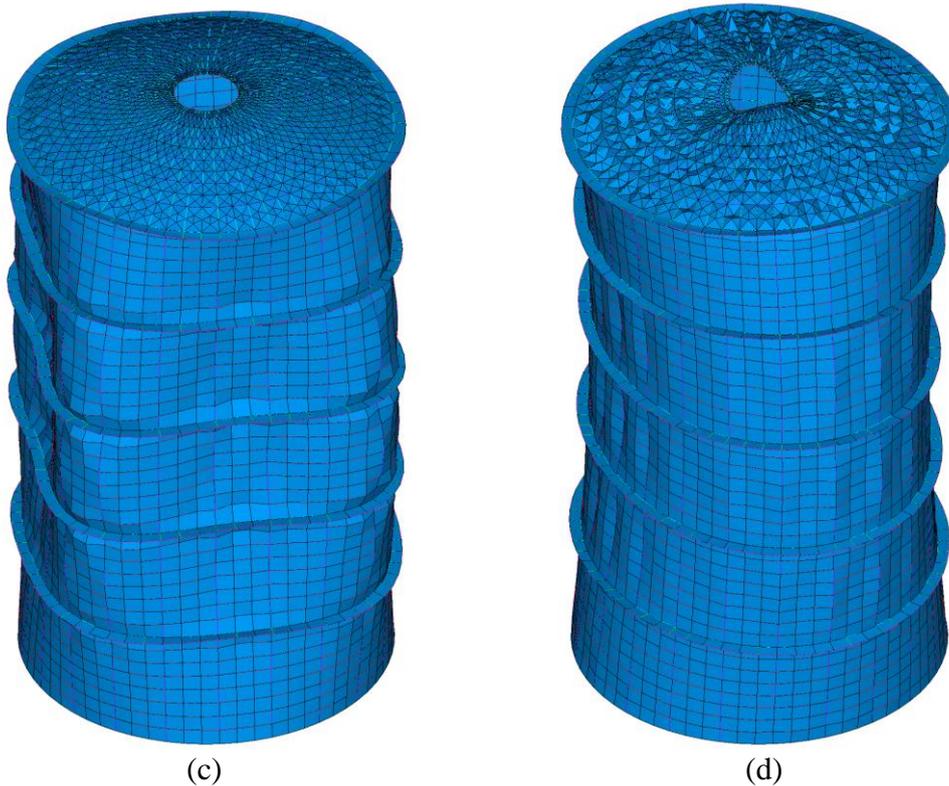
Figure 4.7.4 (cont.) - Mode shapes 5 and 6 ($n_5 = n_6 = 6{,}29$ Hz) (c);
mode shapes 7 and 8 ($n_7 = n_8 = 6{,}70$ Hz) (d).

4.7.5 Dynamic factor and equivalent static actions

The gasholder has a fundamental frequency $n_1 = 4.70$ Hz > 2 Hz; width is $b = 35{,}2$ m > 25 m; total height is 63,75 m < 75 m. Thus, in the lack of more accurate assessments, clause 3.4.1 may be used to give the dynamic factor the value $c_d = 1$. Therefore, according to Equation (3.17), the equivalent static actions coincide with the peak aerodynamic actions.

4.7.6 Vortex shedding

The dynamic response of the structure to vortex shedding should be determined whenever it is possible that a mean wind velocity may occur that is capable of inducing a resonant vortex shedding frequency with the frequency of an across-wind vibration mode.

By applying the criteria given in clause O.1, the first critical velocity caused by resonant vortex shedding with an across-wind vibration mode is given by Equation (O.2), where $n_{L,1} = n_1 = n_2 = 4{,}70$ Hz, $b = 35{,}2$ m is the diameter, St is the Strouhal number. As a first approximation (clause O.2), $St = 0{,}2$. Thus, $v_{cr,1} = 827{,}2$ m/s.

The mean wind velocity at the top of the shell, $h = 59$ m, with design return period $T_R = 500$ years, is equal to $v_{m,l} = 34{,}45 \times 1{,}207 = 41{,}58$ m/s. Thus, since $v_{cr,1} = 827.2$ m/s $> v_{m,l} = 41{,}58$ m/s, no verification is required as regards resonant vortex shedding, Equation (O.3).

4.7.7 Ovalling

The shell of the gasholder is potentially prone to static or dynamic ovalling (clause O.10).

Static ovalling arises because of the distribution of the radial pressures on the external (clause 4.7.2) and internal faces (clause 4.7.3) of the shell. It is therefore necessary to perform an accurate calculation of the stresses generated by these pressures and to carry out suitable local and global checks of the shell.

Dynamic ovalling is analysed by means of two different criteria (clause O.10).

By applying the first criterion, the minimum value of the critical velocity of ovalling (the most hazardous) is given by Equation (O.19), setting $n_{O,1} = n_3 = n_4 = 5,28$ Hz (Figure 4.7.4b), $b = 35,2$ m, $\Omega = 4$. The Strouhal number St is a function of Reynolds number (clause O.2); in this particular case $St = 0,22$. Thus, $v_{O,1} = 211,2$ m/s.

By applying the second criterion, the minimum value of the critical velocity of ovalling is given by Equation (O.20), setting $n_{O,1} = 5,28$ Hz, $\rho_s = 7850$ kg/m^3, $\rho = 1,25$ kg/m^3, $t = 0.005$ m, $b = 35,2$ m, $\xi_{O,1} = 0,002$. Thus, $v_{O,1} = 64,26$ m/s.

The lower value, to be considered in the next verification, is equal to $v_{O,1} = 64,24$ m/s.

The mean wind velocity at the top of the shell, $h = 59$ m, with design return period $T_R = 500$ years is equal to $v_{m,l} = 41,58$ m/s (clause 4.7.5). Thus, since the above critical velocity of ovalling is estimated to be higher than this limit, $v_{O,1} = 64,24$ m/s, the check of dynamic ovalling is satisfied, Equation (O.21).

4.8   CANOPY ROOF

The structure examined in this clause is an agricultural canopy, described in the technical publication "*Particolari costruttivi di strutture in acciaio*" (Detailing of Steel Structures), published by CISIA - *Centro Italiano Sviluppo Impieghi Acciaio* (Italian Centre for the Development of Steel Applications) - Milan (Figures 4.8.1.-4.8.3).

The canopy is the coupling of two duopitch canopies. It is rectangular in plan, $30 \times 22,28$ m. The ridge line is located at a height of 7 m. The eaves are located at a height of 4.7 m. Thus the slope is $\alpha = 22,44°$.

The structural scheme consists of single-bay portal frames whose columns are pinned at their base. In the longitudinal direction, stability is ensured by roof braces and wall shear bracing structures.

The roofing is in fibre-cement sheets on metal purlins.

Analysis is based on clauses 3.1-3.4 and Annexes G, H. The study is conducted, in a preliminary and simplified form, by examining only the aerodynamic actions induced by wind on the roofing sheets installed above the purlins.
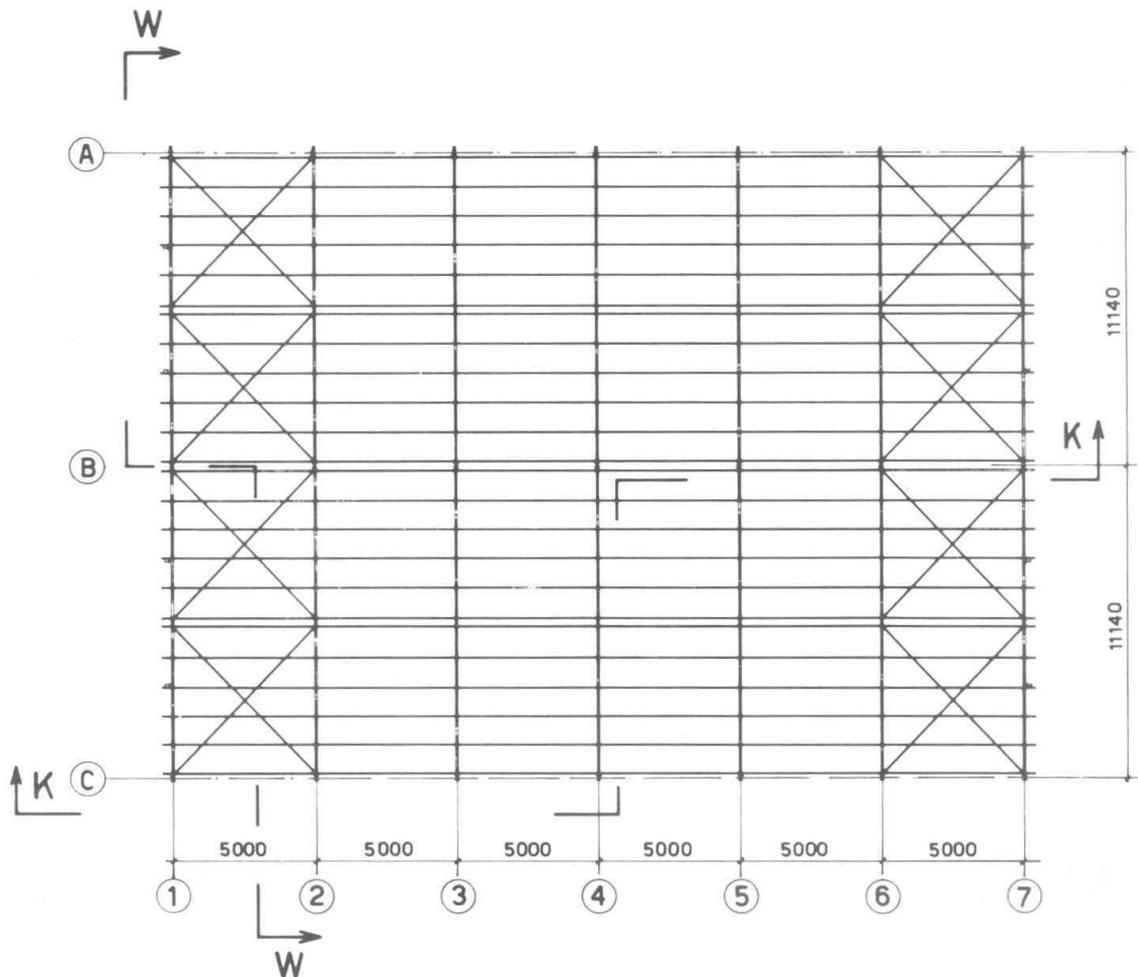
Figure 4.8.1 – Plan of the canopy roof.
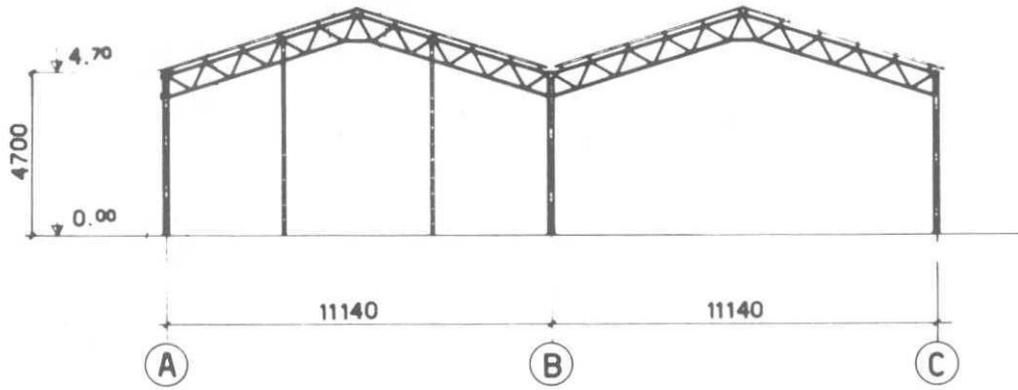
Figure 4.8.2 – Section W-W of the canopy.
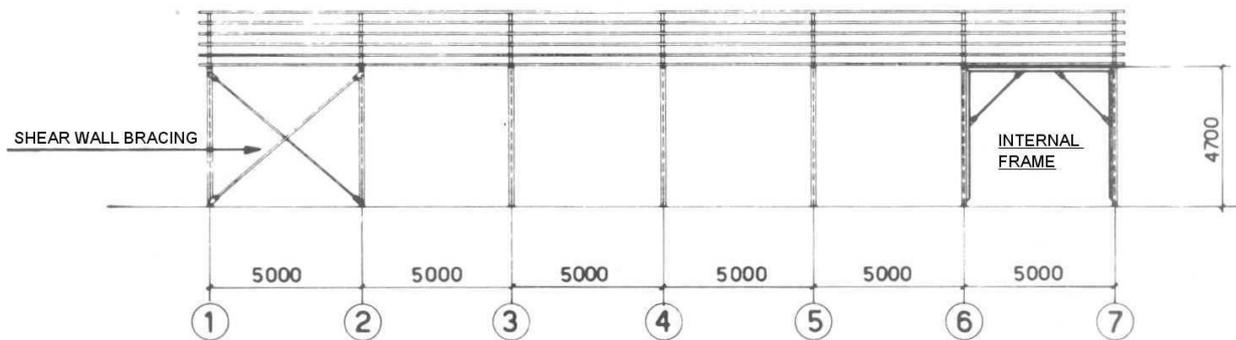
Figure 4.8.3 – Section K-K of the canopy.

Peak overall and local aerodynamic actions are calculated by means of clause 3.3. By using the rules given in clause 3.3.3, the overall forces and moment on the roof are given by Equation (3.13), where q_p is the peak velocity pressure, c_{FX}, c_{FY}, c_{FZ} are the force coefficients in the three directions X, Y, Z, c_{MX}, c_{MY}, c_{MZ} are the moment coefficients around the three directions X, Y, Z, $\bar{z}$ and L are respectively the reference height and length corresponding to the aerodynamic coefficients; the aerodynamic coefficients and reference lengths are calculated by applying Annex G. The local actions on single elements of the roof are calculated by using the rules given in clause 3.3.2; net pressure is given by Equation (3.12), where q_p is the peak velocity pressure, c_{pn} is the overall pressure coefficient, $\bar{z}$ is the reference height; c_{pn} and $\bar{z}$ are calculated by applying Annex H.

The dynamic wind actions are calculated by means of clause 3.4. In particular, by using the rules given in clause 3.4.1, the equivalent static actions are expressed by the Equation (3.17), where c_d is the dynamic factor.

All analyses given below relate to the case in which the wind is at right angles with respect to the ridge lines. The actions associated with the absence of obstacles (degree of blockage $\varphi = 0$) and those associated with the presence of a full blockage ($\varphi = 1$) are considered.

Clause 4.8.1 gives the calculation of overall actions on the roof. Clause 4.8.2 gives the calculation of the local net pressure on the roofing elements. Clause 4.8.3 discusses the calculation of the dynamic factor and the equivalent static actions.

4.8.1 Overall actions on the roof

By applying the indications given in clause G.6.3, the force coefficients for canopies consisting of two adjacent duopitch roofs (of equal slope) are the same as those given in clause G.6.2 for single duopitch canopies, multiplied by the coefficients given in Table G.XIV. In this particular case, these coefficients are all equal to 1.

In accordance with clause G.6.2, the reference height is equal to the height of the eaves, $\bar{z} = h = 4{,}7$ m; therefore, $q_p(\bar{z}) = 778$ N/m^2. The reference area is equal to the area of each slope of the canopy; thus $L^2 = 30 \cdot 11.14/2 = 167{,}1$ m^2. The force coefficients c_F are determined with reference to Table G.XIII and Figure G.28 at $\alpha = 22{,}44°$; they are given in Table 4.8.I for blockage $\varphi = 0$ and $\varphi = 1$. The overall force $F = q_p(\bar{z}) \cdot L^2 \cdot c_F$, perpendicular to each slope of the canopy, takes the values given in Table 4.8.II. This force acts at a distance d/4 = 11.14/4 = 2.785 m from the eaves of each slope in accordance with the outline shown in Figure G.29a.

Table 4.8.I – Force coefficients of the canopy.

Blockage φ	c_F (positive values)	c_F (negative values)
0	0,72	-0,89
1	0,72	-1,40

Table 4.8.II - Forces on each pitch of the canopy (kN).

Blockage φ	F (positive values)	F (negative values)
0	93,6	-115,7
1	93,6	-182,0

4.8.2 Local actions on the roof

By applying the indications given in clause H.4.3, the net pressure coefficients for canopies consisting of two adjacent duopitch roofs (of equal slope) are the same as those given in clause H.6.2 for single duopitch canopies, multiplied by the coefficients given in Table G.XIV. In this particular case, these coefficients are all equal to 1.

In accordance with clause H.4.2, $b = 30$ m, $d = 11.14$ m (Figure H.20), $\bar{z} = h = 4.7$ m (Figure H.21); therefore, $q_p(\bar{z}) = 778$ N/m^2. By using the criterion in Figure H.20, the roof is divided into zones as illustrated in Figure 4.8.4; by means of Table H.VIIIa, the corresponding net pressure coefficients for each of these zones is given in Table 4.8.III. Lastly, by applying Equation (3.12), the net pressure on the roof takes the values given in Table 4.8.IV. By definition, positive pressures act downwards; negative pressures act upwards.
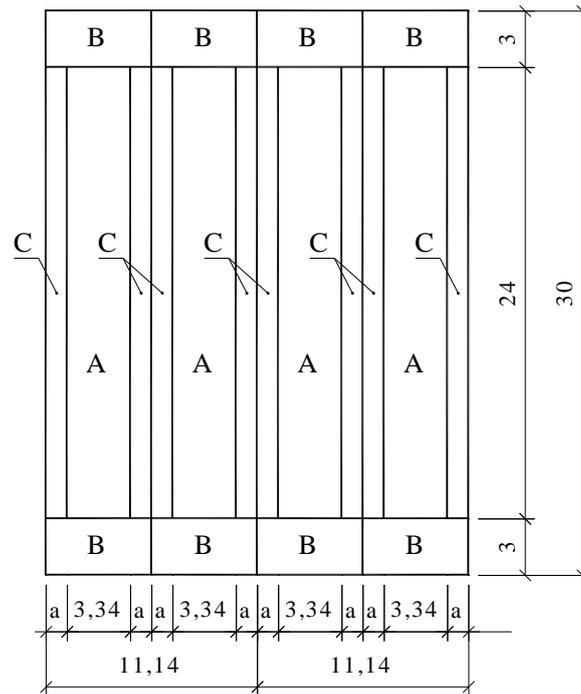
Figure 4.8.4 – Roof zones with uniform net pressure (a = 1.114 m).

Table 4.8.III – Net pressure coefficients on the canopy roof.

Zone	c_{pn} (maximum)	c_{pn} (minimum, $\varphi = 0$)	c_{pn} (minimum, $\varphi = 1$)
A	+1,15	-1,30	-1,40
B	+1,90	-1,85	-2,10
C	+1,55	-1,40	-1,55
D	+0,45	-2,00	-2,05

Table 4.8.III - Net pressure on the canopy roof (N/m^2).

Zone	p_n (maximum)	p_n (minimum, $\varphi = 0$)	p_n (minimum, $\varphi = 1$)
A	+894,7	-1011,4	-1089,2
B	+1478,2	-1439,3	-1633,8
C	+1205,9	-1089,2	-1205,9
D	+350,1	-1556,0	-1594,9

4.8.3 Dynamic factor and equivalent static actions

This Guide, like most International standards, does not provide any guidance towards the value to be given to the dynamic factor c_d. Since these aerodynamic actions are at right angles to the roof slopes, the frequency to be taken into account is that of the dominant vertical oscillations of the canopy. Considering that the columns have high axial stiffness and assuming that the roof structure has high flexural stiffness, as a first approximation one may set $c_d = 1$. Thus, in the lack of more accurate assessments, it may be assumed that the equivalent static actions coincide with the peak aerodynamic actions calculated at clause 4.8.1.

4.9 REINFORCED CONCRETE CHIMNEY

The structure examined in this clause is a power plant reinforced concrete chimney with variable cross section. The structure has a height of 195 m. The external diameter at the base is 12,60 m, with a structural thickness of 0,35 m; the external diameter at the top is 8,70 m, with a structural thickness of 0,15 m. It is assumed that both the diameter and the thickness change linearly between the base and the top of the chimney. Figure 4.9.1 gives the vertical profiles of mass per unit length, m, and of the moment of inertia of the cross section, J_f. For the purpose of a finite element calculations, the chimney is divided into 19 prismatic elements; Table 4.9.I gives, for each element, the heights of the lower node and the upper node, z_i and z_s, and the areas and moments of inertia of the cross section. The elements are numbered starting from the base of the chimney.
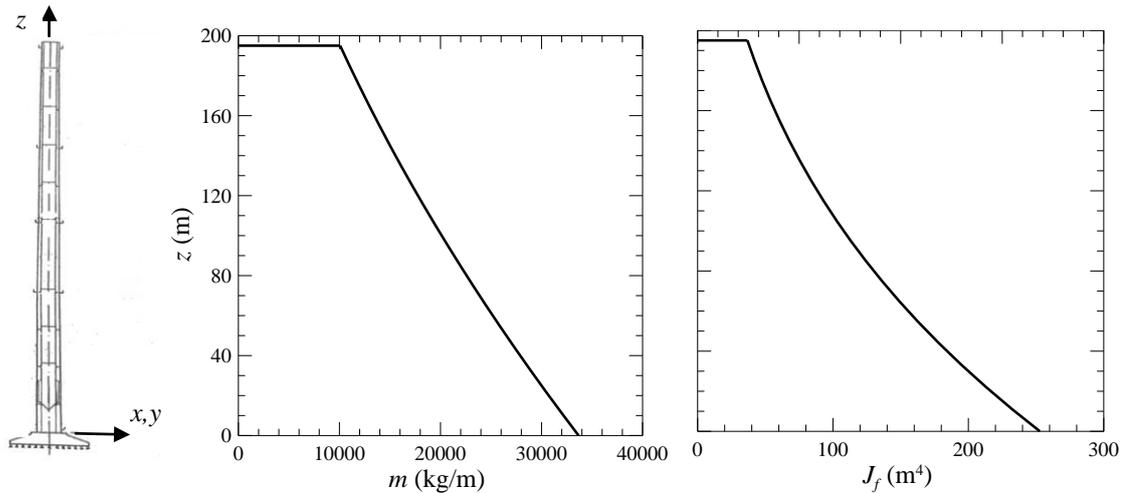
Figure 4.9.1 – Reinforced concrete chimney

Table 4.9.I – Areas and moments of inertia of the reinforced concrete chimney.

Element	z_i -z_s (m)	Area (m^2)	Inertia (m^4)
1	0-11	13,14	242,48
2	11-22	12,49	222,65
3	22-33	11,86	204,01
4	33-44	11,24	186,53
5	44-55	10,63	170,16
6	55-65	10,07	155,51
7	65-75	9,55	142,43
8	75-85	9,03	130,15
9	85-95	8,53	118,64
10	95-105	8,05	107,87
11	105-115	7,57	97,82
12	115-125	7,11	88,44
13	125-135	6,66	79,71
14	135-145	6,22	71,60
15	145-155	5,79	64,09
16	155-165	5,38	57,13
17	165-175	4,98	50,71
18	175-185	4,59	44,80
19	185-195	4,21	39,37

Analysis is performed by applying Annexes G, I, L and O.

Starting from the calculations made in clause 4.2, analysis proceeds in two stages.

In the first stage the along-wind wind actions are determined. In particular, calculations concern the peak aerodynamic actions (clause 4.9.1), the dynamic parameters of the structure (clause 4.9.2), the dynamic factor and the equivalent along-wind static force (clause 4.9.3).

The second stage deals with the determination of the actions for the critical velocities of wind that cause a vortex shedding resonant with the structure vibration. In particular, initial calculations concern the critical wind velocities and the corresponding Scruton numbers (clause 4.9.4). Subsequently, the peak tip deflections are determined, by using both the spectral method (clause 4.9.5) and the harmonic method (clause 4.9.6); these are used to calculate the equivalent across-wind static forces (clause 4.9.7).

4.9.1 Peak aerodynamic actions

By applying the rules given in clause 3.3.4, the peak aerodynamic actions per unit height are given by the Equation (3.14), where q_p is the peak velocity pressure at the current height z of the structure, c_{fX}, c_{fY} and c_{mZ} are the force and moment coefficients per unit height, and l is the reference size.

The peak velocity pressure is given at clause 4.2.7. In particular, for $h = 195$ m e $T_R = 50$ years, $q_p(h) = 2.012$ N/m^2.

The aerodynamic coefficients and reference size are calculated by applying Annex G. In particular, for slender structures and elongated structural elements, clause G.10.1 assigns $c_{fX} = c_{fXo}\cdot\psi_\lambda$, $c_{fY} = c_{fYo}\cdot\psi_\lambda$, $c_{mZ} = c_{mZo}\cdot\psi_\lambda$, (Equation G.18), where c_{fXo}, c_{fYo}, c_{mZo} are the aerodynamic coefficients for structures and elements of ideally infinite length, and ψ_λ is the slenderness reduction coefficient.

The coefficients c_{fXo}, c_{fY} and c_{mZo} and the reference size l for slender structures and elongated elements with a circular cross section are given in clause G.10.6: l is equal to diameter b of the current cross section of the structure; $c_{fYo} = c_{mZo} = 0$ for the polar symmetry of the cross section; c_{fXo} depends on Reynolds number Re and surface roughness k. By applying the rules given in clause 3.3.7, the Reynolds number Re at the top of the structure is given by Equation (3.16), where $b = 8.70$ m, $v_m(h) = 40,91$ m/s; $\upsilon = 15\cdot10^{-6}$ m^2/s. Therefore, $Re = 2,37\cdot10^7$. Assuming that the external surface of the chimney is in smooth concrete, Table G.XVII provides $k = 0.2$ mm; then, at the top of the structure, $k/b = 2,299\cdot10^{-5}$. By applying Equation (G.22b), $c_{fXo} = 0,78$. However, this value depends on the height z above the ground; for simplicity and conservatively it is assumed that this parameter remains constant.

The slenderness coefficient ψ_λ is given at clause G.10.8 for the effective slenderness λ. From Table G.XIX, $\lambda = 0.7\cdot L/l$, where $L = h = 195$ m, $l = b = 8,70$ m (conservatively); thus, $\lambda = 15,69$. Lastly, by applying the Equation (G.23b), $\psi_\lambda = 0,75$.

The force coefficient per unit height in the wind direction is therefore $c_{fX} = c_{fXo}\cdot\psi_\lambda = 0,78\cdot0,75 = 0,58$.

The peak along-wind aerodynamic force per unit height is the product of the peak velocity pressure (clause 4.2.7), the diameter b of the current section (Figure 4.9.1), and the force coefficient per unit height c_{fX}. Consequently:

$$f_X(z) = 778,21 \cdot (12,6 - 0,02 \cdot z) \cdot 0,58 \qquad\qquad \text{for } z \leq 5 \text{ m}$$

$$f_X(z) = 18,22 \cdot \ln\left(\frac{z}{0,1}\right) \cdot \left[\ln\left(\frac{z}{0,1}\right) + 7\right] \cdot (12,6 - 0,02 \cdot z) \cdot 0,58 \qquad \text{for } z > 5 \text{ m}$$

where z is expressed in m and f_x is expressed in N/m.

4.9.2 Dynamic parameters

The dynamic parameters of the chimney are calculated by means of a finite element model and by applying the criteria given in Annex I.

Given the polar symmetry, the vibration modes occur in pairs. Finite element analysis indicates that the first two natural frequencies are $n_1 = n_2 = 0,26$ Hz. The third and fourth natural frequencies are $n_3 = n_4 = 1,22$ Hz. The first two mode shapes are well approximated as $\Phi_1(z)=\Phi_2(z)=(z/h)^\zeta$ (clause I.3.1), where $h = 195$ m and $\zeta = 1,7$ (Figure 4.9.2a) (the choice of the parameter $\zeta = 1,7$ is not consistent with the provision of clause I.3.1, since it is based on more accurate calculations performed with the finite element method). Mode shapes 3 and 4 are reasonably approximated as $\Phi_3(z)=\Phi_4(z)=-5,5 \cdot (z/h)^2 + 8 \cdot (z/h)^3 - 1,5 \cdot (z/h)^4$ (clause I.3.3), where $h = 195$ m (Figure 4.9.2b). Table 4.9.II gives the values taken by the modes at the nodes of the structure; the modes are normalised to an unit tip displacement.
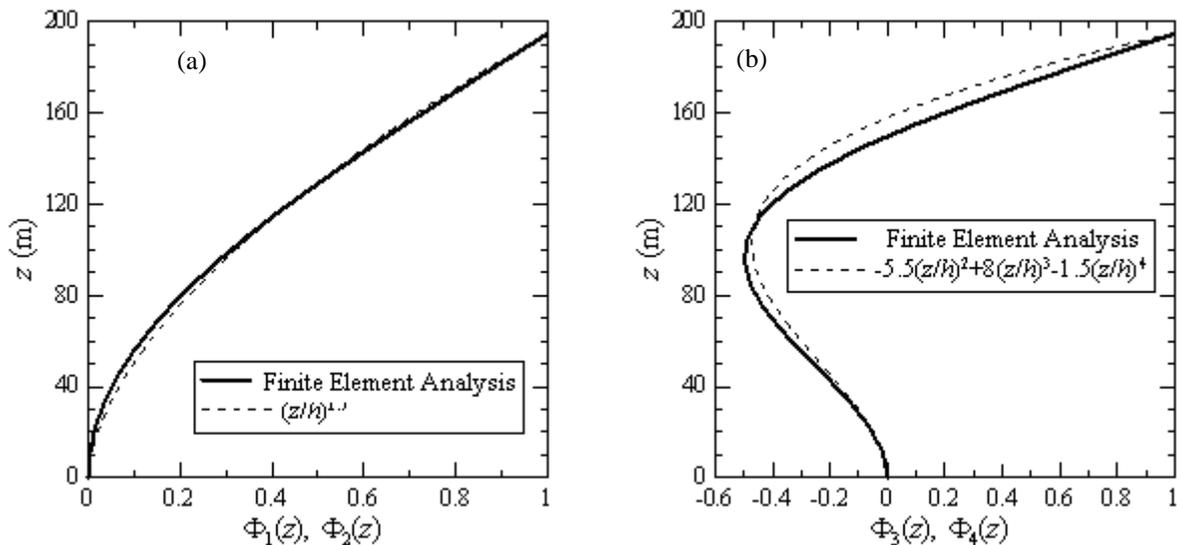
Figure 4.9.2 – First four mode shapes of the reinforced concrete chimney.

Table 4.9.II – Mode shapes of the reinforced concrete chimney.

z (m)	$\Phi_1(z), \Phi_2(z)$	$\Phi_3(z), \Phi_4(z)$
0	0,0000	0,0000
11	0,0040	-0,0167
22	0,0157	-0,0622
33	0,0353	-0,1297
44	0,0625	-0,2109
55	0,0972	-0,2970
65	0,1351	-0,3714
75	0,1787	-0,4343
85	0,2278	-0,4788
95	0,2820	-0,4982
105	0,3410	-0,4872
115	0,4042	-0,4417
125	0,4713	-0,3597
135	0,5416	-0,2409
145	0,6146	-0,0875
155	0,6897	0,0962
165	0,7662	0,3041
175	0,8437	0,5288
185	0,9218	0,7628
195	1,0000	1,0000

The equivalent mass can be calculated directly from its definition, Equation (I.26); approximating the integrals with the Simpson's rule, $m_{e,1} = m_{e,2} = 13.577$ kg/m and $m_{e0.3} = m_{e0.4} = 16.323$ kg/m. On the other hand, by applying the approximate criterion given at clause I.4, the equivalent mass per unit height for the first two modes is equal to the mean value of the mass along the upper third of the chimney (mean of the last seven elements of the chimney, Figure 4.9.1). Inasmuch, $m_{e,1} = m_{e,2} = 13.514$ kg/m. As can be seen, it is a quite accurate approximation.

The critical damping ratio is determined by using the rules given in clause I.6. On the basis of Equation (I.28), it is given by the sum of three contributions.

By applying Table I.III, the structural damping ratio in the first two vibration modes is $\xi_{s,1} = \xi_{s,2} = 0,005$. The same value is taken for the damping ratio for the two upper modes, $\xi_{s,3} = \xi_{s,4} = 0,005$.

The aerodynamic damping ratio is essential for the along-wind oscillations of the structure but on the other hand cannot be taken into account as regards across-wind oscillations caused by resonant vortex shedding. By assuming for simplicity that mode 1 is along-wind and mode 2 is across-wind, the damping ratio ξ_a is given by Equation (I.33), where $c_{fX} = 0,58$, $\rho = 1,25$ kg/m^3, $b = 8,.70$ m (conservatively), $z_e = 0,6 \cdot h = 117$ m (Figure L.2), $v_m(z_e) = 38,15$ m/s (clause 4.2.5), $n_D = 0,26$ Hz, $m_D = 13.514$ kg/m. Thus, $\xi_a = 0,0054$.

It is lastly assumed that no damping device is installed on the structure.

The overall damping ratio is thus $\xi_1 = 0,005 + 0,0054 = 0,0104$ for the calculation of equivalent along-wind static actions, and $\xi_2 = 0,005$ for the calculation of equivalent across-wind static actions associated with resonant vortex shedding.

4.9.3 Dynamic factor and equivalent along-wind static force

The dynamic actions and effects in the along-wind direction are calculated through the rules given in clause 3.4.

In accordance with Equation (3.17), the equivalent along-wind static force per unit height is the product of the peak aerodynamic force per unit height (clause 4.9.1) and the dynamic factor c_d. In this case, $c_d = c_{dD}$, since c_{dD} is the longitudinal (along-wind) dynamic coefficient. In the lack of more accurate assessments, it is determined by applying the criteria in Annex L.

By applying the detailed method (clause L.2), the dynamic factor c_{dD} is given by Equation (L.2). It is assessed by means of the method indicated in Table L.I. The chimney corresponds to the first case in Figure L.2. Table 4.9.III summarises the steps towards the calculation of c_{dD}.

Table 4.6.III - Calculation of the longitudinal (along-wind) dynamic factor.

Equation	Parameter
Figure L.2	$h = 195$ m
	$b = 8,7$ m
	$z_e = 117$ m
(3.5)	$v_m(z_e) = 38,15$ m/s
(3.7)	$I_v(z_e) = 0,142$
(3.8)	$L_v(z_e) = 223,39$ m
F.E. Analysis	$n_D = 0,26$ Hz
(I.29)	$\xi_D = 0,0104$
(L.4)	$B^2 = 0,541$
(L.6)	$S_D = 0,096$
(L.9)	$\eta_h = 5,316$
(L.9)	$\eta_b = 0,237$
(L.7)	$R_h = 0,170$
(L.8)	$R_b = 0,859$
(L.5)	$R_D^2 = 1,061$
(L.11)	$\upsilon_D = 0,212$ Hz
(L.10)	$g_D = 3,298$
(L.3)	$G_D = 2,182$
(L.2)	$c_{dD} = 1,096$

Note that when aerodynamic damping is ignored and calculation of the dynamic factor is then performed with $\xi_D = 0,005$, the result is $c_{dD} = 1,287$.

4.9.4 Critical velocities (vortex shedding) and Scruton numbers

The equivalent static actions associated with vortex shedding in resonance with the structure vibration are assessed by applying the criteria given in Annex O. It is therefore necessary to firstly determine the critical velocities, i.e. the mean wind velocities that cause resonant vortex shedding, and the relative Scruton numbers.

The critical wind velocity for the i-th across-wind vibration mode, $v_{cr,i}$, is given by Equation (O.2), where $n_{L,i}$ is the i-th natural across-wind frequency, b is the diameter, St is the Strouhal number. It is implemented provided that $v_{cr,1} \leq v_{m,l}$, where $v_{m,l}$ is the mean wind velocity at the tip of the structure, with return period $T_R = 500$ years (Equation O.3); then, $v_{m,l} = 49,38$ m/s (clause 4.2.5).

The first across-wind frequency is $n_{L,i} = 0,26$ Hz, and the mode shape is maximum at the tip of the chimney (clause 4.9.2); thus, Equation (O.2) must be applied to the height $z = 195$ m, where $b = 8,70$ m (clause O.1, Figure O.3). Strouhal number is a function of the Reynolds number and therefore of the critical wind velocity; in principle, the resolution of Equation (O.2) requires an iterative calculation. It is possible to proceed as follows: 1) initially set $St = 0,2$, followed by $v_{cr,1} = 11,31$ m/s; 2) determine the Reynolds number by means of Equation (3.16), $Re = 6,56 \cdot 10^6$; 3) calculate the Strouhal number St by means of Table O.I and Figure O.4, $St = 0,22$; 4) the final value of the critical velocity $v_{cr,1} = 10,28$ m/s is obtained at the corresponding $Re = 5.96 \cdot 10^6$ (considering the level of convergence achieved, further iterations are not necessary). Since $v_{cr,1} = 10,28$ m/s $< v_{m,l} = 49,38$ m/s, a specific verification associated with resonant vortex shedding with the first vibration mode is required.

The second across-wind frequency is $n_{L,2} = 1.22$ Hz; Equation (O.2) is applied again to the height $z = 195$ m, where $b = 8,70$ m and $St = 0,22$. The result is a critical velocity of $v_{cr,2} = 48,25$ m/s (considering the level of convergence achieved, further iterations are not necessary). Thus, since $v_{cr,2} = 48,25$ m/s $< v_{m,l} = 49,38$ m/s, the second across-wind mode also needs to be checked against resonant vortex shedding. Higher vibration modes (with higher frequencies) may be excluded from this verification since the critical velocity of the second mode is very close to the limit velocity $v_{m,l}$.

The Scruton number associated with the first across-wind vibration mode, and with the first critical velocity, is given by the Equation (O.4), where $m_{e,1} = 13,514$ kg/m is the equivalent mass per unit height (clause 4.9.2), $\xi_1 = 0,005$ is the damping ratio,not including aerodynamic damping (clause 4.9.2), $\rho = 1,25$ kg/m^3, $b = 8.70$ m; then $Sc_1 = 8,97$. The Scruton number associated with the second across-wind vibration mode, and the second critical velocity, is given by Equation (O.4), where $m_{e,2} = 16,323$ kg/m is the equivalent mass per unit length (clause 4.9.2), $\xi_2 = 0,005$ is the damping factor $\rho = 1,25$ kg/m^3, $b = 8,70$ m; then $Sc_2 = 10,84$. It follows that the effects of vortex shedding must be analysed in detail.

Calculation of the equivalent across-wind static forces caused by critical vortex shedding in the first and second vibration mode is performed by means of the criterion given in clause O.4 (clause 4.9.7). It requires the preliminary calculation of the peak tip deflection. This calculation is performed, for the first vibration mode, by using both the spectral method (clause 4.9.5) and the harmonic method (clause 4.9.6). For the second vibration mode, analysis is limited only to the harmonic method (clause O.4.1).

4.9.5 Peak deflection - spectral method

Calculation of the peak deflection $y_{pL,1}$ by means of the spectral method is based on the rules given in clause O.5, in particular Equation (O.7), where g_L is the peak factor and σ_L is the standard deviation of deflection.

Parameter g_L depends on the Scruton number $Sc_1 = 8,97$ and on the aerodynamic damping parameter $K_a = K_{a,\max} \cdot C_I$ (Equation O.9). Since $Re = 6,56 \cdot 10^6$, $K_{a,\text{Max}} = 1$ (Table O.II, Figure O.8); Furthermore, since $v_{cr,1} = 10,28 > 10$ m/s (Equation O.10, Figure O.9), $C_I = 0.7$; then $K_a = 0,7$. Thus, in accordance with Equation (O.8), $g_L = 2,162$.

The parameter σ_L is given by Equations (O.11)-(O.13) for $a_L = 0,4$, $Sc_1 = 8,97$, $K_a = 0,7$, then $c_1 = -0,0016$; $\rho = 1,25$ kg/m^3, $b = 8,7$ m, $h = 195$ m, $m_{e,1} = 13.514$ kg/m, $K_a = 0,7$, $C_c = 0,01$, $St = 0.22$, then $c_2 = 3,048 \cdot 10^{-6}$. Thus, $\sigma_L/b = 0,028$, $\sigma_L = 0,240$ m.

Lastly, applying the Equation (O.7), $y_{pL,1} = 2,162 \cdot 0,240 = 0,519$ m.

4.9.6 Peak deflection - harmonic method

Calculation of the peak deflection $y_{pL,i}$ by means of the harmonic method is based on the rules given in clause O.6, in particular Equation (O.14). In this case, the harmonic method can be applied to the first and second modes.

For the first across-wind mode, $St = 0,22$, $Sc_1 = 8,97$, $K = 0,13$ (Table O.V). The lateral force coefficient c_{lat} is given by Table O.VI and Figure O.13 for the Reynolds number, since $Re = 6,56 \cdot 10^6$, $c_{lat} = 0,2253$.

The coefficient K_w depends on L_1/b and $\lambda = h/b = 22,41$, where L_1 is the effective correlation length. It is the most critical element to be calculated and it involves, in principle, the application of the iterative method described in clause O.6. It is possible to proceed as follows.

First, let us assign $L_1/b = 6$, assuming that $y_{pL,1}/b < 0.1$. Then determine $K_w = 0,6$ (Table O.V) and, consequently, $y_{pL,1}/b = 0,0405$, Equation (O.14). Since this value is consistent with the initial assumption, $y_{pL,1}/b < 0.1$, it is not necessary to iterate the analysis.

Therefore, $y_{pL,1} = 0,352$ m. As expected, this value is lower than the one given by the spectral method (clause 4.9.5).

For the second across-wind vibration mode, $St = 0,22$, $Sc_2 = 10,84$; the value of the mode shape factor K is calculated using the Equation (O.15), using Figure O.11 and approximating the integrals with the Simpson's rule: $K = 0,166$. The coefficient of lateral shape c_{lat} is given by Table O.VI and Figure O.13 for the Reynolds number; since $Re = 2,80 \cdot 10^7$, $c_{lat} = 0.3$.

In order to calculate coefficient K_w, start by assigning $L_1/b = L_2/b = 6$, consistently with the position of the node of the mode shape (Fig. 4.9.2b); it is also assumed that $y_{pL,2}/b < 0.1$. Then apply Equation (O.16), approximating the integrals with the Simpson's rule and determine $K_w = 0,6$ (Equation O.16). Consequently, $y_{pL,2}/b = 0,0570$, Equation (O.14). Since this value is consistent with the assumption $y_{pL,2}/b < 0,1$, it is not necessary to iterate the analysis.

Therefore, $y_{pL,2} = 0,4955$ m.

4.9.7 Static equivalent across-wind force

The static equivalent across-wind force associated with a vortex shedding resonant with the first across-wind vibration mode, $F_{L,1}$, is given by the Equation (O.5), where m is the mass per unit height given by Figure 4.9.1, $n_{L,1} = 0,26$ Hz, $\Phi_{L,1} = (z/h)^{1.7}$. By applying, the spectral method (clause 4.9.5), $y_{pL,1} = 0,519$ m is conservatively obtained.

The coefficient $C_{TR,1}$ depends on the critical velocity $v_{cr,1} = 10,28$ m/s, on the mean tip wind velocity (with T_R=50 years), $v_{m0.0} = 40,9$ m/s (clause 4.2.5) and on the mean tip wind velocity (with $T_R = 500$ years), $v_{m,l} = 49,38$ m/s. Then, applying the Equation (O.6), $C_{TR,1} = 1$.

Therefore, the static equivalent across-wind force associated with resonant vortex shedding with the first vibration mode is:

$$F_{L,1}(z) = 1,385 \cdot m(z) \cdot \left(\frac{z}{195}\right)^{1,7}$$

where z is expressed in m, m in kg/m and $F_{L,1}$ in N/m.

The static equivalent across-wind force associated with a vortex shedding resonant with the second across-wind vibration mode, $F_{L,2}$, is given by Equation (O.5), where m is the mass per unit length given by Figure 4.9.1, $n_{L,2} = 1,22$ Hz, $\Phi_{L,2} \cong -5,5 \cdot (z/h)^2 + 8 \cdot (z/h)^3 - 1,5 \cdot (z/h)^4$. By applying the harmonic method (clause 4.9.6), $y_{pL,2} = 0,4955$ m.

The coefficient $C_{TR,1}$ depends on the critical wind velocity $v_{cr,1} = 48,25$ m/s, on the mean tip wind velocity (with T_R=50 years), $v_{m0.0} = 40,9$ m/s (clause 4.2.5) and on the mean tip wind velocity (with $T_R = 500$ years), $v_{m,l} = 49,38$ m/s. Then, applying the Equation (O.6), $C_{TR,2} = 0,133$.

Therefore, the static equivalent across-wind force associated with resonant vortex shedding with the second vibration mode is:

$$F_{L,2}(z) = 3,872 \cdot m(z) \cdot \left[-5,5 \cdot \left(\frac{z}{195}\right)^2 + 8 \cdot \left(\frac{z}{195}\right)^3 - 1,5 \cdot \left(\frac{z}{195}\right)^4\right]$$

where z is expressed in m, m in kg/m and $F_{L,2}$ in N/m.

4.10 STEEL CHIMNEY

The structure examined in this clause is a tapered steel chimney, 100 m tall. The tapered portion at the base is 34 m high; the external diameters at the base and at $z = 34$ m are respectively 7,00 m and 3,80 m. The constant-section portion is 66 m tall and has an external diameter of 3,80 m. The structure is entirely welded and has no internal or external lining/cladding. Figure 4.10.1 gives the vertical profiles of mass per unit height, m, and the moment of inertia of the cross section J_f. Table 4.10.I gives the shell thicknesses s at the various sections, between heights z_i and z_s.
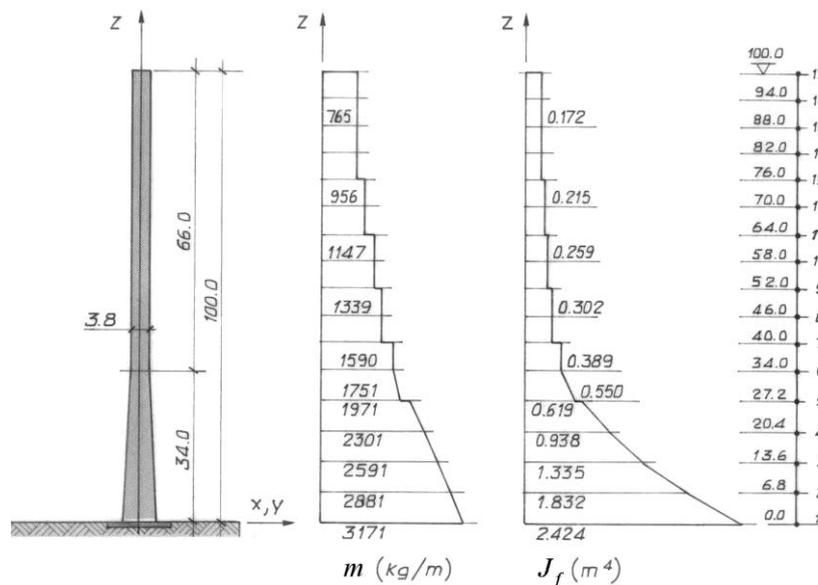
Figure 4.10.1 - Steel chimney .

Table 4.10.I – Shell thicknesses of the steel chimney.

Section	z_i (m)	z_s (m)	s (mm)
1	0,0	27,2	18
2	27,2	40,0	16
3	40,0	52,0	14
4	52,0	64,0	12
5	64,0	76,0	10
6	76,0	100,0	8

Analysis is performed by applying Annexes G, I, L and O.

Starting from the calculations made in clause 4.2, analysis proceeds in two stages.

In the first stage the along-wind wind actions are determined. In particular, the calculations concern the peak aerodynamic actions (clause 4.10.1), the dynamic parameters of the structure (clause 4.10.2), the dynamic factor and the equivalent along-wind static force (clause 4.10.3).

The second stage deals with the determination of the actions of critical wind velocities that cause resonant vortex shedding with the structure vibration. In particular, initial calculations concern the critical wind velocities and the corresponding Scruton numbers (clause 4.10.4). Subsequently, the peak tip deflections are determined, by using both the spectral method (clause 4.10.5) and the harmonic method (clause 4.10.6); these are used to calculate the equivalent across-wind static forces (clause 4.10.7). With the aim of fatigue analyses, clause 4.10.8 assesses the number of load cycles. In clause 4.10.9 a possible vibration mitigation strategy is analyzed. Clause 4.10.10 deals with the analysis of the ovalling of the shell.

4.10.1 Peak aerodynamic actions

By applying the rules given in clause 3.3.4, the peak aerodynamic actions per unit length are given by Equation (3.14), where q_p is the peak velocity pressure at the current height z of the structure, c_{fX}, c_{fY} and c_{mZ} are the force and moment aerodynamic coefficients per unit height, and l is the reference size.

The peak velocity pressure is given at clause 4.2.7. In particular, for $h = 100$ m and $T_R = 50$ years, $q_p(h) = 1.750$ N/m^2.

The aerodynamic coefficients and the reference size are calculated by applying Annex G. In particular, for slender structures and elongated elements, clause G.10.1 assigns $c_{fX} = c_{fXo}\psi_\lambda$, $c_{fY} = c_{fYo}\psi_\lambda$, $c_{mZ} = c_{mZo}\psi_\lambda$, (Equation G.18), where c_{fXo}, c_{fYo}, c_{mZo} are the aerodynamic coefficients for structures and structural elements of infinite length and ψ_λ is the slenderness coefficient.

The coefficients c_{fXo}, c_{fY} and c_{mZo} and the characteristic size l for slender structures and elongated elements with a circular cross section are given in clause G.10.6: l is equal to diameter b of the current cross section of the structure at height z; $c_{fYo} = c_{mZo} = 0$ for the polar symmetry of the cross section; c_{fXo} depends on Reynolds number Re and on surface roughness k. By applying the rules given in clause 3.3.7, the Reynolds number Re at the top of the structure is given by Equation (3.16), where $b = 3,8$ m, $v_m(h) = 37,30$ m/s; $\upsilon = 15 \cdot 10^{-6}$ m^2/s. Therefore, $Re = 9,45 \cdot 10^6$. Assuming that the external surface is made of polished steel, Table G.XVII gives $k = 0,05 \cdot 10^{-3}$ m; thus, at the top of the structure, $k/b = 13,16 \cdot 10^{-6}$. By applying Equation (G.22b), $c_{fXo} = 0.70$. Actually, this value depends on the height z above the ground. For simplicity and conservatively, it is assumed that this parameter is constant.

Coefficient ψ_λ is given at clause G.10.8 for the effective slenderness λ. From Table G.XIX, $\lambda = 0,7L/l$, where $L = h = 100$ m, $l = b = 3,80$ m (conservatively); thus, $\lambda = 18,42$. Lastly, by applying Equation (G.23), $\psi_\lambda = 0,77$.

The along-wind force coefficient is therefore $c_{fX} = c_{fXo}\psi_\lambda = 0,70 \cdot 0,77 = 0,54$.

The peak along-wind aerodynamic force per unit height is the product of the peak velocity pressure (clause 4.2.7), the diameter b of the current cross section of the chimney (Figure 4.10.1), and the force coefficient c_{fX}. Consequently:

$$f_X(z) = 778,21 \cdot (7 - 0,094 \cdot z) \cdot 0,54 \qquad \text{for } z \leq 5 \text{ m}$$

$$f_X(z) = 18,22 \cdot \ln\left(\frac{z}{0,1}\right) \cdot \left[\ln\left(\frac{z}{0,1}\right) + 7\right] \cdot (7 - 0,094 \cdot z) \cdot 0,54 \qquad \text{for } 5 < z < 34 \text{ m}$$

$$f_X(z) = 18,22 \cdot \ln\left(\frac{z}{0,1}\right) \cdot \left[\ln\left(\frac{z}{0,1}\right) + 7\right] \cdot 3,8 \cdot 0,54 \qquad \text{for } z \geq 34 \text{ m}$$

where z is expressed in m and f_x is expressed in N/m.

4.10.2   Dynamic parameters

The dynamic parameters of the chimney are calculated by using a finite element model and by applying the criteria given in Annex I.

Given the polar symmetry, the vibration mode occur in pairs. The first two frequencies are $n_1 = n_2 = 0,77$ Hz. The second two frequencies are $n_3 = n_4 = 3,34$ Hz. The first two mode shapes are therefore well approximated by $\Phi_1(z) = \Phi_2(z) = (z/h)^\zeta$ (clause I.3.1), where $h = 100$ m and $\zeta = 2$.

By applying the criterion given in clause I.4, the equivalent mass per unit height for the first two modes is equal to the mean value of the mass along upper third of the chimney. Thus, by using data reported in Figure 4.10.1, $m_{e,1} = m_{e,2} = 821$ kg/m.

The critical damping ratio is calculated by using the rules given in clause I.6. On the basis of Equation (I.28), it is given by the sum of three different contributions.

By applying Table I.IV, the structural damping ratio in the first two vibration modes is $\xi_{s,1} = \xi_{s,2} = 0,002$.

The aerodynamic damping ratio is essential for the alongwind oscillations of the structure, but cannot be taken into account for across-wind oscillations caused by resonant vortex shedding. By assuming for simplicity that mode 1 is along-wind and mode 2 is across-wind, the damping ratio ξ_a is given by the Equation (I.33), where $c_{fX} = 0,54$, $\rho = 1,25$ kg/m^3, $b = 3,80$ m (conservatively), $z_e = 60$ m (Figure L.2), $v_m(z_e) = 34,54$ m/s (clause 4.2.5), $n_D = 0,77$ Hz, $m_D = 821$ kg/m. Thus, $\xi_a = 0,011$.

In this stage it is assumed that no damping device is installed on the structure.

The overall damping ratio is thus equal to $\xi_1 = 0,002 + 0,011 = 0,013$ for the calculation of equivalent along-wind static actions; however, for the calculation of the equivalent across-wind static actions associated with resonant vortex shedding $\xi_2 = 0,002$.

4.10.3   Dynamic factor and equivalent along-wind static force

The dynamic actions and effects in the along-wind direction are evaluated by using the rules given in clause 3.4.

In accordance with Equation (3.17), the equivalent along-wind static force per unit height is the product of the peak aerodynamic force per unit length (clause 4.9.1) and the dynamic factor c_d. In this case $c_d = c_{dD}$, since c_{dD} is the along-wind dynamic factor. In the lack of more accurate assessments, it is determined by applying the criteria in Annex L.

By applying the detailed method (clause L.2), the dynamic factor c_{dD} is given by Equation L.2. It is calculated using Table L.I. The chimney corresponds to the first case in Figure L.2. Table 4.10.II summarises the steps towards the calculation of c_{dD}.

Table 4.10.II - Calculation of the along-wind dynamic factor.

Equation	Parameter
Figure L.2	$h = 100$ m
	$b = 3,8$ m
	$z_e = 60$ m
(3.5)	$v_m(z_e) = 34,54$ m/s
(3.7)	$I_v(z_e) = 0,156$
(3.8)	$L_v(z_e) = 154,71$ m
(I.4)	$n_D = 0,77$ Hz
(I.28)	$\xi_D = 0,013$
(L.4)	$B^2 = 0,588$
(L.6)	$S_D = 0,059$
(L.9)	$\eta_h = 8,917$
(L.9)	$\eta_b = 0,339$
(L.7)	$R_h = 0,106$
(L.8)	$R_b = 0,808$
(L.5)	$R_D^2 = 0,304$
(L.11)	$\upsilon_D = 0,450$ Hz
(L.10)	$g_D = 3,517$
(L.3)	$G_D = 2,038$
(L.2)	$c_{dD} = 0,974$

Note that, ignoring the aerodynamic part of damping and then calculating the dynamic factor with $\xi_D = 0,002$, the result is $c_{dD} = 1,347$.

4.10.4 Critical velocities (vortex shedding) and Scruton numbers

The equivalent static actions associated with vortex shedding in resonance with the structure are assessed by applying the criteria given in Annex O. It is therefore necessary to firstly determine the critical velocities, that is the mean wind velocities that cause resonance, and the relative Scruton numbers.

The critical wind velocity for the i-th across-wind vibration mode, $v_{cr,i}$, is given by Equation (O.2), where $n_{L,i}$ is the frequency of the i-th across-wind vibration mode, b is the diameter, and St is the Strouhal number. It is implemented provided that $v_{cr,i} \leq v_{m,l}$ where $v_{m,l}$ is the mean wind velocity at the tip of the structure, with return period $T_R = 500$ years (Equation O.3); then, $v_{m,l} = 45,02$ m/s (clause 4.2.5).

The first across-wind frequency is $n_{L,1} = 0,77$ Hz and the mode shape is maximum at the tip of the chimney (clause 4.10.2); thus, Equation (O.2) must be applied to the height $z = 100$ m, where $b = 3,80$ m (clause O.1, Figure O.3). The Strouhal number is a function of the Reynolds number and therefore of the critical wind velocity; in principle, the solution of Equation (O.2) thus requires an iterative calculation. It is possible to proceed as follows: 1) initially set $St = 0,2$, followed by $v_{cr,1} = 14,63$ m/s; 2) determine the Reynolds number by means of Equation (3.16), $Re = 3,7 \cdot 10^6$; 3) calculate the Strouhal number St using Table O.I and Figure O.4, $St = 0,22$; 4) the final value of the

critical velocity $v_{cr,1} = 13,3$ m/s corresponds to $Re = 3,37 \cdot 10^6$ (considering the level of convergence achieved, further iterations are not necessary). Since $v_{cr,1} = 13,3$ m/s $< v_{m,l} = 45,02$ m/s, a specific verification associated with the vortex shedding in resonance with the first vibration mode is required.

The second across-wind frequency is $n_{L,2} = 3,34$ Hz; Equation (O.2) is applied again to at $z = 100$ m, where $b = 3,80$ m and $St = 0,22$. The critical velocity $v_{cr,2} = 57,69$ m/s is obtained (considering the level of convergence achieved, further iterations are not necessary). Therefore, since $v_{cr,2} = 57,69$ m/s $< v_{m,l} = 45,02$ m/s, no specific check for vortex shedding in resonance with the second vibration mode is required. Obviously, the same conclusion applies to higher vibration modes, characterized by higher frequencies.

The Scruton number associated with the first across-wind vibration mode, and the first and only critical velocity, is given by the Equation (O.4), where $m_{e,1} = 821$ kg/m is the equivalent mass per unit length (clause 4.10.2), $\xi_1 = 0,002$ is the damping factor, non including aerodynamic damping (clause 4.10.2), $\rho = 1,25$ kg/m^3, $b = 3,8$ m; then $Sc_1 = 1,14$. It can be concluded that the chimney is potentially prone to shedding induced oscillations.

Calculation of the static equivalent across-wind force caused by critical vortex shedding with the first vibration mode is carried out by using the criterion given in clause O.4 (clause 4.10.7). It requires the preliminary calculation of the peak tip deflection. This calculation is performed by using both the spectral method (clause 4.10.5) and the harmonic method (clause 4.10.6).

4.10.5   Peak deflection - spectral method

Calculation of the peak deflection value $y_{pL,1}$ using the spectral method is based on the rules given in clause O.5, in particular Equation (O.7), where g_L is the peak factor and σ_L is the standard deviation of deflection.

The parameter g_L depends on the Scruton number $Sc = 1,14$ and on the aerodynamic damping parameter $K_a = K_{a,max} C_I$ (Equation O.9). Since $Re = 3,37 \cdot 10^6$, $K_{a,max} = 1$ (Table O.II, Figure O.8); moreover, since $v_{cr,1} = 13,3$ m/s > 10 m/s (Equation O.10, Figure O.9), $C_I = 0,7$; then $K_a = 0,7$. Therefore, by using Equation (O.8), $g_L = 1,42$.

The parameter σ_L is given by Equations (O.11)-(O.13) for $a_L = 0,4$, $Sc_1 = 1,14$, $K_a = 0,7$, thus $c_1 = 0,0696$; $\rho = 1,25$ kg/m^3, $b = 3,80$ m, $h = 100$ m, $m_{e,1} = 821$ kg/m, $K_a = 0,7$, $C_c = 0,01$, $St = 0,22$, then $c_2 = 8,152 \cdot 10^{-6}$. Therefore, $\sigma_L/b = 0,373$, $\sigma_L = 1,418$ m.

Lastly, by applying the Equation (O.7), $y_{pL,1} = 1,42 \cdot 1,418 = 2,014$ m is obtained, a quite large value.

4.10.6   Peak deflection - harmonic method

Calculation of the peak across-wind deflection $y_{pL,1}$ by means of the harmonic method is based on the rules given in clause O.6, in particular Equation (O.14), where $St = 0.22$, $Sc_1 = 1.14$, $K = 0.13$ (Table O.V).

The lateral force coefficient c_{lat} is given by Table O.VI and Figure O.13 for the Reynolds number. Since $Re = 3,37 \cdot 10^6$, $c_{lat} = 0,2$.

Coefficient K_w depends on L_1/b and $\lambda = h/b = 26,32$, where L_1 is the effective correlation length. This is the most critical element to be assessed and involves the application of the iterative method described in clause O.6. It is possible to proceed as follows.

Firstly, let us assign $L_1/b = 6$, assuming that $y_{pL,1}/b < 0.1$. Then determine $K_w = 0,54$ (Table O.V) and, consequently $y_{pL,1}/b = 0,254$ (Equation O.14). Since this value is higher than the initial choice, $y_{pL,1}/b > 0,1$, analysis is iterated by assessing $L_1/b = 7,848$ (Table O.IV, Figure O.12), $K_w = 0,60$ (Table O.V) and, consequently $y_{pL,1}/b = 0,283$ (Equation O.14). Iteration is complete since $K_w \geq 0,60$.

Therefore, $y_{pL,1} = 1,074$ m. As expected, this value is much lower than the one given by the spectral method (clause 4.10.6). Nevertheless, both values seem to be unacceptable.

4.10.7   Static equivalent crosswind force

The static equivalent across-wind force associated with resonant vortex shedding in the first across-wind vibration mode is given by Equation (O.5), where m is the mass per unit height given by Figure 4.10.1, $n_{L,1} = 0,77$ Hz $\Phi_{L,1}(z) = (z/h)^2$. Conservatively, by applying the spectral method (clause 4.10.5), $y_{pL,1} = 2,014$ m.

The coefficient $C_{TR,1}$ depends on the critical velocity $v_{cr,1} = 13,3$ m/s, the tip mean wind velocity (with $T_R = 50$ years), $v_{m,0} = 37,3$ m/s (clause 4.2.5) and the tip mean wind velocity (with $T_R = 500$ years), $v_{m,l} = 45,02$ m/s. Therefore, by applying Equation O.6, $C_{TR,1} = 1$.

In conclusion, the static equivalent across-wind force is:

$$F_L(z) = 47,141 \cdot m(z) \cdot \left(\frac{z}{100}\right)^2$$

where z is expressed in m, m in kg/m and F_L in N/m.

4.10.8   Number of load cycles caused by vortex shedding

Calculation of the number of load cycles caused by resonant vortex shedding during the nominal lifetime of the structure, $V_N = 50$ years, is performed by applying Equations (O.15) and (O.16), where $V_N = 50 \times 32 \cdot 10^6$ s, $n_{L,1} = 0,77$ Hz, $\varepsilon_0 = 0,3$, $v_{cr,1} = 13,3$ m/s, $v_0 = 0,2 \cdot 37,3 = 7,46$ m/s. then, $N = N_1 = 98 \cdot 10^6$.

4.10.9   Mitigation of vibrations

In order to mitigate vibrations caused by wind, without modifying the structural properties of mass and stiffness, it is possible to install a passive control system such as aerodynamic stabilizers or mechanical dampers described in clause O.9.

Aerodynamic stabilizers, such as helical vanes or screens, are limited in that they are effective only against across-wind vibrations caused by vortex shedding. On the contrary, they amplify the along-wind response, giving rise to an increase of the along-wind force coefficient. In this particular case, the use of helical vanes is also not recommended given the very low value of the Scruton number, $Sc_1 = 1,14 < 10$.

The use of a mechanical damper (*Tuned Mass Damper*, TMD) at the chimney tip reduces both along-wind and across-wind vibrations, is effective for all values of the Scruton number and is very common and extensively tested. Such a device, if properly designed, can bring to an overall damping ratio of $\xi_D = \xi_L = 0,05$.

In this case, analysis of the along-wind dynamic response of the chimney results in the value of the dynamic factor $c_{dD} = 0,888$. It ensures a reduction of 9 % compared to the value $c_{dD} = 0,974$ estimated without the TMD (clause 4.10.3).

The advantage of using a TMD is considerably higher for across-wind vibrations caused by vortex shedding, essentially because of the dramatic increase of the Scruton number; as this is proportional to damping, it increases from $Sc_1 = 1,14$ (clause 4.10.4) to $Sc_1 = 28,58$. Thus, applying the spectral method, the peak deflection is equal to $y_{pL,1} = 0,071$ m, compared to $y_{pL,1} = 2,014$ m evaluated without the TMD. By applying the harmonic method, the peak deflection is equal to $y_{pL,1} = 0,039$ m, compared to $y_{pL,1} = 1,172$ m evaluated without the TMD.

4.10.10   Ovalling

The shell of the chimney is potentially susceptible to static or dynamic ovalling (clause O.10).

Static ovalling is ignored, and dynamic ovalling only is considered, by applying the two criteria given in clause O.10.

Initially, the case of an unstiffened metal liner is considered. By applying the criterion indicated at clause I.2.6, the fundamental ovalling frequency, $n_{O,1}$, is given by Equation (I.11), where $b = 3,80$ m; considering the liner section at the tip, the thickness of the shell is $t = 0.008$ m. Therefore, $n_{O,1} = 1,418$ Hz.

By applying the first criterion introduced at clause O.10, the minimum value of the critical ovalling velocity (the most hazardous) is given by Equation (O.19) setting $n_{O,1} = 1,418$ Hz, $b = 3,8$ m, $\Omega = 4$. The Strouhal number St is a function of the Reynolds number (clause O.2); in this case $St = 0,22$. Thus, $v_{O,1} = 6,123$ m/s.

By applying the second criterion introduced at clause O.10, the minimum value of the critical ovalling velocity is given by Equation (O.20) setting $n_{O,1} = 1,418$ Hz, $\rho_s = 7850$ kg/m^3, $\rho = 1,25$ kg/m^3, $t = 0,008$ m, $b = 3,8$ m, $\xi_{O,1} = 0,002$. Thus, $v_{O,1} = 5,273$ m/s.

Note that, in this case, the two critical ovalling velocities are very similar to each other; therefore, the two criteria provide a substantially robust result. The lower value, considered in the next check, is equal to $v_{O,1} = 5,273$ m/s.

The mean wind velocity at the tip of the chimney, $h = 100$ m, with design return period $T_R = 500$ years, is equal to $v_{m,l} = 45,02$ m/s (clause 4.10.4). Thus, since the critical ovalling velocity is lower, the check of Equation (O.21) is not satisfied. An effective technique to overcome this problem is the use of stiffeners. In particular, stiffening rings are expected to increase the value of the fundamental ovalling frequency, $n_{O,1}$, at least enough to increase the critical ovalling velocity, $v_{O,1}$, above the mean wind velocity with $T_R = 500$ years.

4.11 TRUSS GIRDER RAILWAY BRIDGE

The structure examined in this clause is a truss girder bridge of the Treviglio-Bergamo railway, overpassing the A4 Milan-Bergamo-Brescia Motorway (Figure 4.11.1). The structure consists of two statically independent bridges. Each bridge has a 93,10 m span (Figure 4.11.2). The two bridges are longitudinally offset by 11,70 m.

Figure 4.11.1 – View of the twin railway bridges.

FRONT VIEW
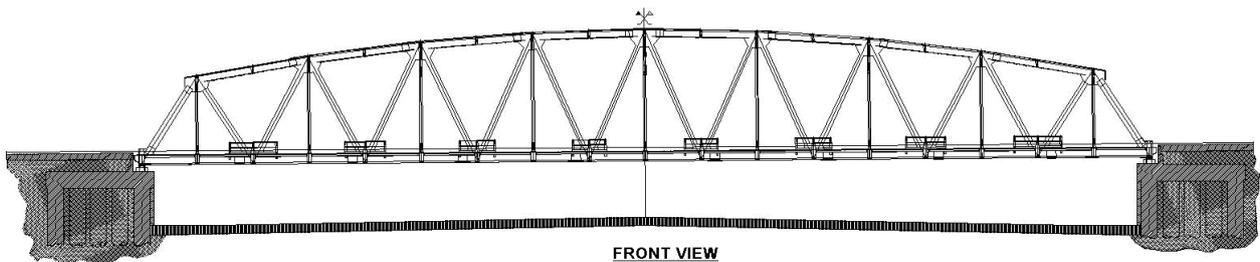
Figure 4.11.2 – Truss girder bridge – longitudinal view.

Each bridge has two load-bearing truss beams with parabolic top chord; thus each beam has a variable height. The two beams are connected together by bracing at the lower and upper levels (Figures 4.11.2 and 4.11.3). The distance between the bottom and top chords (height of the beam) is 8,00 m at the supports and 12,00 m at midspan. The distance between the two truss beams is 5,25 m. The two longitudinal beams are connected through crossbeams at 5,18 m distance centre-to-centre (5,11 m at the two panels at the support ends). Crossbeams also provide support for the deck. Outside and between the two bridges there are inspection gangways along the entire length of the bridges. The intradox of each bridge is at a height of 5,15 m from road level, which coincides with the ground level.
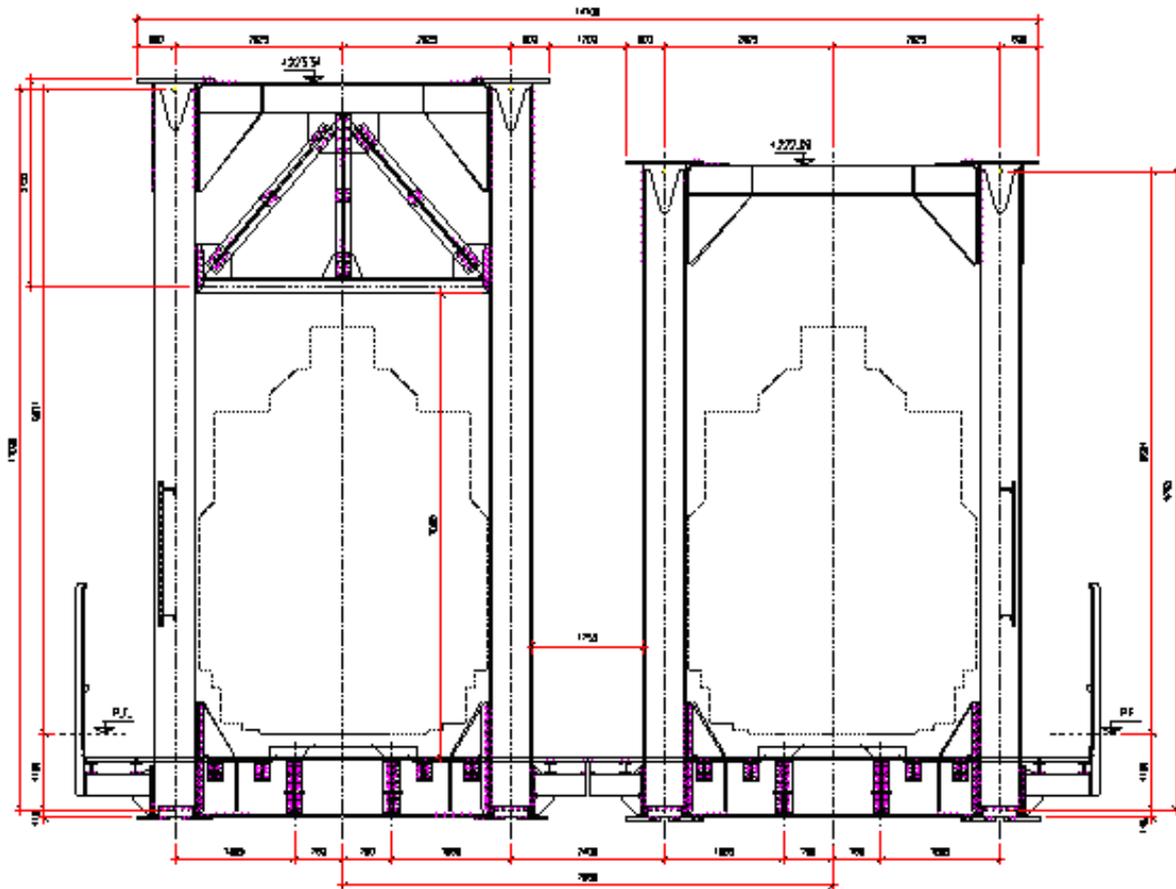
Figure 4.11.3 – Truss girder bridge – cross section.

The structural elements of the bridge consist of hot-formed steel plates and welded composite members from steel plates. The connections between the various structural members are bolted with precision couplings, in compliance with the requirements of Italian standard for the design, construction and testing of railway bridges.

The surfacing of the railway deck and the inspection gangways is made of checker plates to protect the motorway below against the accidental fall of objects. For the same reason, protective metal barriers are installed at the sides of the bridge overlooking the motorway, at heights of 2,00 m to 4,20 m from the bridge deck. Protective barriers are also installed along the parapets of the external gangways.

The ends of the bridges are supported on reinforced concrete piers by means of metal and PTFE bearings with spherical surfaces.

Analysis are performed by applying clauses 3.1-3.4 and Annexes G, I, L, O and P.

Starting from the calculations performed in clause 4.2, clause 4.11.1 gives the peak along-wind aerodynamic actions on the bridge. Clause 4.11.2 summarises the calculations for the dynamic parameters of the structure. Clause 4.11.3 determines the dynamic factor and the static equivalent along-wind forces.

Analysis is performed for three load cases (Table 4.11.I): the first relates to the bridge without the metal barriers and without a train; the second relates to the bridge with the metal barriers and without a train; the third relates to the bridge with both the metal barriers and a train.

Table 4.11.I – Load cases

Load case	Description
1	bridge without metal barriers and without a train
2	bridge with metal barriers and without a train
3	bridge with metal barriers and with a train

The analyses given in clauses 4.11.1 – 4.11.3 refer to the overall wind actions on the bridge. In general terms, however, calculations of the actions and effects of wind on the truss girder beams must also consider the actions and effects of wind on the individual elements comprising the truss girder beams. These actions and their effects must in no case be cumulated with the overall actions and effects.

Clauses 4.11.4 – 4.11.8 illustrate a calculation example referring to a single element. More precisely, clause 4.11.4 gives the calculation for the peak along-wind aerodynamic actions. Clause 4.11.5 summarises the calculations for the dynamic parameters. Clause 4.11.6 gives the calculations for the dynamic factor and the static equivalent along-wind forces. Clauses 4.11.7 and 4.11.8 deal with vortex shedding and galloping, respectively.

The results obtained for the selected element exclude significant dynamic and aeroelastic behaviour. This was to be expected given the stiffness of the element analysed. In general, however, this is not true: more flexible and lighter elements may individually give rise to considerable vibrations. In these cases, deeper analysis of the dynamic and aeroelastic behaviour of each single element is necessary.

4.11.1   Overall peak aerodynamic forces

By applying the rules given in clause 3.3.3, the peak along-wind aerodynamic force, F_X is given by Equation (3.13a), where q_p is the peak velocity pressure, c_{FX} is the along-wind force coefficient, $L^2 = A_n$ is the net reference area associated with the force coefficient. In the lack of more specific and well documented data or of wind tunnel measurements, these values are taken from Annex G.

Given the particular bridge under examination, consisting of twin truss girders with parabolic top chords, located adjacent at a distance less than the height of the trusses themselves, the overall wind actions on the bridge are determined by combining the aerodynamic actions on the individual trusses, calculated according to the rules given in clause G.9. In fact, the limits imposed in clause G.11 do not apply to this example, as they apply only to the types of bridge decks given in Figure G.54.

Analysis was performed by assuming that the wind acts at right angles to the plane of the truss beams. The force coefficient c_{FX} (clause G.9.1) is given by Equation (G.11), where c_{FXo} is the force coefficient for a structure of infinite length, ψ_λ is the slenderness coefficient depending on edge effects.

Load case 1

Edge effects are initially ignored and the calculation is made for the force coefficient c_{FXo} by applying the rules given in clause G.9.2. With reference to Figure G.38, $L = 93,10$ m, $d = 8$ m to the supports and $d = 12$ m at midspan. The gross loaded area of the truss is $A_c = 990$ m^2. The net area of the profiles is estimated to be approximately 264 m^2, to which a 10% is added to take the areas of the gusset plates into account. Thus, the net loaded area is $A_n = 290$ m^2. The resulting density is $\varphi = 0,29$ (Equation G.12). Equation (G.13) therefore indicates that the force coefficient is $c_{FXo} = 1,6$.

The reduction coefficient to take edge effects into account is given by Equation (G.17), where λ is the effective slenderness and φ is the density of the beam. The effective slenderness is calculated on

the basis of the mean height of the beam $l = A_c/L = 10,65$ m, since $L = 93,10$ m; the effective slenderness is therefore $\lambda = 1,4\ L/l = 12,2$ (Table G.XV). Equation (G.17) thus gives (for $\lambda = 12,2$) $\psi_\lambda = 0,991$ for $\varphi = 0,1$ and $\psi_\lambda = 0,916$ for $\varphi = 0,5$. Linear interpolation of the two values gives, for $\varphi = 0,29$, $\psi_\lambda = 0,955$. It follows that the force coefficient is equal to $c_{FX} = 1,60 \times 0,955 = 1,53$ (Equation G.11).

The reference height for the aerodynamic forces is equal to the height above ground of the top chord of the beam, that is $\overline{z}_e = 17,15$ m. Therefore, $q_p(\overline{z}_e) = 1138$ N/m^2. Note that, dividing the truss beam into several parts, it is allowed to attribute the relative reference height to each of these; this leads to a reduction of the peak velocity pressure and consequently of the aerodynamic forces.

By applying Equation (3.13a), the along-wind aerodynamic force acting on the beam directly exposed to the wind is $F_X = 504931$ N.

In order to calculate the aerodynamic force acting on the downwind truss beam, the value calculated above should be multiplied by the sheltering coefficient ψ_s defined by Equation (G.16). The ratio x/d takes the value 0,66 or 0,44, depending on whether d is assessed at the supports or at the centre-line; in any case, it is less than 3. Thus, for a value of the force coefficient equal to $c_{FXo} = 1,6$, it corresponds $\psi_s = 0,19$. The along-wind aerodynamic force acting on the downwind beam is therefore $F_X = 95148$ N.

In conclusion, the total force acting on the structure in the first load case is the sum of the forces acting on the two beams, $F_X = 504931 + 95148 = 600079$ N.

Load case 2

Load case 2 (Table 4.11.I) differs from load case 1 in that the metal barriers are mounted on the structure (Figure 4.11.3). Each bridge has two metal fence barriers. The first barrier, installed along the truss beam, has length $L = 93,1$ m, height $d = 2,20$ m and density $\varphi = 0,30$; the net area is therefore equal to $A_n = 61,446$ m^2. The second barrier, installed along the gangway, has length $L = 93,1$ m, height $d = 3,50$ m and density $\varphi = 0,18$; the net area is therefore equal to $A_n = 58,653$ m^2. The two barriers overlap by 0,70 m; nonetheless, since the fencing of the upwind barrier is not very dense, the small sheltering it offers to the barrier behind it is conservatively ignored.

Ignoring edge effects (clause G.9.2), Equation (G.13) indicates that the force coefficient is equal to $c_{FXo} = 1,6$ for the first barrier ($\varphi = 0,30$), $c_{FXo} = 1,68$ for the second barrier ($\varphi = 0,18$).

The reduction coefficient to take edge effects into account is given by Equation (G.17). The effective slenderness of the first barrier is $\lambda = 1,4\ L/d = 59$; Equation (G.17) therefore gives (for $\lambda = 59$) $\psi_\lambda = 0,998$ for $\varphi = 0,1$ and $\psi_\lambda = 0,964$ for $\varphi = 0,5$; Linear interpolation of the two values gives, for $\varphi = 0,30$, $\psi_\lambda = 0,981$. The slenderness of the second barrier is $\lambda = 1,4\ L/d = 38$; Equation (G.17) therefore gives (for $\lambda = 38$) $\psi_\lambda = 0,996$ for $\varphi = 0,1$ and $\psi_\lambda = 0,951$ for $\varphi = 0,5$; linear interpolation of the two values gives, for $\varphi = 0,18$, $\psi_\lambda = 0,987$.

It follows that the force coefficient for the first metal barrier is equal to $c_{FX} = 1,6 \times 0,981 = 1,57$ (Equation G.11); for the second barrier, it is equal to $c_{FX} = 1,68 \times 0,987 = 1,66$.

The reference height for aerodynamic forces is equal to the height above ground of the top of the barrier, that is $\overline{z}_e = 10,15$ m for the first barrier and $\overline{z}_e = 8,65$ m for the second barrier. Thus, for the first barrier, $q_p(\overline{z}_e) = 978$ N/m^2, while for the second barrier $q_p(\overline{z}_e) = 931$ N/m^2.

By applying Equation (3.13a), the along-wind aerodynamic force acting on the first barrier is $F_X = 94347$ N. The along-wind aerodynamic force acting on the second barrier is $F_X = 90645$ N.

In conclusion, since it is not possible to quantify the sheltering effect of the metal barriers on the truss beams, the total force acting on the structure in the second load case is equal to $F_X = 600079 + 94347 + 90645 = 785071$ N.

Load case 3

Load case 3 (Table 4.11.I) differs from load case 2 in that a train is present on the bridge. Based on the rules given in clause G.11, the height of the train is equal to 4 m. In the lack of more accurate assessments, the train is assumed to resemble an elongated element with a square cross section (clause G.10). The force coefficient per unit length in the wind direction is given by Equation (G.18a), where c_{FXo} is the force coefficient for a structure of infinite length, ψ_λ is the slenderness coefficient as a function of edge effects. Applying the rules given in clause G.10.2, $c_{fXo} = 2,1$. The slenderness coefficient is defined at clause G.10.8 for the effective slenderness λ. Applying Table G.XIX, $\lambda = 1,4$ $L/l = 33$. Finally, the slenderness coefficient is calculated by means of Equation (G.23b) and is $\psi_\lambda = 0,83$. Therefore, $c_{fX} = 2,1 \times 0,83 = 1,74$.

The reference height for the aerodynamic forces is equal to the height of the upper segment of the train, that is $\overline{z}_e = 9,15$ m. Thus, the peak velocity pressure is equal to $q_p(\overline{z}_e) = 948$ N/m^2. By applying Equation (3.14a), the along-wind aerodynamic force per unit length acting on the train is $f_X = 6598$ N/m; therefore, assuming that the train occupies the entire length of the bridge, $L = 93,10$ m, the total force is equal to $F_X = 6598 \times 93,1 = 614281$ N.

The train has a sheltering effect on the downwind beam, while the upwind beam has a sheltering effect on the train. In the lack of more accurate assessments (in particular, results of wind tunnel tests), as a first approximation the total force acting on the train is considered, while the force acting on the two truss beams is reduced by a 4 m high strip along the length of the beams, corresponding to the height of the train. Therefore, the net area of the beam is reduced to $A_n = 240$ m^2. Thus, applying Equation (3.13a), the along-wind aerodynamic force acting on the beam directly exposed to the wind is $F_X = 417874$ N, while that acting on the downwind beam is $F_X = 78743$ N.

In conclusion, if the force on the metal barriers is not added to the force on the train (a rather approximate and somewhat questionable hypothesis), the total force acting on the structure in the third load case is equal to $F_X = 417874 + 78743 + 614281 = 1110898$ N. This load, though calculated as the sum of the components for the two truss beams and the train, should be defined as a total load acting on the structure; it is therefore the task of the designer to decide, on the basis of the particular geometry of the structure, to which structural elements it would be appropriate to apply the wind load.

4.11.2   Overall dynamic parameters

Frequencies and mode shapes of the bridge are evaluated through finite element analyses. Define $n_D = n_1$ as the first longitudinal bending frequency of the truss beams. For the unloaded bridge (load cases 1 and 2), $n_1 = 1,28$ Hz; for the loaded bridge (load case 3), $n_1 = 0,945$ Hz.

The critical damping ratio is calculated by using the rules given in clause I.6. Based on Equation (I.28), it is given by the sum of three components. By applying Table I.V, the structural damping ratio for the first mode is $\xi_{s1} = 0,005$. Aerodynamic damping (clause I.6.5) is conservatively ignored. It is lastly assumed that no damping device is installed on the structure. Thus the total damping ratio coincides with the structural damping ratio.

4.11.3   Dynamic factors and overall alongwind equivalent static forces

The along-wind actions are calculated by using the rules given at clause 3.4.

In accordance with Equation (3.17), the equivalent static actions are expressed by the product of the peak aerodynamic force assessed at Clause 4.11.1 and the dynamic factor c_d. In this case, $c_d = c_{dD}$, since c_{dD} is the along-wind dynamic factor. In the lack of more accurate assessments, it is calculated by applying the criteria in L.2.

In particular, the dynamic factor c_{dD} is given by Equation (L.2). It is calculated by applying the method of Table L.I. The bridge corresponds to the second case of Figure L.2. Table 4.11.II summarises the steps towards the calculation of c_{dD} for the unloaded bridge (load cases 1 and 2) and the loaded bridge (load case 3).

Table 4.11.II - Calculation of the dynamic factor for the unloaded and loaded bridge.

Equation	Parameter (Load cases 1 and 2)	Parameter (Load case 3)
Figure L.2	$h = 10,65$ m	$h = 10,65$ m
	$b = 93,10$ m	$b = 93,10$ m
	$h_1 = 5,15$ m	$h_1 = 5,15$ m
	$z_e = 10,47$ m	$z_e = 10,47$ m
(3.5)	$v_m(z_e) = 25,1$ m/s	$v_m(z_e) = 25,1$ m/s
(3.7)	$I_v(z_e) = 0,215$	$I_v(z_e) = 0,215$
(3.8)	$L_v(z_e) = 59,23$ m	$L_v(z_e) = 59,23$ m
F.E. Analysis	$n_D = 1,28$ Hz	$n_D = 0,945$ Hz
(I.28)	$\xi_D = 0,005$	$\xi_D = 0,005$
(L.4)	$B^2 = 0,438$	$B^2 = 0,438$
(L.6)	$S_D = 0,0639$	$S_D = 0,0768$
(L.9)	$\eta_h = 2,17$	$\eta_h = 1,60$
(L.9)	$\eta_b = 19,0$	$\eta_b = 14,0$
(L.7)	$R_h = 0,356$	$R_h = 0,438$
(L.8)	$R_b = 0,0513$	$R_b = 0,0689$
(L.5)	$R_D^2 = 0,183$	$R_D^2 = 0,369$
(L.11)	$\upsilon_D = 0,695$ Hz	$\upsilon_D = 0,639$ Hz
(L.10)	$g_D = 3,64$	$g_D = 3,62$
(L.3)	$G_D = 2,23$	$G_D = 2,40$
(L.2)	$c_{dD} = 0,890$	$c_{dD} = 0,958$

Table 4.11.III summarises the values of equivalent along-wind static forces. These are given by the product of the peak aerodynamic forces (clause 4.11.1) and the corresponding dynamic factors (Table 4.11.II).

Table 4.11.III – Values of equivalent static forces.

Load case	Peak aerodynamic force (N)	c_{dD}	Equivalent static force (N)
1	600079	0,890	534070
2	785071	0,890	698713
3	1110898	0,958	1064240

4.11.4 Peak aerodynamic forces on a single element

As an example, the aerodynamic actions on the third diagonal of the truss beam are considered, the cross section of which is shown in Figure 4.11.4. The element is 11,04 m long and positioned with its web perpendicular to the plane of the truss beam. Thus, since the wind is perpendicular to the plane of the truss beam, its direction is parallel to the web.
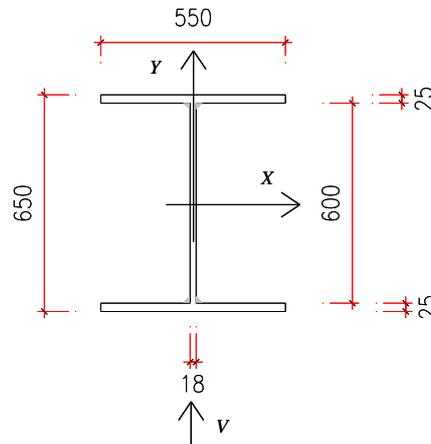

Figure 4.11.4 – Section of the third diagonal.

By applying the rules given in clause 3.3.4, the peak along-wind aerodynamic force per unit length (acting on axis Y) is given by Equation (3.14b), where q_p is the peak velocity pressure, c_{fY} is the along-wind force coefficient, z is the current height of the section above the ground, and l is the reference size (width) of the cross section. In the lack of more specific and well documented data or wind tunnel results, these values are calculated by applying Annex G.

By using the results obtained in clause 4.2.7, at the lower end of the element $z = 5,15$ m, then $q_p(z)$ = 786 N/m^2. At the upper end $z = 14,90$ m, then $q_p(z) = 1094$ N/m^2.

The along-wind force coefficient c_{fY} (clause G.10.1) is given by Equation (G.18b), where c_{fYo} is the along-wind force coefficient for an element of infinite length, ψ_λ is the slenderness coefficient depending on edge effects.

Figure G.50 shows an I-shaped cross-section with the width of the flanges equal to the height of the section. Although this is not the actual situation, in the lack of more accurate data, the values for this case are used. Thus, with oncoming wind parallel to the web, $c_{fYo} = 1,9$; the reference length l of the cross section of the element is also equal to the height b of the cross section. By applying the rules given in clause G.10.8, for $L = 11,04$ m and $l = b = 0,65$ m, the result is $L/l = 16,98$. On the basis of Table G.XIX, for the case of free flow on at least one end (as suggested for ordinary, unfixed joints of truss beams) and a cross section with sharp edges, $\lambda = 2 \cdot L/l = 33,96$. Equation (G.23b) or Figure G.53 gives $\psi_\lambda = 0,833$. It follows that the along-wind force coefficient is $c_{fY} = 1,90 \times 0,833 = 1,58$.

By applying Equation (3.14b), the along-wind aerodynamic force per unit length at the lower end of the element is $f_Y = 786 \times 0,65 \times 1,58 = 807$ N/m, while that acting on the upper end is $f_Y = 1094 \times 0,65 \times 1,58 = 1123$ N/m.

Given the shape of the peak velocity pressure profile, assuming a linear variation of the aerodynamic force along the element axis gives a slight underestimate of the overall aerodynamic force (on the element).

4.11.5 Dynamic parameters of the element

The dynamic parameters of the element were assessed by means of finite element models and by applying the criteria given in Annex I.

As a first approximation, the element is modelled as a prismatic beam with partially fixed joints. The cross section of the element has an area $A = 0,0383$ m^2; the moments of inertia for axes X and Y are respectively $J_x = 3,011 \cdot 10^{-3}$ m^4 e $J_y = 0,693 \cdot 10^{-3}$ m^4. The modulus of elasticity and the mass per unit of volume of the steel are respectively $E = 0.21 \cdot 10^{12}$ N/m^2 and $\rho_s = 7,850$ kg/m^3; thus, the mass per unit length of the element is $m = 300,65$ kg/m. By applying Equation (I.2), the frequencies given in Table 4.11.IV are obtained: n_D and n_L respectively indicate the first along-wind (along Y) and across-wind (along X) frequencies. The same table also gives the results of analysis performed by means of a global finite element model of the bridge.

Table 4.11.IV – Frequencies of the element.

Load case	n_D (Hz)	n_L (Hz)
pin – pin joints	18,69	8,97
fixed - fixed joints	42,37	20,35
finite element model	28,00	14,10

It is interesting to observe that the finite element model provides intermediate values between the theoretical limits. In any case, these are very high frequencies, typical of very stiff elements.

The first bending mode shapes of the element are given in Table I.III. Regardless of the end constraint, the mode has maximum amplitude at midspan.

By applying the criterion given in clause I.4, the equivalent mass per unit length (for any vibration mode) is equal to the mass (uniform) per unit length of the element, then $m_{e,i} = m = 300,65$ kg/m.

The critical damping ratio is calculated by using the rules given in clause I.6. On the basis of Equation (I.28), it is given by the sum of three components. In the lack of specific rules for individual elements and considering that the element has welded joints, it is advisable to conservatively assume a structural damping ratio $\xi_s = 0,002$. Aerodynamic damping (clause I.6.5) is conservatively ignored, and the element is not equipped with damping devices. Thus, the overall damping ratio coincides with the structural damping ratio.

4.11.6 Along-wind equivalent static forces of the element

The element has sufficiently high stiffness (first along-wind frequency higher than 5 Hz). Thus, clause 3.4.1 specifies that the dynamic factor can be given the value $c_d = 1$. The result, applying Equation (3.17), is that the equivalent along-wind static actions coincide with the peak aerodynamic actions.

In any case, assuming $c_d = 1$ is not mandatory, but leads to conservative results. By applying Annex L, it is possible to reduce the value of c_d.

4.11.7 Response of the element to vortex shedding

The response of the element to vortex shedding can be assessed by applying the criteria given in Annex O. It is therefore necessary to firstly determine the critical velocities, that is the mean wind velocities that cause resonance, and the relative Scruton numbers.

The critical wind velocity for the i-th across-wind mode i, $v_{cr,i}$, is given by Equation (O.2), where $n_{L,i}$ is the i-th across-wind frequency, b is the reference dimension (width) of the cross section, and

St is the Strouhal number. It can be implemented provided that $v_{cr,i} \leq v_{m,l}$, where $v_{m,l}$ is the mean wind velocity at the element midspan, $z_m = 10,02$ m, with return period $T_R = 500$ years (Equation O.3); thus, $v_{m,l} = 30,03$ m/s (clause 4.2.5).

The first across-wind frequency is $n_{L,1} = n_L = 14,1$ Hz and the mode shape is maximum at midspan (clause 4.11.5). Table O.I shows that $d/b = 0,650/0,550 = 1,18$ gives $St = 0,106$. Equation (O.2) is used to calculate the value of the first critical velocity $v_{cr,1} = 14,1 \cdot 0,55/0,106 = 73,16$ m/s. Since $v_{cr,1} = 73,16$ m/s $> v_{m,l} = 30,03$ m/s, specific checks for vortex shedding are not necessary. Note that the same result would be achieved if the conservative choice $n_{L,1} = n_L = 8,97$ Hz is made, corresponding to the case of a pinned-pinned element (Table 4.11.IV) (for example, if a finite element model is not available).

4.11.8 Galloping of the element

For a galloping instability to be extremely unlikely (clause P.2) the condition $v_{G,i} > v_{m,l}$ must be satisfied (Equation P.4), where $v_{G,i}$ is the critical velocity of galloping for the *i*-th across-wind mode, $v_{m,l} = 30,03$ m/s (clause 4.11.7). In general, the worst-case condition is that of galloping in the first mode (clause P.2.3).

The critical galloping velocity for the first across-wind mode, $v_{G,1}$, is given by Equation (P.2) where $m_{e,1} = 300,65$ kg/m is the equivalent mass per unit length (clause 4.11.5), $n_{L,1} = n_L = 14,1$ Hz is its first across-wind frequency (clause 4.11.5), $\xi_{L,1} = 0,002$ is the overall damping factor, not including aerodynamic damping (clause 4.11.5), $\rho = 1,25$ kg/m^3 is the air density, $b = 0.55$ m. Moreover, by applying Equation (O.4), the Scruton number for the first across-wind vibration mode is $Sc_1 = 19,98$. Lastly, since the cross section of the element is not among those of Table P.I, the galloping instability factor is assumed to be $a_G = 10$ (clause P.2.2). Thus, $v_{G,1} = 30,99$ m/s $> v_{m,l} = 30,03$ m/s.

It is to be noted that the obtained value is very close to the limit one, and this is due to the lack of specific information about the value to be assumed for parameter a_G; it as advisable to be very prudent in the selection of this parameter.

4.12 BOX GIRDER ROAD BRIDGE

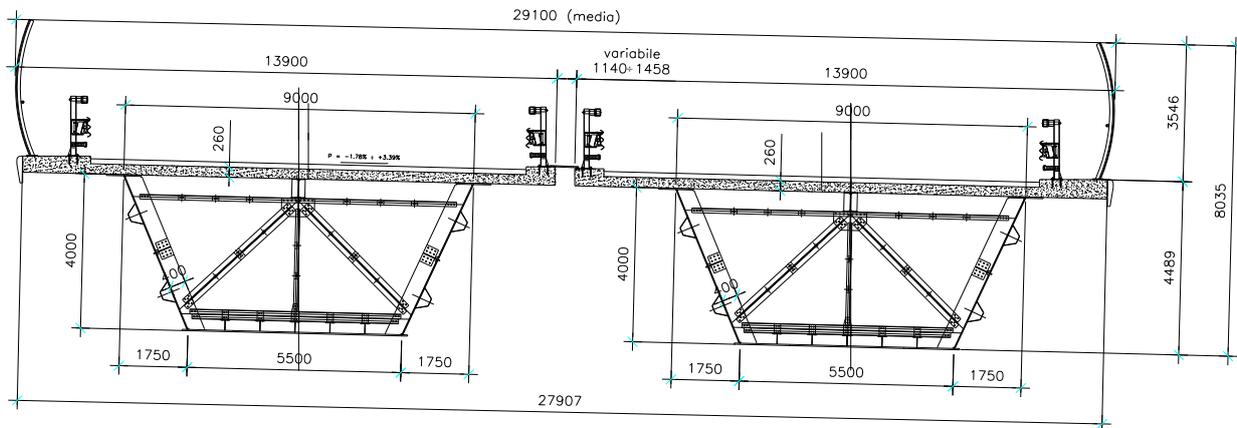The structure examined in this clause is a motorway bridge made of twin box decks (Figure 4.12.1).

Figure 4.12.1 – Cross section of the bridge.

Each deck consists of a trapezoidal steel box 4.000 mm in height; the lower base is 5.500 mm while the upper base is 9.000 mm; the box is completed with a reinforced concrete slab, 260 mm thick and 13.700 mm wide.

The two decks are structurally independent and flank each other at a variable distance of 1.140 to 1.458 mm. The overall width of the cross section therefore varies from 28,94 m to 29,26 m.

In the along-wind direction, the structural scheme of the bridge consists of a continuous beam with two spans on three supports; the two spans have the same length of 76.75 m. The overall length of the bridge is thus 153,50 m (Figure 4.12.2).
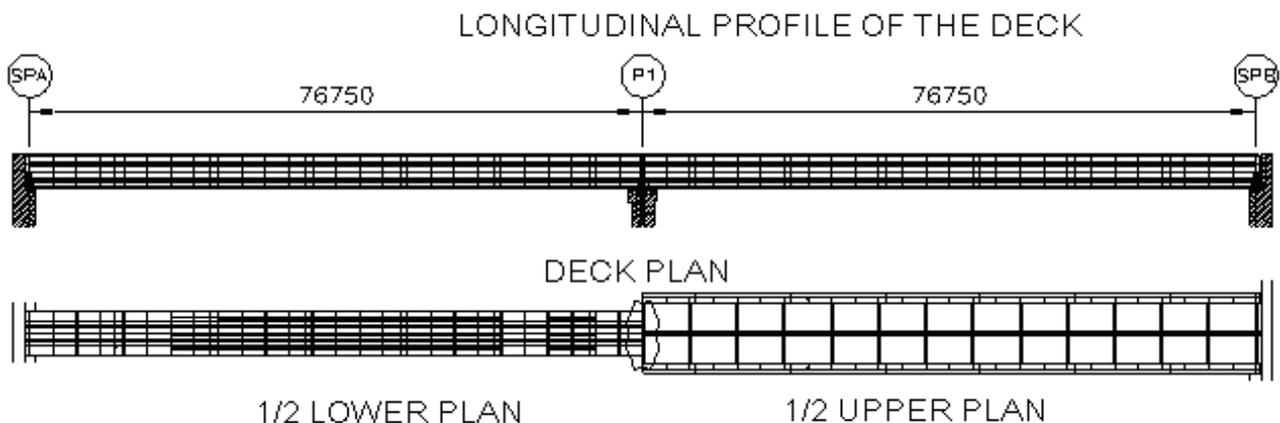
Figure 4.12.2 – Longitudinal view and plan of the bridge.

Two 3.548 mm high wind barriers with a slightly convex shape protect the outer side of each bridge; the cross section of the deck thus has a maximum height of 8.053 mm. The nominal height of road vehicles is 3 m (clause G.11), less than the height of the barriers. Thus, the height of the surface exposed to wind is independent of whether the bridge is loaded or not.

Table 4.12.I summarises the main geometric characteristics of the bridge, by using the symbols reported in Figure G.56.

Table 4.12.I – Geometric characteristics of the bridge.

$d_1 = d_2$	13.900 mm
d_0 (mean)	1.300 mm
$D = d_1 + d_0 + d_2$	29.100 mm
h_{tot}	8.035 mm
$D_G = d_1/2 + d_0 + d_2/2$	15.200 mm
L	76.750 mm

Calculation of wind actions on the deck is performed by using the rules given in clause 3.3.4 and Annexes G, L and P. Note that, in any case, clause G.11 (Bridge decks) in Annex G provides purely preliminary indications.

Starting from the calculations performed at clause 4.2, at clause 4.12.1 the peak aerodynamic wind actions on each deck are determined. Clause 4.12.2 calculates the peak aerodynamic actions transmitted by the decks to the central pier and to each shoulder. Clause 4.12.3 summarises the calculations for the dynamic parameters of the structure. Clause 4.12.4 analyses and discusses the dynamic factors and the equivalent static actions. Clause 4.12.5 calculates the susceptibility of the deck to aeroelastic phenomena (flutter).

4.12.1   Peak aerodynamic actions on each deck

By applying the rules given in clause 3.3.4, the peak aerodynamic actions per unit length are given by Equation (3.14), where f_X, f_Y and m_Z are respectively the along-wind force, the across-wind force and the torque per unit length; q_p is the peak velocity pressure, c_{fX}, c_{fY} and c_{mZ} are the aerodynamic coefficients of force and moment per unit length, and l is the relative reference dimension (which for bridges generally coincides with the width of the deck). In the lack of more specific and well documented data or of results from wind tunnel tests, these values are calculated by applying Annex G.11. The analysis refers to the case where the wind acts perpendicularly to the bridge axis.

The peak velocity pressure is given at clause 4.2.7. The reference height of the deck, $\bar{z}$, is equal to the highest point of the deck at midspan (clause G.11.1), $\bar{z} \cong 25{,}00$ m. Thus, for the reference height, and for $T_R = 50$ years, the peak velocity pressure is equal to $q_p(\bar{z}) = 1.260$ N/m^2.

The distance between the twin decks is equal to $d_0 = 1.3$ m (Table 4.12.I); the width of the two decks is $d_1 = d_2 = 13{,}90$ m; $d_0/\max\{d_1, d_2\} = 1{,}30/13{,}90 = 0{,}094 < 1/4$. Thus, with reference to Equation (G.25), calculation of aerodynamic actions on the decks is performed by means of the method for case b) given in clause G.11.2.

Three quantities have to be calculated in sequence: 1) the wind actions on each deck considered as isolated; 2) the wind actions considering the two decks as a single deck; 3) the wind actions on each deck.

1) <u>Wind actions on each deck considered as isolated</u>

The reference width is equal to $d_1 = 13{,}9$ m. Then, since $h_{tot.} = 8{,}035$ m, $d_1/h_{tot} = 1{,}73$.

By applying the rules given in clause G.11.1, and since $d_1/h_{tot.} = 1{,}73 < 2$, calculation of the force coefficient c_{fX} per unit length is performed by using the criteria for rectangular cross sections (clause G.10.3), Equation G.21. Thus, (for $d/b = 1{,}73$) $c_{fXo} = 1{,}76$. Considering the relevant length of bridge, the reduction arising from edge effects is conservatively ignored. A slenderness coefficient equal to $\psi_\lambda = 1$ is therefore assumed, resulting in $c_{fX} = c_{fXo} = 1{,}76$.

Attention must be paid to the fact that, in the case of a rectangular cross section (clause G.10.3), the coefficient c_{fX} refers to the size at right angles to the flow, b (Figure G.49). Thus, applying the Equation (3.14a) with $l = h_{tot}$, the along-wind force per unit length is equal to $f_{X1} = 17.818$ N/m.

By applying Equations (G.24b) and (G.24c), $c_{fY} = \pm 0,873$ and $c_{mZ} = \pm 0,2$; consequently, by applying Equations (3.14b) and (3.14c), the across-wind (vertical) force and the torque per unit length, referred to d_1, are equal to $f_{Y1} = \pm 15.289$ N/m and $m_{Z1} = \pm 48.689$ N·m/m.

2) <u>Wind actions considering the two decks as a single deck</u>

The reference width is equal to $d = 29,1$ m. Thus, since $h_{tot} = 8,035$ m, $D/h_{tot} = 3,62$.

By applying the rules given in clause G.11.1, and since $D/h_{tot.} = 3,62 > 2$, calculation of the force coefficient c_{fX} is performed by using Equation (G.24a). Thus, (for $d/h_{tot.} = 3,62$) $c_{fX} = 0,41$. Moreover, by applying Equations (G.24b) and (G.24c), $c_{fY} = \pm 1,062$ and $c_{mZ} = \pm 0,2$. Consequently, by applying Equations (3.14a), (3.14b) and (3.14c), the along-wind force, the across-wind (vertical) force and the torque per unit length, referred to D, are equal to $f_{X2} = 15.033$ N/m, $f_{Y2} = \pm 38.939$ N/m and $m_{Z2} = \pm 213.396$ N·m/m.

3) <u>Wind actions on each deck</u>

The wind actions on each deck derive from the calculations performed above by applying Equation (G.26). They are given in Table 4.12.II and must be applied at the centre of gravity of the deck.

Table 4.12.II – Peak aerodynamic actions per unit length (single deck).

Action	Value
f_X	17.818 N/m
f_Y	±30.305 N/m
m_Z	±48.689 N·m/m

The actions given in Table 4.12.II refer to the upwind deck. These values apply also to the other deck, interpreting this load case as associated to wind from the opposite direction to that examined.

4.12.2 Aerodynamic actions transmitted to central piers and to shoulders

Calculation of the peak aerodynamic actions transmitted by the two decks to the common support structures (in this case the central pier and the two end shoulders), is performed by using the relative method at case c), clause G.11.2.

The along-wind force is equal to the higher value between the force calculated considering the two decks together as a single deck of total width D, and the force calculated considering the upwind deck alone as isolated. In the first case, the action transmitted to the central pier is equal to $F_X = 15.033 \cdot (5/4) \cdot 76,75$ N $= 1,44 \cdot 10^6$ N; in the second case, $F_X = 17.818 \cdot (5/4) \cdot 76,75$ N $= 1,71 \cdot 10^6$ N. Thus, $F_X = 1,71 \cdot 10^6$ N. Consequently, the action transmitted to each of the shoulders is equal to $F_X = (3/10) \cdot 1,71 \cdot 10^6$ N $= 0,513 \cdot 10^6$ N.

The across-wind (vertical) force F_Y and the torque M_Z are assessed by considering the two decks together as a single deck of total width D. Thus, $F_Y = \pm 38.939 \cdot (5/4) \cdot 76,75$ N $= \pm 3,74 \cdot 10^6$ N, $M_Z = \pm 213.396 \cdot 76,75$ N·m $= \pm 16,38 \cdot 10^6$ N·m. Consequently, the actions transmitted to each shoulder are equal to $F_Y = \pm (3/10) \cdot 3,74 \cdot 10^6$ N $= \pm 1,12 \cdot 10^6$ N, $M_Z = \pm (1/2) \cdot 16,38 \cdot 10^6$ N·m $= \pm 8,19 \cdot 10^6$ N·m.

Table 4.12.III summarises the actions transmitted by the two decks to the central pier and to each shoulder.

Table 4.12.III – Actions transmitted by the two decks to the central pier and to the shoulders.

Action	Central pier	Shoulder
F_X	$1{,}71 \cdot 10^6$ N	$0{,}513 \cdot 10^6$ N
F_Y	$\pm 3{,}74 \cdot 10^6$ N	$\pm 1{,}12 \cdot 10^6$ N
M_Z	$\pm 16{,}38 \cdot 10^6$ N·m	$\pm 8{,}19 \cdot 10^6$ N·m

4.12.3 Dynamic parameters

The mass per unit length of each unloaded deck is $m = 1.970$ kg/m. The polar mass moment of inertia per unit length of each deck is $I_p = 62.300$ kg·m.

Calculation of the frequencies and vibration modes of the bridge is performed by means of finite element modelling. Table 4.12.IV gives the main frequencies (first vertical mode, first torsional mode and first horizontal mode) of the unloaded bridge (without traffic) and of the bridge at the full load. Figure 4.12.3 illustrates the three mode shapes corresponding to the frequencies given in Table 4.12.IV; the mode shapes without and with traffic are almost the same.

Table 4.12.IV – Main vibration frequencies.

Frequency	Unloaded bridge	Bridge at full load
vertical: $n_{L,1}$	1,21 Hz	1,06 Hz
torsional: $n_{M,1}$	3,74 Hz	3,28 Hz
longitudinal: $n_{D,1}$	4,79 Hz	4,21 Hz

The critical damping ratio is calculated through the rules given in clause I.6. Based on Equation (I.28), it is the sum of three components. By applying Table I.V to a bridge with composite steel-concrete structure, the structural damping ratio for the first mode is equal to $\xi_{s,1} = 0{,}006$. Aerodynamic damping (clause I.6.5) is conservatively ignored, and it is assumed that no damping devices are installed on the structure. Thus, the total damping ratio coincides with the structural damping ratio., $\xi_1 = \xi_{s,1} = 0{,}006$. It is assumed that this value is the same for all modes.
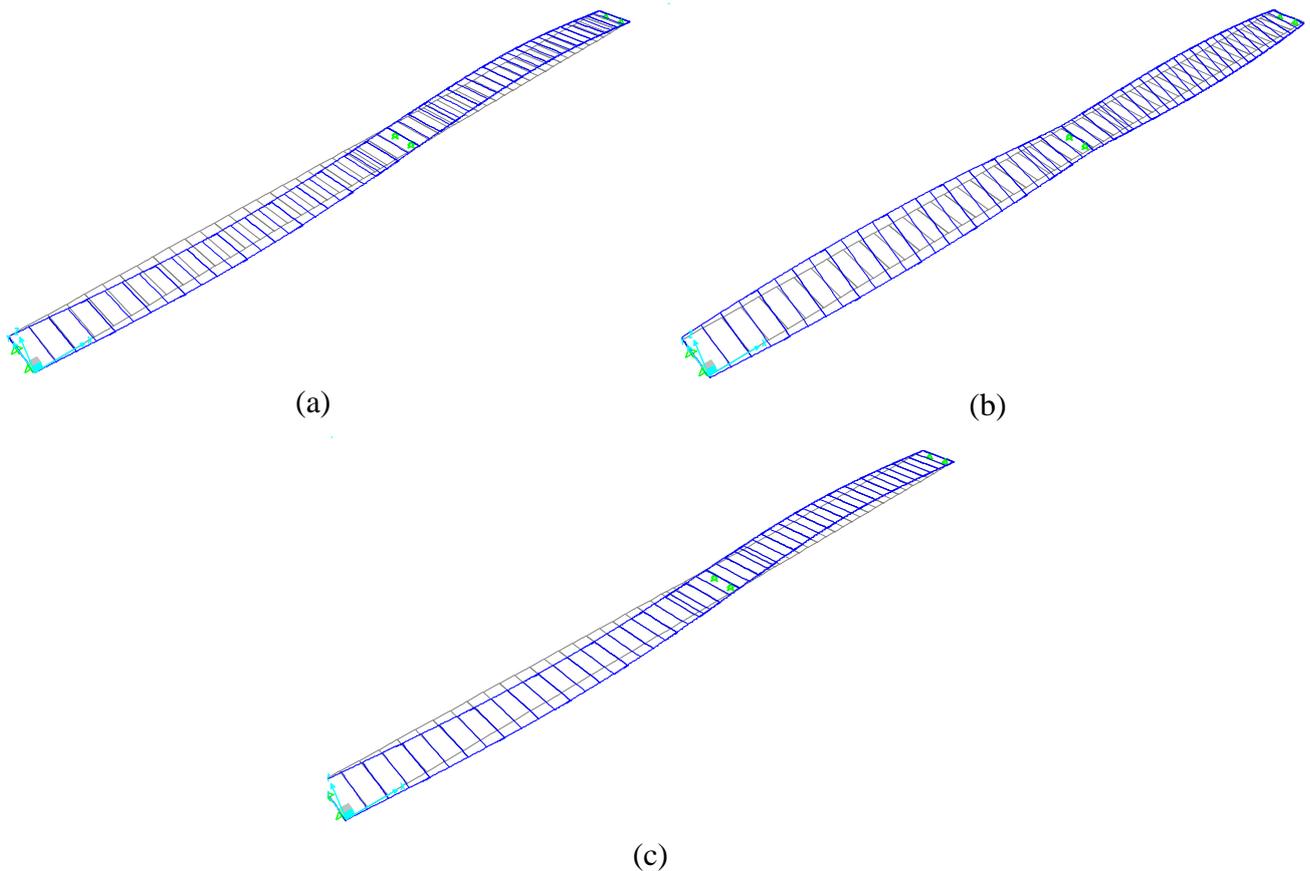
(a)

(b)

(c)

Figure 4.12.3 – Mode shapes of the deck: (a) first mode (first vertical mode); (b) third mode (first torsional mode); (c): sixth mode (first horizontal mode).

4.12.4   Dynamic factors and equivalent static actions

The along-wind actions are calculated by using the rules given at clause 3.4.

In accordance with Equation (3.17), the equivalent static actions are expressed by the product of the peak aerodynamic force calculated at Clause 4.11.1 and the dynamic factor c_d. In this case, $c_d = c_{dD}$, since c_{dD} is the along-wind dynamic factor. In the lack of more accurate assessments, this quantity is determined by applying the criteria in L.2.

In particular, the dynamic factor c_{dD} is given by Equation (L.2). It is calculated by applying the method of Table L.I. The bridge corresponds to the first case in Figure L.2. Table 4.11.IV summarises the steps towards the calculation of c_{dD} for the unloaded and loaded bridge.

Table 4.12.IV - Calculation of the longitudinal (alongwind) dynamic coefficient.

Equation	Parameter (Unloaded bridge)	Parameter (Bridge at full load)
Figure L.2	$h = 8,053$ m	$h = 8,053$ m
	$b = 76,750$ m	$b = 76,750$ m
	$h_1 = 21,00$ m	$h_1 = 21,00$ m
	$z_e \approx 25,00$ m	$z_e \approx 25,00$ m
(3.5)	$v_m(z_e) = 29,82$ m/s	$v_m(z_e) = 29,82$ m/s
(3.7)	$I_v(z_e) = 0,181$	$I_v(z_e) = 0,181$
(3.8)	$L_v(z_e) = 95,59$ m	$L_v(z_e) = 95,59$ m
F.E. Analysis	$n_D = 4,79$ Hz	$n_D = 4,21$ Hz
(I.28)	$\xi_D = 0,006$	$\xi_D = 0,006$
(L.4)	$B^2 = 0,545$	$B^2 = 0,545$
(L.6)	$S_D = 0,023$	$S_D = 0,025$
(L.9)	$\eta_h = 5,175$	$\eta_h = 4,548$
(L.9)	$\eta_b = 49,320$	$\eta_b = 43,348$
(L.7)	$R_h = 0,175$	$R_h = 0,196$
(L.8)	$R_b = 0,020$	$R_b = 0,023$
(L.5)	$R_D^2 = 0,010$	$R_D^2 = 0,014$
(L.11)	$\upsilon_D = 0,654$ Hz	$\upsilon_D = 0,674$ Hz
(L.10)	$g_D = 3,623$	$g_D = 3,631$
(L.3)	$G_D = 1,978$	$G_D = 1,984$
(L.2)	$c_{dD} = 0,872$	$c_{dD} = 0,875$

It is interesting to note that, in this particular case, the presence or otherwise of vehicles plays a more or less negligible role on the along-wind dynamic factor. In any case, since it is less than 1, this coefficient reduces the aerodynamic actions calculated in clauses 4.12.1 and 4.12.2, given the high stiffness of the structure, together with its relevant size.

The product of the along-wind aerodynamic forces (clauses 4.12.1 and 4.12.2) and the along-wind dynamic factor (Table 4.12.IV) provides the equivalent along-wind static forces given in Table 4.12.V.

Table 4.12.V – Equivalent along-wind static forces.

Force per unit length on each deck	$f_X = 17.818 \cdot 0,875 = 15.591$ N/m
Resulting force on the central pier	$F_X = 1,71 \cdot 10^6 \cdot 0,875 = 1,50 \cdot 10^6$ N
Resulting force on each shoulder	$F_X = 0,513 \cdot 10^6 \cdot 0,875 = 0,45 \cdot 10^6$ N

Calculation of the across-wind (vertical) equivalent static and torsional actions requires preliminary calculation of the relative dynamic factors. Unfortunately, at the current state of knowledge, there is no method that can be easily translated into practical rules. This is a problem in this particular case, where across-wind and torsional frequencies are lower than the along-wind frequency, thereby potentially giving rise to higher dynamic amplifications. In the lack of adequate calculation methods, and in the lack of specialist advice, as a approximation it can be set $c_{dL} = c_{dM} = 1$. It is then assumed that the equivalent across-wind and torsional static actions coincide with the corresponding peak aerodynamic actions. Such choice is reasonable, even though there is no guarantee that it is also conservative.

4.12.4   Susceptibility of the deck to flutter

In order to determine the susceptibility of the deck to flutter, the criteria given in Annex P, and in particular in clause P.4, are adopted; they concern the single deck assumed as isolated. Analysis is performed by initially calculating the susceptibility of the deck to torsional flutter (clause P.4.1); the susceptibility of the deck to coupled flutter (clause P.4.2) is then calculated.

By applying the rules given in clause P.4.1, and in particular Equation (P.11), $v_{m,l} = 29,82 \cdot 1,207 = 35,99$ m/s, $d = 13,9$ m, $n_{M,1} = 3,28$ Hz. Thus, the ratio at the left hand side of Equation (P.11) is equal to $0,95 < 3$. It is therefore possible to exclude the occurrence of torsion flutter.

By applying the rules given in clause P.4.2, and since $m = 1.970$ kg/m, $I_p = 62.300$ kg·m and $\rho = 1,25$ kg/m^3, Equation (P.13) gives the dimensionless parameters $r = 0.405$ and $\mu = 16,31$. Moreover, $n_{L,1} = 1,06$ Hz, $h/d = h_{tot.}/d = 8,035/13,900 = 0,58$, thus $\beta_F = 0,30$ (Figure P.6). Therefore, the ratio at the left hand side of Equation (P.12) is equal to $3,094 > 1,5$. The ratio at the left hand side of Equation (P.13) is equal to $2.93 < 20$. The ratio at the left hand side of Equation (P.14) is equal to $0,95$ and it is less than the ratio at the right hand side, which is $1,825$. Thus, since the three inequalities defined by Equations (P.12), (P.13) and (P.14) have been simultaneously verified, it is possible to exclude the occurrence of coupled flutter.

It shall be noted that flutter is a very hazardous phenomenon, especially for suspension and cable-stayed bridges. It is unlikely in a beam bridge such as the one analysed in this clause. Verification is in any case appropriate.